ISSN 2307-8960 (online)

World Journal of *Clinical Cases*

World J Clin Cases 2023 January 26; 11(3): 487-718

Published by Baishideng Publishing Group Inc

World Journal of Clinical Cases

Contents

Thrice Monthly Volume 11 Number 3 January 26, 2023

MINIREVIEWS

ORIGINAL ARTICLE

Retrospective Study

World Journal of Clinical Cases

Thrice Monthly Volume 11 Number 3 January 26, 2023

Contents

World Journal of Clinical Cases

Thrice Monthly Volume 11 Number 3 January 26, 2023

Contents

ABOUT COVER

AIMS AND SCOPE

The primary aim of *World Journal of Clinical Cases* (*WJCC*, *World J Clin Cases*) is to provide scholars and readers from various fields of clinical medicine with a platform to publish high-quality clinical research articles and communicate their research findings online.

WJCC mainly publishes articles reporting research results and findings obtained in the field of clinical medicine and covering a wide range of topics, including case control studies, retrospective cohort studies, retrospective studies, clinical trials studies, observational studies, prospective studies, randomized controlled trials, randomized clinical trials, systematic reviews, meta-analysis, and case reports.

INDEXING/ABSTRACTING

The *WJCC* is now abstracted and indexed in Science Citation Index Expanded (SCIE, also known as SciSearch®), Journal Citation Reports/Science Edition, Current Contents®/Clinical Medicine, PubMed, PubMed Central, Scopus, Reference Citation Analysis, China National Knowledge Infrastructure, China Science and Technology Journal Database, and Superstar Journals Database. The 2022 Edition of Journal Citation Reports® cites the 2021 impact factor (IF) for *WJCC* as 1.534; IF without journal self cites: 1.491; 5-year IF: 1.599; Journal Citation Indicator: 0.28; Ranking: 135 among 172 journals in medicine, general and internal; and Quartile category: Q4. The *WJCC*'s CiteScore for 2021 is 1.2 and Scopus CiteScore rank 2021: General Medicine is 443/826.

RESPONSIBLE EDITORS FOR THIS ISSUE

Production Editor: *Ying-Yi Yuan*; **Production Department Director:** *Xiang Li*; **Editorial Office Director:** *Jin-Lei Wang*.

NAME OF JOURNAL
World Journal of Clinical Cases

ISSN
ISSN 2307-8960 (online)

LAUNCH DATE
April 16, 2013

FREQUENCY
Thrice Monthly

PUBLICATION DATE
January 26, 2023

INSTRUCTIONS TO AUTHORS
https://www.wjgnet.com/bpg/gerinfo/204

GUIDELINES FOR ETHICS DOCUMENTS
https://www.wjgnet.com/bpg/GerInfo/287

GUIDELINES FOR NON-NATIVE SPEAKERS OF ENGLISH
https://www.wjgnet.com/bpg/gerinfo/240

PUBLICATION ETHICS
https://www.wjgnet.com/bpg/GerInfo/288

PUBLICATION MISCONDUCT
https://www.wjgnet.com/bpg/gerinfo/208

ARTICLE PROCESSING CHARGE
https://www.wjgnet.com/bpg/gerinfo/242

STEPS FOR SUBMITTING MANUSCRIPTS
https://www.wjgnet.com/bpg/GerInfo/239

ONLINE SUBMISSION
https://www.f6publishing.com

World Journal of Clinical Cases

Submit a Manuscript: https://www.f6publishing.com

World J Clin Cases 2023 January 26; 11(3): 487-492

DOI: 10.12998/wjcc.v11.i3.487

ISSN 2307-8960 (online)

MINIREVIEWS

Protective effects of combined treatment with ciprofol and mild therapeutic hypothermia during cerebral ischemia-reperfusion injury

Yi-Chao Wang, Meng-Jun Wu, Sheng-Liang Zhou, Zhi-Hui Li

Specialty type: Anesthesiology

Provenance and peer review: Unsolicited article; Externally peer reviewed.

Peer-review model: Single blind

Peer-review report's scientific quality classification

Grade A (Excellent): 0
Grade B (Very good): B
Grade C (Good): C
Grade D (Fair): 0
Grade E (Poor): 0

P-Reviewer: Rezus E, Romania; Seetharaman RV, India

Received: May 6, 2022
Peer-review started: May 6, 2022
First decision: June 9, 2022
Revised: June 13, 2022
Accepted: January 5, 2022
Article in press: January 5, 2023
Published online: January 26, 2023

Yi-Chao Wang, Sheng-Liang Zhou, Zhi-Hui Li, Department of Thyroid & Parathyroid Surgery Center, West China Hospital, Sichuan University, Chengdu 610041, Sichuan Province, China

Yi-Chao Wang, Sheng-Liang Zhou, Zhi-Hui Li, Laboratory of Thyroid and Parathyroid Disease, Frontiers Science Center for Disease-related Molecular Network, West China Hospital, Sichuan University, Chengdu 610041, Sichuan Province, China

Meng-Jun Wu, Department of Anesthesiology, Chengdu Women and Children's Central Hospital, School of Medicine, University of Electronic Science and Technology, Chengdu 610041, Sichuan Province, China

Corresponding author: Zhi-Hui Li, MD, Doctor, Department of Thyroid & Parathyroid Surgery Center, West China Hospital, Sichuan University; Laboratory of Thyroid and Parathyroid Disease, Frontiers Science Center for Disease-related Molecular Network, West China Hospital, Sichuan University. No. 37 Guoxue Lane, Wuhou District, Chengdu 640041, Sichuan Province, China. zhihuiliwt@163.com

Abstract

Despite improvement in cardiopulmonary resuscitation (CPR) performance, cardiac arrest (CA) is still associated with poor prognosis. The high mortality rate is due to multi-organ dysfunction caused by cerebral ischemia and reperfusion injury (I/R). The guidelines for CPR suggest the use of therapeutic hypothermia (TH) as an effective treatment to decrease mortality and the only approach confirmed to reduce I/R injury. During TH, sedative agents (propofol) and analgesia agents (fentanyl) are commonly used to prevent shiver and pain. However, propofol has been associated with a number of serious adverse effects such as metabolic acidosis, cardiac asystole, myocardial failure, and death. In addition, mild TH alters the pharmacokinetics of agents (propofol and fentanyl) and reduces their systemic clearance. For CA patients undergoing TH, propofol can be overdosed, leading to delayed awakening, prolonged mechanical ventilation, and other subsequent complications. Ciprofol (HSK3486) is a novel anesthetic agent that is convenient and easy to administer intravenously outside the operating room. Ciprofol is rapidly metabolized and accumulates at low concentrations after continuous infusion in a stable circulatory system compared to propofol. Therefore, we hypothesized that treatment with HSK3486 and mild TH after CA could protect the brain and other organs.

Key Words: HSK3486; Therapeutic; Cerebral ischemia-reperfusion injury; Hypothesis

Core Tip: Ciprofol (HSK3486) is a novel anesthetic agent that is convenient and easy to administer intravenously outside the operating room. Ciprofol is rapidly metabolized and accumulates at low concentrations after continuous infusion in a stable circulatory system compared to propofol. We hypothesize that HSK3486 can improve survival rates and achieve good neurological outcomes in cardiac arrest patients who receive therapeutic hypothermia.

Citation: Wang YC, Wu MJ, Zhou SL, Li ZH. Protective effects of combined treatment with ciprofol and mild therapeutic hypothermia during cerebral ischemia-reperfusion injury. *World J Clin Cases* 2023; 11(3): 487-492
URL: https://www.wjgnet.com/2307-8960/full/v11/i3/487.htm
DOI: https://dx.doi.org/10.12998/wjcc.v11.i3.487

INTRODUCTION

Cardiac arrest (CA) is associated with poor prognosis. CA accounts for approximately 15% of all deaths and 50% of all cardiac deaths worldwide[1]. Survival rates with good neurological outcomes are low, in the range between 2% and 23%, depending on a variety of regional, social, and medical factors[2,3]. From a pathophysiology perspective, post-CA myocardial injury and brain injury are induced by ischemia/reperfusion injury (I/R injury)[4,5]. The guidelines for cardiopulmonary resuscitation (CPR) suggest that therapeutic hypothermia (TH) is an effective treatment to decrease mortality, and CPR is the only approach confirmed to reduce I/R injury[6,7].

During TH, sedative agents (propofol) and analgesia agents (fentanyl) are commonly used to prevent shiver and pain[6]. However, studies have shown that propofol has been associated with a number of serious adverse effects such as metabolic acidosis, cardiac asystole, myocardial failure, rhabdomyolysis, and death[7-9]. Low-grade myotoxicity can be associated with prolonged (weeks) exposure to propofol in the intensive care unit (ICU), especial in children. Several studies reported that prolonged propofol sedation of coronavirus disease 2019 (COVID-19) patients with long-term mechanical ventilation contributed to critical illness myopathy[8-10]. In addition, it has been shown that mild TH alters the pharmacokinetics of propofol and fentanyl and reduces their systemic clearance in rats after the return of spontaneous circulation (ROSC)[11,12]. For CA patients who have undergone TH, propofol can be overdosed, leading to delayed wakening, prolonged mechanical ventilation, and other subsequent complications, often referred to as propofol syndrome[12].

Ciprofol (HSK3486) (Figure 1), which is a 2,6-disubstituted alkylphenol phenol derivative, is a novel propofol analogue formulated in an injectable emulsion of medium- and long-chain triglycerides[13]. Its pharmacokinetics and distribution indicate that HSK3486 is rapidly metabolized and has low accumulation after continuous infusion[14]. One study reported that HSK3486, like propofol, exerts its sedative effects through binding to gamma-aminobutyric acid type A (GABAA) receptors, but showed higher liposolubility and potency than propofol[15]. Furthermore, to achieve the same level of anesthesia, fewer lipids from the HSK3486 emulsion enter into the circulatory system compared to propofol emulsion[16]. HSK3486 at a maintenance dose of 3-4 mg/kg/h showed good efficacy and safety in the treatment of long-term mechanically ventilated patients in the ICU[16,17]. However, whether HSK3486 can improve survival rates in CA patients who receive TH remains unclear.

HYPOTHESIS

We hypothesize that HSK3486 can improve survival rates and achieve good neurological outcomes in CA patients who receive TH.

RATIONALE FOR THE HYPOTHESIS

The high mortality rate of CA is attributed to whole-body I/R induced multi-organ dysfunction that is referred to as post-cardiac arrest syndrome (PCAS)[18-20]. Post-CA myocardial dysfunction, macrocirculatory dysfunction, and brain injury are the main clinical features of this complex pathophysiological process. Myocardial dysfunction after CA commonly results in death and hemodynamic instability[19]. Increased heart rate and blood pressure after ROSC are attributed to medications and catecholamine release. These effects cause a global stunning of the myocardium that usually resolves and returns to

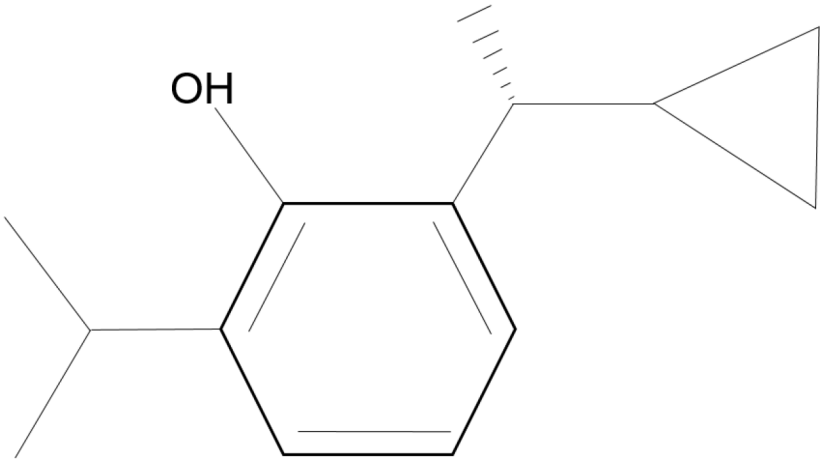

DOI: 10.12998/wjcc.v11.i3.487

Figure 1 The chemical structure of Ciprofol. Ciprofol introduces cyclopropyl on the basis of the chemical structure of propofol to form a chiral structure, which increases the steric effect and enhances the affinity for gamma-aminobutyric acid type A receptors. Ciprofol is a new type of intravenous anesthetic drug with rapid onset of action, rapid recovery, high potency, and less injection pain.

normal after 72 h[20].

Studies have shown that propofol is associated with a number of serious adverse effects such as metabolic acidosis, cardiac asystole, myocardial failure, rhabdomyolysis, and death[7-10]. Low-grade myotoxicity can be associated with prolonged (weeks) exposure to propofol in the ICU[11]. In both clinical and experimental studies where patients and animals have been exposed to long-term (10 d) controlled mechanical ventilation, patients and animals developed critical illness myopathy[8-12]. Thus, for CA patients, propofol infusion syndrome should be reduced to maintain a stable circulatory system, especial when TH treatment has been used.

Ciprofol (HSK3486), which is a 2,6-disubstituted alkylphenol phenol derivative, is a novel propofol analogue formulated in an injectable emulsion of medium- and long-chain triglycerides[13-15]. HSK3486 acts against the α1β2γ2 subtype of GABAA receptors and inhibits a wide range of CYP450 isozymes in mammalian species. Its pharmacokinetics and distribution indicate that HSK3486 is rapidly metabolized and has low accumulation after continuous infusion. One study reported that HSK3486 showed better anesthesia potency over propofol, with an 83% lower ED50. Furthermore, fewer lipids from the HSK3486 emulsion enter into the stable circulatory system compared to a propofol emulsion. Thus, HSK3486 can achieve the same sedative depth during TH after CA and may improve survival rates compared to propofol.

EVALUATION OF THE HYPOTHESIS

This hypothesis can be tested in two ways using rat models of CA. First, we could compare the protective effects of HSK3486 and propofol directly, and second we could test whether the combination of HSK3486 and TH confers greater protection that either HSK3486 or propofol alone.

The CA animal model was established in our previous study[11,21]. Here we would adapt it as follows. After anesthesia, we will induce CA by applying six minutes of asphyxia. We will then use CPR with mechanical ventilation of 100% oxygen, at a frequency of 80 breaths/min, tidal volume of 10 ml/kg, and sternal compressions (with two fingers) at a rate of 200 times/min (attempting to generate systolic arterial pressure peaks > 50 mmHg). We will continue CPR until return of spontaneous circulation (ROSC), defined as achieving a spontaneous mean arterial pressure (MAP) of 60 mmHg, that is maintained for more than 10 min[13,21]. We will simultaneously administer epinephrine (0.02 mg/kg i.v.) with the sternal compressions every 3 min if necessary, and 5% $NaHCO_3$ (1 mmol/kg i.v.) can also be provided if needed. If overall CPR attempts exceed 5 min, the experiment will be stopped. After ROSC, rats will be divided randomly into four groups: S group (sham-operate group), CPR group (infusion with saline 4 ml/kg for 30 min), HSK3486 group (infusion with HSK3486 at 0.4 mg/kg for 30 min), and propofol group (infusion with 2 mg/kg emulsion for 30 min). Survival conditions, behavioral evaluations, echocardiogram, and histopathologic analysis (including TUNEL staining of neurons and cardiomyocytes and Nissl staining of neurons) in each group will be evaluated on days 1 and 7 after ROSC. We will then compare the protective effects of HSK3486 and propofol post-conditioning. In the second set of experiments we will also evaluate the effects of TH. The CA model will be established as described above, but rats will be randomly divided into five groups after ROSC: CPR group, HSK3486 group (infusion with HSK3486 at 2 mg/kg for 30 min), TH group (maintaining rectal temperature at 33

± 0.5℃ for 2 h), HSK3486-TH group (TH will be initiated with HSK3486 infusion at 33 ± 0.5℃ for 2 h), and propofol-TH group (TH will be initiated with propofol infusion at 33 ± 0.5℃ for 2 h). We will conduct the same evaluations at days 1 and 7 as described for first set of experiments. However, during these experiments, the left femoral artery and vein will be separately cannulated with catheters to measure blood pressure and for drug administration. The rectal temperature will be controlled throughout the experiment with the aid of a lamp or ice bag. Rectal temperature, MAP, electrocardiogram, and blood gas levels will be continuously monitored during the experiment.

CONSEQUENCES AND DISCUSSION OF HYPOTHESIS

Despite the advances in treatment of PCAS, a significant proportion of patients still have a poor prognosis. The pathophysiological processes that occur after whole-body I/R injury following CA lead to multi-organ dysfunction. The subsequent reperfusion injury after ROSC causes cardiac and brain dysfunction. HSK3486, as an intravenous anesthetic, has advantages such as rapid metabolism and low accumulation in the circulation compared to propofol.

HSK3486 is a GABAA receptor agonist that has been shown to have an improved anesthetic profile and less injection pain compared to propofol in pre-clinical studies. HSK3486 is formulated in a 10% oil-in-water emulsion with a drug concentration of 10 mg/mL. Compared with lipophilic drugs, such as midazolam, HSK3486 is metabolized at faster rate and reduces the deepening of sedation. HSK3486 has been used for clinical endoscopy, but it has also been recommended for adult patients who may need general anesthesia for fiberoptic bronchoscopy. In a previous trial, Teng *et al*[22] demonstrated the safety of HSK3486 during colonoscopy with good tolerance. In addition, HSK3486 has shown good tolerance in some unpublished studies (NCT03698617, NCT03808844, NCT04048811, and NCT04511728). Furthermore, based on available data, HSK3486 causes less potential damage to cardiovascular and cerebrovascular function, as evidenced by stable hemodynamics and its reported safety profile[23]. Glucuronidation, oxidation, and sulfation are the major metabolic pathways targeted by HSK3486, and its glucuronidation metabolites are generally considered to be nonhypnotic, nontoxic, and rapidly cleared in from the plasma[14]. In summary, HSK3486 may become a promising anesthetic agent.

The available studies provide some useful guidance regarding the appropriate dose for post-conditioning and HSK3486 adaptation. Teng *et al*[22] reported that HSK3486 could be administered at a range of 0.1-0.5 mg/kg during colonoscopy. The study by Li *et al*[23] showed that a sedative effect could be achieved at 0.3 mg/kg in the elderly compared to 0.4 mg/kg in the non-elderly. Thus, 0.4 mg/kg of HSK3486 would be the chosen dose to test in combination with TH. However, due to the lack of research on the appropriate dose of HSK3486 for intravenous administration in CA, more studies are needed to test our hypothesis.

We hypothesize that HSK3486 in combination with TH would confer cardio-protective effects and less risks compared to propofol. The combination of HSK3486 and TH may synergistically prevent neuronal injuries caused by I/R following CA, due to the fact that HSK3486 can be rapidly metabolized. Additionally, this combination could potentially ameliorate the side effects of hypothermia. Therefore, HSK3486 treatment in combination with TH could be a novel treatment for CA patients.

Testing our hypothesis would provide new insight about the treatment of CA, providing a promising prevention strategy for post-arrest myocardial and neuronal reperfusion injury.

LIMITATIONS

Here we propose one hypothesis for using a combined TH treatment after CA, but more experimental data is needed to test our hypothesis, and further studies are needed to elucidate the cardio-protective mechanism of ciprofol in the future.

CONCLUSION

Based on the experimental laboratory data, we hypothesize that HSK3486 administered with TH after CA would improve patient survival rates and lead to good neurological outcomes.

FOOTNOTES

Author contributions: Wang YC designed the study, conducted the data collection, and drafted the manuscript; Wu MJ performed the data collection and helped in the manuscript preparation and data analysis; Zhou SL helped in the manuscript preparation, grammatical revision, and data analysis; Li ZH performed the statistical analysis and helped

in the data collection and in the manuscript preparation; All the authors approved the final version of the paper and agree to be accountable for all aspects of the work thereby ensuring that questions related to the accuracy or integrity of any part of the work are appropriately investigated and resolved.

Conflict-of-interest statement: We declare that we have no financial and personal relationships with other people or organizations that can inappropriately influence our work, there is no professional or other personal interest of any nature or kind in any product, service and/or company that could be construed as influencing the position presented in, or the review of, the manuscript entitled "Protective effects of combined treatment with Ciprofol and mild therapeutic hypothermia during cerebral ischemia-reperfusion injury".

Country/Territory of origin: China

ORCID number: Yi-Chao Wang 0000-0003-2216-5626; Meng-Jun Wu 0000-0002-6899-4318; Sheng-Liang Zhou 0000-0003-2927-4390; Zhi-Hui Li 0000-0003-4080-177X.

S-Editor: Liu JH
L-Editor: A
P-Editor: Liu JH

REFERENCES

1 **Woodruff TM**, Thundyil J, Tang SC, Sobey CG, Taylor SM, Arumugam TV. Pathophysiology, treatment, and animal and cellular models of human ischemic stroke. *Mol Neurodegener* 2011; **6**: 11 [PMID: 21266064 DOI: 10.1186/1750-1326-6-11]
2 **Dalessio L**. Post-Cardiac Arrest Syndrome. *AACN Adv Crit Care* 2020; **31**: 383-393 [PMID: 33313705 DOI: 10.4037/aacnacc2020535]
3 **Xie W**, Zhou P, Sun Y, Meng X, Dai Z, Sun G, Sun X. Protective Effects and Target Network Analysis of Ginsenoside Rg1 in Cerebral Ischemia and Reperfusion Injury: A Comprehensive Overview of Experimental Studies. *Cells* 2018; **7** [PMID: 30545139 DOI: 10.3390/cells7120270]
4 **Zhang WF**, Jin YC, Li XM, Yang Z, Wang D, Cui JJ. Protective effects of leptin against cerebral ischemia/reperfusion injury. *Exp Ther Med* 2019; **17**: 3282-3290 [PMID: 30988703 DOI: 10.3892/etm.2019.7377]
5 **Cadenas S**. ROS and redox signaling in myocardial ischemia-reperfusion injury and cardioprotection. *Free Radic Biol Med* 2018; **117**: 76-89 [PMID: 29373843 DOI: 10.1016/j.freeradbiomed.2018.01.024]
6 **Peberdy MA**, Callaway CW, Neumar RW, Geocadin RG, Zimmerman JL, Donnino M, Gabrielli A, Silvers SM, Zaritsky AL, Merchant R, Vanden Hoek TL, Kronick SL; American Heart Association. Part 9: post-cardiac arrest care: 2010 American Heart Association Guidelines for Cardiopulmonary Resuscitation and Emergency Cardiovascular Care. *Circulation* 2010; **122**: S768-S786 [PMID: 20956225 DOI: 10.1161/CIRCULATIONAHA.110.971002]
7 **Kam PC**, Cardone D. Propofol infusion syndrome. *Anaesthesia* 2007; **62**: 690-701 [PMID: 17567345 DOI: 10.1111/j.1365-2044.2007.05055.x]
8 **Eltzschig HK**, Eckle T. Ischemia and reperfusion--from mechanism to translation. *Nat Med* 2011; **17**: 1391-1401 [PMID: 22064429 DOI: 10.1038/nm.2507]
9 **Lucchetta V**, Bonvicini D, Ballin A, Tiberio I. Propofol infusion syndrome in severe COVID-19. *Br J Anaesth* 2020; **125**: e441-e442 [PMID: 32912604 DOI: 10.1016/j.bja.2020.08.020]
10 **Lönnqvist PA**, Bell M, Karlsson T, Wiklund L, Höglund AS, Larsson L. Does prolonged propofol sedation of mechanically ventilated COVID-19 patients contribute to critical illness myopathy? *Br J Anaesth* 2020; **125**: e334-e336 [PMID: 32600801 DOI: 10.1016/j.bja.2020.05.056]
11 **Yuan J**, Yang MC, Wu MJ, Gou YS. Sedative depth on neurological outcomes in a juvenile rat model of cardiopulmonary resuscitation. *Med Hypotheses* 2019; **132**: 109233 [PMID: 31606702 DOI: 10.1016/j.mehy.2019.109233]
12 **Zhang YJ**, Wu MJ, Li Y, Yu H. Cardiocerebral protection by emulsified isoflurane during cardiopulmonary resuscitation. *Med Hypotheses* 2015; **84**: 20-24 [PMID: 25466299 DOI: 10.1016/j.mehy.2014.11.008]
13 **Bian Y**, Zhang H, Ma S, Jiao Y, Yan P, Liu X, Xiong Y, Gu Z, Yu Z, Huang C, Miao L. Mass balance, pharmacokinetics and pharmacodynamics of intravenous HSK3486, a novel anaesthetic, administered to healthy subjects. *Br J Clin Pharmacol* 2021; **87**: 93-105 [PMID: 32415708 DOI: 10.1111/bcp.14363]
14 **Liao J**, Li M, Huang C, Yu Y, Chen Y, Gan J, Xiao J, Xiang G, Ding X, Jiang R, Li P, Yang M. Pharmacodynamics and Pharmacokinetics of HSK3486, a Novel 2,6-Disubstituted Phenol Derivative as a General Anesthetic. *Front Pharmacol* 2022; **13**: 830791 [PMID: 35185584 DOI: 10.3389/fphar.2022.830791]
15 **Qin L**, Ren L, Wan S, Liu G, Luo X, Liu Z, Li F, Yu Y, Liu J, Wei Y. Design, Synthesis, and Evaluation of Novel 2,6-Disubstituted Phenol Derivatives as General Anesthetics. *J Med Chem* 2017; **60**: 3606-3617 [PMID: 28430430 DOI: 10.1021/acs.jmedchem.7b00254]
16 **Liu Y**, Chen C, Liu N, Tong L, Nie Y, Wu J, Liu X, Gao W, Tang L, Guan X. Efficacy and Safety of Ciprofol Sedation in

ICU Patients with Mechanical Ventilation: A Clinical Trial Study Protocol. *Adv Ther* 2021; **38**: 5412-5423 [PMID: 34417990 DOI: 10.1007/s12325-021-01877-6]

17 **Hu C**, Ou X, Teng Y, Shu S, Wang Y, Zhu X, Kang Y, Miao J. Sedation Effects Produced by a Ciprofol Initial Infusion or Bolus Dose Followed by Continuous Maintenance Infusion in Healthy Subjects: A Phase 1 Trial. *Adv Ther* 2021; **38**: 5484-5500 [PMID: 34559359 DOI: 10.1007/s12325-021-01914-4]

18 **Nolan JP**, Neumar RW, Adrie C, Aibiki M, Berg RA, Böttiger BW, Callaway C, Clark RS, Geocadin RG, Jauch EC, Kern KB, Laurent I, Longstreth WT, Merchant RM, Morley P, Morrison LJ, Nadkarni V, Peberdy MA, Rivers EP, Rodriguez-Nunez A, Sellke FW, Spaulding C, Sunde K, Hoek TV. Post-cardiac arrest syndrome: epidemiology, pathophysiology, treatment, and prognostication. A Scientific Statement from the International Liaison Committee on Resuscitation; the American Heart Association Emergency Cardiovascular Care Committee; the Council on Cardiovascular Surgery and Anesthesia; the Council on Cardiopulmonary, Perioperative, and Critical Care; the Council on Clinical Cardiology; the Council on Stroke. *Resuscitation* 2008; **79**: 350-379 [PMID: 18963350 DOI: 10.1016/j.resuscitation.2008.09.017]

19 **Mai N**, Prifti L, Rininger A, Bazarian H, Halterman MW. Endotoxemia induces lung-brain coupling and multi-organ injury following cerebral ischemia-reperfusion. *Exp Neurol* 2017; **297**: 82-91 [PMID: 28757259 DOI: 10.1016/j.expneurol.2017.07.016]

20 **Nagase M**, Sakurai A, Sugita A, Matsumoto N, Kubo A, Miyazaki Y, Kinoshita K, Yamamoto Y. Oxidative stress and abnormal cholesterol metabolism in patients with post-cardiac arrest syndrome. *J Clin Biochem Nutr* 2017; **61**: 108-117 [PMID: 28955127 DOI: 10.3164/jcbn.17-30]

21 **Idris AH**, Becker LB, Ornato JP, Hedges JR, Bircher NG, Chandra NC, Cummins RO, Dick W, Ebmeyer U, Halperin HR, Hazinski MF, Kerber RE, Kern KB, Safar P, Steen PA, Swindle MM, Tsitlik JE, von Planta I, von Planta M, Wears RL, Weil MH. Utstein-style guidelines for uniform reporting of laboratory CPR research. A statement for healthcare professionals from a Task Force of the American Heart Association, the American College of Emergency Physicians, the American College of Cardiology, the European Resuscitation Council, the Heart and Stroke Foundation of Canada, the Institute of Critical Care Medicine, the Safar Center for Resuscitation Research, and the Society for Academic Emergency Medicine. *Resuscitation* 1996; **33**: 69-84 [PMID: 8959776 DOI: 10.1016/s0300-9572(96)01055-6]

22 **Teng Y**, Ou MC, Wang X, Zhang WS, Liu X, Liang Y, Zuo YX, Zhu T, Liu B, Liu J. Pharmacokinetic and pharmacodynamic properties of ciprofol emulsion in Chinese subjects: a single center, open-label, single-arm dose-escalation phase 1 study. *Am J Transl Res* 2021; **13**: 13791-13802 [PMID: 35035718]

23 **Li X**, Yang D, Li Q, Wang H, Wang M, Yan P, Wu N, Li F, Ma S, Ding Y, Liu J. Safety, Pharmacokinetics, and Pharmacodynamics of a Single Bolus of the γ-aminobutyric Acid (GABA) Receptor Potentiator HSK3486 in Healthy Chinese Elderly and Non-elderly. *Front Pharmacol* 2021; **12**: 735700 [PMID: 34512361 DOI: 10.3389/fphar.2021.735700]

World Journal of Clinical Cases

Submit a Manuscript: https://www.f6publishing.com

World J Clin Cases 2023 January 26; 11(3): 493-505

DOI: 10.12998/wjcc.v11.i3.493

ISSN 2307-8960 (online)

MINIREVIEWS

Non-pulmonary involvement in COVID-19: A systemic disease rather than a pure respiratory infection

Mohamed El-Kassas, Mohamed Alboraie, Mohamed Elbadry, Reem El Sheemy, Mohamed Abdellah, Shimaa Afify, Ahmad Madkour, Mariam Zaghloul, Abeer Awad, Mohamed-Naguib Wifi, Amira Al Balakosy, Mohamed Eltabbakh

Specialty type: Medicine, research and experimental

Provenance and peer review: Invited article; Externally peer reviewed.

Peer-review model: Single blind

Peer-review report's scientific quality classification

Grade A (Excellent): 0
Grade B (Very good): 0
Grade C (Good): C, C
Grade D (Fair): D
Grade E (Poor): 0

P-Reviewer: Navarro-Alvarez N, Mexico; Patel MV, India

Received: July 14, 2022
Peer-review started: July 14, 2022
First decision: October 24, 2022
Revised: November 7, 2022
Accepted: January 5, 2023
Article in press: January 5, 2023
Published online: January 26, 2023

Mohamed El-Kassas, Mohamed Elbadry, Ahmad Madkour, Department of Endemic Medicine, Faculty of Medicine, Helwan University, Cairo 11731, Egypt

Mohamed Alboraie, Mohamed Abdellah, Department of Internal Medicine, Al-Azhar University, Cairo 11884, Egypt

Reem El Sheemy, Department of Tropical Medicine, Minia Faculty of Medicine, Minia University, Minia 61511, Egypt

Shimaa Afify, Department of Gastroenterology, National Hepatology and Tropical Medicine Research Institute, Cairo 11451, Egypt

Mariam Zaghloul, Department of Hepatology, Gastroenterology and Infectious Diseases, Faculty of Medicine, Kafrelsheikh University, Kafrelsheikh 33511, Egypt

Abeer Awad, Mohamed-Naguib Wifi, Department of Internal Medicine, Hepatogastroenterology Unit, Kasr Al-Ainy School of Medicine, Cairo 11451, Egypt

Amira Al Balakosy, Mohamed Eltabbakh, Department of Tropical Medicine, Ain Shams University, Cairo 11451, Egypt

Corresponding author: Abeer Awad, MD, Lecturer, Department of Internal Medicine, Hepatogastroenterology Unit, Kasr Al-Ainy School of Medicine, Cairo University, Kasr Al-Aini Street, Cairo 11451, Egypt. abeer.abdellatif86@gmail.com

Abstract

During the early phase of the coronavirus disease 2019 (COVID-19) pandemic caused by severe acute respiratory syndrome coronavirus 2 (SARS-CoV-2), diagnosis was difficult due to the diversity in symptoms and imaging findings and the variability of disease presentation. Pulmonary manifestations are reportedly the main clinical presentations of COVID-19 patients. Scientists are working hard on a myriad of clinical, epidemiological, and biological aspects to better understand SARS-CoV-2 infection, aiming to mitigate the ongoing disaster. Many reports have documented the involvement of various body systems and organs apart from the respiratory tract including the gastrointestinal, liver, immune system, renal, and neurological systems. Such involvement will result in diverse presentations related to effects on these systems. Other presentations such

as coagulation defects and cutaneous manifestation may also occur. Patients with specific comorbidities including obesity, diabetes, and hypertension have increased morbidity and mortality risks with COVID-19.

Key Words: COVID-19; Non-pulmonary; Extrapulmonary; Clinical manifestations; Systemic disease

Core Tip: Pulmonary involvement was taking the upper hand during the early coronavirus disease 2019 pandemic, which was proven to be a rather multisystemic disease. Due to the helpful research efforts that could help in shifting the developing subject area and proper understanding of the nature of the disease for early diagnosis and controlling the spread of the infection.

Citation: El-Kassas M, Alboraie M, Elbadry M, El Sheemy R, Abdellah M, Afify S, Madkour A, Zaghloul M, Awad A, Wifi MN, Al Balakosy A, Eltabbakh M. Non-pulmonary involvement in COVID-19: A systemic disease rather than a pure respiratory infection. *World J Clin Cases* 2023; 11(3): 493-505
URL: https://www.wjgnet.com/2307-8960/full/v11/i3/493.htm
DOI: https://dx.doi.org/10.12998/wjcc.v11.i3.493

INTRODUCTION

Since January 30, 2020, the World Health Organization has declared the severe acute respiratory syndrome coronavirus 2 (SARS-CoV-2) outbreak as a public health emergency of international concern [1]. This pandemic, which emerged in China, has rapidly spread to affect almost the entire globe within a few weeks. Currently, researchers are working hard on a myriad of aspects, clinical, epidemiological, and biological, to better understand SARS-CoV-2 infection aiming at mitigating the ongoing disaster. As the number of confirmed coronavirus disease 2019 (COVID-19) patients is increasing daily by tens of thousands, clinicians are struggling to understand the possible damage which can complicate SARS-CoV-2 infection[2]. During the early phase of the COVID-19 pandemic, the diagnosis was difficult due to the diversity in symptoms and imaging findings and variability of disease presentation[3,4]. The Centers for Disease Control and Prevention has identified interim clinical presenting features for COVID-19 as fever (83%-99%), cough (59%-82%), fatigue (44%-70%), anorexia (40%-84%), shortness of breath (31%-40%), sputum production (28%-33%) and myalgias (11%-35%)[5]. According to a large Chinese cohort studying disease patterns in more than 44000 patients, disease severity ranged from mild constitutional symptoms and/or mild pneumonia in 81% to shortness of breath and hypoxemia, which complicates about 14% of patients. Acute respiratory distress syndrome (ARDS), respiratory failure, shock, and multi-organ failure occur in only 5% of the affected population[6]. Chest imaging is non-specific in many settings. Although COVID-19 patients can be identified through the detection of bilateral peripheral ground-glass opacities and air-space consolidation, mild or early diseases might lack radiological chest changes[7,8]. Consequently, The American College of Radiology denied computed tomography of the chest as the first-line test for SARS-COV-2. Medical practitioners realize that although the lungs are the most affected organs, the infection can extend to many other organs and systems, including the heart, blood vessels, kidneys, gut, and brain[2].

In this article, we focused on the non-pulmonary involvement in COVID-19 by reviewing the available evidence. Figure 1 summarizes the non-pulmonary involvement in COVID-19.

MATERIALS AND METHODS

The main objectives of the study were to stress the involvement of various body systems and organs in COVID-19 apart from the respiratory tract including the gastrointestinal (GI), liver, immune system, renal, and neurological systems.

Literature search

The literature search was conducted using the PubMed, Scopus, Web of Science (WOS), EBSCO, and Wiley databases. The following search items were used: ("non-pulmonary involvement OR "non-respiratory") AND ("COVID-19 OR "covid 19" OR "covid 19 associated") AND ("a systemic disease rather than a pure respiratory infection" OR "covid 19 associated multi-system inflammatory syndrome in adults" OR "covid 19 associated multi-system inflammatory" OR "covid 19 breakthrough infections"

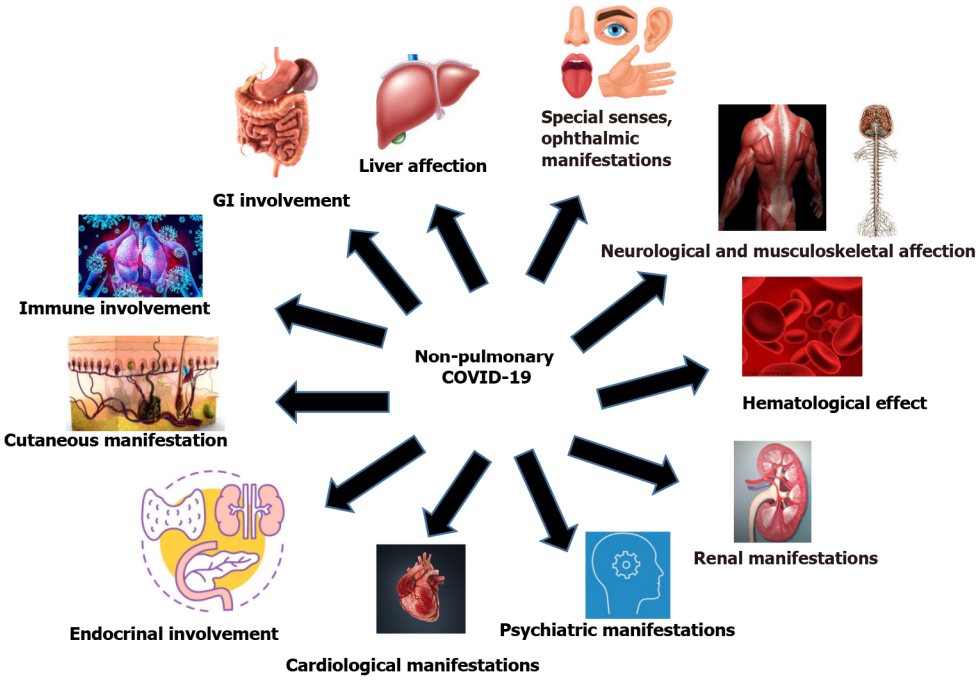

DOI: 10.12998/wjcc.v11.i3.493

Figure 1 Summarizes non-pulmonary involvement in coronavirus disease 2019. GI: Gastrointestinal; COVID-19: coronavirus disease 2019.

OR "covid 19 multi-system"), to retrieve relevant articles regardless the publishing year. For non-English articles, all relevant data were extracted from the English version of the abstract. The full text of these papers was translated into English to retrieve all other needed data. Reviews, meta-analyses, and all other articles containing non-original data were excluded from our review. All retrieved articles were screened and selected by two independent groups of authors (Mohamed El-Kassas and Mohamed Alboraie). Relevant data were extracted into a standardized data collection sheet by two independent authors (Mohamed Elbadry and Mohamed Eltabbakh).

Statistical analysis

Descriptive statistics were used for data analysis.

OBSERVATIONS AND DISCUSSION

GI involvement

In one of the first articles describing the clinical presentation of patients infected with SARS-CoV-2 from Wuhan, diarrhea was one of the clinical presentations[9]. In another study by Gu and his colleague from Shanghai, they described GI manifestations in the form of diarrhea, vomiting, and abdominal pain in COVID-19 patients[10]. With further studies, SARS-CoV-2 RNA was identified in the anal/rectal swabs and stool specimens of COVID-19 patients, even after virus clearance from the upper respiratory tract [11-13]. Genome sequences for SARS-CoV-2 showed that it has about 79.6% similarity to SARS-CoV, encoding and expressing the spike (S) glycoproteins, which help the virus enter human cells through binding to the angiotensin-converting enzyme 2 (ACE2) receptors[14]. ACE2 is highly expressed in type II alveolar cells (AT2) in the lungs and the GI tract, especially the small and large intestines[15]. Previous experience with the severe acute respiratory syndrome (SARS) epidemic in 2003 indicated that coronavirus has tropism in the GI tract. Electron microscopic examination of biopsies and autopsies revealed a rapid increase in the virus in the small intestine and the colon[16,17]. Likewise, Middle Eastern Respiratory Syndrome (MERS in 2013) caused by MERS-CoV can lead to intestinal infection since the human intestinal cells are strongly liable for and support this viral replication[18]. The high susceptibility of the GI tract (GIT) to coronavirus can explain the presence of diarrhea in a proportion of patients infected with COVID-19, despite being less frequent than in SARS. The viral nucleocapsid protein could be stained and identified inside the cytoplasm of epithelial cells of the stomach, duodenum, and rectum[19]. The initial autopsy belonged to an 85-year-old male with COVID-19 revealed areas of dilatation and narrowing of the small bowel[20]. One of the largest and most comprehensive studies evaluating GIT manifestations in COVID-19 patients from Wuhan, with 1141 cases admitted in a single hospital over 7 wk, showed that about 16% of patients presented with GI symptoms only. The most common symptoms were loss of appetite, nausea, and vomiting, which occurred in

about 67% of the patients, diarrhea in 37%, and abdominal pain in 25%[21]. Another study from China stated that 48.5% of patients had GIT symptoms and the most common symptoms were as follows: anorexia (83.8%), diarrhea (29.3%), vomiting (8.1%), and abdominal pain (4.0%), with some patients having multiple symptoms. In this study, 7 patients had only GIT symptoms with no pulmonary symptoms, and those patients needed a longer hospital stay[22]. The same was reported by An *et al*[23], who described 9 adults with COVID-19 who initially presented with only GI manifestations. Five patients became febrile 2-4 d from the onset during their hospital admission, whereas the rest did not show any other symptoms. This should raise awareness about the possibility of SARS-CoV-2 infection in patients presenting with GIT manifestations during the pandemic, which may lead to the spread of infection if not detected early. The last point was specifically mentioned in a separate report describing a patient who suffered abdominal symptoms and was admitted to a surgical department, leading to the infection of more than 10 healthcare workers and 4 patients admitted in the same area[24]. In one of the largest review articles, Yuan and his colleagues analyzed data from 2023 patients, stating whether GI manifestations were present. The incidence of GIT manifestation was between 3% and 79% including anorexia (39.9%-50.2%), diarrhea (2%-49.5%), vomiting (3.6%-66.7%), nausea (1%-29.4%), abdominal pain (2.2%-6.0%), and GI bleeding (4%-13.7%). Both adults and children could present with GI manifestations without pulmonary symptoms. Fecal testing for viral ribonucleic acid (RNA) was as reliable as sputum in detecting SARS-CoV-2. In (36%-53%), fecal polymerase chain reaction (PCR) became positive 2-5 d following positive respiratory specimens. Fecal excretion continued after sputum excretion in (23%-82%) of patients for 1-11 d[25]. Another multicenter study that assessed patients with GIT manifestations in China reported that COVID-19 patients who suffered digestive symptoms had a longer time from symptom onset to admission and evidence of more laboratory derangements, including prolonged coagulation and higher liver enzymes, compared to those without GIT symptoms [22]. In another interesting case report, a 71-year-old woman developed abdominal pain and non-bloody diarrhea, followed by bloody diarrhea, nausea, vomiting, anorexia, and diffuse abdominal pain. Computed tomography showed severe colonic inflammation that was more in the ascending, transverse, and descending colon and had mild right pleural effusion. The patient underwent all investigations as infective diarrhea, which turned negative, and her sigmoidoscopy revealed mild mucosal inflammation. On the 4th day of hospital admission, the patient developed cough, and nasopharyngeal swabs turned positive for SARS-CoV-2[26]. The GI presentation of this case differed from all previously reported cases, thus highlighting the importance of taking all precautions when dealing with patients presenting with any GIT complaints during this pandemic.

Liver effects on patients with COVID-19

There are insufficient data for direct viral-related liver injury in COVID-19 cases. Data from one of the biggest centers in China showed that 2%-11% of COVID-19 cases had liver problems, and 14%-53% had abnormal levels of alanine aminotransferase and aspartate aminotransferase during the disease. Patients with severe COVID-19 had higher values of liver enzymes than mild cases with the disease[27]. Some patients from China have undergone autopsies or post-mortem tissue biopsies to identify the nature of liver injury. The first report was for a 50-year-old man who died from severe COVID-19, and the autopsy specimen showed moderate microvascular steatosis with a mild portal and lobular activity in the liver[28]. Other autopsies revealed hepatomegaly with dark and red hepatocyte degeneration and focal necrosis areas. Also, there was neutrophilic and lymphocytic infiltration in the portal area with congested hepatic sinuses and micro thrombosis. No pathological features of liver failure or injury of bile ducts could be detected in these cases[29].

The liver is considered a target for direct infection, as ACE2 is expressed abundantly in cholangiocytes, which leads to direct cytotoxicity[30]. COVID-19 may cause a severe inflammatory response, which leads to the immune-mediated damage of many organs, including the liver, which is evident by increased peripheral blood levels of many inflammatory markers such as ferritin and many cytokines such as interleukin 2 (IL-2) and IL-6. Also, sepsis is a common complication in severe COVID-19 cases, which may lead to hypoxic and ischemic liver injury, cholestasis, and hepatocellular injury due to severe inflammation. Drug-induced liver injury may be a common cause of liver involvement in COVID-19. Many national recommendations are using multiple antiviral drugs such as oseltamivir, umifenovir, chloroquine, tocilizumab, and lopinavir/ritonavir, which can induce liver injury. Most antipyretic drugs contain paracetamol, which is considered a known cause of hepatotoxicity in high doses[31]. Patients with pre-existing chronic liver disease may be more susceptible to liver damage during COVID-19 infection and its sequelae of immune-mediated damage with severe inflammation[32, 33]. It seems that liver enzyme elevations are usually transient, and severe liver injury is rare with COVID-19. To the best of our knowledge, there are no documented deaths due to hepatic decompensation in cases without pre-existing liver disease. However, regular monitoring of the liver profile is warranted, especially in patients with severe COVID-19 infection[34].

Hematological effect of COVID-19

Hematological effects from SARS-CoV-2 are not a recent finding. Cells with ACE2 receptors might be infected first by the virus, including immune cells. Immune cells produce antibodies that can generate immune hemolysis when they contact red blood cells. Hemoglobin is then infected and attacked. The

viral open reading frame 8 (ORF8) and surface glycoprotein can bind to porphyrin. Simultaneously, ORF1ab, ORF10, and ORF3a proteins can coordinate the attack of the beta chain of hemoglobin, leading to the dissociation of iron and the formation of porphyrin. This attack would cause a loss of hemoglobin, which is essential for carrying oxygen and carbon dioxide. The inability to frequently exchange carbon dioxide and oxygen has a too-intense poisoning and inflammatory effect on the lung cells, eventually resulting in characteristic ground glass-like lung images. The virus can also inhibit normal human heme anabolism[9,35].

That is why recent clinical studies believe that viral damage to the human body is systemic, not confined to the respiratory system. Additionally, overt disseminated intravascular coagulopathy (DIC) was found in 71.4% of non-survivors and 0.6% of survivors upon applying the validated International Society on Thrombosis and Hemostasis DIC score from a single center (the median time to DIC detection was 4 d). Based on these preliminary results, it was assumed that DIC can complicate COVID-19 pneumonia and be associated with mortality. Evidence of DIC, especially elevated D-dimer levels, may also be used to guide therapeutic interventions[36]. It was noticed that older patients with lymphopenia and high lactate dehydrogenase (LDH) levels on admission were associated with severe manifestations and required intensive care unit (ICU) admissions. Also, those patients who required ICU stay had a deeper nadir absolute lymphocytic count, nadir absolute monocyte count and nadir hemoglobin, and higher peak absolute neutrophil count and peak LDH levels compared to patients who did not require ICU[37]. Four possible mechanisms can explain why COVID-19 reduces blood lymphocyte levels: The virus might infect lymphocytes directly, resulting in death. The ACE2 coronavirus receptor is expressed on lymphocytes and may be directly targeted by the viruses[38]. The novel coronavirus virus might directly destroy lymphatic organs such as the thymus and spleen, and this hypothesis needs to be confirmed by pathological dissection in the future. Enhanced lymphocyte apoptosis due to inflammatory cytokines release (*e.g.*, tumor necrosis factor alpha, IL-6, and other pro-inflammatory cytokines) could induce lymphocyte deficiency and lymphocyte inhibitions by metabolic molecules such as hyperlactic acidemia produced by metabolic disorders. In severe forms of COVID-19, patients had elevated blood levels of lactic acid, which might suppress lymphocyte proliferation[39]. The mechanisms mentioned above or beyond might work together or separately to cause lymphopenia, so further research is recommended. That is why lymphopenia is considered an effective and reliable indicator of disease severity and an indication for hospitalization in patients with COVID-19[40].

Renal manifestations of COVID 19

Renal involvement in COVID-19 (coronavirus-nephropathy) has a complex etiology. However, some studies suggest that acute kidney injury (AKI) does not complicate COVID-19, but when it occurs in COVID-19 patients, it is associated with higher morbidity and mortality and is a strong indicator of survival[41]. Renal affection is mutual in COVID-19 patients and manifests mainly with proteinuria in about 44% to 63% of patients, hematuria in 26.9% of patients, elevated serum creatinine (SCr) in 15.5% to 19%, and urea blood nitrogen (BUN) in 14.1% to 27% of the patients. AKI was also reported in 3.2% of infected individuals. Computed tomography (CT) scan of the kidneys illustrated that the renal parenchyma's inflammation and edema were evident in all patients. Renal failure in COVID-19 patients had a greater risk of in-hospital mortality. AKI, proteinuria, hematuria, raised plasma creatinine, and urea nitrogen were evident predictors of in-hospital patients' mortality as well[42,43]. Many mechanisms have been suggested to explain how SARS-CoV-2 impacts renal functions, one of which is attributed to dehydration, which may result from fever; and decreased fluid intake, which leads to a reduction of glomerular filtration rate and causes AKI. This can be reversible in early stages by fluid therapy. However, if dehydration leads to hypoperfusion and ischemia, as in cases of cytokine storm, sepsis and shock, acute tubular necrosis might supervene[44,45]. Rhabdomyolysis and hypoxia are other possibilities, as well as direct virus invasion to the renal tubular cells, interstitium, or glomeruli with direct cytopathic effect. Coronaviruses have a three-dimensional spike protein structure, which is closely bound to human cell receptor 2, where it enters into the cells *via* ACE2 receptors, which are vastly expressed in the renal cells. This explains how the renal cells are targeted and infected by SARS-CoV-2. Although the virus-induced glomerulopathy in the coronaviruses family was low, immune complexes deposition of viral particles or virus-induced specific immunological abnormalities is still possible[46,47]. However, another opinion was that COVID-19 does not induce AKI or deterioration of the renal condition in patients with chronic kidney disease (CKD). In a study including 116 cases confirmed with COVID-19, only 10.8% of patients without CKD showed a mild increase in BUN or SCr, and these elevations were all less than 26 μmol/L within 48 h, which does not match with the AKI standard definition. Only 7.2% of the patients without CKD showed mild albuminuria and gradually returned to normal without needing specific treatment[41].

Cardiological manifestations of COVID-19

The cardiovascular system is sometimes involved during the COVID-19 course by different proposed mechanisms, such as direct myocardial injury by binding to ACE2 receptors, which leads to alteration of signaling pathways that result in acute myocardial injury. Another supposed mechanism is the systemic inflammatory response and cytokine storm, which ultimately leads to multiple end-organ damage proven by the high circulatory levels of proinflammatory cytokines in patients with critical COVID-19.

This may also lead to increased coronary blood flow with increased shear stress that can precipitate plaque rupture and increase vascular thrombosis leading to acute myocardial infarction[48,49]. The hypoxia resulting from acute lung injury may cause a significant imbalance of the oxygen demand-supply ratio to the cardiac muscle and increases cardio-metabolic demand. Electrolyte disturbance, especially hypokalemia (of particular concern in patients with COVID-19), adversely affects various therapies, such as antiviral drugs, which affect QT interval prolongation and corticosteroids, and other therapies can also have deleterious effects on the cardiovascular system[50]. Although cardiovascular risk factors do not increase the chance of getting SARS-CoV-2 infection, they inversely affect the prognosis of COVID-19. These risk factors include diabetes, cardio-cerebrovascular disease, and hypertension, and they were associated with a 2-3 fold greater risk of severe disease, respectively, or requiring ICU admission[6]. Acute myocardial injury is the most commonly described cardiac presentation in COVID-19. Different biomarkers cut-offs and/or electrocardiographic abnormalities have been used to define acute cardiac injury. The most commonly used definition is an elevation of high-sensitivity cardiac troponin above the 99th percentile upper reference limit. The incidence of acute myocardial injury is roughly estimated to be 8%-12% among positive cases of SARS-CoV-2 with a robust unfavorable prognosis of COVID-19. The incidence of ST-segment elevation myocardial infarction in COVID-19 patients seems to be lower, as well as the incidence of left ventricular systolic dysfunction, acute left ventricular failure, and cardiogenic shock. Heart failure has been reported in 52% of COVID-19 patients who subsequently died and 12% of patients discharged from the hospital. Tachy- and bradyarrhythmias were also reported in the severe and morbid form of the disease requiring ICU admission, while acute coronary events and left ventricular systolic dysfunction were not reported and seemed to have very low incidence[51-53]. Interestingly, although myocardial injury is significantly associated with the fatal outcome of COVID-19, the prognosis of patients with underlying cardiovascular disease (excluding myocardial) injury is relatively favorable[54].

Endocrinal involvement in COVID-19

Diabetes, hypertension, and metabolic syndrome significantly impact morbidity and mortality in COVID-19. Hyperglycemia and diabetes are associated with suppression of the immune state and increase the risk of infectious diseases. About 51% of COVID-19 patients reportedly have hyperglycemia, similar to what has been observed with other viral infections such as SARS and MERS. The transient pancreatic cell function impairment can explain the mechanism of hyperglycemia in this situation by the virus itself or by modulation in glucose metabolism. The impact of hyperglycemia in SARS-CoV-2 infection cannot be underestimated due to its effect on the immune status and its further complications[55]. About 50%-60% of impaired glucose tolerance and diabetic patients have a higher incidence of pulmonary infections. Diabetic patients carry a high risk of getting SARS-CoV-2 infection. A study from Wuhan concluded that other diseases accompanied 32% of the infected cases; the highest was for diabetes in 20% of cases, followed by hypertension in 15% and cardiovascular disease in 15% of cases[9]. Another study retrospectively analyzed data from 138 COVID-19 patients and found that 46.4% had one or more underlying diseases, of which diabetes was represented in 10% of cases and 22.2% of ICU cases[24]. Unsurprising that patients with diabetes have a high rate of mortality among SARS-CoV-2 infected patients, it reached 77.7% of critically ill COVID-19 patients[56]. Also, of the 72,314 reported cases of COVID-19 in the Chinese Center for Disease Control and Prevention, diabetic patients had a high mortality rate (7.3% in diabetes mellitus *vs* 2.3% overall)[6].

Generally, there are a lack of data about the effect of obesity on COVID-19 patients. However, some hospitals in Spain showed that obese patients infected with SARS-CoV-2 were more susceptible to severe ARDS, respiratory failure, and even death; this can be explained by sleep apnea syndrome and surfactant dysfunction that occur with severe obesity[57]. Undernourished patients are more susceptible to infection with SARS-CoV-2. Also, COVID-19 itself can lead to malnutrition, which affects outcome and prognosis; therefore, COVID-19 outcome could be improved with improved nutritional status[58].

Unfortunately, there are no currently available data about the outcome of COVID-19 patients with adrenal insufficiency; however, it is expected they may have a high risk for acquiring SARS-CoV-2 infection and high incidence of mortality due to defects in their natural immunity, neutrophils, and natural killer cell action[59]. Similarly, few published data are available about the effect of SARS-CoV infection on male gonads and the risk of infertility. Germ cell destruction, few or no spermatozoon in the seminiferous tubules, a thickened basement membrane, and leukocyte infiltration were found in some SARS-COV-infected patients. This may be explained by sharing the same ACE2 receptor to enter the host cells for reproduction and transmission[60]. Whether a similar effect can occur in SARS-CoV-2 infected patients; needs more research to explore.

Immune involvement in COVID-19

Both innate and adaptive immunity are involved in SARA-CoV-2 infection, with lymphopenia being dominant; however, the severely uncontrollable inflammatory response with markedly elevated levels of proinflammatory cytokines such as IL-6 and IL-1β, as well as IL-2, IL-8, and IL-17, known as cytokine storm, has been seen in severely infected COVID-19 patients. This cytokine storm leads to multiple unwanted harmful effects that can be manifested with severe tissue damage, extensive pulmonary destruction, respiratory failure, multi-organ failure, and even death. In addition to elevated levels of

proinflammatory cytokines, complement activation has also been seen to add another immune-based pathology associated with COVID-19; this may contribute to further hope for using complement inhibitors to decrease inflammatory damage[61].

SARS-CoV-2-specific immunoglobulin G (IgG) and IgM antibodies have been detected in high titer upon analysis of 222 and 173 COVID-19-infected patients; this may be explained by an antibody-mediated immune mechanism that has also been observed with many other viral infections. Hopefully, this can be helpful for antibody-based therapies and vaccine development[62].

Cutaneous manifestation in COVID-19 patients

Available data about the skin manifestations of COVID-19 are scarce. COVID-19 patients may initially present with a skin rash, which may be misdiagnosed as other common skin diseases[9]. A study conducted in Italy collected data from 88 COVID-19 patients; 20.4% developed cutaneous manifestations. Eight patients developed skin manifestations at the onset and ten patients after hospitalization. The developed cutaneous manifestations were variable and included: erythematous rash, widespread urticaria, and chickenpox-like vesicles. Lesions were more evident on the trunk. Most of the lesions were itchy and usually healed in a few days. No correlation was observed between disease severity and cutaneous symptoms. This study reported that skin manifestations recorded in COVID-19 patients are similar to those in common viral infections[63]. A case report from Thailand presented a patient with a petechial skin rash that was first diagnosed as dengue fever because of the endemicity of Dengue in Thailand and the presence of thrombocytopenia, later on, the patient developed respiratory symptoms and all viral causes that might be associated with fever, rash, and the respiratory problem was excluded by laboratory investigation. The final diagnosis of the SARS-COV-2 infection was made using real-time PCR[64]. Urticaria also was reported as a common skin manifestation associated with COVID-19 in Chinese patients[65,66].

Neurological and musculoskeletal systems are affected in COVID-19

Due to the similarities in structure and modes of transmission with SARS-CoV and MERS-CoV, SARS-CoV-2 showed growing evidence of affinity affecting the central nervous system and causing other neurological manifestations. Many early reported data described symptoms of neurological affection, commonly headache, which was severe and intolerable in many cases, dizziness, and unsteadiness of gait[67]. In the first retrospective observational study about the neurological involvement among 214 hospitalized patients in Wuhan, headache was the most common neurologic symptom, affecting 25% of the patients, followed by dizziness in 17%, then a disturbance in their level of consciousness in 8% of cases and acute cerebrovascular events in 3%. Less commonly, ataxia and convulsions occurred in 0.5% of each[68]. In another single-center retrospective observational study, including 221 patients, acute ischemic strokes were found in 5% of patients, with cerebral venous sinus thrombosis in 0.5% and cerebral hemorrhage in 0.5% of cases without the mention of other neurologic deficits. It is worth considering that almost all of these patients were old with accompanying risk factors like hypertension and diabetes mellitus[69]. It was suggested that metabolic and electrolyte imbalances, along with the accompanying hypoxia and/or multiple organ failure in critically ill patients, might represent a plausible explanation for altering mental status[70]. The presence of seizures ranging from subtle subclinical forms to clinically overt seizures and status epilepticus in many patients points to the possibility of having non-convulsive status epilepticus as an explanation, and hence the importance of electroencephalogram monitoring of such patients and the application of Salzburg Consensus Criteria for Non-Convulsive Status Epilecticus[71].

Moreover, some reports have linked Guillain-Barré syndrome and post-infectious acute myelitis to COVID-19. A similar para-infectious association with the Zika virus encouraged the suggestion of a phenomenon with COVID-19 instead of the classic post-infectious form[72,73]. The current piling data and reports of COVID-19 render the pandemic's central nervous system and other neurological manifestations more than just an epiphenomenon as concrete evidence is accumulated. The first reports of substantial evidence include a case of a 24-years-old man who presented with fever and fatigue. COVID-19 RNA was not detected in his nasopharyngeal swab until the 9th day when he was found unconscious and soaking in his vomit with evident neck stiffness and was diagnosed with meningoencephalitis. Despite the negative nasopharyngeal swab, COVID-19 RNA was found in his CSF fluid, while his serum varicella-zoster IgM and anti-herpes simplex virus type 1 were negative. Furthermore, magnetic resonance imaging showed hyperintensity signals in the right lateral ventricle, hippocampus, and right mesial temporal lobe, linking SARS-CoV-2 with his illness[74].

Psychiatric manifestations

During the COVID-19 pandemic, additional anxiety results from fear of acquiring infection, especially in the presence of uncertainty, whether other modes of transmission than droplet infection exist. The uncertain incubation period of the virus and its possible asymptomatic transmission can also cause additional stress. The obligation to social distancing in many countries worldwide resulted in changes in national behavioral patterns and the shutdown of the usual day-to-day functioning[75]. Additionally, reports of shortages in medical protective equipment, medical staff, and hospital beds have raised major

worries worldwide. Lastly, a unique "infodemic" due to a plethora of information from unofficial and unreliable sources poses a significant risk to public mental health during this crisis[76].

The spectrum of psychological distresses can be classified into immediate and long-term effects. Immediate stress during an infectious disease outbreak can include fear and worriedness about a person's health and the health of his family; changes in sleep or eating patterns; difficulty sleeping or concentrating; worsening of chronic health problems; worsening of mental health conditions; and increased use of alcohol, tobacco, or illicit drugs[77]. Panic disorders (resulting from fear of the unknown and the unpredicted) and infomania (the obsessive demand to frequently check media) can also be among the immediate effects. Stigma, xenophobia, and racism related to COVID-19 may also occur. Increased fear and suspicion towards people from China and other countries in which SARS-CoV-2 had widely spread led to social stigmatization and refusal to house, employ, or provide health care for certain races. Theories of conspiracy (mistrust, the detection of real and hidden designs, and the meaning behind the apparent causes) are also present. They have widely spread during the COVID-19 pandemic as different accusations of the virus as a biological war or designed to create an economic crisis are widespread[78]. Studies assessing mental health during the SARS outbreak in 2003 found that the main psychiatric problems were adjustment reactions with increased anxiety levels. Studies have also shown that 10%-35% of SARS survivors reported having features of anxiety, depression, or both during the early recovery phase[79].

Long-term psychiatric consequences of SARS-CoV-2 are still unknown; guided by the last SARS epidemic in 2003, a significant impact on mental health can be expected. In 2003, posttraumatic stress disorder was the most typical psychiatric condition as its cumulative incidence rate of 30 mo after SARS was (47.8%) and then depressive disorders were the second most common impact[80]. Healthcare workers (HCWs) carrying the responsibility to provide care to infected patients and to search for the best therapies for unknown dangerous pathogens are put under significant stress in addition to being exposed to infection. Exposure to infected patients necessitates the social isolation of HCWs with its added psychiatric consequences. When HCWs become infected and turn out to be patients, this change in their role leads to behavior adjustment challenges, frustration, and feeling of helplessness[81].

Special senses

Anosmia and ageusia (loss of smell and taste, respectively) were reported as frequent symptoms in patients with COVID-19[82]. In Italy, of 59 patients with COVID-19, 34% self-reported either smell or taste alteration, and 19% reported both[83]. The same finding was reported by a European multicenter cross-sectional study that showed that out of 417 mild-to-moderate COVID-19 patients, 85.6% reported smell dysfunction, and 88% reported taste dysfunction[82]. An American study on 237 COVID-19 patients showed that anosmia was experienced in 73% of subjects before COVID-19 diagnosis, and it was the initial symptom in about 27% of them[84]. Quantitative smell testing of confirmed 60 COVID-19 patients showed that 98% have some smell dysfunction but not always anosmia[85]. Considering these symptoms as characteristic early diagnostic features of COVID-19 is controversial as the earlier data from china did not stress olfactory or taste disorders in COVID-19 patients. The increasing evidence on the importance of olfactory and gustatory symptoms as a precedent event to the full-blown clinical disease suggests its use as a clinical screening tool to determine the need for early testing, treatment, or quarantine of asymptomatic individuals.

Ophthalmic manifestations

COVID-19 transmission through the ocular route remains uncertain[86]. Animal studies showed that coronaviruses, including SARS-CoV-2, can produce a broad spectrum of ocular manifestations from diseases that involve the anterior segment, like conjunctivitis and anterior uveitis, to posterior segment conditions like retinitis and optic neuritis[87]. The human eye has its intraocular renin-angiotensin system, as ACE2 was detected in the aqueous humor[88]. However, the expression of ACE2 in the conjunctiva or cornea is not well documented. So, ocular infection through ACE2 should be further investigated. A Chinese case series showed that about one-third of patients with COVID-19 had ocular abnormalities. Their ocular manifestations varied between epiphora, conjunctival congestion, or chemosis and were encountered in patients with advanced systemic manifestations[89]. Few case reports have described acute conjunctivitis as a presenting symptom of COVID-19 patients[90,91].

Audio vestibular manifestations

Viral infections are well known for causing sensorineural hearing loss. The evidence of inner ear involvement in COVID-19 patients is scarce and needs further studies. In a recent pilot study that explored the audiological profile of asymptomatic COVID-19 PCR-positive cases, the authors reported a significant worsening of the high-frequency pure-tone thresholds, as well as the transient, evoked otoacoustic emissions amplitudes. This indicates suspected deleterious effects of COVID-19 on the hair cells in the cochlea, but larger studies and follow-ups of these patients after recovery are pivotal to determining the exact mechanism and fate of these effects[92]. Furthermore, Fidan and his colleagues reported a 35-year-old female patient with otalgia and tinnitus. None of the classic COVID-19 symptoms with no comorbidities upon investigation proved to have acute otitis media, bilateral lung involvement

in chest X-ray, and positive RT-PCR result for SARS-CoV-2[93].

CONCLUSION

In this review article, we highlighted multisystemic involvement of COVID-19 infection. Involvement of various body systems and organs apart from the respiratory tract, including the GI, liver, immune system, renal, and neurological systems have been reported with COVID-19 infection.

ACKNOWLEDGEMENTS

The authors acknowledge the tremendous effort and sacrifice of the medical staff working in COVID-19 quarantine hospitals worldwide.

FOOTNOTES

Author contributions: El-Kassas M, Alboraie M, Elbadry M, El Sheemy R, Abdellah M, Afify S, Madkour A, Zaghloul M, Awad A, Wifi MN, Al Balakosy A, and Eltabbakh M equally contributed to writing the manuscript; Alboraie M revised the final manuscript; Awad A submitted the manuscript.

Conflict-of-interest statement: The authors have no conflicts of interest to declare.

Country/Territory of origin: Egypt

ORCID number: Mohamed El-Kassas 0000-0002-3396-6894; Mohamed Alboraie 0000-0002-8490-9822; Mohamed ElBadry 0000-0002-9020-8870; Reem El Sheemy 0000-0001-8158-8878; Mohamed Abdellah 0000-0001-9329-6063; Shimaa Afify 0000-0001-5937-4240; Ahmad Madkour 0000-0001-8416-6013; Mariam Zaghloul 0000-0002-4244-5396; Abeer Awad 0000-0001-9945-9767; Mohamed-Naguib Wifi 0000-0002-3403-7106; Amira Al Balakosy 0000-0002-9229-6237; Mohamed Eltabbakh 0000-0003-2836-807X.

S-Editor: Liu GL
L-Editor: Filipodia
P-Editor: Liu GL

REFERENCES

1 **World Health Organization**. (2020) Novel coronavirus (2019-nCoV) situation reports. [Internet] [accessed 16 May 2020]. Available from: https://www.who.int/emergencies/diseases/
2 **Wadman M**, Couzin-Frankel J, Kaiser J, Matacic C. How does coronavirus kill? *Science AAAS* 2020 [DOI: 10.1126/science.abc3208]
3 **Guan WJ**, Ni ZY, Hu Y, Liang WH, Ou CQ, He JX, Liu L, Shan H, Lei CL, Hui DSC, Du B, Li LJ, Zeng G, Yuen KY, Chen RC, Tang CL, Wang T, Chen PY, Xiang J, Li SY, Wang JL, Liang ZJ, Peng YX, Wei L, Liu Y, Hu YH, Peng P, Wang JM, Liu JY, Chen Z, Li G, Zheng ZJ, Qiu SQ, Luo J, Ye CJ, Zhu SY, Zhong NS; China Medical Treatment Expert Group for Covid-19. Clinical Characteristics of Coronavirus Disease 2019 in China. *N Engl J Med* 2020; **382**: 1708-1720 [PMID: 32109013 DOI: 10.1056/NEJMoa2002032]
4 **Chen N**, Zhou M, Dong X, Qu J, Gong F, Han Y, Qiu Y, Wang J, Liu Y, Wei Y, Xia J, Yu T, Zhang X, Zhang L. Epidemiological and clinical characteristics of 99 cases of 2019 novel coronavirus pneumonia in Wuhan, China: a descriptive study. *Lancet* 2020; **395**: 507-513 [PMID: 32007143 DOI: 10.1016/S0140-6736(20)30211-7]
5 **Center for Disease Control and Prevention**. Management of Patients with Confirmed 2019-nCoV. [Internet] [accessed May 16 2020]. 4/21/2020. Available from: https://www.cdc.gov/coronavirus/2019-ncov/hcp/clinical-guidance-management-patients.html
6 **Wu Z**, McGoogan JM. Characteristics of and Important Lessons From the Coronavirus Disease 2019 (COVID-19) Outbreak in China: Summary of a Report of 72 314 Cases From the Chinese Center for Disease Control and Prevention. *JAMA* 2020; **323**: 1239-1242 [PMID: 32091533 DOI: 10.1001/jama.2020.2648]
7 **Bai HX**, Hsieh B, Xiong Z, Halsey K, Choi JW, Tran TML, Pan I, Shi LB, Wang DC, Mei J, Jiang XL, Zeng QH, Egglin TK, Hu PF, Agarwal S, Xie FF, Li S, Healey T, Atalay MK, Liao WH. Performance of Radiologists in Differentiating

COVID-19 from Non-COVID-19 Viral Pneumonia at Chest CT. *Radiology* 2020; **296**: E46-E54 [PMID: 32155105 DOI: 10.1148/radiol.2020200823]

8 **Shi H**, Han X, Jiang N, Cao Y, Alwalid O, Gu J, Fan Y, Zheng C. Radiological findings from 81 patients with COVID-19 pneumonia in Wuhan, China: a descriptive study. *Lancet Infect Dis* 2020; **20**: 425-434 [PMID: 32105637 DOI: 10.1016/S1473-3099(20)30086-4]

9 **Huang C**, Wang Y, Li X, Ren L, Zhao J, Hu Y, Zhang L, Fan G, Xu J, Gu X, Cheng Z, Yu T, Xia J, Wei Y, Wu W, Xie X, Yin W, Li H, Liu M, Xiao Y, Gao H, Guo L, Xie J, Wang G, Jiang R, Gao Z, Jin Q, Wang J, Cao B. Clinical features of patients infected with 2019 novel coronavirus in Wuhan, China. *Lancet* 2020; **395**: 497-506 [PMID: 31986264 DOI: 10.1016/S0140-6736(20)30183-5]

10 **Gu J**, Han B, Wang J. COVID-19: Gastrointestinal Manifestations and Potential Fecal-Oral Transmission. *Gastroenterology* 2020; **158**: 1518-1519 [PMID: 32142785 DOI: 10.1053/j.gastro.2020.02.054]

11 **Zhang W**, Du RH, Li B, Zheng XS, Yang XL, Hu B, Wang YY, Xiao GF, Yan B, Shi ZL, Zhou P. Molecular and serological investigation of 2019-nCoV infected patients: implication of multiple shedding routes. *Emerg Microbes Infect* 2020; **9**: 386-389 [PMID: 32065057 DOI: 10.1080/22221751.2020.1729071]

12 **Holshue ML**, DeBolt C, Lindquist S, Lofy KH, Wiesman J, Bruce H, Spitters C, Ericson K, Wilkerson S, Tural A, Diaz G, Cohn A, Fox L, Patel A, Gerber SI, Kim L, Tong S, Lu X, Lindstrom S, Pallansch MA, Weldon WC, Biggs HM, Uyeki TM, Pillai SK; Washington State 2019-nCoV Case Investigation Team. First Case of 2019 Novel Coronavirus in the United States. *N Engl J Med* 2020; **382**: 929-936 [PMID: 32004427 DOI: 10.1056/NEJMoa2001191]

13 **Xu Y**, Li X, Zhu B, Liang H, Fang C, Gong Y, Guo Q, Sun X, Zhao D, Shen J, Zhang H, Liu H, Xia H, Tang J, Zhang K, Gong S. Characteristics of pediatric SARS-CoV-2 infection and potential evidence for persistent fecal viral shedding. *Nat Med* 2020; **26**: 502-505 [PMID: 32284613 DOI: 10.1038/s41591-020-0817-4]

14 **Zhou P**, Yang XL, Wang XG, Hu B, Zhang L, Zhang W, Si HR, Zhu Y, Li B, Huang CL, Chen HD, Chen J, Luo Y, Guo H, Jiang RD, Liu MQ, Chen Y, Shen XR, Wang X, Zheng XS, Zhao K, Chen QJ, Deng F, Liu LL, Yan B, Zhan FX, Wang YY, Xiao GF, Shi ZL. A pneumonia outbreak associated with a new coronavirus of probable bat origin. *Nature* 2020; **579**: 270-273 [PMID: 32015507 DOI: 10.1038/s41586-020-2012-7]

15 **Harmer D**, Gilbert M, Borman R, Clark KL. Quantitative mRNA expression profiling of ACE 2, a novel homologue of angiotensin converting enzyme. *FEBS Lett* 2002; **532**: 107-110 [PMID: 12459472 DOI: 10.1016/s0014-5793(02)03640-2]

16 **Hung IF**, Cheng VC, Wu AK, Tang BS, Chan KH, Chu CM, Wong MM, Hui WT, Poon LL, Tse DM, Chan KS, Woo PC, Lau SK, Peiris JS, Yuen KY. Viral loads in clinical specimens and SARS manifestations. *Emerg Infect Dis* 2004; **10**: 1550-1557 [PMID: 15498155 DOI: 10.3201/eid1009.040058]

17 **Leung WK**, To KF, Chan PK, Chan HL, Wu AK, Lee N, Yuen KY, Sung JJ. Enteric involvement of severe acute respiratory syndrome-associated coronavirus infection. *Gastroenterology* 2003; **125**: 1011-1017 [PMID: 14517783 DOI: 10.1016/s0016-5085(03)01215-0]

18 **Zhou J**, Li C, Zhao G, Chu H, Wang D, Yan HH, Poon VK, Wen L, Wong BH, Zhao X, Chiu MC, Yang D, Wang Y, Au-Yeung RKH, Chan IH, Sun S, Chan JF, To KK, Memish ZA, Corman VM, Drosten C, Hung IF, Zhou Y, Leung SY, Yuen KY. Human intestinal tract serves as an alternative infection route for Middle East respiratory syndrome coronavirus. *Sci Adv* 2017; **3**: eaao4966 [PMID: 29152574 DOI: 10.1126/sciadv.aao4966]

19 **Zhao D**, Yao F, Wang L, Zheng L, Gao Y, Ye J, Guo F, Zhao H, Gao R. A Comparative Study on the Clinical Features of Coronavirus 2019 (COVID-19) Pneumonia With Other Pneumonias. *Clin Infect Dis* 2020; **71**: 756-761 [PMID: 32161968 DOI: 10.1093/cid/ciaa247]

20 **Liu Q**, Wang RS, Qu GQ, Wang YY, Liu P, Zhu YZ, Fei G, Ren L, Zhou YW, Liu L. Gross examination report of a COVID-19 death autopsy. *Fa Yi Xue Za Zhi* 2020; **36**: 21-23 [PMID: 32198987 DOI: 10.12116/j.issn.1004-5619.2020.01.005]

21 . Erratum for the Research Article: "Circulating tumor DNA methylation profiles enable early diagnosis, prognosis prediction, and screening for colorectal cancer" by H. Luo, Q. Zhao, W. Wei, L. Zheng, S. Yi, G. Li, W. Wang, H. Sheng, H. Pu, H. Mo, Z. Zuo, Z. Liu, C. Li, C. Xie, Z. Zeng, W. Li, X. Hao, Y. Liu, S. Cao, W. Liu, S. Gibson, K. Zhang, G. Xu, R.-h. Xu. *Sci Transl Med* 2020; **12** [PMID: 32321865 DOI: 10.1126/scitranslmed.abc1078]

22 **Pan L**, Mu M, Yang P, Sun Y, Wang R, Yan J, Li P, Hu B, Wang J, Hu C, Jin Y, Niu X, Ping R, Du Y, Li T, Xu G, Hu Q, Tu L. Clinical Characteristics of COVID-19 Patients With Digestive Symptoms in Hubei, China: A Descriptive, Cross-Sectional, Multicenter Study. *Am J Gastroenterol* 2020; **115**: 766-773 [PMID: 32287140 DOI: 10.14309/ajg.0000000000000620]

23 **An P**, Ji M, Ren H, Su J, Ding NS, Kang J, Yin A, Zhou Q, Shen L, Zhao L, Jiang X, Xiao Y, Tan W, Lv X, Li J, Liu S, Zhou J, Chen H, Xu Y, Liu J, Chen M, Cao J, Zhou Z, Tan S, Yu H, Dong W, Ding Y. Prevention of COVID-19 in patients with inflammatory bowel disease in Wuhan, China. *Lancet Gastroenterol Hepatol* 2020; **5**: 525-527 [PMID: 32311321 DOI: 10.1016/S2468-1253(20)30121-7]

24 **Wang D**, Hu B, Hu C, Zhu F, Liu X, Zhang J, Wang B, Xiang H, Cheng Z, Xiong Y, Zhao Y, Li Y, Wang X, Peng Z. Clinical Characteristics of 138 Hospitalized Patients With 2019 Novel Coronavirus-Infected Pneumonia in Wuhan, China. *JAMA* 2020; **323**: 1061-1069 [PMID: 32031570 DOI: 10.1001/jama.2020.1585]

25 **Tian Y**, Rong L, Nian W, He Y. Review article: gastrointestinal features in COVID-19 and the possibility of faecal transmission. *Aliment Pharmacol Ther* 2020; **51**: 843-851 [PMID: 32222988 DOI: 10.1111/apt.15731]

26 **Carvalho A**, Alqusairi R, Adams A, Paul M, Kothari N, Peters S, DeBenedet AT. SARS-CoV-2 Gastrointestinal Infection Causing Hemorrhagic Colitis: Implications for Detection and Transmission of COVID-19 Disease. *Am J Gastroenterol* 2020; **115**: 942-946 [PMID: 32496741 DOI: 10.14309/ajg.0000000000000667]

27 **Zhang C**, Shi L, Wang FS. Liver injury in COVID-19: management and challenges. *Lancet Gastroenterol Hepatol* 2020; **5**: 428-430 [PMID: 32145190 DOI: 10.1016/S2468-1253(20)30057-1]

28 **Xu Z**, Shi L, Wang Y, Zhang J, Huang L, Zhang C, Liu S, Zhao P, Liu H, Zhu L, Tai Y, Bai C, Gao T, Song J, Xia P, Dong J, Zhao J, Wang FS. Pathological findings of COVID-19 associated with acute respiratory distress syndrome. *Lancet Respir Med* 2020; **8**: 420-422 [PMID: 32085846 DOI: 10.1016/S2213-2600(20)30076-X]

29 **Zhu N**, Zhang D, Wang W, Li X, Yang B, Song J, Zhao X, Huang B, Shi W, Lu R, Niu P, Zhan F, Ma X, Wang D, Xu W,

Wu G, Gao GF, Tan W; China Novel Coronavirus Investigating and Research Team. A Novel Coronavirus from Patients with Pneumonia in China, 2019. *N Engl J Med* 2020; **382**: 727-733 [PMID: 31978945 DOI: 10.1056/NEJMoa2001017]

30 **Chai X**, Hu L, Zhang Y, et al. Specific ACE2 Expression in Cholangiocytes May Cause Liver Damage After 2019-nCoV Infection. bioRxiv; 2020 [DOI: 10.1101/2020.02.03.931766]

31 **Caines A**, Moonka D. Drug Hepatotoxicity: Causality Assessment. *Clin Liver Dis* 2020; **24**: 25-35 [PMID: 31753248 DOI: 10.1016/j.cld.2019.09.001]

32 **Wang FS**, Fan JG, Zhang Z, Gao B, Wang HY. The global burden of liver disease: the major impact of China. *Hepatology* 2014; **60**: 2099-2108 [PMID: 25164003 DOI: 10.1002/hep.27406]

33 **Li J**, Fan JG. Characteristics and Mechanism of Liver Injury in 2019 Coronavirus Disease. *J Clin Transl Hepatol* 2020; **8**: 13-17 [PMID: 32274341 DOI: 10.14218/JCTH.2020.00019]

34 **Sun J**, Aghemo A, Forner A, Valenti L. COVID-19 and liver disease. *Liver Int* 2020; **40**: 1278-1281 [PMID: 32251539 DOI: 10.1111/liv.14470]

35 **Lansiaux E**, Pébaÿ PP, Picard JL, Son-Forget J. COVID-19: beta-thalassemia subjects immunised? *Med Hypotheses* 2020; **142**: 109827 [PMID: 32447232 DOI: 10.1016/j.mehy.2020.109827]

36 **Arachchillage DRJ**, Laffan M. Abnormal coagulation parameters are associated with poor prognosis in patients with novel coronavirus pneumonia. *J Thromb Haemost* 2020; **18**: 1233-1234 [PMID: 32291954 DOI: 10.1111/jth.14820]

37 **Fan BE**, Chong VCL, Chan SSW, Lim GH, Lim KGE, Tan GB, Mucheli SS, Kuperan P, Ong KH. Hematologic parameters in patients with COVID-19 infection. *Am J Hematol* 2020; **95**: E131-E134 [PMID: 32129508 DOI: 10.1002/ajh.25774]

38 **Xu H**, Zhong L, Deng J, Peng J, Dan H, Zeng X, Li T, Chen Q. High expression of ACE2 receptor of 2019-nCoV on the epithelial cells of oral mucosa. *Int J Oral Sci* 2020; **12**: 8 [PMID: 32094336 DOI: 10.1038/s41368-020-0074-x]

39 **Fischer K**, Hoffmann P, Voelkl S, Meidenbauer N, Ammer J, Edinger M, Gottfried E, Schwarz S, Rothe G, Hoves S, Renner K, Timischl B, Mackensen A, Kunz-Schughart L, Andreesen R, Krause SW, Kreutz M. Inhibitory effect of tumor cell-derived lactic acid on human T cells. *Blood* 2007; **109**: 3812-3819 [PMID: 17255361 DOI: 10.1182/blood-2006-07-035972]

40 **Tan L**, Wang Q, Zhang D, Ding J, Huang Q, Tang YQ, Miao H. Lymphopenia predicts disease severity of COVID-19: a descriptive and predictive study. *Signal Transduct Target Ther* 2020; **5**: 33 [PMID: 32296069 DOI: 10.1038/s41392-020-0148-4]

41 **Wang L**, Li X, Chen H, Yan S, Li D, Li Y, Gong Z. Coronavirus Disease 19 Infection Does Not Result in Acute Kidney Injury: An Analysis of 116 Hospitalized Patients from Wuhan, China. *Am J Nephrol* 2020; **51**: 343-348 [PMID: 32229732 DOI: 10.1159/000507471]

42 **Balawender K**, Pliszka A, Krowiak A, Sito M, Grabarek BO, Boroń D. Does SARS-CoV-2 Affect Male Urogenital System? *Curr Pharm Biotechnol* 2022; **23**: 1792-1799 [PMID: 35255789 DOI: 10.2174/1389201023666220307102147]

43 **Cheng Y**, Luo R, Wang K, Zhang M, Wang Z, Dong L, Li J, Yao Y, Ge S, Xu G. Kidney disease is associated with in-hospital death of patients with COVID-19. *Kidney Int* 2020; **97**: 829-838 [PMID: 32247631 DOI: 10.1016/j.kint.2020.03.005]

44 **Li W**, Moore MJ, Vasilieva N, Sui J, Wong SK, Berne MA, Somasundaran M, Sullivan JL, Luzuriaga K, Greenough TC, Choe H, Farzan M. Angiotensin-converting enzyme 2 is a functional receptor for the SARS coronavirus. *Nature* 2003; **426**: 450-454 [PMID: 14647384 DOI: 10.1038/nature02145]

45 **Hamming I**, Timens W, Bulthuis ML, Lely AT, Navis G, van Goor H. Tissue distribution of ACE2 protein, the functional receptor for SARS coronavirus. A first step in understanding SARS pathogenesis. *J Pathol* 2004; **203**: 631-637 [PMID: 15141377 DOI: 10.1002/path.1570]

46 **Menachery VD**, Yount BL Jr, Debbink K, Agnihothram S, Gralinski LE, Plante JA, Graham RL, Scobey T, Ge XY, Donaldson EF, Randell SH, Lanzavecchia A, Marasco WA, Shi ZL, Baric RS. Corrigendum: A SARS-like cluster of circulating bat coronaviruses shows potential for human emergence. *Nat Med* 2016; **22**: 446 [PMID: 27050591 DOI: 10.1038/nm0416-446d]

47 **Valizadeh R**, Baradaran A, Mirzazadeh A, Bhaskar LVKS. Coronavirus-nephropathy; renal involvement in COVID-19. *J Renal Inj Prev* 2020; **9**: e18 [DOI: 10.34172/jrip.2020.18]

48 **Li B**, Yang J, Zhao F, Zhi L, Wang X, Liu L, Bi Z, Zhao Y. Prevalence and impact of cardiovascular metabolic diseases on COVID-19 in China. *Clin Res Cardiol* 2020; **109**: 531-538 [PMID: 32161990 DOI: 10.1007/s00392-020-01626-9]

49 **Xiong TY**, Redwood S, Prendergast B, Chen M. Coronaviruses and the cardiovascular system: acute and long-term implications. *Eur Heart J* 2020; **41**: 1798-1800 [PMID: 32186331 DOI: 10.1093/eurheartj/ehaa231]

50 **Cao LL**, Gaffney LK, Marcus C. Hypokalemia-Induced Rhabdomyolysis in a Child with Autism Affected by the COVID-19 Pandemic. *J Dev Behav Pediatr* 2022; **43**: e356-e360 [PMID: 34740217 DOI: 10.1097/DBP.0000000000001035]

51 **Bonow RO**, Fonarow GC, O'Gara PT, Yancy CW. Association of Coronavirus Disease 2019 (COVID-19) With Myocardial Injury and Mortality. *JAMA Cardiol* 2020; **5**: 751-753 [PMID: 32219362 DOI: 10.1001/jamacardio.2020.1105]

52 **Lippi G**, Plebani M. Laboratory abnormalities in patients with COVID-2019 infection. *Clin Chem Lab Med* 2020; **58**: 1131-1134 [PMID: 32119647 DOI: 10.1515/cclm-2020-0198]

53 **Bansal M**. Cardiovascular disease and COVID-19. *Diabetes Metab Syndr* 2020; **14**: 247-250 [PMID: 32247212 DOI: 10.1016/j.dsx.2020.03.013]

54 **Guo T**, Fan Y, Chen M, Wu X, Zhang L, He T, Wang H, Wan J, Wang X, Lu Z. Cardiovascular Implications of Fatal Outcomes of Patients With Coronavirus Disease 2019 (COVID-19). *JAMA Cardiol* 2020; **5**: 811-818 [PMID: 32219356 DOI: 10.1001/jamacardio.2020.1017]

55 **Ilias I**, Zabuliene L. Hyperglycemia and the novel Covid-19 infection: Possible pathophysiologic mechanisms. *Med Hypotheses* 2020; **139**: 109699 [PMID: 32240876 DOI: 10.1016/j.mehy.2020.109699]

56 **Yang X**, Yu Y, Xu J, Shu H, Xia J, Liu H, Wu Y, Zhang L, Yu Z, Fang M, Yu T, Wang Y, Pan S, Zou X, Yuan S, Shang Y. Clinical course and outcomes of critically ill patients with SARS-CoV-2 pneumonia in Wuhan, China: a single-centered, retrospective, observational study. *Lancet Respir Med* 2020; **8**: 475-481 [PMID: 32105632 DOI: 10.1016/S2213-2600(20)30079-5]

57 **Puig-Domingo M**, Marazuela M, Giustina A. COVID-19 and endocrine diseases. A statement from the European Society of Endocrinology. *Endocrine* 2020; **68**: 2-5 [PMID: 32279224 DOI: 10.1007/s12020-020-02294-5]

58 **Burgos R**, García-Almeida JM, Matía-Martín P, Palma S, Sanz-Paris A, Zugasti A, Alfaro JJ, Fullana AA, Continente AC, Chicetru MJ, Malpartida KG, Faes ÁG, Sánchez VG, López ML, Ortega AJM, Roldán JO, Moreno CS, Llanos PS. Malnutrition management of hospitalized patients with diabetes/hyperglycemia and COVID-19 infection. *Rev Endocr Metab Disord* 2022; **23**: 205-213 [PMID: 35244834 DOI: 10.1007/s11154-022-09714-z]

59 **Bancos I**, Hazeldine J, Chortis V, Hampson P, Taylor AE, Lord JM, Arlt W. Primary adrenal insufficiency is associated with impaired natural killer cell function: a potential link to increased mortality. *Eur J Endocrinol* 2017; **176**: 471-480 [PMID: 28223394 DOI: 10.1530/EJE-16-0969]

60 **Xu J**, Qi L, Chi X, Yang J, Wei X, Gong E, Peh S, Gu J. Orchitis: a complication of severe acute respiratory syndrome (SARS). *Biol Reprod* 2006; **74**: 410-416 [PMID: 16237152 DOI: 10.1095/biolreprod.105.044776]

61 **Cao X**. COVID-19: immunopathology and its implications for therapy. *Nat Rev Immunol* 2020; **20**: 269-270 [PMID: 32273594 DOI: 10.1038/s41577-020-0308-3]

62 **Zhao J**, Yuan Q, Wang H, Liu W, Liao X, Su Y, Wang X, Yuan J, Li T, Li J, Qian S, Hong C, Wang F, Liu Y, Wang Z, He Q, Li Z, He B, Zhang T, Fu Y, Ge S, Liu L, Zhang J, Xia N, Zhang Z. Antibody Responses to SARS-CoV-2 in Patients With Novel Coronavirus Disease 2019. *Clin Infect Dis* 2020; **71**: 2027-2034 [PMID: 32221519 DOI: 10.1093/cid/ciaa344]

63 **Recalcati S**. Cutaneous manifestations in COVID-19: a first perspective. *J Eur Acad Dermatol Venereol* 2020; **34**: e212-e213 [PMID: 32215952 DOI: 10.1111/jdv.16387]

64 **Joob B**, Wiwanitkit V. COVID-19 can present with a rash and be mistaken for dengue. *J Am Acad Dermatol* 2020; **82**: e177 [PMID: 32213305 DOI: 10.1016/j.jaad.2020.03.036]

65 **Lu S**, Lin J, Zhang Z, Xiao L, Jiang Z, Chen J, Hu C, Luo S. Alert for non-respiratory symptoms of coronavirus disease 2019 patients in epidemic period: A case report of familial cluster with three asymptomatic COVID-19 patients. *J Med Virol* 2021; **93**: 518-521 [PMID: 32190904 DOI: 10.1002/jmv.25776]

66 **Zhang JJ**, Dong X, Cao YY, Yuan YD, Yang YB, Yan YQ, Akdis CA, Gao YD. Clinical characteristics of 140 patients infected with SARS-CoV-2 in Wuhan, China. *Allergy* 2020; **75**: 1730-1741 [PMID: 32077115 DOI: 10.1111/all.14238]

67 **Wang HY**, Li XL, Yan ZR, Sun XP, Han J, Zhang BW. Potential neurological symptoms of COVID-19. *Ther Adv Neurol Disord* 2020; **13**: 1756286420917830 [PMID: 32284735 DOI: 10.1177/1756286420917830]

68 **Mao L**, Jin H, Wang M, Hu Y, Chen S, He Q, Chang J, Hong C, Zhou Y, Wang D, Miao X, Li Y, Hu B. Neurologic Manifestations of Hospitalized Patients With Coronavirus Disease 2019 in Wuhan, China. *JAMA Neurol* 2020; **77**: 683-690 [PMID: 32275288 DOI: 10.1001/jamaneurol.2020.1127]

69 **Li Y**, Li M, Wang M, Zhou Y, Chang J, Xian Y, Wang D, Mao L, Jin H, Hu B. Acute cerebrovascular disease following COVID-19: a single center, retrospective, observational study. *Stroke Vasc Neurol* 2020; **5**: 279-284 [PMID: 32616524 DOI: 10.1136/svn-2020-000431]

70 **Asadi-Pooya AA**, Simani L. Central nervous system manifestations of COVID-19: A systematic review. *J Neurol Sci* 2020; **413**: 116832 [PMID: 32299017 DOI: 10.1016/j.jns.2020.116832]

71 **Leitinger M**, Beniczky S, Rohracher A, Gardella E, Kalss G, Qerama E, Höfler J, Hess Lindberg-Larsen A, Kuchukhidze G, Dobesberger J, Langthaler PB, Trinka E. Salzburg Consensus Criteria for Non-Convulsive Status Epilepticus--approach to clinical application. *Epilepsy Behav* 2015; **49**: 158-163 [PMID: 26092326 DOI: 10.1016/j.yebeh.2015.05.007]

72 **Zhao H**, Shen D, Zhou H, Liu J, Chen S. Guillain-Barré syndrome associated with SARS-CoV-2 infection: causality or coincidence? *Lancet Neurol* 2020; **19**: 383-384 [PMID: 32246917 DOI: 10.1016/S1474-4422(20)30109-5]

73 **Jarius S**, Bieber N, Haas J, Wildemann B. MOG encephalomyelitis after vaccination against severe acute respiratory syndrome coronavirus type 2 (SARS-CoV-2): case report and comprehensive review of the literature. *J Neurol* 2022; **269**: 5198-5212 [PMID: 35737110 DOI: 10.1007/s00415-022-11194-9]

74 **Moriguchi T**, Harii N, Goto J, Harada D, Sugawara H, Takamino J, Ueno M, Sakata H, Kondo K, Myose N, Nakao A, Takeda M, Haro H, Inoue O, Suzuki-Inoue K, Kubokawa K, Ogihara S, Sasaki T, Kinouchi H, Kojin H, Ito M, Onishi H, Shimizu T, Sasaki Y, Enomoto N, Ishihara H, Furuya S, Yamamoto T, Shimada S. A first case of meningitis/encephalitis associated with SARS-Coronavirus-2. *Int J Infect Dis* 2020; **94**: 55-58 [PMID: 32251791 DOI: 10.1016/j.ijid.2020.03.062]

75 **Galea S**, Merchant RM, Lurie N. The Mental Health Consequences of COVID-19 and Physical Distancing: The Need for Prevention and Early Intervention. *JAMA Intern Med* 2020; **180**: 817-818 [PMID: 32275292 DOI: 10.1001/jamainternmed.2020.1562]

76 **World Health Organization**. 2019 Novel coronavirus (2019-nCoV): strategic preparedness and response plan. [Internet] [accessed 3 February 2020]. Available from: https://www.who.int/docs/default-source/coronaviruse/srp-04022020.pdf?sfvrsn=7ff55ec0_4

77 **Center of Disease Control and Prevention**. Coronavirus Disease 2019 (COVID-19), stress and Coping. [Internet] [accessed 10 May 2020]. Available from: https://www.cdc.gov/coronavirus/2019-ncov/daily-life-coping/managing-stress-anxiety.html

78 **Jakovljevic M**, Bjedov S, Jaksic N, Jakovljevic I. COVID-19 Pandemia and Public and Global Mental Health from the Perspective of Global Health Securit. *Psychiatr Danub* 2020; **32**: 6-14 [PMID: 32303023 DOI: 10.24869/psyd.2020.6]

79 **Wu KK**, Chan SK, Ma TM. Posttraumatic stress, anxiety, and depression in survivors of severe acute respiratory syndrome (SARS). *J Trauma Stress* 2005; **18**: 39-42 [PMID: 16281194 DOI: 10.1002/jts.20004]

80 **Mak IW**, Chu CM, Pan PC, Yiu MG, Chan VL. Long-term psychiatric morbidities among SARS survivors. *Gen Hosp Psychiatry* 2009; **31**: 318-326 [PMID: 19555791 DOI: 10.1016/j.genhosppsych.2009.03.001]

81 **Wing YK**, Ho SMY. Mental health of patients infected with SARS. In: Chan JCK, Wong VCWT, editors. Challenges of Severe Acute Respiratory Syndrome. Hong Kong: Elsevier (Singapore) Pte Ltd; 2006. p590 [DOI: 10.1016/j.outlook.2003.07.002]

82 **Lechien JR**, Chiesa-Estomba CM, De Siati DR, Horoi M, Le Bon SD, Rodriguez A, Dequanter D, Blecic S, El Afia F, Distinguin L, Chekkoury-Idrissi Y, Hans S, Delgado IL, Calvo-Henriquez C, Lavigne P, Falanga C, Barillari MR, Cammaroto G, Khalife M, Leich P, Souchay C, Rossi C, Journe F, Hsieh J, Edjlali M, Carlier R, Ris L, Lovato A, De

Filippis C, Coppee F, Fakhry N, Ayad T, Saussez S. Olfactory and gustatory dysfunctions as a clinical presentation of mild-to-moderate forms of the coronavirus disease (COVID-19): a multicenter European study. *Eur Arch Otorhinolaryngol* 2020; **277**: 2251-2261 [PMID: 32253535 DOI: 10.1007/s00405-020-05965-1]

83 **Giacomelli A**, Pezzati L, Conti F, Bernacchia D, Siano M, Oreni L, Rusconi S, Gervasoni C, Ridolfo AL, Rizzardini G, Antinori S, Galli M. Self-reported Olfactory and Taste Disorders in Patients With Severe Acute Respiratory Coronavirus 2 Infection: A Cross-sectional Study. *Clin Infect Dis* 2020; **71**: 889-890 [PMID: 32215618 DOI: 10.1093/cid/ciaa330]

84 **Kaye R**, Chang CWD, Kazahaya K, Brereton J, Denneny JC 3rd. COVID-19 Anosmia Reporting Tool: Initial Findings. *Otolaryngol Head Neck Surg* 2020; **163**: 132-134 [PMID: 32340555 DOI: 10.1177/0194599820922992]

85 **Moein ST**, Hashemian SM, Mansourafshar B, Khorram-Tousi A, Tabarsi P, Doty RL. Smell dysfunction: a biomarker for COVID-19. *Int Forum Allergy Rhinol* 2020; **10**: 944-950 [PMID: 32301284 DOI: 10.1002/alr.22587]

86 **Yu AY**, Tu R, Shao X, Pan A, Zhou K, Huang J. A comprehensive Chinese experience against SARS-CoV-2 in ophthalmology. *Eye Vis (Lond)* 2020; **7**: 19 [PMID: 32289038 DOI: 10.1186/s40662-020-00187-2]

87 **Seah I**, Agrawal R. Can the Coronavirus Disease 2019 (COVID-19) Affect the Eyes? *Ocul Immunol Inflamm* 2020; **28**: 391-395 [PMID: 32175797 DOI: 10.1080/09273948.2020.1738501]

88 **Holappa M**, Vapaatalo H, Vaajanen A. Many Faces of Renin-angiotensin System - Focus on Eye. *Open Ophthalmol J* 2017; **11**: 122-142 [PMID: 28761566 DOI: 10.2174/1874364101711010122]

89 **Wu P**, Duan F, Luo C, Liu Q, Qu X, Liang L, Wu K. Characteristics of Ocular Findings of Patients With Coronavirus Disease 2019 (COVID-19) in Hubei Province, China. *JAMA Ophthalmol* 2020; **138**: 575-578 [PMID: 32232433 DOI: 10.1001/jamaophthalmol.2020.1291]

90 **Lescure FX**, Bouadma L, Nguyen D, Parisey M, Wicky PH, Behillil S, Gaymard A, Bouscambert-Duchamp M, Donati F, Le Hingrat Q, Enouf V, Houhou-Fidouh N, Valette M, Mailles A, Lucet JC, Mentre F, Duval X, Descamps D, Malvy D, Timsit JF, Lina B, van-der-Werf S, Yazdanpanah Y. Clinical and virological data of the first cases of COVID-19 in Europe: a case series. *Lancet Infect Dis* 2020; **20**: 697-706 [PMID: 32224310 DOI: 10.1016/S1473-3099(20)30200-0]

91 **Cheema M**, Aghazadeh H, Nazarali S, Ting A, Hodges J, McFarlane A, Kanji JN, Zelyas N, Damji KF, Solarte C. Keratoconjunctivitis as the initial medical presentation of the novel coronavirus disease 2019 (COVID-19). *Can J Ophthalmol* 2020; **55**: e125-e129 [PMID: 32284146 DOI: 10.1016/j.jcjo.2020.03.003]

92 **Mustafa MWM**. Audiological profile of asymptomatic Covid-19 PCR-positive cases. *Am J Otolaryngol* 2020; **41**: 102483 [PMID: 32307189 DOI: 10.1016/j.amjoto.2020.102483]

93 **Fidan V**. New type of corona virus induced acute otitis media in adult. *Am J Otolaryngol* 2020; **41**: 102487 [PMID: 32336572 DOI: 10.1016/j.amjoto.2020.102487]

World Journal of Clinical Cases

Submit a Manuscript: https://www.f6publishing.com

World J Clin Cases 2023 January 26; 11(3): 506-513

DOI: 10.12998/wjcc.v11.i3.506

ISSN 2307-8960 (online)

MINIREVIEWS

Progress and expectation of stem cell therapy for diabetic wound healing

Zhen-Han Xu, Meng-Hui Ma, Yan-Qing Li, Li-Lin Li, Gui-Hua Liu

Specialty type: Endocrinology and metabolism

Provenance and peer review: Invited article; Externally peer reviewed.

Peer-review model: Single blind

Peer-review report's scientific quality classification

Grade A (Excellent): 0
Grade B (Very good): B
Grade C (Good): C
Grade D (Fair): D
Grade E (Poor): E

P-Reviewer: Jabbarpour Z, Iran; Khan I, Pakistan; Trébol J, Spain; Zhang Q, China

Received: August 31, 2022
Peer-review started: August 31, 2022
First decision: September 26, 2022
Revised: November 8, 2022
Accepted: January 9, 2023
Article in press: January 9, 2023
Published online: January 26, 2023

Zhen-Han Xu, Meng-Hui Ma, Yan-Qing Li, Li-Lin Li, Gui-Hua Liu, Reproductive Medicine Center, The Sixth Affiliated Hospital, Sun Yat-Sen University, Guangzhou 510610, Guangdong Province, China

Corresponding author: Gui-Hua Liu, MD, PhD, Associate Chief Physician, Associate Research Scientist, Reproductive Medicine Center, The Sixth Affiliated Hospital, Sun Yat-Sen University, Yuancuner Road, Tianhe District, Guangzhou 510610, Guangdong Province, China. liuguihua@mail.sysu.edu.cn

Abstract

Impaired wound healing presents great health risks to diabetics. Encouragingly, the current clinical successfully found out meaningful method to repair wound tissue, and stem cell therapy could be an effective method for diabetic wound healing with its ability to accelerate wound closure and avoid amputation. This minireview aims at introducing stem cell therapy for facilitating tissue repair in diabetic wounds, discussing the possible therapeutic mechanism and clinical application status and problems.

Key Words: Stem cell; Diabetic wound; Wound healing; Immunoregulation

Core Tip: Diabetic wound is a common complication of diabetes and stem cell therapy is an effective treatment for diabetic wounds. It helps improve wounds mainly by regulating inflammation and blood circulation. At present, many kinds of stem cells have been used and studied, and good results have been achieved. However, there are still problems that need to be solved. Here we discuss the current role and progress of stem cells in the treatment of diabetic wounds.

Citation: Xu ZH, Ma MH, Li YQ, Li LL, Liu GH. Progress and expectation of stem cell therapy for diabetic wound healing. *World J Clin Cases* 2023; 11(3): 506-513
URL: https://www.wjgnet.com/2307-8960/full/v11/i3/506.htm
DOI: https://dx.doi.org/10.12998/wjcc.v11.i3.506

INTRODUCTION

Diabetes with neurological abnormalities as well as peripheral artery disease of the lower extremities[1] can lead to diabetic wounds, particularly diabetic foot ulcers, which are considered one of the most serious complications. The international diabetes federation (IDF) reported that in 2021, there were nearly 536.6 million people living with diabetes[2], and the global diabetic foot ulcer prevalence was 6.3%[3]. Due to some risk factors, including poor glycemic control, peripheral neuropathy, peripheral vascular disease and immunosuppression[4], the progression of diabetic wounds can be accelerated, often resulting in complications demanding an amputation. At present, the treatment for diabetic wounds includes improving vascularization, debridement with pharmacological therapy, negative pressure wound therapy or using growth factors and skin substitutes, aiming at epithelial growth across the ulcer bed[4-7].

Stem cell therapies for wounds have vast prospects by using autologous or allogeneic stem cell transplantation for wound closure. It has been shown to help at all stages of wound healing and plays an important role in inflammation regulation, increasing both epithelialization and angiogenesis[8-11]. This minireview concentrates on the progress of stem cell therapy for facilitating tissue repair in diabetic wounds.

POSSIBLE MECHANISM OF STEM CELL THERAPY

Diabetes patients often suffer hyperglycemia, chronic inflammation, microvascular and macrovascular dysfunction, autonomic and sensory neuropathy, hypoxia and impaired neuropeptide signaling[12]. Necroptosis and apoptosis can be inreased by reactive oxygen species (ROS), advanced glycation end products and methylglyoxal, leading to diabetes complications[13]. Long term hyperglycemia leads to metabolic disorders because of the activation of additional polyol glucose metabolic pathway and the accumulation of toxic sorbitol in nerve tissue cells increases, leading to vascular damage[14,15]. With diabetic peripheral neuropathy as well as peripheral artery disease playing a central role, diabetes patients frequently suffer diabetic foot ulcer[16]. At present, stem cell therapies have been reported to contribute to diabetic wound healing in the following ways.

POSSESSING THE FUNCTION OF ANGIOGENESIS

First, stem cells help secrete vascular endothelial growth factor (VEGF), which promotes angiogenesis and the differentiation of endothelial progenitor cells into endothelial cells[17] and the extracellular matrix through the PI3K/threonine kinase (AKT) signaling pathway[18,19]. And they increase epithelialization, granulation tissue formation and capillary formation[20]. In a high glucose environment, stem cell-secreted exosomes contribute to angiopoiesis in endothelial progenitor cells, and overexpression of the transcription factor nuclear factor-E2-related factor 2 synergizes as a protective factor[21]. Moreover, including angiopoietin-1 (Ang-1), stromal cell-derived factor 1, inducible nitric oxide synthase (iNOS), epidermal growth factor (EGF), keratinocyte growth factor 2, erythropoietin, insulin-like growth factor 1 (IGF-1), basic fibroblast growth factor and placental growth factor, there are still many paracrine cytokines helping angiopoiesis, improving microcirculation in diabetic foot ulcer[22-24].

MODULATING INFLAMMATION

Stem cells are able to switch classically activated macrophages, which are called M1 macrophages and have proinflammatory effects, into optionally activated macrophages, which are called M2 macrophages and have anti-inflammatory effects[8,25-27]. In addition, it has been shown that together with exosomes, stem cells can decrease oxidative stress injuries of endothelial cells, providing immunomodulatory effects[28], and the level of Tregs is also upregulated at the same time[29,30]. Cytokines also play an important role in inflammation, and stem cells have the ability to lower the levels of proinflammatory cytokines, including interleukin-1 (IL-1), IL-6, IFN-β and TNF-α, while increasing the levels of anti-inflammatory cytokines, such as IL-10 and IL-4[31,32]. In a recent study mesenchymal stromal cells (MSCs) expressing IL-6, signaled by activating STAT-3 transcription factor, inhibited ROS by protecting neutrophils from apoptosis, preserving the excessive or inappropriate activation of the oxidative metabolism[33].

IMPROVING THE REMODELING PHASE

By cell differentiation, stem cells can translate into keratinocytes as well as endotheliocytes[34]. It has been reported that microvesicles from stem cells help to reprogram injured cells, thus achieving differentiation[35]. Recent studies have shown that stem cells might offer an important early signal to dermal fibroblast responses for their proliferation and migration[9,18]. Additionally, they lower the levels of matrix metalloproteinase-9 (MMP-9) to decrease proteolysis[36]. By reducing expression of phosphorylated focal adhesion kinase and increase the levels of MMP-2, EGF and IGF-1, MSCs improve the function of keratinocytes[37].

REGULATION OF MICRORNAS

MicroRNAs (miRNAs) have been discovered regulators of gene expression in the regulation of inflammation[38]. Generally, miRNAs promote wound healing by activating multiple pathways directly or indirectly. For example, after MSC treatment it is found that the increased levels of miR-146a result in attenuating expression of proinflammatory and inflammatory genes, including IL-1 receptor-associated kinase 1 (IRAK1), TNF receptor-associated factor 6 (TRAF6), and nuclear factor-κB (NF-κB)[39]. MSCs also enhance diabetic wound healing by improving collagen I content through increasing miR-29b expression[36]. A research has revealed that miR-21-5p promoted angiogenesis through upregulations of vascular endothelial growth factor receptor, activations of serine/ AKT and mitogen-activated protein kinase[40]. In addition, miR-126-3p from MSCs contributes to wound healing by increasing the formation of granulation tissue and angiogenesis[41]. MiRNA mediates the cell microenvironment, regulates the biological activity and phenotype of specific target cells, induces changes in the function of target cells, and leads to a series of biological reactions to play a variety of biological functions[42,43].

In conclusion, stem cells accelerate diabetic wound healing in many ways. Nevertheless, more connections between stem cells and diabetic wounds are under exploration.

STEM CELL THERAPIES FOR DIABETIC WOUNDS IN CLINICAL WORK

Over the past few years, it has been revealed that different types of stem cell therapies have been used in clinical work[44], as shown in Table 1. Although clinical data drew the conclusion that using stem cells benefits diabetic wounds, various types of stem cells with diversified methods still need to be identified. Attention should be given to adverse effects that have appeared in some research. For example, increased exudation from diabetic wounds may be associated with stem cells[45]. However, some clinical studies and analyses support its safety[46-48]. There are several types of cells used in clinical work. For example, adipose-derived mesenchymal stromal cells (ADMSCs) have been proven to be able to accelerate the time to wound closure[49] and the level of wound healing[50]. By intravascular and intralesional injection, umbilical cord mesenchymal stromal cells (UCMSCs) can not only improve the completion of wound closure[51] but also increase the number of vessels[52]. One case in which bone marrow mesenchymal stem cells (BMMSCs) were used for diabetic wound healing showed a good result in the next 10 years[53]. In addition, it has been revealed that BMMSC therapy might be better tolerated and more effective than bone marrow-derived mononuclear cells (BMMNCs) for increasing lower limb perfusion and promoting foot ulcer healing in diabetic patients with critical limb ischemia [54]. By treating with different doses of granulocyte colony stimulating factor (G-CSF), peripheral blood stem cells can be gained to promote the establishment of collateral circulation[55].

Although stem cell therapy has been shown to be a relatively safe treatment for diabetic wounds, unavoidable transplantation complications have appeared in diabetics, including febrile neutropenia, alopecia and gastrointestinal reaction[56]. A clinical trial reported one diabetes patient died of pseudomonas sepsis in the course of neutropenia after autologous hematopoietic stem cell transplantation[57]. Thus, complications as well as adverse events still can't be ignored while the safety of stem cell transplantation has been reported in some studies[58].

CONCLUSION

Stem Cell therapy could be an effective treatment for diabetic wounds[59,60], which contains endless medical value together with a wide scientific perspective accelerating diabetic wound healing. Stem cells have also demonstrated their therapeutic potential in the field even if infection is present[61]. However, there are still problems that need to be solved.

First, the mechanisms of stem cell therapy are still considered as a vital part of the theoretical basis of clinical study. Although animal experiments and clinical trials provide us with great results, studies based on the molecular level should be carried out to gain more molecular mechanisms.

Table 1 Recent clinical trials regarding stem cell therapies for diabetic wounds

Ref.	Type of stem cells	Number of cases	Mean age (year)	Methods of treatment	Possible mechanism	Outcome	Adverse events	Conciusion
Uzun *et al* [49], 2021	ADMSCs	10	57.5	Intralesional injection	The release of angiogenic cytokines, increasing epithelialization, granulation tissue formation, anti-inflammatory, and anti-apoptotic effects	Time to wound closure (d): ADMSCs group (n = 10): 31.0 ± 10.7; Control group (n = 10): 54.8 ± 15.0; P = 0.002	No found	Allogeneic ADMSCs injection is a safe and effective method with a positive contribution to wound-healing time in the treatment of chronic diabetic foot ulcers
Suzdaltseva *et al*[51], 2020	UCMSCs	31	58.5	Intralesional injection	The release of angiogenic cytokines, cell differentiation, and immunomodulation	Complete wound closure or significant improvement (% in group)[a]: UCMSCs group (n = 59): 22%; Placebo group (n = 49): 8.2%; P < 0.05	No found	Locally delivered allogeneic UCMSCs can contribute to chronic wound repair and provide an additional support toward new therapeutic strategies
Moon *et al* [50], 2019	ADMSCs	30	59.9	Topical	Synthesizing higher amounts of collagen, fibroblast growth factor, and vascular endothelial growth factor in vitro	Complete wound closure at Week 12 (% in group): ADMSCs group (n = 30): 82%; Control group (n = 29): 53%; P < 0.05	No found	Allogeneic ADMSCs might be effective and safe to treat diabetic foot ulcers
Chen *et al* [53], 2018	BMMSCs	1	64	Intramuscular injection	The release of angiogenic cytokines, differentiation and angiogen	No recurrence in the next 10-yr follow-up span	No found	Autologous BMMSC transplantation therapy may be an effective measure for recurrent bullosis diabeticorum
Qin *et al* [52], 2016	UCMSCs	28	75	Intravascular and intralesional injection	The release of signalling or growth factors, and differentiation of injected precursor cells into functional tissue	Increased number of vessels: Experimental group (n = 28): 9.3 ± 2.7; Control group (n = 25): 5.9 ± 3.3; P < 0.05	No found	UCMSC transplantation after angioplasty is a safe and effective clinical therapy for severe diabetic foot
Xu *et al*[55], 2016	Peripheral blood stem cells	63	69	Intralesional injection	Angiogenesis and vascularization	CTA score[b]: Pre-transplantation (n = 63): 1.22 ± 0.15; Post-transplantation (n = 63): 2.35 ± 0.784; P < 0.01	No found	Autologous peripheral blood stem cell transplantation can promote the establishment of collateral circulation in patients with diabetic foot
Lu *et al*[54], 2011	BMMSCs	18	63	Intramuscular injection	The release of angiogenic cytokines, differentiation and angiogenesis	Angiographic score of MRA in limbs at 24 wk[b]: BMMSCs (n = 18): 1.9 ± 0.5; BMMNCs (n = 19): 1.5 ± 0.6; P = 0.018	No found	BMMSCs therapy may be better tolerated and more effective than BMMNCs for increasing lower limb perfusion and promoting foot ulcer healing in diabetic patients with critical limb ischemia

[a]108 patients, including 31 patients (28.7%) suffering from diabetic foot, were randomized to the umbilical cord mesenchymal stromal cell group and placebo group.

[b]0 points, no new collateral vessels; 1 point, little new collateral circulation; 2 points, moderate new collateral circulation; 3 points, abundant new collateral circulation.

ADMSCs: Adipose-derived mesenchymal stromal cells; UCMSCs: Umbilical cord mesenchymal stromal cells; BMMSCs: Bone marrow mesenchymal stem cells; CTA: Computed tomography angiography; MRA: Magnetic resonance angiography; BMMNCs: Bone marrow-derived mononuclear cells.

Second, the safety of treatment cannot be ignored, although only a few adverse events have been reported, which urges more clinical trials. At the same time, more specific therapeutic doses and administration routes should be revealed, which accounts for how to reduce side effects and adverse reactions. For example, on account of its differentiative capacity, surgical dressing with stem cells may have the ability to decrease bleeding as well as accelerate operative incision closure, since it has been reported that advanced dressings for the delivery of progenitor cells are at the point in research[62]. Moreover, considering patients with cancer who cannot receive stem cell treatment[63], alternative solutions need to be identified.

Third, it is still important for physicians to simplify the approach of gathering as well as preconditioning stem cells because preconditioning MSCs with pretreatment agents significantly hastened healing in delayed-healing wounds[64]. In addition, evidence has shown that the ability of stem cells in elderly people to proliferate and differentiate diminishes with age[65]. Therefore, the differences between autotransplantation and allotransplantation should be taken into consideration to improve the success rate of transplantation.

Last, the questions of ethics also matter. Promising and effective stem cell therapy has raised serious ethical problems[66]. Not only do social responsibility and moral constraints regularize approaches of treatment, but relevant laws and medical guidelines also need to be improved.

The answers to these questions will lead to better and more appropriate treatments for different patients.

FOOTNOTES

Author contributions: Xu ZH, Ma MH, Li YQ, Li LL and Liu GH designed the research study; Xu ZH, Ma MH, Li YQ and Li LL performed the research; Xu ZH and Ma MH contributed literature search; Xu ZH, Li LL and Liu GH contributed data analysis; Xu ZH and Li YQ wrote the manuscript; All authors have read and approve the final manuscript.

Supported by The National Natural Science Foundation of China, No. 82171604.

Conflict-of-interest statement: All the authors declare that there are no conflicts of interest associated with this manuscript.

Country/Territory of origin: China

ORCID number: Zhen-Han Xu 0000-0002-6445-3557; Meng-Hui Ma 0000-0002-6369-1000; Yan-Qing Li 0000-0003-3222-5610; Li-Lin Li 0000-0003-3298-297X; Gui-Hua Liu 0000-0003-1811-8763.

S-Editor: Liu JH
L-Editor: A
P-Editor: Liu JH

REFERENCES

1 **Edmonds M**, Manu C, Vas P. The current burden of diabetic foot disease. *J Clin Orthop Trauma* 2021; **17**: 88-93 [PMID: 33680841 DOI: 10.1016/j.jcot.2021.01.017]
2 Global diabetes data report 2000 — 2045. Available from: https://diabetesatlas.org/data/
3 **Zhang P**, Lu J, Jing Y, Tang S, Zhu D, Bi Y. Global epidemiology of diabetic foot ulceration: a systematic review and meta-analysis (†). *Ann Med* 2017; **49**: 106-116 [PMID: 27585063 DOI: 10.1080/07853890.2016.1231932]
4 **Lim JZ**, Ng NS, Thomas C. Prevention and treatment of diabetic foot ulcers. *J R Soc Med* 2017; **110**: 104-109 [PMID: 28116957 DOI: 10.1177/0141076816688346]
5 **Cho H**, Blatchley MR, Duh EJ, Gerecht S. Acellular and cellular approaches to improve diabetic wound healing. *Adv Drug Deliv Rev* 2019; **146**: 267-288 [PMID: 30075168 DOI: 10.1016/j.addr.2018.07.019]
6 **Cavanagh PR**, Lipsky BA, Bradbury AW, Botek G. Treatment for diabetic foot ulcers. *Lancet* 2005; **366**: 1725-1735 [PMID: 16291067 DOI: 10.1016/S0140-6736(05)67699-4]
7 **Maksimova N**, Krasheninnikov M, Zhang Y, Ponomarev E, Pomytkin I, Melnichenko G, Lyundup A. Early passage autologous mesenchymal stromal cells accelerate diabetic wound re-epithelialization: A clinical case study. *Cytotherapy* 2017; **19**: 1548-1550 [PMID: 28986173 DOI: 10.1016/j.jcyt.2017.08.017]
8 **Krasilnikova OA**, Baranovskii DS, Lyundup AV, Shegay PV, Kaprin AD, Klabukov ID. Stem and Somatic Cell Monotherapy for the Treatment of Diabetic Foot Ulcers: Review of Clinical Studies and Mechanisms of Action. *Stem Cell Rev Rep* 2022; **18**: 1974-1985 [PMID: 35476187 DOI: 10.1007/s12015-022-10379-z]
9 **Smith AN**, Willis E, Chan VT, Muffley LA, Isik FF, Gibran NS, Hocking AM. Mesenchymal stem cells induce dermal fibroblast responses to injury. *Exp Cell Res* 2010; **316**: 48-54 [PMID: 19666021 DOI: 10.1016/j.yexcr.2009.08.001]
10 **Javazon EH**, Keswani SG, Badillo AT, Crombleholme TM, Zoltick PW, Radu AP, Kozin ED, Beggs K, Malik AA, Flake AW. Enhanced epithelial gap closure and increased angiogenesis in wounds of diabetic mice treated with adult murine bone marrow stromal progenitor cells. *Wound Repair Regen* 2007; **15**: 350-359 [PMID: 17537122 DOI: 10.1111/j.1524-475X.2007.00237.x]

11 **Yang J**, Chen Z, Pan D, Li H, Shen J. Umbilical Cord-Derived Mesenchymal Stem Cell-Derived Exosomes Combined Pluronic F127 Hydrogel Promote Chronic Diabetic Wound Healing and Complete Skin Regeneration. *Int J Nanomedicine* 2020; **15**: 5911-5926 [PMID: 32848396 DOI: 10.2147/IJN.S249129]

12 **Baltzis D**, Eleftheriadou I, Veves A. Pathogenesis and treatment of impaired wound healing in diabetes mellitus: new insights. *Adv Ther* 2014; **31**: 817-836 [PMID: 25069580 DOI: 10.1007/s12325-014-0140-x]

13 **Volpe CMO**, Villar-Delfino PH, Dos Anjos PMF, Nogueira-Machado JA. Cellular death, reactive oxygen species (ROS) and diabetic complications. *Cell Death Dis* 2018; **9**: 119 [PMID: 29371661 DOI: 10.1038/s41419-017-0135-z]

14 **Brem H**, Tomic-Canic M. Cellular and molecular basis of wound healing in diabetes. *J Clin Invest* 2007; **117**: 1219-1222 [PMID: 17476353 DOI: 10.1172/JCI32169]

15 **Jhamb S**, Vangaveti VN, Malabu UH. Genetic and molecular basis of diabetic foot ulcers: Clinical review. *J Tissue Viability* 2016; **25**: 229-236 [PMID: 27372176 DOI: 10.1016/j.jtv.2016.06.005]

16 **Schaper NC**, Van Netten JJ, Apelqvist J, Lipsky BA, Bakker K; International Working Group on the Diabetic Foot (IWGDF). Prevention and management of foot problems in diabetes: A Summary Guidance for Daily Practice 2015, based on the IWGDF guidance documents. *Diabetes Res Clin Pract* 2017; **124**: 84-92 [PMID: 28119194 DOI: 10.1016/j.diabres.2016.12.007]

17 **Ge Q**, Zhang H, Hou J, Wan L, Cheng W, Wang X, Dong D, Chen C, Xia J, Guo J, Chen X, Wu X. VEGF secreted by mesenchymal stem cells mediates the differentiation of endothelial progenitor cells into endothelial cells *via* paracrine mechanisms. *Mol Med Rep*(e-pub ahead of print 14 November 2017) [DOI: 10.3892/mmr.2017.8059]

18 **Wang J**, Wu H, Peng Y, Zhao Y, Qin Y, Zhang Y, Xiao Z. Hypoxia adipose stem cell-derived exosomes promote high-quality healing of diabetic wound involves activation of PI3K/Akt pathways. *J Nanobiotechnology* 2021; **19**: 202 [PMID: 34233694 DOI: 10.1186/s12951-021-00942-0]

19 **Zhang W**, Bai X, Zhao B, Li Y, Zhang Y, Li Z, Wang X, Luo L, Han F, Zhang J, Han S, Cai W, Su L, Tao K, Shi J, Hu D. Cell-free therapy based on adipose tissue stem cell-derived exosomes promotes wound healing *via* the PI3K/Akt signaling pathway. *Exp Cell Res* 2018; **370**: 333-342 [PMID: 29964051 DOI: 10.1016/j.yexcr.2018.06.035]

20 **Guillamat-Prats R**. The Role of MSC in Wound Healing, Scarring and Regeneration. *Cells* 2021; **10** [PMID: 34359898 DOI: 10.3390/cells10071729]

21 **Li X**, Xie X, Lian W, Shi R, Han S, Zhang H, Lu L, Li M. Exosomes from adipose-derived stem cells overexpressing Nrf2 accelerate cutaneous wound healing by promoting vascularization in a diabetic foot ulcer rat model. *Exp Mol Med* 2018; **50**: 1-14 [PMID: 29651102 DOI: 10.1038/s12276-018-0058-5]

22 **Kinnaird T**, Stabile E, Burnett MS, Shou M, Lee CW, Barr S, Fuchs S, Epstein SE. Local delivery of marrow-derived stromal cells augments collateral perfusion through paracrine mechanisms. *Circulation* 2004; **109**: 1543-1549 [PMID: 15023891 DOI: 10.1161/01.CIR.0000124062.31102.57]

23 **Schlosser S**, Dennler C, Schweizer R, Eberli D, Stein JV, Enzmann V, Giovanoli P, Erni D, Plock JA. Paracrine effects of mesenchymal stem cells enhance vascular regeneration in ischemic murine skin. *Microvasc Res* 2012; **83**: 267-275 [PMID: 22391452 DOI: 10.1016/j.mvr.2012.02.011]

24 **Chen L**, Tredget EE, Wu PY, Wu Y. Paracrine factors of mesenchymal stem cells recruit macrophages and endothelial lineage cells and enhance wound healing. *PLoS One* 2008; **3**: e1886 [PMID: 18382669 DOI: 10.1371/journal.pone.0001886]

25 **Maggini J**, Mirkin G, Bognanni I, Holmberg J, Piazzón IM, Nepomnaschy I, Costa H, Cañones C, Raiden S, Vermeulen M, Geffner JR. Mouse bone marrow-derived mesenchymal stromal cells turn activated macrophages into a regulatory-like profile. *PLoS One* 2010; **5**: e9252 [PMID: 20169081 DOI: 10.1371/journal.pone.0009252]

26 **Liu W**, Yu M, Xie D, Wang L, Ye C, Zhu Q, Liu F, Yang L. Melatonin-stimulated MSC-derived exosomes improve diabetic wound healing through regulating macrophage M1 and M2 polarization by targeting the PTEN/AKT pathway. *Stem Cell Res Ther* 2020; **11**: 259 [PMID: 32600435 DOI: 10.1186/s13287-020-01756-x]

27 **Louiselle AE**, Niemiec SM, Zgheib C, Liechty KW. Macrophage polarization and diabetic wound healing. *Transl Res* 2021; **236**: 109-116 [PMID: 34089902 DOI: 10.1016/j.trsl.2021.05.006]

28 **Yan C**, Xv Y, Lin Z, Endo Y, Xue H, Hu Y, Hu L, Chen L, Cao F, Zhou W, Zhang P, Liu G. Human Umbilical Cord Mesenchymal Stem Cell-Derived Exosomes Accelerate Diabetic Wound Healing *via* Ameliorating Oxidative Stress and Promoting Angiogenesis. *Front Bioeng Biotechnol* 2022; **10**: 829868 [PMID: 35174145 DOI: 10.3389/fbioe.2022.829868]

29 **Xiong J**, Hu H, Guo R, Wang H, Jiang H. Mesenchymal Stem Cell Exosomes as a New Strategy for the Treatment of Diabetes Complications. *Front Endocrinol (Lausanne)* 2021; **12**: 646233 [PMID: 33995278 DOI: 10.3389/fendo.2021.646233]

30 **Nojehdehi S**, Soudi S, Hesampour A, Rasouli S, Soleimani M, Hashemi SM. Immunomodulatory effects of mesenchymal stem cell-derived exosomes on experimental type-1 autoimmune diabetes. *J Cell Biochem* 2018; **119**: 9433-9443 [PMID: 30074271 DOI: 10.1002/jcb.27260]

31 **Liu L**, Yu Y, Hou Y, Chai J, Duan H, Chu W, Zhang H, Hu Q, Du J. Human umbilical cord mesenchymal stem cells transplantation promotes cutaneous wound healing of severe burned rats. *PLoS One* 2014; **9**: e88348 [PMID: 24586314 DOI: 10.1371/journal.pone.0088348]

32 **Aggarwal S**, Pittenger MF. Human mesenchymal stem cells modulate allogeneic immune cell responses. *Blood* 2005; **105**: 1815-1822 [PMID: 15494428 DOI: 10.1182/blood-2004-04-1559]

33 **Raffaghello L**, Bianchi G, Bertolotto M, Montecucco F, Busca A, Dallegri F, Ottonello L, Pistoia V. Human mesenchymal stem cells inhibit neutrophil apoptosis: a model for neutrophil preservation in the bone marrow niche. *Stem Cells* 2008; **26**: 151-162 [PMID: 17932421 DOI: 10.1634/stemcells.2007-0416]

34 **Isakson M**, de Blacam C, Whelan D, McArdle A, Clover AJ. Mesenchymal Stem Cells and Cutaneous Wound Healing: Current Evidence and Future Potential. *Stem Cells Int* 2015; **2015**: 831095 [PMID: 26106431 DOI: 10.1155/2015/831095]

35 **Camussi G**, Deregibus MC, Cantaluppi V. Role of stem-cell-derived microvesicles in the paracrine action of stem cells. *Biochem Soc Trans* 2013; **41**: 283-287 [PMID: 23356298 DOI: 10.1042/BST20120192]

36 **Xu J**, Zgheib C, Hodges MM, Caskey RC, Hu J, Liechty KW. Mesenchymal stem cells correct impaired diabetic wound

healing by decreasing ECM proteolysis. *Physiol Genomics* 2017; **49**: 541-548 [PMID: 28842435 DOI: 10.1152/physiolgenomics.00090.2016]

37 **Kato J**, Kamiya H, Himeno T, Shibata T, Kondo M, Okawa T, Fujiya A, Fukami A, Uenishi E, Seino Y, Tsunekawa S, Hamada Y, Naruse K, Oiso Y, Nakamura J. Mesenchymal stem cells ameliorate impaired wound healing through enhancing keratinocyte functions in diabetic foot ulcerations on the plantar skin of rats. *J Diabetes Complications* 2014; **28**: 588-595 [PMID: 25027388 DOI: 10.1016/j.jdiacomp.2014.05.003]

38 **Sheedy FJ**, O'Neill LA. Adding fuel to fire: microRNAs as a new class of mediators of inflammation. *Ann Rheum Dis* 2008; **67** Suppl 3: iii50-iii55 [PMID: 19022814 DOI: 10.1136/ard.2008.100289]

39 **Xu J**, Wu W, Zhang L, Dorset-Martin W, Morris MW, Mitchell ME, Liechty KW. The role of microRNA-146a in the pathogenesis of the diabetic wound-healing impairment: correction with mesenchymal stem cell treatment. *Diabetes* 2012; **61**: 2906-2912 [PMID: 22851573 DOI: 10.2337/db12-0145]

40 **Huang C**, Luo W, Wang Q, Ye Y, Fan J, Lin L, Shi C, Wei W, Chen H, Wu Y, Tang Y. Human mesenchymal stem cells promote ischemic repairment and angiogenesis of diabetic foot through exosome miRNA-21-5p. *Stem Cell Res* 2021; **52**: 102235 [PMID: 33601096 DOI: 10.1016/j.scr.2021.102235]

41 **Tao SC**, Guo SC, Li M, Ke QF, Guo YP, Zhang CQ. Chitosan Wound Dressings Incorporating Exosomes Derived from MicroRNA-126-Overexpressing Synovium Mesenchymal Stem Cells Provide Sustained Release of Exosomes and Heal Full-Thickness Skin Defects in a Diabetic Rat Model. *Stem Cells Transl Med* 2017; **6**: 736-747 [PMID: 28297576 DOI: 10.5966/sctm.2016-0275]

42 **Ferguson SW**, Wang J, Lee CJ, Liu M, Neelamegham S, Canty JM, Nguyen J. The microRNA regulatory landscape of MSC-derived exosomes: a systems view. *Sci Rep* 2018; **8**: 1419 [PMID: 29362496 DOI: 10.1038/s41598-018-19581-x]

43 **Phinney DG**, Di Giuseppe M, Njah J, Sala E, Shiva S, St Croix CM, Stolz DB, Watkins SC, Di YP, Leikauf GD, Kolls J, Riches DW, Deiuliis G, Kaminski N, Boregowda SV, McKenna DH, Ortiz LA. Mesenchymal stem cells use extracellular vesicles to outsource mitophagy and shuttle microRNAs. *Nat Commun* 2015; **6**: 8472 [PMID: 26442449 DOI: 10.1038/ncomms9472]

44 **Kosaric N**, Kiwanuka H, Gurtner GC. Stem cell therapies for wound healing. *Expert Opin Biol Ther* 2019; **19**: 575-585 [PMID: 30900481 DOI: 10.1080/14712598.2019.1596257]

45 **Askø Andersen J**, Rasmussen A, Frimodt-Møller M, Engberg S, Steeneveld E, Kirketerp-Møller K, O'Brien T, Rossing P. Novel topical allogeneic bone-marrow-derived mesenchymal stem cell treatment of hard-to-heal diabetic foot ulcers: a proof of concept study. *Stem Cell Res Ther* 2022; **13**: 280 [PMID: 35765085 DOI: 10.1186/s13287-022-02951-8]

46 **Dubský M**, Jirkovská A, Bem R, Fejfarová V, Pagacová L, Nemcová A, Sixta B, Chlupac J, Peregrin JH, Syková E, Jude EB. Comparison of the effect of stem cell therapy and percutaneous transluminal angioplasty on diabetic foot disease in patients with critical limb ischemia. *Cytotherapy* 2014; **16**: 1733-1738 [PMID: 25304666 DOI: 10.1016/j.jcyt.2014.08.010]

47 **Marino G**, Moraci M, Armenia E, Orabona C, Sergio R, De Sena G, Capuozzo V, Barbarisi M, Rosso F, Giordano G, Iovino F, Barbarisi A. Therapy with autologous adipose-derived regenerative cells for the care of chronic ulcer of lower limbs in patients with peripheral arterial disease. *J Surg Res* 2013; **185**: 36-44 [PMID: 23773718 DOI: 10.1016/j.jss.2013.05.024]

48 **Carstens MH**, Quintana FJ, Calderwood ST, Sevilla JP, Ríos AB, Rivera CM, Calero DW, Zelaya ML, Garcia N, Bertram KA, Rigdon J, Dos-Anjos S, Correa D. Treatment of chronic diabetic foot ulcers with adipose-derived stromal vascular fraction cell injections: Safety and evidence of efficacy at 1 year. *Stem Cells Transl Med* 2021; **10**: 1138-1147 [PMID: 33826245 DOI: 10.1002/sctm.20-0497]

49 **Uzun E**, Güney A, Gönen ZB, Özkul Y, Kafadar İH, Günay M, Mutlu M. Intralesional allogeneic adipose-derived stem cells application in chronic diabetic foot ulcer: Phase I/2 safety study. *Foot Ankle Surg* 2021; **27**: 636-642 [PMID: 32826167 DOI: 10.1016/j.fas.2020.08.002]

50 **Moon KC**, Suh HS, Kim KB, Han SK, Young KW, Lee JW, Kim MH. Potential of Allogeneic Adipose-Derived Stem Cell-Hydrogel Complex for Treating Diabetic Foot Ulcers. *Diabetes* 2019; **68**: 837-846 [PMID: 30679183 DOI: 10.2337/db18-0699]

51 **Suzdaltseva Y**, Zhidkih S, Kiselev SL, Stupin V. Locally Delivered Umbilical Cord Mesenchymal Stromal Cells Reduce Chronic Inflammation in Long-Term Nonhealing Wounds: A Randomized Study. *Stem Cells Int* 2020; **2020**: 5308609 [PMID: 32148521 DOI: 10.1155/2020/5308609]

52 **Qin HL**, Zhu XH, Zhang B, Zhou L, Wang WY. Clinical Evaluation of Human Umbilical Cord Mesenchymal Stem Cell Transplantation After Angioplasty for Diabetic Foot. *Exp Clin Endocrinol Diabetes* 2016; **124**: 497-503 [PMID: 27219884 DOI: 10.1055/s-0042-103684]

53 **Chen Y**, Ma Y, Li N, Wang H, Chen B, Liang Z, Ren R, Lu D, Boey J, Armstrong DG, Deng W. Efficacy and long-term longitudinal follow-up of bone marrow mesenchymal cell transplantation therapy in a diabetic patient with recurrent lower limb bullosis diabeticorum. *Stem Cell Res Ther* 2018; **9**: 99 [PMID: 29631615 DOI: 10.1186/s13287-018-0854-9]

54 **Lu D**, Chen B, Liang Z, Deng W, Jiang Y, Li S, Xu J, Wu Q, Zhang Z, Xie B, Chen S. Comparison of bone marrow mesenchymal stem cells with bone marrow-derived mononuclear cells for treatment of diabetic critical limb ischemia and foot ulcer: a double-blind, randomized, controlled trial. *Diabetes Res Clin Pract* 2011; **92**: 26-36 [PMID: 21216483 DOI: 10.1016/j.diabres.2010.12.010]

55 **Xu SM**, Liang T. Clinical observation of the application of autologous peripheral blood stem cell transplantation for the treatment of diabetic foot gangrene. *Exp Ther Med* 2016; **11**: 283-288 [PMID: 26889255 DOI: 10.3892/etm.2015.2888]

56 **Gu B**, Miao H, Zhang J, Hu J, Zhou W, Gu W, Wang W, Ning G. Clinical benefits of autologous haematopoietic stem cell transplantation in type 1 diabetes patients. *Diabetes Metab* 2018; **44**: 341-345 [PMID: 29331269 DOI: 10.1016/j.diabet.2017.12.006]

57 **Snarski E**, Milczarczyk A, Hałaburda K, Torosian T, Paluszewska M, Urbanowska E, Król M, Boguradzki P, Jedynasty K, Franek E, Wiktor-Jedrzejczak W. Immunoablation and autologous hematopoietic stem cell transplantation in the treatment of new-onset type 1 diabetes mellitus: long-term observations. *Bone Marrow Transplant* 2016; **51**: 398-402 [PMID: 26642342 DOI: 10.1038/bmt.2015.294]

58 **Jin L**, Wang X, Qiao Z, Deng Y. The safety and efficacy of mesenchymal stem cell therapy in diabetic lower extremity

vascular disease: a meta-analysis and systematic review. *Cytotherapy* 2022; **24**: 225-234 [PMID: 34656420 DOI: 10.1016/j.jcyt.2021.08.001]

59 **Gadelkarim M**, Abushouk AI, Ghanem E, Hamaad AM, Saad AM, Abdel-Daim MM. Adipose-derived stem cells: Effectiveness and advances in delivery in diabetic wound healing. *Biomed Pharmacother* 2018; **107**: 625-633 [PMID: 30118878 DOI: 10.1016/j.biopha.2018.08.013]

60 **El Hage R**, Knippschild U, Arnold T, Hinterseher I. Stem Cell-Based Therapy: A Promising Treatment for Diabetic Foot Ulcer. *Biomedicines* 2022; **10** [PMID: 35884812 DOI: 10.3390/biomedicines10071507]

61 **Amini A**, Chien S, Bayat M. Potential of stem cells for treating infected Diabetic Foot Wounds and Ulcers: a systematic review. *Mol Biol Rep* 2022; **49**: 10925-10934 [PMID: 36008608 DOI: 10.1007/s11033-022-07721-6]

62 **Kirby GT**, Mills SJ, Vandenpoel L, Pinxteren J, Ting A, Short RD, Cowin AJ, Michelmore A, Smith LE. Development of Advanced Dressings for the Delivery of Progenitor Cells. *ACS Appl Mater Interfaces* 2017; **9**: 3445-3454 [PMID: 28068055 DOI: 10.1021/acsami.6b14725]

63 **Mohr A**, Zwacka R. The future of mesenchymal stem cell-based therapeutic approaches for cancer - From cells to ghosts. *Cancer Lett* 2018; **414**: 239-249 [PMID: 29175461 DOI: 10.1016/j.canlet.2017.11.025]

64 **Amini A**, Chien S, Bayat M. Effectiveness of preconditioned adipose-derived mesenchymal stem cells with photobiomodulation for the treatment of diabetic foot ulcers: a systematic review. *Lasers Med Sci* 2022; **37**: 1415-1425 [PMID: 34697696 DOI: 10.1007/s10103-021-03451-6]

65 **You D**, Jang MJ, Lee J, Jeong IG, Kim HS, Moon KH, Suh N, Kim CS. Periprostatic implantation of human bone marrow-derived mesenchymal stem cells potentiates recovery of erectile function by intracavernosal injection in a rat model of cavernous nerve injury. *Urology* 2013; **81**: 104-110 [PMID: 23122545 DOI: 10.1016/j.urology.2012.08.046]

66 **de Miguel-Beriain I**. The ethics of stem cells revisited. *Adv Drug Deliv Rev* 2015; **82-83**: 176-180 [PMID: 25446134 DOI: 10.1016/j.addr.2014.11.011]

World Journal of Clinical Cases

Submit a Manuscript: https://www.f6publishing.com

World J Clin Cases 2023 January 26; 11(3): 514-527

DOI: 10.12998/wjcc.v11.i3.514

ISSN 2307-8960 (online)

MINIREVIEWS

Prevention, diagnostic evaluation, management and prognostic implications of liver disease in critically ill patients with COVID-19

Asimina Valsamaki, Maria Xanthoudaki, Katerina G Oikonomou, Panagiotis J Vlachostergios, Antonios Papadogoulas, Periklis Katsiafylloudis, Ioanna Voulgaridi, Apostolia-Lemonia Skoura, Apostolos Komnos, Panagiotis Papamichalis

Specialty type: Critical care medicine

Provenance and peer review: Invited article; Externally peer reviewed.

Peer-review model: Single blind

Peer-review report's scientific quality classification

Grade A (Excellent): 0
Grade B (Very good): B
Grade C (Good): C
Grade D (Fair): 0
Grade E (Poor): 0

P-Reviewer: Dasuqi SA, Saudi Arabia; Tusabe F

Received: October 12, 2022
Peer-review started: October 12, 2022
First decision: November 26, 2022
Revised: December 5, 2022
Accepted: January 10, 2023
Article in press: January 10, 2023
Published online: January 26, 2023

Asimina Valsamaki, Maria Xanthoudaki, Katerina G Oikonomou, Antonios Papadogoulas, Periklis Katsiafylloudis, Apostolos Komnos, Panagiotis Papamichalis, Intensive Care Unit, General Hospital of Larissa, Larissa 41221, Greece

Panagiotis J Vlachostergios, Division of Hematology and Medical Oncology, Department of Medicine, Weill Cornell Medicine, New York, NY 10065, United States

Ioanna Voulgaridi, Department of Microbiology, General Hospital of Larissa, Larissa 41221, Greece

Apostolia-Lemonia Skoura, Transfusion Medicine Department, University Hospital of Larissa, Larissa 41110, Greece

Corresponding author: Panagiotis Papamichalis, MD, PhD, Consultant Physician-Scientist, Doctor, Intensive Care Unit, General Hospital of Larissa, Tsakalof 1, Larissa 41221, Greece. ppapamih@med.uth.gr

Abstract

Coronavirus disease 2019 (COVID-19), caused by severe acute respiratory syndrome coronavirus 2, broke out in December 2019 in Wuhan city of China and spread rapidly worldwide. Therefore, by March 2020, the World Health Organization declared the disease a global pandemic. Apart from the respiratory system, various other organs of the human body are also seriously affected by the virus. Liver injury in patients with a severe form of COVID-19 is estimated to be 14.8%-53.0%. Elevated levels of total bilirubin, aspartate aminotransferase and alanine aminotransferase and low levels of serum albumin and prealbumin are the main laboratory findings. Patients with pre-existing chronic liver disease and cirrhosis are much more prone to develop severe liver injury. This literature review presented the recent scientific findings regarding the pathophysiological mechanisms responsible for liver injury in critically ill patients with COVID-19, the various interactions between drugs used to treat the disease and the function of the liver and the specific tests providing the possibility of early diagnosis of severe liver injury in these patients. Moreover, it highlighted the burden that COVID-19 put on health systems worldwide and its effect on transplant programs and the care provided to critically ill patients in general and particularly to those with chronic liver disease.

Key Words: Coronavirus disease 2019; Severe acute respiratory syndrome coronavirus 2; Liver disease; Intensive care unit; Liver unit; Prealbumin

Core Tip: The liver follows the respiratory system with a lower but considerable frequency of affection by severe acute respiratory syndrome coronavirus 2. Coronavirus disease 2019 causes acute and acute-on-chronic liver injury. The pathophysiological mechanisms are complex. Certain biomarkers such as fibrosis-4 score and non-invasive point-of-care methods such as ultrasonography or transient elastography can be extremely helpful in the early diagnosis of liver injury and the assessment of its progression. Health systems, intensive care units, liver units and transplant programs were seriously affected by the pandemic. The clinician should recognize the symptoms and signs of liver injury early and take the appropriate measures to reverse it.

Citation: Valsamaki A, Xanthoudaki M, Oikonomou KG, Vlachostergios PJ, Papadogoulas A, Katsiafylloudis P, Voulgaridi I, Skoura AL, Komnos A, Papamichalis P. Prevention, diagnostic evaluation, management and prognostic implications of liver disease in critically ill patients with COVID-19. *World J Clin Cases* 2023; 11(3): 514-527
URL: https://www.wjgnet.com/2307-8960/full/v11/i3/514.htm
DOI: https://dx.doi.org/10.12998/wjcc.v11.i3.514

INTRODUCTION

In December 2019, an epidemic of pneumonia of unknown origin broke out in Wuhan city, in the Hubei province of China, causing global concern because of its ease of transmission and the significant rates of morbidity and mortality that accompanied it. To diagnose and control this highly infectious disease, patients were immediately isolated, and their clinical and epidemiological data were studied thoroughly. The immediate mobilization of the global scientific community rapidly identified the cause (severe acute respiratory syndrome coronavirus 2 [SARS-CoV-2]) of coronavirus disease 2019 (COVID-19)[1]. In the immediate aftermath, the disease spread very rapidly to all the regions of the world, forcing the World Health Organization to declare the COVID-19 outbreak as a "global pandemic" on March 11, 2020.

Over the next years, the pandemic greatly affected the health systems of all the countries of the world causing until September 16, 2022 more than 611550000 cases and more than 6525000 deaths[2,3]. SARS-CoV-2 has been associated with three primary modes of transmission, known as "contact," "droplet" and "airborne" transmission[4].

Among the organs affected by COVID-19 is the liver, with several early scientific reports describing various degrees of liver dysfunction and injury[5]. The liver is responsible for the regulation of levels of many chemical substances and biomarkers in the human blood, carrying out crucial functions including but not limited to: the production and excretion of bile; the excretion of bilirubin, cholesterol, hormones and drugs; the metabolism of fats, proteins and carbohydrates; enzyme activation; the storage of glycogen, vitamins and minerals; synthesis of plasma proteins, such as albumin and clotting factors; the conversion of ammonia to urea; blood detoxification and purification; and the metabolism of hemoglobin for the use of its iron content. Chronic liver diseases are prevalent all over the world, imposing a significant burden on healthcare systems. According to Mohammed *et al*[6], patients with known chronic liver disease present a higher risk of complications from COVID-19 in comparison with the general population, with a mortality rate as high as 12%. Mortality from secondary liver injury in the intensive care unit (ICU) is significantly higher, ranging between 27%-48% for critically ill patients with cholestasis and between 40%-60% for critically ill patients with hypoxic liver injury[7].

This literature review presented the recent scientific findings regarding the pathophysiological mechanisms responsible for the induction of liver injury in critically ill patients with COVID-19, the various interactions between drugs used to treat the disease and the function of the liver, the tests providing the possibility of early diagnosis of severe liver injury in these patients, and the effect of the pandemic on health systems, transplant programs and critically ill patients with or without pre-existing chronic liver disease.

An advanced search strategy was made to identify studies published until August 2022 using the key words "COVID-19," "Liver" and "Intensive Care Unit" in the PubMed electronic bibliographic database. Initially, 560 studies were identified. These studies were reviewed based on their title and abstract, thus excluding 301 studies. The full texts of the remaining 259 studies were assessed for

eligibility based on their relevance to the subject of our review, particularly focusing on critical illness and liver disease. Most of these studies were excluded because they referred to patients with mild or moderate COVID-19. A total of 97 studies were finally included and analyzed for this systematic review. Overall, limited evidence exists regarding liver disease, critical illness and COVID-19.

EFFECT OF COVID-19 ON THE LIVER

SARS-CoV-2 just like its predecessors SARS-CoV (responsible for the SARS epidemic in 2003) and MERS-CoV (responsible for the Middle East respiratory syndrome epidemic in 2012) is a coronavirus and shares sequence homology and genome similarities with them[5]. The main symptoms caused by SARS-CoV-2, affecting men more severely than women, include fever, upper and lower respiratory symptomatology (cough, rhinorrhea, sore throat, flu-like symptoms and dyspnea), general muscle aches, anosmia, ageusia and increased likelihood of occurrence of vascular thrombosis.

Several reports regarding SARS-CoV and MERS-CoV reported that both of them caused liver injury in a significant number of patients. For example, Chau *et al*[8] reported 3 cases of hepatitis directly associated with SARS disease and revealed that various degrees of impairment of liver function had been reported in up to 60% of the patients suffering from SARS. Alsaad *et al*[9], after 14 years reported portal and lobular hepatitis at post-mortem histopathological findings in a 33-year-old male patient who died from MERS-CoV infection.

In May 2020, the results of a multicenter observational cohort study from 208 hospitals in the United Kingdom (20133 patients) were published. They investigated the outcome of patients with severe disease who were admitted to these hospitals[10]. Their median age was 73 years (range: 0–104 years), and 60% of them were men. The mortality rate in the cohort was 26%, whereas 41% of the patients were discharged alive, and the rest (34%) continued to be hospitalized at the end of the study. Liver disease was among the pathological conditions associated with increased in-hospital mortality, along with sex (male sex), age, obesity and chronic pulmonary, chronic kidney and chronic cardiac diseases.

Liver injury caused in patients severely affected by COVID-19 is estimated to be at levels of 14.8%-53.0%[11]. The imaging findings in these patients include hepatomegaly, gall bladder thickness and prominence of the common bile duct in the ultrasonography, along with pericholecystic fat stranding and hypodensity of the liver in the computed tomography (CT) images[12].

According to Nardo *et al*[13], the most likely pathophysiological mechanisms involved in causing liver injury after severe infection from SARS-CoV-2 are as follows:

(1) Moderate hepatic steatosis: There is growing evidence that SARS-CoV-2 modifies the function and the activity of the mitochondria, downregulating nuclear-encoded mitochondrial genes that are associated with cellular respiration[14]. Another cause of steatosis seems to be the induction of endoplasmic reticulum stress by SARS-CoV-2, which in turn has been shown to cause lipogenesis in the hepatic cells[15]. Finally, another proposed possible mechanism is directly associated with the characteristic "cytokine storm"/cytokine release syndrome (CRS) observed in the severe forms of COVID-19. Interleukin (IL)-6 produced by the cytokine storm most probably causes hyperactivation of the mammalian target of rapamycin, which can induce lipogenesis inside the hepatic cell[16]. In conclusion, the above-mentioned process of excessive lipogenesis seems to be detrimental to the function of the hepatic cell and the liver as a whole, and on the other hand it enhances the potential of the virus, providing it with the necessary nutrient material to achieve its replication and exocytosis[13,17].

(2) Cholestasis and bile duct alterations: Apart from IL-6, during the cytokine storm a large number of other inflammatory cytokines are released, including IL-1 and tumor necrosis factor-alpha. These cytokines cause hepatocellular cholestasis, closely resembling cholestasis observed in severe cases of sepsis[18]. An additional pathophysiological lesion that has been observed in these patients comes from the so-called "triple hit" to the bile ducts, consisting of hypoxia due to respiratory failure, systemic inflammatory response syndrome resulting in inflammation and fibrosis of the bile ducts and direct infection of the cholangiocytes from the virus[19].

(3) Hypoxic hepatitis (HH): Pathophysiologically, the causes of HH during the course of severe COVID-19 are multifactorial, including acute respiratory failure, severe sepsis, heart failure, including right-sided heart failure, acute respiratory distress syndrome (ARDS), a hyper-coagulate state, deteriorating the congestion of the liver and the hemodynamic effects of positive-pressure ventilation[20].

(4) The gut–liver axis: Symptomatology from the gastrointestinal tract is common in patients with severe COVID-19, with relevant rates ranging from 4.9% to 74.0%. The most common symptoms are nausea, vomiting, diarrhea, loss of appetite and abdominal pain[21]. It is speculated that the damage caused by SARS-CoV-2 to the epithelial barrier of the small intestine may lead to the transmission of the virus into the hepatocytes through the portal vein, aggravating the lesions of the liver parenchyma. In addition, alterations in gut microbiota caused either by drugs for COVID-19 or by the virus itself may play a significant role through the gut-liver axis.

(5) Injury induced by treating medications: As SARS-CoV-2 is novel to the scientific community and no specific therapy for COVID-19 has been found, numerous different drugs have been used in several cases outside their officially approved indications. Typical examples are the antimalarial drug hydroxy-

chloroquine, antibiotics (mainly from the family of macrolides), antiviral agents such as lopinavir, ritonavir and remdesivir, immunomodulating medications such as tocilizumab and dexamethasone and even anti-inflammatory and antipyretics in high doses[22]. Many of them presented already-known hepatotoxic side effects. For example, corticosteroids have been implicated as a cause of glycogenosis or steatosis[23], whereas tocilizumab is reported to cause drug-induced liver injury (DILI) in critically ill patients with COVID-19[24]. Specific reference should be made to paracetamol, the most commonly used analgesic and antipyretic medication in the elderly, prescribed in many cases in high doses and for a long time. According to Mian *et al*[25], old age and frailty decrease the clearance of paracetamol at percentages of 29.0%-45.7%, varying between 0.20-0.38 L/h/kg in older patients in comparison with values between 0.28-0.7 L/h/kg in younger patients. Another important influence of aging is on the volume of distribution of paracetamol, which decreases in older patients because of its incomplete distribution into body fat, with a consequent increase in the plasma concentration of paracetamol in the elderly.

In the United States of America, severe DILI presents the leading cause of acute liver failure (ALF), ahead of all the other causes even viral hepatitis. More than 1000 pharmaceutical agents have been identified as causes of serious liver disease, a figure that will increase significantly in the near future, as the pharmaceutical industry is constantly developing new drugs for use by the general population and patients. There are two main types of adverse reactions induced by drugs[26,27]: (1) Type A (intrinsic adverse reactions) are dose dependent and produce predictable toxicities; and (2) Type B (idiosyncratic adverse reactions) are difficult to be explained by their pharmacologic response or their dose and are associated with patient, drug or environmental risk factors, making them difficult to be predicted.

In order to predict the occurrence of a severe DILI early and take the appropriate preventive measures, various methods have been proposed. Hy's Law is one of the most commonly used, named after Dr. Hyman Zimmerman. It is based on the observation that patients with elevated serum total bilirubin who have received a medication causing hepatocellular (not hepatobiliary) injury, with the absence of other possible causes that could explain these disorders, are at high risk for fatal or requiring transplantation DILI, with mortality ranging between 10%-50%[28]. Another valuable tool is the LiverTox free online database, which allows clinicians to be informed about the latest data of the hepatotoxicity of various pharmaceutical agents, while at the same time they are assisted in the diagnosis and treatment of DILI[29].

Another important area of scientific research is the way by which liver dysfunction of any etiology has the potential to affect the accumulation and the toxicity of various drugs. According to Bosilkovska *et al*[30], the physiologic changes that accompany any hepatic impairment alter the disposition of most of the drugs. Portosystemic shunting decreases the initial metabolism, increasing the oral bioavailability of highly extracted drugs, whereas a coexisting disorder in the production of drug-binding proteins can change the distribution of the drug. In addition, both the amount and the function of enzymes that are produced by the liver and are responsible for the metabolism of drugs are affected by hepatic damage. The final result is the reduction of drug clearance, along with increased plasma drug concentration, which are both difficult to be predicted. Thus, the pharmacologic properties of most of the drugs are altered during severe liver disease.

In conclusion, the mechanism of liver injury during COVID-19 is twofold[31]. Either SARS-CoV-2 directly attacks the hepatic cells and the cholangiocytes, or it causes damage to the liver parenchyma by activating (and dysregulating) the patient's immune system, probably in a similar way to the severe lung injury caused by the cytokine storm process. In several cases, the damage is caused by a combination of the above two mechanisms. In other cases, the liver is affected by the medication used against COVID-19.

The histopathological features that have been described in critically ill patients with COVID-19 and concurrent hepatic involvement are various and, in most cases, nonspecific. Characteristic and specific for the disease is the detection of SARS-CoV-2 RNA in liver tissue in up to 55% of patients with severe liver injury[32]. Lagana *et al*[32] in a series of 40 critically ill patients who died from complications of COVID-19 reported that the most common hepatic histopathological findings were: (1) Macrovesicular steatosis (75% of the patients); (2) Lobular and portal necroinflammation (50% of the patients); and (3) Vascular pathology (primarily sinusoidal microthrombi) in a significantly smaller number of patients (15%). Finally, in another post-mortem report, the commonest findings in 22 critically ill patients who died from the disease were liver parenchymal congestion along with sinusoidal congestion and congestion of the small hepatic veins, extravasation of red cells into the Disse's space, necrosis of a large number of hepatic cells and macro- and micro- vacuolar steatosis[33]. Nevertheless, all the above-mentioned findings seemed to be because of the combination of the organism's systemic response to inflammation and its comorbidities, rather than the direct action of SARS-CoV-2 on the liver[34].

DIAGNOSTIC AND PROGNOSTIC TOOLS FOR LIVER INJURY IN PATIENTS WITH COVID-19

Studies on the evolution of liver injury from SARS-CoV-2 and on factors that can predict the outcome

are relatively few. Various outcome measures have been studied[35] including liver function tests (LFTs). A broad spectrum of abnormal LFTs has been described in patients with COVID-19. Aminotransferases (aspartate aminotransferase [AST] and alanine aminotransferase [ALT]), alkaline phosphatase, gamma-glutamyl transpeptidase (GGT) and bilirubin have been the most extensively studied markers of liver function in patients with COVID-19. Various studies have demonstrated a correlation between liver injury and disease severity, albeit most of these data are not strictly limited to critically ill patients[36-39]. In several studies including severe and non-severe patients with COVID-19 strong association was found between LFT (particularly AST) abnormalities and disease severity and mortality[40-44]. Lok *et al*[45], reporting similar results, suggested that immune system dysregulation may be a plausible contributing factor to the former association.

The role of microRNAs, which are considered to alter the immune response, is notable. To the best of our knowledge, only one study has found an association between liver-derived miR-122 and patient mortality in a cohort including patients with severe COVID-19[46]. Whereas the role of microRNAs in the inflammatory process is well documented, their specific role in COVID-19 is yet to be clarified.

Focusing on critically ill patients, a wide range of abnormal LFTs has been reported, whereas the vast majority of published data deliberate on aminotransferases. The prevalence of abnormal LFTs seems to be higher in ICU patients than in ward patients with COVID-19, according to a large meta-analysis including 31 studies from various countries[47]. In a study including 166 patients requiring mechanical ventilation, AST and ALT elevation served as predictive factors for the requirement of invasive mechanical ventilation[48]. Similar results were reported by Yip *et al*[49]. An independent association was found between aminotransferases elevation and ICU admission, mechanical ventilation and/or death. In addition, an association was found between aminotransferase elevation and lopinavir/ritonavir plus interferon beta and corticosteroid use, and the researchers suggested a cautious use of medications to minimize hepatotoxicity.

Nevertheless, Roman *et al*[50], in a study including exclusively critically ill patients with laboratory-proven liver damage, failed to demonstrate a correlation between liver injury severity and mortality. Azad Allarakia *et al*[51] examined plausible associations between routine laboratory tests and disease severity. No difference was found regarding LFTs between ICU and ward patients; however, confounding factors were not adjusted. Similarly, in a study conducted early during the pandemic era, no association was found between disease severity and LFTs[52].

Regarding mortality, in a large cohort including 3812 patients with COVID-19, an association between elevated ALT, AST, GGT levels and ICU admission was reported, and AST elevation was associated with the risk of death after adjusting for confounding factors such as age, obesity and previous liver disease[41]. Following the aforementioned study, in the study of Salik *et al*[53], which included exclusively critically ill patients, liver dysfunction and liver injury were associated with higher 7-d and 28-d mortality in comparison with patients with COVID-19 without liver biochemistry abnormalities. Interestingly, in the study of Kasapoglu *et al*[54], although ICU patients had higher values of AST and GGT, only GGT among LFTs was found to be predictive of mortality in ICU patients.

In addition to the aforementioned biomarkers, interest has been drawn to the role of albumin and prealbumin as prognostic markers of COVID-19 outcome. Hypoalbuminemia is common among critically ill patients with COVID-19. There are various mechanisms not directly related to hepatocellular damage that lead to hypoalbuminemia in these patients, including malnutrition, extravasation due to capillary leakage and a decreased rate of synthesis. Furthermore, measurements of serum albumin in hospitalized patients are often affected by exogenous albumin administration. Prealbumin is a precursor of albumin with a shorter half-life and can be used to assess protein status during a shorter time-frame. Low prealbumin levels were associated with disease severity and may be of prognostic value as they were identified as independent predictors of mortality in critically ill patients with COVID-19[55,56].

Various non-invasive fibrosis estimators include the fibrosis-4 (FIB-4) score, the FORNS index for liver fibrosis, the AST to platelet ratio index (APRI) score, the nonalcoholic fatty liver disease (NAFLD) fibrosis score (NFS) and the AST to ALT ratio.

Of the above-mentioned biomarkers and scores, the FIB-4 score attracted interest and applicability. It is a scoring system that uses four simple parameters, readily available in all in-patients: the age, the platelet count, and the values of AST and ALT. A score of < 1.45 has a negative predictive value of more than 90% for advanced fibrosis of the liver, whereas a score of > 3.25 has a positive predictive value of 65%, with 97% specificity[57].

Crisan *et al*[58] published the results of a retrospective cohort study (370 consecutive patients with COVID-19, from whom 289 presented with abnormal liver biomarkers at admission) to evaluate the predictive value of the various liver tests and estimators. They concluded that an elevated FIB-4 score (values > 3.25) and elevated AST were the only two tests that were independently associated with higher mortality in these patients. The FIB-4 score is a valuable tool that can help clinicians identify existing undiagnosed liver disease or the possibility of rapid deterioration of liver function during COVID-19, so that patients with abnormal values receive priority in their inpatient management[58].

Findings in association with the value of the FIB-4 score were also verified in the systematic review and meta-analysis of Liu *et al*[59], who concluded that along with the FIB-4 score, the APRI score, the NFS and the FORNS index could also serve as indicators for identifying patients at high risk of

developing severe COVID-19 with worse outcomes. More specifically, one unit elevation of the APRI score increases the risk of death by 178%, higher NFS (≥ -1.5) increases the risk of developing severe COVID-19 by ten-fold, and an increase of the FORNS index by one point increases the risk of death by 41%.

CRITICALLY ILL PATIENTS WITH ACUTE LIVER DISEASE AND COVID-19

Acute liver injury (ALI) has been reported in approximately 19% of patients with COVID-19; however, the percentage increases dramatically, up to 89.2%, in ICU patients[60,61]. The spectrum of ALI in critically ill patients with COVID-19 is wide, varying from simple elevations of LFTs to ALF, the need for advanced support and even the need for transplantation[62-64]. For patients with severe liver injury (approximately 6.4% of all patients with distorted liver biochemistry), a severe disease course is expected[65]. The correlation of impaired liver function with sudden death in patients with COVID-19 is another outstanding association[66]. Most studies reported a predominance of the hepatocellular pattern[67]. However, other distributions of liver injury pattern have been reported as well[62].

HH as a clinical presentation of COVID-19 is observed in approximately 5.9% of ICU patients with COVID-19 and has a significant effect on patient survival[68]. The diagnosis is made when the following criteria are met: (1) A massive but transiently elevated ALT level (more than 20-fold the upper limit of normal); (2) The presence of respiratory, cardiac or circulatory failure; and (3) Exclusion of other causes of liver injury[69]. The close monitoring of cardiac and respiratory function and early etiologic management of hemodynamic instability/shock is crucial for patient survival when HH is suspected [68].

Secondary sclerosing cholangitis is another devastating form of liver disease in COVID-19, which is associated with considerable morbidity and mortality. Contributing pathophysiological mechanisms include bile duct ischemia and toxic bile formation[70]. The underlying histopathological findings consist of ischemic damage to the perihilar bile ducts[71]. Ursodeoxycholic acid (UDCA) has been reported to give promising results; however, for a proportion of these patients, transplantation is required[72]. Rare but devastating clinical presentations include liver abscess with necrosis[73] and vascular thrombotic events in abdominal vessels such as portal and mesenteric vein thrombosis[74].

ALF is a life-threatening condition characterized by hepatic encephalopathy and coagulopathy in patients without pre-existing liver disease[75]. During the pandemic, an increased incidence of hepatitis of unknown etiology in the pediatric population has been reported with subsequent liver failure and the need for liver transplantation (LT) for a proportion of these children. This raised great concern about the possible vulnerability of children to this extremely severe complication. Although adenovirus is the main etiological agent suspected to be responsible, the association with COVID-19 and the role of other contributing factors remain to be clarified[76]. In adults, there are reports on other viruses as causative factors of ALF, such as the infection from or the reactivation of herpes simplex virus-1 following the immunosuppression that patients with COVID-19 receive for treating the CRS[77].

When assessing critically ill patients with COVID-19 and ALI, the diagnostic approach basically remains the same as for any patient who has ALI and is severely ill. However, some differences exist that must be pointed out.

Current guidelines recommend against unnecessary imaging [*e.g.*, ultrasound (unless performed at the bedside), CT-magnetic resonance (MR) imaging/MR cholangiopancreatography][78]. The transport of these patients requires special knowledge, equipment and experience and should be kept for patients where the examination results may change the patient's management.

Approaches that do not require patient transportation are preferred. An approach regarding the hemodynamic monitoring of these patients uses invasive cardiac monitors based on the thermodilution method. These methods are invasive, expensive and present septic and other catheter-related complications. Moreover, they have limitations in critically ill patients with liver failure such as the presence of ascites (extravascular third space fluid) or hepatic hydrothorax (extravascular lung water), which confuse the measurements and the lack of validation of these techniques on such patients. Remote point-of-care ultrasonography (POCUS) by a hepatologist or an ICU physician, with real-time interpretation by a cardiologist through telemedicine, is a trend that has been adopted in the COVID-19 era[79]. Information on the hemodynamic status and the cause of the hemodynamic compromise of these patients is safely and accurately collected. Basic diagnoses such as pulmonary embolism or myocardial infarction are made at the bedside. The evaluation of intravascular volume status helps to differentiate between prerenal acute kidney injury and hepatorenal syndrome or between transfusion-related acute lung injury and transfusion-associated circulatory overload. In addition, this powerful and non-invasive tool contributes to the prompt identification of liver-related pathologies, including portal vein or hepatic vein thrombosis, the presence of ascites, suspected pneumothorax and hemothorax. This approach has provided several solutions for liver units and ICUs during the pandemic.

Another non-invasive method that has been evaluated for the assessment of liver injury during COVID-19 is the vibration-controlled transient elastography/FibroScan. It may serve as a tool for identifying patients with elevated liver stiffness and thus at greater risk of developing ALI and

progressing to severe COVID-19 with worse clinical outcomes, even when no history of pre-existing liver disease is present[80,81].

No special recommendations or measures exist which could prevent liver injury from COVID-19. The prophylaxis of the liver can only be achieved through measures that prevent infection from SARS-CoV-2. Thus, current guidelines suggest using personal protective equipment for healthcare personnel in the liver and other departments, cancelling all elective/nonurgent procedures and vaccinating with the approved vaccines the vulnerable population with or without pre-existing liver disease[78,82]. Another approach is the use of dietary supplements as prophylaxis for severe disease and liver involvement. Among the supplements used for the prevention of COVID-19, several pieces of evidence exist on the possible protective role of vitamins C and D in humans, whereas in animal models, xanthohumol has an anti-inflammatory action on liver injury[83].

Accordingly, no separate protocols exist for the treatment of liver injury from COVID-19. The implementation of the general therapeutic protocols for the disease is applicable[84], with special care for liver protection and early detection of liver injury in patients with COVID-19[85]. In cases of patients with progressive ALF, when the applied standard supportive care (hemodynamic, nutritional, respiratory support, avoidance of all unnecessary hepatotoxic factors) does not lead to the resolution of ALF, LT can be the final solution[75]. Removing hepatotoxic metabolites such as conjugated or unconjugated bilirubin, bile acids, phenols, fatty acids, cytokines, ammonia or amino acids with the use of extracorporeal blood purification techniques presents an interesting alternative approach, particularly when LT is not a feasible option or even as a bridging therapy toward transplantation[86,87]. These techniques eliminate not only hepatic metabolites but also inflammatory mediators responsible for the CRS, leading to the preservation of organ function and prevention of organ failure, while advanced support is offered in patients with COVID-19[86].

CRITICALLY ILL PATIENTS WITH CHRONIC LIVER DISEASE AND COVID-19

Acute-on-chronic liver failure has been reported in patients with pre-existing liver disease[40]. Particularly in patients with cirrhosis, the associated state of immunosuppression in conjunction with COVID-19 can lead to acute decompensation, most frequently manifested as worsening ascites with spontaneous bacterial peritonitis and to hepatic failure in patients with impaired and limited reserves [40,88]. Liver injury has been observed in 26.7% of patients with severe pneumonia[88]. Despite the lack of coagulation factors in decompensated liver disease, a hypercoagulable state may be present in COVID-19, and hepatic impairment may be associated with greater activation of the coagulation pathways[75,89].

In critically ill patients with COVID-19, pre-existing liver disease and evidence of liver impairment, LFTs must be frequently monitored[85]. Typically, no specific treatment is indicated, and emphasis should be placed on cause-directed therapy.

UDCA may be added as a treatment in patients with liver injury because of its anti-inflammatory and immunomodulatory properties[88]. In the ICU setting, treatment with vasopressors should be administered with caution in patients with cirrhosis and COVID-19, to avoid detrimental effects on cardiac output. Moreover, caution should be taken while administering immunosuppressive agents, such as tocilizumab and baricitinib, as they may cause the reactivation of chronic hepatitis B. In such cases, antiviral prophylaxis is indicated[88].

In terms of prognosis, it has been hypothesized that patients with chronic liver disease may be particularly vulnerable to developing severe COVID-19[90]. Higher mortality rates have been observed in patients with COVID-19, pre-existing chronic liver disease and cirrhosis caused by chronic hepatitis B and C[40]. Moreover, patients with NAFLD present a higher risk for progression to severe COVID-19 [91]. Patients with cirrhosis having ARDS have a worse prognosis than patients without cirrhosis, and pre-existing liver fibrosis is independently associated with a significantly higher risk of death in patients with severe COVID-19 admitted to the ICU[92].

An approach to liver disease in critically ill patients with COVID-19 is proposed by the authors (Figure 1).

EFFECT OF THE PANDEMIC ON HEALTH SYSTEMS, ICUS, LIVER UNITS AND TRANSPLANT PROGRAMS

During the pandemic, health systems and ICUs were overburdened by critically ill patients. Higher mortality risk was observed and was associated with ICU patient load[4,93,94]. In line with this, patients with chronic liver disease had significantly high mortality during the pandemic, leading to suggestions regarding their primary and emergency care and their access to intensive care and high-dependency units[95]. In addition, the effect of the pandemic was significant on the treatment of complications of chronic liver disease such as hepatocellular carcinoma (HCC); surveillance for HCC and treatment of

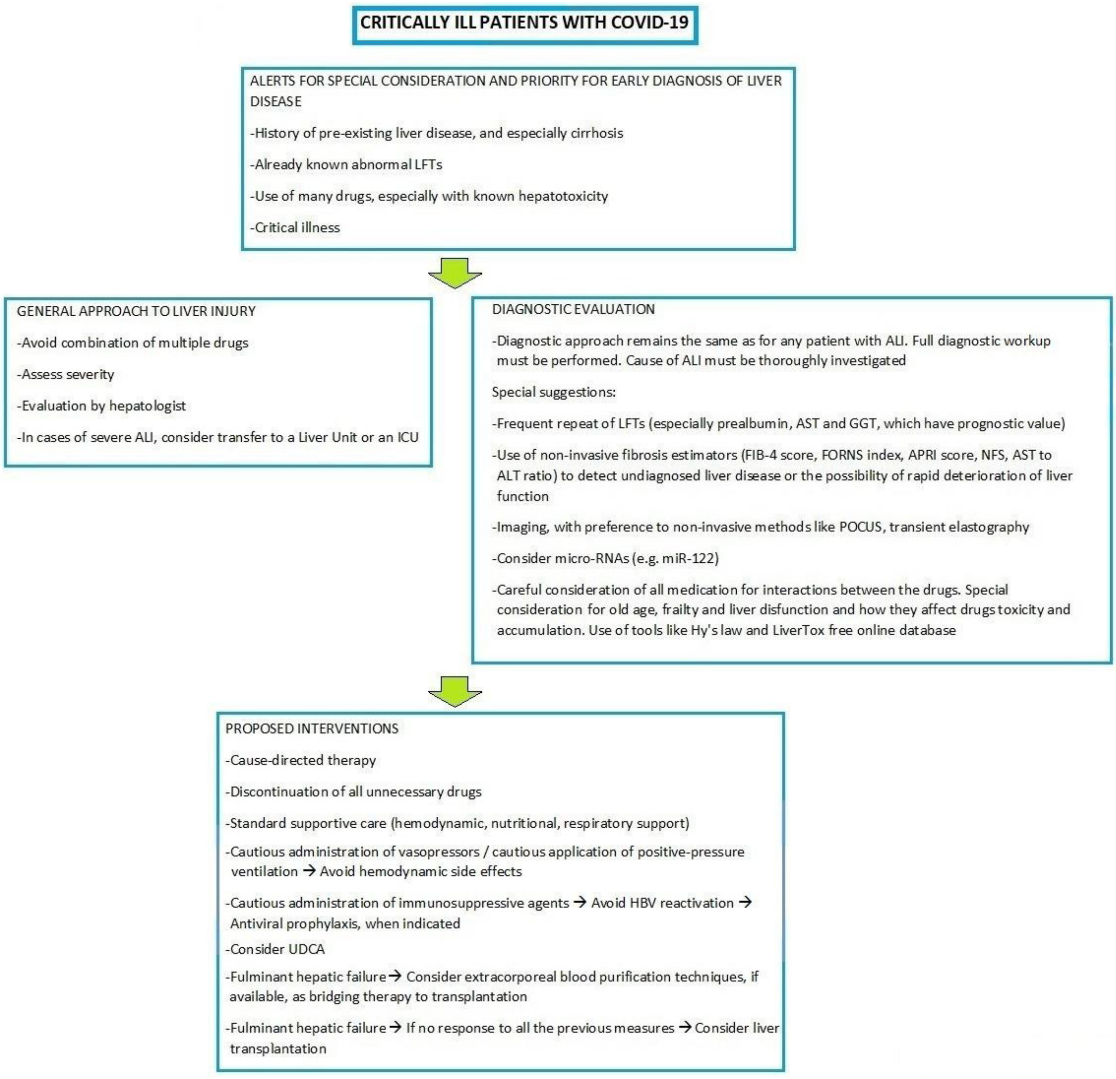

DOI: 10.12998/wjcc.v11.i3.514

Figure 1 Proposed approach to liver disease in critically ill patients with coronavirus disease 2019. Apart from general rules regarding all patients, special measures can help clinicians identify and confront liver disease in severely ill patients with coronavirus disease 2019. ALI: Acute liver injury; ALT: Alanine aminotransferase; APRI: Aspartate aminotransferase to platelet ratio index; AST: Aspartate aminotransferase; COVID-19: Coronavirus disease 2019; FIB-4: Fibrosis-4; GGT: Gamma-glutamyl transpeptidase; HBV: Hepatitis B virus; ICU: Intensive care unit; LFTs: Liver function tests; NFS: Nonalcoholic fatty liver disease fibrosis score; POCUS: Point-of-care ultrasonography; UDCA: Ursodeoxycholic acid.

early-stage HCC were modified. Another significant change was the extensive use of telemedicine to minimize patients' and healthcare workers' exposure to COVID-19[96].

Transplant programs and care provided to LT recipients were also greatly affected. Living donor LT was suspended in some centers worldwide[96]. As a response to these issues, national protocols were specially prepared[97], and transplantation centers implemented special strategies to increase their successful transplantation rates[98]. Recommendations point out the need for the restoration of LT programs; however, prioritization of patients with poor short-term prognosis (with acute/acute-on-chronic liver failure, high Model for End-stage Liver Disease score and HCC at the upper limits of the Milan criteria) may be necessary in some cases[67].

In general, transplant recipients present higher rates of severe disease and higher mortality rates than nontransplant patients; thus, their exposure to COVID-19 should remain minimal[78]. Immunosuppression should be reduced only under special circumstances, *e.g.*, symptomatic COVID-19, and with caution[78,99]. COVID-19 screening should be performed for both donors and recipients. Charts regarding LT organ offers are available to optimize the management of the procedures associated with LT in the COVID-19 era[78].

CONCLUSION

Apart from the upper and lower respiratory system, the liver is also greatly affected by COVID-19. The pathophysiological mechanisms include cholestasis, bile duct alterations, hepatic steatosis, involvement of the gut-liver axis, HH and hepatitis induced by the drugs that are used to treat the actual disease. The hepatocyte seems to be affected both directly, by SARS-CoV-2 itself, and by the disruption and dysregulation of the immune system. Not only patients with or without pre-existing liver disease individually but also health systems and transplant programs were greatly affected by the pandemic, and great effort has been made, which needs to be continued to minimize the consequences. Scientific research over the past 2 years has shown that certain biomarkers can be extremely useful in the early diagnosis of liver injury and the evaluation of its progression. Non-invasive assessment with transient elastography or POCUS is the trend for evaluating particularly patients in the ICU setting where biopsy is difficult to perform because of coagulation abnormalities and transport for CT or MR imaging is difficult and potentially dangerous. Although in most cases, liver involvement in COVID-19 is mild, the clinician should be able to recognize the symptoms and signs of liver dysfunction early and not focus exclusively on symptomatology from the respiratory system.

ACKNOWLEDGEMENTS

This paper is dedicated to the memory of the exceptional doctor Tilemachos Zafeiridis (1974-2021), 1 year after his premature death, to remind us how much we miss him.

FOOTNOTES

Author contributions: Papamichalis P and Oikonomou KG designed the review; Papadogoulas A, Katsiafylloudis P, Voulgaridi I and Skoura AL gathered the data; Papamichalis P, Oikonomou KG, Valsamaki A and Xanthoudaki M analyzed, interpreted the data and wrote the final version of the manuscript; Oikonomou KG and Vlachostergios PJ performed English editing; Komnos A critically reviewed the paper; All authors have read and approved the final manuscript.

Conflict-of-interest statement: The authors declare having no conflicts of interest.

Country/Territory of origin: Greece

ORCID number: Asimina Valsamaki 0000-0001-8814-0371; Maria Xanthoudaki 0000-0002-8734-6463; Katerina G Oikonomou 0000-0002-2142-1387; Panagiotis J Vlachostergios 0000-0002-1704-1517; Antonios Papadogoulas 0000-0002-8781-6269; Periklis Katsiafylloudis 0000-0003-1042-8193; Ioanna Voulgaridi 0000-0002-7352-0934; Apostolia-Lemonia Skoura 0000-0003-2480-0072; Apostolos Komnos 0000-0002-7225-3213; Panagiotis Papamichalis 0000-0001-7296-419X.

S-Editor: Chang KL
L-Editor: Filipodia
P-Editor: Chang KL

REFERENCES

1 **Ciotti M**, Ciccozzi M, Terrinoni A, Jiang WC, Wang CB, Bernardini S. The COVID-19 pandemic. *Crit Rev Clin Lab Sci* 2020; **57**: 365-388 [PMID: 32645276 DOI: 10.1080/10408363.2020.1783198]
2 **Cucinotta D**, Vanelli M. WHO Declares COVID-19 a Pandemic. *Acta Biomed* 2020; **91**: 157-160 [PMID: 32191675 DOI: 10.23750/abm.v91i1.9397]
3 COVID-19 Map [cited Sep 17, 2022]. Johns Hopkins Coronavirus Resource Center. [Internet]. Available from: https://gisanddata.maps.arcgis.com/apps/dashboards/bda7594740fd40299423467b48e9ecf6
4 **Tusabe F**, Tahir IM, Akpa CI, Mtaki V, Baryamujura J, Kamau B, Lidoroh S, Kobugabe PL, Maaga NO, Bongomin F. Lessons Learned from the Ebola Virus Disease and COVID-19 Preparedness to Respond to the Human Monkeypox Virus Outbreak in Low- and Middle-Income Countries. *Infect Drug Resist* 2022; **15**: 6279-6286 [PMID: 36329989 DOI: 10.2147/IDR.S384348]
5 **Cheng ZJ**, Shan J. 2019 Novel coronavirus: where we are and what we know. *Infection* 2020; **48**: 155-163 [PMID:

32072569 DOI: 10.1007/s15010-020-01401-y]
6 **Mohammed A**, Paranji N, Chen PH, Niu B. COVID-19 in Chronic Liver Disease and Liver Transplantation: A Clinical Review. *J Clin Gastroenterol* 2021; **55**: 187-194 [PMID: 33394628 DOI: 10.1097/MCG.0000000000001481]
7 **Perez Ruiz de Garibay A**, Kortgen A, Leonhardt J, Zipprich A, Bauer M. Critical care hepatology: definitions, incidence, prognosis and role of liver failure in critically ill patients. *Crit Care* 2022; **26**: 289 [PMID: 36163253 DOI: 10.1186/s13054-022-04163-1]
8 **Chau TN**, Lee KC, Yao H, Tsang TY, Chow TC, Yeung YC, Choi KW, Tso YK, Lau T, Lai ST, Lai CL. SARS-associated viral hepatitis caused by a novel coronavirus: report of three cases. *Hepatology* 2004; **39**: 302-310 [PMID: 14767982 DOI: 10.1002/hep.20111]
9 **Alsaad KO**, Hajeer AH, Al Balwi M, Al Moaiqel M, Al Oudah N, Al Ajlan A, AlJohani S, Alsolamy S, Gmati GE, Balkhy H, Al-Jahdali HH, Baharoon SA, Arabi YM. Histopathology of Middle East respiratory syndrome coronovirus (MERS-CoV) infection - clinicopathological and ultrastructural study. *Histopathology* 2018; **72**: 516-524 [PMID: 28858401 DOI: 10.1111/his.13379]
10 **Docherty AB**, Harrison EM, Green CA, Hardwick HE, Pius R, Norman L, Holden KA, Read JM, Dondelinger F, Carson G, Merson L, Lee J, Plotkin D, Sigfrid L, Halpin S, Jackson C, Gamble C, Horby PW, Nguyen-Van-Tam JS, Ho A, Russell CD, Dunning J, Openshaw PJ, Baillie JK, Semple MG; ISARIC4C investigators. Features of 20 133 UK patients in hospital with covid-19 using the ISARIC WHO Clinical Characterisation Protocol: prospective observational cohort study. *BMJ* 2020; **369**: m1985 [PMID: 32444460 DOI: 10.1136/bmj.m1985]
11 **Velarde-Ruiz Velasco JA**, García-Jiménez ES, Remes-Troche JM. Hepatic manifestations and impact of COVID-19 on the cirrhotic patient. *Rev Gastroenterol Mex (Engl Ed)* 2020; **85**: 303-311 [PMID: 32553772 DOI: 10.1016/j.rgmx.2020.05.002]
12 **Lei P**, Zhang L, Han P, Zheng C, Tong Q, Shang H, Yang F, Hu Y, Li X, Song Y. Liver injury in patients with COVID-19: clinical profiles, CT findings, the correlation of the severity with liver injury. *Hepatol Int* 2020; **14**: 733-742 [PMID: 32886333 DOI: 10.1007/s12072-020-10087-1]
13 **Nardo AD**, Schneeweiss-Gleixner M, Bakail M, Dixon ED, Lax SF, Trauner M. Pathophysiological mechanisms of liver injury in COVID-19. *Liver Int* 2021; **41**: 20-32 [PMID: 33190346 DOI: 10.1111/liv.14730]
14 **Miller B**, Silverstein A, Flores M, Xiang W, Cao K, Kumagai H, Mehta HH, Yen K, Kim SJ, Cohen P. SARS-CoV-2 induces a unique mitochondrial transcriptome signature. 2020 Preprint. Available from: Research Square [DOI: 10.21203/rs.3.rs-36568/v1]
15 **Malhi H**, Kaufman RJ. Endoplasmic reticulum stress in liver disease. *J Hepatol* 2011; **54**: 795-809 [PMID: 21145844 DOI: 10.1016/j.jhep.2010.11.005]
16 **Peterson TR**, Sengupta SS, Harris TE, Carmack AE, Kang SA, Balderas E, Guertin DA, Madden KL, Carpenter AE, Finck BN, Sabatini DM. mTOR complex 1 regulates lipin 1 localization to control the SREBP pathway. *Cell* 2011; **146**: 408-420 [PMID: 21816276 DOI: 10.1016/j.cell.2011.06.034]
17 **Campos-Varela I**, Villagrasa A, Simon-Talero M, Riveiro-Barciela M, Ventura-Cots M, Aguilera-Castro L, Alvarez-Lopez P, Nordahl EA, Anton A, Bañares J, Barber C, Barreira-Diaz A, Biagetti B, Camps-Relats L, Ciudin A, Cocera R, Dopazo C, Fernandez A, Jimenez C, Jimenez MM, Jofra M, Gil C, Gomez-Gavara C, Guanozzi D, Guevara JA, Lobo B, Malagelada C, Martinez-Camprecios J, Mayorga L, Miret E, Pando E, Pérez-Lopez A, Pigrau M, Prio A, Rivera-Esteban JM, Romero A, Tasayco S, Vidal-Gonzalez J, Vidal L, Minguez B, Augustin S, Genesca J. The role of liver steatosis as measured with transient elastography and transaminases on hard clinical outcomes in patients with COVID-19. *Therap Adv Gastroenterol* 2021; **14**: 17562848211016567 [PMID: 34104210 DOI: 10.1177/17562848211016567]
18 **Cheung A**, Flamm S. Hepatobiliary Complications in Critically Ill Patients. *Clin Liver Dis* 2019; **23**: 221-232 [PMID: 30947873 DOI: 10.1016/j.cld.2018.12.005]
19 **Méndez-Sánchez N**, Valencia-Rodríguez A, Qi X, Yoshida EM, Romero-Gómez M, George J, Eslam M, Abenavoli L, Xie W, Teschke R, Carrion AF, Keaveny AP. What Has the COVID-19 Pandemic Taught Us so Far? *J Clin Transl Hepatol* 2020; **8**: 0024 [PMID: 32309152 DOI: 10.14218/JCTH.2020.00024]
20 **Kariyawasam JC**, Jayarajah U, Abeysuriya V, Riza R, Seneviratne SL. Involvement of the Liver in COVID-19: A Systematic Review. *Am J Trop Med Hyg* 2022; **106**: 1026-1041 [PMID: 35203056 DOI: 10.4269/ajtmh.21-1240]
21 **Oikonomou KG**, Papamichalis P, Zafeiridis T, Xanthoudaki M, Papapostolou E, Valsamaki A, Bouliaris K, Papamichalis M, Karvouniaris M, Vlachostergios PJ, Skoura AL, Komnos A. Gastroenterology and liver disease during COVID-19 and in anticipation of post-COVID-19 era: Current practice and future directions. *World J Clin Cases* 2021; **9**: 4918-4938 [PMID: 34307544 DOI: 10.12998/wjcc.v9.i19.4918]
22 **Provenzani A**, Polidori P. Covid-19 and drug therapy, what we learned. *Int J Clin Pharm* 2020; **42**: 833-836 [PMID: 32382873 DOI: 10.1007/s11096-020-01049-6]
23 **Garcia-Cortes M**, Robles-Diaz M, Stephens C, Ortega-Alonso A, Lucena MI, Andrade RJ. Drug induced liver injury: an update. *Arch Toxicol* 2020; **94**: 3381-3407 [PMID: 32852569 DOI: 10.1007/s00204-020-02885-1]
24 **Muhović D**, Bojović J, Bulatović A, Vukčević B, Ratković M, Lazović R, Smolović B. First case of drug-induced liver injury associated with the use of tocilizumab in a patient with COVID-19. *Liver Int* 2020; **40**: 1901-1905 [PMID: 32478465 DOI: 10.1111/liv.14516]
25 **Mian P**, Allegaert K, Spriet I, Tibboel D, Petrovic M. Paracetamol in Older People: Towards Evidence-Based Dosing? *Drugs Aging* 2018; **35**: 603-624 [PMID: 29916138 DOI: 10.1007/s40266-018-0559-x]
26 **Iasella CJ**, Johnson HJ, Dunn MA. Adverse Drug Reactions: Type A (Intrinsic) or Type B (Idiosyncratic). *Clin Liver Dis* 2017; **21**: 73-87 [PMID: 27842776 DOI: 10.1016/j.cld.2016.08.005]
27 **Egan LJ**. Mechanisms of drug toxicity or intolerance. *Dig Dis* 2011; **29**: 172-176 [PMID: 21734381 DOI: 10.1159/000323881]
28 **Robles-Diaz M**, Lucena MI, Kaplowitz N, Stephens C, Medina-Cáliz I, González-Jimenez A, Ulzurrun E, Gonzalez AF, Fernandez MC, Romero-Gómez M, Jimenez-Perez M, Bruguera M, Prieto M, Bessone F, Hernandez N, Arrese M, Andrade RJ; Spanish DILI Registry; SLatinDILI Network; Safer and Faster Evidence-based Translation Consortium. Use of Hy's law and a new composite algorithm to predict acute liver failure in patients with drug-induced liver injury.

Gastroenterology 2014; **147**: 109-118.e5 [PMID: 24704526 DOI: 10.1053/j.gastro.2014.03.050]
29 National Institute of Diabetes and Digestive and Kidney Diseases. LiverTox: Clinical and Research Information on Drug-Induced Liver Injury. (2012). [cited Sep 17, 2022]. Available from: http://www.ncbi.nlm.nih.gov/books/NBK547852/
30 **Bosilkovska M**, Walder B, Besson M, Daali Y, Desmeules J. Analgesics in patients with hepatic impairment: pharmacology and clinical implications. *Drugs* 2012; **72**: 1645-1669 [PMID: 22867045 DOI: 10.2165/11635500-000000000-00000]
31 **Su YJ**, Chang CW, Chen MJ, Lai YC. Impact of COVID-19 on liver. *World J Clin Cases* 2021; **9**: 7998-8007 [PMID: 34621856 DOI: 10.12998/wjcc.v9.i27.7998]
32 **Lagana SM**, Kudose S, Iuga AC, Lee MJ, Fazlollahi L, Remotti HE, Del Portillo A, De Michele S, de Gonzalez AK, Saqi A, Khairallah P, Chong AM, Park H, Uhlemann AC, Lefkowitch JH, Verna EC. Hepatic pathology in patients dying of COVID-19: a series of 40 cases including clinical, histologic, and virologic data. *Mod Pathol* 2020; **33**: 2147-2155 [PMID: 32792598 DOI: 10.1038/s41379-020-00649-x]
33 **Falasca L**, Nardacci R, Colombo D, Lalle E, Di Caro A, Nicastri E, Antinori A, Petrosillo N, Marchioni L, Biava G, D'Offizi G, Palmieri F, Goletti D, Zumla A, Ippolito G, Piacentini M, Del Nonno F. Postmortem Findings in Italian Patients With COVID-19: A Descriptive Full Autopsy Study of Cases With and Without Comorbidities. *J Infect Dis* 2020; **222**: 1807-1815 [PMID: 32914853 DOI: 10.1093/infdis/jiaa578]
34 **Tarik Aslan A**, Yasemin Balaban H. An overview of SARS-COV-2-related hepatic injury. *Hepatol Forum* 2021; **2**: 122-127 [PMID: 35784909 DOI: 10.14744/hf.2021.2021.0020]
35 **Jothimani D**, Venugopal R, Abedin MF, Kaliamoorthy I, Rela M. COVID-19 and the liver. *J Hepatol* 2020; **73**: 1231-1240 [PMID: 32553666 DOI: 10.1016/j.jhep.2020.06.006]
36 **Henry BM**, de Oliveira MHS, Benoit S, Plebani M, Lippi G. Hematologic, biochemical and immune biomarker abnormalities associated with severe illness and mortality in coronavirus disease 2019 (COVID-19): a meta-analysis. *Clin Chem Lab Med* 2020; **58**: 1021-1028 [PMID: 32286245 DOI: 10.1515/cclm-2020-0369]
37 **Lei F**, Liu YM, Zhou F, Qin JJ, Zhang P, Zhu L, Zhang XJ, Cai J, Lin L, Ouyang S, Wang X, Yang C, Cheng X, Liu W, Li H, Xie J, Wu B, Luo H, Xiao F, Chen J, Tao L, Cheng G, She ZG, Zhou J, Wang H, Lin J, Luo P, Fu S, Ye P, Xiao B, Mao W, Liu L, Yan Y, Chen G, Huang X, Zhang BH, Yuan Y. Longitudinal Association Between Markers of Liver Injury and Mortality in COVID-19 in China. *Hepatology* 2020; **72**: 389-398 [PMID: 32359177 DOI: 10.1002/hep.31301]
38 **Sharma A**, Jaiswal P, Kerakhan Y, Saravanan L, Murtaza Z, Zergham A, Honganur NS, Akbar A, Deol A, Francis B, Patel S, Mehta D, Jaiswal R, Singh J, Patel U, Malik P. Liver disease and outcomes among COVID-19 hospitalized patients - A systematic review and meta-analysis. *Ann Hepatol* 2021; **21**: 100273 [PMID: 33075578 DOI: 10.1016/j.aohep.2020.10.001]
39 **Mendizabal M**, Piñero F, Ridruejo E, Anders M, Silveyra MD, Torre A, Montes P, Urzúa A, Pages J, Toro LG, Díaz J, Gonzalez Ballerga E, Miranda-Zazueta G, Peralta M, Gutiérrez I, Michelato D, Venturelli MG, Varón A, Vera-Pozo E, Tagle M, García M, Tassara A, Brutti J, Ruiz García S, Bustios C, Escajadillo N, Macias Y, Higuera-de la Tijera F, Gómez AJ, Dominguez A, Castillo-Barradas M, Contreras F, Scarpin A, Schinoni MI, Toledo C, Girala M, Mainardi V, Sanchez A, Bessone F, Rubinstein F, Silva MO. Prospective Latin American cohort evaluating outcomes of patients with COVID-19 and abnormal liver tests on admission. *Ann Hepatol* 2021; **21**: 100298 [PMID: 33359234 DOI: 10.1016/j.aohep.2020.100298]
40 **Garrido M**, Pereira Guedes T, Alves Silva J, Falcão D, Novo I, Archer S, Rocha M, Maia L, Sarmento-Castro R, Pedroto I. Impact of Liver Test Abnormalities and Chronic Liver Disease on the Clinical Outcomes of Patients Hospitalized with COVID-19. *GE Port J Gastroenterol* 2021; **158**: 1-12 [PMID: 34192127 DOI: 10.1159/000513593]
41 **Paštrovic F**, Lucijanic M, Atic A, Stojic J, Barisic Jaman M, Tjesic Drinkovic I, Zelenika M, Milosevic M, Medic B, Loncar J, Mijic M, Filipec Kanizaj T, Kralj D, Lerotic I, Virovic Jukic L, Ljubicic N, Luetic K, Grgic D, Majerovic M, Ostojic R, Krznaric Z, Luksic I, Piskac Zivkovic N, Keres T, Grabovac V, Persec J, Barsic B, Grgurevic I. Prevalence and Prognostic Impact of Deranged Liver Blood Tests in COVID-19: Experience from the Regional COVID-19 Center over the Cohort of 3812 Hospitalized Patients. *J Clin Med* 2021; **10** [PMID: 34575333 DOI: 10.3390/jcm10184222]
42 **Ampuero J**, Sánchez Y, García-Lozano MR, Maya-Miles D, Romero Gómez M. Impact of liver injury on the severity of COVID-19: a systematic review with meta-analysis. *Rev Esp Enferm Dig* 2021; **113**: 125-135 [PMID: 33267597 DOI: 10.17235/reed.2020.7397/2020]
43 **Balderramo D**, Mattos AZ, Mulqui V, Chiesa T, Plácido-Damián Z, Abarca J, Bolomo A, Carlino Y, Bombassaro IZ, Wiltgen D, Castillo LT, Díaz K, Acuña J, Manero E, Prieto J, Carrera E, Díaz-Ferrer J, Debes JD. Abnormal Liver Tests during Hospitalization Predict Mortality in Patients with COVID-19: A Multicenter Study from South America. *Can J Gastroenterol Hepatol* 2021; **2021**: 1622533 [PMID: 34621710 DOI: 10.1155/2021/1622533]
44 **Chaibi S**, Boussier J, Hajj WE, Abitbol Y, Taieb S, Horaist C, Jouannaud V, Wang P, Piquet J, Maurer C, Lahmek P, Nahon S. Liver function test abnormalities are associated with a poorer prognosis in Covid-19 patients: Results of a French cohort. *Clin Res Hepatol Gastroenterol* 2021; **45**: 101556 [PMID: 33139241 DOI: 10.1016/j.clinre.2020.10.002]
45 **Lok J**, Gess M. Liver dysfunction in COVID-19: a useful prognostic marker of severe disease? *Frontline Gastroenterol* 2021; **12**: 293-298 [PMID: 34249314 DOI: 10.1136/flgastro-2020-101689]
46 **Gutmann C**, Khamina K, Theofilatos K, Diendorfer AB, Burnap SA, Nabeebaccus A, Fish M, McPhail MJW, O'Gallagher K, Schmidt LE, Cassel C, Auzinger G, Napoli S, Mujib SF, Trovato F, Sanderson B, Merrick B, Roy R, Edgeworth JD, Shah AM, Hayday AC, Traby L, Hackl M, Eichinger S, Shankar-Hari M, Mayr M. Association of cardiometabolic microRNAs with COVID-19 severity and mortality. *Cardiovasc Res* 2022; **118**: 461-474 [PMID: 34755842 DOI: 10.1093/cvr/cvab338]
47 **Dong ZY**, Xiang BJ, Jiang M, Sun MJ, Dai C. The Prevalence of Gastrointestinal Symptoms, Abnormal Liver Function, Digestive System Disease and Liver Disease in COVID-19 Infection: A Systematic Review and Meta-Analysis. *J Clin Gastroenterol* 2021; **55**: 67-76 [PMID: 33116063 DOI: 10.1097/MCG.0000000000001424]
48 **Higuera-de la Tijera F**, Servín-Caamaño A, Reyes-Herrera D, Flores-López A, Robiou-Vivero EJA, Martínez-Rivera F, Galindo-Hernández V, Chapa-Azuela O, Chávez-Morales A, Rosales-Salyano VH. Impact of liver enzymes on SARS-CoV-2 infection and the severity of clinical course of COVID-19. *Liver Res* 2021; **5**: 21-27 [PMID: 33520337 DOI: 10.1016/j.livres.2021.01.001]

49 **Yip TC**, Lui GC, Wong VW, Chow VC, Ho TH, Li TC, Tse YK, Hui DS, Chan HL, Wong GL. Liver injury is independently associated with adverse clinical outcomes in patients with COVID-19. *Gut* 2021; **70**: 733-742 [PMID: 32641471 DOI: 10.1136/gutjnl-2020-321726]

50 **Roman A**, Moldovan S, Santini A, Stoian M, Dobru D. Impact of the Severity of Liver Injury in COVID-19 Patients Admitted to an Intensive Care Unit During the SARS-CoV2 Pandemic Outbreak. *J Crit Care Med (Targu Mures)* 2021; **7**: 211-216 [PMID: 34722924 DOI: 10.2478/jccm-2021-0021]

51 **Azad Allarakia BM**, Gattan HS, Abdeen RH, Al-Ahmadi BM, Shater AF, Bazaid MB, Althomali OW, Bazaid AS. Predicting Intensive Care Unit Admission for COVID-19 Patients from Laboratory Results. *Dis Markers* 2022; **2022**: 4623901 [PMID: 35634446 DOI: 10.1155/2022/4623901]

52 **Zhao Y**, Zhou J, Pan L, Zhang Y, Wang H, Wu W, He J, Chen J, Huang H. Detection and analysis of clinical features of patients with different types of coronavirus disease 2019. *J Med Virol* 2021; **93**: 401-408 [PMID: 32589755 DOI: 10.1002/jmv.26225]

53 **Salık F**, Uzundere O, Bıçak M, Akelma H, Akgündüz M, Korhan Z, Kandemir D, Kaçar CK. Liver function as a predictor of mortality in COVID-19: A retrospective study. *Ann Hepatol* 2021; **26**: 100553 [PMID: 34624543 DOI: 10.1016/j.aohep.2021.100553]

54 **Kasapoglu B**, Yozgat A, Tanoglu A, Can G, Sakin YS, Kekilli M. Gamma-glutamyl-transferase may predict COVID-19 outcomes in hospitalised patients. *Int J Clin Pract* 2021; **75**: e14933 [PMID: 34605109 DOI: 10.1111/ijcp.14933]

55 **Fan H**, Cai J, Tian A, Li Y, Yuan H, Jiang Z, Yu Y, Ruan L, Hu P, Yue M, Chen N, Li J, Zhu C. Comparison of Liver Biomarkers in 288 COVID-19 Patients: A Mono-Centric Study in the Early Phase of Pandemic. *Front Med (Lausanne)* 2020; **7**: 584888 [PMID: 33521010 DOI: 10.3389/fmed.2020.584888]

56 **Li T**, Guo Y, Zhuang X, Huang L, Zhang X, Wei F, Yang B. Abnormal liver-related biomarkers in COVID-19 patients and the role of prealbumin. *Saudi J Gastroenterol* 2020; **26**: 272-278 [PMID: 32769260 DOI: 10.4103/sjg.SJG_239_20]

57 **McPherson S**, Stewart SF, Henderson E, Burt AD, Day CP. Simple non-invasive fibrosis scoring systems can reliably exclude advanced fibrosis in patients with non-alcoholic fatty liver disease. *Gut* 2010; **59**: 1265-1269 [PMID: 20801772 DOI: 10.1136/gut.2010.216077]

58 **Crisan D**, Avram L, Grapa C, Dragan A, Radulescu D, Crisan S, Grosu A, Militaru V, Buzdugan E, Stoicescu L, Radulescu L, Ciovicescu F, Jivanescu DB, Mocan O, Micu B, Donca V, Marinescu L, Macarie A, Rosu M, Nemes A, Craciun R. Liver Injury and Elevated FIB-4 Define a High-Risk Group in Patients with COVID-19. *J Clin Med* 2021; **11** [PMID: 35011894 DOI: 10.3390/jcm11010153]

59 **Liu M**, Mei K, Tan Z, Huang S, Liu F, Deng C, Ma J, Yu P, Liu X. Liver Fibrosis Scores and Hospitalization, Mechanical Ventilation, Severity, and Death in Patients with COVID-19: A Systematic Review and Dose-Response Meta-Analysis. *Can J Gastroenterol Hepatol* 2022; **2022**: 7235860 [PMID: 35369116 DOI: 10.1155/2022/7235860]

60 **Çelik I**, Öztürk R. From asymptomatic to critical illness: decoding various clinical stages of COVID-19. *Turk J Med Sci* 2021; **51**: 3284-3300 [PMID: 34445855 DOI: 10.3906/sag-2107-137]

61 **Qian SZ**, Hong WD, Lingjie-Mao, Chenfeng-Lin, Zhendong-Fang, Pan JY. Clinical Characteristics and Outcomes of Severe and Critical Patients With 2019 Novel Coronavirus Disease (COVID-19) in Wenzhou: A Retrospective Study. *Front Med (Lausanne)* 2020; **7**: 552002 [PMID: 33015108 DOI: 10.3389/fmed.2020.552002]

62 **Bender JM**, Worman HJ. Coronavirus Disease 2019 and Liver Injury: A Retrospective Analysis of Hospitalized Patients in New York City. *J Clin Transl Hepatol* 2021; **9**: 551-558 [PMID: 34447685 DOI: 10.14218/JCTH.2020.00171]

63 **Shehab M**, Alrashed F, Shuaibi S, Alajmi D, Barkun A. Gastroenterological and hepatic manifestations of patients with COVID-19, prevalence, mortality by country, and intensive care admission rate: systematic review and meta-analysis. *BMJ Open Gastroenterol* 2021; **8** [PMID: 33664052 DOI: 10.1136/bmjgast-2020-000571]

64 **Sikkema BJB**, Sint Nicolaas JJ, van Wijngaarden PP. No association between COVID-19 related liver injury and the course of disease: a retrospective study. *Scand J Gastroenterol* 2021; **56**: 68-71 [PMID: 33119428 DOI: 10.1080/00365521.2020.1842489]

65 **Phipps MM**, Barraza LH, LaSota ED, Sobieszczyk ME, Pereira MR, Zheng EX, Fox AN, Zucker J, Verna EC. Acute Liver Injury in COVID-19: Prevalence and Association with Clinical Outcomes in a Large U.S. Cohort. *Hepatology* 2020; **72**: 807-817 [PMID: 32473607 DOI: 10.1002/hep.31404]

66 **Yang N**, Tian K, Jin M, Zhang X, Zhang F, Shi X, Wang X, Niu S, Shi J, Hu K, Liu K, Peng P, Wang Y, Zhang H, Tian J. Sudden death of COVID-19 patients in Wuhan, China: A retrospective cohort study. *J Glob Health* 2021; **11**: 05006 [PMID: 33828847 DOI: 10.7189/jogh.11.05006]

67 **Boettler T**, Marjot T, Newsome PN, Mondelli MU, Maticic M, Cordero E, Jalan R, Moreau R, Cornberg M, Berg T. Impact of COVID-19 on the care of patients with liver disease: EASL-ESCMID position paper after 6 months of the pandemic. *JHEP Rep* 2020; **2**: 100169 [PMID: 32835190 DOI: 10.1016/j.jhepr.2020.100169]

68 **Huang H**, Li H, Chen S, Zhou X, Dai X, Wu J, Zhang J, Shao L, Yan R, Wang M, Wang J, Tu Y, Ge M. Prevalence and Characteristics of Hypoxic Hepatitis in COVID-19 Patients in the Intensive Care Unit: A First Retrospective Study. *Front Med (Lausanne)* 2020; **7**: 607206 [PMID: 33681238 DOI: 10.3389/fmed.2020.607206]

69 **Zhang Y**, Liu J, Yu L, Zhou N, Ding W, Zheng S, Shi D, Li L. Prevalence and characteristics of hypoxic hepatitis in the largest single-centre cohort of avian influenza A(H7N9) virus-infected patients with severe liver impairment in the intensive care unit. *Emerg Microbes Infect* 2016; **5**: e1 [PMID: 26733380 DOI: 10.1038/emi.2016.1]

70 **Edwards K**, Allison M, Ghuman S. Secondary sclerosing cholangitis in critically ill patients: a rare disease precipitated by severe SARS-CoV-2 infection. *BMJ Case Rep* 2020; **13** [PMID: 33168538 DOI: 10.1136/bcr-2020-237984]

71 **Bütikofer S**, Lenggenhager D, Wendel Garcia PD, Maggio EM, Haberecker M, Reiner CS, Brüllmann G, Buehler PK, Gubler C, Müllhaupt B, Jüngst C, Morell B. Secondary sclerosing cholangitis as cause of persistent jaundice in patients with severe COVID-19. *Liver Int* 2021; **41**: 2404-2417 [PMID: 34018314 DOI: 10.1111/liv.14971]

72 **Hunyady P**, Streller L, Rüther DF, Groba SR, Bettinger D, Fitting D, Hamesch K, Marquardt JU, Mücke VT, Finkelmeier F, Sekandarzad A, Wengenmayer T, Bounidane A, Weiss F, Peiffer KH, Schlevogt B, Zeuzem S, Waidmann O, Hollenbach M, Kirstein MM, Kluwe J, Kütting F, Mücke MM. Secondary sclerosing cholangitis following COVID-19 disease: a multicenter retrospective study. *Clin Infect Dis* 2022 [PMID: 35809032 DOI: 10.1093/cid/ciac565]

73 **Liemarto AK**, Budiono BP, Chionardes MA, Oliviera I, Rahmasiwi A. Liver abscess with necrosis in post COVID-19: A case report. *Ann Med Surg (Lond)* 2021; **72**: 103107 [PMID: 34840781 DOI: 10.1016/j.amsu.2021.103107]

74 **Harouachi A**, Bouhout T, Hadj Kacem H, Serji B, Berkhli H, Madani H, El Harroudi T. Acute hepatitis with portal and mesenteric vein thrombosis revealing SARS-CoV-2 infection: Case report and literature review. *Ann Med Surg (Lond)* 2022; **77**: 103706 [PMID: 35531429 DOI: 10.1016/j.amsu.2022.103706]

75 **Haji Esmaeil Memar E**, Mamishi S, Sharifzadeh Ekbatani M, Alimadadi H, Yaghmaei B, Chegini V, Janani S, Mahmoudi S. Fulminant hepatic failure: A rare and devastating manifestation of Coronavirus disease 2019 in an 11-year-old boy. *Arch Pediatr* 2020; **27**: 502-505 [PMID: 33069564 DOI: 10.1016/j.arcped.2020.09.009]

76 **Romaní Vidal A**, Vaughan A, Innocenti F, Colombe S, Nerlander L, Rachwal N, Ciancio BC, Mougkou A, Carvalho C, Delgado E, Mook P, de Muylder G, Peeters M, Tenev T, Golkocheva-Markova E, Vorobieva Solholm Jensen V, Koch A, Figoni J, Brouard C, Nikolopoulou G, Zisouli A, Murphy N, Broderick A, Goldberg L, Rich R, Hecht Sagie L, Tosti ME, Suligoi B, Joosten R, Pijnacker R, Fjeldheim I, Heen E, Stępień M, Polański P, Tato Marinho R, Vieira Martins J, Varela C, Avellón A, Andersson E, Jansson Mörk M, Mandal S, Watson C, Coughlan L, Chand M, Neill C, Bradley DT, Li K, O'Leary M, McInnes N, Williams CJ, Moore C, Gjini A, Duffell E, Pebody R. Hepatitis of unknown aetiology in children - epidemiological overview of cases reported in Europe, 1 January to 16 June 2022. *Euro Surveill* 2022; **27** [PMID: 35929429 DOI: 10.2807/1560-7917.ES.2022.27.31.2200483]

77 **Busani S**, Bedini A, Biagioni E, Serio L, Tonelli R, Meschiari M, Franceschini E, Guaraldi G, Cossarizza A, Clini E, Maiorana A, Gennari W, De Maria N, Luppi M, Mussini C, Girardis M; Modena Covid-19 Working Group (MoCo19). Two Fatal Cases of Acute Liver Failure Due to HSV-1 Infection in COVID-19 Patients Following Immunomodulatory Therapies. *Clin Infect Dis* 2021; **73**: e252-e255 [PMID: 32840571 DOI: 10.1093/cid/ciaa1246]

78 **Fix OK**, Hameed B, Fontana RJ, Kwok RM, McGuire BM, Mulligan DC, Pratt DS, Russo MW, Schilsky ML, Verna EC, Loomba R, Cohen DE, Bezerra JA, Reddy KR, Chung RT. Clinical Best Practice Advice for Hepatology and Liver Transplant Providers During the COVID-19 Pandemic: AASLD Expert Panel Consensus Statement. *Hepatology* 2020; **72**: 287-304 [PMID: 32298473 DOI: 10.1002/hep.31281]

79 **Premkumar M**, Kajal K, Kulkarni AV, Gupta A, Divyaveer S. Point-of-Care Echocardiography and Hemodynamic Monitoring in Cirrhosis and Acute-on-Chronic Liver Failure in the COVID-19 Era. *J Intensive Care Med* 2021; **36**: 511-523 [PMID: 33438491 DOI: 10.1177/0885066620988281]

80 **Effenberger M**, Grander C, Fritsche G, Bellmann-Weiler R, Hartig F, Wildner S, Seiwald S, Adolph TE, Zoller H, Weiss G, Tilg H. Liver stiffness by transient elastography accompanies illness severity in COVID-19. *BMJ Open Gastroenterol* 2020; **7** [PMID: 32665398 DOI: 10.1136/bmjgast-2020-000445]

81 **Demirtas CO**, Keklikkiran C, Ergenc I, Erturk Sengel B, Eskidemir G, Cinel I, Odabasi Z, Korten V, Yilmaz Y. Liver stiffness is associated with disease severity and worse clinical scenarios in coronavirus disease 2019: A prospective transient elastography study. *Int J Clin Pract* 2021; **75**: e14363 [PMID: 33993597 DOI: 10.1111/ijcp.14363]

82 **Cornberg M**, Buti M, Eberhardt CS, Grossi PA, Shouval D. EASL position paper on the use of COVID-19 vaccines in patients with chronic liver diseases, hepatobiliary cancer and liver transplant recipients. *J Hepatol* 2021; **74**: 944-951 [PMID: 33563499 DOI: 10.1016/j.jhep.2021.01.032]

83 **Rossi RE**, Chen J, Caplin ME. The Role of Diet and Supplements in the Prevention and Progression of COVID-19: Current Knowledge and Open Issues. *Prev Nutr Food Sci* 2022; **27**: 137-149 [PMID: 35919576 DOI: 10.3746/pnf.2022.27.2.137]

84 **Dalekos GN**, Stefos A, Georgiadou S, Lygoura V, Michail A, Ntaios G, Samakidou A, Giannoulis G, Gabeta S, Vlychou M, Petinaki E, Leventogiannis K, Giamarellos-Bourboulis EJ, Gatselis NK. Lessons from pathophysiology: Use of individualized combination treatments with immune interventional agents to tackle severe respiratory failure in patients with COVID-19. *Eur J Intern Med* 2021; **88**: 52-62 [PMID: 33820686 DOI: 10.1016/j.ejim.2021.03.026]

85 **Mameli S**, Marcialis MA, Bassareo PP, Fanos V. COVID-19 and hepatic damage: what we know? *Panminerva Med* 2021 [PMID: 33470582 DOI: 10.23736/S0031-0808.21.04239-7]

86 **Ronco C**, Bagshaw SM, Bellomo R, Clark WR, Husain-Syed F, Kellum JA, Ricci Z, Rimmelé T, Reis T, Ostermann M. Extracorporeal Blood Purification and Organ Support in the Critically Ill Patient during COVID-19 Pandemic: Expert Review and Recommendation. *Blood Purif* 2021; **50**: 17-27 [PMID: 32454500 DOI: 10.1159/000508125]

87 **Tampe D**, Korsten P, Bremer SCB, Winkler MS, Tampe B. Kinetics of Bilirubin and Ammonia Elimination during Hemadsorption Therapy in Secondary Sclerosing Cholangitis Following ECMO Therapy and Severe COVID-19. *Biomedicines* 2021; **9** [PMID: 34944657 DOI: 10.3390/biomedicines9121841]

88 **Ozkurt Z**, Çınar Tanrıverdi E. COVID-19: Gastrointestinal manifestations, liver injury and recommendations. *World J Clin Cases* 2022; **10**: 1140-1163 [PMID: 35211548 DOI: 10.12998/wjcc.v10.i4.1140]

89 **Váncsa S**, Hegyi PJ, Zádori N, Szakó L, Vörhendi N, Ocskay K, Földi M, Dembrovszky F, Dömötör ZR, Jánosi K, Rakonczay Z Jr, Hartmann P, Horváth T, Erőss B, Kiss S, Szakács Z, Németh D, Hegyi P, Pár G. Pre-existing Liver Diseases and On-Admission Liver-Related Laboratory Tests in COVID-19: A Prognostic Accuracy Meta-Analysis With Systematic Review. *Front Med (Lausanne)* 2020; **7**: 572115 [PMID: 33282888 DOI: 10.3389/fmed.2020.572115]

90 **Simon TG**, Hagström H, Sharma R, Söderling J, Roelstraete B, Larsson E, Ludvigsson JF. Risk of severe COVID-19 and mortality in patients with established chronic liver disease: a nationwide matched cohort study. *BMC Gastroenterol* 2021; **21**: 439 [PMID: 34814851 DOI: 10.1186/s12876-021-02017-8]

91 **Sharma P**, Kumar A, Anikhindi S, Bansal N, Singla V, Shivam K, Arora A. Effect of COVID-19 on Pre-existing Liver disease: What Hepatologist Should Know? *J Clin Exp Hepatol* 2021; **11**: 484-493 [PMID: 33398223 DOI: 10.1016/j.jceh.2020.12.006]

92 **Romero-Cristóbal M**, Clemente-Sánchez A, Piñeiro P, Cedeño J, Rayón L, Del Río J, Ramos C, Hernández DA, Cova M, Caballero A, Garutti I, García-Olivares P, Hortal J, Guerrero JE, García R, Bañares R, Rincón D. Possible unrecognised liver injury is associated with mortality in critically ill COVID-19 patients. *Therap Adv Gastroenterol* 2021; **14**: 17562848211023410 [PMID: 34178116 DOI: 10.1177/17562848211023410]

93 **Wilde H**, Mellan T, Hawryluk I, Dennis JM, Denaxas S, Pagel C, Duncan A, Bhatt S, Flaxman S, Mateen BA, Vollmer SJ. The association between mechanical ventilator compatible bed occupancy and mortality risk in intensive care patients with COVID-19: a national retrospective cohort study. *BMC Med* 2021; **19**: 213 [PMID: 34461893 DOI:

10.1186/s12916-021-02096-0]

94 **Bravata DM**, Perkins AJ, Myers LJ, Arling G, Zhang Y, Zillich AJ, Reese L, Dysangco A, Agarwal R, Myers J, Austin C, Sexson A, Leonard SJ, Dev S, Keyhani S. Association of Intensive Care Unit Patient Load and Demand With Mortality Rates in US Department of Veterans Affairs Hospitals During the COVID-19 Pandemic. *JAMA Netw Open* 2021; **4**: e2034266 [PMID: 33464319 DOI: 10.1001/jamanetworkopen.2020.34266]

95 **Williams R**, Alessi C, Alexander G, Allison M, Aspinall R, Batterham RL, Bhala N, Day N, Dhawan A, Drummond C, Ferguson J, Foster G, Gilmore I, Goldacre R, Gordon H, Henn C, Kelly D, MacGilchrist A, McCorry R, McDougall N, Mirza Z, Moriarty K, Newsome P, Pinder R, Roberts S, Rutter H, Ryder S, Samyn M, Severi K, Sheron N, Thorburn D, Verne J, Williams J, Yeoman A. New dimensions for hospital services and early detection of disease: a Review from the Lancet Commission into liver disease in the UK. *Lancet* 2021; **397**: 1770-1780 [PMID: 33714360 DOI: 10.1016/S0140-6736(20)32396-5]

96 **Akbulut S**, Garzali IU, Hargura AS, Aloun A, Yilmaz S. Screening, Surveillance, and Management of Hepatocellular Carcinoma During the COVID-19 Pandemic: a Narrative Review. *J Gastrointest Cancer* 2022; 1-12 [PMID: 35499649 DOI: 10.1007/s12029-022-00830-2]

97 **Abd Elbaset HS**, Sultan AM, Montasser IF, Soliman HEM, Elayashy M, Makhlouf NA; Scientific Committee of Ministry of Health (MOH) National Project of Waiting Lists, Egypt. Egyptian protocol for living donor liver transplantation (LDLT) during SARS-CoV-2 pandemic. *Egypt Liver J* 2021; **11**: 14 [PMID: 34777866 DOI: 10.1186/s43066-020-00074-4]

98 **Muller X**, Tilmans G, Chenevas-Paule Q, Lebossé F, Antonini T, Poinsot D, Rode A, Guichon C, Schmitt Z, Ducerf C, Mohkam K, Lesurtel M, Mabrut JY. Strategies for liver transplantation during the SARS-CoV-2 outbreak: Preliminary experience from a single center in France. *Am J Transplant* 2020; **20**: 2989-2996 [PMID: 32476233 DOI: 10.1111/ajt.16082]

99 **Pereira MR**, Mohan S, Cohen DJ, Husain SA, Dube GK, Ratner LE, Arcasoy S, Aversa MM, Benvenuto LJ, Dadhania DM, Kapur S, Dove LM, Brown RS Jr, Rosenblatt RE, Samstein B, Uriel N, Farr MA, Satlin M, Small CB, Walsh TJ, Kodiyanplakkal RP, Miko BA, Aaron JG, Tsapepas DS, Emond JC, Verna EC. COVID-19 in solid organ transplant recipients: Initial report from the US epicenter. *Am J Transplant* 2020; **20**: 1800-1808 [PMID: 32330343 DOI: 10.1111/ajt.15941]

World Journal of Clinical Cases

Submit a Manuscript: https://www.f6publishing.com

World J Clin Cases 2023 January 26; 11(3): 528-533

DOI: 10.12998/wjcc.v11.i3.528

ISSN 2307-8960 (online)

MINIREVIEWS

Exosomal miRNA in early-stage hepatocellular carcinoma

Zhi-Qiang Wu, Yi-Xin Zhu, Yun Jin, Yin-Chu Zhan

Specialty type: Gastroenterology and hepatology

Provenance and peer review: Invited article; Externally peer reviewed.

Peer-review model: Single blind

Peer-review report's scientific quality classification

Grade A (Excellent): 0
Grade B (Very good): B
Grade C (Good): C, C
Grade D (Fair): 0
Grade E (Poor): 0

P-Reviewer: Luo L, China; Mohammed HA, Saudi Arabia; Wang ZX, China

Received: October 28, 2022
Peer-review started: October 28, 2022
First decision: December 19, 2022
Revised: December 26, 2022
Accepted: January 5, 2023
Article in press: January 5, 2023
Published online: January 26, 2023

Zhi-Qiang Wu, Yi-Xin Zhu, Yin-Chu Zhan, Department of Surgery, The Second People's Hospital of Quzhou, Quzhou 324000, Zhejiang Province, China

Yun Jin, Department of Surgery, The Second Affiliated Hospital, Zhejiang University, School of Medicine, Hangzhou 310009, Zhejiang Province, China

Corresponding author: Yin-Chu Zhan, MD, Director, Surgeon, Department of Surgery, The Second People's Hospital of Quzhou, No. 338 Xin'an Avenue, Qujiang District, Quzhou 324000, Zhejiang Province, China. qzhospzyc@163.com

Abstract

The incidence and mortality of hepatic carcinoma (HCC) remain high, and early diagnosis of HCC is seen as a key approach in improving clinical outcomes. However, the sensitivity and specificity of current early screening methods for HCC are not satisfactory. In recent years, research around exosomal miRNA has gradually increased, and these molecules have emerged as attractive candidates for early diagnosis and treatment of HCC. This review summarizes the feasibility of using miRNAs in peripheral blood exosomes as early diagnostic tools for HCC.

Key Words: Hepatic carcinoma; Early diagnosis; Exosomal miRNA; Biomarker

Core Tip: The prognosis of hepatic carcinoma (HCC) is poor and surgical resection is the only potential radical cure. Early diagnosis of HCC is a key approach in improving clinical outcomes. However, the sensitivity and specificity of current early screening methods for HCC are not satisfactory. Exosomal miRNAs have become a candidate for early diagnosis and treatment of HCC. This review summarizes the feasibility of using miRNAs in peripheral blood exosomes as early diagnostic tools for HCC.

Citation: Wu ZQ, Zhu YX, Jin Y, Zhan YC. Exosomal miRNA in early-stage hepatocellular carcinoma. *World J Clin Cases* 2023; 11(3): 528-533
URL: https://www.wjgnet.com/2307-8960/full/v11/i3/528.htm
DOI: https://dx.doi.org/10.12998/wjcc.v11.i3.528

INTRODUCTION

Hepatocellular carcinoma (HCC) is one of the most common malignant tumors in the world, with the seventh highest incidence and second highest mortality among all malignant cancer types[1,2]. About 905000 patients are newly diagnosed with liver cancers each year around the world, with 75% of these being accounted for by HCC alone, and altogether causing about 830000 deaths[3]. Infection with hepatitis B virus (HBV) is the most common cause of HCC, and more than half of the world's new cases of HCC were detected in China[4]. The high incidence and mortality of HCC pose a significant threat to the health of Chinese people and place a heavy burden on society[5].

It is considered that the best stage for treatment of HCC is Stage I, or subclinical liver cancer[6]. However, HCC symptoms in this period are not obvious, and most patients are not diagnosed until the middle or late stages. Therefore, development of more effective screening methods that allow earlier detection of HCC represents an important research focus. The five-year survival rate for patients with early-stage HCC is more than 70%, but this rate drops to less than 12.5% for patients with advanced HCC[7].

Tumor markers represent one approach for the early diagnosis of HCC, allowing earlier detection of primary tumors, recurrent tumors, and metastatic tumors than other methods. Yet, the accuracy of prediction and diagnosis achieved by tumor markers could still be improved, and such improvements would confer parallel improvements in prognosis and patient outcomes (Table 1)[8-12]. Alpha-fetoprotein (AFP), which has been widely used as a marker for HCC diagnosis and monitoring, is not highly sensitive to early HCC, and may also be increased in patients without HCC but with chronic viral hepatitis and cirrhosis[13]. As such, AFP can lead to misdiagnoses or unclear clinical interpretation, particularly if detected alone[14]. Despite the obvious limitations of using AFP as an early screening marker for HCC, its ubiquity has precluded its replacement by other clinical markers. At present, a variety of molecular markers are used in the diagnosis of HCC, but they all have the problems of low sensitivity and insufficient specificity. The sensitivity of AFP-L3, a glycoform of AFP, for the diagnosis of early HCC is less than 28%[15]. Another biomarker, protein induced by vitamin K absence II (PIVKA II), is also relatively insensitive for diagnosing early HCC[7]. Therefore, it is an urgent research direction to identify tumor markers with high sensitivity and specificity for the early diagnosis of HCC.

RELATIONSHIP BETWEEN RNA AND HCC

In recent years, non-coding RNA has attracted ever-increasing attention in the field of biological medicine. Our understanding of these RNA molecules has progressed rapidly, yielding a new understanding of cellular life and providing new opportunities for the diagnosis and treatment of various diseases. Among such non-coding RNA, the most extensively studied, to date, is microRNA (miRNA) - a class of small non-coding single-stranded RNA molecules containing 19-25 nucleotides. They are formed from double-stranded RNA precursors composed of 70-100 nucleotides in a hairpin structure. The sequences of miRNA are highly conserved across different species, suggesting that these very small molecules may play important roles in various cellular processes such as development, proliferation, differentiation, and apoptosis[16]. Significant differences in miRNA expression profiles have also been identified in some diseases[17,18], indicating that miRNA may be used as biomarkers for the diagnosis and prognosis of such diseases, including malignant tumors. Due to their structure, miRNAs can stably exist in the blood circulation, but the form of miRNAs in the circulation is not clear. Since RNA exposed to the blood is degraded within a short period of time, some researchers have pointed out that the stable existence of miRNAs in plasma must indicate the presence of protective macromolecules. Increasing evidence has shown that the main components of such protective macromolecular complexes are exosomes[19].

The correlation between miRNA and HCC was first proposed by Murakami, who analyzed the expression of microRNAs in tumor and adjacent tissues of HCC patients, as well as the liver tissues of hepatitis patients. It was found that miRNA-99a was positively correlated with the degree of pathological differentiation of HCC, while miRNA-20, miRNA-18 and pre-miRNA-18 were negatively correlated with the differentiation of HCC and positively correlated with the occurrence of HCC[20]. Since then, additional studies have confirmed close associations between miRNAs and HCC. These miRNAs can be roughly divided into two categories: "non-liver-specific miRNAs," such as miRNA-21, miRNA-221/222, and let-7, which are abnormally expressed in various tumors such as liver cancer, pancreatic cancer, and lung cancer[21-23], and "liver-specific miRNAs," which are only abnormally expressed in HCC. An example of a liver-specific miRNA is miRNA-122, which is up-regulated in HCC and suppresses the expression of the proto-oncogene c-myc through transcriptional activators[24]. Studies have shown that miRNA-122 is up-regulated in 70% of human liver cancer tissues and 100% of liver cancer cell models[25].

HCC is the result of multiple genetic mutations, which can occur in oncogenes or tumor suppressor genes, growth factors or their receptors, and myriad signaling pathways controlling cellular prolif-

Table 1 Biomarkers for the diagnosis of hepatocellular carcinoma

Biomarker	Ref.	Country	Sensitivity (%)	Specificity (%)
AFP	Trevisani *et al*[8]	Italy	60	90
DCP	Feng *et al*[9]	China	83	91
AFP-L3	Toyoda *et al*[10]	Japan	41	85
GP73	Marrero *et al*[11]	United States	62	88
miR-21-5p	Ghosh *et al*[12]	India	74	68

AFP: Alpha-fetoprotein; DCP: Des-γ-carboxyprothrombin.

eration or behavior. Gene mutations also play a very important role in the progression of a tumor. When the expression of a gene or a class of molecules is silenced or enhanced, the possibility of tumorigenesis is present[26], and microRNA is gradually becoming the focus of this kind of research. miRNAs - small RNA molecules with very simple structures that regulate hundreds of mRNAs - play an unusual role in gene expression networks. Abnormally expressed miRNA may play a role similar to oncogenes such as myc or tumor suppressor genes such as p53, inducing or inhibiting liver tumorigenesis according to the specific cellular function of the target gene or genes regulated by that specific miRNA[27]. Meanwhile, and critically, miRNA can also influence the therapeutic effects of chemotherapy and intervene in the process of drug tolerance[28,29].

Regarding the use of miRNAs as molecular markers for tumors, miRNA-21 has gained attention as the first miRNA used in the clinic[30]. Many studies have confirmed that miRNA-21 is an oncogene, promoting liver tumor growth and metastasis by inhibiting the tumor suppressor genes PTEN and MAP2K3[31,32]. In 2012, Tomimaru *et al*[33] found that expression of miRNA-21 was increased in the plasma and tumor tissues of HCC patients, and that there was a correlation between them. Further investigation revealed that plasma miRNA-21 had clinical application value and could be used to diagnose HCC. Several additional studies have also shown that various miRNAs can be used for the diagnosis or prognosis of HCC patients. For example, serum miRNA-122 can also be used as a tumor marker for the diagnosis of HCC[34], while miRNA-125 and miRNA-233 can further be used for the early diagnosis of HCC patients who are HBV-positive[35]. miR-140 can also be used to determine the prognosis of HCC patients[36].

EXOSOMAL MIRNA IN HCC

The stability of miRNAs in plasma depends on exosomes. Exosomes are bilayer lipid membrane-coated vesicles with diameters of about 30-100 nm that can be released out of the cell and into the blood, urine, saliva, and other body fluids. It is generally believed that exosomes are composed of such lipid molecules as well as myriad amino acids and proteins, among which the common markers of exosomes have been identified as CD9, CD63, CD81, CD82, and others[37]. Nucleic acids in exosomes include mRNA, DNA, miRNA and other non-coding RNAs. Exosomes can carry these functional substances between cells and mediate communication between cells, thus regulating protein synthesis, cellular proliferation and differentiation, antiviral activity, and myriad other physiological and pathological activities.

Exosomal miRNAs have multiple potential functions in cell-to-cell communication. As such, they can be used to detect pathophysiological changes in the body, track changes in tumors, and aid in the diagnosis and prognosis of various diseases[38]. Down-regulation of exosomal miRNA expression has been shown to play a certain role in the mechanism of tumorigenesis[39]. Because exosomes and their contents (mainly miRNAs) can reflect the state of the cell they were released from – including whether that cell was of a tumorigenic or healthy state - exosomal miRNAs may hold a high value in the clinical diagnosis of tumors[40]. Detection of exosomes derived from tumor cells and their miRNA levels may become a novel biological tool with clinical potential and utility in people at high risk of cancer[41].

Protein and miRNA profiles in exosomes produced by HCC cells have been shown to be significantly different from those produced by normal cells[42,43]. Such exosomes can be ingested and internalized by other cells to deliver genes with certain functions[44]. Similar to the screening of serum tumor markers for liver cancer, exosomal miRNA can also be used as a valuable, non-invasive biomarker to distinguish the type and grade of liver inflammation, and then assist in the early diagnosis of liver cancer. Studies have also shown that circulating miRNAs may become biomarkers for HCC diagnosis due to the large number of miRNA variants in HCC cells[45]. Ghosh *et al*[12] identified a liver-specific exosomal miRNA, miR-21-5p, as an early circulating diagnostic marker for HCC with low AFP. The sensitivity, specificity, and accuracy of miR-21-5p differential diagnosis of HCC are 74%, 68%, and 71%,

respectively.

CONCLUSION

In conclusion, although many miRNAs have been identified as tumor markers for early diagnosis of liver cancer in recent years, most of them have some defects and deficiencies, meaning that there is no clear consensus on which one or few miRNAs can improve the early diagnostics of HCC. Remaining challenges include a lack of further study on the specificity and sensitivity of target miRNAs in the diagnosis of liver cancer, a lack of robust clinical comparison between candidate miRNAs and the current tumor marker, AFP, and an expensive and cumbersome detection method for target miRNAs in HCC patients. As increased attention is placed upon exosomal miRNAs and their application at home and abroad, it is necessary and urgent to fully explore and realize the potential for exosomal miRNAs in the early diagnosis and treatment of liver cancer in clinical practice.

FOOTNOTES

Author contributions: Wu ZQ and Zhu YX designed and reviewed the manuscript; Wu ZQ, Zhu YX, and Jin Y wrote the paper; All authors read and approved the manuscript; Wu ZQ and Zhu YX contributed equally to this work.

Supported by the Quzhou Science and Technology Guided Project Planning, No. 2019133.

Conflict-of-interest statement: We declare that we have no conflict of interest related to this work.

Country/Territory of origin: China

ORCID number: Yun Jin 0000-0002-3073-4043; Yin-Chu Zhan 0000-0002-6017-1907.

S-Editor: Liu JH
L-Editor: A
P-Editor: Liu JH

REFERENCES

1 **Mohammed HA**, Almahmoud SA, Arfeen M, Srivastava A, El-Readi MZ, Ragab EA, Shehata SM, Mohammed SAA, Mostafa EM, El-khawaga HA, Khan RA. Phytochemical profiling, molecular docking, and in vitro anti-hepatocellular carcinoid bioactivity of Suaeda vermiculata extracts. *Arab J Chem* 2022; **15** [DOI: 10.1016/j.arabjc.2022.103950]
2 **Mohammed HA**, Khan RA. Anthocyanins: Traditional Uses, Structural and Functional Variations, Approaches to Increase Yields and Products' Quality, Hepatoprotection, Liver Longevity, and Commercial Products. *Int J Mol Sci* 2022; **23** [PMID: 35216263 DOI: 10.3390/ijms23042149]
3 **Sung H**, Ferlay J, Siegel RL, Laversanne M, Soerjomataram I, Jemal A, Bray F. Global Cancer Statistics 2020: GLOBOCAN Estimates of Incidence and Mortality Worldwide for 36 Cancers in 185 Countries. *CA Cancer J Clin* 2021; **71**: 209-249 [PMID: 33538338 DOI: 10.3322/caac.21660]
4 **Feng RM**, Zong YN, Cao SM, Xu RH. Current cancer situation in China: good or bad news from the 2018 Global Cancer Statistics? *Cancer Commun (Lond)* 2019; **39**: 22 [PMID: 31030667 DOI: 10.1186/s40880-019-0368-6]
5 **El-Serag HB**, Rudolph KL. Hepatocellular carcinoma: epidemiology and molecular carcinogenesis. *Gastroenterology* 2007; **132**: 2557-2576 [PMID: 17570226 DOI: 10.1053/j.gastro.2007.04.061]
6 **Bruix J**, Sherman M; American Association for the Study of Liver Diseases. Management of hepatocellular carcinoma: an update. *Hepatology* 2011; **53**: 1020-1022 [PMID: 21374666 DOI: 10.1002/hep.24199]
7 **Wang W**, Wei C. Advances in the early diagnosis of hepatocellular carcinoma. *Genes Dis* 2020; **7**: 308-319 [PMID: 32884985 DOI: 10.1016/j.gendis.2020.01.014]
8 **Trevisani F**, D'Intino PE, Morselli-Labate AM, Mazzella G, Accogli E, Caraceni P, Domenicali M, De Notariis S, Roda E, Bernardi M. Serum alpha-fetoprotein for diagnosis of hepatocellular carcinoma in patients with chronic liver disease: influence of HBsAg and anti-HCV status. *J Hepatol* 2001; **34(4)**: 570-575 [PMID: 11394657 DOI: 10.1016/s0168-8278(00)00053-2]
9 **Feng H**, Li B, Li Z, Wei Q, Ren L. PIVKA-II serves as a potential biomarker that complements AFP for the diagnosis of hepatocellular carcinoma. *BMC Cancer* 2021; **21(1)**: 401 [PMID: 33849479 DOI: 10.1186/s12885-021-08138-3]

10 **Toyoda H**, Kumada T, Tada T, Kaneoka Y, Maeda A, Kanke F, Satomura S. Clinical utility of highly sensitive Lens culinaris agglutinin-reactive alpha-fetoprotein in hepatocellular carcinoma patients with alpha-fetoprotein < 20 ng/mL. *Cancer Sci* 2011; **102(5)**: 1025-1031 [PMID: 21244578 DOI: 10.1111/j.1349-7006.2011.01875.x]

11 **Marrero JA**, Romano PR, Nikolaeva O, Steel L, Mehta A, Fimmel CJ, Comunale MA, D'Amelio A, Lok AS, Block TM. GP73, a resident Golgi glycoprotein, is a novel serum marker for hepatocellular carcinoma. *J Hepatol* 2005; **43(6)**: 1007-1012 [PMID: 16137783 DOI: 10.1016/j.jhep.2005.05.028]

12 **Ghosh S**, Bhowmik S, Majumdar S, Goswami A, Chakraborty J, Gupta S, Aggarwal S, Ray S, Chatterjee R, Bhattacharyya S, Dutta M, Datta S, Chowdhury A, Dhali GK, Banerjee S. The exosome encapsulated microRNAs as circulating diagnostic marker for hepatocellular carcinoma with low alpha-fetoprotein. *Int J Cancer* 2020; **147**: 2934-2947 [PMID: 32441313 DOI: 10.1002/ijc.33111]

13 **European Association for the Study of the Liver**; European Organisation for Research and Treatment of Cancer. EASL-EORTC clinical practice guidelines: management of hepatocellular carcinoma. *J Hepatol* 2012; **56**: 908-943 [PMID: 22424438 DOI: 10.1016/j.jhep.2011.12.001]

14 **Motomura T**, Shirabe K, Mano Y, Muto J, Toshima T, Umemoto Y, Fukuhara T, Uchiyama H, Ikegami T, Yoshizumi T, Soejima Y, Maehara Y. Neutrophil-lymphocyte ratio reflects hepatocellular carcinoma recurrence after liver transplantation *via* inflammatory microenvironment. *J Hepatol* 2013; **58**: 58-64 [PMID: 22925812 DOI: 10.1016/j.jhep.2012.08.017]

15 **Marrero JA**, Feng Z, Wang Y, Nguyen MH, Befeler AS, Roberts LR, Reddy KR, Harnois D, Llovet JM, Normolle D, Dalhgren J, Chia D, Lok AS, Wagner PD, Srivastava S, Schwartz M. Alpha-fetoprotein, des-gamma carboxyprothrombin, and lectin-bound alpha-fetoprotein in early hepatocellular carcinoma. *Gastroenterology* 2009; **137**: 110-118 [PMID: 19362088 DOI: 10.1053/j.gastro.2009.04.005]

16 **Whittaker S**, Marais R, Zhu AX. The role of signaling pathways in the development and treatment of hepatocellular carcinoma. *Oncogene* 2010; **29**: 4989-5005 [PMID: 20639898 DOI: 10.1038/onc.2010.236]

17 **Lander ES**. Cutting the Gordian helix--regulating genomic testing in the era of precision medicine. *N Engl J Med* 2015; **372**: 1185-1186 [PMID: 25689017 DOI: 10.1056/NEJMp1501964]

18 **Baltimore D**, Berg P, Botchan M, Carroll D, Charo RA, Church G, Corn JE, Daley GQ, Doudna JA, Fenner M, Greely HT, Jinek M, Martin GS, Penhoet E, Puck J, Sternberg SH, Weissman JS, Yamamoto KR. Biotechnology. A prudent path forward for genomic engineering and germline gene modification. *Science* 2015; **348**: 36-38 [PMID: 25791083 DOI: 10.1126/science.aab1028]

19 **Gibbings DJ**, Ciaudo C, Erhardt M, Voinnet O. Multivesicular bodies associate with components of miRNA effector complexes and modulate miRNA activity. *Nat Cell Biol* 2009; **11**: 1143-1149 [PMID: 19684575 DOI: 10.1038/ncb1929]

20 **Murakami Y**, Yasuda T, Saigo K, Urashima T, Toyoda H, Okanoue T, Shimotohno K. Comprehensive analysis of microRNA expression patterns in hepatocellular carcinoma and non-tumorous tissues. *Oncogene* 2006; **25**: 2537-2545 [PMID: 16331254 DOI: 10.1038/sj.onc.1209283]

21 **Huang Y**, Yang YB, Zhang XH, Yu XL, Wang ZB, Cheng XC. MicroRNA-21 gene and cancer. *Med Oncol* 2013; **30**: 376 [PMID: 23277281 DOI: 10.1007/s12032-012-0376-8]

22 **Garofalo M**, Quintavalle C, Romano G, Croce CM, Condorelli G. miR221/222 in cancer: their role in tumor progression and response to therapy. *Curr Mol Med* 2012; **12**: 27-33 [PMID: 22082479 DOI: 10.2174/156652412798376170]

23 **Wang X**, Cao L, Wang Y, Wang X, Liu N, You Y. Regulation of let-7 and its target oncogenes (Review). *Oncol Lett* 2012; **3**: 955-960 [PMID: 22783372 DOI: 10.3892/ol.2012.609]

24 **Wang B**, Hsu SH, Wang X, Kutay H, Bid HK, Yu J, Ganju RK, Jacob ST, Yuneva M, Ghoshal K. Reciprocal regulation of microRNA-122 and c-Myc in hepatocellular cancer: role of E2F1 and transcription factor dimerization partner 2. *Hepatology* 2014; **59**: 555-566 [PMID: 24038073 DOI: 10.1002/hep.26712]

25 **Fornari F**, Gramantieri L, Giovannini C, Veronese A, Ferracin M, Sabbioni S, Calin GA, Grazi GL, Croce CM, Tavolari S, Chieco P, Negrini M, Bolondi L. MiR-122/cyclin G1 interaction modulates p53 activity and affects doxorubicin sensitivity of human hepatocarcinoma cells. *Cancer Res* 2009; **69**: 5761-5767 [PMID: 19584283 DOI: 10.1158/0008-5472.CAN-08-4797]

26 **Shiraha H**, Yamamoto K, Namba M. Human hepatocyte carcinogenesis (review). *Int J Oncol* 2013; **42**: 1133-1138 [PMID: 23426905 DOI: 10.3892/ijo.2013.1829]

27 **Lujambio A**, Lowe SW. The microcosmos of cancer. *Nature* 2012; **482**: 347-355 [PMID: 22337054 DOI: 10.1038/nature10888]

28 **Meng F**, Henson R, Lang M, Wehbe H, Maheshwari S, Mendell JT, Jiang J, Schmittgen TD, Patel T. Involvement of human micro-RNA in growth and response to chemotherapy in human cholangiocarcinoma cell lines. *Gastroenterology* 2006; **130**: 2113-2129 [PMID: 16762633 DOI: 10.1053/j.gastro.2006.02.057]

29 **Xia L**, Zhang D, Du R, Pan Y, Zhao L, Sun S, Hong L, Liu J, Fan D. miR-15b and miR-16 modulate multidrug resistance by targeting BCL2 in human gastric cancer cells. *Int J Cancer* 2008; **123**: 372-379 [PMID: 18449891 DOI: 10.1002/ijc.23501]

30 **Lawrie CH**, Gal S, Dunlop HM, Pushkaran B, Liggins AP, Pulford K, Banham AH, Pezzella F, Boultwood J, Wainscoat JS, Hatton CS, Harris AL. Detection of elevated levels of tumour-associated microRNAs in serum of patients with diffuse large B-cell lymphoma. *Br J Haematol* 2008; **141**: 672-675 [PMID: 18318758 DOI: 10.1111/j.1365-2141.2008.07077.x]

31 **Meng F**, Henson R, Wehbe-Janek H, Ghoshal K, Jacob ST, Patel T. MicroRNA-21 regulates expression of the PTEN tumor suppressor gene in human hepatocellular cancer. *Gastroenterology* 2007; **133**: 647-658 [PMID: 17681183 DOI: 10.1053/j.gastro.2007.05.022]

32 **Xu G**, Zhang Y, Wei J, Jia W, Ge Z, Zhang Z, Liu X. MicroRNA-21 promotes hepatocellular carcinoma HepG2 cell proliferation through repression of mitogen-activated protein kinase-kinase 3. *BMC Cancer* 2013; **13**: 469 [PMID: 24112539 DOI: 10.1186/1471-2407-13-469]

33 **Tomimaru Y**, Eguchi H, Nagano H, Wada H, Kobayashi S, Marubashi S, Tanemura M, Tomokuni A, Takemasa I, Umeshita K, Kanto T, Doki Y, Mori M. Circulating microRNA-21 as a novel biomarker for hepatocellular carcinoma. *J Hepatol* 2012; **56**: 167-175 [PMID: 21749846 DOI: 10.1016/j.jhep.2011.04.026]

34 **Qi P**, Cheng SQ, Wang H, Li N, Chen YF, Gao CF. Serum microRNAs as biomarkers for hepatocellular carcinoma in

Chinese patients with chronic hepatitis B virus infection. *PLoS One* 2011; **6**: e28486 [PMID: 22174818 DOI: 10.1371/journal.pone.0028486]

35 **Giray BG**, Emekdas G, Tezcan S, Ulger M, Serin MS, Sezgin O, Altintas E, Tiftik EN. Profiles of serum microRNAs; miR-125b-5p and miR223-3p serve as novel biomarkers for HBV-positive hepatocellular carcinoma. *Mol Biol Rep* 2014; **41**: 4513-4519 [PMID: 24595450 DOI: 10.1007/s11033-014-3322-3]

36 **Yang H**, Fang F, Chang R, Yang L. MicroRNA-140-5p suppresses tumor growth and metastasis by targeting transforming growth factor β receptor 1 and fibroblast growth factor 9 in hepatocellular carcinoma. *Hepatology* 2013; **58**: 205-217 [PMID: 23401231 DOI: 10.1002/hep.26315]

37 **Kwizera EA**, O'Connor R, Vinduska V, Williams M, Butch ER, Snyder SE, Chen X, Huang X. Molecular Detection and Analysis of Exosomes Using Surface-Enhanced Raman Scattering Gold Nanorods and a Miniaturized Device. *Theranostics* 2018; **8**: 2722-2738 [PMID: 29774071 DOI: 10.7150/thno.21358]

38 **Eldh M**, Olofsson Bagge R, Lässer C, Svanvik J, Sjöstrand M, Mattsson J, Lindnér P, Choi DS, Gho YS, Lötvall J. MicroRNA in exosomes isolated directly from the liver circulation in patients with metastatic uveal melanoma. *BMC Cancer* 2014; **14**: 962 [PMID: 25510783 DOI: 10.1186/1471-2407-14-962]

39 **Kogure T**, Yan IK, Lin WL, Patel T. Extracellular Vesicle-Mediated Transfer of a Novel Long Noncoding RNA TUC339: A Mechanism of Intercellular Signaling in Human Hepatocellular Cancer. *Genes Cancer* 2013; **4**: 261-272 [PMID: 24167654 DOI: 10.1177/1947601913499020]

40 **Li Y**, Zhang L, Liu F, Xiang G, Jiang D, Pu X. Identification of endogenous controls for analyzing serum exosomal miRNA in patients with hepatitis B or hepatocellular carcinoma. *Dis Markers* 2015; **2015**: 893594 [PMID: 25814782 DOI: 10.1155/2015/893594]

41 **Julich H**, Willms A, Lukacs-Kornek V, Kornek M. Extracellular vesicle profiling and their use as potential disease specific biomarker. *Front Immunol* 2014; **5**: 413 [PMID: 25225495 DOI: 10.3389/fimmu.2014.00413]

42 **Chen W**, Mao Y, Liu C, Wu H, Chen S. Exosome in Hepatocellular Carcinoma: an update. *J Cancer* 2021; **12**: 2526-2536 [PMID: 33854614 DOI: 10.7150/jca.54566]

43 **Liu C**, Wu H, Mao Y, Chen W, Chen S. Exosomal microRNAs in hepatocellular carcinoma. *Cancer Cell Int* 2021; **21**: 254 [PMID: 33964930 DOI: 10.1186/s12935-021-01941-9]

44 **Wang F**, Li L, Piontek K, Sakaguchi M, Selaru FM. Exosome miR-335 as a novel therapeutic strategy in hepatocellular carcinoma. *Hepatology* 2018; **67**: 940-954 [PMID: 29023935 DOI: 10.1002/hep.29586]

45 **Lang FM**, Hossain A, Gumin J, Momin EN, Shimizu Y, Ledbetter D, Shahar T, Yamashita S, Parker Kerrigan B, Fueyo J, Sawaya R, Lang FF. Mesenchymal stem cells as natural biofactories for exosomes carrying miR-124a in the treatment of gliomas. *Neuro Oncol* 2018; **20**: 380-390 [PMID: 29016843 DOI: 10.1093/neuonc/nox152]

World Journal of Clinical Cases

Submit a Manuscript: https://www.f6publishing.com

World J Clin Cases 2023 January 26; 11(3): 534-544

DOI: 10.12998/wjcc.v11.i3.534

ISSN 2307-8960 (online)

MINIREVIEWS

Impact of multidrug resistance on the management of bacterial infections in cirrhosis

Carlos Terra, Ângelo Zambam de Mattos, Marcelo Souza Chagas, Andre Torres, Denusa Wiltgen, Barbara Muniz Souza, Renata Mello Perez

Specialty type: Gastroenterology and hepatology

Provenance and peer review: Invited article; Externally peer reviewed.

Peer-review model: Single blind

Peer-review report's scientific quality classification

Grade A (Excellent): A
Grade B (Very good): B, B
Grade C (Good): 0
Grade D (Fair): D
Grade E (Poor): 0

P-Reviewer: Bukhari SM, Pakistan; Kreisel W, Germany; Sahle Z, Ethiopia

Received: November 10, 2022
Peer-review started: November 10, 2022
First decision: November 26, 2022
Revised: December 22, 2022
Accepted: January 5, 2023
Article in press: January 5, 2023
Published online: January 26, 2023

Carlos Terra, Marcelo Souza Chagas, Andre Torres, Barbara Muniz Souza, Gastroenterology-Liver Unit, State University of Rio de Janeiro, Rio de Janeiro 20551-030, Rio de Janeiro, Brazil

Carlos Terra, Liver Unit, Casa de Saúde São José-Rede Santa Catarina, Rio de Janeiro 22271-080, Rio de Janeiro, Brazil

Carlos Terra, Ângelo Zambam de Mattos, Marcelo Souza Chagas, Andre Torres, Denusa Wiltgen, Barbara Muniz Souza, Renata Mello Perez, Alliance of Brazilian Centers for Cirrhosis Car, The ABC Group, Rio de Janeiro 20551-030, Rio de Janeiro, Brazil

Carlos Terra, Liver Unit, Federal Hospital of Lagoa, Rio de Janeiro 22470-050, Rio de Janeiro, Brazil

Ângelo Zambam de Mattos, Graduate Program in Medicine: Hepatology, Federal University of Health Sciences of Porto Alegre, Porto Alegre 90020-090, Rio Grande do Sul, Brazil

Ângelo Zambam de Mattos, Gastroenterology and Hepatology Unit, Irmandade Santa Casa de Misericórdia de Porto Alegre, Porto Alegre 90020-090, Rio Grande do Sul, Brazil

Marcelo Souza Chagas, Internal Medicine, Federal Hospital of Lagoa, Rio de Janeiro 22470-050, Rio de Janeiro, Brazil

Denusa Wiltgen, Department of Internal Medicine, Federal University of Health Sciences of Porto Alegre, Porto Alegre 90020-090, Brazil

Renata Mello Perez, Hepatology Division, Federal University of Rio de Janeiro, Rio de Janeiro 21941-617, Rio de Janeiro, Brazil

Renata Mello Perez, IDOR, D'Or Institute for Research and Education, Rio de Janeiro 22281-100, Rio de Janeiro, Brazil

Corresponding author: Carlos Terra, MD, PhD, Associate Professor, Doctor, Gastroenterology-Liver Unit, State University of Rio de Janeiro, Boulevard 28 Setembro, 77-3rd floor-Vila Isabel, Rio de Janeiro 20551-030, Rio de Janeiro, Brazil. carlosterrario@hotmail.com

Abstract

Patients with cirrhosis have an increased risk of infection and differently from other complications, that over the years are improving in their outcomes, infections in cirrhotic patients are still a major cause of hospitalization and death

(up to 50% in-hospital mortality). Infections by multidrug-resistant organisms (MDRO) have become a major challenge in the management of cirrhotic patients with significant prognostic and cost-related impact. About one third of cirrhotic patients with bacterial infections is infected with MDR bacteria and their prevalence has increased in recent years. MDR infections have a worse prognosis compared to infections by non-resistant bacteria because they are associated with lower rate of infection resolution. An adequate management of cirrhotic patients with infections caused by MDR bacteria depends on the knowledge of some epidemiological aspects, such as the type of infection (spontaneous bacterial peritonitis, pneumonia, urinary tract infection and spontaneous bacteremia), bacteriological profile of antibiotic resistance at each health care unit and site of infection acquisition (community acquired, healthcare associated or nosocomial). Furthermore, regional variations in the prevalence of MDR infections determine that the choice of empirical antibiotic therapy must be adapted to the local microbiological epidemiology. Antibiotic treatment is the most effective measure to treat infections caused by MDRO. Therefore, optimizing antibiotic prescribing is critical to effectively treat these infections. Identification of risk factors for multidrug resistance is essential to define the best antibiotic treatment strategy in each case and the choice of an effective empirical antibiotic therapy and its early administration is cardinal to reduce mortality. On the other hand, the supply of new agents to treat these infections is very limited. Thus, specific protocols that include preventive measures must be implemented in order to limit the negative impact of this severe complication in cirrhotic patients.

Key Words: Cirrhosis; Infection; Multidrug-resistance; Bacterial; Antibiotics; Microbiota

Core Tip: Infections by multidrug-resistant organisms (MDRO) have become a major challenge in the management of cirrhotic patients with significant prognostic and cost-related impact. This review presents the main epidemiological data, clinical impact, risk factors, and the best management of cirrhotic patients infected with MDR bacteria.

Citation: Terra C, de Mattos ÂZ, Chagas MS, Torres A, Wiltgen D, Souza BM, Perez RM. Impact of multidrug resistance on the management of bacterial infections in cirrhosis. *World J Clin Cases* 2023; 11(3): 534-544
URL: https://www.wjgnet.com/2307-8960/full/v11/i3/534.htm
DOI: https://dx.doi.org/10.12998/wjcc.v11.i3.534

INTRODUCTION

The rising prevalence of multidrug-resistant organisms (MDRO) (resistant at least to one agent in three or more antimicrobial categories), extensively drug-resistant organisms (a resistance profile that compromised at least one agent in all but two or fewer antimicrobial categories), and pan drug-resistant organisms (PDRO) (resistant to all known antimicrobial agents) represents a global threat to human health[1,2]. At same time, active agents against MDRO are limited despite an increase in the availability of novel antibiotics in recent years.

Reports from the United States and Europe estimate a death toll of 29-33 patients each year associated with antimicrobial resistant microorganisms, with a huge attributable healthcare cost[2-5]. The so called "ESKAPE" pathogens [*Enterococcus faecium, Staphylococcus aureus* (*S. aureus*), *Klebsiella pneumoniae, Acinetobacter baumannii, Pseudomonas aeruginosa, and Enterobacteriaceae species*] are especially worrisome: The acquisition of antimicrobial resistance genes, in association to the classical mechanisms of antimicrobial resistance (inactivation or alteration of the antimicrobial molecule, bacterial target site modifications, reduced antibiotic penetration/accumulation, and the formation of bacterial biofilms), make ESKAPE pathogens challenging to surveillance and subsequent infections difficult to treat. The SKAPE pathogens have developed resistance against almost all antibiotics used in the clinical setting (oxazolidinones, lipopeptides, macrolides, fluoroquinolones, B-lactams, and also to antibiotics that are considered "the last line of defense", like carbapenems, glycopeptides and polymyxins). Face to the increased burden of disease and death rates due to treatment failure, the Word Health Organization has designated the SKAPE group as "priority organisms" to focus and guide research and development related to new antibiotics[1].

Over the last years cirrhosis complications are improving their outcomes with new strategies and technologies. However, infections in cirrhotic patients are still a major cause of hospitalization and death (up to 50% in-hospital mortality)[6]. Although the reasons for these imbalanced morbidity and

mortality are not totally elucidated, MDR infections may play an important role. In a recent multicentric study that assessed the epidemiology of bacterial infections in hospitalized cirrhotic patients, the overall prevalence of MDRO was 34%[7]. Another report concerning critically ill patients with decompensated cirrhosis points to 46% of isolates being MDROs at admissions. Meanwhile, MDRO isolates responsible for infection during intensive care unit stay were at 60%[8]. Different studies confirm the ominous prognosis of cirrhotic patients with infections by MDRO[9,10] (Table 1) Antimicrobial standard prescription for infection in liver cirrhosis doesn't routinely comprehend the MDRO spectrum. Cirrhosis itself increases the risk for sepsis and septic shock and when associated with an inappropriate choice of empirical antimicrobial treatment may be determinant of a worst outcome.

In this review, we describe the epidemiology, clinical settings and the current evidence-based strategies for early recognition and treatment alternatives for MDR infection in cirrhotic patients.

EPIDEMIOLOGY

Bacterial infections affect 25%-35% of hospitalized patients with cirrhosis and lead to a four-fold increase in their mortality when compared to noninfected counterparts[11]. The prognostic impact of infections is such that they are considered defining events of state 6 (end-state, late decompensation) in the clinical course of cirrhosis[12]. Moreover, infections (together with alcoholic hepatitis) are the most important drivers of acute decompensation of cirrhosis and acute-on-chronic liver failure (ACLF)[9,13,14].

Despite the evolution in medical care, there is evidence suggesting that mortality associated with infections in individuals with cirrhosis might be increasing. Our group, for instance, has demonstrated that mortality associated with spontaneous bacterial peritonitis increased from 22% to 40% in a decade [15,16]. An explanation for this finding might be the growing importance of infections caused by MDRO. In our setting, after evaluating 5800 isolates from hospitalized patients, we have shown that 38% and 44% of individuals with and without cirrhosis respectively were infected with MDRO. Furthermore, in that study, 20% of *Escherichia coli* and *Klebsiella sp* strains infecting patients with cirrhosis were extended-spectrum beta-lactamase (ESBL)-producing bacteria, and 44% of *S. aureus* strains were methicillin-resistant[17].

Additionally, a recent European study has clearly demonstrated that infections associated with MDRO are increasing in individuals with cirrhosis. The study evaluated two prospective multicenter cohorts of patients hospitalized for acute decompensation of cirrhosis or ACLF. The first cohort consisted of 1146 individuals evaluated in 2011, of which 39.7% were infected. The second cohort consisted of 883 individuals evaluated in 2018, of which 32.2% were infected. In that study, infections associated with MDRO were diagnosed in 29.2% of subjects with positive cultures in the 2011 cohort and in 37.9% of those pertaining to the 2018 cohort[10].

On a global level, another prospective cohort study has demonstrated the relevance of infections associated with MDRO in individuals with cirrhosis worldwide. The authors included 1302 infected patients with cirrhosis from 46 different centers in Europe, America and Asia. The most common infections were spontaneous bacterial peritonitis [spontaneous bacterial peritonitis (SBP), 27%], urinary tract infection (22%) and pneumonia (19%), and 57% of isolates consisted of Gram-negative bacteria. Among individuals with positive cultures, 34% were infected with MDRO, most commonly ESBL-producing *Enterobacteriaceae*, methicillin-resistant *S. aureus*, vancomycin-resistant *Enterococci*, *Pseudomonas aeruginosa*, and *Acinetobacter baumannii*. The prevalence of infections caused by MDRO was higher in Asia (51%), than in Europe (29%) or America (27%). Independent risk factors for infections with MDRO were being from Asia (and mostly from India, where MDRO were present in 73% of isolates), using antibiotics in the three months previous to hospital admission, being exposed to healthcare facilities, and the site of infection (pneumonia, skin and soft tissue infection and urinary tract infection had higher odds of being caused by MDRO)[7].

Africa and Oceania are poorly represented in studies evaluating the prevalence of MDRO in patients with cirrhosis. However, a recent retrospective cohort study has demonstrated a low prevalence of MDRO in blood cultures of patients with cirrhosis hospitalized in Australia (5.6% of admissions). Despite the low prevalence, the study has shown a significant increase in infections caused by MDRO over a decade[18], similarly to what had been previously verified in Europe[10].

PROGNOSTIC IMPACT OF MULTIDRUG RESISTANT BACTERIAL INFECTIONS

Different abnormalities related to the immune system and the occurrence of bacterial translocation from the intestinal lumen increase the susceptibility to infections in cirrhotic patients[19]. Bacterial infections are very common in cirrhosis affecting approximately 1/3 of patients with decompensated cirrhosis and are responsible for significant mortality. In a review study Arvaniti *et al*[11] evaluated 178 studies with more than 11000 patients with cirrhosis and found that infections increase mortality four-fold. In these patients delayed antibiotic treatment and inadequate empirical therapy are independently associated

Table 1 Prevalence and prognosis of multidrug-resistant organisms infections in cirrhosis

Ref.	Study design	*n*	MDR infection (%)	Mortality (%)	Comments
Piano *et al*[7]	Single center study	75	35.0	86.0	ACLF grade 2 and 3 were more frequent in MDRO infected patients
Cassini *et al* [3]	Meta-analysis	671 689	NA	4.9	Estimate the incidence of infections caused by selected antibiotic-resistant bactéria in countries of the EU and EEA in 2015
Trebicka *et al*[9]	European multicenter	376	18.9	40.8 at 28.0 d; 48.7 at 90.0 d	In infection-induced ACLF, the prevalence of MDR strains was significantly higher; severe sepsis (40.7% *vs* 21.6%), ACLF (72.3% *vs* 42.0%) and 90-d mortality (48.7% *vs* 30.7%) were more frequent in infections caused by MDR strains compared to non-MDR strains
Costabeber *et al*[17]	Retrospective	474	37.5	-	To evaluate the resistance profile of bacteria isolated from cirrhotic patients admitted to a referral hospital in Brazil
Trebicka *et al*[9]	European multicenter	520	14.8	35.1 at 28.0 d	MDROs were not significantly different between specific infections in the different European regions; MDROs were more frequently isolated in the ICU (23.8% *vs* 12.2%) and nosocomial infections (21.3% *vs* 8.3% and 6.6% in CA and HCA infections, respectively); MDROs were more prevalent in infections causing severe sepsis/shock (30.3% *vs* 12.2%) or ACLF (20.5% *vs* 9.4%)
Johnson *et al* [18]	Retrospective	3951	5.6	27.7	Presence of MDR bacteria in the blood was not associated with in-hospital mortality

ACLF: Acute on chronic liver failure; EU: European Union; EEA: European Economic Area; MDR: Multi-drug resistant; MDRO: Multi drug resistant organism; ICU: Intensive care unit; CA: Community acquired; HCA: Health-care associated; NA: Not available.

with mortality[20,21].

As stated before, recent studies suggest that about 34% of cirrhotic patients with bacterial infections are infected with MDRO[7]. Infections by MDRO have a worse prognosis because they are associated with lower rate of infection resolution with traditional empirical antibiotic treatment. In the first series (2005-2007) of a Spanish study, failure to antibiotic treatment was higher (30% *vs* 8%) in MDR infections than in susceptible bacterial infections. In addition, this study found a higher frequency of septic shock (26% *vs* 10%) and higher hospital mortality rate (25% *vs* 12%) in MDR infections compared to infections by non-resistant bacteria. An important finding of the second series (2010-2011) of this study was the higher prevalence of MDRO in nosocomial infections (39%) compared to HCA (a type of infection that occurs in patients with a previous contact with a healthcare environment, *e.g.*, hospitalization or short-term admission for at least 2 d in the previous 90 d, residence in a nursing home or a long-term care facility, or chronic hemodialysis) and community-acquired infections (20% and 0%, respectively)[22]. Similarly, an intercontinental study evaluated 1302 infected cirrhotic patients and confirmed that infections caused by MDRO were associated with a lower efficacy (40% *vs* 68%) and a longer duration (12 d[7-18] *vs* 10 d[7-15]) of empirical antibiotic treatment. Furthermore, patients with bacterial infections by multi-resistant strains had a higher incidence of septic shock (27% *vs* 13%) and higher in-hospital and 28-d mortality rate (31% *vs* 21% and 34% *vs* 22%, respectively)[7]. Finally, a meta-analysis on the impact of infections by MDRO on mortality in cirrhosis found a four times increased risk of mortality associated with bacterial resistance compared to non-resistant bacterial infections[11].

RISK FACTORS FOR MULTIDRUG RESISTANT BACTERIAL INFECTIONS

MDR infection results from an interaction of different risk factors that act synergistically. Although some risk factors have been identified, we still far from completely understand all the mechanisms involved, and there is still much to research in this field. Identifying risk factors for multidrug resistance is essential to define the best antibiotic treatment strategy in each case[21].

Previous use of antibiotics is a well-known driver for multidrug resistant infection in different clinical settings. A strong association of MDRO with previous antibiotic therapy was also observed in cirrhotic patients. Extended use of broad-spectrum antibiotics[23] and exposure to systemic antibiotics treatment for at least five days, especially in the previous three months, were highlighted as risk factors[7,24]. Prior use of beta-lactam antibiotics is especially important and has been identified as an independent predictor in the multivariate analysis[22,25]. These findings reinforce the importance of the judicious use of antibiotics in preventing MDRO emergence, with avoidance of overuse and early de-escalation strategies.

Another important risk factor for MDR infections is the previous occurrence of infections by resistant bacteria. In the multivariate analysis, infection caused by MDR bacteria in the last 6 mo increases the risk by 2.45 times[22].

Current or recent contact with the healthcare system is another important risk factor for MDR infections. A strong association between MDR infections and hospital admission has been shown in several studies[10,26,27]. Patients with nosocomial infection, hospitalization for more than 48 h, and those discharged in the last 30 d are at increased risk for MDR infections. In addition, an increased risk has been reported in patients admitted to the intensive care unit. The risk of MDR infections is also related to the duration of hospitalization and the invasiveness of the procedures performed.

Non-hospitalized patients with healthcare-associated (HCA) infections have an intermediate rate (14%-41%) of infections caused by MDRO, which is lower than in nosocomial infections (23%-39%) but higher than that observed in community-acquired infections (0%-16%). Therefore, the risk of MDR infection is directly related to where the infection was acquired (nosocomial or community-acquired)[22,26,28].

Although the association of quinolone prophylaxis with MDR infection was not identified with the use of norfloxacin for six months in a placebo-controlled trial[29] and in an epidemiological study[7], the prophylactic use of antibiotics has been pointed out as a risk factor for MDR infections in other studies [22,25,30].

The bacteriological profile of antibiotic resistance in each geographic region also influences the risk of multidrug resistance. Patients from India, other Asian centers, and South America had an increased risk of MDR bacteria[7]. The bacteriological profile of antibiotic resistance at each health care unit is also an important point, and this local antibiotic resistance profile should be considered in the estimation of the MDR risk of each patient[7,31].

MDR risk is also related to the site of the infection. For example, MDR infections were more commonly observed in patients with pneumonia, skin and soft tissue infections than in those with SBP or spontaneous bacteremia[7,27].

A higher prevalence of proton pump inhibitors (PPI) use among patients with MDR infection has been reported[24], suggesting that PPI could be a risk factor for infections caused by MDRO. However, this association still needs to be better explored in further studies.

MDR infections are more commonly observed in patients with worse liver function, however it is difficult to establish whether liver function is an independent risk factor for MDR because patients with more severe liver disease have more frequent hospitalizations and are more exposed to the use of antibiotics. In the study of Piano *et al*[7], liver function was not independently associated with MDR infections in the multivariate analysis although patients with MDR infections presented higher Child and MELD-Na scores. Therefore, even if it is not an independent risk factor, MDR infection is often associated with more severe liver disease.

Table 2 shows the main risk factors for MDR infections.

MANAGEMENT

Empirical antibiotic therapy

In the early phases of bacterial infections in patients with cirrhosis, typical signs of infection (like fever) may not be present. Bacterial infections can precipitate and/or constitute part of the process of acute decompensation of cirrhosis, and an appropriate work-up for infections (*e.g.*, diagnostic paracentesis; chest X-ray; urinalysis; blood, ascites and urine cultures) should be made in all patients hospitalized for decompensated liver disease[32].

Optimizing the prescription of antibiotics is cardinal to effectively treat infections, protect patients from harms caused by unnecessary antibiotic use, and combat antibiotic resistance. As the prevalence of MDRO differs throughout the world, the choice of an empirical antibiotic therapy should be tailored to the local microbiological epidemiology, and it should also be influenced by the type of infection (*e.g.*, SBP, urinary tract infection, pneumonia, soft tissue infection), the severity of infection, and the potential risk factors for infections caused by MDRO[32,33] (Table 1).

Effective antibiotics need to be administered as early as possible. In a retrospective cohort study of 126 cirrhotic patients with SBP-associated septic shock, each hour of delay in the appropriate antimicrobial therapy was associated with 1.86 times increase in hospital mortality[34]. In a worldwide study of hospitalized patients with cirrhosis, the administration of adequate empirical antibiotic treatment was found to be an independent and the only potentially modifiable predictor of in-hospital and 28-d mortality[7].

In the whole Canonic series, MDROs were more prevalent in infections causing severe sepsis/septic shock and/or ACLF and associated to lower resolution rate and higher mortality at 28 d, especially if treated with inadequate empirical antibiotic strategies[10]. A multicenter retrospective study of 865 consecutive patients with a first presentation of SBP in Korea pointed that empirical carbapenem treatment was significantly associated to lower in-hospital mortality than third-generation cephalosporins of among 314 critically ill patients (CLIF-SOFA scores ≥ 7; 23.1% *vs* 38.8%; aOR, 0.84;

Table 2 Risk factors for multidrug-resistant infection in cirrhosis

No.	Risk factors for MDR infection in cirrhosis
1	Prior (3 mo) use of broad-spectrum antibiotics
2	Prior infection by MDROs (6 mo)
3	Nosocomial infection
4	Recent contact with the healthcare system
5	Site of infection (pneumonia, skin, and soft tissue infections)
6	Geographic region
7	Prophylactic use of antibiotics (?)/proton pump inhibitors use?

MDR: Multi-drug resistant; MDRO: Multi drug resistant organism.

95%CI, 0.75-0.94; $P = 0.002$)[35].

In the treatment of HCA infections in an Italian population of cirrhotic patients, with a prevalence of MDRO of 40%-46%, empirical broad-spectrum therapy (imipenem/cilastatin ± vancomycin) significantly reduced in-hospital mortality when compared to third generation cephalosporins, particularly in patients with sepsis. It also reduced the rate of treatment failure and length of stay[36]. In a prospective randomized controlled trial (RCT) that enrolled 32 patients with nosocomial SBP, the broad-spectrum antibiotic therapy (meropenem plus daptomycin) was more effective than ceftazidime (86.7% *vs* 25%, $P < 0.001$). Furthermore, meropenem plus daptomycin was effective in 90% of nonresponders to ceftazidime. The response to first-line treatment was an independent predictor of survival[37].

The isolation of MDRO in rectal and nasal swabs could also guide empirical antibiotic strategies in cirrhotic patients. In a study of two European cohorts comprising a total of 907 critically ill patients, including 550 patients with cirrhosis, rectal colonization by MDRO was highly prevalent in cirrhotic patients, ranging from 28.7% to 31.1% in intensive care unit admissions, and MDRO carriage increased the short-term risk of subsequent infection by the colonizing organism[38].

Patients with cirrhosis and severe infections may benefit from therapeutic strategies aimed at optimizing the antibiotics' pharmacokinetic/pharmacodynamic target. The use of high antibiotic doses within the first 48-72 h after the diagnosis of infection and the continuous or extended infusions of beta-lactams are more likely to achieve and to maintain serum drug levels above the minimum inhibitory concentration compared to standard bolus administration 6. In a secondary analysis of a European prospective multicenter study of patients with cirrhosis and bloodstream infection, the empirical continuous/extended infusion of piperacillin-tazobactam or carbapenems was associated with lower mortality compared to traditional dosing schedules (adjusted hazard ratio, 0.41; 95%CI, 0.110-0.936; $P = 0.04$), and it was particularly useful in those patients who were critically ill[39].

After completing 48-72 h of antibiotic therapy, early de-escalation can be considered based on clinical evolution and available antibiotic susceptibility tests. Short-term treatment is another key measure to prevent antibiotic resistance[7,40,41]. In the 1990s, a randomized controlled trial of 100 patients with SBP showed that a short-course (5-d) treatment is as effective as long-course (10-d) therapy and significantly less expensive[42]. In non-SBP infections, the optimal duration of antibiotic therapy has not been established, but data from the general population suggests that a 7-d course is adequate for most infections[32].

Figure 1 and Table 3 summarizes the management of patients with cirrhosis and bacterial infection.

Non-antibiotic approach

The emergence and spread of MDRO in cirrhosis require the implementation of measures aimed to prevent its complications. Pharmacological and non-pharmacological strategies are needed, including hand hygiene and barrier precaution, restriction of antibiotic use to high-risk populations, de-escalating antibiotic therapy based on rapid microbiological tests, study of non-antibiotic prophylaxis measures, broad and strict infection control policies, and programs of epidemiological surveillance[25].

Non-antibiotic drugs with potential benefit on infections in cirrhosis: Although antibiotic treatment is the most effective measure for controlling established MDR infection, other drugs have shown potential benefits in preventing infections in cirrhosis. A lower occurrence of SBP has been demonstrated in patients using non-selective beta-blockers (NSBB)[43]. This benefit of NSBB has been related to its potential effect in improving intestinal motility, improving intestinal permeability, and reducing bacterial translocation[44,45]. Statins also seem to have a beneficial effect against bacterial infection[46] that is attributed to its anti-inflammatory and immunomodulatory properties.

Table 3 Recommended empirical antibiotic treatment for bacterial infection in cirrhosis

Type of infection	Community-acquired infection	Nosocomial and HCA infection or sepsis
SBP, spontaneous bacterial empyema and spontaneous bacteremia	Cefotaxime or Amoxicilin/clavulanic acid	Piperacillin/tazobactam or Meropenem ± Vancomycin or Daptomycin or Linezolid[1]
UTI	Fosfomycin or cotrimoxazole	Uncomplicated: Nitrofurantoin or Fosfomycin; if sepsis: Piperacillin/tazobactam or Meropenem ± Glycopeptide
Pneumonia	Amoxicilin/clavulanic acid; Ceftriaxone + Macrolide; Levofloxacin; Moxifloxacin	Piperacillin/tazobactam or Meropenem or Ceftazidime + Ciprofloxacin; Glycopeptides or Linezolid[1] should be added in patients with risk factors for MRSA[2]
Skin and soft tissue infections	Amoxicilin/clavulanic acidor ± Clindamycin	Meropenem or Piperacillin/tazobactam + Glycopeptide or Daptomycin or Linezolid[1] ± Cindamycin; if necrotizing fascitis: Meropenem + Daptomycin + Clindamycin

[1]Vancomycin, teicoplanin or daptomycin in areas with a high prevalence Methicillin-resistant Staphylococcus aureus and vancomycin-susceptible enterococci. Vancomycin must be replaced by linezolid in areas with a high prevalence of vancomycin-resistant enterococci.
[2]Ventilator-associated pneumonia, previous antibiotic therapy, nasal Methicillin-resistant Staphylococcus aureus carriage.
HCA: Health care associated; MRSA: Methicillin-resistant Staphylococcus aureus; SBP: Spontaneous bacterial peritonitis; UTI: Urinary tract infection.

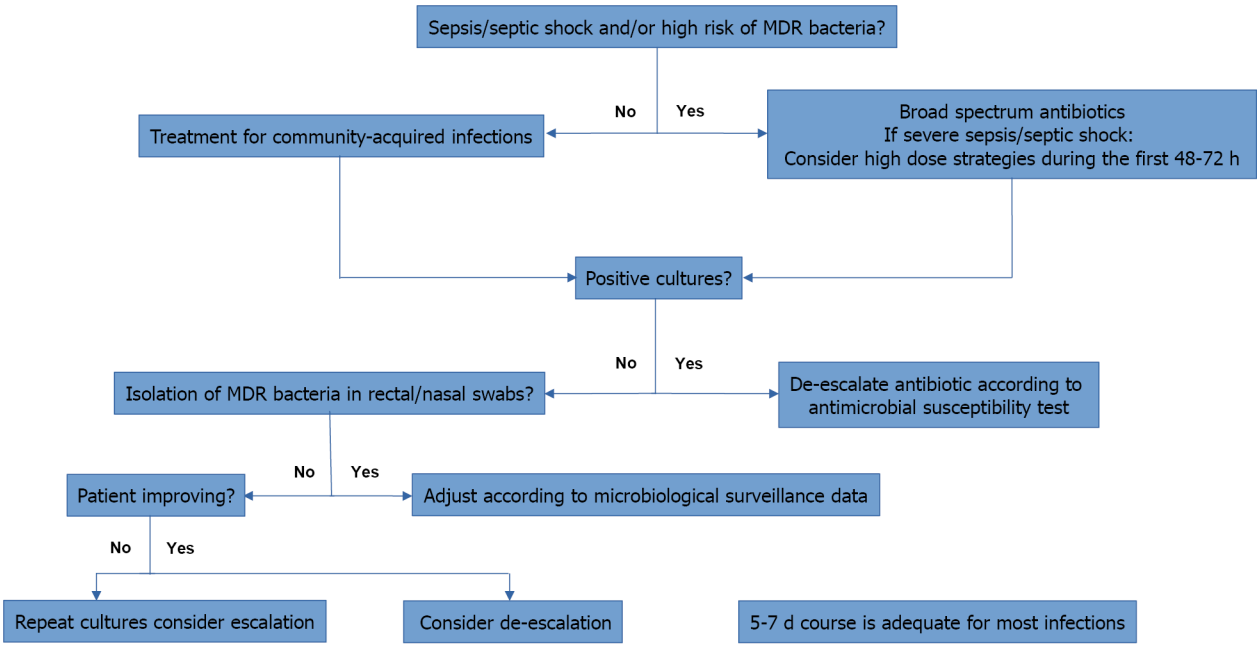

DOI: 10.12998/wjcc.v11.i3.534

Figure 1 Suggested algorithm for the management of patients with cirrhosis and bacterial infections. MDR: Multidrug-resistant.

Non-pharmacological measures: Non-pharmacological measures are based on preventive strategies and procedures focusing on intestinal colonization with MDRO. The most important preventive measure is the restrictive and judicious antibiotic use since the main driver for the emergence of MDR infections is the widespread use of antibiotics.

The main non-pharmacological measures focus on gut microbiota[27]. A healthy microbiome is essential to prevent colonization and infection by MDRO[25]. Different approaches focusing on the modulation of the intestinal microbiome were studied, such as probiotics, prebiotics/synbiotics dietary regimens, and fecal microbiota transplant (FMT)[45].

Although some studies have shown favorable results with probiotics, there are also negative studies. This controversy is probably related to different probiotics used and the different number and concentration of the species. Further studies are necessary to define the ideal combination, dose, and duration of administration.

FMT involves the safe transfer of exogenous bacterial flora from a healthy donor to another patient, in capsule or liquid formulations. The rationale for using this technique is the central role of the gastrointestinal colonization in the development of MDR infections. It has been demonstrated that colonization by MDRO is associated with increased risk of infection by the colonizing bacteria in the

short-term[38]. FMT has the potential effect of promoting MDRO decolonization.

A systematic review with meta-analysis[47] of five studies, with a total number of 52 patients, evaluated whether FMT decolonizes antibiotic-resistant bacteria from the gut of colonized adults. Evidence from this meta-analysis indicates a potential benefit of FMT as a decolonization intervention, with few adverse effects. Despite the low quality of evidence appointed by this meta-analysis, these preliminary results suggest that FMT is a promising approach that deserves further analysis in RCTs.

In cirrhotic patients, a preliminary study of FMT in patients with advanced cirrhosis on lactulose and rifaximin demonstrated that FMT restored antibiotic-associated disruption in microbial diversity and function[48]. The impact of FMT in the reduction of gut microbial antibiotic resistance genes was later reported in two trials: a capsule FMT trial and an enema FMT trial with 20 patients each. This study demonstrated that, despite differences in routes of administration, antibiotic resistance gene abundance was reduced after FMT compared to pre-FMT baseline and non-FMT groups in decompensated cirrhosis[49].

Another possible approach, although still requiring further studies, is phage therapy. This technique is based on the use of bacteriophages which are viruses that infect bacteria[50]. The bacteriophages replicate inside the bacteria leading to their destruction. It is an old technique that was left aside with the advent of antibiotics, but nowadays it has been considered again as a therapeutic option to face the serious problem of antibiotic multidrug resistance[51,52]. Although specific studies in cirrhotic patients are not available, phage therapy represents a possible future alternative therapy for controlling MDRO [53].

CONCLUSION

In this review, we describe the epidemiology, clinical settings and the current evidence-based strategies for early recognition and treatment alternatives for MDR infection in cirrhotic patients.

FOOTNOTES

Author contributions: Terra C, de Mattos ÂZ, Chagas MS, Torres A, Wiltgen D, Souza BM, and Perez RM performed the research, analyzed the data, and wrote the manuscript; all authors have read and approve the final manuscript.

Conflict-of-interest statement: All authors report no relevant conflicts of interest for this article.

Country/Territory of origin: Brazil

ORCID number: Carlos Terra 0000-0003-3069-128X; Ângelo Zambam de Mattos 0000-0002-3063-0199; Marcelo Souza Chagas 0000-0002-1418-1696; Andre Torres 0000-0002-4994-7137; Denusa Wiltgen 0000-0002-7334-2779; Barbara Muniz Souza 0000-0001-7061-1788; Renata Mello Perez 0000-0002-3367-9991.

S-Editor: Chen YL
L-Editor: A
P-Editor: Chen YL

REFERENCES

1 **Magiorakos AP**, Srinivasan A, Carey RB, Carmeli Y, Falagas ME, Giske CG, Harbarth S, Hindler JF, Kahlmeter G, Olsson-Liljequist B, Paterson DL, Rice LB, Stelling J, Struelens MJ, Vatopoulos A, Weber JT, Monnet DL. Multidrug-resistant, extensively drug-resistant and pandrug-resistant bacteria: an international expert proposal for interim standard definitions for acquired resistance. *Clin Microbiol Infect* 2012; **18**: 268-281 [PMID: 21793988 DOI: 10.1111/j.1469-0691.2011.03570.x]

2 **Kadri SS**. Key Takeaways From the U.S. CDC's 2019 Antibiotic Resistance Threats Report for Frontline Providers. *Crit Care Med* 2020; **48**: 939-945 [PMID: 32282351 DOI: 10.1097/CCM.0000000000004371]

3 **Cassini A**, Högberg LD, Plachouras D, Quattrocchi A, Hoxha A, Simonsen GS, Colomb-Cotinat M, Kretzschmar ME, Devleesschauwer B, Cecchini M, Ouakrim DA, Oliveira TC, Struelens MJ, Suetens C, Monnet DL; Burden of AMR Collaborative Group. Attributable deaths and disability-adjusted life-years caused by infections with antibiotic-resistant bacteria in the EU and the European Economic Area in 2015: a population-level modelling analysis. *Lancet Infect Dis*

2019; **19**: 56-66 [PMID: 30409683 DOI: 10.1016/S1473-3099(18)30605-4]
4 **Weist K**, Högberg LD. ECDC publishes 2015 surveillance data on antimicrobial resistance and antimicrobial consumption in Europe. *Euro Surveill* 2016; **21** [PMID: 27918266 DOI: 10.2807/1560-7917.ES.2016.21.46.30399]
5 **Serra-Burriel M**, Keys M, Campillo-Artero C, Agodi A, Barchitta M, Gikas A, Palos C, López-Casasnovas G. Impact of multi-drug resistant bacteria on economic and clinical outcomes of healthcare-associated infections in adults: Systematic review and meta-analysis. *PLoS One* 2020; **15**: e0227139 [PMID: 31923281 DOI: 10.1371/journal.pone.0227139]
6 **Fernández J**, Piano S, Bartoletti M, Wey EQ. Management of bacterial and fungal infections in cirrhosis: The MDRO challenge. *J Hepatol* 2021; **75** Suppl 1: S101-S117 [PMID: 34039482 DOI: 10.1016/j.jhep.2020.11.010]
7 **Piano S**, Singh V, Caraceni P, Maiwall R, Alessandria C, Fernandez J, Soares EC, Kim DJ, Kim SE, Marino M, Vorobioff J, Barea RCR, Merli M, Elkrief L, Vargas V, Krag A, Singh SP, Lesmana LA, Toledo C, Marciano S, Verhelst X, Wong F, Intagliata N, Rabinowich L, Colombato L, Kim SG, Gerbes A, Durand F, Roblero JP, Bhamidimarri KR, Boyer TD, Maevskaya M, Fassio E, Kim HS, Hwang JS, Gines P, Gadano A, Sarin SK, Angeli P; International Club of Ascites Global Study Group. Epidemiology and Effects of Bacterial Infections in Patients With Cirrhosis Worldwide. *Gastroenterology* 2019; **156**: 1368-1380.e10 [PMID: 30552895 DOI: 10.1053/j.gastro.2018.12.005]
8 **Fischer P**, Pandrea S, Dan Grigorescu M, Stefanescu H, Tefas C, Hadade A, Procopet B, Ionescu D. The threat of carbapenem resistance in Eastern Europe in patients with decompensated cirrhosis admitted to intensive care unit. *Dig Liver Dis* 2022; **54**: 1385-1391 [PMID: 35732546 DOI: 10.1016/j.dld.2022.05.011]
9 **Trebicka J**, Fernandez J, Arroyo V; PREDICT STUDY group of the EASL-CLIF CONSORTIUM. Reply to: Correspondence on 'The PREDICT study uncovers three clinical courses of acutely decompensated cirrhosis that have distinct pathophysiology'. *J Hepatol* 2021; **74**: 480-481 [PMID: 33279257 DOI: 10.1016/j.jhep.2020.11.019]
10 **Fernández J**, Prado V, Trebicka J, Amoros A, Gustot T, Wiest R, Deulofeu C, Garcia E, Acevedo J, Fuhrmann V, Durand F, Sánchez C, Papp M, Caraceni P, Vargas V, Bañares R, Piano S, Janicko M, Albillos A, Alessandria C, Soriano G, Welzel TM, Laleman W, Gerbes A, De Gottardi A, Merli M, Coenraad M, Saliba F, Pavesi M, Jalan R, Ginès P, Angeli P, Arroyo V; European Foundation for the Study of Chronic Liver Failure (EF-Clif). Multidrug-resistant bacterial infections in patients with decompensated cirrhosis and with acute-on-chronic liver failure in Europe. *J Hepatol* 2019; **70**: 398-411 [PMID: 30391380 DOI: 10.1016/j.jhep.2018.10.027]
11 **Arvaniti V**, D'Amico G, Fede G, Manousou P, Tsochatzis E, Pleguezuelo M, Burroughs AK. Infections in patients with cirrhosis increase mortality four-fold and should be used in determining prognosis. *Gastroenterology* 2010; **139**: 1246-1256, 1256.e1 [PMID: 20558165 DOI: 10.1053/j.gastro.2010.06.019]
12 **D'Amico G**, Morabito A, D'Amico M, Pasta L, Malizia G, Rebora P, Valsecchi MG. Clinical states of cirrhosis and competing risks. *J Hepatol* 2018; **68**: 563-576 [PMID: 29111320 DOI: 10.1016/j.jhep.2017.10.020]
13 **Moreau R**, Jalan R, Gines P, Pavesi M, Angeli P, Cordoba J, Durand F, Gustot T, Saliba F, Domenicali M, Gerbes A, Wendon J, Alessandria C, Laleman W, Zeuzem S, Trebicka J, Bernardi M, Arroyo V; CANONIC Study Investigators of the EASL-CLIF Consortium. Acute-on-chronic liver failure is a distinct syndrome that develops in patients with acute decompensation of cirrhosis. *Gastroenterology* 2013; **144**: 1426-1437, 1437.e1 [PMID: 23474284 DOI: 10.1053/j.gastro.2013.02.042]
14 **O'Leary JG**, Reddy KR, Garcia-Tsao G, Biggins SW, Wong F, Fallon MB, Subramanian RM, Kamath PS, Thuluvath P, Vargas HE, Maliakkal B, Tandon P, Lai J, Thacker LR, Bajaj JS. NACSELD acute-on-chronic liver failure (NACSELD-ACLF) score predicts 30-day survival in hospitalized patients with cirrhosis. *Hepatology* 2018; **67**: 2367-2374 [PMID: 29315693 DOI: 10.1002/hep.29773]
15 **Coral G**, de Mattos AA, Damo DF, Viégas AC. [Prevalence and prognosis of spontaneous bacterial peritonitis. Experience in patients from a general hospital in Porto Alegre, RS, Brazil (1991-2000)]. *Arq Gastroenterol* 2002; **39**: 158-162 [PMID: 12778307 DOI: 10.1590/s0004-28032002000300005]
16 **Musskopf MI**, Fonseca FP, Gass J, de Mattos AZ, John JA, de Mello Brandão AB. Prognostic factors associated with in-hospital mortality in patients with spontaneous bacterial peritonitis. *Ann Hepatol* 2012; **11**: 915-920 [PMID: 23109456]
17 **Costabeber AM**, Mattos AA, Sukiennik TC. Prevalence of bacterial resistance in hospitalized Cirrhotic patients in southern brazil: A new challenge. *Rev Inst Med Trop Sao Paulo* 2016; **58**: 36 [PMID: 27253738 DOI: 10.1590/S1678-9946201658036]
18 **Johnson AL**, Ratnasekera IU, Irvine KM, Henderson A, Powell EE, Valery PC. Bacteraemia, sepsis and antibiotic resistance in Australian patients with cirrhosis: a population-based study. *BMJ Open Gastroenterol* 2021; **8** [PMID: 34876410 DOI: 10.1136/bmjgast-2021-000695]
19 **Thulstrup AM**, Sørensen HT, Schønheyder HC, Møller JK, Tage-Jensen U. Population-based study of the risk and short-term prognosis for bacteremia in patients with liver cirrhosis. *Clin Infect Dis* 2000; **31**: 1357-1361 [PMID: 11096002 DOI: 10.1086/317494]
20 **Bartoletti M**, Giannella M, Lewis R, Caraceni P, Tedeschi S, Paul M, Schramm C, Bruns T, Merli M, Cobos-Trigueros N, Seminari E, Retamar P, Muñoz P, Tumbarello M, Burra P, Torrani Cerenzia M, Barsic B, Calbo E, Maraolo AE, Petrosillo N, Galan-Ladero MA, D'Offizi G, Bar Sinai N, Rodríguez-Baño J, Verucchi G, Bernardi M, Viale P; ESGBIS/BICHROME Study Group. A prospective multicentre study of the epidemiology and outcomes of bloodstream infection in cirrhotic patients. *Clin Microbiol Infect* 2018; **24**: 546.e1-546.e8 [PMID: 28818628 DOI: 10.1016/j.cmi.2017.08.001]
21 **Arabi YM**, Dara SI, Memish Z, Al Abdulkareem A, Tamim HM, Al-Shirawi N, Parrillo JE, Dodek P, Lapinsky S, Feinstein D, Wood G, Dial S, Zanotti S, Kumar A; Cooperative Antimicrobial Therapy of Septic Shock (CATSS) Database Research Group. Antimicrobial therapeutic determinants of outcomes from septic shock among patients with cirrhosis. *Hepatology* 2012; **56**: 2305-2315 [PMID: 22753144 DOI: 10.1002/hep.25931]
22 **Fernández J**, Acevedo J, Castro M, Garcia O, de Lope CR, Roca D, Pavesi M, Sola E, Moreira L, Silva A, Seva-Pereira T, Corradi F, Mensa J, Ginès P, Arroyo V. Prevalence and risk factors of infections by multiresistant bacteria in cirrhosis: a prospective study. *Hepatology* 2012; **55**: 1551-1561 [PMID: 22183941 DOI: 10.1002/hep.25532]
23 **Zhong L**, Men TY, Li H, Peng ZH, Gu Y, Ding X, Xing TH, Fan JW. Multidrug-resistant gram-negative bacterial infections after liver transplantation - spectrum and risk factors. *J Infect* 2012; **64**: 299-310 [PMID: 22198738 DOI: 10.1016/j.jinf.2011.12.005]

24 **Figueiredo LM**, Rafael MA, Alexandrino G, Branco JC, Carvalho R, Costa MN, Martins A. Risk factors for the emergence of multidrug-resistant organisms in liver cirrhosis. *Gastroenterol Hepatol* 2022; **45**: 186-191 [PMID: 34052400 DOI: 10.1016/j.gastrohep.2021.04.006]

25 **Fernández J**, Bert F, Nicolas-Chanoine MH. The challenges of multi-drug-resistance in hepatology. *J Hepatol* 2016; **65**: 1043-1054 [PMID: 27544545 DOI: 10.1016/j.jhep.2016.08.006]

26 **Jalan R**, Fernandez J, Wiest R, Schnabl B, Moreau R, Angeli P, Stadlbauer V, Gustot T, Bernardi M, Canton R, Albillos A, Lammert F, Wilmer A, Mookerjee R, Vila J, Garcia-Martinez R, Wendon J, Such J, Cordoba J, Sanyal A, Garcia-Tsao G, Arroyo V, Burroughs A, Ginès P. Bacterial infections in cirrhosis: a position statement based on the EASL Special Conference 2013. *J Hepatol* 2014; **60**: 1310-1324 [PMID: 24530646 DOI: 10.1016/j.jhep.2014.01.024]

27 **Gallaher CE**, Shawcross DL. Management of Multidrug-Resistant Infections in Cirrhosis. *Semin Liver Dis* 2022; **42**: 173-187 [PMID: 35130574 DOI: 10.1055/a-1765-0056]

28 **Merli M**, Lucidi C, Giannelli V, Giusto M, Riggio O, Falcone M, Ridola L, Attili AF, Venditti M. Cirrhotic patients are at risk for health care-associated bacterial infections. *Clin Gastroenterol Hepatol* 2010; **8**: 979-985 [PMID: 20621200 DOI: 10.1016/j.cgh.2010.06.024]

29 **Moreau R**, Elkrief L, Bureau C, Perarnau JM, Thévenot T, Saliba F, Louvet A, Nahon P, Lannes A, Anty R, Hillaire S, Pasquet B, Ozenne V, Rudler M, Ollivier-Hourmand I, Robic MA, d'Alteroche L, Di Martino V, Ripault MP, Pauwels A, Grangé JD, Carbonell N, Bronowicki JP, Payancé A, Rautou PE, Valla D, Gault N, Lebrec D; NORFLOCIR Trial Investigators. Effects of Long-term Norfloxacin Therapy in Patients With Advanced Cirrhosis. *Gastroenterology* 2018; **155**: 1816-1827.e9 [PMID: 30144431 DOI: 10.1053/j.gastro.2018.08.026]

30 **Salerno F**, Borzio M, Pedicino C, Simonetti R, Rossini A, Boccia S, Cacciola I, Burroughs AK, Manini MA, La Mura V, Angeli P, Bernardi M, Dalla Gasperina D, Dionigi E, Dibenedetto C, Arghittu M; AISF Investigators. The impact of infection by multidrug-resistant agents in patients with cirrhosis. A multicenter prospective study. *Liver Int* 2017; **37**: 71-79 [PMID: 27364035 DOI: 10.1111/Liv.13195]

31 **Aguirre-García J**. Comment on: Ruelas-Villavicencio A L, et. al. "In whom, how and how often is surveillance for hepatocellular carcinoma cost-effective? *Ann Hepatol* 2005; **4**: 289 [PMID: 16432498 DOI: 10.1016/j.aohep.2022.100719]

32 **Piano S**, Tonon M, Angeli P. Changes in the epidemiology and management of bacterial infections in cirrhosis. *Clin Mol Hepatol* 2021; **27**: 437-445 [PMID: 33504138 DOI: 10.3350/cmh.2020.0329]

33 **Miranda-Zazueta G**, León-Garduño LAP, Aguirre-Valadez J, Torre-Delgadillo A. Bacterial infections in cirrhosis: Current treatment. *Ann Hepatol* 2020; **19**: 238-244 [PMID: 32317149 DOI: 10.1016/j.aohep.2019.09.011]

34 **Karvellas CJ**, Abraldes JG, Arabi YM, Kumar A; Cooperative Antimicrobial Therapy of Septic Shock (CATSS) Database Research Group. Appropriate and timely antimicrobial therapy in cirrhotic patients with spontaneous bacterial peritonitis-associated septic shock: a retrospective cohort study. *Aliment Pharmacol Ther* 2015; **41**: 747-757 [PMID: 25703246 DOI: 10.1111/apt.13135]

35 **Kim SW**, Yoon JS, Park J, Jung YJ, Lee JS, Song J, Lee HA, Seo YS, Lee M, Park JM, Choi DH, Kim MY, Kang SH, Yang JM, Song DS, Chung SW, Kim MA, Jang HJ, Oh H, Lee CH, Lee YB, Cho EJ, Yu SJ, Kim YJ, Yoon JH, Lee JH. Empirical Treatment With Carbapenem vs Third-generation Cephalosporin for Treatment of Spontaneous Bacterial Peritonitis. *Clin Gastroenterol Hepatol* 2021; **19**: 976-986.e5 [PMID: 32623007 DOI: 10.1016/j.cgh.2020.06.046]

36 **Merli M**, Lucidi C, Di Gregorio V, Lattanzi B, Giannelli V, Giusto M, Farcomeni A, Ceccarelli G, Falcone M, Riggio O, Venditti M. An empirical broad spectrum antibiotic therapy in health-care-associated infections improves survival in patients with cirrhosis: A randomized trial. *Hepatology* 2016; **63**: 1632-1639 [PMID: 26529126 DOI: 10.1002/hep.28332]

37 **Piano S**, Fasolato S, Salinas F, Romano A, Tonon M, Morando F, Cavallin M, Gola E, Sticca A, Loregian A, Palù G, Zanus G, Senzolo M, Burra P, Cillo U, Angeli P. The empirical antibiotic treatment of nosocomial spontaneous bacterial peritonitis: Results of a randomized, controlled clinical trial. *Hepatology* 2016; **63**: 1299-1309 [PMID: 26084406 DOI: 10.1002/hep.27941]

38 **Prado V**, Hernández-Tejero M, Mücke MM, Marco F, Gu W, Amoros A, Toapanta D, Reverter E, Peña-Ramirez C, Altenpeter L, Bassegoda O, Mezzano G, Aziz F, Juanola A, Rodríguez-Tajes S, Chamorro V, López D, Reyes M, Hogardt M, Kempf VAJ, Ferstl PG, Zeuzem S, Martínez JA, Vila J, Arroyo V, Trebicka J, Fernandez J. Rectal colonization by resistant bacteria increases the risk of infection by the colonizing strain in critically ill patients with cirrhosis. *J Hepatol* 2022; **76**: 1079-1089 [PMID: 35074475 DOI: 10.1016/j.jhep.2021.12.042]

39 **Bartoletti M**, Giannella M, Lewis RE, Caraceni P, Tedeschi S, Paul M, Schramm C, Bruns T, Merli M, Cobos-Trigueros N, Seminari E, Retamar P, Muñoz P, Tumbarello M, Burra P, Torrani Cerenzia M, Barsic B, Calbo E, Maraolo AE, Petrosillo N, Galan-Ladero MA, D'Offizi G, Zak-Doron Y, Rodriguez-Baño J, Baldassarre M, Verucchi G, Domenicali M, Bernardi M, Viale P; ESGBIS/BICHROME study group. Extended Infusion of β-Lactams for Bloodstream Infection in Patients With Liver Cirrhosis: An Observational Multicenter Study. *Clin Infect Dis* 2019; **69**: 1731-1739 [PMID: 30649218 DOI: 10.1093/cid/ciz032]

40 **Fernández J**, Tandon P, Mensa J, Garcia-Tsao G. Antibiotic prophylaxis in cirrhosis: Good and bad. *Hepatology* 2016; **63**: 2019-2031 [PMID: 26528864 DOI: 10.1002/hep.28330]

41 **Allaire M**, Cadranel JF, Nguyen TTN, Garioud A, Zougmore H, Heng R, Perignon C, Ollivier-Hourmand I, Dao T. Management of infections in patients with cirrhosis in the context of increasing therapeutic resistance: A systematic review. *Clin Res Hepatol Gastroenterol* 2020; **44**: 264-274 [PMID: 31706985 DOI: 10.1016/j.clinre.2019.10.003]

42 **Runyon BA**, McHutchison JG, Antillon MR, Akriviadis EA, Montano AA. Short-course versus long-course antibiotic treatment of spontaneous bacterial peritonitis. A randomized controlled study of 100 patients. *Gastroenterology* 1991; **100**: 1737-1742 [PMID: 2019378 DOI: 10.1016/0016-5085(91)90677-d]

43 **Senzolo M**, Cholongitas E, Burra P, Leandro G, Thalheimer U, Patch D, Burroughs AK. beta-Blockers protect against spontaneous bacterial peritonitis in cirrhotic patients: a meta-analysis. *Liver Int* 2009; **29**: 1189-1193 [PMID: 19508620 DOI: 10.1111/j.1478-3231.2009.02038.x]

44 **Reiberger T**, Ferlitsch A, Payer BA, Mandorfer M, Heinisch BB, Hayden H, Lammert F, Trauner M, Peck-Radosavljevic M, Vogelsang H; Vienna Hepatic Hemodynamic Lab. Non-selective betablocker therapy decreases intestinal permeability and serum levels of LBP and IL-6 in patients with cirrhosis. *J Hepatol* 2013; **58**: 911-921 [PMID: 23262249 DOI:

10.1016/j.jhep.2012.12.011]
45 **Yan K**, Garcia-Tsao G. Novel prevention strategies for bacterial infections in cirrhosis. *Expert Opin Pharmacother* 2016; **17**: 689-701 [PMID: 26799197 DOI: 10.1517/14656566.2016.1145663]
46 **Motzkus-Feagans C**, Pakyz AL, Ratliff SM, Bajaj JS, Lapane KL. Statin use and infections in Veterans with cirrhosis. *Aliment Pharmacol Ther* 2013; **38**: 611-618 [PMID: 23889738 DOI: 10.1111/apt.12430]
47 **Tavoukjian V**. Faecal microbiota transplantation for the decolonization of antibiotic-resistant bacteria in the gut: a systematic review and meta-analysis. *J Hosp Infect* 2019; **102**: 174-188 [PMID: 30926290 DOI: 10.1016/j.jhin.2019.03.010]
48 **Bajaj JS**, Kakiyama G, Savidge T, Takei H, Kassam ZA, Fagan A, Gavis EA, Pandak WM, Nittono H, Hylemon PB, Boonma P, Haag A, Heuman DM, Fuchs M, John B, Sikaroodi M, Gillevet PM. Antibiotic-Associated Disruption of Microbiota Composition and Function in Cirrhosis Is Restored by Fecal Transplant. *Hepatology* 2018; **68**: 1549-1558 [PMID: 29665102 DOI: 10.1002/hep.30037]
49 **Bajaj JS**, Shamsaddini A, Fagan A, Sterling RK, Gavis E, Khoruts A, Fuchs M, Lee H, Sikaroodi M, Gillevet PM. Fecal Microbiota Transplant in Cirrhosis Reduces Gut Microbial Antibiotic Resistance Genes: Analysis of Two Trials. *Hepatol Commun* 2021; **5**: 258-271 [PMID: 33553973 DOI: 10.1002/hep4.1639]
50 **Principi N**, Silvestri E, Esposito S. Advantages and Limitations of Bacteriophages for the Treatment of Bacterial Infections. *Front Pharmacol* 2019; **10**: 513 [PMID: 31139086 DOI: 10.3389/fphar.2019.00513]
51 **Golkar Z**, Bagasra O, Pace DG. Bacteriophage therapy: a potential solution for the antibiotic resistance crisis. *J Infect Dev Ctries* 2014; **8**: 129-136 [PMID: 24518621 DOI: 10.3855/jidc.3573]
52 **Kortright KE**, Chan BK, Koff JL, Turner PE. Phage Therapy: A Renewed Approach to Combat Antibiotic-Resistant Bacteria. *Cell Host Microbe* 2019; **25**: 219-232 [PMID: 30763536 DOI: 10.1016/j.chom.2019.01.014]
53 **Fauconnier A**, Nagel TE, Fauconnier C, Verbeken G, De Vos D, Merabishvili M, Pirnay JP. The Unique Role That WHO Could Play in Implementing Phage Therapy to Combat the Global Antibiotic Resistance Crisis. *Front Microbiol* 2020; **11**: 1982 [PMID: 33013742 DOI: 10.3389/fmicb.2020.01982]

World Journal of Clinical Cases

Submit a Manuscript: https://www.f6publishing.com

World J Clin Cases 2023 January 26; 11(3): 545-555

DOI: 10.12998/wjcc.v11.i3.545

ISSN 2307-8960 (online)

MINIREVIEWS

Could there be an interplay between periodontal changes and pancreatic malignancies?

Bogdan Silviu Ungureanu, Dorin Nicolae Gheorghe, Flavia Mirela Nicolae, Sandu Râmboiu, Petru Adrian Radu, Valeriu Marin Șurlin, Victor Dan Eugen Strâmbu, Dan Ionut Gheonea, Alexandra Roman, Petra Șurlin

Specialty type: Medicine, research and experimental

Provenance and peer review: Invited article; Externally peer reviewed.

Peer-review model: Single blind

Peer-review report's scientific quality classification

Grade A (Excellent): 0
Grade B (Very good): B, B
Grade C (Good): 0
Grade D (Fair): 0
Grade E (Poor): 0

P-Reviewer: Ksiazek M, Poland; Sun SY, China

Received: November 18, 2022
Peer-review started: November 18, 2022
First decision: December 10, 2022
Revised: December 19, 2022
Accepted: January 10, 2023
Article in press: January 10, 2023
Published online: January 26, 2023

Bogdan Silviu Ungureanu, Dan Ionut Gheonea, Department of Gastroenterology, University of Medicine and Pharmacy of Craiova, Craiova 200349, Romania

Dorin Nicolae Gheorghe, Flavia Mirela Nicolae, Petra Șurlin, Department of Periodontology, Research Center of Periodontal-Systemic Implications, University of Medicine and Pharmacy of Craiova, Craiova 200349, Romania

Sandu Râmboiu, Valeriu Marin Șurlin, Department 1st of Surgery, University of Medicine and Pharmacy of Craiova, Craiova 200349, Romania

Petru Adrian Radu, Victor Dan Eugen Strâmbu, Department of General Surgery, "Carol Davila" University of Medicine and Pharmacy, Bucharest 020021, Romania

Alexandra Roman, Department of Periodontology, "Iuliu Haţieganu" University of Medicine and Pharmacy, Cluj-Napoca 400012, Romania

Corresponding author: Flavia Mirela Nicolae, MD, Doctor, Researcher, Department of Periodontology, Research Center of Periodontal-Systemic Implications, University of Medicine and Pharmacy of Craiova, Str. Petru Rareș, nr. 2, Craiova 200349, Romania.
flavia.nicolae23@yahoo.com

Abstract

The term "periodontal disease" refers to a group of chronic inflammatory illnesses caused by specific microorganisms from subgingival biofilm, that affect the tooth-supporting tissues. Recent research has also shown that periodontal infection plays a role in aggravating systemic disease states at distal sites, reinforcing the significance of the oral cavity for general health. Additionally, it has been suggested that gastroenterological malignancies may be promoted by hemato-genous, enteral or lymphatic translocation of periopathogens. In the past 25 years, the global burden of pancreatic cancer (PC) has more than doubled, making it one of the major causes of cancer-related mortality. Periodontitis has been linked to at least 50% increased risk of PC and it could be considered a risk factor for this malignancy. A recent study performed on 59000 African American women with a follow up of 21 years showed that participants who had poor dental health had higher chances of PC. The findings, according to researchers, might be related to the inflammation that some oral bacteria trigger. Regarding the mortality of PC, periodontitis considerably raises the chance of dying from PC. Microbiome

alterations in the gut, oral cavity and pancreatic tissues of PC patients occur when compared to healthy flora, demonstrating a link between PC and microecology. Inflammation may also contribute to PC development, although the underlying pathway is not yet known. The function of the microbiome in PC risk has drawn more focus over the last decade. Future risk of PC has been linked to the oral microbiome, specifically increased levels of *Porphyromonas gingivalis* and *Aggregatibacter actinomycetemcomitans* and decreased relative abundance of *Leptotrichia* and *Fusobacteria*, suggesting that it may have an impact on the inflammatory condition by expanding, altering, and regulating the commensal microbiome. Patients who received periodontal treatment had significantly decreased incidence rate ratios for PC. By analyzing patterns in the microbiome composition throughout PC development and establishing strategies to enhance the cancer-associated microbial system, we can increase the efficacy of therapy and eventually find an application for the microbial system. The development of immunogenomics and gut microgenomics in the life sciences will result in a significant advancement in our understanding of how microbial systems and immunotherapy interact, and it may also have intriguing therapeutic implications for extending the lifetime of PC patients.

Key Words: Periodontal disease; Pancreatic cancer; Microbiome; Periodontitis; Periopathogens; Periodontal medicine

Core Tip: It has been suggested that gastroenterological malignancies may be promoted by hematogenous, enteral or lymphatic translocation of periopathogens. Periodontitis has been linked to at least 50% increased risk of pancreatic cancer (PC) and it could be considered a risk factor for this malignancy. Future risk of PC has been linked to the oral microbiome, specifically increased levels of *Porphyromonas gingivalis* and *Aggregatibacter actinomycetemcomitans* and decreased relative abundance of *Leptotrichia* and *Fusobacteria*. By analyzing patterns in the microbiome composition throughout PC development and establishing strategies to enhance the cancer-associated microbial system, we can increase the efficacy of therapy.

Citation: Ungureanu BS, Gheorghe DN, Nicolae FM, Râmboiu S, Radu PA, Șurlin VM, Strâmbu VDE, Gheonea DI, Roman A, Șurlin P. Could there be an interplay between periodontal changes and pancreatic malignancies? *World J Clin Cases* 2023; 11(3): 545-555
URL: https://www.wjgnet.com/2307-8960/full/v11/i3/545.htm
DOI: https://dx.doi.org/10.12998/wjcc.v11.i3.545

INTRODUCTION

The term "periodontal disease" refers to a group of inflammatory illnesses that affect the tooth-supporting tissues, ultimately leading to tooth loss and even resulting in systemic inflammation. Up to 90% of people worldwide are affected by the two most common periodontal disorders, gingivitis and periodontitis[1]. The cornerstone of avoiding periodontitis is the treatment of gingivitis, a reversible inflammation of the gingiva that takes place before periodontitis. By gradually destroying the alveolar bone and periodontal ligament, periodontitis-which is typically caused by Gram-negative bacteria-can result in recession, increased probing depth, or both[1].

Periodontal disease is initiated and progresses due to a dysbiosis of the commensal oral microbiota, which subsequently interacts with the host's immune system[2,3]. Diverse bacteria (or certain gene combinations within the community) may be capable of having various functions within the periodontal ecosystem that collaborate to generate and establish a microbiota that promotes disease. Numerous microbial species were found in the oral cavity, but most of them are commensal bacteria such as *Streptococcus, Capnocytophaga, Eikenella corrodens* and *Veillonella parvula*; nevertheless, in condition of some imbalances, they could also become pathogens for the tooth supporting tissues[4]. One of the crucial requirements for the development of a potentially pathogenic community is the ability of certain species to modify host responses in ways that compromise immune surveillance and tip the balance from homeostasis to dysbiosis[5]. *Porphyromonas gingivalis* (*P. gingivalis*), *Treponema denticola* and *Tanerella forsythia*, Gram-negative and anaerobiotic bacteria, possess a higher virulency and aggressiveness and are also involved in periopathogenesis[4].

Numerous mechanisms, including the systemic dissemination of periodontal pathogens and the systemic leakage of local inflammatory mediators, have been involved in the strong association between periodontitis and a number of systemic disorders[6]. Periodontal and systemic diseases have a two-way relationship; periodontal disease can have negative effects on the overall systemic health, and some systemic conditions increase the risk of periodontal disease onset[6,7]. Recent research has also shown that periodontal infection plays a role in aggravating systemic disease states at distal sites, including cardiovascular disease, adverse pregnancy outcomes, diabetes mellitus, Alzheimer's disease, inflammatory bowel diseases, and various cancer types, reinforcing the significance of the oral cavity for general health[6-9]. Additionally, it has been suggested that gastroenterological malignancies may be promoted by hematogenous (oral-blood axis *via* the perturbed periodontal tissues), enteral (oral-gut axis *via* saliva) or lymphatic (*via* the lymphatic drainage system) translocation of periopathogens[10-12].

In the past 25 years, the global burden of pancreatic cancer (PC) has more than doubled, making it one of the major causes of cancer-related mortality[13]. It comprises for almost 2% of all malignancies and is linked to 5% of deaths caused by cancer[14]. North America, Europe, and Australia have the highest incidence rates of PC[14,15]. While the ageing process of the global population could increase the incidence, other major risk factor, specifically smoking, obesity, diabetes and drinking alcohol should be considered for their modifiable nature[13,15].

Only around 20% of patients are initially diagnosed with early-stage PC, which is surgically resectable, thus explaining the low survival rates[13]. Even after a potentially radical treatment, the majority of patients eventually relapse, and their 5-year survival rate is only 2%–9%[14]. During the initial stages of the disease and its progression to advanced pancreatic metastasis, when tumor cells are very invasive, the majority of patients don't exhibit any apparent symptoms. Considering that it is one of the life-threatening malignant tumors, early diagnosis is imperative[13-15]. Pancreatic ductal adenocarcinomas account for over 90% of pancreatic malignancies[13].

Viral infections have been shown to express a strong relationship with cancer, but also certain bacteria can stimulate or trigger uncontrolled cell development by escaping the immune system or preventing apoptosis. Since periodontitis is a chronic oral bacterial infection, a potential link between periodontitis and PC has been proposed[9].

AIM

The purpose of this current review is to update and organize the most recent data on periodontal disease and its implications in PC in order to highlight the fact that there is sufficient evidence to establish a connection between them, through the action of periodontal pathogens, taking into account that periopathogens are essential for the onset and progression of periodontal disease, and their involvement in various systemic disorders has already been proven. This would encourage more exploration into the negative impact of periodontal disease on the development of PC in individuals with both disorders. The findings of future studies may have significant implications for periodontal and gastroenterological practice. For instance, periodontal screening for patients with this type of cancer and periodontal therapy, when necessary, may help lower the risk of PC's adverse evolution while also improving the quality of life for these patients.

PERIODONTAL DISEASE AND PC: EPIDEMIOLOGIC DATA

Periodontitis has been linked to various malignancies, with risk ranging between 14% and 20%[16,17]. Periodontitis has been linked to at least 50% increased risk of PC and it could be considered a risk factor for this malignancy[1,16,17], whereas other studies reported no significant association between periodontal disease and PC[1,18]. Periodontal disease risk is linked to a number of variables that are known to increase the risk of PC, such as smoking, alcohol drinking, and diabetes. The oral microbiome is thus affected by these exposures and circumstances, leading to dysbiosis and a relative increase in the amount of oral pathogenic microorganisms[19,20].

A 10 years follow-up study showed that the risk of all or specific gastro-intestinal malignancies, including PC, was not significantly associated with the severity of chronic periodontitis. After sex and age stratification, this null connection remained consistent[21]. No associations were found between the risk of PC and the eight single nucleotide polymorphisms, which provide the strongest explanation for a genetic predisposition to developing chronic or aggressive periodontitis[22].

Patients with PC may exhibit increased bleeding on probing when exposed to minimal amounts of dental plaque, which could point to periodontitis' excessive activity, often known as a hyperactive phenotype. Although dysfunctions of the CD14 axis receptor, nuclear factor kappa B (NF-kB) factors, and NOTCH pathway proteins are hypothesized, the source of high bleeding on probing index values at a relatively low plaque index rate is unknown at this time[23].

A cohort study that followed 5889441 individuals for a median of 7.2 years discovered that, compared to those with a healthy dental status, people with root canal infections, mild inflammation, and periodontitis in the under-50 age group had a 58% higher risk of developing PC, while those with periodontitis had a 56% higher risk. Only the subgroup of those with periodontitis exhibited a 20% elevated risk in the 50–70 age range. In all age categories, people with fewer teeth seemed to be at a higher risk[12]. Another study found that having periodontal disease was linked to a higher risk of developing PC in people 65 years of age or older, but not in people under 65[24].

A recent study performed on 59000 African American women with a follow up of 21 years showed that participants who had poor dental health had higher chances of PC[25]. Participants who reported both gum disease and tooth loss had a 58% higher chance of receiving a PC diagnosis[25]. Furthermore, compared to women who had neither periodontal disease nor tooth loss, those who reported periodontal gum disease but no tooth loss had a 77% higher chance of being diagnosed with PC[25]. Their research revealed that PC diagnoses were twice as likely to occur in women without periodontal disease but with absent teeth. Furthermore, the risk was significantly increased among patients who had at least 5 extracted teeth[25]. The findings, according to researchers, might be related to the inflammation that some oral bacteria trigger[25]. In an older research paper, when periodontal disease and recent tooth loss were evaluated together, the risk of PC significantly rose, with a risk ratio of 2.71 compared to people who had neither periodontal disease nor recent tooth loss. These findings imply that recent tooth loss may be a sign of severe periodontal disease[26].

Compared to the link between tooth loss and PC, the relationship between periodontal disease and PC has showed more consistent evidence[16,24,27,28]. According to a meta-analysis, the summary relative risk for periodontitis and PC was 1.74, while the risk for edentulism was 1.54[18]. Nevertheless, data is inconsistent as other research reported no associations between tooth loss and PC[27,28].

So far, research indicates that, independently of other recognized risk factors, like smoking, periodontal disease may contribute to the development of PC[26,29]. A prospective research of 48375 male health professionals revealed that those who had a history of periodontal disease at baseline had a 64% higher risk of PC[26,27,30]. In people who had never smoked, there was a stronger correlation between periodontal disease and PC[26,27,30]. Smoking is also linked to a two-fold increase in the risk of PC[26].

In a research with a long follow-up (10 years) and a substantial population-based cohort (568273 participants), there was a strong positive association between periodontitis and cancer mortality, particularly PC mortality[31]. After adjusting for age, sex, and additional controls for smoking, education, race/ethnicity, and body mass index (BMI), orodigestive cancer mortality was higher in patients with periodontal disease. Furthermore, the severity of periodontal disease enhanced the risks for orodigestive cancer mortality[32]. With age, sex, smoking, education, race/ethnicity and BMI adjustments, the mortality for PC in periodontal patients increased by nearly four times[32].

Regarding the mortality of PC, periodontitis considerably raises the chance of dying from PC[1].

HUMAN MICROBIOME AND PC

Multiple diverse organisms, such as bacteria, viruses, fungus, and protozoa, compose the human microbiota, as the presence of certain microorganisms was reported even before birth, in the human placenta[14,33,34]. They are essential for maintaining human health and preventing illnesses. Bacteria's ability to cause cancer is linked to both individual species and dysbiotic ecosystems[11]. Some hepatitis viruses, particular oral, gastrointestinal, and pancreatic microorganisms may have an etiological role in PC development[14,33,35].

Microbial diversity in the colon and other internal organs is decreased as a result of human microbial system dysregulation and, in PC patients, the imbalance of the intestinal microbiota is common[14,33,35]. Regardless of the severity of PC, the bacterial DNA patterns in the pancreatic and duodenal tissue of the same participants were comparable, indicating that bacteria may be traveling from the gut to the pancreas[36]. Microbiome alterations in the gut, oral cavity and pancreatic tissues of PC patients occur when compared to healthy flora, demonstrating a link between PC and microecology (Table 1). Inflammation may also contribute to PC development, although the underlying pathway is not yet known[37].

According to scientific research, the human microbiota has a key contribution to the onset, progression, and prognosis of PC[14,33,35,38]. The NYU Langone study found that, in contrast to other research linking poor oral health to PC, oral microbiome dysbiosis actually occurred before the malignancy took hold[30].

The function of the microbiome in PC risk has drawn more focus over the last decade. Using 16S rRNA fluorescent probes and quantitative real-time polymerase chain reaction, it was discovered that PC patients had an intrapancreatic bacterial load that was 1000 times higher than that of normal pancreatic tissue. The mean relative proportions of certain taxa varied between the healthy cohort, pancreatic benign neoplasm, and PC[35]. A recent case-control study found that there were discrepancies in the overall bacterial communities between those with PC and controls. While the presence of *Enterobacteriaceae*, *Lachnospiraceae G7*, *Bacteroidaceae*, or *Staphylococcaceae* was linked to an increased risk

Table 1 Selected studies assessing various methods for detecting bacteria in different types of gastroenterological cancers

Ref.	Types of samples and methods used	Bacteria detected in patients with PC	Types of digestive cancers
Del Castillo *et al*[36], 2019	16S rRNA gene sequencing was performed on tissue samples (pancreatic duct, duodenum, pancreas), swabs (bile duct, jejunum, stomach), and stool samples	*Lactobacillus, Porphyromonas, Fusobacterium, Prevotella*	Pancreatic cancer
Torres *et al* [37], 2015	16S rRNA gene sequencing was performed on saliva samples	*Leptotrichia, Porphyromonas*	Pancreatic cancer
Vogtmann *et al* [39], 2020	16S rRNA gene sequencing was performed on saliva samples		Pancreatic adenocarcinoma
Fan *et al*[43], 2018	16S rRNA gene sequencing was performed on pre-diagnostic oral wash samples	*Porphyromonas gingivalis, Aggregatibacter actinomycetemcomitans*	Pancreatic adenocarcinoma
Farrell *et al* [47], 2012	16S rRNA gene sequencing was performed on saliva samples	*Streptococcus mitis, Granulicatella adiacens, Neisseria elongata*	Pancreatic cancer
Tan *et al*[48], 2022	16S rRNA gene sequencing was performed on oral wash samples, resected cancer tissue and matched normal adjacent tissues	*Porphyromonas gingivalis,Firmicutes, Proteobacteria, Neisseria, Haemophilus, Aggregatibacter, Pseudomonas, Sphingomonas Bacteroidota*	Pancreatic cancer
Mitsuhashi *et al*[52], 2015	Genomic DNA was extracted from pancreatic tissues specimens	*Fusobacterium*	Pancreatic ductal adenocarcinoma
Yamamura *et al*[53], 2017	Genomic DNA was obtained using a cotton swab in the oral cavity and from cancerous tissues	*Fusobacterium*	Esophageal, gastric, colorectal, liver and pancreatic cancer
Gaiser *et al* [58], 2019	Microbial DNA was isolated from cyst fluid and plasma	*Fusobacterium nucleatum, Granulicatella adiacens*	Pancreatic cystic neoplasms

PC: Pancreatic cancer.

of PC, increased relative levels of *Haemophilus* were linked to a lower risk[39]. Currently, *Neisseria elongata*, *P. gingivalis, Streptococcus mitis* and *Fusobacterium* are the key pathogens implicated in PC and it was postulated that *Fusobacterium* can significantly decrease a patient's survival time when it comes to the prognostic evaluation of PC[11,14].

By causing DNA damage, epigenetic alterations of phagocytosis-related genes, immunological response, chromatin organization, cellular proliferation, and higher DNA mutation rates, the microbiome can influence cancer's development. The microbiome can also potentially cause signaling pathway disruption, enhanced local inflammation, and impaired epithelial barrier function[11]. According to one study, the point mutations in the PC patient's p53 tumor suppressor gene may be caused by the peptidyl arginine deaminase enzymes that are specific to oral periopathogen *P. gingivalis* [40].

According to one study, periodontitis, PC and chronic pancreatitis may all share the excessive inflammatory response brought on by the mutations of certain genes, *Q705K* and *F359L*, which are amino acids in *NLRP2* and *NLRP3*. It has been shown that rs35829419 (*Q705K*, *NLRP3*) polymorphism is more common in people with PC, while rs17699678 (*F359L*, *NLRP2*) polymorphism is more common in people with chronic pancreatitis[41].

By triggering systemic inflammation or, alternatively, by increasing the synthesis of bacterial metabolites, such as nitrosamines, reactive oxygen species sulfides, butyrate or acetaldehydes, chronic periodontitis through periopathogens may facilitate pancreatic carcinogenesis[9-11,18]. According to various theories, nitrosamines, acetaldehyde and gastric acidity play a significant role in the development of PC[9,18,27,42], as they can cause DNA alkylation, mutations, damage or impaired repair, which can result in inflammation or tumorigenesis[11].

Although the underlying mechanism connecting periodontitis to gastrointestinal cancers is not fully understood, and it is still uncertain which stage of periodontitis may affect cancer risk, gastroenterological malignancies have a high biological plausibility in relation to oral infections and inflammation[1,19]. Blood antibodies to certain oral pathogens and poor oral health status were linked to an elevated risk of PC[19,43]. A person's chance of developing PC was increased by 70% and 80%, respectively, whether they had oral mucosal lesions, or tongue lesions caused by Candida[1]. PC development was positively associated with tooth loss, although seropositivity to *Helicobacter pylori* was not significantly correlated with tooth loss[44]. Recent research could not establish a link between *Helicobacter pylori* and a higher risk of PC[45].

Future risk of PC has been linked to the oral microbiome, specifically increased levels of *P. gingivalis* and *Aggregatibacter actinomycetemcomitans* (*A. actinomycetemcomitans*) and decreased relative abundance of *Leptotrichia* and *Fusobacteria*, suggesting that it may have an impact on the inflammatory condition by

expanding, altering, and regulating the commensal microbiome[11-13,29]. It's noteworthy that *Leptotrichia* species, which are opportunistic pathogenic bacteria, are also frequently discovered in immunosuppressed individuals[46]. Using direct bacterial DNA analysis from samples of people's saliva taken years before diagnosis, a cohort research found strong associations between two periopathogens, *P. gingivalis* and *A. actinomycetemcomitans*, and PC[1,10,43]. This connection is also confirmed by a research which found that pre-diagnostic blood samples from those diagnosed with PC had more antigens to *P. gingivalis* than samples from controls[13]; in contrast, phylum *Fusobacteria* appeared to be linked with a reduced chance of developing PC[10,33]. There are still unanswered doubts regarding the mechanism underlying this connection and whether there is a direct causal correlation[13].

Oral microbiome profiles in patients with PC and controls significantly differ, according to scientific research[47]. Combining immunological dysregulation, genomic damage, and microbial variations between PC cases, early PC cases, and healthy controls, these factors point to a mechanistic role for oral microbiome components in PC development[11].

Bacteria can have a significant impact on carcinogenesis' mechanisms[43,45]. The bacterial "driver-passenger model" best describes this method of collaboration, in which the "driver" pathogen, such as *A. actinomycetemcomitans*, causes DNA damage in the host cells. A more stable ecosystem results from the modifications this driving pathogen makes to the microenvironment around the host cell. These changes make it easier for other germs to proliferate and survive. Once the cancer cells have been located, the "passenger" bacteria, such as *F. nucleatum*, will operate as a connecting organism between the early colonization microorganisms (*A. actinomycetemcomitans*) and the late colonizing microbes (*P. gingivalis*). *P. gingivalis* has the ability to block cancer cell death and encourage tumor growth[43,45]. The three microorganisms could have a significant synergistic impact on the onset and progression of cancer. This means that a diversified microbial environment is both more stable and harmful than a single species of bacterium, which may be a key element in the development of cancer[45].

Porphyromonas gingivalis

A recent study revealed that numerous bacterial taxa which were often detected in the tumoral milieu were also discovered in the oral microbiome, raising the possibility of bacterial translocation from the mouth to the pancreas. Unexpectedly, *P. gingivalis*, one major periodontal pathogen, which usually colonizes the oral cavity, was found in the saliva samples, normal surrounding tissues and the malignant tissues of PC patients in the same report[42,48]. The oral-derived migration of *P. gingivalis* into the pancreas as well as its capacity to cause PC were further shown. The explanation is that *P. gingivalis* induces the aggregation of neutrophils and the release of neutrophil elastase, which eventually promotes pancreatic neoplasms[48].

There is growing evidence that PC and periodontal infections are closely related[12] as *Leptotrichia* and *Porphyromonas* were more prevalent in PC patients' saliva than in healthy controls' saliva[37].

A 1.6-fold higher risk of PC was found in one of the biggest prospective cohort analyses to date when *P. gingivalis* taxa were directly detected in saliva using 16S RNA genes[43]. Unlike past studies assessing bacterial DNA in cancer patients' saliva, this cohort study was distinctive in that saliva samples were taken up to 10 years before a cancer diagnosis[28,43].

Participants who had *P. gingivalis* in their oral microbiome were shown to have a 59% higher chance of developing PC than those who did not[32]. In a European cohort research, those with high levels of antibodies to *P. gingivalis* (> 200 ng/mL) had a twofold increased probability of developing PC[1,10,30,33].

Although the dose-response was not linear and tended to flatten at higher immunoglobulin G (IgG) levels, a cohort research demonstrated a threefold increase in orodigestive cancer mortality, including pancreatic tumors, with rising *P. gingivalis* IgG levels[28,30,32].

Periodontal disease, oral pathogenic microorganisms, and PC have all been linked in a direct manner *via* biological pathways that have been hypothesized. One theory proposes a novel apoptosis-resistant mechanism that promotes immunosuppression and oncogenesis, with *P. gingivalis* serving as the common link[1]. Inhibiting epithelial cells' ability to undergo apoptosis, which has an essential function in defending malignant cells, is one of *P. gingivalis*' major carcinogenic effects. Some signaling pathways that *P. gingivalis* activates are implicated in immune evasion, tumorigenesis, cell invasion of tumor cells, and induction of apoptosis[49].

The bacteria *P. gingivalis* was discovered to be enriched in the abundant intratumor microbiota composition in human PC tissue. *P. gingivalis* may create a tumor microenvironment that is pro-inflammatory and elevate neutrophil elastase levels, eventually promoting the development of PC[42,48]. It was discovered that *P. gingivalis* survives inside PC cells, a property that can be improved *in vitro* and is amplified by hypoxia, a key aspect of PC[50]. The capacity of the bacteria to survive intracellularly and to increase Akt signaling and cyclin D1 expression, two essential pathways associated with PC development, are connected to the enhancement of proliferation. *P. gingivalis* infection of tumor cells led to enhanced growth in vivo. The scientists concluded that *P. gingivalis* directly influences PC cells in a pro-tumorigenic manner[50]. PC cell proliferation was considerably increased by live *P. gingivalis*, but surprisingly, this effect was not mediated by Toll-like receptor 2, an innate immune receptor that is activated in response to *P. gingivalis* on immune and cancer cells and is necessary for the bacterium to

cause alveolar bone resorption[50].

Another link between *P. gingivalis* and tumors is the metabolism of possibly carcinogenic compounds produced by this bacteria[49]. Following the administration of lipopolysaccharide from *P. gingivalis*, increased expressions of certain genes (*Reg*3A and G) were reported, thus the authors suggested that it could play an important role in *P. gingivalis*-lipopolysaccharide-related PC in mice[51].

P. gingivalis was definitely able to influence the host immunological responses, according to RNA sequencing. After *P. gingivalis* infection, neutrophil chemokines (Cxcl1, Cxcl2, Cxcr2, *etc*.) were discovered to be strongly elevated, but genes linked to gram-negative bacterial defense and antitumorigenic activities, such as lymphocyte chemotaxis and cell cytosis, were significantly suppressed. In PC mouse models, *P. gingivalis* specifically bypasses the host immune system and severely reduces the host's ability to fight tumors[48].

High frequencies of mutations in the tumor suppressor gene p53 were found in PC patients, leading researchers to draw the conclusion that alteration of the p53 gene is a crucial event in the development of human pancreatic tumors[49]. Furthermore, *P. gingivalis* decreases p53 levels while increasing the cell cycle's S-phase advancement[11].

Both *F. nucleatum* and *P. gingivalis* possess strong antiapoptotic properties as well as capabilities of immune evasion and disruption[11].

Fusobacterium nucleatum

Fusobacterium species were examined by Mitsuhashi *et al*[52] in 283 PC patients and their results found a detection rate of 8.8% in tumor tissue and 28% in normal adjacent tissues. When using multivariate Cox regression analysis, it was shown that the presence of these bacteria is associated with a greater mortality, in comparison with *Fusobacterium*-negative group[52]. Conversely, a recent study did not detect *F. nucleatum* DNA in PC tissues. They hypothesized that *F. nucleatum* would contribute to the development of gastroenterological tract cancer but not pancreatic or liver cancer[53], although Mitsuhashi *et al*[52] stated that the bacterium could be considered a prognostic marker of PC[52].

Moreover, greater abundance of *Fusobacteria* and its genus *Leptotrichia* was linked to a lower risk of PC, according to a cohort study that used direct bacterial DNA sequencing from samples of people's saliva obtained years before diagnosis[42,43]. In contrast, *F. nucleatum*-positive pancreatic ductal adenocarcinomas were linked to elevated cancer-specific mortality rates[11,46].

Fusobacterium species were more frequently discovered in pancreatic tail cancer than in head or body cancer, despite the lack of a significant association. Uncertainty surrounds the high incidence of *Fusobacterium* species in pancreatic tail tumors. The difference in vascular supply between the pancreas tail and head or body could represent one possibility for this observation[52].

Aggregatibacter actinomycetemcomitans

Moreover, although the connection was not as strong as for *P. gingivalis*, people who exhibited *A. actinomycetemcomitans* in their oral microbiome also had at least a 50% higher relative chance of developing PC[32]. When *A. actinomycetemcomitans* taxa were directly detected in saliva using 16S RNA genes, one of the biggest cohort analyses to date found a 2-fold increased risk of PC[43]. In contrast to past studies measuring bacterial DNA in cancer patients' saliva, the samples used in this cohort study were taken up to 10 years before the cancer diagnosis[28].

Through the insertion of DNA double-strand breaks *via* CDT activity, *A. actinomycetemcomitans* Y4 can cause genomic instability, a significant phase in the tumorigenesis[11].

Bacterial toxins, such the cytolethal distending toxin released by *A. actinomycetemcomitans*, can disrupt the balance of the host's immune system, harm antigen-presenting cells, and prevent lymphocyte proliferation[11]. Moreover, their lipopolysaccharide may help accelerate carcinogenesis through NF-kB signaling and TLR4 binding, both of which are elevated in the tumor microenvironment[11].

THERAPEUTIC APPROACHES

Previous research has demonstrated a connection between microbes and the development and spread of PC. The development of biomarkers that may control how responsive cancers are to therapeutic drugs may be regulated by the human microbial system, which is particularly advantageous for enhancing PC's clinical efficiency. Chemotherapy and immunotherapy can be paired with microbial systems, which may provide PC patients a significant amount of hope. But there is still a lot of disagreement in this area[14].

Early detection

It has been established that intestinal microbiota contributes to PC by producing tumor-specific immunity and systemic immunity, although the mechanism is yet unknown. In an effort to develop new therapeutic approaches, future research will concentrate on how microbiota influences the development and maintenance of immunological tolerance. In order to create more targeted techniques of response modulation, a thorough investigation of the PC-associated microflora can be performed to pinpoint

particular communities that contribute either positively or negatively to the onset and progression of PC [14]. The biggest chance of increasing survival rates would arise from early identification of PC. A particular oral microbiota analysis might be developed to enable the early diagnosis of cancer since mouth dysbiosis appears to be more pronounced in individuals with gastrointestinal tumors[29].

To determine if the presence of specific microbial species may be used as a biomarker for the early diagnosis of PC, the salivary bacterial profiles of 108 people were examined; 8 of them received a PC diagnosis, 22 were healthy controls and the other had other diseases. When compared to healthy participants or patients with other disorders, the ratio of *Leptotrichia* and *Porphyromonas* was considerably greater in the saliva of subjects with a future PC diagnosis[20,37]. *P. gingivalis* may serve as a biomarker for the emergence and progression of PC[49].

Similar shifts may be observed in individuals with preneoplastic lesions, such as intraductal papillary mucinous neoplasms, if alterations in the oral microbiota are connected to the probability of developing PC[20].

Saliva is a biofluid that is simple to acquire, making it perfect for the early identification of a variety of illnesses, including bacterial and viral infections, cardiovascular, renal, autoimmune disorders and, especially, malignancies[54-56]. Eight metabolites (leucine with isoleucine, tryptophan, valine, glutamic acid, phenylalanine, glutamine, and aspartic acid) were found in a research that thoroughly investigated salivary metabolites and identified metabolic patterns unique to several types of malignancies, including PCs. According to this, salivary metabolites could be considered cancer-specific markers[55].

Gut microbiome modulation

The identification of biomarkers for predicting future PC risk and prognosis is made possible by microbiota research, which offers the chance to fully explain the underlying processes. According to prior research, PC is linked to bacteria that may alter a tumor's susceptibility to therapeutic medicines. Through appropriate adjustment, the effectiveness of this deadly disease's therapy can be greatly improved. The development and application of novel antibiotics, prebiotics, probiotics or microbial transplantation in conjunction with chemotherapy and immunotherapy may hold considerable potential for PC patients[35,46,57].

Reducing the pancreatic inflammatory microbiome may be a viable treatment option for individuals with an early precursor of PC, like pancreatic cysts-intraductal papillary mutinous neoplasms-, because of the demonstrated co-occurrence and enrichment of oral bacterial species in their microbiome[58].

Pushalkar *et al*[59] showed that intestinal bacteria may invade the pancreas, and that in PC tissue, both in animal models and in people, there is an increased abundance of bacteria compared with control cases with a different microbiome community in PC samples compared to controls. Furthermore, compared to healthy animals, PC mouse models have a higher capacity for the gut microbiota to translocate to the pancreas[20,59]. In one investigation, the significance of the *P. gingivalis*-inflammatory system-pancreas axis in the progression of PC was clarified, and it was suggested that lowering *P. gingivalis* infections or inflammatory state would help with PC prevention and therapy[48].

Additionally, PC developed more slowly in germ-free mutated animals. Oral antibiotic therapy also showed a protective effect against tumor growth, while gut microbiome repopulation with PC mouse feces increased cancer progression[20].

It was discovered that microbe-free mice did not respond to immunotherapeutic medications, but mice that were administered *Bacteroides fragilis* responded positively. According to Sivan *et al*[60], *Bifidobacterium* increased the effectiveness of cancer immunotherapy in mice, which suggested that microbes, particularly gut bacteria, may be triggering the immune response by causing enterocytes to produce specific message molecules or send signals to immune cells, which enhances their capacity to fight tumors[35,60]. Due primarily to its poor response to chemotherapy, PC is often a fatal disease. Recent research suggests that the tumor microenvironment may be a significant factor in developing gemcitabine chemoresistance[57].

By analyzing patterns in the microbiome composition throughout PC development and establishing strategies to enhance the cancer-associated microbial system, we can increase the efficacy of therapy and eventually find an application for the microbial system. The development of immunogenomics and gut micro-genomics in the life sciences will result in a significant advancement in our understanding of how microbial systems and immunotherapy interact, and it may also have intriguing therapeutic implications for extending the lifetime of PC patients[14].

Periodontal treatment

Enhancing our knowledge of the connection between periodontal disease and other risk factors and how they affect cancer risk, as well as identifying potential bacteria that may be involved in carcinogenesis, may also open up new opportunities for early cancer detection (through the discovery of biomarkers), and provide information on whether active treatment for periodontal disease will lessen the burden of cancer[28,46]. It is uncertain to say at this point if the burden of cancer would decrease with the treatment of periodontitis[28].

Using the Taiwanese NHIRD, a research project investigated the link between periodontal disease and cancer, particularly PC, and the impact of periodontal disease therapy, which was defined as at least 10 procedures like scaling and periodontal flap surgery. Patients who received treatment had

significantly decreased incidence rate ratios for PC and adjusted hazard ratios. The modified model did not, however, take smoking into account[19,61].

CONCLUSION

These researches support the hypothesis that certain characteristics of the human microbiome play a significant role in shaping the immune response in a manner that facilitates tumor development. Given the growing epidemiological data linking periodontal disease to PC and the rapid unraveling of new molecular links between periopathogens and cancer development, the impact of bacterial infection on pancreatic carcinogenesis has to be given more consideration. More research in this field is expected to improve our knowledge of this aggressive malignancy and provide us with new chances for early identification and/or the development of treatments.

FOOTNOTES

Author contributions: Șurlin P, Șurlin VM, Gheonea DI contributed to conceiving the study; Nicolae FM, Ungureanu BS, Râmboiu S contributed to the investigation; Strâmbu VDE, Gheonea DI, Roman A contributed to the supervision; Nicolae FM, Gheorghe DN, Șurlin P wrote the original draft; Nicolae FM, Ungureanu BS, Radu PA, Șurlin P edited the original draft; All authors have read and agreed to the published version of the manuscript.

Conflict-of-interest statement: All the authors report no relevant conflicts of interest for this article.

Country/Territory of origin: Romania

ORCID number: Bogdan Silviu Ungureanu 0000-0003-2648-5408; Dorin Nicolae Gheorghe 0000-0003-1569-1601; Flavia Mirela Nicolae 0000-0002-4675-4292; Sandu Râmboiu 0000-0002-0795-1648; Petru Adrian Radu 0000-0003-4006-5397; Dan Ionut Gheonea 0000-0003-1942-6629; Alexandra Roman 0000-0002-0649-9426; Petra Șurlin 0000 0003 3469 8008.

S-Editor: Fan JR
L-Editor: A
P-Editor: Fan JR

REFERENCES

1 **Zhang Y**, Sun C, Song EJ, Liang M, Shi T, Min M, Sun Y. Is periodontitis a risk indicator for gastrointestinal cancers? *J Clin Periodontol* 2020; **47**: 134-147 [PMID: 31697412 DOI: 10.1111/jcpe.13217]
2 **Highfield J**. Diagnosis and classification of periodontal disease. *Aust Dent J* 2009; **54** Suppl 1: S11-S26 [PMID: 19737262 DOI: 10.1111/j.1834-7819.2009.01140.x]
3 **Kinane DF**, Stathopoulou PG, Papapanou PN. Periodontal diseases. *Nat Rev Dis Primers* 2017; **3**: 17038 [PMID: 28805207 DOI: 10.1038/nrdp.2017.38]
4 **Kolenbrander PE**, Palmer RJ Jr, Periasamy S, Jakubovics NS. Oral multispecies biofilm development and the key role of cell-cell distance. *Nat Rev Microbiol* 2010; **8**: 471-480 [PMID: 20514044 DOI: 10.1038/nrmicro2381]
5 **Hajishengallis G**, Lamont RJ. Beyond the red complex and into more complexity: the polymicrobial synergy and dysbiosis (PSD) model of periodontal disease etiology. *Mol Oral Microbiol* 2012; **27**: 409-419 [PMID: 23134607 DOI: 10.1111/j.2041-1014.2012.00663.x]
6 **Sedghi LM**, Bacino M, Kapila YL. Periodontal Disease: The Good, The Bad, and The Unknown. *Front Cell Infect Microbiol* 2021; **11**: 766944 [PMID: 34950607 DOI: 10.3389/fcimb.2021.766944]
7 **Hegde R**, Awan KH. Effects of periodontal disease on systemic health. *Dis Mon* 2019; **65**: 185-192 [PMID: 30384973 DOI: 10.1016/j.disamonth.2018.09.011]
8 **Nwizu N**, Wactawski-Wende J, Genco RJ. Periodontal disease and cancer: Epidemiologic studies and possible mechanisms. *Periodontol 2000* 2020; **83**: 213-233 [PMID: 32385885 DOI: 10.1111/prd.12329]
9 **Pizzo G**, Guiglia R, Lo Russo L, Campisi G. Dentistry and internal medicine: from the focal infection theory to the periodontal medicine concept. *Eur J Intern Med* 2010; **21**: 496-502 [PMID: 21111933 DOI: 10.1016/j.ejim.2010.07.011]
10 **Yu TC**, Zhou YL, Fang JY. Oral pathogen in the pathogenesis of colorectal cancer. *J Gastroenterol Hepatol* 2022; **37**: 273-279 [PMID: 34837266 DOI: 10.1111/jgh.15743]
11 **Teles FRF**, Alawi F, Castilho RM, Wang Y. Association or Causation? *J Dent Res* 2020; **99**: 1411-1424 [PMID: 32811287 DOI: 10.1177/0022034520945242]

12 **Yu J**, Ploner A, Chen MS, Zhang J, Sandborgh-Englund G, Ye W. Poor dental health and risk of pancreatic cancer: a nationwide registry-based cohort study in Sweden, 2009-2016. *Br J Cancer* 2022; **127**: 2133-2140 [PMID: 36273086 DOI: 10.1038/s41416-022-02018-8]

13 **Klein AP**. Pancreatic cancer epidemiology: understanding the role of lifestyle and inherited risk factors. *Nat Rev Gastroenterol Hepatol* 2021; **18**: 493-502 [PMID: 34002083 DOI: 10.1038/s41575-021-00457-x]

14 **Zhao Z**, Liu W. Pancreatic Cancer: A Review of Risk Factors, Diagnosis, and Treatment. *Technol Cancer Res Treat* 2020; **19**: 1533033820962117 [PMID: 33357065 DOI: 10.1177/1533033820962117]

15 **Kamisawa T**, Wood LD, Itoi T, Takaori K. Pancreatic cancer. *Lancet* 2016; **388**: 73-85 [PMID: 26830752 DOI: 10.1016/S0140-6736(16)00141-0]

16 **Michaud DS**, Fu Z, Shi J, Chung M. Periodontal Disease, Tooth Loss, and Cancer Risk. *Epidemiol Rev* 2017; **39**: 49-58 [PMID: 28449041 DOI: 10.1093/epirev/mxx006]

17 **Corbella S**, Veronesi P, Galimberti V, Weinstein R, Del Fabbro M, Francetti L. Is periodontitis a risk indicator for cancer? *PLoS One* 2018; **13**: e0195683 [PMID: 29664916 DOI: 10.1371/journal.pone.0195683]

18 **Maisonneuve P**, Amar S, Lowenfels AB. Periodontal disease, edentulism, and pancreatic cancer: a meta-analysis. *Ann Oncol* 2017; **28**: 985-995 [PMID: 28453689 DOI: 10.1093/annonc/mdx019]

19 **Bracci PM**. Oral Health and the Oral Microbiome in Pancreatic Cancer: An Overview of Epidemiological Studies. *Cancer J* 2017; **23**: 310-314 [PMID: 29189325 DOI: 10.1097/PPO.0000000000000287]

20 **Archibugi L**, Signoretti M, Capurso G. The Microbiome and Pancreatic Cancer: An Evidence-based Association? *J Clin Gastroenterol* 2018; **52** Suppl 1, Proceedings from the 9th Probiotics, Prebiotics and New Foods, Nutraceuticals and Botanicals for Nutrition & Human and Microbiota Health Meeting, held in Rome, Italy from September 10 to 12, 2017: S82-S85 [PMID: 30001289 DOI: 10.1097/MCG.0000000000001092]

21 **Chou SH**, Tung YC, Wu LS, Chang CJ, Kung S, Chu PH. Severity of chronic periodontitis and risk of gastrointestinal cancers: A population-based follow-up study from Taiwan. *Medicine (Baltimore)* 2018; **97**: e11386 [PMID: 29979428 DOI: 10.1097/MD.0000000000011386]

22 **Corlin L**, Ruan M, Tsilidis KK, Bouras E, Yu YH, Stolzenberg-Solomon R, Klein AP, Risch HA, Amos CI, Sakoda LC, Vodička P, Rish PK, Beck J, Platz EA, Michaud DS. Two-Sample Mendelian Randomization Analysis of Associations Between Periodontal Disease and Risk of Cancer. *JNCI Cancer Spectr* 2021; **5** [PMID: 34222791 DOI: 10.1093/jncics/pkab037]

23 **Miskiewicz A**, Szparecki G, Durlik M, Rydzewska G, Ziobrowski I, Górska R. The correlation between pancreatic dysfunction markers and selected indices of periodontitis. *Adv Clin Exp Med* 2018; **27**: 313-319 [PMID: 29558037 DOI: 10.17219/acem/64937]

24 **Chang JS**, Tsai CR, Chen LT, Shan YS. Investigating the Association Between Periodontal Disease and Risk of Pancreatic Cancer. *Pancreas* 2016; **45**: 134-141 [PMID: 26474422 DOI: 10.1097/MPA.0000000000000419]

25 **Gerlovin H**, Michaud DS, Cozier YC, Palmer JR. Oral Health in Relation to Pancreatic Cancer Risk in African American Women. *Cancer Epidemiol Biomarkers Prev* 2019; **28**: 675-679 [PMID: 30923045 DOI: 10.1158/1055-9965.EPI-18-1053]

26 **Meyer MS**, Joshipura K, Giovannucci E, Michaud DS. A review of the relationship between tooth loss, periodontal disease, and cancer. *Cancer Causes Control* 2008; **19**: 895-907 [PMID: 18478344 DOI: 10.1007/s10552-008-9163-4]

27 **Michaud DS**, Joshipura K, Giovannucci E, Fuchs CS. A prospective study of periodontal disease and pancreatic cancer in US male health professionals. *J Natl Cancer Inst* 2007; **99**: 171-175 [PMID: 17228001 DOI: 10.1093/jnci/djk021]

28 **Chung M**, York BR, Michaud DS. Oral Health and Cancer. *Curr Oral Health Rep* 2019; **6**: 130-137 [PMID: 31871854 DOI: 10.1007/s40496-019-0213-7]

29 **Mascitti M**, Togni L, Troiano G, Caponio VCA, Gissi DB, Montebugnoli L, Procaccini M, Lo Muzio L, Santarelli A. Beyond Head and Neck Cancer: The Relationship Between Oral Microbiota and Tumour Development in Distant Organs. *Front Cell Infect Microbiol* 2019; **9**: 232 [PMID: 31297343 DOI: 10.3389/fcimb.2019.00232]

30 **Michaud DS**. Role of bacterial infections in pancreatic cancer. *Carcinogenesis* 2013; **34**: 2193-2197 [PMID: 23843038 DOI: 10.1093/carcin/bgt249]

31 **Heikkilä P**, But A, Sorsa T, Haukka J. Periodontitis and cancer mortality: Register-based cohort study of 68,273 adults in 10-year follow-up. *Int J Cancer* 2018; **142**: 2244-2253 [PMID: 29322513 DOI: 10.1002/ijc.31254]

32 **Ahn J**, Segers S, Hayes RB. Periodontal disease, Porphyromonas gingivalis serum antibody levels and orodigestive cancer mortality. *Carcinogenesis* 2012; **33**: 1055-1058 [PMID: 22367402 DOI: 10.1093/carcin/bgs112]

33 **Vogtmann E**, Goedert JJ. Epidemiologic studies of the human microbiome and cancer. *Br J Cancer* 2016; **114**: 237-242 [PMID: 26730578 DOI: 10.1038/bjc.2015.465]

34 **Xiao J**, Fiscella KA, Gill SR. Oral microbiome: possible harbinger for children's health. *Int J Oral Sci* 2020; **12**: 12 [PMID: 32350240 DOI: 10.1038/s41368-020-0082-x]

35 **Wei MY**, Shi S, Liang C, Meng QC, Hua J, Zhang YY, Liu J, Zhang B, Xu J, Yu XJ. The microbiota and microbiome in pancreatic cancer: more influential than expected. *Mol Cancer* 2019; **18**: 97 [PMID: 31109338 DOI: 10.1186/s12943-019-1008-0]

36 **Del Castillo E**, Meier R, Chung M, Koestler DC, Chen T, Paster BJ, Charpentier KP, Kelsey KT, Izard J, Michaud DS. The Microbiomes of Pancreatic and Duodenum Tissue Overlap and Are Highly Subject Specific but Differ between Pancreatic Cancer and Noncancer Subjects. *Cancer Epidemiol Biomarkers Prev* 2019; **28**: 370-383 [PMID: 30373903 DOI: 10.1158/1055-9965.EPI-18-0542]

37 **Torres PJ**, Fletcher EM, Gibbons SM, Bouvet M, Doran KS, Kelley ST. Characterization of the salivary microbiome in patients with pancreatic cancer. *PeerJ* 2015; **3**: e1373 [PMID: 26587342 DOI: 10.7717/peerj.1373]

38 **Nagata N**, Nishijima S, Kojima Y, Hisada Y, Imbe K, Miyoshi-Akiyama T, Suda W, Kimura M, Aoki R, Sekine K, Ohsugi M, Miki K, Osawa T, Ueki K, Oka S, Mizokami M, Kartal E, Schmidt TSB, Molina-Montes E, Estudillo L, Malats N, Trebicka J, Kersting S, Langheinrich M, Bork P, Uemura N, Itoi T, Kawai T. Metagenomic Identification of Microbial Signatures Predicting Pancreatic Cancer From a Multinational Study. *Gastroenterology* 2022; **163**: 222-238 [PMID: 35398347 DOI: 10.1053/j.gastro.2022.03.054]

39 **Vogtmann E**, Han Y, Caporaso JG, Bokulich N, Mohamadkhani A, Moayyedkazemi A, Hua X, Kamangar F, Wan Y,

Suman S, Zhu B, Hutchinson A, Dagnall C, Jones K, Hicks B, Shi J, Malekzadeh R, Abnet CC, Pourshams A. Oral microbial community composition is associated with pancreatic cancer: A case-control study in Iran. *Cancer Med* 2020; **9**: 797-806 [PMID: 31750624 DOI: 10.1002/cam4.2660]

40 **Öğrendik M**. Oral bacteria in pancreatic cancer: mutagenesis of the p53 tumour suppressor gene. *Int J Clin Exp Pathol* 2015; **8**: 11835-11836 [PMID: 26617937]

41 **Miskiewicz A**, Szparecki G, Durlik M, Rydzewska G, Ziobrowski I, Górska R. The Q705K and F359L Single-Nucleotide Polymorphisms of NOD-Like Receptor Signaling Pathway: Association with Chronic Pancreatitis, Pancreatic Cancer, and Periodontitis. *Arch Immunol Ther Exp (Warsz)* 2015; **63**: 485-494 [PMID: 26253076 DOI: 10.1007/s00005-015-0355-9]

42 **Olsen I**, Yilmaz Ö. Possible role of Porphyromonas gingivalis in orodigestive cancers. *J Oral Microbiol* 2019; **11**: 1563410 [PMID: 30671195 DOI: 10.1080/20002297.2018.1563410]

43 **Fan X**, Alekseyenko AV, Wu J, Peters BA, Jacobs EJ, Gapstur SM, Purdue MP, Abnet CC, Stolzenberg-Solomon R, Miller G, Ravel J, Hayes RB, Ahn J. Human oral microbiome and prospective risk for pancreatic cancer: a population-based nested case-control study. *Gut* 2018; **67**: 120-127 [PMID: 27742762 DOI: 10.1136/gutjnl-2016-312580]

44 **Stolzenberg-Solomon RZ**, Dodd KW, Blaser MJ, Virtamo J, Taylor PR, Albanes D. Tooth loss, pancreatic cancer, and Helicobacter pylori. *Am J Clin Nutr* 2003; **78**: 176-181 [PMID: 12816788 DOI: 10.1093/ajcn/78.1.176]

45 **Sun Z**, Xiong C, Teh SW, Lim JCW, Kumar S, Thilakavathy K. Mechanisms of Oral Bacterial Virulence Factors in Pancreatic Cancer. *Front Cell Infect Microbiol* 2019; **9**: 412 [PMID: 31867287 DOI: 10.3389/fcimb.2019.00412]

46 **Herremans KM**, Riner AN, Cameron ME, McKinley KL, Triplett EW, Hughes SJ, Trevino JG. The oral microbiome, pancreatic cancer and human diversity in the age of precision medicine. *Microbiome* 2022; **10**: 93 [PMID: 35701831 DOI: 10.1186/s40168-022-01262-7]

47 **Farrell JJ**, Zhang L, Zhou H, Chia D, Elashoff D, Akin D, Paster BJ, Joshipura K, Wong DT. Variations of oral microbiota are associated with pancreatic diseases including pancreatic cancer. *Gut* 2012; **61**: 582-588 [PMID: 21994333 DOI: 10.1136/gutjnl-2011-300784]

48 **Tan Q**, Ma X, Yang B, Liu Y, Xie Y, Wang X, Yuan W, Ma J. Periodontitis pathogen Porphyromonas gingivalis promotes pancreatic tumorigenesis *via* neutrophil elastase from tumor-associated neutrophils. *Gut Microbes* 2022; **14**: 2073785 [PMID: 35549648 DOI: 10.1080/19490976.2022.2073785]

49 **Zhou Y**, Luo GH. Porphyromonas gingivalis and digestive system cancers. *World J Clin Cases* 2019; **7**: 819-829 [PMID: 31024953 DOI: 10.12998/wjcc.v7.i7.819]

50 **Gnanasekaran J**, Binder Gallimidi A, Saba E, Pandi K, Eli Berchoer L, Hermano E, Angabo S, Makkawi HA, Khashan A, Daoud A, Elkin M, Nussbaum G. Intracellular Porphyromonas gingivalis Promotes the Tumorigenic Behavior of Pancreatic Carcinoma Cells. *Cancers (Basel)* 2020; **12** [PMID: 32824786 DOI: 10.3390/cancers12082331]

51 **Hiraki D**, Uehara O, Kuramitsu Y, Morikawa T, Harada F, Yoshida K, Akino K, Chiba I, Asaka M, Abiko Y. P. gingivalis Lipopolysaccharide Stimulates the Upregulated Expression of the Pancreatic Cancer-Related Genes Regenerating Islet-Derived 3 A/G in Mouse Pancreas. *Int J Mol Sci* 2020; **21** [PMID: 33027970 DOI: 10.3390/ijms21197351]

52 **Mitsuhashi K**, Nosho K, Sukawa Y, Matsunaga Y, Ito M, Kurihara H, Kanno S, Igarashi H, Naito T, Adachi Y, Tachibana M, Tanuma T, Maguchi H, Shinohara T, Hasegawa T, Imamura M, Kimura Y, Hirata K, Maruyama R, Suzuki H, Imai K, Yamamoto H, Shinomura Y. Association of Fusobacterium species in pancreatic cancer tissues with molecular features and prognosis. *Oncotarget* 2015; **6**: 7209-7220 [PMID: 25797243 DOI: 10.18632/oncotarget.3109]

53 **Yamamura K**, Baba Y, Miyake K, Nakamura K, Shigaki H, Mima K, Kurashige J, Ishimoto T, Iwatsuki M, Sakamoto Y, Yamashita Y, Yoshida N, Watanabe M, Baba H. Fusobacterium nucleatum in gastroenterological cancer: Evaluation of measurement methods using quantitative polymerase chain reaction and a literature review. *Oncol Lett* 2017; **14**: 6373-6378 [PMID: 29151903 DOI: 10.3892/ol.2017.7001]

54 **Karpiński TM**. Role of Oral Microbiota in Cancer Development. *Microorganisms* 2019; **7** [PMID: 30642137 DOI: 10.3390/microorganisms7010020]

55 **Sugimoto M**, Wong DT, Hirayama A, Soga T, Tomita M. Capillary electrophoresis mass spectrometry-based saliva metabolomics identified oral, breast and pancreatic cancer-specific profiles. *Metabolomics* 2010; **6**: 78-95 [PMID: 20300169 DOI: 10.1007/s11306-009-0178-y]

56 **Chen Y**, Chen X, Yu H, Zhou H, Xu S. Oral Microbiota as Promising Diagnostic Biomarkers for Gastrointestinal Cancer: A Systematic Review. *Onco Targets Ther* 2019; **12**: 11131-11144 [PMID: 31908481 DOI: 10.2147/OTT.S230262]

57 **Choy ATF**, Carnevale I, Coppola S, Meijer LL, Kazemier G, Zaura E, Deng D, Giovannetti E. The microbiome of pancreatic cancer: from molecular diagnostics to new therapeutic approaches to overcome chemoresistance caused by metabolic inactivation of gemcitabine. *Expert Rev Mol Diagn* 2018; **18**: 1005-1009 [PMID: 30392417 DOI: 10.1080/14737159.2018.1544495]

58 **Gaiser RA**, Halimi A, Alkharaan H, Lu L, Davanian H, Healy K, Hugerth LW, Ateeb Z, Valente R, Fernández Moro C, Del Chiaro M, Sällberg Chen M. Enrichment of oral microbiota in early cystic precursors to invasive pancreatic cancer. *Gut* 2019; **68**: 2186-2194 [PMID: 30872392 DOI: 10.1136/gutjnl-2018-317458]

59 **Pushalkar S**, Hundeyin M, Daley D, Zambirinis CP, Kurz E, Mishra A, Mohan N, Aykut B, Usyk M, Torres LE, Werba G, Zhang K, Guo Y, Li Q, Akkad N, Lall S, Wadowski B, Gutierrez J, Kochen Rossi JA, Herzog JW, Diskin B, Torres-Hernandez A, Leinwand J, Wang W, Taunk PS, Savadkar S, Janal M, Saxena A, Li X, Cohen D, Sartor RB, Saxena D, Miller G. The Pancreatic Cancer Microbiome Promotes Oncogenesis by Induction of Innate and Adaptive Immune Suppression. *Cancer Discov* 2018; **8**: 403-416 [PMID: 29567829 DOI: 10.1158/2159-8290.CD-17-1134]

60 **Sivan A**, Corrales L, Hubert N, Williams JB, Aquino-Michaels K, Earley ZM, Benyamin FW, Lei YM, Jabri B, Alegre ML, Chang EB, Gajewski TF. Commensal Bifidobacterium promotes antitumor immunity and facilitates anti-PD-L1 efficacy. *Science* 2015; **350**: 1084-1089 [PMID: 26541606 DOI: 10.1126/science.aac4255]

61 **Hwang IM**, Sun LM, Lin CL, Lee CF, Kao CH. Periodontal disease with treatment reduces subsequent cancer risks. *QJM* 2014; **107**: 805-812 [PMID: 24722845 DOI: 10.1093/qjmed/hcu078]

World Journal of Clinical Cases

Submit a Manuscript: https://www.f6publishing.com

World J Clin Cases 2023 January 26; 11(3): 556-565

DOI: 10.12998/wjcc.v11.i3.556

ISSN 2307-8960 (online)

ORIGINAL ARTICLE

Retrospective Study

Qixue Shuangbu decoction and acupuncture combined with Western medicine in acute severe stroke patients

Li-Kun Gou, Chun Li

Specialty type: Critical care medicine

Provenance and peer review: Unsolicited article; Externally peer reviewed.

Peer-review model: Single blind

Peer-review report's scientific quality classification

Grade A (Excellent): 0
Grade B (Very good): B
Grade C (Good): C
Grade D (Fair): 0
Grade E (Poor): 0

P-Reviewer: Monetta L, Canada; Scheitz JF, Germany

Received: May 6, 2022
Peer-review started: May 6, 2022
First decision: May 30, 2022
Revised: June 18, 2022
Accepted: December 21, 2022
Article in press: December 21, 2022
Published online: January 26, 2023

Li-Kun Gou, Chun Li, Department of Critical Care Medicine, Lanzhou Second People's Hospital, Lanzhou 730046, Gansu Province, China

Corresponding author: Chun Li, MD, Chief Doctor, Department of Critical Care Medicine, Lanzhou Second People's Hospital, No. 388 Jingyuan Road, Lanzhou 730046, Gansu Province, China. lanzhoulichun@126.com

Abstract

BACKGROUND

Stroke is a common and frequently occurring disease of the nervous system and one of the three major diseases leading to human death. The incidence and mortality of stroke in China increase with age. Overall, 70 % of patients with stroke have serious disability, which results in heavy burden to their families and the society.

AIM

To analyze the effects of Qixue Shuangbu decoction and acupuncture combined with Western medicine on immune indexes and digestive tract function in patients with acute severe stroke.

METHODS

A total of 68 patients with acute severe stroke admitted to Lanzhou Second People's Hospital between March 2018 and September 2021 were selected and divided into the control and observation groups according to a random number table method. The control group was administered routine Western medicine treatment, such as dehydration, lowering intracranial pressure, anticoagulation, improving cerebral blood circulation and cerebral nerve protection according to the "Guidelines for the Diagnosis and Treatment of Acute Ischemic Stroke in China." The observation group was administered Qixue Shuangbu decoction *via* nasal feeding tube on the basis of the routine Western medicine treatment with simultaneous acupuncture. The two groups were compared.

RESULTS

The acute physiology and chronic health evaluation II, organ dysfunction syndrome score, National Institutes of Health Stroke Scale, and traditional Chinese medicine syndrome scores of the two groups were significantly decreased compared with those measured before treatment, and the complements C3 and C4, and immunoglobulins (Ig) M and G were significantly increased

compared with those observed before treatment ($P < 0.05$). After treatment, the scores of the observation group were lower than those of the control group, and the complement and Ig levels were higher than those of the control group ($P < 0.05$). The levels of diamine oxidase (DAO), D-lactic acid (D-LA), and calcitonin gene-related peptide (CGRP) in the two groups were significantly higher than those before treatment, while the levels of lipopolysaccharide, ubiquitin carboxyl-terminal hydrolase 1 (UCH-L1), tumor necrosis factor-α (TNF-α), interleukin (IL) -2, and IL-8 were significantly lower than those before treatment ($P < 0.05$). After treatment, DAO, D-LA, and CGRP were higher in the observation group than in the control group, while lipopolysaccharide, UCH-L1, TNF-α, IL-2, and IL-8 were lower than in the control group ($P < 0.05$). The hospitalization time of individuals in the observation group was shorter than that of the control group ($P < 0.05$).

CONCLUSION

Qixue Shuangbu decoction and acupuncture combined with Western medicine for the treatment of acute severe stroke can regulate intestinal flora, reduce inflammation, improve intestinal mucosal barrier function and immune function related indicators, and promote recovery.

Key Words: Qixue Shuangbu Decoction; Acupuncture; Western medicine; Acute severe stroke; Intestinal flora; Degree of inflammation; Immune function

Core Tip: Severe stroke is an acute and critical disease of the nervous system, which is a group of diseases that cause brain tissue damage due to the sudden rupture of brain vessels or the failure of blood to flow into the brain due to vascular obstruction. Traditional Chinese medicine believes that the disease belongs to the category of "stroke." There is evidence that lack of multi-factor endowment, aging, and yang hyperactivity wind, or drinking of syrup, overeating fat, climate change and other incentives result in viscera dysfunction, qi and blood disturbance, disturbing the brain orifices, and channeling the meridians for stroke.

Citation: Gou LK, Li C. Qixue Shuangbu decoction and acupuncture combined with Western medicine in acute severe stroke patients. *World J Clin Cases* 2023; 11(3): 556-565
URL: https://www.wjgnet.com/2307-8960/full/v11/i3/556.htm
DOI: https://dx.doi.org/10.12998/wjcc.v11.i3.556

INTRODUCTION

Severe stroke is a common disease of the nervous system with high mortality. Due to the most common sensory and motor dysfunction caused by neurological impairment, patients cannot eat independently; therefore, they require nutritional support treatment. However, long-term nutritional support treatment leads to abnormal intestinal flora, imbalance of gastrointestinal hormone secretion, and eventually systemic inflammatory response and even flora disorder[1]. The disease belongs to "apoplexy" category of traditional Chinese medicine. Because the brain is the capital of the gods, the disorder of qi and blood leads to the occurrence of apoplexy and the imbalance of qi movement in spleen and stomach. Additionally, the stagnation of intestinal dross leads to the accumulation of blood stasis and heat, which disturbs the gods. Both form a vicious circle. Therefore, traditional Chinese medicine (TCM) advocates the principle of promoting qi and activating blood, dredging the fu organs and reducing turbidity. Qi and blood Shuangbu decoction is mainly used to supplement qi and blood deficiency in patients with stroke, and acupuncture treatment focuses on regulating gastrointestinal function[2]. In this study, the effects of Qixue Shuangbu decoction and acupuncture combined with Western medicine on patients with acute severe stroke were assessed. The immune function and digestive tract function indexes were selected as the observation objects to analyze the therapeutic effect of integrated traditional Chinese and Western medicine to provide the corresponding basis for clinical practice.

MATERIALS AND METHODS

General information

A total of 68 patients with acute severe stroke admitted to Lanzhou Second People's Hospital between March 2018 and September 2021 were selected and divided into two groups according to the random number table method. A total of 34 cases were included in the control group, of whom 19 and 15 were men and women, respectively, and were aged 42–75 years (average, 60.84 ± 5.32 years). The time from onset to treatment was 0.5–6 h, with an average of 2.74 ± 0.46 h. The locations of lesions were the basal ganglia, lobe, and brainstem in 19, 10, and 5 cases, respectively. The Glasgow coma scale (GCS) was 6.25 ± 1.04. A total of 34 cases were included in the observation group, of whom 17 were men and 17 were women, aged 41–75 years (average, 61.01 ± 5.05 years). The time from onset to treatment was 0.5–6 h, with an average of 2.69 ± 0.47 h, and the locations of lesions were the basal ganglia, brain lobe, and brain stem for 17, 12, 5 cases, respectively. The gCS score was 6.22 ± 1.01 points. General data were balanced between the two groups, with no statistical significance being observed ($P > 0.05$).

The inclusion criteria were as follows: (1) Stroke defined in line with the "Chinese guidelines for the diagnosis and treatment of acute ischemic stroke 2014" criteria for ischemic stroke[3]: (a) acute onset; (b) focal neurological deficit; (c) unlimited duration of symptoms or signs; (d) excluding non-vascular causes; and (e) excluding cerebral hemorrhage; (2) stroke defined in line with the "common diagnostic criteria of traditional Chinese medicine" in the Qixue deficiency syndrome standard[4], including dizziness, fatigue, insomnia, amnesia, shortness of breath, pale lips, pale tongue, weak pulse, and other syndromes; (3) ≥ 40 years of age, ≤ 75 years of age; (4) GCS score of ≤ 8 and National Institutes of Health Stroke Scale (NIHSS) score of ≥ 17; and (5) family members sign informed consent.

The exclusion criteria were as follows: (1) A history of mental illness; (2) a history of serious underlying digestive diseases or abdominal surgery; (3) complicated with severe visceral lesions; and (4) thyroid dysfunction, coagulation dysfunction, malignant tumors, or severe malnutrition.

Methods

In the control group, routine Western medicine treatment, including dehydration and intracranial pressure reduction, anticoagulation, improvement of cerebral blood circulation, and cerebral nerve protection, was adopted. Patients were administered enteral nutrition support treatment. Enteral nutrition suspension (commodity name: Nengquanli, Newdihiya Pharmaceutical Co., Ltd., Batch No. 20180318) was administered 1500–2500 mL/day with 50–100 mL/h dripping speed using a gastric tube.

In the observation group, the patients were administered with Qixue Shuangbu decoction using a nasal feeding tube and simultaneous acupuncture treatment was performed. Prescriptions of Qixue Shuangbu decoction included *Codonopsis* (15 g), *Atractylodes* (15 g), *Poria* (12 g), *Angelica* (12 g), *Paeoniae Alba* (12 g), *Rehmannia glutinosa* (15 g), *Chuanxiong* (9 g), and *Radix Glycyrrhizae* (6 g). The above drugs were decocted for 150 mL and administered using a nasal feeding tube daily for 14 d. The acupuncture points were Neiguan, Zusanli, Guanyuan, Qihai, Shangjuxu, Zhongwan, and Xiawan. One-time acupuncture was performed using the twirling small lifting insertion technique, following the use of a gas needle for 20 min. Acupuncture was performed twice a day as a continuous treatment of 14 d.

Observation indicators

Acute physiology and chronic health evaluation II (APACHE II)[5] and organ dysfunction syndrome (MODS)[6] scores were used to evaluate the overall severity of the disease and severity of organ failure. The two scores were proportional to the overall severity of the disease and severity of organ failure, respectively. NIHSS[7] was used to evaluate the degree of neurological deficit, and it was proportional to the degree of neurological deficit. TCM syndrome score was estimated based on symptoms, including dizziness, laziness, amnesia, fatigue, insomnia, dreaminess, blurred vision, palpitations, shortness of breath, loss of appetite, slim body, and luxuriant face. The above symptoms were categorized from light to heavy using the Likert 4 grade scoring method, ranging from 0–3 points.

The incidence of gastrointestinal complications (diarrhea, constipation, gastrointestinal bleeding, vomiting), pressure sores, ventilator-associated pneumonia (VAP), offline success rate, hospitalization time, and 28-d mortality in the two groups were recorded[8].

Detection method

Fasting venous blood (3 mL) was extracted from patients and centrifuged at 2000 r/min for 30 min. Hitachi 7600i automatic biochemical analyzer was used for determination of biochemical parameters. The kit was provided by Nanjing Jiancheng Biological Products Co., Ltd. The calcitonin gene-related peptide (CGRP), ubiquitin carboxyl-terminal hydrolase 1 (UCH-L1), tumor necrosis factor-α (TNF-α), interleukin (IL)-2, IL-8, diamine oxidase (DAO), and D-lactic acid (D-LA) were estimated using enzyme-linked immunosorbent assay. The changes of the lipopolysaccharide concentration were determined using a radioimmunoassay. The changes of complement C3, complement C4, immunoglobulin (Ig) M, and IgG were detected by flow cytometry.

The patient's feces weighing 1 g were diluted with 5 mL of distilled water and inoculated in appropriate culture medium to determine the number of *Bifidobacterium*, *Lactobacillus*, *Enterococcus*, and *Enterobacter*.

Statistical analysis

The data were processed using the SPSS19.0 software. The data were assessed for normal distribution and uniform variance was described using mean ± SD. The *t* test was used for comparison, and the number of cases (%) for enumeration data were used for description. The χ^2 test was used for comparison, and statistical significance was set at $P < 0.05$.

RESULTS

Comparison of scores between and within groups

Before treatment, APACHE II, MODS, NIHSS, and TCM syndrome scores were not significantly different between the groups ($P > 0.05$). Table 1 shows that APACHE II, MODS, NIHSS, and TCM syndrome scores were significantly lower than those before treatment for both groups ($P < 0.05$). After treatment, the scores of the observation group were lower than those of the control group ($P < 0.05$).

Comparison of complement and Ig system indexes between and within groups

Complement (complement C3, complement C4) and Ig system (IgM, IgG) indexes were not significantly different before treatment ($P > 0.05$). Table 2 shows that the complement and Ig system indexes were significantly higher than those before treatment in both groups ($P < 0.05$). After treatment, complement C3, complement C4, IgM, and IgG were higher in the observation group than in the control group ($P < 0.05$).

Comparison of intestinal mucosal barrier function indexes between groups and within groups

Before treatment, the intestinal mucosal barrier function indexes were not significantly different between the groups ($P > 0.05$). Table 3 shows that DAO and D-LA were significantly increased ($P < 0.05$), while lipopolysaccharide was significantly decreased ($P < 0.05$) in the two groups. After treatment, DAO and D-LA were higher in the observation group than in the control group, while lipopolysaccharide was lower than that in the control group ($P < 0.05$).

Comparison of CGRP, UCH-L1, TNF-α, IL-2, IL-8 between and within groups

Before treatment, CGRP, UCH-L1, TNF-α, IL-2 and IL-8 were not significantly different ($P > 0.05$). Table 4 shows that CGRP was significantly increased ($P < 0.05$), and UCH-L1, TNF-α, IL-2 and IL-8 were significantly decreased ($P < 0.05$) in the two groups. After treatment, CGRP was higher, while UCH-L1, TNF-α, IL-2 and IL-8 were lower in the observation group than in the control group ($P < 0.05$).

Comparison of intestinal flora between groups and within groups

The number of intestinal flora before treatment were not significantly different between the groups ($P > 0.05$). As shown in Table 5, *Bifidobacterium*, *Lactobacillus*, and *Enterococcus* numbers were significantly higher in the two groups than those before treatment ($P < 0.05$), while the number of *Bacteroides* was significantly lower than that before treatment ($P < 0.05$). After treatment, *Bifidobacterium*, *Lactobacillus*, and *Enterococcus* numbers were higher in the observation group than in the control group, while the number of *Bacteroides* was lower than in the control group ($P < 0.05$).

Comparison of the incidence of gastrointestinal complications and pressure ulcers between groups

There were seven cases of gastrointestinal complications and one case of pressure sore in the control group. The overall complication rate was 23.53%, which was higher than that of the observation group (8.82%); however, no statistical significance was reached ($P > 0.05$) (Table 6).

Comparison of VAP incidence, weaning success rate, hospital stay, and 28-d mortality between groups

The incidence of VAP and the success rate of weaning were higher in the observation group than those in the control group, while the 28-d mortality rate was lower than that in the control group; however, no statistical significance was reached ($P > 0.05$). The hospitalization time of the observation group was significantly shorter than that of the control group ($P < 0.05$) (Table 7).

Table 1 Comparison of scores between and within groups (mean ± SD)

Indicators	Time	Control group (*n* = 34)	Observation group (*n* = 34)	*t* value	*P* value
APACHE II score (points)	Before treatment	17.58 ± 3.21	17.62 ± 3.08	0.052	0.958
	After treatment	13.25 ± 2.14[a]	10.11 ± 1.83[a]	6.502	0.000
MODS score (points)	Before treatment	14.55 ± 2.53	14.48 ± 2.61	0.112	0.911
	After treatment	9.89 ± 1.67[a]	8.21 ± 1.43[a]	4.456	0.000
NIHSS score (points)	Before treatment	19.97 ± 2.07	20.01 ± 2.13	0.079	0.938
	After treatment	10.74 ± 1.74[a]	8.56 ± 1.55[a]	5.455	0.000
TCM syndrome points (points)	Before treatment	24.12 ± 2.58	23.97 ± 2.61	0.238	0.812
	After treatment	11.41 ± 1.25[a]	7.85 ± 1.06[a]	12.666	0.000

[a]*P* < 0.05 *vs* before treatment.
APACHE II: Acute physiology and chronic health evaluation II; MODS: Organ dysfunction syndrome; NIHSS: National Institutes of Health Stroke Scale; TCM: Traditional Chinese medicine.

Table 2 Comparison of complement and immunoglobulins system indexes between and within groups (mean ± SD)

Indicators	Time	Control group (*n* = 34)	Observation group (*n* = 34)	*t* value	*P* value
Complement C3 (g/L)	Before treatment	1.04 ± 0.12	1.02 ± 0.13	0.659	0.512
	After treatment	1.28 ± 0.17[a]	1.43 ± 0.21[a]	3.237	0.002
Complement C4 (g/L)	Before treatment	0.22 ± 0.05	0.23 ± 0.04	0.911	0.366
	After treatment	0.31 ± 0.07[a]	0.37 ± 0.09[a]	3.068	0.003
IgM (g/L)	Before treatment	0.74 ± 0.11	0.73 ± 0.14	0.327	0.744
	After treatment	1.11 ± 0.15[a]	1.36 ± 0.18[a]	6.221	0.000
IgG (g/L)	Before treatment	9.74 ± 0.41	9.68 ± 0.38	0.626	0.534
	After treatment	10.64 ± 0.52[a]	11.47 ± 0.61[a]	6.038	0.000

[a]*P* < 0.05 *vs* before treatment.
Ig: Immunoglobulins.

Table 3 Comparison of intestinal mucosal barrier function indexes between groups and within groups (mean ± SD)

Indicators	Time	Control group (*n* = 34)	Observation group (*n* = 34)	*t* value	*P* value
DAO (U/mL)	Before treatment	3.28 ± 0.34	3.31 ± 0.30	0.386	0.701
	After treatment	4.15 ± 0.38[a]	4.63 ± 0.45[a]	4.752	0.000
D-LA (mmol/L)	Before treatment	0.18 ± 0.07	0.19 ± 0.06	0.632	0.529
	After treatment	0.27 ± 0.08[a]	0.36 ± 0.10[a]	4.098	0.000
Lipopolysaccharide (ng/L)	Before treatment	17.41 ± 4.52	17.35 ± 4.67	0.054	0.957
	After treatment	11.14 ± 2.05[a]	8.21 ± 1.61[a]	6.554	0.000

[a]*P* < 0.05 *vs* before treatment.
DAO: Diamine oxidase; D-LA: D-lactic acid.

DISCUSSION

Severe stroke refers to the brain tissue necrosis or softening caused by hypoxia and ischemia due to cerebral blood circulation disorder, which is a common cerebrovascular disease in clinic. The occurrence of patients with stroke is generally developed on the basis of atherosclerosis changes. Inflammatory reaction is one of the reasons for cell loss, which has a serious impact on life safety and physical and

Table 4 Comparison of calcitonin gene-related peptide, ubiquitin carboxyl-terminal hydrolase 1, tumor necrosis factor-α, interleukin-2, interleukin-8 between and within groups (mean ± SD)

Indicators	Time	Control group (*n* = 34)	Observation group (*n* = 34)	*t* value	*P* value
CGRP (pg/mL)	Before treatment	21.52 ± 5.36	20.97 ± 5.71	0.409	0.683
	After treatment	28.26 ± 6.17[a]	36.58 ± 6.78[a]	5.292	0.000
UCH-L1 (μg/L)	Before treatment	0.40 ± 0.18	0.41 ± 0.13	0.263	0.794
	After treatment	0.25 ± 0.11[a]	0.17 ± 0.10[a]	3.138	0.003
TNF-α (pg/mL)	Before treatment	44.52 ± 5.89	42.97 ± 6.01	1.074	0.287
	After treatment	21.02 ± 4.15[a]	14.63 ± 3.85[a]	6.582	0.000
IL-2 (pg/mL)	Before treatment	15.89 ± 2.16	15.81 ± 2.24	0.150	0.881
	After treatment	10.13 ± 1.92[a]	6.78 ± 1.52[a]	7.977	0.000
IL-8 (pg/mL)	Before treatment	5.23 ± 0.82	5.18 ± 0.91	0.238	0.813
	After treatment	4.64 ± 0.53[a]	3.47 ± 0.42[a]	10.088	0.000

[a]*P* < 0.05 *vs* before treatment.

CGRP: Calcitonin gene-related peptide; UCH-L1: Ubiquitin carboxyl-terminal hydrolase 1; TNF-α: Tumor necrosis factor-α; IL: Interleukin.

Table 5 Comparison of intestinal flora between groups and within groups (mean ± SD)

Indicators	Time	Control group (*n* = 34)	Observation group (*n* = 34)	*t* value	*P* value
Bifidobacterium (× 10^7 CFU)	Before treatment	9.74 ± 1.14	9.67 ± 1.21	0.246	0.807
	After treatment	11.11 ± 1.25[a]	12.78 ± 1.34[a]	5.314	0.000
Lactobacillus (× 10^7 CFU)	Before treatment	9.42 ± 1.14	9.36 ± 1.08	0.223	0.824
	After treatment	10.78 ± 1.27[a]	12.63 ± 1.41[a]	5.685	0.000
Enterococcus (× 10^7 CFU)	Before treatment	8.85 ± 1.14	8.79 ± 1.21	0.210	0.834
	After treatment	9.75 ± 1.21[a]	11.41 ± 1.37[a]	5.296	0.000
Bacteroides (× 10^7 CFU)	Before treatment	7.96 ± 0.21	8.02 ± 0.26	1.047	0.299
	After treatment	6.41 ± 0.17[a]	6.02 ± 0.14[a]	10.326	0.000

[a]*P* < 0.05 *vs* before treatment.

Table 6 Comparison of the incidence of gastrointestinal complications and pressure ulcers between groups, *n* (%)

Group	Gastrointestinal complications				Pressure ulcer	Total complications
	Diarrhea	Constipate	Gastrointestinal bleeding	Vomit		
Control group (*n* = 34)	2 (5.88)	1 (2.94)	1 (2.94)	3 (8.82)	1 (2.94)	8 (23.53)
Observation group (*n* = 34)	1 (2.94)	0 (0.00)	0 (0.00)	2 (5.88)	0 (0.00)	3 (8.82)
χ^2 value						2.711
P value						0.100

mental health of patients[9]. Most critically ill patients experience disturbance of consciousness, swallowing dysfunction, and metabolic exuberance; therefore, they have higher nutritional needs. However, limited intake leads to high stress response, resulting in malnutrition and reduced immune function[10]. Western medicine mainly relies on intestinal nutrition support in the aspect of supplemental nutrition; however, it can cause reproduction of pathogenic bacteria and formation of flora disorder, which would eventually lead to excessive activation of systemic inflammatory response. At the same time, the loss of neurological function in patients with stroke would lead to the inactivation of gastrointestinal hormones and change in neurotransmitter secretion, affecting the function of human

Table 7 Comparison of ventilator-associated pneumonia incidence, weaning success rate, hospital stay, and 28-d mortality between groups, *n* (%)

Group	Incidence of VAP	Offline success rate	Hospital stay (d)	28 d case fatality rate (%)
Control group (n = 34)	11 (32.35)	18 (52.94)	20.56 ± 5.82	7 (20.59)
Observation group (n = 34)	5 (14.71)	23 (67.65)	16.78 ± 4.53	2 (5.88)
χ^2/t value	2.942	1.536	2.989	3.202
P value	0.086	0.215	0.004	0.074

VAP: Ventilator-associated pneumonia.

intestinal mucosa and causing intestinal flora disorder.

TCM believes that stroke belongs to the category of stroke. In early stages of the disease, wind, fire, phlegm, and silt are the main factors, while in late stages, deficiency and silt are the main factors. TCM theory believes that qi is the handsome of blood, blood is the mother of qi, qi is the blood, qi is the vitality and movement, and qi deficiency is unable to promote the operation of blood, which will lead to blood stasis. This study adopts the TCM treatment method of Qixue Shuangbu decoction combined with acupuncture treatment. Qixue Shuangbu decoction consists of Sijunzi decoction and Siwu decoction. Reinforcing qi by *Dangshen*, strengthening healthy qi and expelling pathogenic factors, reinforcing qi by *Shaoyao Ganhuayin*, replenishing blood by *Danggui Shudihuan*g and activating blood by *Chuanxiong*. *Rhizoma Atractylodis Macrocephalae* and *Poria* can nourish qi and blood by invigorating spleen, while stir-fried licorice can reconcile various drugs. Ginger and jujube can support spleen and stomach, give consideration to tonifying qi and blood, play the role of nourishing blood, invigorating spleen and kidney, tonifying qi and blood, and harmonizing qi and blood[11-14].

Acupuncture treatment is the external treatment of TCM. This study selected acupoints that are commonly used in the treatment of gastrointestinal diseases. Zusanli is a strong point, can strengthen the body, spleen and stomach, while Shangjuxushichangchangchangxiahe point can reconcile gastrointestinal function. Guanyuan and Qihai can strengthen the spleen and kidney, while Buyuanqi and Zhongwan can reduce adverse stomach. Xiawan is Tongzhi and Neiguan and can open the orifices to wake up the min. Therefore, the acupuncture treatment of the above acupoints helps regulate the intestinal function of patients and improve the imbalance of flora. This study found that DAO and D-LA were higher, while lipopolysaccharide was lower in the observation group than in the control group after treatment, indicating that the regulation of TCM combined therapy on intestinal flora was significant. The above indicators are commonly used for the observation of intestinal mucosal loss. There is a bidirectional regulation between the human intestinal tract and the brain. Reducing intestinal loss through combined treatment can be administered back to the brain, thereby reducing the neurological deficit symptoms of patients[15,16].

In this study, the APACHE II, MODS, NIHSS and TCM syndrome scores were significantly decreased in the two groups compared with those before treatment, and the scores in the observation group were lower than those in the control group after treatment, indicating that the combined treatment of TCM had good effects on improving the symptoms of neurological deficit and reducing the severity of patients. Chinese medicine prescriptions can improve blood flow, improve vascular reserve capacity of patients, and alleviate the corresponding clinical signs caused by stroke. In this study, the complement and Ig system indexes of the two groups were significantly improved compared with those before treatment. The complement C3, complement C4, IgM and IgG were higher in the observation group than those in the control group after treatment, indicating that the immune function of the patients was significantly improved after TCM combined treatment. TCM and acupuncture treatment can promote the secretion of IL-2, thereby promoting lymphocyte proliferation and differentiation, as well as antibody formation, and playing an important role in human immune response. In this study, the changes of inflammatory factors in patients were also analyzed. TNF-α, IL-2, and IL-8 are the commonly used cellular inflammatory factors in clinic. The increase in their concentration suggested that the inflammatory response in patients was aggravated, and it could mediate the cascade activation process of inflammatory response. UCH-L1 was mainly expressed in the brain, testis, or ovary tissue, belonging to neuron-specific protein, which was of great significance to maintain the normal function of the nervous system. CGRP was a vasodilator polypeptide substance in the peripheral and central nervous system, which could form a strong antagonistic effect on cardiovascular and cerebrovascular contraction. Therefore, the severe response of patients in this study was reduced. The decrease of vasoconstrictive substance concentration suggests the possible mechanism of TCM combined therapy [17,18].

This study also analyzed the complications. The two main complications were gastrointestinal complications and pressure sores, which could be alleviated through active treatment. In contrast, the observation group showed significantly shortened hospitalization time, indicating that the combined

treatment of TCM used multiple ways to regulate the clinical signs and symptoms of patients helping reduce the hospitalization time of patients. In terms of the changes of bacterial flora in patients after treatment, *Bifidobacterium*, *Lactobacillus,* and *Enterococcus* numbers were higher in the observation group than in the control group, and the number of *Bacteroides* was lower than in the control group. Under normal conditions, beneficial and harmful bacteria in the human body were inhibited and reached a balance. The balance of bacterial flora is helpful for the digestion and absorption in the human body. Through the combined treatment of TCM, the beneficial bacteria in patients with severe stroke were increased, and the reproduction of harmful bacteria was inhibited, so as to protect the gastrointestinal function and promote the absorption of nutrients, which played an important role in maintaining the balance of bacterial flora in the human body[19,20].

In this study, patients with severe stroke were selected as the research objects, and the improvement effect of the combined treatment of TCM on patients was emphatically analyzed. At the same time, a variety of observation indexes were selected, including inflammatory factors, immune factors, intestinal flora, and other factors, which further confirmed the effect of the combined treatment of TCM and Western medicine, and could provide certain basis for the clinical comprehensive treatment of severe stroke. However, the number of cases included in this study is limited, and the cases derived from the same hospital, which may introduce a bias in case selection, and the follow-up time was relatively short. Follow-up studies should have been further confirmed by increasing the quality of life and living ability of patients outside the hospital.

CONCLUSION

In summary, Qixue Shuangbu decoction and acupuncture combined with Western medicine in the treatment of acute severe stroke can regulate intestinal flora, reduce inflammation, improve intestinal mucosal barrier function and immune function related indicators, and promote recovery.

ARTICLE HIGHLIGHTS

Research background

Stroke is a common and frequently occurring disease of the nervous system and one of the three major diseases leading to human death.

Research motivation

The effects of Qixue Shuangbu decoction and acupuncture combined with Western medicine on immune indexes and digestive tract function in patients with acute severe stroke were analyze.

Research objectives

This study aimed to observe the curative effect of Qixue Shuangbu Decoction and acupuncture combined with Western medicine on acute severe stroke, with the purpose of improving the clinical therapeutic effect.

Research methods

The observation group was administered Qixue Shuangbu decoction *via* nasal feeding tube on the basis of the routine Western medicine treatment with simultaneous acupuncture. The two groups were compared.

Research results

After treatment, the scores of the observation group were lower than those of the control group, and the complement and Ig levels were higher than those of the control group. The levels of diamine oxidase, D-lactic acid, and calcitonin gene-related peptide in the two groups were significantly higher than those before treatment, while the levels of lipopolysaccharide, ubiquitin carboxyl-terminal hydrolase 1, tumor necrosis factor-α, interleukin (IL) -2, and IL-8 were significantly lower than those before treatment.

Research conclusions

Qixue Shuangbu decoction and acupuncture combined with Western medicine for the treatment of acute severe stroke can regulate intestinal flora.

Research perspectives

The immune function and digestive tract function indexes were selected as the observation objects to analyze the therapeutic effect of integrated traditional Chinese and Western medicine to provide the corresponding basis for clinical practice.

FOOTNOTES

Author contributions: Gou LK and Li C design the study; Gou LK drafted the manuscript; Gou LK and Li C collected the data; Li C analyzed and interpreted data, Gou LK and Li C wrote and revised the manuscript.

Supported by Lanzhou Science and Technology Development Plan Project, No. 2020-ZD-126.

Institutional review board statement: The study was reviewed and approved by the Lanzhou Second People's Hospital Institutional Review Board.

Informed consent statement: All study participants, or their legal guardian, provided informed written consent prior to study enrollment.

Conflict-of-interest statement: The authors declare no conflict of interest.

Data sharing statement: No additional data are available.

Country/Territory of origin: China

ORCID number: Li-Kun Gou 0000-0003-1802-349X; Chun Li 0000-0003-3481-6131.

S-Editor: Wang JL
L-Editor: A
P-Editor: Wang JL

REFERENCES

1 **Khandelwal P**, Martínez-Pías E, Bach I, Prakash T, Hillen ME, Martínez-Galdámez M, Arenillas JF. Severe Epistaxis after Tissue Plasminogen Activator administration for Acute Ischemic Stroke in SARS-COV-2 Infection. *Brain Circ* 2021; **7**: 135-138 [PMID: 34189359 DOI: 10.4103/bc.bc_17_21]
2 **Elsaid N**, Mustafa W, Saied A. Radiological predictors of hemorrhagic transformation after acute ischemic stroke: An evidence-based analysis. *Neuroradiol J* 2020; **33**: 118-133 [PMID: 31971093 DOI: 10.1177/1971400919900275]
3 **Riou-Comte N**, Zhu F, Cherifi A, Richard S, Nace L, Audibert G, Achit H, Costalat V, Arquizan C, Beaufils O, Consoli A, Lapergue B, Loeb T, Rouchaud A, Macian F, Cailloce D, Biondi A, Moulin T, Desmettre T, Marnat G, Sibon I, Combes X, Lebedinsky AP, Vuillemet F, Kempf N, Pierot L, Moulin S, Lemmel P, Mazighi M, Blanc R, Sabben C, Schluck E, Bracard S, Anxionnat R, Guillemin F, Hossu G, Gory B; DIRECT ANGIO Investigators. Direct transfer to angiosuite for patients with severe acute stroke treated with thrombectomy: the multicentre randomised controlled DIRECT ANGIO trial protocol. *BMJ Open* 2021; **11**: e040522 [PMID: 33722864 DOI: 10.1136/bmjopen-2020-040522]
4 **Obayashi S**, Takahashi R, Onuki M. Upper limb recovery in early acute phase stroke survivors by coupled EMG-triggered and cyclic neuromuscular electrical stimulation. *NeuroRehabilitation* 2020; **46**: 417-422 [PMID: 32310196 DOI: 10.3233/NRE-203024]
5 **Forti P**, Maioli F, Nativio V, Maestri L, Coveri M, Zoli M. Association of prestroke glycemic status with stroke mortality. *BMJ Open Diabetes Res Care* 2020; **8** [PMID: 32079614 DOI: 10.1136/bmjdrc-2019-000957]
6 **Naito Y**, Kamiya M, Morishima N, Ishikawa T. Association between out-of-bed mobilization and complications of immobility in acute phase of severe stroke: A retrospective observational study. *J Stroke Cerebrovasc Dis* 2020; **29**: 105112 [PMID: 32912565 DOI: 10.1016/j.jstrokecerebrovasdis.2020.105112]
7 **Amarenco P**, Denison H, Evans SR, Himmelmann A, James S, Knutsson M, Ladenvall P, Molina CA, Wang Y, Johnston SC; THALES Steering Committee and Investigatorsa. Ticagrelor Added to Aspirin in Acute Nonsevere Ischemic Stroke or Transient Ischemic Attack of Atherosclerotic Origin. *Stroke* 2020; **51**: 3504-3513 [PMID: 33198608 DOI: 10.1161/STROKEAHA.120.032239]
8 **Shen S**, Hou N. Adverse Drug Reactions Caused by Antimicrobials Treatment for Ventilator-Associated Pneumonia. *Front Pharmacol* 2022; **13**: 921307 [PMID: 35712710 DOI: 10.3389/fphar.2022.921307]
9 **Ansari S**, McConnell DJ, Velat GJ, Waters MF, Levy EI, Hoh BL, Mocco J. Intracranial stents for treatment of acute ischemic stroke: evolution and current status. *World Neurosurg* 2011; **76**: S24-S34 [PMID: 22182268 DOI: 10.1016/j.wneu.2011.02.031]
10 **Moshayedi P**, Liebeskind DS, Jadhav A, Jahan R, Lansberg M, Sharma L, Nogueira RG, Saver JL. Decision-Making Visual Aids for Late, Imaging-Guided Endovascular Thrombectomy for Acute Ischemic Stroke. *J Stroke* 2020; **22**: 377-386 [PMID: 33053953 DOI: 10.5853/jos.2019.03503]
11 **Warach SJ**, Dula AN, Milling TJ Jr. Tenecteplase Thrombolysis for Acute Ischemic Stroke. *Stroke* 2020; **51**: 3440-3451 [PMID: 33045929 DOI: 10.1161/STROKEAHA.120.029749]
12 **Liao Z**, Bu Y, Li M, Han R, Zhang N, Hao J, Jiang W. Remote ischemic conditioning improves cognition in patients with

subcortical ischemic vascular dementia. *BMC Neurol* 2019; **19**: 206 [PMID: 31443692 DOI: 10.1186/s12883-019-1435-y]

13 **Saver JL**, Adeoye O. Intravenous Thrombolysis Before Endovascular Thrombectomy for Acute Ischemic Stroke. *JAMA* 2021; **325**: 229-231 [PMID: 33464293 DOI: 10.1001/jama.2020.22388]

14 **Rioux B**, Keezer MR, Gioia LC. Occult cancer diagnosed following acute ischemic stroke. *CMAJ* 2020; **192**: E1037-E1039 [PMID: 32900764 DOI: 10.1503/cmaj.200725]

15 **Salwi S**, Cutting S, Salgado AD, Espaillat K, Fusco MR, Froehler MT, Chitale RV, Kirshner H, Schrag M, Jasne A, Burton T, Grory BM, Saad A, Jayaraman MV, Madsen TE, Dakay K, McTaggart R, Yaghi S, Khatri P, Mistry AM, Mistry EA. Mechanical Thrombectomy in Ischemic Stroke Patients with Severe Pre-Stroke Disability. *J Stroke Cerebrovasc Dis* 2020; **29**: 104952 [PMID: 32689611 DOI: 10.1016/j.jstrokecerebrovasdis.2020.104952]

16 **Yamagami H**, Sakaguchi M, Furukado S, Hoshi T, Abe Y, Hougaku H, Hori M, Kitagawa K. Statin therapy increases carotid plaque echogenicity in hypercholesterolemic patients. *Ultrasound Med Biol* 2008; **34**: 1353-1359 [PMID: 18378381 DOI: 10.1016/j.ultrasmedbio.2008.01.019]

17 **Scaravilli V**, Guzzardella A, Madotto F, Beltrama V, Muscatello A, Bellani G, Monti G, Greco M, Pesenti A, Bandera A, Grasselli G. Impact of dexamethasone on the incidence of ventilator-associated pneumonia in mechanically ventilated COVID-19 patients: a propensity-matched cohort study. *Crit Care* 2022; **26**: 176 [PMID: 35698155 DOI: 10.1186/s13054-022-04049-2]

18 **Ahmed Y**, Bardia N, Judge C, Ahmad S, Malozzi C, Calderon E. *Aerococcus urinae*: A Rare Cause of Endocarditis Presenting With Acute Stroke. *J Med Cases* 2021; **12**: 65-70 [PMID: 34434432 DOI: 10.14740/jmc3612]

19 **Ebinger M**, Siegerink B, Kunz A, Wendt M, Weber JE, Schwabauer E, Geisler F, Freitag E, Lange J, Behrens J, Erdur H, Ganeshan R, Liman T, Scheitz JF, Schlemm L, Harmel P, Zieschang K, Lorenz-Meyer I, Napierkowski I, Waldschmidt C, Nolte CH, Grittner U, Wiener E, Bohner G, Nabavi DG, Schmehl I, Ekkernkamp A, Jungehulsing GJ, Mackert BM, Hartmann A, Rohmann JL, Endres M, Audebert HJ; Berlin_PRehospital Or Usual Delivery in stroke care (B_PROUD) study group. Association Between Dispatch of Mobile Stroke Units and Functional Outcomes Among Patients With Acute Ischemic Stroke in Berlin. *JAMA* 2021; **325**: 454-466 [PMID: 33528537 DOI: 10.1001/jama.2020.26345]

20 **Ehtesham M**, Mohmand M, Raj K, Hussain T, Kavita F, Kumar B. Clinical Spectrum of Hyponatremia in Patients with Stroke. *Cureus* 2019; **11**: e5310 [PMID: 31592365 DOI: 10.7759/cureus.5310]

World Journal of Clinical Cases

Submit a Manuscript: https://www.f6publishing.com

World J Clin Cases 2023 January 26; 11(3): 566-575

DOI: 10.12998/wjcc.v11.i3.566

ISSN 2307-8960 (online)

ORIGINAL ARTICLE

Retrospective Study

Successful treatment of patients with refractory idiopathic membranous nephropathy with low-dose Rituximab: A single-center experience

Yao-Wei Wang, Xin-Hui Wang, Hong-Xia Wang, Ren-Huan Yu

Specialty type: Medicine, research and experimental

Provenance and peer review: Unsolicited article; Externally peer reviewed.

Peer-review model: Single blind

Peer-review report's scientific quality classification

Grade A (Excellent): 0
Grade B (Very good): B
Grade C (Good): C
Grade D (Fair): 0
Grade E (Poor): 0

P-Reviewer: Doh K, South Korea; Guo X, China

Received: September 6, 2022
Peer-review started: September 6, 2022
First decision: October 11, 2022
Revised: October 14, 2022
Accepted: December 15, 2022
Article in press: December 15, 2022
Published online: January 26, 2023

Yao-Wei Wang, Xin-Hui Wang, Hong-Xia Wang, Ren-Huan Yu, China Department of Nephrology, Xiyuan Hospital of China Academy of Chinese Medical Sciences, Beijing 100091, China

Corresponding author: Ren-Huan Yu, PhD, Professor, China Department of Nephrology, Xiyuan Hospital of China Academy of Chinese Medical Sciences, No. 1 Xiyuan Playground, Haidian District, Beijing 100091, China. tezhongeyu@vip.sina.com

Abstract

BACKGROUND

The recognition of idiopathic membranous nephropathy (IMN) as an autoimmune disease has paved the way for the use of B-cell-depleting agents, such as Rituximab (RTX), which is now a first-line drug for treating IMN with proven safety and efficacy. Nevertheless, the usage of RTX for the treatment of refractory IMN remains controversial and challenging.

AIM

To evaluate the efficacy and safety of a new low-dose RTX regimen for the treatment of patients with refractory IMN.

METHODS

A retrospective study was performed on refractory IMN patients that accepted a low-dose RTX regimen (RTX, 200 mg, once a month for five months) in the Xiyuan Hospital of Chinese Academy of Chinese Medical Sciences' Department of Nephrology from October 2019 to December 2021. To assess the clinical and immune remission data, we performed a 24 h urinary protein quantification (UTP) test and measured the serum albumin (ALB) and serum creatinine (SCr) levels, phospholipase A2 receptor (PLA2R) antibody titer, and $CD19^+$ B-cell count every three months.

RESULTS

A total of nine refractory IMN patients were analyzed. During follow-up conducted twelve months later, the results from the 24 h UTP decreased from baseline [8.14 ± 6.05 g/d to 1.24 ± 1.34 g/d ($P < 0.05$)] and the ALB levels increased from baseline [28.06 ± 8.42 g/L to 40.93 ± 5.85 g/L ($P < 0.01$)]. Notably, after administering RTX for six months, the SCr decreased from 78.13 ± 16.49 μmol/L to 109.67 ± 40.87 μmol/L ($P < 0.05$). All of the nine patients were positive

for serum anti-PLA2R at the beginning, and four patients had normal anti-PLA2R titer levels at six months. The level of $CD19^+$ B-cells decreased to 0 at three months, and $CD19^+$ B-cell count remained at 0 up until six months of follow-up.

CONCLUSION
Our low-dose RTX regimen appears to be a promising treatment strategy for refractory IMN.

Key Words: Refractory nephrotic syndrome; Idiopathic membranous nephropathy; Low-dose rituximab

Core Tip: According to the Kidney Disease Improving Global Outcomes 2021 guidelines, Rituximab (RTX) is now the first-line therapy for patients with idiopathic membranous nephropathy (IMN). However, the use of RTX for the treatment of patients with refractory IMN remains challenging. We conducted a retrospective study on nine patients with refractory IMN to explore the efficacy and safety of a new low-dose RTX regimen (RTX, 200 mg, once a month for five months), and conclude that our low-dose RTX regimen is a promising treatment strategy for refractory IMN.

Citation: Wang YW, Wang XH, Wang HX, Yu RH. Successful treatment of patients with refractory idiopathic membranous nephropathy with low-dose Rituximab: A single-center experience. *World J Clin Cases* 2023; 11(3): 566-575
URL: https://www.wjgnet.com/2307-8960/full/v11/i3/566.htm
DOI: https://dx.doi.org/10.12998/wjcc.v11.i3.566

INTRODUCTION

Idiopathic membranous nephropathy (IMN) is a common pathological type of glomerular disease, and its incidence rate has been continuously increasing yearly[1]. In the past 10 years, the proportion of adult patients with IMN with renal puncture has risen from 12.2%–24.9%, ranking second among those with primary glomerular diseases[2]. Currently, IMN is considered to be an autoimmune disease[3]. The M-type phospholipase A2 receptor (PLA2R) on the cell surface of podocytes is the major target antigen in IMN and can be found in 70%–80% of IMN patients[4]. Additionally, new antigens. Such as thrombospondin type-1 domain-containing 7A, neural epidermal growth factor-like 1 protein, and semaphorin 3b have also been recently discovered[5,6], further rationalizing the use of B-cell-depleting agents.

Rituximab (RTX) is an anti-CD20 monoclonal antibody that is used to treat several autoimmune disorders[7]. Since 2004, some reports have explored the use of RTX in patients with refractory nephrotic syndrome, and the preliminary results showed that RTX may lead to remission and reduce immunosuppressive drug use[8,9]. According to the Kidney Disease Improving Global Outcomes 2021 guidelines, RTX is now the first-line therapy for patients with IMN, and the remission rate can reach 60%–80% at 12 mo[10]. However, 35%–40% of IMN patients still show no response to RTX. Refractory IMN is characterized by recurrence or resistance to RTX-based and other traditional immunosuppressive therapies, including prednisone (Pre), cyclophosphamide (CTX), and calcineurin inhibitors (CNIs)[11]. In Asia, 5%–14% of refractory patients progress to end-stage renal disease (ESRD) within 10–15 years[12]. Therefore, new therapies are urgently needed to treat IMN.

When introduced to IMN treatment, standard doses for RTX (375 mg/m^2 every week for four weeks or 1 g fixed-dose with a repeat dose in two weeks) were drawn from the preexisting dosages for treating other autoimmune diseases, such as anti-neutrophil cytoplasmic antibody-associated vasculitis, rheumatoid arthritis (RA), autoimmune cytopenia, and focal segmental glomerulosclerosis[13]. Recently, few case series studies have proven the effectiveness of low-dose RTX regimens with repeated injections in treating patients with refractory IMN and showed that low-dose RTX could effectively improve the remission rate and peripheral blood B-cell elimination[14]. Currently, for the treatment of RA, a low-dose RTX regimen (500 mg twice daily) has replaced the original dose (1000 mg twice daily) and become the new standard. Kurosu *et al*[15] reported a case of steroid-resistant Nephrotic syndrome, where the kidney pathology showed minimal changes in glomerulopathy. The patient achieved complete remission (CR) with a single dose of RTX of 375 mg/m^2. Wang *et al*[16] reported the case of a 51-year-old man diagnosed with refractory IMN. The patient received a single dose of 100 mg RTX, after which the B-cells declined rapidly, and a gradual reduction in proteinuria was also observed. Katsuno *et al*[17] reported three patients with refractory IMN who were treated with single-dose RTX (500–600 mg) where two of the patients achieved complete and incomplete remission.

Based on previous studies, we evaluated the efficacy and safety of low-dose RTX in patients with refractory IMN. The regimen included 200 mg RTX once a month for five months. Compared to traditional regimens, our regimen appears to be a promising treatment strategy for refractory IMN.

MATERIALS AND METHODS

Patients

This was a retrospective case series study that included patients with refractory IMN who were admitted at the Xiyuan Hospital of the Chinese Academy of Chinese Medical Science Department of Nephrology from October 2019 to December 2021 (n = 9).

Acceptance and discharge standards

The inclusion criteria were as follows: (1) Patients with histologically proven IMN and a PLA2R antibody-positive status (Anti-PLA2R titer > 20 RU/mL); (2) Patients diagnosed with refractory IMN, broadly defined, who still presented with the nephrotic syndrome after six months of regular corticosteroid and immunosuppressive therapies, including those with Pre, CTX, cyclosporine, tacrolimus, mycophenolate mofetil, and RTX[10]; (3) Patients who signed the informed consent form for the low-dose RTX regimen and fully understood the risks of treatment; and (4) Patients with a follow-up period of > 1 year with an interval of < three months or > four visits between visits *per* year. The patients had complete clinical data, including routine blood test results, liver and kidney function test results, 24 h urinary protein quantitation (UTP) test results, serum anti-PLA2R antibody titer, and $CD19^+$ B-cell counts. The exclusion criteria were as follows: (1) Presence of secondary membranous nephropathy, such as lupus nephritis, hepatitis B virus, hepatitis C, and tumors; (2) Glomerular diseases combined with other types; (3) Severe infections; and (4) Allergic reactions constitution.

Intervention

The low-dose RTX regimen was administered with a dose of 200 mg once a month for five months. Notably, after the patients were treated with RTX, the dosage of the primary therapeutic immunosuppressant was gradually decreased in all patients. If the patient's blood pressure remained > 130/80 mmHg, an appropriate angiotensin receptor blocker was added to the regime to stabilize blood pressure.

Every three months, clinical data such as 24 h UTP, serum ALB and serum creatinine (SCr) levels, PLA2R antibody titer, and $CD19^+$ B-cell count were evaluated.

Efficacy evaluation criteria

The primary outcome was complete clinical remission. A composite remission was defined either as a complete response (CR) or partial response (PR). Proteinuria of < 0.3 g/d is defined as CR, while PR is defined as a 24 h UTP of 0.3 g-3.5 g/d, or 24 h UTP decreased by more than 50% compared to baseline. No reaction was defined as a decrease in proteinuria of less than 30% or renal function deterioration.

The secondary outcomes were 24 h UTP, ALB and SCr levels, Anti-PLA2R titer, $CD19^+$ B-cell count, adverse events, and a composite endpoint of 40% reduction in estimated glomerular filtration rate, doubling of SCr, ESRD, and death.

Statistical methods

Statistical analyses were performed using IBM SPSS Statistics for Windows, version 23.0 (IBM Corp., Armonk, N.Y., United States). Data is presented as the mean ± SD unless otherwise indicated. The comparison of each indicator before and after treatment was performed using a paired sample t-test, and unsatisfactory results were expressed as the median. The paired rank-sum test was used to compare before and after the treatment. Qualitative data was expressed as percentages (%). Comparisons between the groups were performed using the chi-square test, and the test level was set to 0.05.

RESULTS

Baseline characteristics

Nine patients with refractory IMN were treated with low-dose RTX at our center between October 2019 and December 2021. The baseline features of the patients are listed in Table 1. There were five men and four women, with an average age of 44.0 ± 11.7 years. Of these, six patients were diagnosed with IMN by kidney biopsy, and the other three patients were diagnosed with a serum anti-PLA2R titer > 100 RU/mL. Furthermore, all nine (100%) patients tested positive for serum anti-PLA2R at the beginning of the trial. Before the administration of RTX, all nine patients had received regular corticosteroid and immunosuppressive therapy for at least six months prior and still presented with the nephrotic

Table 1 Baseline characteristics

Patient No.	Age (yr)	Sex	PLA2R	Duration (mo)	Previous treatment	Effect	Side effect	Current treatment
1	57	M	+	12	(1) RTX 500 mg iv twice in two months; and (2) Pre 40 mg/d + CSA 150 mg/d	SR	Serum glucose up	Pre + TAC
2	28	M	+	54	(1) Pre 20 mg/d + TAC 2 mg/d; and (2) Pre 24 mg/d + TAC 2 mg/d	SR	Cushing's syndrome	Pre + TAC
3	40	M	+	21	(1) CSA 150 mg/d; (2) Pre 20 mg/d + CTX 100 mg/d; and (3) Pre 30 mg + TAC 2 mg/d	SR	Hypertension	Pre + TAC
4	60	F	+	51	(1) TAC 2 mg/d; and (2) Pre 20 mg + CSA 150 mg/d	SR	Steroid-induced diabetes	Non
5	31	M	+	9	(1) CsA 150 mg/d; (2) Pre 48 mg/d + TAC 2 mg/d; and (3) Pre 48 mg/d + CTX 100 mg/d	SD	Steroid-induced diabetes; liver damage; Hypertension	Pre + TAC
6	29	F	+	31	(1) Pre 15 mg/d + CSA 150 mg/d; (2) Pre 40 mg/d + LEF 30 mg/d; and (3) Pre 25 mg/d + TAC 2 mg/d	SD	Cushing's syndrome; Hypertension	Pre
7	49	M	+	44	(1) Pre 40 mg/d + CSA 150 mg/d; and (2) Pre 24 mg/d + TAC 2 mg/d	SD	Cushing's syndrome; Steroid-induced diabetes	Pre + TAC
8	49	F	+	35	(1) Pre 50 mg/d + CTX 1000 mg iv; (2) Pre 30 mg/d + CSA 150 mg/d; and (3) TAC 3 mg/d	SR	Cushing's syndrome; Liver damage; Steroid-induced diabetes	Non
9	36	F	+	18	(1) Pre 24 mg/d + CSA 100 mg/d; and (2) TAC 2 mg/d	SR	Non	Non

M: Male; F: Femle; PLA2R: Phospholipase A2 receptor; RTX: Rituximab; Pre: Prednisone; CAS: Cyclosporine; TAC: Tacrolimus; LEF: Leflunomide; SR: Steroid-resistant; SD: Steroid-dependent.

syndrome; therefore, they were diagnosed with refractory IMN. Of these, six patients were steroid-resistant and three patients were steroid-dependent.

Furthermore, at baseline, all nine patients experienced adverse reactions triggered by the above treatment, including two with elevated serum glucose levels, one with hypertension, one with Cushing syndrome; one combined with steroid-induced diabetes, hypertension, and an abnormal liver function; one combined with hypertension and Cushing syndrome; one combined with steroid-induced diabetes and Cushing syndrome; and one combined with steroid-induced diabetes, an abnormal liver function, and an abnormal liver function.

Clinical outcomes during follow-up

The clinical outcomes of the nine patients during the twelve months of follow-up are listed in Table 2 and Supplementary Table 1. The proportion of patients who achieved CR or PR over time, as well as the trends of the remission rate, 24 h UTP, ALB, and SCr levels are shown in Figure 1. The PR and CR rates gradually increased with a lengthened treatment time. The remission rates were 56% (5/9; PR 5) at three months, 67% at six months (6/9; PR 6), 89% at nine and twelve months (8/9; CR 3 and PR 5). One patient did not complete the course of treatment due to adverse infusion reactions.

The comparison of the clinical outcomes at twelve months of follow-up is shown in Table 3. In the eight patients treated with a low dose of RTX for six months, the 24 h UTP and ALB levels showed no significant changes when compared with those before treatment. Nine months later, the 24 h UTP decreased from 8.14 ± 6.05 g/d to 1.74 ± 1.81 g/d ($P < 0.05$), and the ALB level improved from 28.06 ± 8.42 g/L to 36.84 ± 6.74 g/L ($P < 0.05$). At the end of the twelve-month follow-up, 24 h UTP decreased to 1.24 ± 1.34, and ALB improved to 40.93 ± 5.85 g/L, which are significant differences compared with those before treatment ($P < 0.05$ and $P < 0.01$, respectively). This means that the longer the follow-up period, the higher the remission rate. Notably, after administering RTX, there was a significant difference in the SCr levels when compared with those before treatment ($P < 0.05$).

Immunologic remission during follow-up

We used serum PLA2R antibodies and $CD19^+$ B-cells to assess immune remission. As shown in Table 4, all nine patients had elevated serum PLA2R antibody titers at the beginning of the trial. Concerning the anti-PLA2R titers before RTX administration, three patients had low titers of anti-PLA2R (≤ 50 IU/L), two patients had medium titers of anti-PLA2R (50–150 IU/L), and four patients had a high titer of anti-PLA2R (> 150 IU/L). Of them, eight patients were followed up for six months, and the titers of anti-PLA2R decreased after administering RTX. Furthermore, at the three-month follow-up, one patient (No. 6) tested negative for the PLA2R antibody; at the six-month follow-up, four patients (No. 1, 6, 8, and 9)

Table 2 Clinical outcomes

Patient No.	Before administering of RTX (0 mo)			After administering of RTX (6 mo)				Follow-up (12 mo)			
	24 h UTP (g/d)	ALB (g/L)	Scr (μmol/L)	24 h UTP (g/d)	ALB (g/L)	Scr (μmol/L)	Remission	24 h UTP (g/d)	ALB (g/L)	Scr (μmol/L)	Remission
1	15.2	13.9	97	2.3	25.1	64	PR	1.88	44	66	PR
2	7.1	29	78	3.6	36.9	72	NR	2	36.2	83	PR
3	17	16	202	9.9	24.3	93	NR	4	29.9	116	PR
4	6.7	26	142	-	-	-	-	-	-	-	-
5	5.7	35	84	1.03	45.1	64	PR	0.09	49.5	90	CR
6	1.8	37.4	78	1.3	42	82	PR	0.6	40.1	75	PR
7	3.5	32.5	90	1.8	35.1	69	PR	0.27	44.1	88	CR
8	15	26.9	91	6.2	29.4	70	PR	0.9	41.4	82	PR
9	1.3	35.8	125	0.64	39.1	111	PR	0.175	42.2	124	CR

UTP: Urinary protein quantitation; RTX: Rituximab; ALB: Albumin; Scr: Serum creatinine; PR: Partial remission; CR: Complete remission; NR: No remission.

Table 3 Comparison of clinical outcomes during follow-up

Outcome	0 (mo)	3 (mo)	6 (mo)	9 (mo)	12 (mo)
24 h UTP (g/d)	8.14 ± 6.05	5.65 ± 4.99	3.35 ± 3.20	1.74 ± 1.81[a]	1.24 ± 1.34[a]
ALB (g/L)	28.06 ± 8.42	32.39 ± 8.7	34.63 ± 7.69	36.84 ± 6.74[a]	40.93 ± 5.85[b,c]
Scr (μmol/L)	109.67 ± 40.87	97.38 ± 27.34	78.13 ± 16.49[a]	84.5 ± 16.96	90.5 ± 19.81
Remission rate (%)	–	56% (5/9)	67% (6/9)	89% (8/9)	89% (8/9)

[a]$P < 0.05$ *vs* 0 mo.
[b]$P < 0.01$ *vs* 0 mo.
[c]$P < 0.05$ *vs* 3 mo.
Data were analysed by one-way ANOVA followed by post hoc LSD test (albumin and serum creatinine) and presented as the mean ± SD. Data were analysed by Kruskal Wallis H test (24 h urinary protein quantitation).
UTP: Urinary protein quantitation; ALB: Albumin; Scr: Serum creatinine.

were negative for the PLA2R antibody. The level of $CD19^+$ B-cells decreased to 0 at three months, and remained the same until six months of follow-up.

Adverse events

During the median (8.7 ± 3.7 mo) period of follow-up, among the nine patients who experienced adverse reactions, one patient presented with shivering. Shivering occurred during the first infusion of RTX, but no dyspnea or fever occurred simultaneously. Symptoms were relieved 10 min after terminating the RTX treatment, and no RTX was infused afterwards; the patient did not complete the treatment. Two patients had a fever, which occurred within 24 h of RTX infusion. The body temperature was 37.5–38.5 °C, but returned to normal within 48 h without administering antibiotics. The fever did not recur.

DISCUSSION

IMN is the most common cause of primary nephrotic syndrome in adults. The prognosis of patients with IMN varies greatly, with around 1/3 of the patients progressing to ESRD within 10–15 years, and another 1/3 being relieved of symptoms[3]. To date, alkylating agents are the only drugs with a proven efficacy in preventing the development of ESRD[18]. Therefore, corticosteroid therapy combined with alkylating agents has been recognized as the treatment of choice for decades. Other immunosuppressive agents[19], such as CNIs, have been tested only in trials using proteinuria reduction as an alternative

Table 4 Serum anti-phospholipase A2 receptor titer and CD 19$^+$ B-cell count during administering of Rituximab

Patient No.	Before administering of RTX (0 mo)		Administering of RTX (3 mo)		After administering of RTX (6 mo)	
	Anti-PLA2R titer (RU/mL)	CD19$^+$ B (pcs/μL)	PLA2R antibody (RU/mL)	CD19$^+$ B (pcs/μL)	PLA2R antibody (RU/mL)	CD19$^+$ B (pcs/μL)
1	1400	418	104	0	Negative	0
2	180	6	96	0	82	0
3	215	169	67	0	48	0
4	500	422	-	-	-	-
5	32	114	27	0	20	0
6	45	28	Negative	0	Negative	0
7	52	460	22	0	17	0
8	130	192	38	0	Negative	0
9	36	258	21	0	Negative	0

RTX: Rituximab; PLA2R: Phospholipase A2 receptor.

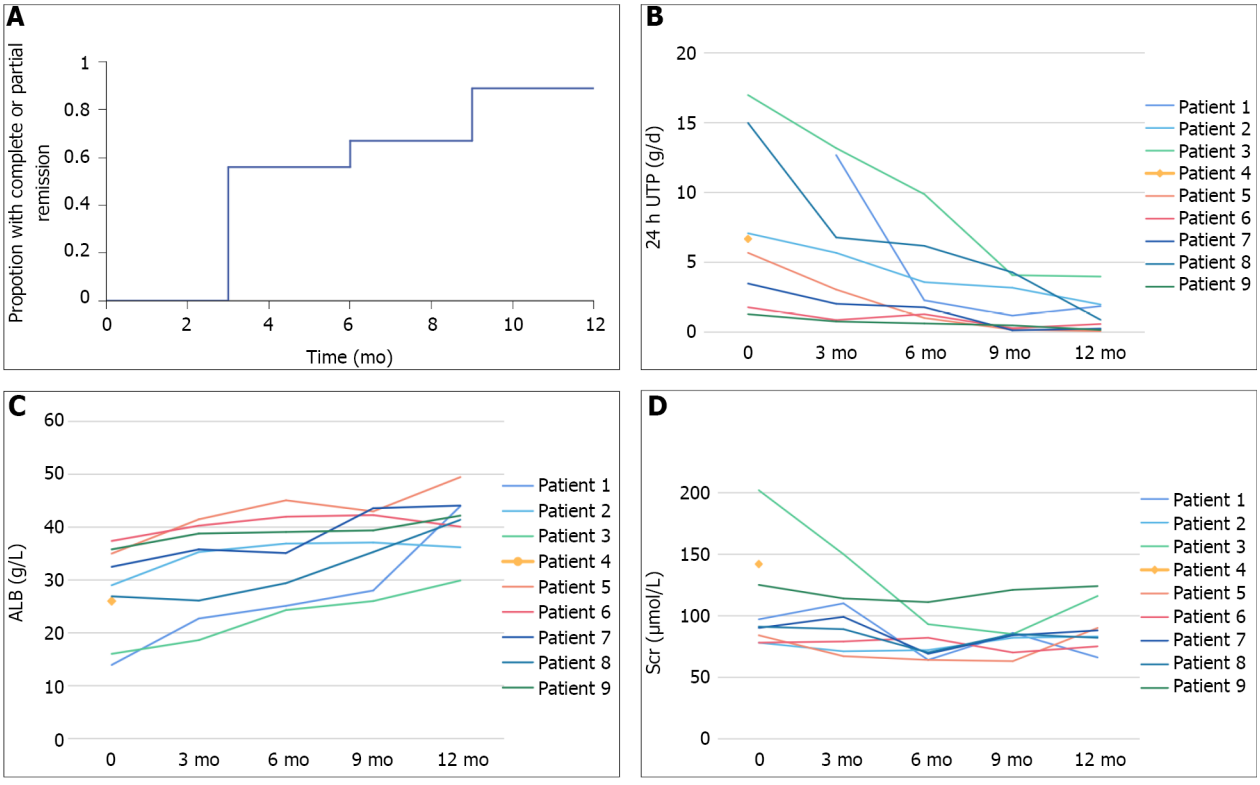

DOI: 10.12998/wjcc.v11.i3.566

Figure 1 Clinical outcomes. A: Kaplan-Meier curve for complete or partial remission; B: 24 h urinary protein quantification trend after Rituximab (RTX) in 9 patients with refractory idiopathic membranous nephropathy (IMN); C: Albumin trend after RTX in 9 patients with refractory IMN; D: Serum creatinine trend after RTX in 9 patients with refractory IMN. UTP: Urinary protein quantification; ALB: Albumin; SCr: Serum creatinine.

endpoint.

Although an effective immunosuppressive treatment scheme for IMN has been established clinically, 20%–30% of IMN patients are resistant to standard immunosuppressive therapy or often relapse[20]; these patients were diagnosed with refractory IMN. In Asia, 5%–14% of refractory IMN patients will progress to ESRD. Therefore, effective and safe therapeutic strategies for refractory IMN must be explored. In the past decade, significant advances in understanding of IMN have established that it is an autoantibody-driven disease[21,22]. As a result, there is a clear choice for treating B-cell depletion. Currently, RTX is the most important immunosuppressive treatment for IMN. The results of the MENTOR trial provide the basis for RTX being the first-line treatment in patients with IMN[23].

Although the results of RTX are promising, it should be noted that approximately 30%–40% of cases experience treatment failure, which means that other treatment regimens are needed. Currently, some studies have focused on the paradigm shift from RTX to new alternatives or combined drugs in treating patients with refractory IMN to overcome drug resistance. However, the second course of RTX may achieve remission even in the setting of resistant RTX after the first course[24].

The natural course of IMN varies greatly; thus, it is not suitable for all patients to receive a unified treatment and the optimal RTX dose for the treatment of IMN remains controversial. Different RTX application regimens were used across various studies, ranging from a single dose of 375 mg/m^2 to a repeated dose of 375 mg/m^2 for four weeks after six months. A prospective clinical study evaluated the low-dose RTX regimen (375 mg/m^2, once) compared with the standard RTX regimen (375 mg/m^2, four times)[25]. If the consumption of B-cells is insufficient, the same dose can be used in the low-dose RTX group. The results showed that among the twelve patients who were administered with low-dose RTX, only one needed a second dose to achieve complete B-cell depletion, and at 1 year, the remission rate of the two groups was the same. They also concluded that a single-dose RTX regimen was extremely cost-effective and may limit the production of antichimeric antibodies, lowering the risk of adverse reactions. Similarly, another retrospective study compared forty-two patients administered low-dose RTX (375 mg/m^2)[26]. The control group was treated with steroid hormones combined with alkylating agents or a standard RTX regimen (375 mg/m^2, four times). At twenty-four months, there was no significant difference in clinical outcomes between the two groups. All patients treated with RTX showed complete B-cell depletion in the first month, but B-cell recovery occurred earlier in the low-dose group than in the standard group. Recently, some case reports and case series studies have proven the effectiveness of low dose but RTX regimens with repeated injections in treating patients with refractory IMN. These regimens seem to extend the inhibition of B-cells. We explored a new RTX regimen (200 mg once a month for five months) for treating patients with refractory IMN in our hospital.

Nine patients with refractory PLAR-associated MN were included in this analysis. In the data provided twelve months after baseline, the remission rate was 56% (5/9; PR 5) at three months, 67% at six months (6/9; PR 6), and 89% at nine and twelve months (8/9; CR 3 and PR 5). Another patient did not complete the treatment because of infusion reactions. In a review of currently available studies, the overall remission rates (complete and partial) of RTX at twelve months of treatment for patients with IMN consistently ranged from 44%–85%. Few studies have reported that among patients with refractory IMN, the efficacy rate of RTX can only reach 40%. The remission rate of the low-dose RTX regimen at our center was significantly higher than that reported in previous studies.

In addition, we observed that clinical remission in patients with refractory IMN was slower than in patients with immune remission. We used serum PLA2R antibody titer and CD19$^+$ B-cell counts to assess immune remission. The level of CD19$^+$ B-cells decreased to 0 at three months, which was maintained until six months of follow-up. At the beginning of the trial, all nine patients were positive for the PLA2R antibody. The titers of anti-PLA2R decreased after administering low-dose RTX, and one patient (No. 6) had a normal anti-PLA2R titer after three months, while four patients (No. 1, 6, 8, and 9) had a normal anti-PLA2R titer after six months. However, when compared with the previous situation, the 24 h UTP and ALB levels showed no significant changes at six months. Until nine months post-treatment, 24 h UTP decreased from 8.14 ± 6.05 g/d to 1.74 ± 1.81 g/d ($P < 0.05$), while ALB has increased from 28.06 ± 8.42 g/L to 36.84 ± 6.74 g/L ($P < 0.05$). At the end of the twelve-month follow-up period, the clinical outcomes were significantly enhanced when compared to those before treatment. This means that the longer the follow-up time, the higher the remission rate that was observed. Notably, none of the eight patients had a recurrence until the to date.

Compared with the standardized dose (375 mg/m^2 every week for four weeks, or 1 g fixed-dose with a repeat dose in two weeks), our low-dose RTX regimen lasted for a longer time (*i.e.*, B-cell levels remained low for a longer period of time), which meant that the disease was less likely to relapse. Furthermore, when compared to the high-dose RTX and traditional immunosuppressive regimens, our low-dose RTX regimen also has advantages in terms of security. Although effective immunosuppressive regimens for IMN have been established clinically, the preceding therapeutic options have significant disadvantages, which limit their application, especially in patients with renal insufficiency. At the beginning of the trial, eight patients had a side reaction associated with previous immunosuppressive treatment. During the twelve-month follow-up that tracked adverse reactions, there was only one case of shivering. Notably, after administering RTX for six months, the SCr level decreased from 78.13 ± 16.49 μmol/L to 109.67 ± 40.87 μmol/L ($P < 0.05$). In this study, we found that our low-dose RTX regimen for the treatment of refractory IMN significantly improved the clinical outcomes and further increased the remission rate. Moreover, treatment with our low-dose RTX regimen is more cost-effective than that with high-dose RTX.

However, it is worth noting that this research also has few limitations that must be considered. First of all, since our study was retrospective in nature and the sample size was small ($n = 9$), the statistical analysis of data may have biases and inadequacies in terms of generalization. Second, the clinical outcomes were monitored after 1 year; however, the data on immunological indicators, including serum anti-PLA2R titer and CD19$^+$ B-cell count, were monitored only after six months. The long-term prognosis of our low-dose RTX regimen in treating refractory IMN patients is still yet to be explored. To confirm these results and deepen our understanding about this treatment option, we need to conduct

large-scale clinical trials and further clarify the mechanism of action of RTX in refractory IMN.

CONCLUSION

The treatment of patients with refractory IMN using RTX remains controversial and challenging. Conventional immunosuppressive treatment strategies have been applied for several years and have clinically established therapeutic efficacy. In conclusion, we found that our low-dose RTX regimen significantly improved clinical outcomes and further increased the remission rate of patients with IMN. Moreover, treatment with our low-dose RTX regimen is more cost-effective than that with high-dose RTX.

ARTICLE HIGHLIGHTS

Research background

The recognition of idiopathic membranous nephropathy (IMN) as an autoimmune disease has paved the way for the use of B-cell depleting agents such as Rituximab (RTX), which is now a first-line drug for IMN patients with proven safety and efficacy.

Research motivation

RTX for the treatment of refractory IMN patients remains controversial and challenging.

Research objectives

To evaluate the efficacy and safety of a new low-dose RTX regimen for the treatment of refractory IMN patients.

Research methods

A retrospective study was performed on refractory IMN patients that accepted Low-dose RTX regimen (RTX, 200 mg, once a month for five months).

Research results

A total of 9 refractory IMN patients were analyzed. At 12 mo of follow-up data from baseline, the 24 h urinary protein quantification was decreased from 8.14 ± 6.05 g/d to 1.24 ± 1.34 g/d ($P < 0.05$), and the albumin was improved from 28.06 ± 8.42 g/L to 40.93 ± 5.85 g/L ($P < 0.01$). Notably, after administering RTX for 6 mo, the serum creatinine decreased from 78.13 ± 16.49 μmol/L to 109.67 ± 40.87 μmol/L ($P < 0.05$). All of the 9 patients were serum anti-phospholipase A2 receptor (PLA2R) positive at the beginning, and 4 patients had a normal anti-PLA2R titer at six months. The level of $CD19^+$ B-cells decreased to 0 at three months, and the count of $CD19^+$ B-cells lasted to 0 until six months of follow-up.

Research conclusions

We found that our low-dose RTX regimen for the treatment of refractory IMN significantly improved clinical outcomes and further increased the remission rate.

Research perspectives

Treatment with our low-dose RTX regimen is more cost-effective than high-dose RTX.

FOOTNOTES

Author contributions: Wang HX and Wang YW contributed to the conception and design of the study; Wang HX, Wang YW, and Wang XH contributed to data collection, analysis, and interpretation; Wang YW and Wang XH wrote the manuscript; Yu RH critically revised the manuscript for important intellectual content; All authors revised the manuscript and approved the submitted version.

Supported by National Key Research and Development Program of China, No. 2019YFC1708503.

Institutional review board statement: The study protocol was approved by the ethics review board of Xiyuan Hospital, China's Academy of Chinese Medical Sciences (Beijing, China, approved No. 2022XLA130-2). All of the procedures were performed in accordance with the Declaration of Helsinki and relevant policies in China.

Informed consent statement: A written informed consent was obtained from the patient for publication of this case report.

Conflict-of-interest statement: All the authors report no relevant conflicts of interest for this article.

Data sharing statement: The datasets generated and/or analyzed during the current study are available from the corresponding author upon reasonable request.

Country/Territory of origin: China

ORCID number: Ren-Huan Yu 0000-0003-0879-5357.

S-Editor: Fan JR
L-Editor: A
P-Editor: Fan JR

REFERENCES

1 **Hu R**, Quan S, Wang Y, Zhou Y, Zhang Y, Liu L, Zhou XJ, Xing G. Spectrum of biopsy proven renal diseases in Central China: a 10-year retrospective study based on 34,630 cases. *Sci Rep* 2020; **10**: 10994 [PMID: 32620914 DOI: 10.1038/s41598-020-67910-w]
2 **Xu X**, Wang G, Chen N, Lu T, Nie S, Xu G, Zhang P, Luo Y, Wang Y, Wang X, Schwartz J, Geng J, Hou FF. Long-Term Exposure to Air Pollution and Increased Risk of Membranous Nephropathy in China. *J Am Soc Nephrol* 2016; **27**: 3739-3746 [PMID: 27365535 DOI: 10.1681/ASN.2016010093]
3 **Glassock RJ**. Diagnosis and natural course of membranous nephropathy. *Semin Nephrol* 2003; **23**: 324-332 [PMID: 12923720 DOI: 10.1016/s0270-9295(03)00049-4]
4 **Kao L**, Lam V, Waldman M, Glassock RJ, Zhu Q. Identification of the immunodominant epitope region in phospholipase A2 receptor-mediating autoantibody binding in idiopathic membranous nephropathy. *J Am Soc Nephrol* 2015; **26**: 291-301 [PMID: 25205735 DOI: 10.1681/ASN.2013121315]
5 **Sethi S**. New 'Antigens' in Membranous Nephropathy. *J Am Soc Nephrol* 2021; **32**: 268-278 [PMID: 33380523 DOI: 10.1681/ASN.2020071082]
6 **Suzuki T**, Han W, Watanabe S, Terashita M, Nakata M, Ichikawa D, Shirai S, Shibagaki Y. Clinical characteristics of thrombospondin type-1 domain-containing 7A-associated membranous nephropathy. *Ren Fail* 2020; **42**: 966-968 [PMID: 32935600 DOI: 10.1080/0886022X.2020.1819318]
7 **Chisari CG**, Sgarlata E, Arena S, Toscano S, Luca M, Patti F. Rituximab for the treatment of multiple sclerosis: a review. *J Neurol* 2022; **269**: 159-183 [PMID: 33416999 DOI: 10.1007/s00415-020-10362-z]
8 **Fervenza FC**, Cosio FG, Erickson SB, Specks U, Herzenberg AM, Dillon JJ, Leung N, Cohen IM, Wochos DN, Bergstralh E, Hladunewich M, Cattran DC. Rituximab treatment of idiopathic membranous nephropathy. *Kidney Int* 2008; **73**: 117-125 [PMID: 17943078 DOI: 10.1038/sj.ki.5002628]
9 **Fervenza FC**, Abraham RS, Erickson SB, Irazabal MV, Eirin A, Specks U, Nachman PH, Bergstralh EJ, Leung N, Cosio FG, Hogan MC, Dillon JJ, Hickson LJ, Li X, Cattran DC; Mayo Nephrology Collaborative Group. Rituximab therapy in idiopathic membranous nephropathy: a 2-year study. *Clin J Am Soc Nephrol* 2010; **5**: 2188-2198 [PMID: 20705965 DOI: 10.2215/CJN.05080610]
10 **Waldman M**, Beck LH Jr, Braun M, Wilkins K, Balow JE, Austin HA 3rd. Membranous nephropathy: Pilot study of a novel regimen combining cyclosporine and Rituximab. *Kidney Int Rep* 2016; **1**: 73-84 [PMID: 27942609 DOI: 10.1016/j.ekir.2016.05.002]
11 **Hofstra JM**, Branten AJ, Wirtz JJ, Noordzij TC, du Buf-Vereijken PW, Wetzels JF. Early *vs* late start of immunosuppressive therapy in idiopathic membranous nephropathy: a randomized controlled trial. *Nephrol Dial Transplant* 2010; **25**: 129-136 [PMID: 19666912 DOI: 10.1093/ndt/gfp390]
12 **Shi B**, Zhang RR, Liang Y, Wang XH, Lang R, Yu RH. Efficacy of Traditional Chinese Medicine Regimen Jian Pi Qu Shi Formula for Refractory Patients with Idiopathic Membranous Nephropathy: A Retrospective Case-Series Study. *Evid Based Complement Alternat Med* 2018; **2018**: 5854710 [PMID: 30344612 DOI: 10.1155/2018/5854710]
13 **Genberg H**, Hansson A, Wernerson A, Wennberg L, Tydén G. Pharmacodynamics of rituximab in kidney allotransplantation. *Am J Transplant* 2006; **6**: 2418-2428 [PMID: 16925569 DOI: 10.1111/j.1600-6143.2006.01497.x]
14 **Rojas-Rivera JE**, Carriazo S, Ortiz A. Treatment of idiopathic membranous nephropathy in adults: KDIGO 2012, cyclophosphamide and cyclosporine A are out, rituximab is the new normal. *Clin Kidney J* 2019; **12**: 629-638 [PMID: 31583088 DOI: 10.1093/ckj/sfz127]
15 **Kurosu N**, Sugiura H, Iwasaki C, Asamiya Y, Kojima C, Moriyama T, Itabashi M, Tsukada M, Takei T, Ogawa T, Yoshida T, Uchida K, Tsuchiya K, Nitta K. Successful use of single-dose rituximab for the maintenance of remission in a patient with steroid-resistant nephrotic syndrome. *Intern Med* 2009; **48**: 1901-1904 [PMID: 19881243 DOI: 10.2169/internalmedicine.48.2435]
16 **Wang XP**, Hu ZX, Guo DY, Tao Y. Remission of Refractory Membranous Nephropathy by Low-dose Rituximab: A Case Report. *Chin Med J (Engl)* 2016; **129**: 871-873 [PMID: 26996486 DOI: 10.4103/0366-6999.178967]

17 **Katsuno T**, Ozaki T, Kim H, Kato N, Suzuki Y, Akiyama S, Ishimoto T, Kosugi T, Tsuboi N, Ito Y, Maruyama S. Single-dose Rituximab Therapy for Refractory Idiopathic Membranous Nephropathy: A Single-center Experience. *Intern Med* 2017; **56**: 1679-1686 [PMID: 28674357 DOI: 10.2169/internalmedicine.56.7908]

18 **Kidney Disease: Improving Global Outcomes (KDIGO) Glomerular Diseases Work Group**. KDIGO 2021 Clinical Practice Guideline for the Management of Glomerular Diseases. *Kidney Int* 2021; **100**: S1-S276 [PMID: 34556256 DOI: 10.1016/j.kint.2021.05.021]

19 **Couser WG**. Primary Membranous Nephropathy. *Clin J Am Soc Nephrol* 2017; **12**: 983-997 [PMID: 28550082 DOI: 10.2215/CJN.11761116]

20 **Gao S**, Cui Z, Wang X, Zhang YM, Wang F, Cheng XY, Meng LQ, Zhou FD, Liu G, Zhao MH. Rituximab Therapy for Primary Membranous Nephropathy in a Chinese Cohort. *Front Med (Lausanne)* 2021; **8**: 663680 [PMID: 34095173 DOI: 10.3389/fmed.2021.663680]

21 **Teisseyre M**, Cremoni M, Boyer-Suavet S, Ruetsch C, Graça D, Esnault VLM, Brglez V, Seitz-Polski B. Advances in the Management of Primary Membranous Nephropathy and Rituximab-Refractory Membranous Nephropathy. *Front Immunol* 2022; **13**: 859419 [PMID: 35603210 DOI: 10.3389/fimmu.2022.859419]

22 **Paulina XMR**, Anupama P, Xuefei T. New insights into the immunity and podocyte in glomerular health and disease: From pathogenesis to therapy in proteinuric kidney disease. *Integr Med Nephrol Androl* 2021; **8**: 5

23 **Fervenza FC**, Appel GB, Barbour SJ, Rovin BH, Lafayette RA, Aslam N, Jefferson JA, Gipson PE, Rizk DV, Sedor JR, Simon JF, McCarthy ET, Brenchley P, Sethi S, Avila-Casado C, Beanlands H, Lieske JC, Philibert D, Li T, Thomas LF, Green DF, Juncos LA, Beara-Lasic L, Blumenthal SS, Sussman AN, Erickson SB, Hladunewich M, Canetta PA, Hebert LA, Leung N, Radhakrishnan J, Reich HN, Parikh SV, Gipson DS, Lee DK, da Costa BR, Jüni P, Cattran DC; MENTOR Investigators. Rituximab or Cyclosporine in the Treatment of Membranous Nephropathy. *N Engl J Med* 2019; **381**: 36-46 [PMID: 31269364 DOI: 10.1056/NEJMoa1814427]

24 **Boyer-Suavet S**, Andreani M, Lateb M, Savenkoff B, Brglez V, Benzaken S, Bernard G, Nachman PH, Esnault V, Seitz-Polski B. Neutralizing Anti-Rituximab Antibodies and Relapse in Membranous Nephropathy Treated With Rituximab. *Front Immunol* 2019; **10**: 3069 [PMID: 31998325 DOI: 10.3389/fimmu.2019.03069]

25 **Cravedi P**, Ruggenenti P, Sghirlanzoni MC, Remuzzi G. Titrating rituximab to circulating B cells to optimize lymphocytolytic therapy in idiopathic membranous nephropathy. *Clin J Am Soc Nephrol* 2007; **2**: 932-937 [PMID: 17702725 DOI: 10.2215/CJN.01180307]

26 **Fenoglio R**, Baldovino S, Sciascia S, De Simone E, Del Vecchio G, Ferro M, Quattrocchio G, Naretto C, Roccatello D. Efficacy of low or standard rituximab-based protocols and comparison to Ponticelli's regimen in membranous nephropathy. *J Nephrol* 2021; **34**: 565-571 [PMID: 32594370 DOI: 10.1007/s40620-020-00781-6]

World Journal of Clinical Cases

Submit a Manuscript: https://www.f6publishing.com

World J Clin Cases 2023 January 26; 11(3): 576-597

DOI: 10.12998/wjcc.v11.i3.576

ISSN 2307-8960 (online)

ORIGINAL ARTICLE

Retrospective Study

Bowel inflammatory presentations on computed tomography in adult patients with severe aplastic anemia during flared inflammatory episodes

Xi-Chen Zhao, Cheng-Jiang Xue, Hui Song, Bin-Han Gao, Fu-Shen Han, Shu-Xin Xiao

Specialty type: Hematology

Provenance and peer review: Unsolicited article; Externally peer reviewed.

Peer-review model: Single blind

Peer-review report's scientific quality classification

Grade A (Excellent): 0
Grade B (Very good): B
Grade C (Good): C
Grade D (Fair): D
Grade E (Poor): 0

P-Reviewer: Ishfaq A, United States; Patel GR, India

Received: October 19, 2022
Peer-review started: October 19, 2022
First decision: November 25, 2022
Revised: December 3, 2022
Accepted: January 5, 2023
Article in press: January 5, 2023
Published online: January 26, 2023

Xi-Chen Zhao, Department of Hematology, The Central Hospital of Qingdao West Coast New Area, Qingdao 266555, Shandong Province, China

Cheng-Jiang Xue, Department of Neurosurgery, The Central Hospital of Qingdao West Coast New Area, Qingdao 266555, Shandong Province, China

Hui Song, Bin-Han Gao, Department of Radiology, The Central Hospital of Qingdao West Coast New Area, Qingdao 266555, Shandong Province, China

Fu-Shen Han, Department of Pneumology, The Central Hospital of Qingdao West Coast New Area, Qingdao 266555, Shandong Province, China

Shu-Xin Xiao, Department of Hematology, The Affiliated Hospital of Qingdao University, Qingdao 266000, Shandong Province, China

Corresponding author: Shu-Xin Xiao, MD, Chief Physician, Department of Hematology, The Affiliated Hospital of Qingdao University, No. 16 Jiangsu Road, Qingdao 266000, Shandong Province, China. xsxa@sina.com

Abstract

BACKGROUND

Patients with severe aplastic anemia (SAA) frequently present with inflammatory episodes, and during flared inflammatory episodes, hematopoietic function is further exacerbated. The gastrointestinal tract is the most common site for infectious and inflammatory diseases, and its structural and functional features confer on it the most potent capacity to affect hematopoietic and immune functions. Computed tomography (CT) is a readily accessible approach to provide highly useful information in detecting morphological changes and guiding further work-ups.

AIM

To explore CT imaging presentations of gut inflammatory damage in adult SAA patients during inflammatory episodes.

METHODS

We retrospectively evaluated the abdominal CT imaging presentations of 17

hospitalized adult patients with SAA in search of the inflammatory niche when they presented with systemic inflammatory stress and exacerbated hematopoietic function. In this descriptive manuscript, the characteristic images that suggested the presence of gastrointestinal inflammatory damage and related imaging presentations of individual patients were enumerated, analyzed and described.

RESULTS

All eligible patients with SAA had CT imaging abnormalities that suggested the presence of an impaired intestinal barrier and increased epithelial permeability. The inflammatory damages were concurrently present in the small intestine, the ileocecal region and the large intestines. Some readily identified imaging signs, such as bowel wall thickening with mural stratification ("water holo sign", "fat holo sign", intramural gas and subserosal pneumatosis) and mesenteric fat proliferation (fat stranding and "creeping fat sign"), fibrotic bowel wall thickening, "balloon sign", rugged colonic configuration, heterogeneity in the bowel wall texture, and adhered and clustered small bowel loop (including various patterns of "abdominal cocoon"), occurred at a high incidence, which suggested that the damaged gastrointestinal tract is a common inflammatory niche responsible for the systemic inflammatory stresses and the exacerbated hematopoietic failure in patients with SAA. Particularly, the "fat holo sign" was present in 7 patients, a rugged colonic configuration was present in 10 patients, the adhesive bowel loop was present in 15 patients, and extraintestinal manifestations suggestive of tuberculosis infections were present in 5 patients. According to the imaging features, a suggestive diagnosis of Crohn's disease was made in 5 patients, ulcerative colitis in 1 patient, chronic periappendiceal abscess in 1 patient, and tuberculosis infection in 5 patients. Other patients were diagnosed with chronic enteroclolitis with acutely aggravated inflammatory damage.

CONCLUSION

Patients with SAA had CT imaging patterns that suggested the presence of active chronic inflammatory conditions and aggravated inflammatory damage during flared inflammatory episodes.

Key Words: Aplastic anemia; Computed tomography; Bowel inflammatory damage; Fat holo sign; Balloon sign; Abdominal cocoon

Core Tip: Patients with severe aplastic anemia frequently present with inflammatory episodes. The gastrointestinal tract is the most common site for infectious and inflammatory diseases, and its structural and functional features confer on it the most potent capacity to affect hematopoietic and immune functions. We retrospectively reviewed the bowel morphological changes on computed tomography in seventeen patients with severe aplastic anemia during flared inflammatory episodes. All patients demonstrated imaging abnormalities that suggested the presence of active chronic inflammatory conditions and aggravated inflammatory damage in the gastrointestinal tract. These inflammatory conditions likely contributed to their systemic inflammatory stresses and exacerbated hematopoietic failure.

Citation: Zhao XC, Xue CJ, Song H, Gao BH, Han FS, Xiao SX. Bowel inflammatory presentations on computed tomography in adult patients with severe aplastic anemia during flared inflammatory episodes. *World J Clin Cases* 2023; 11(3): 576-597

URL: https://www.wjgnet.com/2307-8960/full/v11/i3/576.htm

DOI: https://dx.doi.org/10.12998/wjcc.v11.i3.576

INTRODUCTION

Aplastic anemia (AA) is the paradigm of hematopioetic failure resulting from the immune-mediated destruction of hematopoietic progenitor cells, leading to heavily suppressed blood cell productivity and peripheral cytopenia. In patients with severe AA (SAA), fulminant infections, frequently in the absence of localized symptoms and signs, and refractory to broad-spectrum antibiotics, are the most common complications and the main causes of death. Infections in SAA are usually attributed to severely impaired granulopoiesis, and it frequently has a poor response to recombinant human granulocyte colony-stimulating factor (rhG-CSF) treatment[1-3]. However, successful treatment of the underlying

infections can significantly improve the hematological profile and even achieve a complete hematological remission in some patients, providing strong evidence that aggravated inflammatory reactions are responsible, at least in a fraction of patients, for the exacerbated hematopoietic suppression[4-6]. Very recently, initiation and perpetuation of AA pathogenesis has been found to be associated with gut inflammatory disorders (GIDs)[7,8]. However, the role of GIDs in AA pathogenesis is overlooked likely due to the high prevalence and good tolerance of GIDs and the low incidence of AA.

The gastrointestinal tract hosts the most enriched and complex microbial community in the human body. Not only pathogenic microbes but also dysbiotic commensal bacteria and various chemical components can compromise the intestinal barrier[9,10]. In the setting of impaired intestinal barrier structure and function, antigens from commensal microbes and undigested food as a source of continuous antigen supply can translocate to the lamina propria, blood, and remote organs and come into intimate contact with host immune cells, thereby initiating and perpetuating autoimmunity[11,12] and amplifying aberrant immune responses[13]. The gastrointestinal tract also hosts the most enriched lymphoid tissues and hence can provide sufficient activated immune cells to sustain exaggerated immune responses. Because the body is constantly confronted with various harmful environmental factors, the gastrointestinal tract is the most common site for infectious and inflammatory diseases[9,10].

Active GIDs, whether as a consequence or as an incentive factor in the process of gut dysbiosis and epithelial damage, can lead to morphological manifestations that can be detected by various imaging modalities. The imaging presentations are usually nonspecific, and arriving at an etiopathological diagnosis usually necessitates the comprehensive analysis of data from clinical, endoscopic, pathological and laboratory investigations, and is frequently dependent on the results of specific laboratory tests and the responses to specific treatments. However, computed tomography (CT) is a readily accessible approach able to provide highly useful information not only in detecting the distribution, extent, degree, and patterns of the gastrointestinal lesions and the adjacent inflammatory changes that prompt a radiological diagnosis but also in guiding further work-ups for pathognomonic diagnosis, identifying complications, evaluating treatment responses and monitoring disease activities in the subsequent follow-ups[14-16]. In this study, we explored the CT imaging manifestations of the gastrointestinal tract in adult patients with SAA during flared inflammatory episodes and showed that all patients had imaging abnormalities suggesting the presence of active chronic gut inflammatory conditions and acutely aggravated inflammatory damages.

MATERIALS AND METHODS

Participants

In this retrospective study, we reviewed the abdominal CT images in 17 hospitalized adult SAA patients who were treated at our center from October 2019 to March 2022, including 8 males and 9 females, with a median age of 55 years (ranging from 34 to 78 years). They were hospitalized due to rapidly exacerbated cytopenia, aggravated fatigue, varying degrees of febrile episodes and elevated inflammatory indices, indicating the presence of systemic inflammatory responses[1-3]. Each patient was definitively diagnosed with SAA for more than 2 years, and the SAA progressed from non-SAA (NSAA) after the patients experienced various accelerating episodes. In addition to supportive care, they were routinely treated with cyclosporine (3-4 mg/kg/d), stanozolol (6-8 mg/d) and eltrombopag (50 mg/d) in the SAA stage, in the absence of any therapeutic responses. In the patients with very SAA (VSAA), recombinant human granulocyte colony-stimulating factor (rhG-CSF, 100-200 μg/d) was added, without an evident increase in granulocytes. Patients who had diseases of portal hypertension, hepatic disease, pancreatic disease, cardiopulmonary disease, heart failure, severe hypoalbuminemia and ischemic enteropathy were excluded, because these diseases can cause stratified bowel wall thickening by blood congestion in the gastrointestinal tract, which may confound the imaging presentations of inflammatory lesions[16-18]. Abdominal CT was performed to search for the inflammatory niche before antibiotic and other treatments.

The modified Camitta criteria were used to assess severity of AA[3]: The diagnostic criteria for SAA were absolute neutrophil count (ANC) < 0.5×10^9/L, platelets (Plts) < 20×10^9/L, and absolute reticulocyte count (Ret) < 20×10^9/L. The diagnostic criteria for VSAA were ANC < 0.2×10^9/L in addition to the above hematological presentations.

Study procedure

CT imaging modalities: Conventional CT was performed for all patients in the search of the inflammatory niche during flared inflammatory episodes. If the conventional CT was sufficient to determine the radiological changes, contrast-enhanced CT was waived in order to reduce the radiation exposure. If the conventional CT was unable to determine the imaging abnormalities due to the difficulty in the discrimination of a massive lesion from contents in the intestinal lumen or due to the suspicion of a massive lesion being malignant, contrast-enhanced CT was performed. Meanwhile, endoscopic examination of the large intestine and ileocecal region was performed. Contrast-enhanced CT was performed in 1 patient in this study. Multiplanar reconstruction was performed for the assessment and

expression of the radiological manifestations.

CT image reviewing process: Each patient's CT images were reviewed, and the imaging abnormalities were collected independently by each of the six authors: Xi-Chen Zhao, Cheng-Jiang Xue, Hui Song, Bin-Han Gao, Fu-Sen Han, and Shu-Xin Xiao. After several rounds of extensive consultation, the imaging abnormalities suggesting the presence of GIDs were decided by the first and corresponding author. In patients with evident chest CT presentations that likely had pathogenic relationships with the bowel inflammatory damages; those chest CT abnormalities were also enumerated and described.

Radiological manifestations suggesting the gut involvement of inflammatory disorders: After careful assessment of the radiographs and after extensive consultations within our research group with reference to the patients' symptoms and signs, the following imaging presentations were considered to have abnormalities suggestive of the presence of GIDs.

First, the criteria for the diagnosis of bowel wall thickening met one of the following criteria[17-21]: (1) Bowel wall thickness greater than 3 mm in adequately distended intestinal segments; (2) bowel wall thickness greater than 4 mm in underdistended intestinal segments; (3) cross-sectional diameter greater than 6 mm in collapsed small intestines; and (4) cross-sectional diameter greater than 5 mm in collapsed large intestines.

The bowel wall thickening may be focal or segmental, symmetrical or asymmetrical, concentric or eccentric, homogeneous or heterogeneous. The following signs were helpful in the identification of the location and extent of the diseased bowel segments: (1) Mesenteric inflammatory changes indicative of transmural inflammation: "fat stranding"[22,23], "creeping fat sign"[24-26] and "comb sign"[27,28]; (2) mural stratification indicative of edematous bowel wall (water holo sign) and submucosal fat deposition (fat holo sign)[17-21]; (3) intramural gas and/or subserosal pneumatosis indicative of aerogenous bacterial proliferation in the bowel wall[14-16]; (4) gas-liquid levels in the intestinal lumen indicative of intestinal dynamical abnormalities; (5) heterogeneity in the bowel wall texture especially with segmentally gas-filled and segmentally liquid-filled intestinal lumen; (6) inflamed diverticulitis; (7) epiplioic appendagitis; (8)"empty colon sign" or narrowed bowel lumen[15,16]; (9) adhesive bowel loop, especially with mesenteric inflammatory changes and/or adjacent peritoneal fibrotic thickening ("abdominal cocoon")[29-32]; and (10) rugged colonic configuration, especially with mesenteric inflammatory changes and/or adjacent peritoneal fibrotic thickening.

Second, the "balloon sign" refers to a segment of a paper-thin bowel wall (a highly dilated and thinned bowel segment filled with gas) wrapped by a large cluster of circumferentially distributed hypervascular mesenteric fat stranding[33-36]. The hypervascular mesenteric fat deposition suggests the presence of active chronic transmural inflammatory damage in the diseased intestinal segments[22-26].

Third, peritoneal involvement: Including peritoneal thickening, ascites particularly loculated ascites and peritoneal nodularity.

In the evaluation of bowel inflammatory damage, particular attention was given to imaging abnormalities in the large intestines and ileocecal region, since in these sites, the lymphoid tissues are the most enriched and the microbial community is the most abundant; therefore, inflammatory damage and compromised epithelial integrity in these intestinal segments has the most potent capability to supply sufficient intestine-derived antigens and to activate sufficient immune cells and hence has the most potent capability to affect hematopoietic and immune functions[9,10].

This study was approved by the Institutional Review Board of The Central Hospital of Qingdao West Coast New Area and followed the Declaration of Helsinki (No. 2022-10-08). The requirement for written informed consent was waived by the Review Board since this was a retrospective study, and no information about patient identification was revealed in the manuscript.

Statistical analysis

Categorical data are presented as numbers with percentages, and continuous data are presented as medians with interquartile ranges.

RESULTS

General characteristics of patients

General information, severity of AA, disease duration, complete blood cell count (CBC) results when abdominal CT was performed, major gastrointestinal presentations and suggested radiological diagnosis are listed in Table 1. Seventeen patients (8 men and 9 women) with a median age of 55 years, ranging from 34 years to 78 years were enrolled. The total AA duration ranged from 8 years to 23 years, with a median duration of 13 years, and the total SAA duration ranged from 2 years to 9 years, with a median duration of 5 years. Among all patients, 5 had VSAA. Abdominal tenderness was present in all patients, but abdominal pain was present in only 8 patients, in accordance with the good tolerance of GIDs. Abnormalities in the frequency and property of the feces were present in 11 patients.

Table 1 Clinical characteristics and rediological diagnosis of the studied patients

No.	Sex/age	Hematological diagnosis	Total duration (yr)	SAA duration (yr)	CBC results					Abdominal symptoms	Suggested radiological diagnosis	Extraintestinal abnormalities
					WBC	ANC	Hb	Plts	Rets			
01	M/54	VSAA	23	8	0.66	0.14	44	5	3.17	AP, AT	CAA	
02	M/46	SAA	16	6	1.24	0.55	42	11	6.16	AT	CEC	
03	F/78	VSAA	11	3	0.65	0.17	41	8	1.81	AP, AT	CD	
04	F/38	SAA	17	6	1.62	0.71	45	18	4.18	AP, AT	CEC	
05	M/71	VSAA	14	4	0.57	0.08	42	2	1.92	AT	UC, ATB?	+
06	M/65	SAA	21	8	1.38	0.42	46	13	5.47	AP, AT	CEC	
07	F/52	SAA	11	5	1.48	0.44	53	21	4.62	AT	CEC	
08	M/61	SAA	21	7	1.73	0.77	62	16	2.28	AT	CD, ATB?	+
09	F/55	SAA	9	3	1.17	0.43	48	6	11.75	AT	CEC	
10	M/77	VSAA	8	4	0.42	0.16	40	4	1.78	AT	CD	
11	M/57	SAA	12	2	1.14	0.36	45	14	6.32	AP, AT	CEC	
12	F/48	SAA	12	6	0.92	0.44	40	3	2.08	AT	CD	
13	F/34	SAA	18	7	0.92	0.31	62	7	1.59	AP, AT	ATB?	+
14	F/40	SAA	13	4	0.86	0.27	44	2	6.03	AP, AT	CD	
15	F/42	SAA	20	9	0.82	0.39	51	18	2.14	AT	CEC	
16	M/68	VSAA	10	3	0.47	0.14	39	6	3.44	AT	CEC, ATB?	+
17	F/36	SAA	11	3	1.38	0.31	46	9	8.41	AP, AT	ATB?	+

M: Male; F: Female; SAA: Severe aplastic anemia; VSAA: Very-severe aplastic anemia; WBC: White blood cells (× 10^9/L); CBC: Complete blood cell count; WBC: White blood cell count; ANC: Absolute neutrophil count (× 10^9/L); Hb: Hemoglobulin (g/L); Plt: Platelets (× 10^9/L); Ret: Absolute reticulocyte count (× 10^9/L); AP: Abdominal pain; AT: Abdominal tenderness; CAA: Chronic appendiceal abscess; CEC: Chronic enterocolitis; ATB: Abdominal tuberculosis; CD: Crohn's disease; UC: Ulcerative colitis.

CT imaging abnormalities reflecting gut involvement of inflammatory conditions

Characteristic images are enumerated, analyzed and described in the Discussion section. All patients recruited in this study presented with evident imaging abnormalities that suggested the presence of inflammatory damages in the gastrointestinal tract. Noticeably, inflammatory involvement of the large intestine and the ileocecal region was present in all patients. Inflammatory lesions were also present in the small intestine in all patients, suggesting that the inflammatory pathogenesis was most likely initiated at the proximal gastrointestinal tract. According to the imaging features, a suggestive diagnosis

of Crohn's disease was made in 5 patients, ulcerative colitis in 1 patient, chronic periappendiceal abscess in 1 patient, and tuberculosis infection in 5 patients. Other patients were diagnosed with chronic enterocolitis with acutely aggravated inflammatory damage. The suggested radiological diagnosis is listed in Table 1.

DISCUSSION

The severity of cellular immune-mediated hematopoietic suppression in patients with AA commonly fluctuates in parallel with the waxing and waning of physical and mental stresses, and these stresses are obviously driven by active chronic inflammatory conditions and their recurrently aggravated episodes. In flared inflammatory episodes, blood cell production is heavily suppressed, and cytopenia worsens. With effective treatment of the inflammatory episodes, blood cell productivity can be significantly improved. Along with the increased frequency of and decreased intervals between these inflammatory episodes, patients eventually enter into an advanced stage, in which immune-mediated hematological damage is exacerbated and the sensitivity to previous effective treatments is lost[1,2,37,38].

This is not surprising because the blood cells themselves are immune cells, and their production is regulated largely in response to a variety of microbial attacks. When confronting an acute and limited infection, host hematopoiesis skews its proliferation and differentiation toward the production of innate immune cells to fight against the invading microbes at the expense of reduced self-renewal capacity[39,40]. After the infected pathogens are cleared out, the activated host immune system quickly returns to the homeostatic state, and the skewed blood cell production ends. However, in the setting of active chronic inflammatory conditions or overwhelming infections, host hematopoiesis can be heavily suppressed and exhausted due to prolonged and exaggerated immune responses and the subsequently overproduced proinflammatory mediators[41-43], resulting in heavily decreased marrow cellularity and increased peripheral cytopenia in genetically susceptible subjects, which are the characteristic morphological and immunological changes seen in AA[1-3]. The sustenance of an active inflammatory condition in which the degree and duration of immune responses are sufficient to induce severe aplastic cytopenia critically necessitates sufficient activated immune cells and a continuous antigen supply.

The gastrointestinal tract provides the largest interface bridging the host neuro-endocrine-immune system with environmental factors and is constantly confronted with a variety of environmental challenges. The gastrointestinal tract also hosts the body's most abundant gut-associated lymphoid tissues and microbial community[9,10]. These structural and functional characteristics make the gastrointestinal tract the most vulnerable site for pathogen invasion and chemical injuries and the most common source of a continuous antigen supply. Therefore, the gastrointestinal tract becomes the most important site for pathological interactions between host immune cells and pathogenic antigens.

The gastrointestinal tract is the most common site for chronic and active inflammatory niches not only due to various pathogenic microbial attacks and chemical injuries but also due to dysbiotic commensal microbes and autoimmunity. Such abundant lymphoid tissues and microbial communities confer on the gastrointestinal tract the ability to provide sufficient activated immune cells and a continuous antigen supply and thereby have the most potent capacity to continuously release excessive proinflammatory cytokines.

Under chronic and active inflammatory conditions, upregulated human leukocyte antigen and pattern recognition receptors on hematopoietic progenitors enhance their responsiveness to pathogenic stimulation[44-46], and upregulated Fas molecules accelerate their apoptotic cell death[45], eventually resulting in the exhaustion of hematopoietic progenitor cells. The severity of GIDs is largely affected by changes in a variety of environmental factors, such as food supplements[47-49], antibiotic abuse[50,51], mental stresses[52,53] and pathogen invasion, leading to the fluctuant property of GIDs, in accordance with the fluctuant property of AA.

AA has been reported to be associated with gut inflammatory diseases, including inflammatory bowel disease, celiac disease and neutropenic enterocolitis[8]. In our previously reported case, intermittent treatments with a gut-cleansing preparation achieved reproducible hematological remissions, providing direct evidence for the role of GIDs in the initiation and perpetuation of AA pathophysiology[4]. Merely gluten-free diets[5] or resection of diseased intestinal segments[6] can achieve excellent hematological improvement, providing convincing evidence that GIDs play an indispensable role in the sustenance of AA pathophysiology.

In this pathogenic process, impaired intestinal integrity and increased epithelial permeability play pivotal roles[11,12]. These GID-associated morphological changes could be detected by various imaging modalities. Abdominal CT is a readily accessible and highly efficient imaging modality for detecting morphological changes in the gastrointestinal tract[14-16,19,20]. In this study, we explored the abdominal imaging presentations in patients with SAA in search of the inflammatory niche when the patients presented with systemic inflammatory stresses. We selected patients with SAA experiencing flared episodes because during this stage, morphological changes due to the gut inflammation are probably more serious and hence more easily identified by radiological examination.

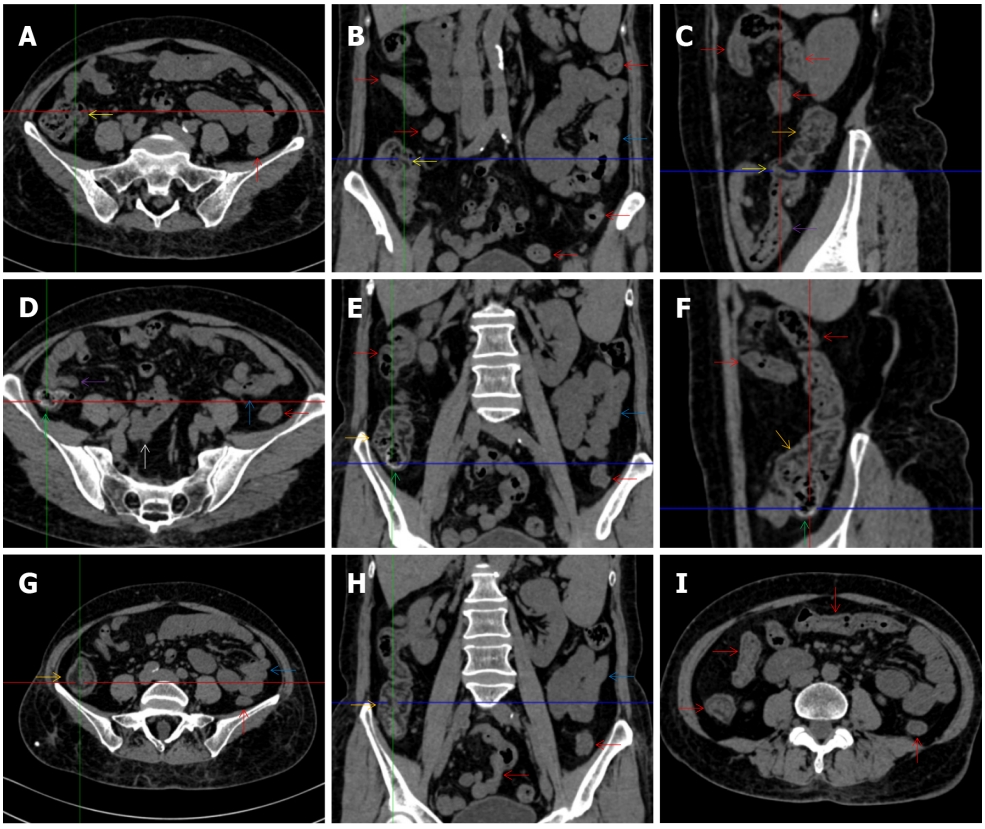

DOI: 10.12998/wjcc.v11.i3.576

Figure 1 Characteristic images of case 4. A-C: Characteristic images of the ileocecal region. The ileocecal valve (yellow arrows), the proximal ascending colon (orange arrows) and the terminal ileum (purple arrows) were significantly thickened and stratified by submucosal fat deposition, forming the so-called "fat holo sign". From the distal ascending colon to the sigmoid colon (red arrows), the wall was thickened and stratified with "water holo sign". The small intestine was heterogeneous in bowel wall texture, and gas-filled in some segments and liquid-filled in other segments, and a segment of adhesive bowel loop was found in the middle jejunum (blue arrows); D-F: Characteristic images of the asending colon. The irregular contour and the fibrotic thickening of the mucosal folds made the colonic configuration rugged. The mucosa of the cecum and the appendiceal root was fibrously thickened (green arrows), and the appendix was gas-filled. Thickened omentum surrounded the ileocecal region and the ascending colon. A segment of adhesive bowel loop was found in the proximal ileum (a white arrow). The mucosa of the proximal ileum in the adhered bowel loop was fibrotically thickened, with mesenteric fat deposition and adjacent peritoneal thickening forming the so-called "abdominal cocoon"; G and H: Typical fat holo sign in the ascending colon. The "fat holo sign" was more typical in the middle ascending colon; I: Thickened and stratified larger intestine. From the distal ascending colon to the sigmoid colon (red arrows), the wall was thickened and stratified by edematous submucosal tissues, forming the so-called "water holo sign". In some segments, the colon was emptied. Paracolonic fat stranding was present from the cecum to the sigmoid colon. The disproportionately less severe paracolonic fat stranding suggested that the edematous colon most likely occurred during an acute episode.

In the evaluation of abdominal CT imaging abnormalities, particular attention has been given to inflammatory abnormalities in the ileocecal region and the colonic segments because they host the most enriched microbial community and lymphoid tissues[9,10,19]; therefore, inflammatory diseases and compromised intestinal barriers in these bowel segments have the most potent capacity to provide sufficient intestine-derived antigens and activated immune cells to affect hematopoietic and immune functions irrespective of whether they are primary damage or secondary to dysbiotic gut microbiota. As demonstrated by this study, all patients with SAA during flared inflammatory episodes had evident morphological abnormalities that could reflect the presence of a severely damaged intestinal structure and function in the ileocecal region and the colonic segments. All patients also presented with inflammatory damages in the proximal small intestine, suggesting that inflammatory damages in the upper gastrointestinal tract led to the inflammatory damages in the downstream intestinal segments, probably by altering the gut microbial composition[54-56]. In the following sections, we described the characteristic CT imaging findings in each patient in the category of readily identified morphological presentations.

All patients demonstrated CT imaging abnormalities that suggested the presence of gut inflammatory damage in the large intestine. Colonic wall thickening with mural stratification, intramual gas and paracolonic fat stranding is the common presentation of colonic involvement of inflammatory damage. A stratified bowel wall can be caused by submucosal fat deposition (fat holo sign) or submucosal edematous tissues (water holo sign)[17-19]. The water holo sign was present in 8 patients [Figure 1 (case 4), Figure 2 (case 3), Figure 3 (case 6), Figure 4 (case 9), Figure 5 (case 15), Figure 6 (case 2), Figure 7 (case 1), and Figure 8 (case 12)], commonly accompanying intramural gas and subserosal peumatosis, which indicated the presence of aerogenous bacterial proliferation in the colonic wall irrespective of primary

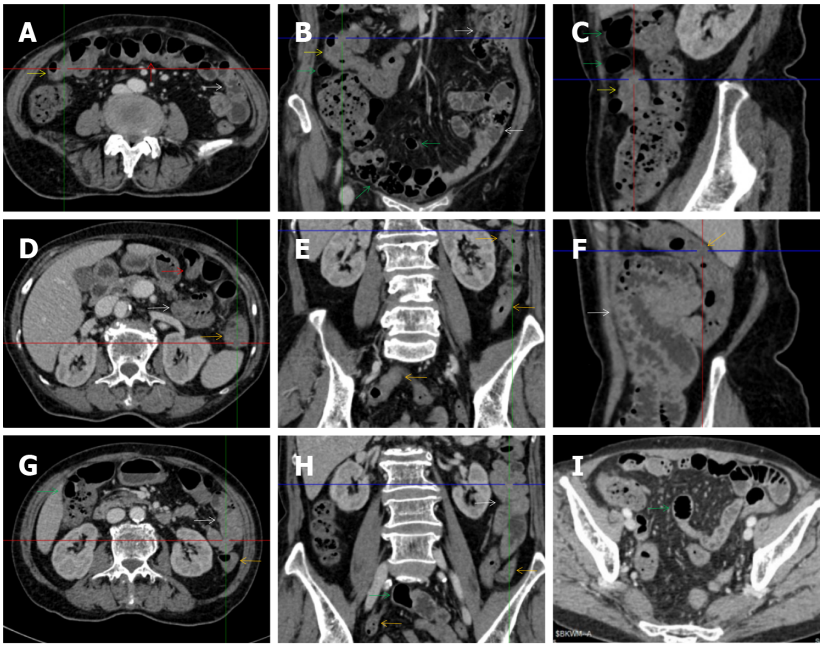

DOI: 10.12998/wjcc.v11.i3.576

Figure 2 Characteristic images of case 3. A-C: Characteristic images of the thickened transverse colon. The segmentally thickened, stratified (water holo sign) and emptied colon with paracolonic fat stranding was present in the hepatic flexure (yellow arrows) in which an inflamed polypoid lesion was found on endoscopic examination, followed by the asymmetrically thickened wall and gas-filled lumen of the transverse colon (red arrows) in which the colonic villi were absent; D-F: Characteristic images of the thickened descending colon. The wall of the descending and sigmoid colon was thickened and stratified with mesenteric fat stranding (orange arrows), with the most striking segment being in the splenic flexure; G and H: Characteristic images of an adhesive bowel loop. While the ileum was gas-filled and distended (green arrows), the adhesive jejunal loop (white arrows) was heterogeneous in bowel wall texture and liquid-filled with multiple gas-liquid levels and accrescent plica. Increased mesenteric fat and vasculature were adjacent to the adhered jejunal loop; I: Characteristic image of a balloon sign. Clustering and hypervascular mesenteric fat proliferation wrapped a segment of paper-thin ileum, forming the so-called "balloon sign". Balloon sign was also present in the hepatic flexure.

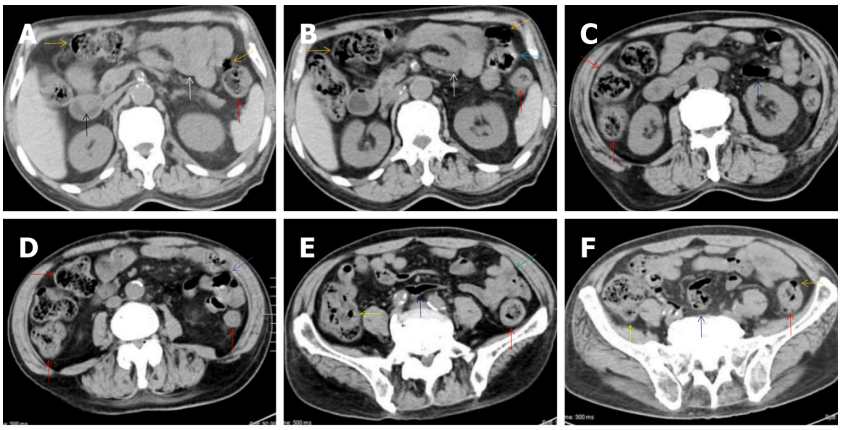

DOI: 10.12998/wjcc.v11.i3.576

Figure 3 Characteristic images of case 6. A and B: Characteristic images of the upper abdomen. Several inflamed diverticula (orange arrows) were present in the colonic segments. In the duodenum-jejunum junction (a blue arrow), the bowel wall was fibrotically thickened and the lumen was gas-filled. In the bulb part of the duodenum, a polypoid mass (a black arrow) protruded into the lumen. A segment of adhesive jejunal loop was present in the proximal jejunum (white arrows); C and D: Characteristic images of the thickened colon. The wall from the cecum to the descending colon was significantly thickened with mural stratification, intramural gas and pericolonic fat stranding. A segment of adhesive bowel loop was present in the middle jejunum (a purple arrow) in which the bowel wall was asymmetrically thickened and the lumen was gas-filled with particularly prominent mesenteric fat stranding; E: Characteristic images of the ileocecal region. Stratified thickening of the ileocecal valve and the terminal ileum was gas-filled (yellow arrows). The third segments of adhesive bowel loop were present in the distal jejunum (a green arrow); F: Characteristic image of a balloon sign. The sigmoid colon was dilated and the wall was paper-thin (navy blue arrows), with clustering pericolonic fat stranding forming the so-called "balloon sign".

infection or infection secondary to dysbiotic microbiota, acute episodes or chronic damage[22,23]. The fat holo sign which suggested the existence of active chronic gut inflammation was detected in 7 patients [Figure 1 (case 4), Figure 9 (case 13), Figure 4 (case 9), Figure 10 (case 11), Figure 11 (case 17), Figure 7 (case 1), and Figure 12 (case 16)]. In these 7 patients, the fat holo sign was located in the

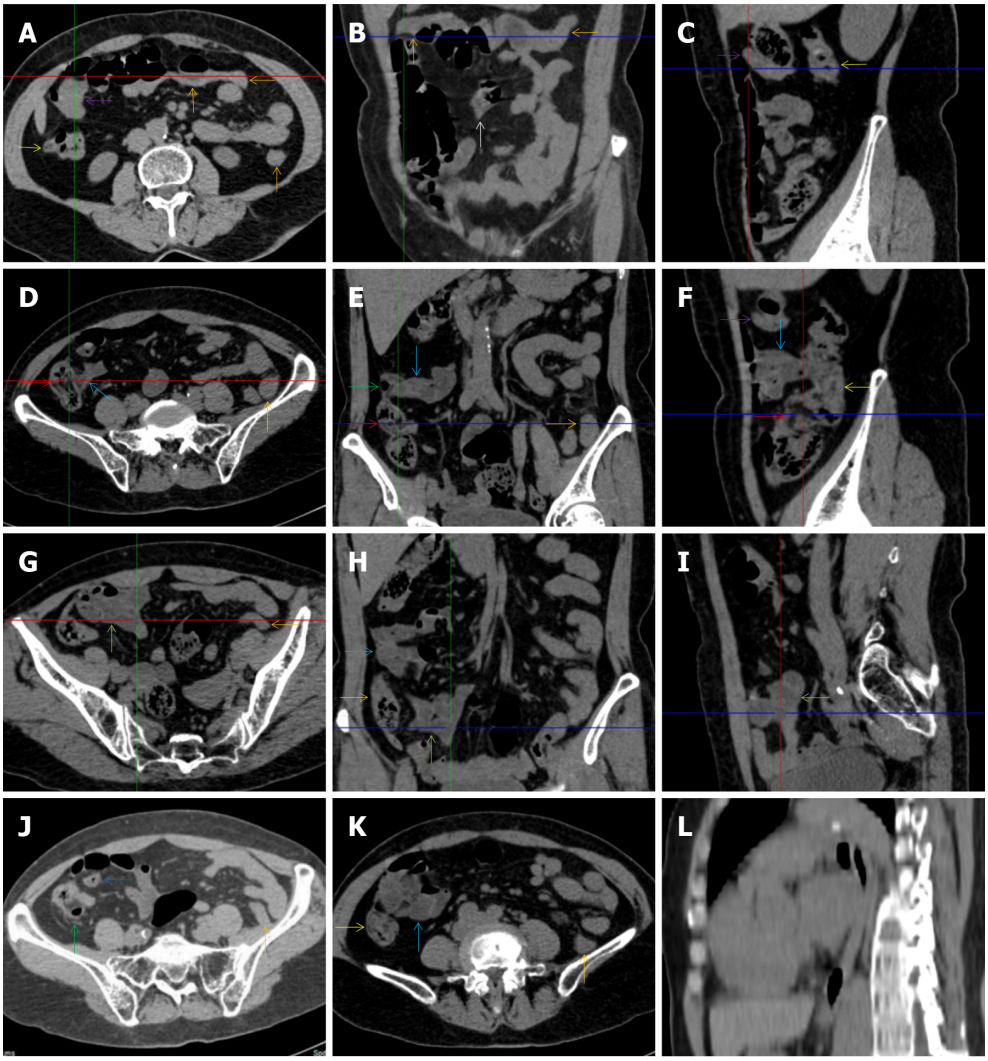

DOI: 10.12998/wjcc.v11.i3.576

Figure 4 Characteristic images of case 9. A-C: Characteristic images of an empty colon sign. The segmentally wall-thickened, stratified and emptied colon in the hepatic flexure (purple arrows) followed by the collapsed transverse (adjacent to the dilated ileum in which gas-liquid levels could be recognized) and descending colon (orange arrows), forming the so-called "empty colon sign". A short segment of asymmetrically thickened wall was present in the proximal ileum (a white arrow), around which the hypervascular fat stranding was especially prominent, distal to which the ileal lumen was gas-filled, and proximal to which the ileal lumen was liquid-filled; D-F: Characteristic images of the ileocecal region. The ileocecal valve and the terminal ileum were thickened and stratified by submucosal fat deposition (red arrows). Omental thickening was especially prominent in the ileocecal region. The wall of the ascending colon was thickened and, in some segments, stratified with submucosal fat deposition, and in other segments, stratified with submucosal edematous tissue (yellow arrows). Several inflamed diverticula (green arrows) were present in the cecum and ascending colon. The distal ileum was strictured (blue arrows), proximal to which the ileal lumen was liquid-filled; G-I: Characteristic images of adhesive bowel loops. The fibrotic mucosa and liquid-filled lumen of the adhesive bowel loops were present in the proximal ileum (powder blue arrows) and distal ileum (jade-green arrows); J: Characteristic image of a balloon sign. A large cluster of circumferentially distributed hypervascular fat stranding wrapped a segment of the dilated lumen and paper-thin bowel wall of the sigmoid colon, forming the so-called "balloon sign". An inflamed diverticula was present in the cecum, with strikingly thickened omentim (a green arrow); K: Characteristic image of an adhesive bowel loop in the proximal ileum. A segment of adhesive bowel loop in the proximal ileum, together with the fibrotically thickened peritoneum, formed the so-called "abdominal cocoon"; L: Characteristic image of esophagus. Hypertrophic lesions presented in two segments of the esophagus, together with the inflammatory lesions in the jejunum suggesting that the initiating factor in the upper gastrointestinal tract affected the functions of the downstream intestinal segments.

ileocecal region and proximal ascending colon.

The "balloon sign" is characterized by circumferentially distributed clustering of hypervascular mesenteric fat proliferation wrapping a short segment of highly distended paper-thin bowel wall[33,34]. The "balloon sign" can also be seen in a large subserosal pneumatosis[35,36]. The circumferentially distributed clustering of hypervascular fat proliferation suggests the presence of an active chronic inflammatory condition in diseased intestinal segments. The balloon sign was present in 7 patients. The paper-thin bowel wall can be the wall of either the small or large intestine. In Figure 2 (case 3), the paper-thin bowel wall was present in the proximal ileum. In Figure 13 (case 14), the paper-thin bowel wall was present in the ascending colon. In Figure 11 (case 17), the paper-thin bowel wall was present in the hepatic flexure. In Figure 3 (case 6), Figure 4 (case 9), Figure 8 (case 7) and Figure 14 (case 8), the paper-thin bowel wall was present in the sigmoid colon.

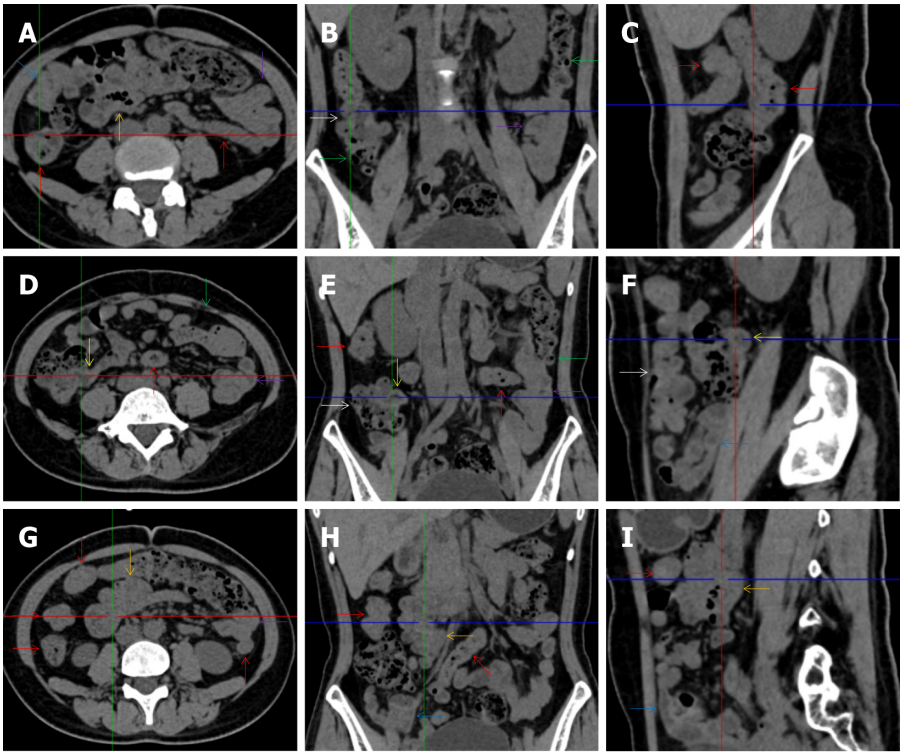

DOI: 10.12998/wjcc.v11.i3.576

Figure 5 Characteristic images of case 15. A-C: Characteristic images of the ascending colon. The ascending colon was rugged with omental thickening and paracolonic fat stranding, and the colonic wall was thickened with mural stratification and intramural gas (white arrows). From the hepatic flexure to the sigmoid colon (red arrows), the bowel wall was thickened and stratified with several inflamed diverticula (green arrows) in these colonic segments. Three segments of adhesive bowel loops were visualized: one in the distal ileum (blue arrows), the other two in the middle ileum (orange arrows) and the jejunum (purple arrows); D-F: Characteristic images of the ileocecal region. The ileocecal valve and the terminal ileal wall were fibrotically thickened (yellow arrows), proximal to which the ileal lumen was liquid-filled; G-I: Characteristic images of the adhesive bowel loops in the middle and distal ileum. The bowel loop in the middle ileum was adhered and clustered (orange arrows), with the bowel wall being highly heterogeneous in texture and the mucosa being hyperdense. The bowel loop in the distal ileum was adhered, the lumen was liquid-filled, and the bowel wall was fibrotically thickened, together with the fibrotically thickened peritoneum forming the so-called "abdominal cocoon" (blue arrows).

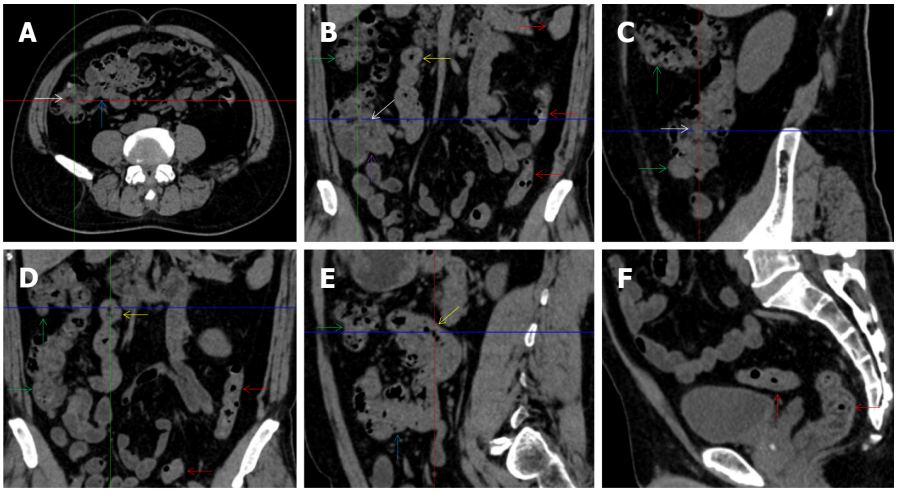

DOI: 10.12998/wjcc.v11.i3.576

Figure 6 Characteristic images of case 2. A-C: Characteristic images of the ileocecal region. The ileocecal valve and the terminal ileal wall were thickened and stratified (white arrows), the ileal mucosa was hyperdense and the ileal lumen was liquid-filled. The adhered and clustered distal ileum and cecum with the fibrotically thickened peritoneum (a purple arrow) formed the so-called "abdominal cocoon"; D and E: Characteristic images of the ascending colon and the adhesive bowel loops. In the ascending colon (green arrows), the wall was thickened and stratified with "water holo sign", the mucosa was hyperdense and the configuration was rugged, with paracolonic fat stranding, omental thickening and subserosal pneumatoses. The wall of the descending and sigmoid colon (red arrows) was also thickened and stratified. In two segments of the adhesive bowel loop (blue arrows and yellow arrows), the bowel wall was heterogeneously thickened and the lumen was gas-filled, suggesting the presence of heterogeneity in small bowel wall texture; F: A particularly striking edematous segment was present in the rectum.

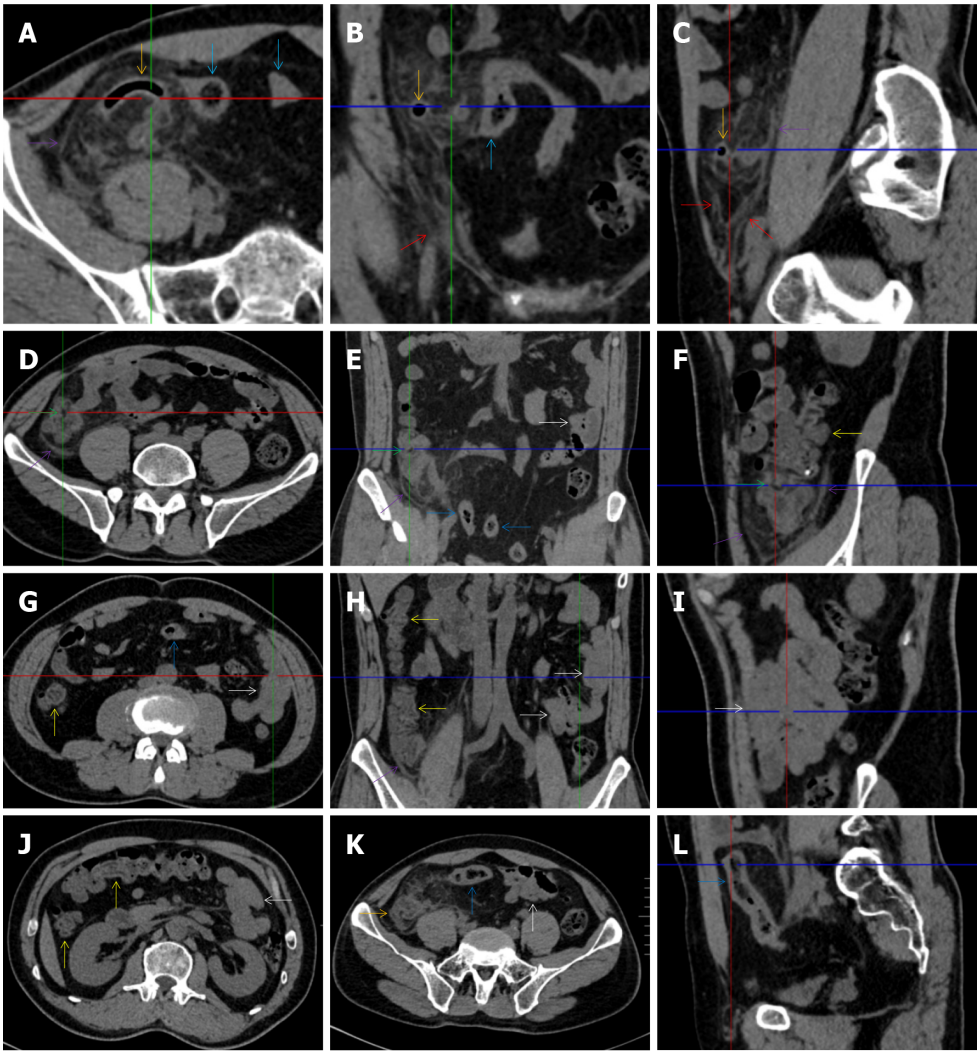

DOI: 10.12998/wjcc.v11.i3.576

Figure 7 Characteristic images of case 1. A-C: Characteristic images of the ileocecal region. A massive cluster of fat stranding that was wrapped by the strikingly thickened omentum (purple arrows) was centered on the homogeneously wall-thickened and gas-filled appendix (orange arrows), leading to the diagnosis of a chronic periappendiceal abscess. The periappendiceal inflammatory changes extended to the scrotum along the inguinal canal (red arrows). In the adjacent sigmoid colon, the wall was thickened and stratified with the water holo sign, and the lumen was gas-filled (blue arrows); D-F: Characteristic images of the ascending colon. The ileocecal valve was thickened and strictured (green arrows), proximal to which the ileal lumen was liquid-filled. Bowel wall thickening with irregular mucosal folds, emptied lumen, mural stratification (fat holo sign) and paracolonic fat stranding that was disproportionately less severe than the severity of the colonic wall thickening was present in the ascending colon (yellow arrows). In the descending colon, the wall was also fibrotically thickened; G-I: Characteristic images of an adhesive bowel segment. A segment of adhesive bowel loop with fibrotic bowel wall thickening, peritoneal thickening and hypervascular mesenteric fat stranding was present in the jejunum (white arrows), together with the segmentally gas-filled, segmentally liquid-filled jejunal lumen, suggesting the inflammatory involvement of the upper gastrointestinal tract; J: Characteristic image of the thickened transverse colon. Bowel wall thickening with emptied lumen, mural stratification (water holo sign) and paracolonic fat stranding that was disproportionately less severe than the severity of the colonic wall thickening was present in the transverse colon, suggesting the involvement of a transmural inflammatory condition; K and L: The thickened and stratified sigmoid colon. Of the sigmoid colon adjacent to the massive inflammatory lesion, the wall was thickened and stratified with the water holo sign, and the lumen was gas-filled.

The "empty colon sign" refers to a colonic segment in which any contents are absent, usually in a segmentally wall-thickened colon or following a focally wall-thickened colon. Malignant masses are the most common cause. However, inflammatory diseases can also cause empty colon signs, especially in segmental thickening of the colonic wall with edematous submucosal tissues and prominent mesenteric fat stranding[15-18]. In this study, 6 patients presented with an empty colon sign. In Figure 9 (case 13), the empty colon sign was exhibited a thickened, stratified and emptied colonic segment in the hepatic flexure, followed by the collapsed proximal transverse colon. In Figure 4 (case 9), the collapsed transverse and descending colon followed the segmentally wall-thickened colon in the hepatic flexure, and endoscopic examination later demonstrated a polypoid lesion in the diseased colonic segment. In Figure 7 (case 1), the empty colon sign was exhibited as a long segment of the thickened, stratified and emptied ascending and proximal transverse colon. In Figure 1 (case 4), Figure 2 (case 3) and Figure 5 (case 15), the empty colon sign was exhibited a segmentally thickened, stratified and emptied colon in the hepatic flexure.

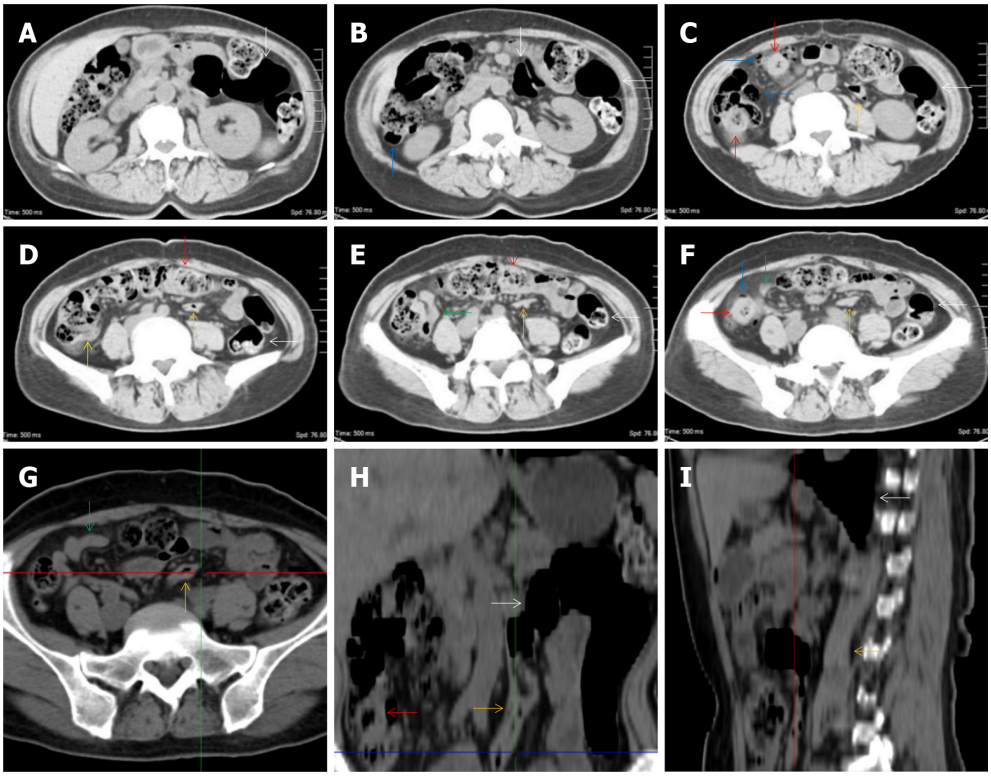

DOI: 10.12998/wjcc.v11.i3.576

Figure 8 Characteristic images of case 7. A-F: Characteristic images of the ileocecal region and the large colon. The ileocecal valve was thickened and stratified (yellow arrow). The distal ileum was thickened and strictured (green arrows) with a large cluster of misty exudative lesions surrounding the cecum and distal ileum, and the proximal small intestine was liquid-filled with multiple gas-liquid levels. From the cecum to the distal descending colon, the mucosa and the villi were hyperdense, with several focally wall-thickened and stratified colonic segments (red arrows) and several inflamed diverticula (blue arrows). An obstructively thickened segment of the sigmoid colon (orange arrows) with prominent paracolonic hypervascular fat stranding was distal to the remarkably distended lumen and paper-thin bowel wall of the sigmoid colon (white arrows); G-I: Reconstructed images of the obstructively thickened sigmoid colon. From the reconstructed images, the obstructively thickened segment of the sigmoid colon (orange arrows) and the proximal distended sigmoid colon (white arrows) were better visualized. The misty exudative lesions and the surrounded cecum and distal ileum were also better visualized (green arrows).

The "creeping fat sign" represents an imaging presentation in which proliferated fat deposition leads to the widening of the bowel loop[24]. The appearance of the creeping fat sign signifies the presence of chronic transmural inflammation in diseased intestinal segments[16,18,24,25]. In Figure 15 (case 10), the silt-like fat deposition led to the widening of the small bowel loop. In the ileal segment, the wall was thickened, and the lumen was dilated. In Figure 14 (case 8), similar imaging features were shared with those in Figure 15 (case 10). However, Figure 14 (case 8) presented concomitantly with infectious lesions in the pleura, indicative of the reactivation of old tuberculosis.

Diffused bowel inflammatory damage in Crohn's disease predominantly affects the small intestine, and the ileocecal valve and large intestine are commonly involved. The "creeping fat sign" is the characteristic imaging presentation in the diagnosis of Crohn's disease[24,25]. In Figure 15 (case 10), the "creeping fat" manifested as silt-like fat deposition. However, most patients manifested perienteric hypervascular fat proliferation wrapping the fibrotically thickened wall and dilated lumen of the ileal segment. Four patients (cases 8, 9, 12, and 14) were found to have this radiological feature. In Figure 14 (case 8), this form of creeping fat was present in the distal jejunum, whereas in the other 3 patients [Figure 15 (case 9), Figure 16 (case 12) and Figure 13 (case 14)], creeping fat was present in the ileum. They also presented with other forms of inflammatory changes in the small and large intestines.

While the diffuse bowel inflammatory lesions of Crohn's disease predominate in the small intestine, the bowel inflammatory lesions of ulcerative colitis predominate in the colon. Fibrotic thickening of the colonic wall is a common imaging presentation, usually with striking paracolonic hypervascular mesenteric fat proliferation, indicating chronic lesions in nature, different from those of acute colonic infectious diseases[15-19]. The ileocecal region and small intestine are commonly involved in various forms of inflammatory damages. These imaging features were present in Figure 17 (case 5). In addition to fibrotic thickening of the colonic wall and the dilated colonic lumen, peritoneal thickening and loculated ascites in the iliac fossa and pelvic cavity indicated peritoneal involvement of inflammatory lesions. The hypertrophic lesion in the pluera with pleural effusion suggested the presence of tuberculosis infection. These imaging features indicated that tuberculosis infection likely initiated the gut inflammatory condition in this case.

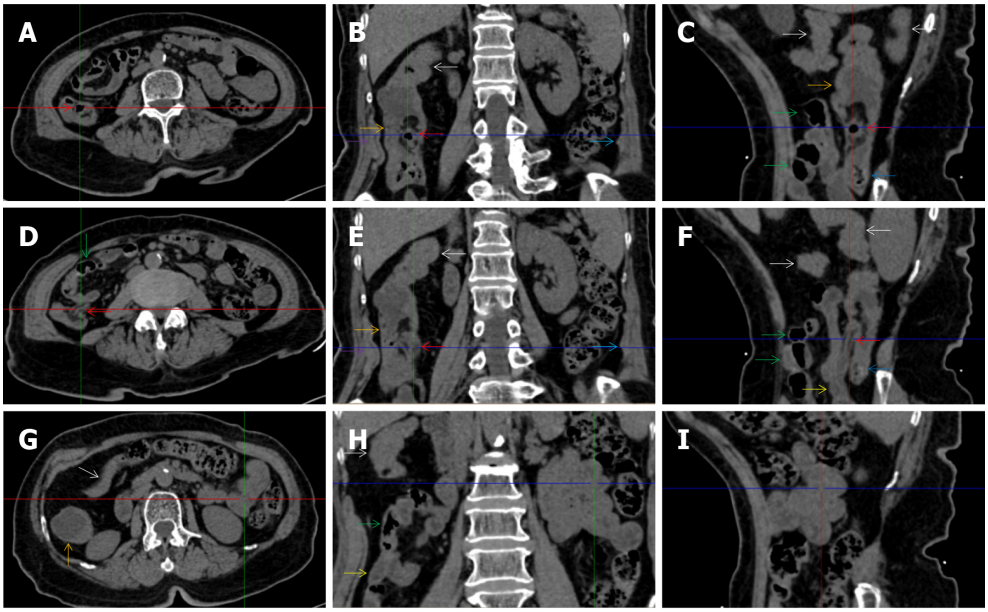

DOI: 10.12998/wjcc.v11.i3.576

Figure 9 Characteristic images of case 13. A-C: Characteristic images of the ileocecal valve and ascending colon. There was edematous fat deposition around the ileocecal valve and the terminal ileum, forming the so-called "fat holo sign". A massive necrotic lesion in the colonic wall was adjacent to the edematous fat deposition, and the serosal colonic wall was hypertrophically thickened (orange arrows). The adjacent parietal peritoneum (purple arrows) and the left parietal peritoneum (navy blue arrows) were also hypertrophically thickened. The mucosa of the cecum was fibrotically thickened (blue arrow); D-F: Characteristic images of the distal ileum. Strictured thickening of the ileocecal valve and terminal ileum (red arrows) led to the distal ileum being liquid-filled. Proximal to the liquid-filled distal ileum (yellow arrows) was the asymmetrically wall-thickened and gas-filled ileum (green arrows). Heterogeneity of the small bowel wall was observed; G-I: Characteristic images of an "abdominal cocoon". A segment of adhesive bowel loop was present in the middle jejunum, together with the fibrotically thickened bowel and peritoneal involvement forming the so-called "cauliflower sign". Edematously thickened colonic wall and emptied colonic lumen were present from the proximal ascending colon to the hepatic flexure, followed by a segment of the collapsed transverse colon (white arrows), forming the so-called "empty colon sign".

Marked irregular mucosal contour and fibrotically thickened mucosal folds of the large intestine, commonly with colonic wall thickening and subserosal pneumatosis, makes the colonic configuration rugged. This rugged colonic configuration especially with peritoneal thickening could suggest an existence of active and chronic inflammatory conditions in diseased colonic segment. It commonly occurs in the ascending colon and coexists omental involvement and pronounced paracolonic fat stranding. This easily recognized imaging presentation is highly useful in the identification of colonic inflammatory damages which is distinguishable from edematous thickening of the colonic wall with dispropositionately less severe paracolonic fat stranding in acute enterocolotis[14-18]. In patients presented with this imaging presentation, inflammatory lesions also involved other colonic segments, the ileocecal region and small intestine. The rugged configuration of the ascending colon presented in 10 patients [Figure 1 (case 4), Figure 2 (case 3), Figure 4 (case 9), Figure 5 (case 15), Figure 10 (case 11), Figure 6 (case 2), Figure 11 (case 17), Figure 7 (case 1), Figure 14 (case 8) and Figure 12 (case 16)], suggesting that it is common imaging presentations in patients with SAA, in accordance with the high prevalence of inflammatory and infectious diseases in the ileocecal region and the proximal ascending colon.

The "adhesive bowel loop" refers to a segment of small bowel that was adhered and clustered. Various bowel wall abnormalities could be present in the adhered and clustered small bowel segments. Heterogeneity in the bowel wall texture was commonly striking in the adhered small bowel segment. The lumen could be either gas-filled or liquid-filled and frequently alternated. Gas-liquid levels are frequently present in the lumen of the small bowel, indicating the presence of dynamical abnormalities. Bowel wall thickening and transmural inflammatory changes, such as mesenteric fat deposition, increased vasculature and fibrotic peritoneal thickening, were usually particularly striking in the adhered bowel segments. A segment of adhesive bowel loop with peritoneal involvement forms the so-called "abdominal cocoon"[29-32]. In this study, various abdominal cocoons, such as the "accordion sign", "cauliflower sign" and "bottle gourd sign", were found. An adhesive bowel loop was present in 15 patients [Figure 1 (case 4), Figure 9 (case 13), Figure 2 (case 3), Figure 3 (case 6), Figure 4 (case 9), Figure 16 (case 12), Figure 13 (case 14), Figure 5 (case 15), Figure 10 (case 11), Figure 6 (case 2), Figure 11 (case 17), Figure 7 (case 1), Figure 8 (case 7), Figure 14 (case 8), and Figure 17 (case 16)]. The high incidence of an adhesive bowel loop suggested the presence of high prevalence of chronic active bowel inflammatory damage in the small intestine in patients with SAA. In the 2 patients without an adhesive bowel loop, Figure 15 (case 10) and Figure 17 (case 5) presented with striking hypervascular mesenteric fat proliferation and a widened bowel loop (creeping fat sign), also indicating the presence of active

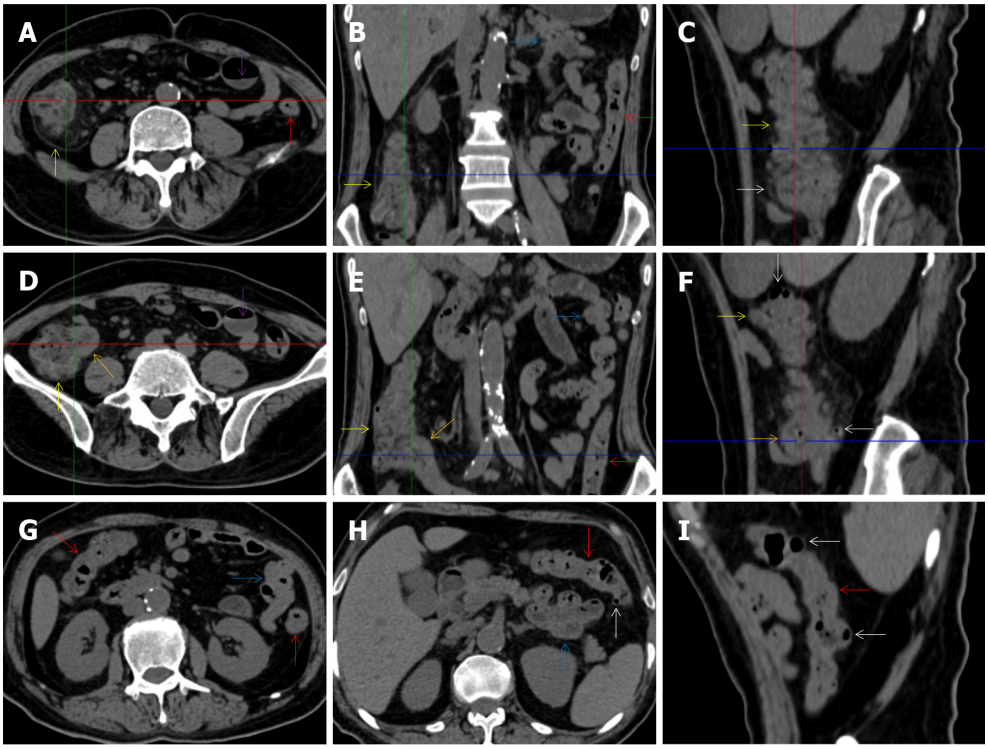

DOI: 10.12998/wjcc.v11.i3.576

Figure 10 Characteristic images in case 11. A-C: Characteristic images of the ascending colon. The ascending colon was rugged with fibrotically and irregularly thickened colonic mucosa, circumferentially distributed omental thickening and paracolonic fat stranding (yellow arrows), and other colonic segments were thickened and stratified with water holo sign (red arrows); D-F: Characteristic images of the ileocecal region. The ileocecal valve and the terminal ileal wall were strikingly thickened and stratified (orange arrows). Bowel wall thickening, mural stratification, heterogeneity in bowel wall texture and gas-liquid levels (purple arrows) were found in the small intestine; G-I: Stratified thickening of the large intestine. From the hepatic flexure to the sigmoid colon, the colonic wall was thickened and stratified with water holo sign (red arrows). Several inflamed diverticula was present in the colonic segments (white arrows). A segment of adhesive bowel loop was present in the middle jejunum (blue arrows), together with the peritoneal involvement forming the so-called "cauliflower sign".

chronic inflammatory involvement of the small intestine[24-26]. Although these inflammatory lesions in the small bowel might not serve as the major factors in the regulation of hematopoietic and immune functions, they exert an important role that affects the downstream gut microbial community and thereby affects downstream intestinal barrier function[54-56].

The ileocecal region is the most common site for various infectious and inflammatory diseases[9,10,14,16]. In this study, all patients with SAA presented with inflammatory involvement of the ileoceal region. Among them, 2 patients presented with inflammatory lesions in the ileocecal region as the predominant imaging presentation. In Figure 7 (case 1), the prominent inflammatory lesion was a large omentum-encapsulated inflammatory mass centered on the homogeneously wall-thickened appendix and extending to the scrotum along the inguinal canal. In Figure 8 (case 7), the particularly prominent inflammatory lesion was a cluster of misty fat stranding wrapping the thickened and strictured distal ileum.

Concomitant extraabdominal presentations may confer useful information for a suggestive etiopathological diagnosis. In this study, pleural involvement of hypertrophic lesions was present in 4 patients [Figure 5 (case 5), Figure 11 (case 17), Figure 14 (case 8), and Figure 12 (case 16)], strongly suggestive of tuberculosis infection. However, no tuberculotic lesions were present in their lungs. In addition to the pleural involvement, 1 patients [Figure 9 (case 13)] presented with peritoneal involvement of hypertrophic lesions, also suggesting the presence of tuberculosis infection.

Taken together, this radiological study demonstrated the gut involvement of various inflammatory changes in all patients with SAA. The inflammatory lesions concurrently affected the large intestine, ileocaecal region and small intestine. Although compromised intestinal integrity in the ileocecal region and large intestine exerts a major role in the development of hematological and immunological diseases [9-13], inflammatory damage and dysfunction in the upper gastrointestinal tract can affect the pathophysiologies of the downstream intestinal integrity[54-56] and thereby exert an indirect impact on hematological and immunological function. In susceptible individuals, active chronic gut inflammatory conditions may initiate and perpetuate hematological damage, and aggravated gut damages may induce flared episodes[4-8].

During flared episodes, the imaging features suggested the presence of chronic gut inflammatory conditions and acutely aggravated inflammatory damages. Some readily recognized imaging signs, such as bowel wall thickening with mural stratification ("water holo sign", "fat holo sign", intramural

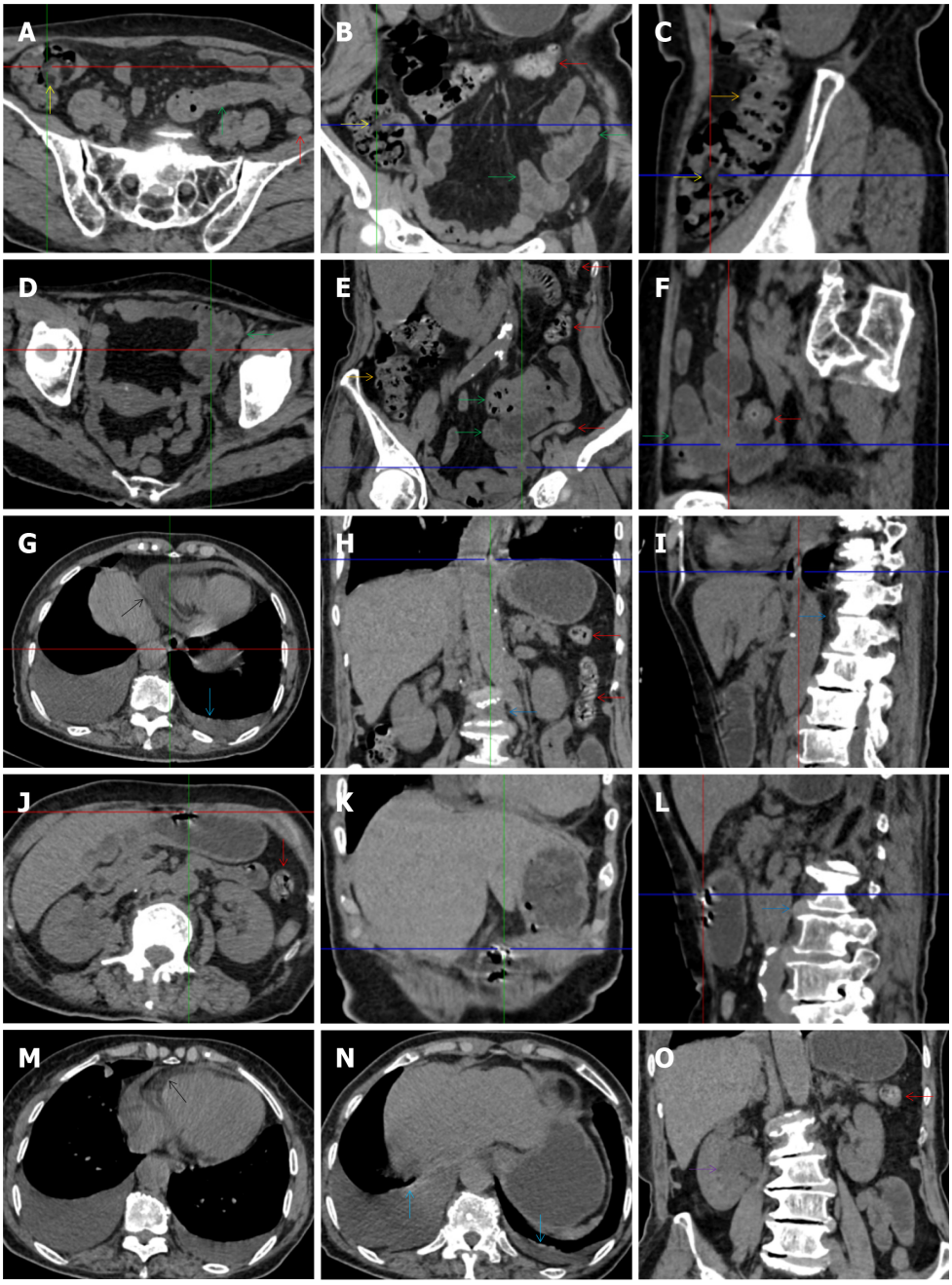

DOI: 10.12998/wjcc.v11.i3.576

Figure 11 Characteristic images in case 17. A-C: Characteristic images of the ileocecal region and the ascending colon. Circumferentially distributed fat deposition wrapped the ileocecal valve (yellow arrows), forming the so-called "fat holo sign". The terminal ileum was thickened, and the strictured ileocecal valve and terminal ileum led to the small intestines being liquid-filled. Heterogeneity and hypertrophic lesions of the small intestines were easily recognized. The ascending colon was rugged with paracolonic fat stranding and peritoneal thickening, and the colonic wall was thickened and stratified with edematous submucosal tissue and intramural gas (orange arrows). From the transverse to the sigmoid colon (red arrows), the colonic wall was fibrotically thickened, with multiple inflamed diverticula in this colonic segment; D-F: Characteristic images of an adhered jejunal segment. A long segment of the adhered jejunal loop was present in the left iliac fossa and pelvic cavity (green arrows). In the adhesive jejunal loop, the lumen was gas-filled in the proximal segment and liquid-filled in the distal segment. Hypervascular mesenteric fat stranding and fibrotic peritoneal thickening were present in this bowel segment, forming the so-called "abdominal cocoon". Fibrotic wall thickening was present in the entire jejunal segment and accrescent pili were visualized in the adhesive jejunal loop and the proximal jejunum; G-I: Erosive lesions in extraintestinal organs. Erosive lesions on the background of the calcified lesions were found in the esophagus. Hypertrophic lesions and seromembranous effusion were visualized in the pericardium (black arrows) and the pleura (light blue arrows). Exudative lesions were also present in the vertebral column (blue arrows); J-L: Erosive lesions in the stomach. Erosive lesions on the background of the calcified lesions were also found in the stomach; M-O: Exudative lesions in extraintestinal organ. Hypertrophic lesions and seromembranous effusion were visualized in the pericardium (black arrows) and the pleura (light blue arrows). Exudative lesions were also present in the renal pelvis and urinary tract (a purple arrow). These radiological features led to the diagnosis of reactive tuberculosis infections in the gastrointestinal tract, urinary tract, peritoneum, vertebral column, pleura and pericardium.

gas and subserosal pneumatoses) and mesenteric fat proliferation (fat stranding and "creeping fat sign"), "balloon sign", rugged colonic configuration and adhesive bowel loop (including various patterns of abdominal cocoon), occurred at a high incidence, which suggested that the gastrointestinal

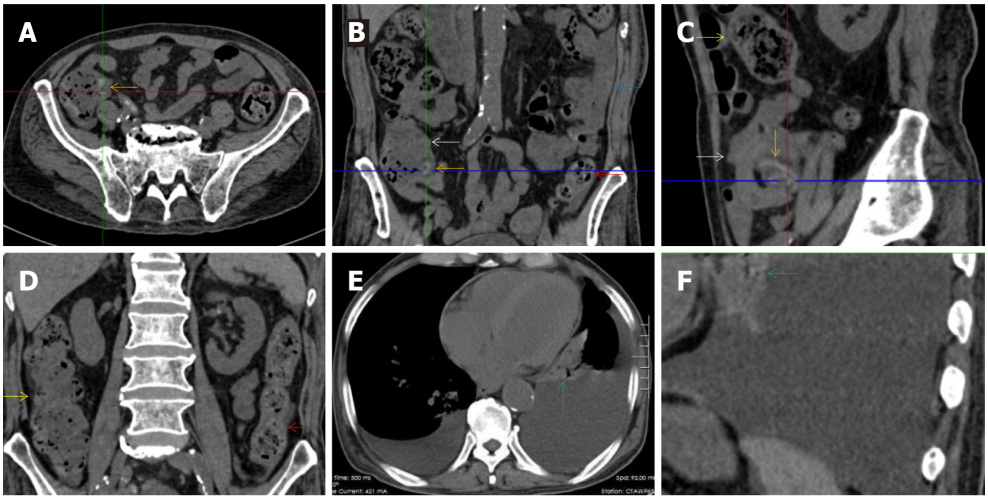

DOI: 10.12998/wjcc.v11.i3.576

Figure 12 Characteristic images in case 16. A-C: Characteristic images of the ileocecal region and the small intestine. The ileocecal valve was fibrotic and thickened with edematous fat deposition, forming the so-called "fat holo sign" (orange arrows), and the distal ileum was adhesive with mesenteric fat stranding and peritoneal thickening (white arrow), forming the so-called "abdominal cocoon". Intestinal adhesion with bowel wall thickening, peritoneal involvement and mesenteric fat stranding was also found in the jejunum (blue arrow). Heterogeneity in the bowel wall texture was particularly prominent in the adhesive bowel segments; D: Characteristic image of the large intestine. The ascending colon was rugged and the colonic wall was thickened and stratified, with adjacent omental thickening (yellow arrows). The descending colonic wall were significantly thickened and stratified with mucosal hyperdensity and paracolonic fat stranding (red arrows); E and F: Characteristic images of the chest computed tomography (CT) scan. Chest CT revealed that the pleural effusion was predominantly in the left cavity and hypertrophic lesions involved both the left pleura and the pericardium (green arrows).

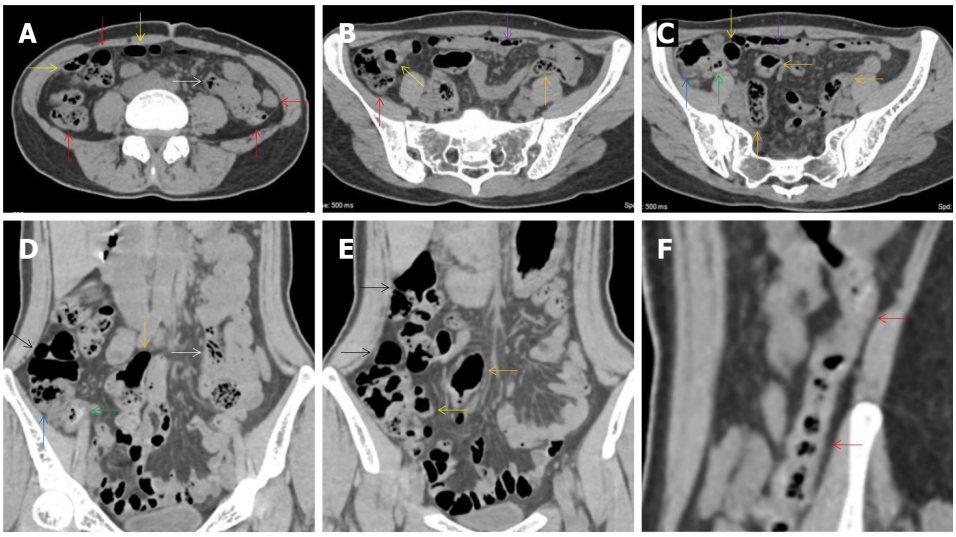

DOI: 10.12998/wjcc.v11.i3.576

Figure 13 Characteristic images of case 14. A-C: Characteristic images of the bowel inflammatory lesions. The ileocecal valve and the ileal wall were fibrotically thickened and the ileal lumen was gas-filled (yellow arrows), with a large cluster of hypervascular perienteric fat proliferation wrapping the wall-thickened and lumen-dilated ileum. The cecum (blue arrows) and appendix (green arrows) were also fibrotically thickened and stratified, with peripheral fat stranding. Gas-liquid levels were present in the lumen of the proximal ileum and distal jejunum (purple arrows). However, the adhesive jejunal loop was liquid-filled with prominent hypervascular mesenteric fat proliferation. In a segment of the jejunum (white arrows), the bowel wall was thickened, the lumen was gas-filled and the mesenteric fat stranding was especially prominent. Thickened peritoneum was adjacent to the adhesive jejunal loop, forming the so-call "abdominal cocoon" and the enlarged mesenteric vascularity formed the so-called "comb sign". The ascending colon was dilated with a paper-thin bowel wall (black arrows), forming the so-called "balloon sign". From the hepatic flexure to the distal descending colon (red arrows), the bowel was thickened and stratified (water holo sign), with paracolonic fat stranding and peritoneal thickening being particular prominent in the hepatic flexure. The sigmoid colon was fibrotically thickened and dilated (orange arrows); D and E: Characteristic images in coronally reconstructed images. The coronally reconstructed images better outlined the above-mentioned imaging features; F: Characteristic image of the descending colon in coronally reconstructed section. A coronally reconstructed image better outlined the thickened and stratified descending colon.

tract is common inflammatory niche responsible for the systemic inflammatory stresses in patients with SAA. Successful treatment of their gut inflammatory conditions significantly improves their hematological profile[4-6], providing convincing evidence for a role of gut inflammation in hematopoietic suppression.

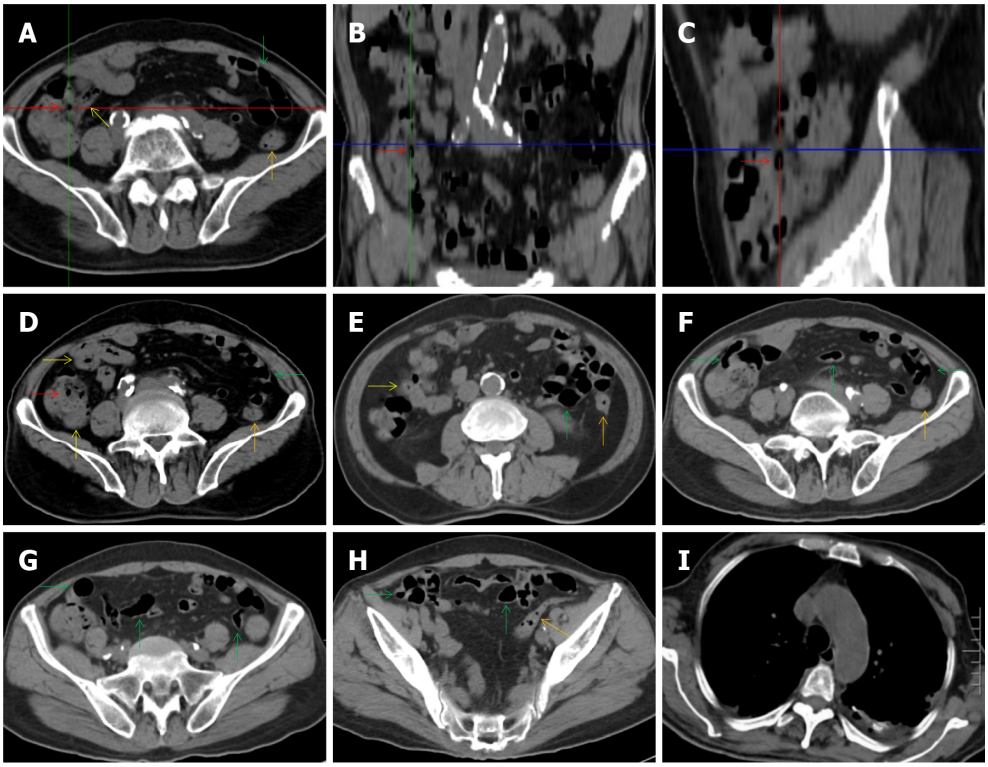

DOI: 10.12998/wjcc.v11.i3.576

Figure 14 Characteristic images in case 8. A-C: Characteristic images of the ileocecal region and the small intestine. The ileocecal valve (red arrows) was thickened, strictured and stratified. The distal ileum (yellow arrows) were significantly thickened with intramural gas and wrapped by prominent mesenteric fat stranding, which suggested the presence of aggravated inflammatory damage in the distal ileum and ileocecal region; D-H: Characteristic images of the small intestine. In the ileocecal region, the ileum adhered to the cecum, and the cecum was thickened and stratified. In other colonic segments (orange arrows), the bowel wall was also thickened and stratified, and the lumen was dilated in some segments and collapsed in other segments. From the jejunum to the proximal ileum (green arrows), the wall was fibrotic and thickened and the lumen was gas-filled. Several segments of adhesive bowel loop were present in the small bowel. Noticeably, panabdominal silt-like hypervascular fat deposition wrapped the adhesive and widened small bowel loop (creeping fat sign), which suggested the presence of chronic transmural inflammatory damage and a diagnosis of Crohn's disease; I: Characteristic image of the chest computed tomography (CT) scan. Chest CT showed exudative lesions in the left pleura in the context of calcified lesions, indicating the reactivation of an old tuberculosis infection.

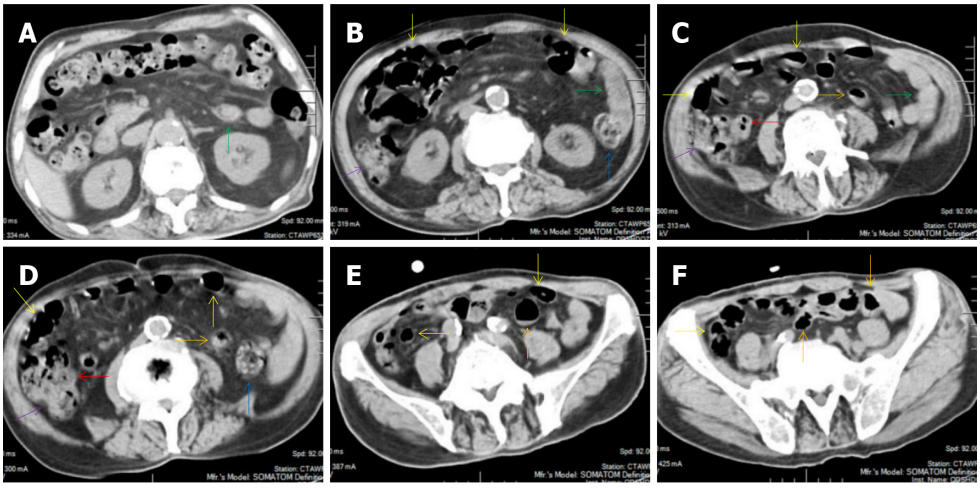

DOI: 10.12998/wjcc.v11.i3.576

Figure 15 Characteristic images of case 10. A and B: Characteristic images of the fat deposition. The most noticeable radiological finding was the panabdominal silt-like hypervascular fat deposition, leading to the widening of the bowel loop of the jejunum and the proximal ileum, forming the so-called "creeping fat sign". The ileum was fibritically thickened and dilated, and the duodenum and the proximal jejunum were liquid-filled (green arrows); C and D: Characteristic images of the ileocecal region. The ileocecal valve and the terminal ileum were significantly thickened, stratified and strictured (red arrows), and proximal to the thickened terminal ileum, the ileal lumen was dilated and gas-filled and the mucosa was hyperdense (yellow arrows). The ascending colonic wall was also thickened (purple arrows). In a short segment of the descending colon (blue arrows), accrescent villi were especially prominent; E and F: Characteristic images of the small intestine. The proximal ileum and the distal jejunum (orange arrows) were thickened and gas-filled.

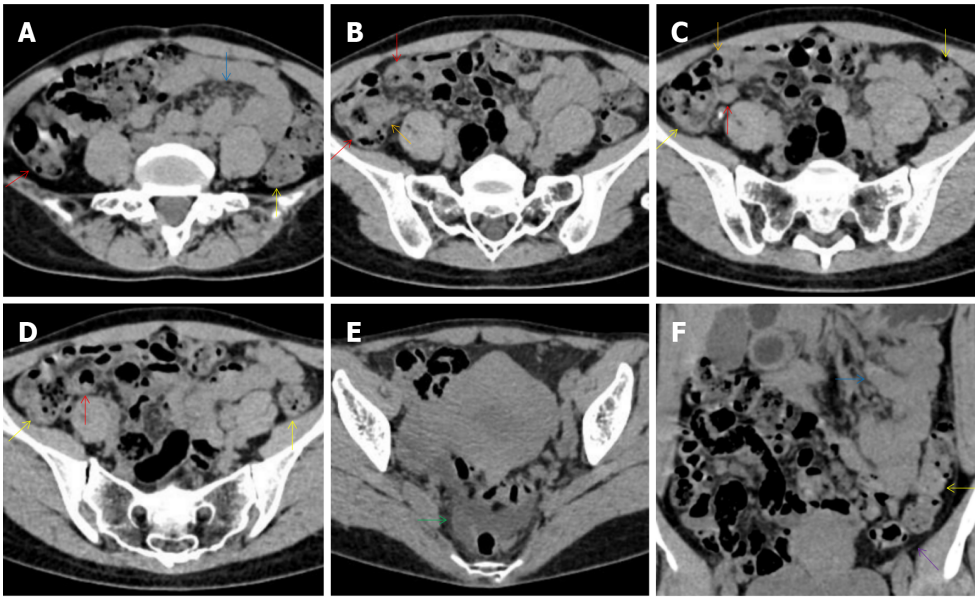

DOI: 10.12998/wjcc.v11.i3.576

Figure 16 Characteristic images of case 12. A-D: Characteristic images of the bowel inflammatory lesions. The ileocecal valve and the terminal ileal wall (red arrows) were thickened, stratified and strictured. Proximal to the strictured terminal ileum, the ileal lumen was dilated and gas-filled, and the mucosa was hyperdense. A large cluster of hypervasular mesenteric fat proliferation wrapped the dilated and gas-filled ileum. The jejunum was liquid-filled and the jejunual loop was adhesive. A cluster of hypervascular fat stranding wrapped a short segment of the jejunum (blue arrows), suggesting that the transmural inflammation was more serious in this jejunal segment. The colonic wall was also thickened and stratified, with intramural gas and subserosal pneumatosis (yellow arrows); E: Characteristic image of the pelvic liquid collection. Mild liquid collection was present in the pelvic cavity (a green arrow), together with the thickened peritoneum (a purple arrow) suggesting the presence of peritoneal involvement; F: Characteristic image in coronally reconstructed section. A coronally reconstructed image better outlined the above-mentioned imaging features.

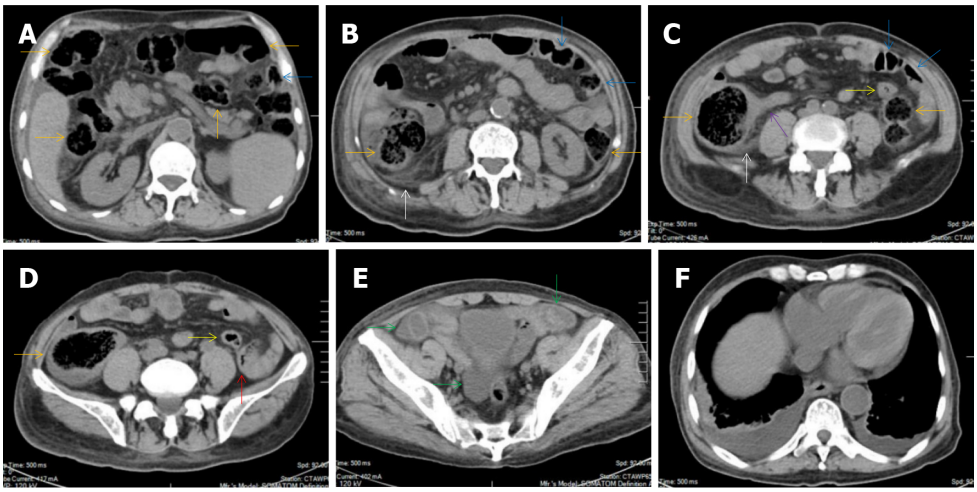

DOI: 10.12998/wjcc.v11.i3.576

Figure 17 Characteristic images of case 5. A-D: Characteristic images of the bowel inflammatory lesions. From the cecum to the descending colon, the lumen was dilated, the mucosa was hyperdence and the wall was thickened and stratified in some segments (orange arrows), with striking mesenteric fat stranding. There was a hypertrophic lesion (a red arrow) in the terminal descending colon. The mucosa of the proximal sigmoid colon was hyperdense and the lumen was gas-filled (blue arrows), following which was a short segment of strictured sigmoid colon (yellow arrows). The ileocecal valve and the terminal ileum were thickened and strictured but without mural stratification (a purple arrow), proximal to which the small intestine was liquid-filled. In the ileocecal region, the colonic wall was thickened with smudgy peritoneal thickening (white arrows); E: Characteristic image of the pelvic liquid collection. Mild ascites was present in both the right and left iliac fossa (green arrows), together with a thickened peritoneum suggesting the presence of peritoneal involvement; F: Characteristic image of the chest computed tomography (CT) scan. Chest CT showed the presence of pleural effusion in the bilateral cavities and bilateral pleural hypertrophic thickening. Enlarged blood vessels extended to the hypertrophic lesions.

Although not able to provide an etiopathological diagnosis, abdominal CT can provide useful information for exploring gut inflammatory conditions and guiding further work-ups. In this study, a suggestive diagnosis of Crohn's disease was made in 5 patients, ulcerative colitis in 1 patient, chronic periappendiceal abscess in 1 patient, and tuberculosis infection in 5 patients[57-59]. Although the

presence of abdominal cocoons has been reported to have a high probability of tuberculosis infection[31, 32] and there was a high incidence of abdominal cocoons present in this study, it was difficult to make a presumptive diagnosis of tuberculosis infection in patients with abdominal cocoons other than the abovementioned 5 patients.

This study had several limitations. First, although CT has some advantages in the detection of the site, extent, degree and peripheral changes of gut inflammatory damage, the exact pathogenic factors cannot be identified, and arriving at an etiopathological diagnosis frequently requires other laboratory tests. This study lacked the endoscopic, pathological and other definitive diagnostic examinations largely due to the contraindication of invasive operative procedures resulting from the very low platelet count and the platelet transfusion refractoriness of these patients. Second, the number of studied patients was quite small, leading to the incidence of each imaging sign being less representative of the actual incidence. Third, the treatment responses by suggested radiological diagnosis were not summarized.

CONCLUSION

All patients with SAA during inflammatory episodes demonstrated gut involvement of both active chronic inflammatory conditions and acute inflammatory damage, providing further evidence to demonstrate the role of GIDs in the pathogenesis of immune-mediated hematopoietic failure. Although arriving at an etiopathological diagnosis frequently requires other laboratory tests, abdominal CT imaging can provide highly useful information for the exploration of gut inflammatory damage and is very helpful for the suggestion of an effective treatment modality. In patients with aggravated cytopenia and clinical presentations suggestive of the presence of inflammatory responses, inflammatory diseases in the gastrointestinal tract should be considered, abdominal CT should be performed, and imaging signs that suggest the presence of gut inflammatory lesions should be carefully identified.

ARTICLE HIGHLIGHTS

Research background

The gastrointestinal tract hosts the body's most enriched lymphoid tissues and microbial community and therefore can provide sufficient activated immune cells and continuous intestine-derived antigens to influence the host hematopoietic and immune functions. The gastrointestinal tract is the most common site for infectious and inflammatory diseases. Morphological changes on computed tomography (CT) images can provide useful information that reflects the distribution, extent, and severity of the bowel inflammation and even suggests a pathogenic diagnosis.

Research motivation

Initiation and perpetuation of aplastic anemia (AA) pathogenesis has been found to be associated with gut inflammatory disorders (GIDs). GIDs have a powerful impact on hematopoietic and immune functions. Treatment of GIDs can improve hematological profile and immunological derangement.

Research objectives

To explore CT imaging presentations of gut inflammatory damage in adult patients with severe AA (SAA) and to provoke awareness of GIDs in the pathogenesis of hematological and autoimmune disorders.

Research methods

We retrospectively evaluated the abdominal CT imaging presentations of 17 hospitalized adult patients with SAA in search of the inflammatory niche when they presented with systemic inflammatory stress and exacerbated hematopoietic function.

Research results

All eligible patients with SAA had CT imaging abnormalities that suggested the presence of an impaired intestinal barrier and increased epithelial permeability. The inflammatory damages were concurrently present in the small intestine, the ileocecal region and the large intestines.

Research conclusions

All patients with SAA had CT imaging patterns that suggested the presence of active chronic inflammatory conditions and aggravated inflammatory damage during flared inflammatory episodes. In patients with aggravated cytopenia and clinical presentations suggestive of the presence of inflammatory responses, inflammatory diseases in the gastrointestinal tract should be considered, abdominal CT should be performed, and imaging signs that suggest the presence of gut inflammatory lesions

should be carefully identified.

Research perspectives

Abdominal CT imaging presentations in association with hematopoietic failure and autoimmune diseases warrant extensive investigations.

FOOTNOTES

Author contributions: Zhao XC and Xiao SX developed the idea; Zhao XC and Xue CJ organized the study; Zhao XC, Xue CJ, Song H, Gao BH, Han FS, and Xiao SX reviewed and consulted the CT images; Zhao XC drafted the manuscript; Xiao SX revised and approved the final manuscript; all authors have read and approved the final version of the manuscript.

Supported by the Specialized Scientific Research Fund Projects of the Medical Group of Qingdao University, No. YLJT20201002.

Institutional review board statement: The study was reviewed and approved by the Central Hospital of Qingdao West Coast New Area Institutional Review Board (Approval No. 2022-10-08).

Informed consent statement: The requirement of written informed consent was waived by The Ethics Committee of The Central Hospital of Qingdao West Coast New Area since this was a retrospective study and no information linked to the patients' identity was revealed in the manuscript.

Conflict-of-interest statement: The authors have no conflicts of interest to declare that are relevant to the content of this article.

Data sharing statement: No additional data are available.

Country/Territory of origin: China

ORCID number: Xi-Chen Zhao 0000-0002-3304-2851; Cheng-Jiang Xue 0000-0002-8763-9901; Hui Song 0000-0002-6347-4006; Bin-Han Gao 0000-0002-7916-546X; Fu-Shen Han 0000-0002-5630-5730; Shu-Xin Xiao 0000-0003-0821-6968.

S-Editor: Chen YL
L-Editor: A
P-Editor: Zhao S

REFERENCES

1 **Giudice V**, Selleri C. Aplastic anemia: Pathophysiology. *Semin Hematol* 2022; **59**: 13-20 [PMID: 35491054 DOI: 10.1053/j.seminhematol.2021.12.002]
2 **Patel BA**, Giudice V, Young NS. Immunologic effects on the haematopoietic stem cell in marrow failure. *Best Pract Res Clin Haematol* 2021; **34**: 101276 [PMID: 34404528 DOI: 10.1016/j.beha.2021.101276]
3 **Killick SB**, Bown N, Cavenagh J, Dokal I, Foukaneli T, Hill A, Hillmen P, Ireland R, Kulasekararaj A, Mufti G, Snowden JA, Samarasinghe S, Wood A, Marsh JC; British Society for Standards in Haematology. Guidelines for the diagnosis and management of adult aplastic anaemia. *Br J Haematol* 2016; **172**: 187-207 [PMID: 26568159 DOI: 10.1111/bjh.13853]
4 **Zhao XC**, Zhao L, Sun XY, Xu ZS, Ju B, Meng FJ, Zhao HG. Excellent response of severe aplastic anemia to treatment of gut inflammation: A case report and review of the literature. *World J Clin Cases* 2020; **8**: 425-435 [PMID: 32047795 DOI: 10.12998/wjcc.v8.i2.425]
5 **Salmeron G**, Patey N, de Latour RP, Raffoux E, Gluckman E, Brousse N, Socié G, Robin M. Coeliac disease and aplastic anaemia: a specific entity? *Br J Haematol* 2009; **146**: 122-124 [PMID: 19438483 DOI: 10.1111/j.1365-2141.2009.07719.x]
6 **Tokar B**, Aydoğdu S, Paşaoğlu O, Ilhan H, Kasapoğlu E. Neutropenic enterocolitis: is it possible to break vicious circle between neutropenia and the bowel wall inflammation by surgery? *Int J Colorectal Dis* 2003; **18**: 455-458 [PMID: 12750931 DOI: 10.1007/s00384-003-0502-3]
7 **Espinoza JL**, Elbadry MI, Nakao S. An altered gut microbiota may trigger autoimmune-mediated acquired bone marrow failure syndromes. *Clin Immunol* 2016; **171**: 62-64 [PMID: 27506961 DOI: 10.1016/j.clim.2016.08.008]
8 **Zhao XC**, Sun XY, Zhao L, Meng FJ. Gut inflammation in the pathogenesis of acquired aplastic anemia. *Chin Med J (Engl)* 2020; **133**: 1878-1881 [PMID: 32568881 DOI: 10.1097/CM9.0000000000000772]

9 **Shen L**. Functional morphology of the gastrointestinal tract. *Curr Top Microbiol Immunol* 2009; **337**: 1-35 [PMID: 19812978 DOI: 10.1007/978-3-642-01846-6_1]
10 **Guven-Maiorov E**, Tsai CJ, Nussinov R. Structural host-microbiota interaction networks. *PLoS Comput Biol* 2017; **13**: e1005579 [PMID: 29023448 DOI: 10.1371/journal.pcbi.1005579]
11 **Fasano A**. All disease begins in the (leaky) gut: role of zonulin-mediated gut permeability in the pathogenesis of some chronic inflammatory diseases. *F1000Res* 2020; **9** [PMID: 32051759 DOI: 10.12688/f1000research.20510.1]
12 **Mu Q**, Kirby J, Reilly CM, Luo XM. Leaky Gut As a Danger Signal for Autoimmune Diseases. *Front Immunol* 2017; **8**: 598 [PMID: 28588585 DOI: 10.3389/fimmu.2017.00598]
13 **Vogelzang A**, Guerrini MM, Minato N, Fagarasan S. Microbiota - an amplifier of autoimmunity. *Curr Opin Immunol* 2018; **55**: 15-21 [PMID: 30248521 DOI: 10.1016/j.coi.2018.09.003]
14 **Duffin C**, Mirpour S, Catanzano T, Moore C. Radiologic Imaging of Bowel Infections. *Semin Ultrasound CT MR* 2020; **41**: 33-45 [PMID: 31964493 DOI: 10.1053/j.sult.2019.10.004]
15 **Yu SJ**, Heo JH, Choi EJ, Kim JH, Lee HS, Kim SY, Lim JH. Role of multidetector computed tomography in patients with acute infectious colitis. *World J Clin Cases* 2022; **10**: 3686-3697 [PMID: 35647171 DOI: 10.12998/wjcc.v10.i12.3686]
16 **Hines JJ Jr**, Mikhitarian MA, Patel R, Choy A. Spectrum and Relevance of Incidental Bowel Findings on Computed Tomography. *Radiol Clin North Am* 2021; **59**: 647-660 [PMID: 34053611 DOI: 10.1016/j.rcl.2021.03.012]
17 **Fernandes T**, Oliveira MI, Castro R, Araújo B, Viamonte B, Cunha R. Bowel wall thickening at CT: simplifying the diagnosis. *Insights Imaging* 2014; **5**: 195-208 [PMID: 24407923 DOI: 10.1007/s13244-013-0308-y]
18 **Mills A**, Mellnick VM, Itani M. Imaging of Bowel Wall Thickening in the Hospitalized Patient. *Radiol Clin North Am* 2020; **58**: 1-17 [PMID: 31731894 DOI: 10.1016/j.rcl.2019.08.006]
19 **Agarwala R**, Singh AK, Shah J, Mandavdhare HS, Sharma V. Ileocecal thickening: Clinical approach to a common problem. *JGH Open* 2019; **3**: 456-463 [PMID: 31832544 DOI: 10.1002/jgh3.12186]
20 **Marín-Díez E**, Crespo Del Pozo J. Diagnostic approach to small-bowel wall thickening: beyond Crohn's disease and cancer. *Radiologia (Engl Ed)* 2021 [PMID: 33546910 DOI: 10.1016/j.rx.2020.11.010]
21 **Wang X**, Yuan M, Mi H, Suo S, Eteer K, Li S, Lu Q, Xu J, Hu J. The feasibility of differentiating colorectal cancer from normal and inflammatory thickening colon wall using CT texture analysis. *Sci Rep* 2020; **10**: 6346 [PMID: 32286352 DOI: 10.1038/s41598-020-62973-1]
22 **Thornton E**, Mendiratta-Lala M, Siewert B, Eisenberg RL. Patterns of fat stranding. *AJR Am J Roentgenol* 2011; **197**: W1-14 [PMID: 21700969 DOI: 10.2214/AJR.10.4375]
23 **Pereira JM**, Sirlin CB, Pinto PS, Jeffrey RB, Stella DL, Casola G. Disproportionate fat stranding: a helpful CT sign in patients with acute abdominal pain. *Radiographics* 2004; **24**: 703-715 [PMID: 15143223 DOI: 10.1148/rg.243035084]
24 **Xiong S**, Tan J, Wang Y, He J, Hu F, Wu X, Liu Z, Lin S, Li X, Chen Z, Mao R. Fibrosis in fat: From other diseases to Crohn's disease. *Front Immunol* 2022; **13**: 935275 [PMID: 36091035 DOI: 10.3389/fimmu.2022.935275]
25 **Suau R**, Pardina E, Domènech E, Lorén V, Manyé J. The Complex Relationship Between Microbiota, Immune Response and Creeping Fat in Crohn's Disease. *J Crohns Colitis* 2022; **16**: 472-489 [PMID: 34528668 DOI: 10.1093/ecco-jcc/jjab159]
26 **Ha CWY**, Martin A, Sepich-Poore GD, Shi B, Wang Y, Gouin K, Humphrey G, Sanders K, Ratnayake Y, Chan KSL, Hendrick G, Caldera JR, Arias C, Moskowitz JE, Ho Sui SJ, Yang S, Underhill D, Brady MJ, Knott S, Kaihara K, Steinbaugh MJ, Li H, McGovern DPB, Knight R, Fleshner P, Devkota S. Translocation of Viable Gut Microbiota to Mesenteric Adipose Drives Formation of Creeping Fat in Humans. *Cell* 2020; **183**: 666-683.e17 [PMID: 32991841 DOI: 10.1016/j.cell.2020.09.009]
27 **Knox C**, Almeida J. The Comb Sign. *Clin Gastroenterol Hepatol* 2021; **19**: A29-A30 [PMID: 32634621 DOI: 10.1016/j.cgh.2020.06.054]
28 **Ueda Y**, Yanagi H. The comb sign in a patient with Crohn's disease. *J Gen Fam Med* 2022; **23**: 120-121 [PMID: 35261863 DOI: 10.1002/jgf2.499]
29 **Basara Akin I**, Altay C, Celik A, Secil M. Computed Tomography Features of Encapsulating Peritoneal Sclerosis. *Can Assoc Radiol J* 2019; **70**: 233-238 [PMID: 30922787 DOI: 10.1016/j.carj.2018.11.005]
30 **Ethiraj D**, Indiran V. Abdominal Cocoon: "Cauliflower Sign" on Contrast-Enhanced Computed Tomography Scan. *GE Port J Gastroenterol* 2020; **28**: 76-77 [PMID: 33564710 DOI: 10.1159/000507636]
31 **Gorsi U**, Gupta P, Mandavdhare HS, Singh H, Dutta U, Sharma V. The use of computed tomography in the diagnosis of abdominal cocoon. *Clin Imaging* 2018; **50**: 171-174 [PMID: 29602067 DOI: 10.1016/j.clinimag.2018.03.014]
32 **Sharma V**, Singh H, Mandavdhare HS. Tubercular Abdominal Cocoon: Systematic Review of an Uncommon Form of Tuberculosis. *Surg Infect (Larchmt)* 2017; **18**: 736-741 [PMID: 28759335 DOI: 10.1089/sur.2017.110]
33 **Ling J**, Dyer RB. The "hot air balloon" sign. *Abdom Radiol (NY)* 2019; **44**: 2663-2664 [PMID: 30850891 DOI: 10.1007/s00261-019-01972-x]
34 **LoVerde ZJ**, Dyer RB. "Lâcher de ballons" or "release of balloons" sign. *Abdom Radiol (NY)* 2018; **43**: 2208-2209 [PMID: 29260277 DOI: 10.1007/s00261-017-1428-5]
35 **Rodríguez-Otero Luppi C**, Rodríguez Blanco M, Bollo Rodríguez J, Méndez A, Merlo Más J. Laparoscopic resection of a giant colonic diverticulum - the 'lifting balloon' sign - a video vignette. *Colorectal Dis* 2019; **21**: 1096-1098 [PMID: 31120633 DOI: 10.1111/codi.14716]
36 **Heylen CE**, Pringot J, Van Belle K. The Lifting Balloon: Sign of a Giant Colonic Diverticulum. *J Belg Soc Radiol* 2017; **101**: 26 [PMID: 30039018 DOI: 10.5334/jbr-btr.1363]
37 **Wang J**, Erlacher M, Fernandez-Orth J. The role of inflammation in hematopoiesis and bone marrow failure: What can we learn from mouse models? *Front Immunol* 2022; **13**: 951937 [PMID: 36032161 DOI: 10.3389/fimmu.2022.951937]
38 **Espinoza JL**, Kotecha R, Nakao S. Microbe-Induced Inflammatory Signals Triggering Acquired Bone Marrow Failure Syndromes. *Front Immunol* 2017; **8**: 186 [PMID: 28286502 DOI: 10.3389/fimmu.2017.00186]
39 **Boiko JR**, Borghesi L. Hematopoiesis sculpted by pathogens: Toll-like receptors and inflammatory mediators directly activate stem cells. *Cytokine* 2012; **57**: 1-8 [PMID: 22079335 DOI: 10.1016/j.cyto.2011.10.005]

40 **Chiba Y**, Mizoguchi I, Hasegawa H, Ohashi M, Orii N, Nagai T, Sugahara M, Miyamoto Y, Xu M, Owaki T, Yoshimoto T. Regulation of myelopoiesis by proinflammatory cytokines in infectious diseases. *Cell Mol Life Sci* 2018; **75**: 1363-1376 [PMID: 29218601 DOI: 10.1007/s00018-017-2724-5]

41 **Esplin BL**, Shimazu T, Welner RS, Garrett KP, Nie L, Zhang Q, Humphrey MB, Yang Q, Borghesi LA, Kincade PW. Chronic exposure to a TLR ligand injures hematopoietic stem cells. *J Immunol* 2011; **186**: 5367-5375 [PMID: 21441445 DOI: 10.4049/jimmunol.1003438]

42 **MacNamara KC**, Racine R, Chatterjee M, Borjesson D, Winslow GM. Diminished hematopoietic activity associated with alterations in innate and adaptive immunity in a mouse model of human monocytic ehrlichiosis. *Infect Immun* 2009; **77**: 4061-4069 [PMID: 19451243 DOI: 10.1128/IAI.01550-08]

43 **Rodriguez S**, Chora A, Goumnerov B, Mumaw C, Goebel WS, Fernandez L, Baydoun H, HogenEsch H, Dombkowski DM, Karlewicz CA, Rice S, Rahme LG, Carlesso N. Dysfunctional expansion of hematopoietic stem cells and block of myeloid differentiation in lethal sepsis. *Blood* 2009; **114**: 4064-4076 [PMID: 19696201 DOI: 10.1182/blood-2009-04-214916]

44 **Maratheftis CI**, Andreakos E, Moutsopoulos HM, Voulgarelis M. Toll-like receptor-4 is up-regulated in hematopoietic progenitor cells and contributes to increased apoptosis in myelodysplastic syndromes. *Clin Cancer Res* 2007; **13**: 1154-1160 [PMID: 17317824 DOI: 10.1158/1078-0432.CCR-06-2108]

45 **Giudice V**, Feng X, Lin Z, Hu W, Zhang F, Qiao W, Ibanez MDPF, Rios O, Young NS. Deep sequencing and flow cytometric characterization of expanded effector memory CD8(+)CD57(+) T cells frequently reveals T-cell receptor Vβ oligoclonality and CDR3 homology in acquired aplastic anemia. *Haematologica* 2018; **103**: 759-769 [PMID: 29419434 DOI: 10.3324/haematol.2017.176701]

46 **Chaturvedi CP**, Tripathy NK, Minocha E, Sharma A, Rahman K, Nityanand S. Altered Expression of Hematopoiesis Regulatory Molecules in Lipopolysaccharide-Induced Bone Marrow Mesenchymal Stem Cells of Patients with Aplastic Anemia. *Stem Cells Int* 2018; **2018**: 6901761 [PMID: 30416525 DOI: 10.1155/2018/6901761]

47 **Adolph TE**, Zhang J. Diet fuelling inflammatory bowel diseases: preclinical and clinical concepts. *Gut* 2022; **71**: 2574-2586 [PMID: 36113981 DOI: 10.1136/gutjnl-2021-326575]

48 **Sugihara K**, Kamada N. Diet-Microbiota Interactions in Inflammatory Bowel Disease. *Nutrients* 2021; **13** [PMID: 34062869 DOI: 10.3390/nu13051533]

49 **Zhang P**. Influence of Foods and Nutrition on the Gut Microbiome and Implications for Intestinal Health. *Int J Mol Sci* 2022; **23** [PMID: 36076980 DOI: 10.3390/ijms23179588]

50 **Mamieva Z**, Poluektova E, Svistushkin V, Sobolev V, Shifrin O, Guarner F, Ivashkin V. Antibiotics, gut microbiota, and irritable bowel syndrome: What are the relations? *World J Gastroenterol* 2022; **28**: 1204-1219 [PMID: 35431513 DOI: 10.3748/wjg.v28.i12.1204]

51 **Gobbo MM**, Bomfim MB, Alves WY, Oliveira KC, Corsetti PP, de Almeida LA. Antibiotic-induced gut dysbiosis and autoimmune disease: A systematic review of preclinical studies. *Autoimmun Rev* 2022; **21**: 103140 [PMID: 35830954 DOI: 10.1016/j.autrev.2022.103140]

52 **Black J**, Sweeney L, Yuan Y, Singh H, Norton C, Czuber-Dochan W. Systematic review: the role of psychological stress in inflammatory bowel disease. *Aliment Pharmacol Ther* 2022; **56**: 1235-1249 [PMID: 36082403 DOI: 10.1111/apt.17202]

53 **Bonaz B**. Anti-inflammatory effects of vagal nerve stimulation with a special attention to intestinal barrier dysfunction. *Neurogastroenterol Motil* 2022; **34**: e14456 [PMID: 36097404 DOI: 10.1111/nmo.14456]

54 **Fakharian F**, Asgari B, Nabavi-Rad A, Sadeghi A, Soleimani N, Yadegar A, Zali MR. The interplay between Helicobacter pylori and the gut microbiota: An emerging driver influencing the immune system homeostasis and gastric carcinogenesis. *Front Cell Infect Microbiol* 2022; **12**: 953718 [PMID: 36046747 DOI: 10.3389/fcimb.2022.953718]

55 **Peng W**, Zhao X, Li X. Helicobacter bilis Contributes to the Occurrence of Inflammatory Bowel Disease by Inducing Host Immune Disorders. *Biomed Res Int* 2022; **2022**: 1837850 [PMID: 35983246 DOI: 10.1155/2022/1837850]

56 **Qi Y**, Zang SQ, Wei J, Yu HC, Yang Z, Wu HM, Kang Y, Tao H, Yang MF, Jin L, Zen K, Wang FY. High-throughput sequencing provides insights into oral microbiota dysbiosis in association with inflammatory bowel disease. *Genomics* 2021; **113**: 664-676 [PMID: 33010388 DOI: 10.1016/j.ygeno.2020.09.063]

57 **Eraksoy H**. Gastrointestinal and Abdominal Tuberculosis. *Gastroenterol Clin North Am* 2021; **50**: 341-360 [PMID: 34024445 DOI: 10.1016/j.gtc.2021.02.004]

58 **Gupta P**, Kumar S, Sharma V, Mandavdhare H, Dhaka N, Sinha SK, Dutta U, Kochhar R. Common and uncommon imaging features of abdominal tuberculosis. *J Med Imaging Radiat Oncol* 2019; **63**: 329-339 [PMID: 30932343 DOI: 10.1111/1754-9485.12874]

59 **Deshpande SS**, Joshi AR, Deshpande SS, Phajlani SA. Computed tomographic features of abdominal tuberculosis: unmask the impersonator! *Abdom Radiol (NY)* 2019; **44**: 11-21 [PMID: 30027495 DOI: 10.1007/s00261-018-1700-3]

World Journal of Clinical Cases

Submit a Manuscript: https://www.f6publishing.com

World J Clin Cases 2023 January 26; 11(3): 598-609

DOI: 10.12998/wjcc.v11.i3.598

ISSN 2307-8960 (online)

ORIGINAL ARTICLE

Retrospective Study

Clinical outcomes of AngioJet pharmacomechanical thrombectomy *versus* catheter-directed thrombolysis for the treatment of filter-related caval thrombosis

Jin-Yong Li, Jian-Long Liu, Xuan Tian, Wei Jia, Peng Jiang, Zhi-Yuan Cheng, Yun-Xin Zhang, Xiao Liu, Mi Zhou

Specialty type: Surgery

Provenance and peer review: Unsolicited article; Externally peer reviewed.

Peer-review model: Single blind

Peer-review report's scientific quality classification

Grade A (Excellent): 0
Grade B (Very good): 0
Grade C (Good): C, C
Grade D (Fair): 0
Grade E (Poor): E

P-Reviewer: Kharlamov AN, Netherlands; Shariati MBH, Iran

Received: October 30, 2022
Peer-review started: October 30, 2022
First decision: December 13, 2022
Revised: December 22, 2022
Accepted: January 5, 2023
Article in press: January 5, 2023
Published online: January 26, 2023

Jin-Yong Li, Jian-Long Liu, Xuan Tian, Wei Jia, Peng Jiang, Zhi-Yuan Cheng, Yun-Xin Zhang, Xiao Liu, Mi Zhou, Department of Vascular Surgery, Beijing Jishuitan Hospital, Beijing 100035, China

Corresponding author: Xuan Tian, Doctor, Associate Professor, Department of Vascular Surgery, Beijing Jishuitan Hospital, No. 31 East Street, Xinjiekou, Xicheng District, Beijing 100035, China. doctor_tx@sina.com

Abstract

BACKGROUND

The inferior vena cava filter is utilized worldwide to intercept thrombi and to reduce the risk of fatal pulmonary embolism (PE). However, filter-related thrombosis is a complication of filter implantation. Endovascular methods such as AngioJet rheolytic thrombectomy (ART) and catheter-directed thrombolysis (CDT) can treat filter-related caval thrombosis, but the clinical outcomes of both treatment modalities have not been determined.

AIM

To compare the treatment outcomes of AngioJet rheolytic thrombectomy *vs* catheter-directed thrombolysis in patients with filter-related caval thrombosis.

METHODS

In this single-center retrospective study, 65 patients (34 males and 31 females; mean age: 59.0 ± 13.43 years) with intrafilter and inferior vena cava thrombosis were enrolled between January 2021 and August 2022. These patients were assigned to either the AngioJet group (n = 44) or the CDT group (n = 21). Clinical data and imaging information were collected. Evaluation measures included thrombus clearance rate, periprocedural complications, urokinase dosage, incidence of PE, limb circumference difference, length of stay, and filter removal rate.

RESULTS

Technical success rates were 100% in the AngioJet and CDT groups. In the AngioJet group, grade II and grade III thrombus clearance was achieved in 26

(59.09%) and 14 (31.82%) patients, respectively. In the CDT group, grade II and grade III thrombus clearance was accomplished in 11 (52.38%) patients and 8 (38.10%) patients, respectively (P > 0.05).The peridiameter difference of the thigh was significantly reduced in patients from both groups after treatment (P < 0.05). The median dosage of urokinase was 0.08 (0.02, 0.25) million U in the AngioJet group and 1.50 (1.17, 1.83) million U in the CDT group (P < 0.05). Minor bleeding was shown in 4 (19.05%) patients in the CDT group, and when it was compared with that in the AngioJet group, the difference was statistically significant (P < 0.05). No major bleeding occurred. Seven (15.91%) patients in the AngioJet group had hemoglobinuria and 1 (4.76%) patient in the CDT group had bacteremia. There were 8 (18.18%) patients with PE in the AngioJet group and 4 (19.05%) patients in the CDT group before the intervention (P > 0.05). Computed tomography angiopulmonography (CTA) showed that PE was resolved after the intervention. New PE occurred in 4 (9.09%) patients in the AngioJet group and in 2 (9.52%) patients in the CDT group after theintervention (P > 0.05). These cases of PE were asymptomatic. The mean length of stay was longer in the CDT group (11.67 ± 5.34 d) than in the AngioJet group (10.64 ± 3.52 d) (P < 0.05). The filter was successfully retrieved in the first phase in 10 (47.62%) patients in the CDT group and in 15 (34.09%) patients in the AngioJet group (P > 0.05).Cumulative removal was accomplished in 17 (80.95%) out of 21 patients in the CDT group and in 42 (95.45%) out of 44 patients in the ART group (P > 0.05). The median indwelling time for patients with successful retrieval was 16 (13139) d in the CDT group and 59 (12231) d in the ART group (P > 0.05).

CONCLUSION

Compared with catheter-directed thrombolysis, AngioJet rheolytic thrombectomy can achieve similar thrombus clearance effects, improve the filter retrieval rate, reduce the urokinase dosage and lower the risk of bleeding events in patients with filter-related caval thrombosis.

Key Words: Inferior vena cava filter; Thrombosis; AngioJet rheolytic thrombectomy; Catheter-directed thrombolysis; Clinical outcome

Core Tip: This is a retrospective study. A total of 65 patients were enrolled to evaluate the clinical outcomes of different treatment methods in patients with filter-related caval thrombosis. We compared the data of patients between the AngioJet rheolytic thrombectomy group (n = 44) and the catheter-directed thrombolysis group (n = 21). The current results showed no difference in thrombus clearance or filter retrieval rate. However, the results showed significant differences in urokinase dosage, peridiameter difference of the thigh, minor bleeding, and length of stay.

Citation: Li JY, Liu JL, Tian X, Jia W, Jiang P, Cheng ZY, Zhang YX, Liu X, Zhou M. Clinical outcomes of AngioJet pharmacomechanical thrombectomy *versus* catheter-directed thrombolysis for the treatment of filter-related caval thrombosis. *World J Clin Cases* 2023; 11(3): 598-609
URL: https://www.wjgnet.com/2307-8960/full/v11/i3/598.htm
DOI: https://dx.doi.org/10.12998/wjcc.v11.i3.598

INTRODUCTION

Patients with deep venous thrombosis (DVT) have a high risk of lethal acute pulmonary embolism (PE) if left untreated[1-3]. Anticoagulants are the mainstay of prophylaxis in DVT[4,5]. At present, inferior vena cava (IVC) filters are used to reduce the risk of fatal PE in high-risk patients[6,7]. However, permanent placement of IVC filters may lead to some complications, such as fracture or migration, organ injury, and thrombotic events[8-10]. The incidence of filter-related caval thrombosis ranges from 1% to 30%, depending on the type of filter[11-13]. Filter-related thrombosis can cause caval occlusion associated with some complications, including renal dysfunction and pelvic congestion syndrome[14].

Therefore, early thrombus clearance is essential to restore the patency of the caval outflow. It is difficult to treat filter-related thrombosis because of the large vessel lumen and the large thrombus burden. The methods of thrombus clearanceinclude open surgical thrombectomy, catheter-directed thrombolysis (CDT), and percutaneous mechanical thrombectomy (PMT)[15]. Open surgical thrombectomy ensures satisfactory long-term clinical outcomes for patients who are not eligible for endovascular measures[16]. Although CDT is an effective treatment for filter-related caval thrombosis that can restore blood flow, it increases the risk of bleeding events[13,14,17]. PMT is effective for

resolving filter-related caval thrombosis, reducing the dosage of thrombolytic drugs and the risk of bleeding events[18].

A meta-analysis recently reported the treatment outcomes of AngioJet *vs* CDT for lower extremity deep venous thrombosis (LEDVT)[19]. Based on our clinical experience, PMT can reduce the risk of bleeding and may be a good option. What's more, it is unclear whether CDT and PMT lead to major bleeding or fatal PE in patients with filter-related caval thrombosis. However, the clinical outcomes of both treatment modalities have not been determined in these patients until now. Therefore, we aimed to compare ART with CDT in patients with filter-related thrombosis on treatment outcomes for providing a basis for clinical practice and research.

MATERIALS AND METHODS

Patients

This is a single-center retrospective study. Patients with traumatic lower-limb fractures and simultaneous DVT who were admitted to Beijing Jishuitan Hospital between January 2021 and August 2022 were enrolled in the present study. The presence of DVT was confirmed with bilateral color Doppler ultrasound or venography. These patients received an IVC filter before surgical fixation. The IVC filter was deployed in all patients using the standard technique, and the femoral vein of the healthy limb was used as the access site for filter placement. Filter removal was attempted within 2 wk after fracture surgery in all patients, and venography revealed intrafilter and IVC thrombosis. Sixty-five patients (59.0 years ± 13.43 years) were identified for inclusion in the study. General patient information data, including sex, age, affected limbs, risk factors (fracture types), scope of thrombosis, filter types, and duration of symptoms (defined as the time from detection oflower extremity DVT to thrombus clearance), were collected (Table 1). This study received ethical approval from the Ethics Committee of our hospital.

The inclusion criteria were as follows: (1) Unilateral lower extremity fracture and simultaneous DVT (femoral and/or popliteal venous thrombosis) in the acute stage; (2) complete medical records; (4) life expectancy > 1 year; (5) no serious complications of vital organs; (6) no anticoagulant or thrombolysis contraindication after surgical fixation of fractures; and (7) no previous history of thrombosis.

The exclusion criteria were as follows: (1) Bilateral lower extremity DVT; (2) thrombosis throughout the iliofemoral vein; (3) history of pregnancy or any hemorrhage; (4) life expectancy < 1 year; and (5) contraindications related therapeutic drugs.

These patients were assigned to either the AngioJet group (n = 44) or the CDT group (n = 21). The study profile was shown in Figure 1. Evaluation measures included thrombus clearance rate, periprocedural complications, urokinase dosage, incidence of PE, limb circumference difference, length of stay, and filter removal rate. The procedure of intervention was as follows (Table 2).

AngioJet rheolytic thrombectomy

A 6-Fr AngioJet thrombectomy catheter (Boston Scientific, Natick, MA, United States) was inserted into the IVC thrombus *via* the femoral vein. The power-pulsed spraying thrombolytic mode was used, and saline-containing urokinase (100 mL of normal saline + 200000 U of urokinase) was injected into the IVC thrombus at a speed of 1 mm/s. The dosage of normal saline-containing urokinase depended on the extent of the thrombus. After waiting for 15-20 min, a mechanical rheolytic thrombectomy was performed for aspiration of the thrombus. If the thrombus remained, we repeated the aspiration 2-3 times. If the inferior vena cava angiography showed that the thrombus remained, a 10F guiding catheter (OptEase™ Retrieval Catheter, Cordis Corporation, FL, United States) was used to suck the thrombus out under guidance of an exchange guidewire (Terumo, Japan) *via* femoral vein access. The catheter connected a 20 mL injector, and constant negative pressure of the syringe was maintained for repeated thrombus suction. Finally, inferior vena cava angiography was implemented to assess thrombus clearance (Figure 2).

CDT

We placed a thrombolytic catheter (UniFuse, AngioDynamics, Latham, NY, United States) in the thrombus *via* the femoral vein. Urokinase was constantly injected through the catheter at a rate of 500000 U/d. Angiography was implemented every 24 h to evaluate the thrombolytic effect (Figure 3). Thrombolysis was terminated when the plasma fibrinogen level was less than 1 g/L, the IVC was unobstructed, or there were serious complications. If the inferior vena cava angiography showed that the thrombus remained, a 10F guiding catheter was used to suck the thrombus out under the guidance of an exchange guidewire (Terumo, Japan) *via* femoral vein access. The catheter connected to a 20 mL injector was maintained for repeated thrombus suction. Eventually, inferior vena cava angiography was performed to evaluate the thrombus clearance effect.

Table 1 General data of patients in the two groups, *n* (%)

	CDT group (*n* = 21)	AngioJet group (*n* = 44)	χ^2/t	*P* values
Age (yr old)	55.24 ± 11.92	56.84 ± 14.19	-0.447	0.656
Male	13 (61.90)	21 (47.73)	1.145	0.285
Affected limbs (left)	10 (47.62)	20 (45.54)	0.027	0.87
Duration of symptoms	11.23 ± 2.17	11.59 ± 2.08	-0.63	0.531
Risk factors (fracture types)				
Below the knee	6 (28.57)	8 (18.18)	0.913	0.657
Knee	6 (28.57)	14 (31.82)		
Above the knee	9 (42.86)	22 (50.0)		
Scope of thrombosis				
Femoral/popliteal/calf	5 (23.81)	6 (13.64)	0.448	0.503
Popliteal/calf	16 (76.19)	38 (86.36)		
Filter types				
Denali	22 (100.0)	41 (93.18)	–	0.545

CDT: Catheter-directed thrombolysis.

Table 2 Intervention related data between these two groups of patients, *n* (%)

	CDT group (*n* = 21)	AngioJet group (*n* = 44)	χ^2/t	*P* values
Scope of thrombosis				
intra-filter thrombosis	18 (85.71)	38 (86.36)	0	1
intra-filter and IVC thrombosis	3 (14.29)	6 (13.64)		
Pulmonary embolism	4 (19.05)	8 (18.18)	0	1
Left lung	2 (9.52)	3 (6.82)	–	0.655
Embolism of lobar artery	1 (4.76)	2 (0.45)	–	1
Embolism of segmental artery	3 (14.29)	6 (13.64)	0	1
Median urokinase dosage (million U, range)	1.50 (1.17, 1.83)	0.08 (0.02, 0.25)	-6.495	0
Large-lumen catheter aspiration thrombus	11 (52.38)	33 (75.0)	3.326	0.068
D-Dimer (before intervention)	12.10 (2.29, 30.93)[a]	8.87 (2.01, 18.88)[b]	-4.472	0
D-Dimer (after intervention)	8.37 (2.67, 15.98)[a]	7.14 (0.43, 22.05)[b]	-3.407	0.001

[a]$P < 0.01$, before treatment *vs* after treatment in the catheter-directed thrombolysis group.
[b]$P < 0.01$, before treatment *vs* after treatment in the AngioJet group.
CDT: Catheter-directed thrombolysis; IVC: Inferior vena cava.

Filter retrieval

Filter retrieval was performed when the patient was considered low risk for PE. The criteria were as follows: (1) Decreasing trend or normal serum D-dimer levels; (2) IVC thrombus clearance of more than 95% after ART or CDT; and (3) disappearance or organization of the previously visualized lower-limb thrombus. The same placement technique as before was applied for venous access for the filter retrieval procedures. All procedures were performed through the femoral vein. Briefly, after venous access and the introduction of the angiography catheter, initial venography was performed to evaluate the patency of the IVC. The filter was retrieved using the Günther Tulip Retrieval System (William Cook Europe, Denmark). If the above conditions were not met, anticoagulation therapy was continued, ultrasound or venography was further assessed for the associated risks, and filter removal was performed at an optional stage.

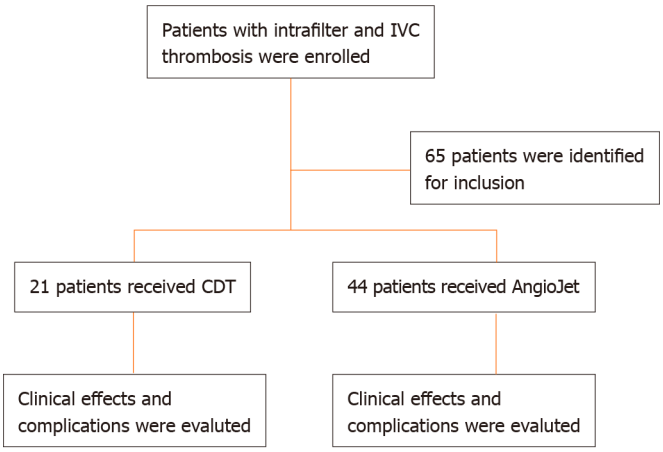

DOI: 10.12998/wjcc.v11.i3.598

Figure 1 Study profile. IVC: Inferior vena cava; CDT: Catheter-directed thrombolysis.

Anticoagulant therapy

During hospitalization, low molecular weight heparin was routinely given after fracture surgery, and anticoagulation therapy with 20 mg rivaroxaban was initiated daily after thrombus clearance. Oral anticoagulant was taken for at least 3 mo after filter removal.

Observation indicators and evaluation criteria

Technical success is defined as uncomplicated implementation of the AngioJet device or CDT for thrombectomy through femoral vein access. CTA and D-dimer tests were performed before and after the operation within 3 d. D-dimer was analyzed with a Sysmex CS-5100 System. The laboratory reference range was 0 to 0.55 mg/mL. The difference in circumference between the affected and unaffected thighs at 15 cm above the patella was measured before and after treatment. The thrombus clearance effect was assessed according to the outcomes of the first and last venography. The degree of thrombus clearance was divided into three types: Grade I (partial clearance (< 50%), grade II (most clearance (50%-99%), and grade III (complete clearance (100%)[20]. The occurrence of complications was evaluated, including minor bleeding (epistaxis, gum bleeding, and hematoma), major bleeding (retroperitoneal or intracranial bleeding), hemoglobinuria, bacteremia, allergic reaction, serious cardiovascular or respiratory complications, and death. Filter removal of the first phase was defined as immediate retrieval within 3 d after thrombus removal. After anticoagulation and thrombus clearance, all filters were removed, and the cumulative removal rate was calculated by the proportion of successful filter retrieval. The indwelling time of the filter was the time from placement to retrieval. The follow-up time was more than one month, and patients also underwent routine D-dimer tests every month after discharge.

Statistical analysis

Continuous variables are presented as medians, minimums, and maximums for nonparametric distributions and were compared by using the Mann-Whitney test. Continuous variables are presented as the means and standard deviations for parametric distributions, and comparisons were made using the independent *t* test. Categorical variables are evaluated as frequencies and percentages and compared by using the chi-square test or Fisher's exact test. Statistical significance was defined as $P < 0.05$. All statistical analyses were processed with SPSS 23.0 software (SPSS Inc., Chicago, IL, United States).

RESULTS

Patients

Sixty-five (65) patients diagnosed with traumatic lower-limb fracture and simultaneous DVT between January 2021 and August 2022 were enrolled in the study. Forty-four patients (56.84 ± 14.19 years) were included in the AngioJet group, and 21 patients (55.24 ± 11.92 years) were included in the CDT group. The left lower extremity was affected in 10 patients (47.76%) in the CDT group and in 20 patients (45.54%) in the ART group ($P > 0.05$). Risk factors associated with acute DVT in the two groups were fractures below the knee (28.57% *vs* 18.18%, $P > 0.05$), fractures of the knee (28.57% *vs* 31.82%, $P > 0.05$), and fractures above the knee (42.86% *vs* 50.0%, $P > 0.05$). The scope of thrombosis in both groups included the femoral/popliteal/calf vein (23.81% *vs* 13.64%, $P > 0.05$) and popliteal/calf vein (76.19% *vs* 86.36%, $P > 0.05$). Filters of Denali were implanted in 22 patients in the CDT group and 44 in the ART

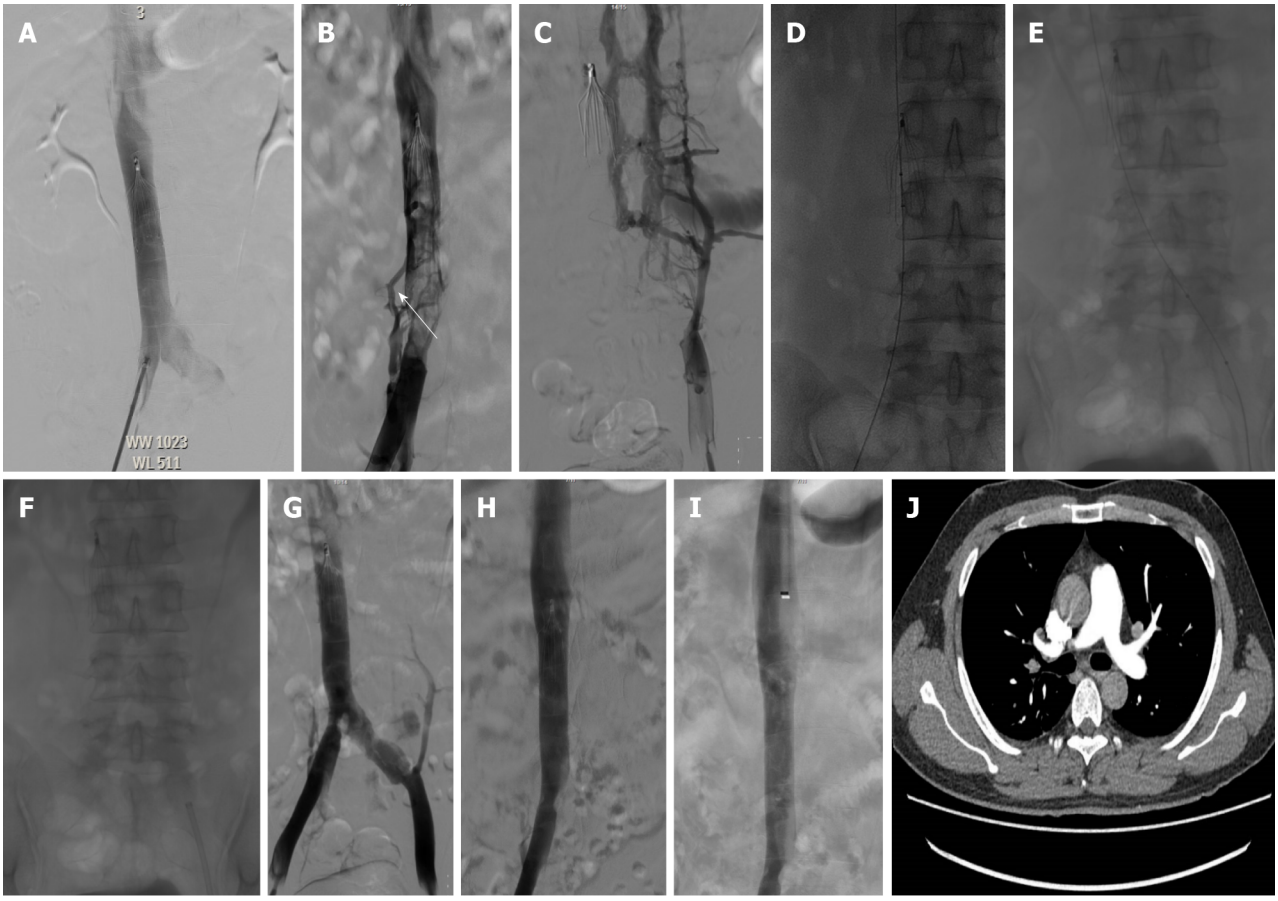

DOI: 10.12998/wjcc.v11.i3.598

Figure 2 Angiography was performed to evaluate the thrombus clearance of AngioJet. A: A 31-year-old male patient with acute traumatic lower-limb fracture and simultaneous deep venous thrombosis received an inferior vena cava (IVC) filter before surgical fixation; B and C: Filter removal was attempted within 2 weeks after fracture surgery, and angiography showed filter-related IVC-iliac vein thrombosis (white arrow); D and E: A 6-Fr AngioJet thrombectomy catheter was placed for thrombus clearance; F: The 10F guiding catheter was placed and withdrawn, and the thrombus was aspirated under negative pressure until it exited the body, which could be repeated 2-3 times; G and H: The venography showed the complete clearance thrombus of filter-related IVC-iliac vein thrombosis; I: The venography showed that the IVC vein was unobstructed after filter retrieval; J: Computed tomography angiopulmonography did not show pulmonary embolism after intervention.

group (100% *vs* 93.18%, $P > 0.05$). The general information is shown in Table 1.

The scope of thrombosis in both groups included intrafilter thrombosis (85.71% *vs* 86.36%, $P > 0.05$) and intrafilter and IVC thrombosis (14.29% *vs* 13.64%, $P > 0.05$). There were 8 (18.18%) patients with PE in the AngioJet group and 4 (19.05%) patients in the CDT group before the intervention ($P > 0.05$). CTA showed that these cases of PE were resolved after the intervention. The PE was located at the level of segmental or lobar arteries in these patients ($P > 0.05$). The median dosage of urokinase was 0.08 (0.02, 0.25) million U in the AngioJet group and 1.50 (1.17, 1.83) million U in the CDT group ($P < 0.05$). Compared to 33 (75.0%) patients in the AngioJet group, 11 (52.38%) patients in the CDT group were treated with large-lumen catheter suction after thrombus clearance ($P > 0.05$). In the CDT group, the median D-dimer levels were 12.10 (2.29, 30.93) and 8.37 (2.67, 15.98) mg/mL before and after treatment, respectively ($P < 0.05$). In the AngioJet group, the median D-dimer levels were 8.87 (2.01, 18.88) and 7.14 (0.43, 22.05) mg/mL before and after treatment, respectively ($P < 0.05$) (Table 2).

Evaluation of clinical outcomes

The technical success rates were 100% in the AngioJet and CDT groups. Thrombus clearance of patients in the CDT and AngioJet groups reached grade I (9.52% *vs* 9.09%), grade II (52.38% *vs* 59.09%), and grade III (38.10% *vs* 31.82%), respectively ($P > 0.05$). In the AngioJet group, the differences in thigh circumference were 4.76 ± 0.77 cm and 1.58 ± 0.51 cm before and after treatment, respectively ($P < 0.05$). In the CDT group, the peridiameter differences of the thigh were 4.51 ± 0.65 cm and 1.44 ± 0.36 cm, respectively ($P < 0.05$).

In the AngioJet group, 7 patients (15.91) developed hemoglobinuria after the procedure, which was relieved after rehydration and hydration, and no hemoglobinuria was found in the CDT group. Bacteremia was found in one patient (4.76%) in the CDT group, which was relieved by anti-infection after catheter removal. In the CDT group, minor bleeding was observed in 4 (19.05%) patients, including

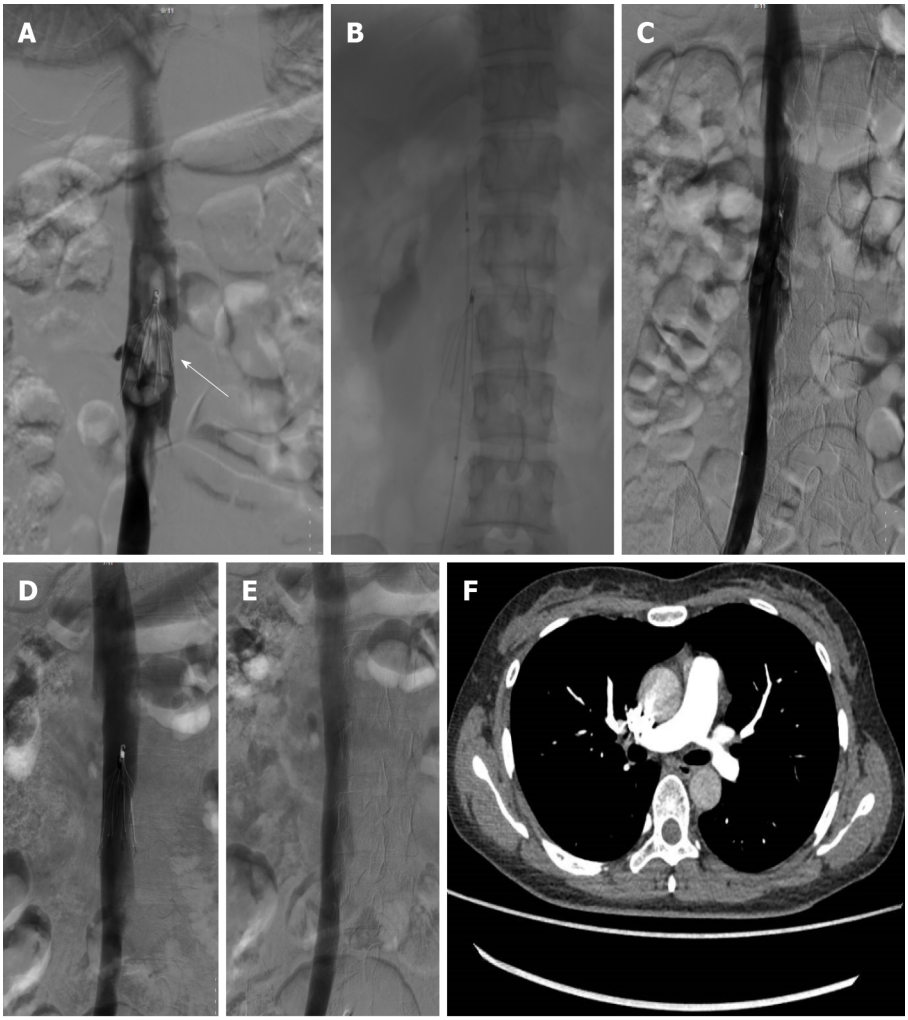

DOI: 10.12998/wjcc.v11.i3.598

Figure 3 Angiography was implemented to assess the thrombus clearance of catheter-directed thrombolysis. A: A 36-year-old male patient with acute traumatic lower-limb fracture and simultaneous deep venous thrombosis received an inferior vena cava (IVC) filter before surgical fixation. Filter removal was attempted within 2 wk after fracture surgery, and venography showed IVC-related caval thrombosis; B: A thrombolytic catheter was placed in the thrombosed segment *via* the right femoral vein, and urokinase was continuously injected; C: The venography showed that the most clearance thrombus of filter-related thrombosis; D: The patient was given anticoagulation therapy with rivaroxaban 20 mg daily after catheter-directed thrombolysis. The venography showed that the complete thrombus clearance of filter-related thrombosis 7 wk later; E: The venography showed that the IVC vein was unobstructed after the filter removal; F: Computed tomography angiopulmonography did not show pulmonary embolism after intervention.

epistaxis in 2 patients, gum bleeding in one patient, and hematoma at the puncture site in one patient, and the difference was significant compared with the AngioJet group ($P < 0.05$). New PE occurred in 4 patients (9.09) in the AngioJet group and in 2 patients (9.52) in the CDT group and was asymptomatic in each case. These PEs were located at the level of segmental arteries in these patients ($P > 0.05$). The mean length of stay was longer in the CDT group (11.67 ± 5.34 d) than in the AngioJet group (10.64 ± 3.52 d) ($P < 0.05$).

Immediate filter retrieval was successful in 10 out of 21 patients (47.62% success rate) after the procedure in the CDT group and 15 out of 44 patients (34.09% success rate) in the ART group ($P > 0.05$). Cumulative removal was achieved in 17 (80.95% success rate) out of 21 patients in the CDT group and 42 (95.45% success rate) out of 44 patients in the AngioJet group ($P > 0.05$). Filter retrieval was unsuccessful in one patient due to superior vena cava malformation and was not conducted in 3 CDT patients due to organized thrombus, which prevented the capture of the retrieval hook, and in 2 AngioJet patients because of an organized thrombus on the hook. The median indwelling time for patients in whom retrieval was successful was 16 d (range 13-139 d) in the CDT group and 59 d (range 12-231 d) in the ART group ($P > 0.05$). The therapeutic effects and complications are shown in Table 3.

The median follow-up time was 4(1,10) months. At the 1-mo follow-up, no major bleeding, symptomatic PE, recurrent thrombosis or other serious complications was observed after the procedure in either group. Two (4.5%) patients in the AngioJet group developed recurrent swelling of the affected limb 1 mo after the intervention. The ultrasound showed venous reflux of the lower extremities. There was no skin ulceration or pigmentation in the calf after treatment in either group.

Table 3 Therapeutic effect and complications of patients in the two groups, *n* (%)

	CDT group (*n* = 21)	AngioJet group (*n* = 44)	χ^2/t	*P* values
Thrombus clearance grade				
Grade I (< 50%)	2 (9.52)	4 (9.09)	0.281	0.922
Grade II (50%-99%)	11 (52.38)	26 (59.09)		
Grade III (100%)	8 (38.10)	14 (31.82)		
Complications				
Haemoglobinuria	0	7 (15.91)	–	0.086
Any bleed	4 (19.05)	0	–	0.009
Bacteraemia	1 (4.76)	0	–	0.323
PE after treatment	2 (9.52)	4 (9.09)	–	1
Left lung	2 (9.52)	0	–	0.101
Embolism of segmental artery	2 (9.52)	4 (9.09)	–	1
Difference of circumference between affected and unaffected thigh (cm)				
Before treatment	4.51 ± 0.65[c]	4.76 ± 0.77[d]	-1.267	0.21
After treatment	1.44 ± 0.36[d]	1.58 ± 0.51[d]	-1.089	0.28
Length of stay (d)	11.67 ± 5.34	10.64 ± 3.52	2.215	0.03
Filter removal				
the first phase	10 (47.62)	15 (34.09)	1.099	0.294
the cumulative removal	17 (80.95)	42 (95.45)	–	0.08
IVCF retention time (d)	16 (13, 139)	59 (12, 231)	-0.991	0.322
D-dimer after 1 mo (mg/L)	0.24 (0.09, 2.15)	0.26 (0.09, 2.62)	-4.346	0

[c]$P < 0.01$, before treatment *vs* after treatment in the catheter-directed thrombolysis group.
[d]$P < 0.01$, before treatment *vs* after treatment in the AngioJet group.
CDT: Catheter-directed thrombolysis; IVCF: Inferior vena cava filter; PE: Pulmonary embolism.

DISCUSSION

A high incidence of DVT has been reported in trauma patients, especially those with lower-limb fractures. With transient trauma contraindicating anticoagulant use, temporary perioperative IVC filter placement is the best prophylactic option for these patients[12,21]. IVC filter placement, however, may lead to numerous complications[22]. Filter-related thrombosis is one of the complications after implantation, with an incidence of approximately 10% in these patients[12]. Moreover, filter-related thrombosis also causes serious complications, such as caval occlusion or shock[14,23]. Prompt treatment of thrombi and retrieval of IVC filters can reduce the risk of filter-related thrombosis. The more effective methods for treating acute IVC filter-related thrombosis are CDT or ART[18,24]. No relevant literature evaluating the clinical efficacy of the two methods has been found thus far.

In our study, endovascular intervention resulted in good clinical outcomes, with a high incidence of thrombus clearance in patients in both groups. Studies have shown that grade II/III thrombus clearance was achieved in 80%-91% of acute LEDVT patients who underwent ART and in 83%-97% of acute LEDVT patients who underwent CDT[20,25]. The results of this study show that the extent of thrombus clearance in patients with IVC thrombosis is similar to that of patients with LEDVT. However, there have also been studies reporting 100% clearance of grade II/III IVC thrombosis[18,26]. This is somewhat different from our study and may be related to the selection of patients, the time of thrombosis, and the choice of thrombolytic drugs. In our study, manual aspiration thrombectomy (MAT) was performed according to the effect of thrombus removal after the operation. MAT through a large vascular sheath and guiding catheter is an adjunctive procedure for thrombus removal. It is also a necessary and effective means of thrombus clearance because of the large lumen and thrombus burden of the IVC in the treatment of filter-related thrombosis. In one study, the researchers repeated that MAT could achieve more than 95% thrombus clearance, which was shown in venography in patients with acute iliofemoral DVT[27]. However, in another study, the researchers mentioned that MAT had a good thrombusclearance rate but was less effective than ART for the treatment of IVC filter-related

thrombosis (74.13 ± 19.74% *vs* 84.58 ± 11.90%, $P < 0.05$)[18]. ART or CDT combined with MAT can achieve good clinical outcomes, but further studies are needed to confirm this hypothesis in the future.

CDT can rapidly achieve complete thrombolysis without pure anticoagulation but increases the potential risk of bleeding, which may be life-threatening[28]. It has been reported that the incidence of bleeding events in CDT ranges from 9.7% to 21.1% in patients with LEDVT[20,25-26]. Our study showed that the bleeding complication rate was 19.05%, which was similar to that of LEDVT, and no major bleeding events occurred. In addition to bleeding complications, the management of CDT is also a tricky problem, mainly reflected in the restriction of patient movement because of indwelling catheters, bleeding or hematoma, and catheter-related bacteremia. In this study, one patient (4.76%) in the CDT group developed postoperative catheter-related bacteremia, which was cured by antibiotic treatment. When catheter-related infection occurs, it is necessary to remove the catheter, which may affect thrombolytic treatment. Therefore, catheter-related bacteremia should be avoided. ART can quickly reduce the volume of thrombi, which can achieve better clinical outcomes for inferior vena cava-iliac vein thrombosis[29]. Transient hemoglobinuria is one of the common complications of ART, and studies have reported an incidence of 9.1%-19%[18,20]. ART lowers urokinase dosage but causes discomfort, such as chest tightness, during the procedure in patients with IVC thrombosis. If these conditions occur, the procedure should be stopped, and thrombus removal can be resumed when the symptoms are relieved.

Winters *et al*[30] found that the retrieval rate improved from 23% to 45% over the past five years. It was reported in another study that the retrieval rate of the filter increased from 6.9% to 22.1% in the past 5 years[31]. This indicates that the retrievable rate is still low. Because it is difficult to complete DVT treatment within a short retrieval window, one might lose the best chance of filter retrieval. Meanwhile, a large number of retrievable filters were converted to permanent filters due to capturing thrombi or displaced or tilted filters[32]. Therefore, it is very important to perform thrombus clearance for filter-related thrombosis, which can improve the removal rate of the filter. In our study, the cumulative filter removal rate was 80.95% in the CDT group and 95.45% in the ART group. In addition, it is necessary to choose a filter such as Denali with a long indwelling time and a high removal rate as much as possible [33].

Lindsey *et al*[34] reported that the incidence of trapped IVC filter thrombus was 38% in patients with symptomatic lower extremity DVT who underwent endovascular interventions. At present, the occurrence of PE due to thrombus clearance in patients with intrafilter and IVC thrombosis has not been clinically reported. In our study, the incidence of PE was approximately 9% after ART or CDT in these patients. These PEs were asymptomatic, located in the pulmonary segmental or lobar arteries and relieved with conservative anticoagulation. After oral rivaroxaban anticoagulation, the patient's D-dimer level nearly dropped to normal within one month. This suggests that adequate anticoagulation after thrombus clearance is essential.

There are still several limitations in this study. First, it is a single-center retrospective analysis, which makes it prone to patient selection bias and artificial judgment bias for thrombus removal. LEDVT is different from intrafilter and IVC thrombosis. Thrombus clearance assessment for LEDVT may not be appropriate for IVC thrombosis. In the future, it is necessary to explore objective methods for evaluating thrombus clearance. Second, the sample size of the study was limited. Third, due to the short follow-up period, PTS and venous insufficiency were not evaluated. At present, there is a lack of large-scale studies and long-term follow-up on the venous patency rate and incidence of PTS after IVC thrombosis removal.

CONCLUSION

In summary, we reported the advantages and disadvantages of the two surgical methods in the treatment of patients with filter-related thrombosis. Compared with catheter-directed thrombolysis, ART can attain similar thrombus clearance effects, improve the filter retrieval rate, reduce the dosage of thrombolytic drugs and lower the risk of bleeding. ART and CDT did not cause fatal symptomatic PE in these patients. Because CDT has a greater risk of bleeding, ART may be an alternative treatment for these patients. However, ART, CDT, MAT and conservative treatment with anticoagulants are effective treatments for patients with IVC thrombosis. Which method is more advantageous? Large-sample prospective trials are needed to further confirm the clinical outcome of these treatment modalities.

ARTICLE HIGHLIGHTS

Research background

Filter-related thrombosis is a complication of filter implantation. Early thrombus removal is implemented to restore the patency of the caval outflow. AngioJet rheolytic thrombectomy (ART) and catheter-directed thrombolysis (CDT) are endovascular treatment methods for filter-related caval

thrombosis, but the clinical outcomes of both treatment modalities have not been determined.

Research motivation

We have performed both CDT and ART for filter-related thrombosis at our center. To date, there are few studies comparing the clinical outcomes of the two surgical methods, and the results are expected to be reported.

Research objectives

The aim of this study is to compare the clinical outcomes of AngioJet rheolytic thrombectomy with those of catheter-directed thrombolysis in patients with filter-related caval thrombosis.

Research methods

Sixty-five patients (34 males and 31 females; mean age: 59.0 ± 13.43 years) with intrafilter and inferior vena cava thrombosis were enrolled between January 2021 and August 2022. Of these, patients were divided into the AngioJet group (n = 44) and the CDT group (n = 21). Clinical data and imaging information were collected. Evaluation measures included thrombus clearance rate, periprocedural complications, urokinase dosage, incidence of PE, limb circumference difference, length of stay, and filter removal rate.

Research results

There was no significant difference in thrombus clearance between the two groups (P > 0.05). The peridiameter difference of the thigh was significantly reduced in the patients of both groups after treatment (P < 0.05). The median dosage of urokinase was significantly lower in the ART group (0.08 (0.02, 0.25) million U) than in the CDT group (1.50 (1.17, 1.83) million U) (P < 0.05). Minor bleeding was shown in 4 (19.05%) patients in the CDT group, and when it was compared with that in the AngioJet group, the difference was statistically significant (P < 0.05). There was no case of symptomatic PE after the procedure in either group. The mean length of stay was 11.67 ± 5.34 d in the CDT group and 10.64 ± 3.52 d in the AngioJet group (P < 0.05). Cumulative removal was accomplished in 17 (80.95%) out of 21 patients in the CDT group and in 42 (95.45%) out of 44 patients in the AngioJet group (P > 0.05).

Research conclusions

Compared with catheter-directed thrombolysis, AngioJet rheolytic thrombectomy can achieve similar thrombus clearance effects, improve the filter retrieval rate, reduce the urokinase dosage and lower the risk of bleeding events in patients with filter-related caval thrombosis.

Research perspectives

Further large, prospective clinical studies of the clinical outcomes of CDT and ART are needed.

FOOTNOTES

Author contributions: All listed authors have read and approved the final draft of the manuscript; Tian X, and Liu JL contributed to the conception of the research idea and critical revision of the manuscript; Zhou M and Liu X contributed to the data collection and initial draft; Cheng ZY contributed to statistical analysis, critical revision, and final draft of the manuscript; Li JY wrote the manuscript; Jiang P, Jia W, and Zhang YX reviewed and edited the manuscript.

Supported by Beijing Municipal Administration of Hospital Incubating Program, No, PX2022015.

Institutional review board statement: This study secured ethical approval from the Ethics Committee of Beijing Jishuitan Hospital.

Informed consent statement: All study participants provided informed written consent about personal and medical data collection prior to study enrolment.

Conflict-of-interest statement: All the authors declare that they have no competing interests.

Data sharing statement: The datasets used and/or analyzed during the current study are available from the corresponding author upon reasonable request.

Country/Territory of origin: China

ORCID number: Jin-Yong Li 0000-0003-2530-2796; Jian-Long Liu 0000-0002-5004-2132; Xuan Tian 0000-0002-7710-476X; Wei Jia 0000-0003-4084-194X; Peng Jiang 0000-0002-1742-8236; Zhi-Yuan Cheng 0000-0001-6634-0583; Yun-Xin Zhang 0000-0003-3471-1401; Xiao Liu 0000-0001-9228-6234; Mi Zhou 0000-0002-7901-6763.

S-Editor: Liu JH
L-Editor: A
P-Editor: Liu JH

REFERENCES

1 **Patel K**, Fasanya A, Yadam S, Joshi AA, Singh AC, DuMont T. Pathogenesis and Epidemiology of Venous Thromboembolic Disease. *Crit Care Nurs Q* 2017; **40**: 191-200 [PMID: 28557890 DOI: 10.1097/CNQ.0000000000000158]
2 **Melman WP**, Ettema HB, Verheyen CC. Symptomatic venous thromboembolism after trauma surgery: a study on 56.884 procedures. *Acta Orthop Belg* 2020; **86**: 363-368 [PMID: 33581018]
3 **Barrera LM**, Perel P, Ker K, Cirocchi R, Farinella E, Morales Uribe CH. Thromboprophylaxis for trauma patients. *Cochrane Database Syst Rev* 2013; CD008303 [PMID: 23543562 DOI: 10.1002/14651858.CD008303.pub2]
4 **Madan S**, Shah S, Dale P, Partovi S, Parikh SA. Use of novel oral anticoagulant agents in venous thromboembolism. *Cardiovasc Diagn Ther* 2016; **6**: 570-581 [PMID: 28123977 DOI: 10.21037/cdt.2016.11.17]
5 **Kearon C**, Akl EA, Comerota AJ, Prandoni P, Bounameaux H, Goldhaber SZ, Nelson ME, Wells PS, Gould MK, Dentali F, Crowther M, Kahn SR. Antithrombotic therapy for VTE disease: Antithrombotic Therapy and Prevention of Thrombosis, 9th ed: American College of Chest Physicians Evidence-Based Clinical Practice Guidelines. *Chest* 2012; **141**: e419S-e496S [PMID: 22315268 DOI: 10.1378/chest.11-2301]
6 **Charalel RA**, Durack JC, Mao J, Ross JS, Meltzer AJ, Sedrakyan A. Statewide Inferior Vena Cava Filter Placement, Complications, and Retrievals: Epidemiology and Recent Trends. *Med Care* 2018; **56**: 260-265 [PMID: 29356721 DOI: 10.1097/MLR.0000000000000867]
7 **Decousus H**, Leizorovicz A, Parent F, Page Y, Tardy B, Girard P, Laporte S, Faivre R, Charbonnier B, Barral FG, Huet Y, Simonneau G. A clinical trial of vena caval filters in the prevention of pulmonary embolism in patients with proximal deep-vein thrombosis. Prévention du Risque d'Embolie Pulmonaire par Interruption Cave Study Group. *N Engl J Med* 1998; **338**: 409-415 [PMID: 9459643 DOI: 10.1056/NEJM199802123380701]
8 **Abudayyeh I**, Takruri Y, Weiner JB. Heart block and cardiac embolization of fractured inferior vena cava filter. *SAGE Open Med Case Rep* 2016; **4**: 2050313X16686017 [PMID: 28228959 DOI: 10.1177/2050313X16686017]
9 **Shimizu T**, Kubota K, Suzuki T, Matsumoto T, Shiraki T, Sakuraoka Y, Mori S, Iso Y, Kato M, Ishizuka M, Aoki T. A technique for taping inferior vena cava caudal to the duodenum: duodenal penetration by IVC filter strut after retroperitoneal lymph node dissection-usefulness of the mesenteric approach. *Surg Case Rep* 2019; **5**: 69 [PMID: 31020425 DOI: 10.1186/s40792-019-0626-5]
10 **Knavel EM**, Woods MA, Kleedehn MG, Ozkan OS, Laeseke PF. Complex Inferior Vena Cava Filter Retrieval Complicated by Migration of Filter Fragment into the Aorta and Subsequent Distal Embolization. *J Vasc Interv Radiol* 2016; **27**: 1865-1868 [PMID: 27886952 DOI: 10.1016/j.jvir.2016.07.024]
11 **King RW**, Wooster MD, Veeraswamy RK, Genovese EA. Contemporary rates of inferior vena cava filter thrombosis and risk factors. *J Vasc Surg Venous Lymphat Disord* 2022; **10**: 313-324 [PMID: 34425266 DOI: 10.1016/j.jvsv.2021.07.016]
12 **Huang J**, Kong J, Zhang X, Liu C, Zhao Z, Liu L, Xiao L, Han X. Risk factors for inferior vena cava filter thrombosis in traumatic fracture patients with deep venous thrombosis of lower extremity: A single-center experience. *Vascular* 2022; 17085381221128056 [PMID: 36171637 DOI: 10.1177/17085381221128056]
13 **Patel SH**, Patel R. Inferior vena cava filters for recurrent thrombosis: current evidence. *Tex Heart Inst J* 2007; **34**: 187-194 [PMID: 17622366]
14 **Xiao L**, Shen J, Tong JJ, Zhang Z, Mu XL, Yi ZJ, Bai S, Xu K. Transcatheter thrombolytic therapy for symptomatic thrombo-occlusion of inferior vena cava filter. *Exp Ther Med* 2013; **5**: 533-538 [PMID: 23403505 DOI: 10.3892/etm.2012.843]
15 **Kakkos SK**, Gohel M, Baekgaard N, Bauersachs R, Bellmunt-Montoya S, Black SA, Ten Cate-Hoek AJ, Elalamy I, Enzmann FK, Geroulakos G, Gottsäter A, Hunt BJ, Mansilha A, Nicolaides AN, Sandset PM, Stansby G; Esvs Guidelines Committee, de Borst GJ, Bastos Gonçalves F, Chakfé N, Hinchliffe R, Kolh P, Koncar I, Lindholt JS, Tulamo R, Twine CP, Vermassen F, Wanhainen A, Document Reviewers, De Maeseneer MG, Comerota AJ, Gloviczki P, Kruip MJHA, Monreal M, Prandoni P, Vega de Ceniga M. Editor's Choice - European Society for Vascular Surgery (ESVS) 2021 Clinical Practice Guidelines on the Management of Venous Thrombosis. *Eur J Vasc Endovasc Surg* 2021; **61**: 9-82 [PMID: 33334670 DOI: 10.1016/j.ejvs.2020.09.023]
16 **Wagenhäuser MU**, Dimopoulos C, Antakyali K, Meyer-Janiszewski YK, Mulorz J, Ibing W, Ertas N, Spin JM, Schelzig H, Duran M. Clinical outcomes after direct and indirect surgical venous thrombectomy for inferior vena cava thrombosis. *J Vasc Surg Venous Lymphat Disord* 2019; **7**: 333-343.e2 [PMID: 30853561 DOI: 10.1016/j.jvsv.2018.11.005]
17 **Baekgaard N**, Broholm R, Just S, Jørgensen M, Jensen LP. Long-term results using catheter-directed thrombolysis in 103 Lower limbs with acute iliofemoral venous thrombosis. *Eur J Vasc Endovasc Surg* 2010; **39**: 112-117 [PMID: 19879780 DOI: 10.1016/j.ejvs.2009.09.015]
18 **Liu Z**, Fu G, Gong M, Zhao B, Gu J, Wang T, Zhou Y, He X, Kong J. AngioJet Rheolytic Thrombectomy to Treat Inferior Vena Cava Filter-Related Thrombosis: Efficacy and Safety Compared With Large-Lumen Catheter Suction. *Front*

Cardiovasc Med 2022; **9**: 837455 [PMID: 35387438 DOI: 10.3389/fcvm.2022.837455]

19 **Li GQ**, Wang L, Zhang XC. AngioJet Thrombectomy Versus Catheter-Directed Thrombolysis for Lower Extremity Deep Vein Thrombosis: A Meta-Analysis of Clinical Trials. *Clin Appl Thromb Hemost* 2021; **27**: 10760296211005548 [PMID: 33813903 DOI: 10.1177/10760296211005548]

20 **Zhu J**, Ni CF, Dai ZY, Yao LZ, Li WH. A case-controlled study on AngioJet rheolytic thrombectomy and catheter-directed thrombolysis in the treatment of acute lower extremity deep venous thrombosis. *Vascular* 2020; **28**: 177-182 [PMID: 31674880 DOI: 10.1177/1708538119877322]

21 **Jia W**, Liu J, Tian X, Jiang P. Tempofilter II implantation in patients with lower extremity fractures and proximal deep vein thrombosis. *Diagn Interv Radiol* 2014; **20**: 245-250 [PMID: 24675164 DOI: 10.5152/dir.2013.13289]

22 **Grewal S**, Chamarthy MR, Kalva SP. Complications of inferior vena cava filters. *Cardiovasc Diagn Ther* 2016; **6**: 632-641 [PMID: 28123983 DOI: 10.21037/cdt.2016.09.08]

23 **Higashi H**, Yoshii T, Inaba S, Morofuji T, Morioka H, Saito M, Sumimoto T. Life-threatening shock due to inferior vena cava filter thrombosis. *Heart Lung Vessel* 2015; **7**: 263-265 [PMID: 26495274]

24 **Li WD**, Li CL, Qian AM, Zhang YQ, Li XQ. Catheter-directed thrombolysis combined with manual aspiration thrombectomy for acute inferior vena cava filter thrombosis. *Int Angiol* 2016; **35**: 605-612 [PMID: 26576664]

25 **Xu Y**, Wang X, Shang D, Liu J, Chen W, Han X. Outcome of AngioJet mechanical thrombus aspiration in the treatment of acute lower extremities deep venous thrombosis. *Vascular* 2021; **29**: 415-423 [PMID: 32957848 DOI: 10.1177/1708538120958595]

26 **Shi W**, Lou W, He X, Liu C, Gu J. The management of filter-related caval thrombosis complicated by heparin-induced thrombocytopenia and thrombosis. *Int J Clin Exp Med* 2015; **8**: 13078-13088 [PMID: 26550230]

27 **Zhu QH**, Zhou CY, Chen Y, Wang J, Mo HY, Luo MH, Huang W, Yu XF. Percutaneous manual aspiration thrombectomy followed by stenting for iliac vein compression syndrome with secondary acute isolated iliofemoral deep vein thrombosis: a prospective study of single-session endovascular protocol. *Eur J Vasc Endovasc Surg* 2014; **47**: 68-74 [PMID: 24183245 DOI: 10.1016/j.ejvs.2013.09.030]

28 **Amin VB**, Lookstein RA. Catheter-directed interventions for acute iliocaval deep vein thrombosis. *Tech Vasc Interv Radiol* 2014; **17**: 96-102 [PMID: 24840964 DOI: 10.1053/j.tvir.2014.02.006]

29 **Huang CY**, Hsu HL, Kuo TT, Lee CY, Hsu CP. Percutaneous pharmacomechanical thrombectomy offers lower risk of post-thrombotic syndrome than catheter-directed thrombolysis in patients with acute deep vein thrombosis of the lower limb. *Ann Vasc Surg* 2015; **29**: 995-1002 [PMID: 25765634 DOI: 10.1016/j.avsg.2015.01.014]

30 **Winters JP**, Morris CS, Holmes CE, Lewis P, Bhave AD, Najarian KE, Shields JT, Charash W, Cushman M. A multidisciplinary quality improvement program increases the inferior vena cava filter retrieval rate. *Vasc Med* 2017; **22**: 51-56 [PMID: 27811236 DOI: 10.1177/1358863X16676658]

31 **Ahmed O**, Wadhwa V, Patel K, Patel MV, Turba UC, Arslan B. Rising Retrieval Rates of Inferior Vena Cava Filters in the United States: Insights From the 2012 to 2016 Summary Medicare Claims Data. *J Am Coll Radiol* 2018; **15**: 1553-1557 [PMID: 29606636 DOI: 10.1016/j.jacr.2018.01.037]

32 **Ho KM**, Tan JA, Burrell M, Rao S, Misur P. Venous thrombotic, thromboembolic, and mechanical complications after retrievable inferior vena cava filters for major trauma. *Br J Anaesth* 2015; **114**: 63-69 [PMID: 24980424 DOI: 10.1093/bja/aeu195]

33 **Stavropoulos SW**, Chen JX, Sing RF, Elmasri F, Silver MJ, Powell A, Lynch FC, Abdel Aal AK, Lansky A, Muhs BE; DENALI Trial Investigators. Analysis of the Final DENALI Trial Data: A Prospective, Multicenter Study of the Denali Inferior Vena Cava Filter. *J Vasc Interv Radiol* 2016; **27**: 1531-1538.e1 [PMID: 27569678 DOI: 10.1016/j.jvir.2016.06.028]

34 **Lindsey P**, Echeverria A, Poi MJ, Matos J, Bechara CF, Cheung M, Lin PH. Thromboembolic Risk of Endovascular Intervention for Lower Extremity Deep Venous Thrombosis. *Ann Vasc Surg* 2018; **49**: 247-254 [PMID: 29197610 DOI: 10.1016/j.avsg.2017.10.004]

World Journal of Clinical Cases

Submit a Manuscript: https://www.f6publishing.com

World J Clin Cases 2023 January 26; 11(3): 610-620

DOI: 10.12998/wjcc.v11.i3.610

ISSN 2307-8960 (online)

ORIGINAL ARTICLE

Clinical Trials Study

Efficacy and safety of propofol target-controlled infusion combined with butorphanol for sedated colonoscopy

Feng Guo, De-Feng Sun, Yan Feng, Lin Yang, Jing-Lin Li, Zhong-Liang Sun

Specialty type: Medicine, research and experimental

Provenance and peer review: Unsolicited article; Externally peer reviewed.

Peer-review model: Single blind

Peer-review report's scientific quality classification

Grade A (Excellent): A
Grade B (Very good): 0
Grade C (Good): 0
Grade D (Fair): D
Grade E (Poor): 0

P-Reviewer: Musa Y, Nigeria; Ubiali MLC, Brazil

Received: October 12, 2022
Peer-review started: October 12, 2022
First decision: November 11, 2022
Revised: December 19, 2022
Accepted: January 5, 2023
Article in press: January 5, 2023
Published online: January 26, 2023

Feng Guo, Department of Anesthesiology, No. 967 Hospital, Joint Logistics Support Force of Chinese People's Liberation Army, Dalian 116011, Liaoning Province, China

De-Feng Sun, Yan Feng, Jing-Lin Li, Zhong-Liang Sun, Department of Anesthesiology, The First Affiliated Hospital of Dalian Medical University, Dalian 116011, Liaoning Province, China

Lin Yang, Department of Neuroelectrophysiology, The First Affiliated Hospital of Dalian Medical University, Dalian 11601, Liaoning Province, China

Corresponding author: De-Feng Sun, MS, Professor, Department of Anesthesiology, The First Affiliated Hospital of Dalian Medical University, No. 5 Longbin Road, Jinzhou District, Dalian 116011, Liaoning Province, China. sundefengyl@163.com

Abstract

BACKGROUND

Propofol is a short-acting, rapid-recovering anesthetic widely used in sedated colonoscopy for the early detection, diagnosis and treatment of colon diseases. However, the use of propofol alone may require high doses to achieve the induction of anesthesia in sedated colonoscopy, which has been associated with anesthesia-related adverse events (AEs), including hypoxemia, sinus bradycardia, and hypotension. Therefore, propofol co-administrated with other anesthetics has been proposed to reduce the required dose of propofol, enhance the efficacy, and improve the satisfaction of patients receiving colonoscopy under sedation.

AIM

To evaluate the efficacy and safety of propofol target-controlled infusion (TCI) in combination with butorphanol for sedation during colonoscopy.

METHODS

In this controlled clinical trial, a total of 106 patients, who were scheduled for sedated colonoscopy, were prospectively recruited and assigned into three groups to receive different doses of butorphanol before propofol TCI: Low-dose butorphanol group (5 μg/kg, group B1), high-dose butorphanol group (10 μg/kg, group B2), and control group (normal saline, group C). Anesthesia was achieved by propofol TCI. The primary outcome was the median effective concentration (EC50) of propofol TCI, which was measured using the up-and-down sequential method. The secondary outcomes included AEs in perianesthesia and recovery characteristics.

RESULTS

The EC50 of propofol for TCI was 3.03 μg/mL [95% confidence interval (CI): 2.83-3.23 μg/mL] in group B2, 3.41 μg/mL (95%CI: 3.20-3.62 μg/mL) in group B1, and 4.05 μg/mL (95%CI: 3.78-4.34 μg/mL) in group C. The amount of propofol necessary for anesthesia was 132 mg [interquartile range (IQR), 125-144.75 mg] in group B2 and 142 mg (IQR, 135-154 mg) in group B1. Furthermore, the awakening concentration was 1.1 μg/mL (IQR, 0.9-1.2 μg/mL) in group B2 and 1.2 μg/mL (IQR, 1.025-1.5 μg/mL) in group B1. Notably, the propofol TCI plus butorphanol groups (groups B1 and B2) had a lower incidence of anesthesia AEs, when compared to group C. Furthermore, no significant differences were observed in the rates of AEs in perianesthesia, including hypoxemia, sinus bradycardia, hypotension, nausea and vomiting, and vertigo, among group C, group B1 and group B2.

CONCLUSION

The combined use with butorphanol reduces the EC50 of propofol TCI for anesthesia. The decrease in propofol might contribute to the reduced anesthesia-related AEs in patients undergoing sedated colonoscopy.

Key Words: Colonoscopy; Sedated colonoscopy; Propofol; Butorphanol; Target-controlled infusion; Effective concentration; Adverse event

Core Tip: Propofol target-controlled infusion co-administrated with butorphanol significantly reduces the dose of propofol required for achieving anesthesia in patients undergoing sedated colonoscopy, leading to the enhancement of efficacy, and reduction in anesthesia-related adverse events when using propofol alone. Therefore, these findings may be beneficial for clinicians in inducing anesthesia, eventually improving the care and satisfaction of patients receiving diagnostic or therapeutic colonoscopic procedures for colorectal diseases.

Citation: Guo F, Sun DF, Feng Y, Yang L, Li JL, Sun ZL. Efficacy and safety of propofol target-controlled infusion combined with butorphanol for sedated colonoscopy. *World J Clin Cases* 2023; 11(3): 610-620
URL: https://www.wjgnet.com/2307-8960/full/v11/i3/610.htm
DOI: https://dx.doi.org/10.12998/wjcc.v11.i3.610

INTRODUCTION

Colonoscopy is an essential endoscopic tool for the screening, early diagnosis, and treatment of colorectal diseases, especially colorectal cancer, which is the second most common cause of cancer-related mortality worldwide[1,2]. It has been noted that conventional colonoscopy has a number of limitations, including high degree of patient discomfort during the colonoscopic procedure, prolonged insertion, and difficult or even failed cecal intubation[3,4]. In order to reduce patient discomfort and facilitate cecal intubation, colonoscopy with anesthesia or performed under sedation has gained increasing acceptance and popularity in recent years[4,5]. Indeed, patients under sedation during diagnostic or therapeutic endoscopic procedures generally experience minimal or even no discomfort[4,5]. Numerous studies have evaluated the efficacy and safety of anesthetics for sedation colonoscopy, such as propofol, which is a short-acting rapid-recovering anesthetic[6-12]. The results of previous studies suggest that propofol, particularly delivered by target-controlled infusion (TCI), which is a drug delivery technique applied to achieve the desired anesthetic drug concentration by using a pharmacokinetic model and considering the patient characteristics [*i.e.*, age, gender and body mass index (BMI)], is an effective anesthetic with rapid onset and short recovery[11,13-18]. Compared to conventional methods of administrating drugs during anesthesia, such as bolus injection with a syringe and continuous infusion with an infusion pump, TCI provides a relatively constant concentration at the target site, and a more rapid recovery time.

Despite the mentioned advantages, various adverse events (AEs) can occur, including hypoxemia, sinus bradycardia, and hypotension[11,12]. These AEs have been associated with the required high dose of propofol for the induction of anesthesia, when used as the sole anesthetic during colonoscopic procedures[11,12]. Hence, propofol co-administrated with other anesthetics has been sought to reduce the dose of propofol required for anesthesia, enhance the efficacy, and improve the satisfaction of patients undergoing endoscopic procedures[19-24]. For instance, butorphanol, a synthetic opioid, has

higher affinity for opioid receptors, when compared to opioids. Compared to morphine, butorphanol has higher analgesic potency, a similar duration of action, and lower respiratory depression. Furthermore, butorphanol is a mixed opioid agonist/antagonist, which includes an agonistic action on the kappa-opioid receptor and agonistic/antagonistic effects on the mu-opioid receptor. This exerts an analgesic effect mainly by agonizing the kappa-opioid receptor. In addition, butorphanol can be used to mitigate the respiratory depression of mu-opioid agonists. The advantages of butorphanol include low toxicity and low potential for abuse. Previous studies have revealed that compared to other synthetic opioid analgesic drugs (*e.g.*, sufentanil), butorphanol has less anesthesia-related AEs, such as respiratory depression, decreased gastrointestinal activity and smooth muscle spasm, itchy skin, urinary retention, physical and physiological dependence, nausea, and vomiting[25,26]. Furthermore, butorphanol has been widely used in anesthesia for patients undergoing gastrointestinal endoscopy.

The present controlled clinical trial aimed to determine the effects of different doses of butorphanol on the efficacy of propofol TCI based on the median effective concentration (EC50) and safety, in terms of anesthesia-related AEs, in patients undergoing colonoscopic procedures under sedation. These results may be beneficial for clinicians in inducing anesthesia, eventually improving the care for patients receiving diagnostic or therapeutic colonoscopic procedures for colorectal diseases.

MATERIALS AND METHODS

Patients and study design

For the present controlled clinical trial, patients who underwent sedated colonoscopy were prospectively recruited from the First Affiliated Hospital of Dalian Medical University (Dalian, Liaoning Province, China) between December 2020 and March 2021. During the patient enrollment, the following inclusion criteria were used: (1) 18-65 years old; (2) Scheduled to undergo sedated colonoscopy; and (3) American Society of Anesthesiologists (ASA) I-II, graded according to the ASA Physical Status (PS) Classification System. Patients who presented with the following clinical conditions were excluded from the clinical trial: (1) Obstructive sleep apnea hypopnea syndrome; (2) Liver failure, kidney failure, or both; (3) Severe cardio/cerebrovascular diseases categorized as class III or higher, according to the New York Heart Association classification system; (4) Medical history of chronic pain or mental illness; (5) Regular intake of sedatives and painkillers; (6) Medical history of vertigo or motion sickness; (7) BMI of ≥ 30 kg/m^2; (8) Pregnant patients; and (9) Patients who were unwilling to provide a written informed consent. The enrolled patients were assigned to three groups, based on the time sequence: (1) Group B1, received low-dose butorphanol (propofol TCI plus butorphanol, 5 μg/kg); (2) Group B2, received high-dose butorphanol (propofol TCI plus butorphanol, 10 μg/kg); and (3) Group C, the control group [normal saline (NS)]. The Propofol Medium and Long Chain Fat Emulsion Injection (Batch No. J20160089) was obtained from Beijing Fresenius Kabi Pharmaceutical Co. Ltd. (Beijing, China). The Butorphanol Tartrate Injection (Batch no. h20143106) was manufactured by Jiangsu Hengrui Pharmaceutical Co., Ltd. (Nanjing, Jiangsu, China).

The present study was reviewed and approved by the Ethics Committee of the First Affiliated Hospital of Dalian Medical University, with approval no: PJ-KS-KY-2020-144 (X). A written informed consent was obtained from each participant prior to the initiation of the clinical trial. The clinical trial was registered with the Chinese Clinical Trial Registry (ChiCTR 2000034849, 21/07/2020). The present study was conducted in accordance with the guidelines of the Declaration of Helsinki.

Anesthesia procedure

The Propofol Medium and Long Chain Fat Emulsion Injection (Batch no. J20160089) was obtained from Beijing Fresenius Kabi Pharmaceutical Co. Ltd. (Beijing, China). The Butorphanol Tartrate Injection (Trade name: Nuoyang; 2 mL:4 mg; Batch no. h20143106) was manufactured by Jiangsu Hengrui Pharmaceutical Co., Ltd. (Nanjing, Jiangsu, China).

For the anesthesia, at 10 min before the colonoscopy, the patients intravenously received butorphanol at a dose of 5 μg/kg in group B1 and 10 μg/kg in group B2, and patients in group C received NS. Upon arrival in the examination room, an oxygen mask was placed on the patient at a flow rate of 5 L/min. Then, the patient's routine electrocardiogram, heart rate (HR), non-invasive blood pressure and pulse oximetry (SpO_2) were monitored during the procedure. A computer-controlled TCI pump (Guangxi Weili Fangzhou Technology, Guangxi, China) was initiated. Then, propofol TCI was administered with an initial plasma target concentration of 3.0 μg/mL for the first case in each group. This was used as the first dose of propofol. When the target concentration of propofol was achieved, the colonoscopy was performed. The administration of propofol TCI was stopped when the colonoscope reached the ileocecal region, and colonoscopic withdrawal began.

Assessment of primary outcome

The primary aim of the present study was to determine the EC50 of propofol for TCI, which is necessary for half maximal effectiveness. The EC50 of propofol for TCI in each group was measured using the up-and-down sequential method, which has a widely used sequential design for studies on the EC50 of

anesthesia. The initial plasma target concentration designated for each group was 3.0 μg/mL. Purposeful movements (*e.g.*, the head or limbs) were defined as "responsive", while no purposeful movements were defined as "non-responsive". If "responsive" was found in a particular patient, the target plasma concentration of propofol was increased for the next patient by 0.5 μg/mL. In contrast, once "non-responsive" was identified in a particular patient, the target plasma concentration of propofol for the next patient was decreased by 0.5 μg/mL. The process was repeated until eight crossover points were attained. The number of patients needed for the present study could not be calculated beforehand. The target propofol concentration in plasma for consecutive patients in each group and the response to the procedures were determined and used to calculate the EC50 and 95% confidence interval (CI).

Assessment of secondary outcomes

The secondary outcomes included the following measurements: (1) Amount of propofol used during the colonoscopic procedure; (2) Awakening concentration of propofol, which was referred to as the effect-site concentration of propofol in association with eye opening in response to verbal command; (3) Anesthesia-related AEs in perianesthesia, including hypoxemia, sinus bradycardia, hypotension, nausea and vomiting, and vertigo; and (4) Mean arterial pressure (MAP) and HR at different time points, including prior to anesthesia (T0), immediately after consciousness disappeared in response to the induction of anesthesia (T1), when the colonoscope reached the ileocecal region (T2), and when consciousness was regained (T3).

Statistical analysis

Statistical analysis was performed using the GraphPad Prism software (San Diego, CA, United States). Quantitative data were expressed as mean ± SD, or median and interquartile range (IQR), as appropriate. Analysis of variance or Kruskal-Wallis test, and post-hoc test with Bonferroni adjustment were performed to compare quantitative data. The numerical data were analyzed by χ^2 test, while *K*-test was used to compare the EC50 values of propofol for TCI among the three groups (group C, group B1 and group B2). The logarithm for each target concentration (logx), total number of cases (n), effective rate (P), and difference between the logarithm of two adjacent target concentrations (d) were calculated, as follows: (1) Logarithm of EC50: log EC50 = ΣnlogX/Σn; (2) Standard error of logEC50: SlogEC50 = d $\sqrt{\sum \frac{p(1-p)}{(n-1)}}$; and (3) Logarithm of 95%CI of EC50: (logEC50 - 1.96 × Slog EC50, logEC50 + 1.96 × SlogEC50). EC50 and 95%CI were the negative logarithms. A P value of < 0.05 was considered statistically significant between groups.

RESULTS

Demographic and clinical characteristics of patients

A total of 106 patients who underwent sedated colonoscopy were enrolled for the present clinical study. The baseline demographic and clinical characteristics of patients in group C (n = 38), group B1 (n = 36), and group B2 (n = 32) are summarized in Table 1. The mean age of patients was 55.9 years old (SD = 4.3 years old) in group C, 56.9 years old (SD = 4.2 years old) in group B1, and 56.6 years old (SD = 4.8 years old) in group B2. There were no significant differences in baseline demographic characteristics among the groups (all, P > 0.05). The mean BMI was 21.8 kg/m^2 (SD = 1.4 kg/m^2) for patients in group C, 21.3 kg/m^2 (SD = 1.4 kg/m^2) for patients in group B1, and 21.2 kg/m^2 (SD = 1.3 kg/m^2) for patients in group B2. No significant difference was observed among the groups (all, P > 0.05). In addition, there was no significant difference in the proportion of patients with ASA I or II, based on the ASA PS Classification System and the operation time among groups (all, P > 0.05).

Comparison of primary outcomes

For the EC50 for propofol in TCI, the concentrations needed to achieve half maximal effectiveness were compared among the groups. The target propofol concentrations in the plasma of patients for the calculation of the EC50 are presented in Figure 1. As shown in Table 2, the EC50 for propofol in TCI was 4.05 μg/mL (95%CI: 3.78-4.34 μg/mL) in group C, 3.41 μg/mL (95%CI: 3.20-3.62 μg/mL) in group B1, and 3.03 μg/mL (95%CI: 2.83-3.23 μg/mL) in group B2. The statistical analysis revealed that the EC50 in group B2 was significantly lower, when compared to the EC50 in group B1 and group C (P < 0.05, Table 2). Furthermore, the amount of propofol necessary for anesthesia was determined as 132 mg (IQR, 125-144.75 mg) in group B2, which was significantly lower, when compared to the amount in group B1 (142 mg; IQR, 135-154 mg) (P < 0.05, Table 2, Figure 2). These results suggest that the intravenous infusion of 10 μg/kg of butorphanol reduced the need for high-dose propofol for anesthesia, when compared to 5 μg/kg of butorphanol. In addition, the awakening concentration of propofol was 1.1 μg/mL (IQR, 0.9-1.2 μg/mL) in group B2. This concentration was lower than that in group B1 (1.2 μg/mL;

Table 1 Demographic and clinical characteristics of patients in the different groups

Groups	*n*	Age (yr)	Gender (M/F)	BMI (kg/m²)	ASA (I/II)	Operation time (min)
Group C	38	55.9 ± 4.3	18/20	21.8 ± 1.4	26/12	12 (10-14)
Group B1	36	56.9 ± 4.2	17/19	21.3 ± 1.4	24/12	11 (10-12)
Group B2	32	56.6 ± 4.8	15/17	21.2 ± 1.3	21/11	11 (10-12)
P value		0.591	0.999	0.200	0.969	0.218

M: Male; F: Female; BMI: Body mass index; ASA: American Society of Anesthesiologists Physical Status Classification.

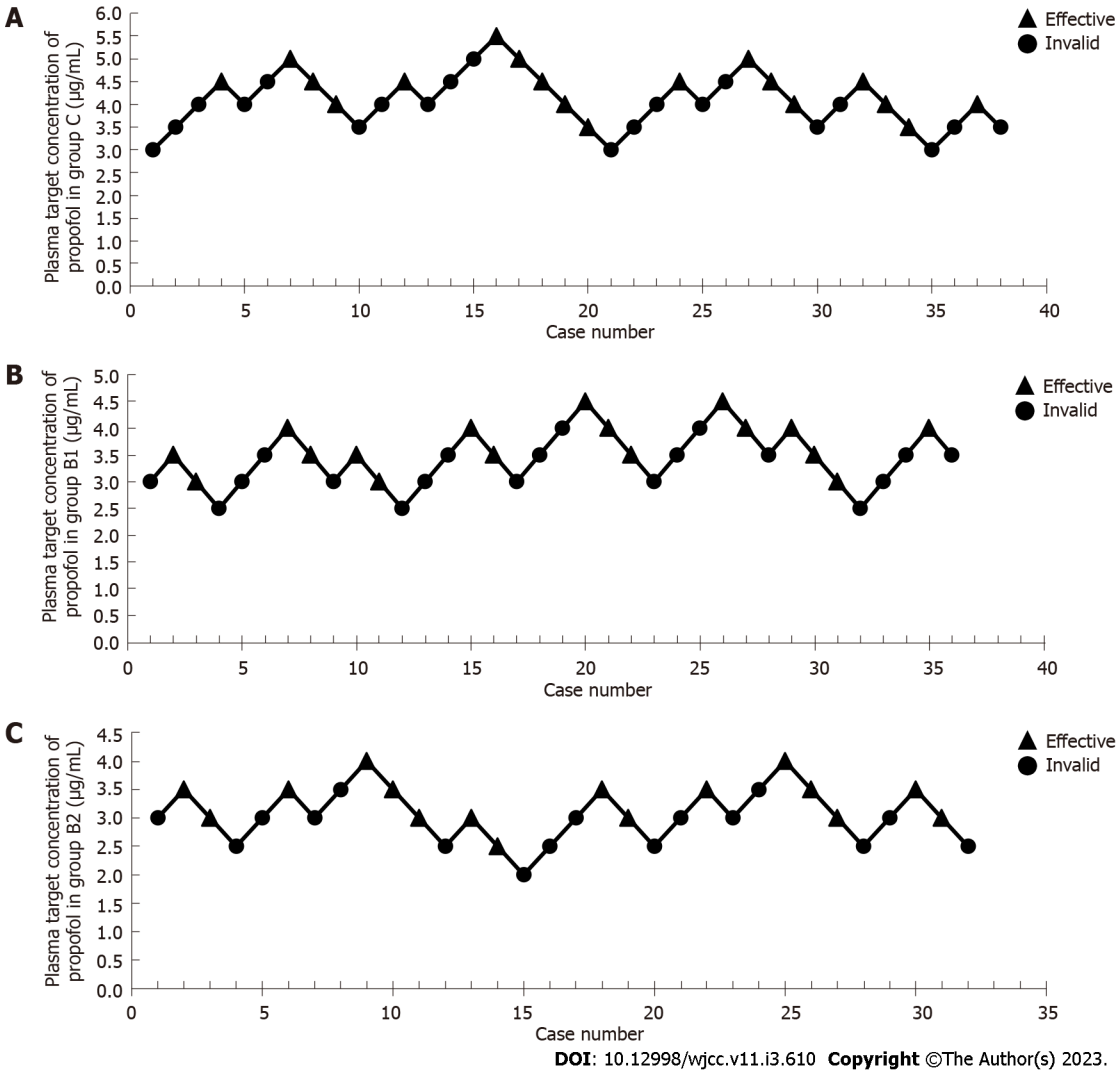

DOI: 10.12998/wjcc.v11.i3.610

Figure 1 Target propofol concentrations in plasma for consecutive patients of each group and the response to the procedures. A: Target propofol concentrations in plasma for consecutive patients in the control group (group C); B: Target propofol concentrations in plasma for consecutive patients in group B1; C: Target propofol concentrations in plasma for consecutive patients in group B2. The target propofol concentrations in plasma for consecutive patients in each group and the response to the procedures were used to calculate the median effective concentration (EC50), which is the concentration required to achieve the half maximal effectiveness of propofol. The resulting EC50 for each group and 95% confidence intervals are presented in Table 2.

IQR, 1.025-1.500 μg/mL) ($P < 0.05$, Figure 2).

Comparison of secondary outcomes

MAP and HR were compared at different time points (T0, T1, T2 and T3) during the procedure among the groups. As shown in Figure 3 and Table 3, the MAP values at time points T1 and T2 were significantly lower in group C, when compared to groups B1 and B2 ($P < 0.05$). In addition, the HR value at time point T1 was significantly lower in group C, when compared to groups B1 and B2 ($P <$

Table 2 Comparison of median effective concentration, dose for anesthesia, and awakening concentration of propofol among the different groups

Groups	*n*	EC_{50} (μg/mL)	95%CI (μg/mL)	Amount of propofol necessary for anesthesia (mg)	Awakening concentration of propofol (μg/mL)
Group C	38	4.05	3.78-4.34	151.0 (142.0-160.5)	1.200 (0.975-1.300)
Group B1	36	3.41[1]	3.20-3.62	142 (135-154)[1,3]	1.200 (1.025-1.500)[3]
Group B2	32	3.03[1,2]	2.83-3.23	132.00 (125.00-144.75)[1,2]	1.1 (0.9-1.2)[2]

[1]$P < 0.05$ *vs* the control group (group C).
[2]$P < 0.05$ *vs* group B1.
[3]$P < 0.05$ *vs* group B2.
Awakening concentration of propofol was defined as the effect-site concentration of propofol in association with eye opening in response to verbal command. CI: Confidence interval; EC50: Effective concentration

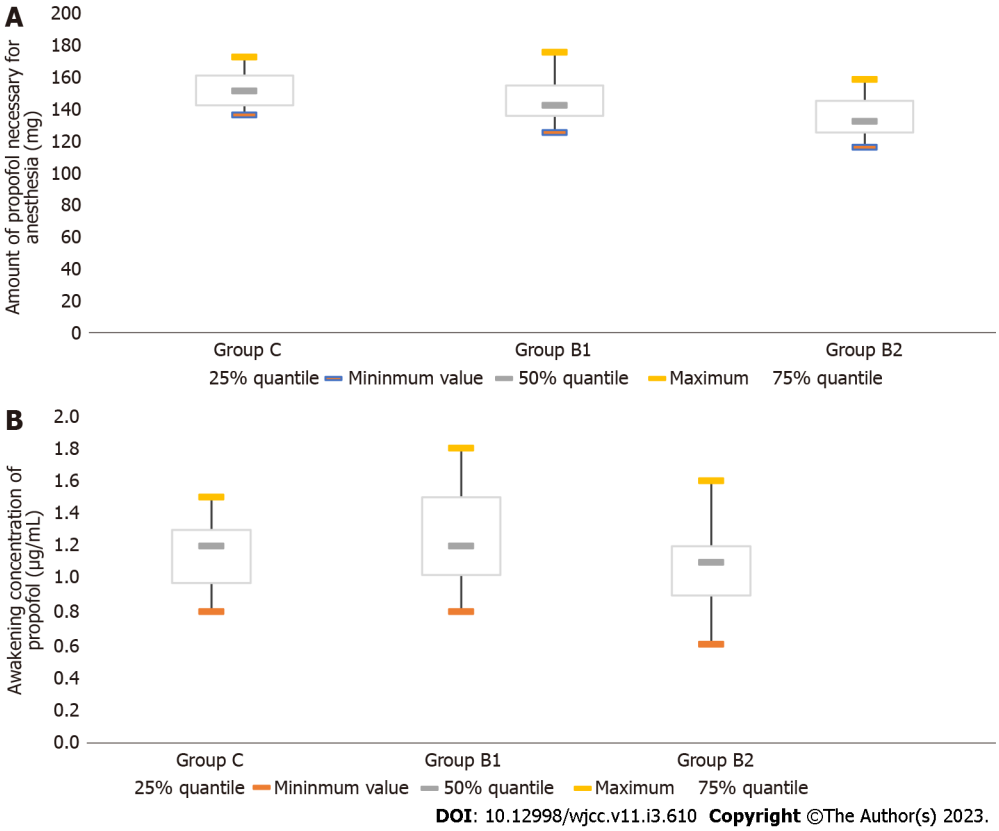

DOI: 10.12998/wjcc.v11.i3.610

Figure 2 Bar graphs for the amount of propofol used during the sedated colonoscopy and the awakening concentration of propofol in each group. A: The amount of propofol used during the sedated colonoscopy in each group; B: The awakening concentration of propofol in each group. The amount of propofol used for the sedated colonoscopic procedure and the awakening concentration of propofol in group C, group B1 and group B2 are illustrated in the bar graphs. The lowest mean amount of propofol used for sedated colonoscopic procedures was observed in group B2, and there was a significant difference among the groups. The wakening concentration of propofol was defined as the effect-site concentration of propofol in association with eye opening in response to verbal command. The mean awakening concentration of propofol was lower in group B2, when compared to group B1.

0.05).

Next, a comparison of AEs (*e.g.*, hypoxemia, sinus bradycardia, hypotension, nausea and vomiting, and vertigo) in perianesthesia was performed among the groups, and the resulting data are summarized in Table 4. Overall, the incidence of each AE did not significantly differ among the groups (all, $P > 0.05$). Notably, the incidence of hypoxemia was higher in group C (13.2%), when compared to group B1 (5.6%) and group B2 (9.4%). In addition, one patient (2.6%) had hypotension in group C, while none of the patients had hypotension in groups B1 and B2. The reduction in anesthesia AEs, especially hypoxemia and hypotension, in groups B1 and B2 could have been attributed to the decrease in propofol required for anesthesia, when used in combination with butorphanol, during the colonoscopic procedure.

Table 3 Comparison of mean arterial pressure and heart rate among the different groups

	Groups	T0	T1	T2	T3
MAP (mmHg)	Group C	90.4 ± 6.1	73.4 ± 6.1[1]	77.0 ± 5.8[1]	88.6 ± 5.4
	Group B1	89.4 ± 5.4	81.7 ± 4.1	85.3 ± 4.0	88.3 ± 3.8
	Group B2	89.5 ± 5.1	78.3 ± 5.0[2]	82.4 ± 4.2[2]	88.5 ± 4.1
HR (bpm)	Group C	81.8 ± 8.8	68.8 ± 7.2[1]	72.1 ± 6.9	79.9 ± 6.0
	Group B1	80.3 ± 9.0	73.2 ± 8.5	74.9 ± 8.0	78.3 ± 6.2
	Group B2	81.9 ± 9.3	74.7 ± 9.8	76.2 ± 8.2	80.1 ± 6.1

[1]$P < 0.05$ *vs* groups B1 and B2.
[2]$P < 0.05$ *vs* group B1.
T0, prior to anesthesia; T1, immediately after losing consciousness in response to induction of anesthesia; T2, the colonoscope reached the ileocecal; T3, consciousness regained. MAP: Mean arterial pressure; HR: Heart rate; bpm: Beats per minute.

Table 4 Comparison of frequency of adverse events in perianesthesia among the different groups

Groups	*n*	Hypoxemia	Sinus bradycardia	Hypotension	Nausea, vomiting	Vertigo
Group C	38	5 (13.2%)	1 (2.6%)	1 (2.6%)	2 (5.3%)	4 (10.5%)
Group B1	36	2 (5.6%)	0 (0%)	0 (0%)	1 (2.8%)	3 (8.3%)
Group B2	32	3 (9.4%)	2 (6.3%)	0 (0%)	2 (6.3%)	3 (9.4%)

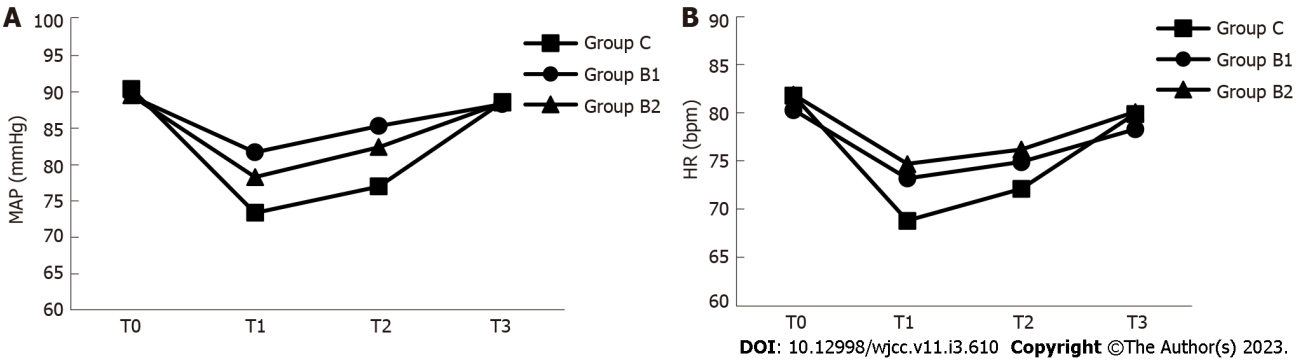

DOI: 10.12998/wjcc.v11.i3.610

Figure 3 The mean arterial pressure and heart rate at different time points during the procedures in each group are shown. A: The mean arterial pressure at different time points during the procedures in each group; B: The heart rate at different time points during the procedures in each group. The mean arterial pressure (MAP) and heart rate (HR) were examined at the following four time points: prior to anesthesia (T0), immediately after consciousness disappeared in response to induction of anesthesia (T1), when the colonoscope reached the ileocecal region (T2), and when consciousness was regained (T3). The MAP represents the average arterial pressure throughout one cardiac cycle, with a normal range of 70-110 mmHg. The MAP values at time points T1 and T2 were significantly lower in group C, when compared to groups B1 and B2 ($P < 0.05$). The HR value at time point of T1 was significantly lower in group C, when compared to groups B1 and B2 ($P < 0.05$).

DISCUSSION

The efficacy and safety of propofol TCI co-administrated with different doses of butorphanol have not yet been evaluated for sedated colonoscopy in the Chinese population. To the best of our knowledge, the present study is the first controlled clinical trial that investigated the effects of different doses of butorphanol on the efficacy and safety of propofol TCI for sedated colonoscopy in Chinese patients. The main novel findings are summarized, as follows. Butorphanol co-administrated with propofol for TCI can significantly improve the efficacy of propofol TCI, as supported by the following evidence: (1) Patients with anesthesia induced by propofol TCI plus high-dose butorphanol had a significantly lower EC50 of propofol for TCI *vs* patients induced by propofol TCI plus low-dose butorphanol and controls (all, $P < 0.05$); and (2) The amount of propofol needed for anesthesia was significantly lower in group B2 *vs* group B1. In addition, the rates for anesthesia-related AEs, including hypoxemia, sinus bradycardia, hypotension, nausea and vomiting, and vertigo, were similar in group C, group B1 and group B2. It is noteworthy that patients in group C had a higher incidence of hypoxemia and hypotension, when

compared to the other two groups. Furthermore, there is a possibility that the lower incidence of anesthesia AEs (hypoxemia and hypotension) is associated with the reduced amount of propofol due to the co-administration of butorphanol with propofol.

The primary aim of the present clinical trial was to determine the effects of the co-administration of butorphanol on the required dose of TCI propofol to achieve sedation during colonoscopic procedures. The TCI system can be programmed using either of the two main pharmacokinetic models: The Marsh model and Schnider model[13,14]. The Marsh model has weight as a model parameter, while the Schnider model has multiple parameters (*e.g.*, age, weight, height, and lean body mass). Chen *et al*[27] examined the performance of the Marsh model and Schnider model for TCI propofol, and suggested that the Marsh model was overall superior to the Schnider model, and more suitable for TCI propofol [27]. Therefore, in the present study, the Marsh model was selected as the pharmacokinetic model to program the TCI system for propofol. It was found that the duration of action and recovery time of propofol were significantly shorter for the TCI of propofol, when compared to the conventional infusion of propofol[11,14,17,18,28]. In addition, the co-administration of propofol with other anesthetics has been shown to reduce the required dose of propofol for targeted anesthesia, and improve patient satisfaction during diagnostic and therapeutic endoscopy[11,19-24,29]. Considering the various advantages of butorphanol, which are mainly associated with less anesthesia-related AEs (*e.g.*, respiratory depression, smooth muscle spasm, skin itches, urinary retention, physical and physiological dependence, nausea and vomiting)[25,26], the co-administration of butorphanol with propofol was examined in the present study. The up-and-down sequential method was used to determine the EC50, which is a commonly used measurement to evaluate the potency of a drug. The results revealed a significant reduction in the required propofol dose, when used in combination with both low-dose (5 μg/kg) and high-dose (10 μg/kg) butorphanol. Given that different anesthetics have various interactions, further studies are needed to determine the optimal combination of different anesthetics, such as propofol and butorphanol, and ensure the effectiveness and safety.

Despite these promising findings, the present study has several limitations. First, the baseline psychological state was not evaluated in the enrolled patients. Considering that preoperative anxiety has been shown to affect the dose of propofol required to achieve anesthesia induction, patients presenting with anxiety may need a higher dose of propofol. Second, the depth of sedation during the colonoscopic procedure was not monitored. Third, although the present study revealed that the butorphanol co-administration with propofol for TCI improved the efficacy without increasing the incidence of anesthesia-related complications, the level of patient satisfaction was not examined. Although propofol and butorphanol exhibited "synergic effects", the interaction between these two anesthetics should be further assessed, in order to ensure the potency and safety of this anesthesia for patients. Future studies with a larger sample size are presently being performed in our center to gain more insight into the combination of propofol TCI and butorphanol for sedation during colposcopy.

CONCLUSION

Overall, the present clinical study revealed that butorphanol co-administrated with propofol TCI can reduce the EC50 of propofol for anesthesia without causing additional anesthesia-related complications in patients undergoing sedated colonoscopy. These findings may assist clinicians in performing anesthesia induction for colonoscopy, eventually helping to improve the care for patients who must receive colonoscopic procedures for colorectal diseases.

ARTICLE HIGHLIGHTS

Research background

Propofol, known as an effective anesthetic with rapid onset and short recovery, has been used in sedated colonoscopy. However, when used alone, high-dose propofol is usually needed for anesthesia, and this may cause anesthesia-related adverse events (AEs).

Research motivation

This clinical study was intended to reduce the required dose of propofol by co-administration with butorphanol in patients receiving colonoscopy under sedation.

Research objectives

The objective of this clinical trial was to assess the efficacy and safety of propofol target-controlled infusion (TCI) in combination with butorphanol for sedation during colonoscopy.

Research methods

One hundred six patients were assigned into three groups to receive different doses of butorphanol before propofol TCI: Low-dose butorphanol group (B1), high-dose butorphanol group (B2), and control group (C). The primary outcome included the median effective concentration (EC50) of propofol TCI, and the secondary outcomes were AEs in perianesthesia and recovery characteristics.

Research results

The EC50 of propofol for TCI was 3.03 μg/mL in group B2, 3.41 μg/ in group B1, and 4.05 μg/mL in group C. The amount of propofol necessary for anesthesia was 132 mg in group B2, lower than 142 mg in group B1. Notably, the propofol TCI plus butorphanol groups (groups B1 and B2) had a lower incidence of anesthesia AEs, when compared to group C. Moreover, there were no significant differences among the three groups in the rates of AEs in perianesthesia, including hypoxemia, sinus bradycardia, hypotension, nausea and vomiting, and vertigo.

Research conclusions

This study has shown that propofol in combination with butorphanol reduces the EC50 of propofol TCI for anesthesia in patients undergoing sedated colonoscopy, and in turn may decrease anesthesia-related AEs in patients undergoing sedated colonoscopy.

Research perspectives

Propofol in combination with butorphanol may improve care for patients undergoing colonoscopic procedures for colorectal diseases.

FOOTNOTES

Author contributions: Guo F and Sun DF are general project manager; Sun DF and Li JL contributed to the study-related decision making and evaluation of examination (including laboratory) results; Guo F, Feng Y and Yang L performed patient screening/enrollment, Guo F and Feng Y participated in the collection of patient medical source documents/research data, (electronic) case report form data entry/correction, and research document management; Sun DF, Li JL and Yang L involved in the assessment of adverse events/serious adverse events, and reporting of safety information; Li JL and Yang L performed the physical examination; Sun ZL communicated with the ethics committee; Guo F and Yang L have contributed equally to this work and share first authorship.

Institutional review board statement: The present study was reviewed and approved by the Ethics Committee of the First Affiliated Hospital of Dalian Medical University, with approval no: PJ-KS-KY-2020-144 (X).

Clinical trial registration statement: The clinical trial was registered with the Chinese Clinical Trial Registry (ChiCTR 2000034849, 21/07/2020).

Informed consent statement: A written informed consent was obtained from each participant prior to the initiation of the clinical trial.

Conflict-of-interest statement: All the authors report no relevant conflicts of interest for this article.

Data sharing statement: The datasets used and/or analyzed during the current study are available from the corresponding author on reasonable request.

CONSORT 2010 statement: The authors have read the CONSORT 2010 Statement, and the manuscript was prepared and revised according to the CONSORT 2010 Statement.

Country/Territory of origin: China

ORCID number: Feng Guo 0000-0002-8290-725X; De-Feng Sun 0000-0002-5147-2409; Yan Feng 0000-0002-9873-8905; Lin Yang 0000-0003-4232-6052; Jing-Lin Li 0000-0003-3020-3530; Zhong-Liang Sun 0000-0002-3657-6963.

S-Editor: Wang JJ
L-Editor: A
P-Editor: Wang JJ

REFERENCES

1 **Bray F**, Ferlay J, Soerjomataram I, Siegel RL, Torre LA, Jemal A. Global cancer statistics 2018: GLOBOCAN estimates of incidence and mortality worldwide for 36 cancers in 185 countries. *CA Cancer J Clin* 2018; **68**: 394-424 [PMID: 30207593 DOI: 10.3322/caac.21492]

2 **Jemal A**, Ward EM, Johnson CJ, Cronin KA, Ma J, Ryerson B, Mariotto A, Lake AJ, Wilson R, Sherman RL, Anderson RN, Henley SJ, Kohler BA, Penberthy L, Feuer EJ, Weir HK. Annual Report to the Nation on the Status of Cancer, 1975-2014, Featuring Survival. *J Natl Cancer Inst* 2017; **109** [PMID: 28376154 DOI: 10.1093/jnci/djx030]

3 **Yang C**, Sriranjan V, Abou-Setta AM, Poluha W, Walker JR, Singh H. Anxiety Associated with Colonoscopy and Flexible Sigmoidoscopy: A Systematic Review. *Am J Gastroenterol* 2018; **113**: 1810-1818 [PMID: 30385831 DOI: 10.1038/s41395-018-0398-8]

4 **Ferreira AO**, Cravo M. Sedation in gastrointestinal endoscopy: Where are we at in 2014? *World J Gastrointest Endosc* 2015; **7**: 102-109 [PMID: 25685266 DOI: 10.4253/wjge.v7.i2.102]

5 **Moon SH**. Sedation regimens for gastrointestinal endoscopy. *Clin Endosc* 2014; **47**: 135-140 [PMID: 24765595 DOI: 10.5946/ce.2014.47.2.135]

6 **Schilling D**. Propofol-based sedation in gastrointestinal endoscopy: getting safer and safer. *Digestion* 2014; **89**: 272-273 [PMID: 25011629 DOI: 10.1159/000362541]

7 **Pace NL**, Stylianou MP. Advances in and limitations of up-and-down methodology: a précis of clinical use, study design, and dose estimation in anesthesia research. *Anesthesiology* 2007; **107**: 144-152 [PMID: 17585226 DOI: 10.1097/01.anes.0000267514.42592.2a]

8 **Padmanabhan A**, Frangopoulos C, Shaffer LET. Patient Satisfaction With Propofol for Outpatient Colonoscopy: A Prospective, Randomized, Double-Blind Study. *Dis Colon Rectum* 2017; **60**: 1102-1108 [PMID: 28891855 DOI: 10.1097/DCR.0000000000000909]

9 **Leslie K**, Allen ML, Hessian EC, Peyton PJ, Kasza J, Courtney A, Dhar PA, Briedis J, Lee S, Beeton AR, Sayakkarage D, Palanivel S, Taylor JK, Haughton AJ, O'Kane CX. Safety of sedation for gastrointestinal endoscopy in a group of university-affiliated hospitals: a prospective cohort study. *Br J Anaesth* 2017; **118**: 90-99 [PMID: 28039246 DOI: 10.1093/bja/aew393]

10 **Li XT**, Ma CQ, Qi SH, Zhang LM. Combination of propofol and dezocine to improve safety and efficacy of anesthesia for gastroscopy and colonoscopy in adults: A randomized, double-blind, controlled trial. *World J Clin Cases* 2019; **7**: 3237-3246 [PMID: 31667174 DOI: 10.12998/wjcc.v7.i20.3237]

11 **Zhang K**, Xu H, Li HT. Safety and efficacy of propofol alone or in combination with other agents for sedation of patients undergoing colonoscopy: an updated meta-analysis. *Eur Rev Med Pharmacol Sci* 2020; **24**: 4506-4518 [PMID: 32373988 DOI: 10.26355/eurrev_202004_21033]

12 **Lundström S**, Twycross R, Mihalyo M, Wilcock A. Propofol. *J Pain Symptom Manage* 2010; **40**: 466-470 [PMID: 20816571 DOI: 10.1016/j.jpainsymman.2010.07.001]

13 **Struys MM**, De Smet T, Glen JI, Vereecke HE, Absalom AR, Schnider TW. The History of Target-Controlled Infusion. *Anesth Analg* 2016; **122**: 56-69 [PMID: 26516804 DOI: 10.1213/ANE.0000000000001008]

14 **Mu JJ**, Jiang T, Deng LP, Choi SW, Irwin MG, Yuen VM. A comparison of two techniques for induction of anaesthesia with target-controlled infusion of propofol. *Anaesthesia* 2018; **73**: 1507-1514 [PMID: 29956318 DOI: 10.1111/anae.14355]

15 **Liu N**, Rinehart J. Closed-Loop Propofol Administration: Routine Care or a Research Tool? *Anesth Analg* 2016; **122**: 4-6 [PMID: 26678459 DOI: 10.1213/ANE.0000000000000665]

16 **Swinhoe CF**, Peacock JE, Glen JB, Reilly CS. Evaluation of the predictive performance of a 'Diprifusor' TCI system. *Anaesthesia* 1998; **53** Suppl 1: 61-67 [PMID: 9640119 DOI: 10.1111/j.1365-2044.1998.53s104.x]

17 **Moerman AT**, Herregods LL, De Vos MM, Mortier EP, Struys MM. Manual versus target-controlled infusion remifentanil administration in spontaneously breathing patients. *Anesth Analg* 2009; **108**: 828-834 [PMID: 19224790 DOI: 10.1213/ane.0b013e318198f6dc]

18 **Müller T**, Ludwig A, Biro P. Two distinct application habits for propofol: an observational study. *Eur J Anaesthesiol* 2010; **27**: 265-269 [PMID: 19952755 DOI: 10.1097/EJA.0b013e3283354736]

19 **Zhou X**, Li BX, Chen LM, Tao J, Zhang S, Ji M, Wu MC, Chen M, Zhang YH, Gan GS, Song XY. Etomidate plus propofol versus propofol alone for sedation during gastroscopy: a randomized prospective clinical trial. *Surg Endosc* 2016; **30**: 5108-5116 [PMID: 27005294 DOI: 10.1007/s00464-016-4861-6]

20 **Haytural C**, Aydınlı B, Demir B, Bozkurt E, Parlak E, Dişibeyaz S, Saraç A, Özgök A, Kazancı D. Comparison of Propofol, Propofol-Remifentanil, and Propofol-Fentanyl Administrations with Each Other Used for the Sedation of Patients to Undergo ERCP. *Biomed Res Int* 2015; **2015**: 465465 [PMID: 26576424 DOI: 10.1155/2015/465465]

21 **Lonardo NW**, Mone MC, Nirula R, Kimball EJ, Ludwig K, Zhou X, Sauer BC, Nechodom K, Teng C, Barton RG. Propofol is associated with favorable outcomes compared with benzodiazepines in ventilated intensive care unit patients. *Am J Respir Crit Care Med* 2014; **189**: 1383-1394 [PMID: 24720509 DOI: 10.1164/rccm.201312-2291OC]

22 **van den Berg JP**, Vereecke HE, Proost JH, Eleveld DJ, Wietasch JK, Absalom AR, Struys MM. Pharmacokinetic and pharmacodynamic interactions in anaesthesia. A review of current knowledge and how it can be used to optimize anaesthetic drug administration. *Br J Anaesth* 2017; **118**: 44-57 [PMID: 28039241 DOI: 10.1093/bja/aew312]

23 **Smith C**, McEwan AI, Jhaveri R, Wilkinson M, Goodman D, Smith LR, Canada AT, Glass PS. The interaction of fentanyl on the Cp50 of propofol for loss of consciousness and skin incision. *Anesthesiology* 1994; **81**: 820-8; discussion 26A [PMID: 7943832]

24 **Bouillon TW**, Bruhn J, Radulescu L, Andresen C, Shafer TJ, Cohane C, Shafer SL. Pharmacodynamic interaction between propofol and remifentanil regarding hypnosis, tolerance of laryngoscopy, bispectral index, and electroencephalographic approximate entropy. *Anesthesiology* 2004; **100**: 1353-1372 [PMID: 15166553 DOI: 10.1097/00000542-200406000-00006]

25 **Agarwal A**, Raza M, Dhiraaj S, Pandey R, Gupta D, Pandey CK, Singh PK, Singh U. Pain during injection of propofol: the effect of prior administration of butorphanol. *Anesth Analg* 2004; **99**: 117-119 [PMID: 15281515 DOI: 10.1213/01.ANE.0000117002.03919.49]

26 **Zhu X**, Chen L, Zheng S, Pan L. Comparison of ED95 of Butorphanol and Sufentanil for gastrointestinal endoscopy sedation: a randomized controlled trial. *BMC Anesthesiol* 2020; **20**: 101 [PMID: 32359348 DOI: 10.1186/s12871-020-01027-5]

27 **Chen SL**, Lin WW, Wang CL, Lin CL. Comparison of accuracy of Marsh model versus Schnider model for propofol target-controlled infusion system. *Chin J Anesthesiol* 2015; **35**: 1466-1469 [DOI: 10.3760/CMA.J.ISSN.0254-1416.2015.12.015]

28 **Xu Z**, Liu F, Yue Y, Ye T, Zhang B, Zuo M, Xu M, Hao R, Xu Y, Yang N, Che X. C50 for propofol-remifentanil target-controlled infusion and bispectral index at loss of consciousness and response to painful stimulus in Chinese patients: a multicenter clinical trial. *Anesth Analg* 2009; **108**: 478-483 [PMID: 19151275 DOI: 10.1213/ane.0b013e31818f8a30]

29 **Yoon SW**, Choi GJ, Lee OH, Yoon IJ, Kang H, Baek CW, Jung YH, Woo YC. Comparison of propofol monotherapy and propofol combination therapy for sedation during gastrointestinal endoscopy: A systematic review and meta-analysis. *Dig Endosc* 2018; **30**: 580-591 [PMID: 29526045 DOI: 10.1111/den.13050]

World Journal of Clinical Cases

Submit a Manuscript: https://www.f6publishing.com

World J Clin Cases 2023 January 26; 11(3): 621-628

DOI: 10.12998/wjcc.v11.i3.621

ISSN 2307-8960 (online)

ORIGINAL ARTICLE

Observational Study

Application of a hospital–community–family trinity rehabilitation nursing model combined with motor imagery therapy in patients with cerebral infarction

Wen-Wen Li, Min Li, Xiao-Juan Guo, Fu-De Liu

Specialty type: Neurosciences

Provenance and peer review: Unsolicited article; Externally peer reviewed.

Peer-review model: Single blind

Peer-review report's scientific quality classification

Grade A (Excellent): 0
Grade B (Very good): 0
Grade C (Good): C, C
Grade D (Fair): 0
Grade E (Poor): 0

P-Reviewer: Albuquerque K, United States; Palmer T, United Kingdom

Received: November 10, 2022
Peer-review started: November 10, 2022
First decision: November 25, 2022
Revised: December 17, 2022
Accepted: December 23, 2022
Article in press: December 23, 2022
Published online: January 26, 2023

Wen-Wen Li, Min Li, Xiao-Juan Guo, Fu-De Liu, Department of Neurology, The First Affilated Hospital of Xi'an Jiaotong University, Xi'an 710061, Shaanxi Province, China

Corresponding author: Fu-De Liu, MHSc, Attending Doctor, Department of Neurology, The First Affilated Hospital of Xi'an Jiaotong University, No. 277 West Yanta Rd, Xi'an 710061, Shaanxi Province, China. liufude1011@163.com

Abstract

BACKGROUND

Rehabilitation nursing is considered an indispensable part of the cerebral infarction treatment system. The hospital–community–family trinity rehabilitation nursing model can provide continuous nursing services across hospitals, communities, and families for patients.

AIM

To explore the application of a hospital–community–family rehabilitation nursing model combined with motor imagery therapy in patients with cerebral infarction.

METHODS

From January 2021 to December 2021, 88 patients with cerebral infarction were divided into a study (n = 44) and a control (n = 44) group using a simple random number table. The control group received routine nursing and motor imagery therapy. The study group was given hospital–community–family trinity rehabilitation nursing based on the control group. Motor function (FMA), balance ability (BBS), activities of daily living (BI), quality of life (SS-QOL), activation status of the contralateral primary sensorimotor cortical area to the affected side, and nursing satisfaction were evaluated before and after intervention in both groups.

RESULTS

Before intervention, FMA and BBS were similar ($P > 0.05$). After 6 months' intervention, FMA and BBS were significantly higher in the study than in the control group (both $P < 0.05$). Before intervention, BI and SS-QOL scores were not different between the study and control group ($P > 0.05$). However, after 6 months' intervention, BI and SS-QOL were higher in the study than in the control group ($P < 0.05$). Before intervention, activation frequency and volume were similar between the study and the control group ($P > 0.05$). After 6 months'

intervention, the activation frequency and volume were higher in the study than in the control group ($P < 0.05$). The reliability, empathy, reactivity, assurance, and tangibles scores for quality of nursing service were higher in the study than in the control group ($P < 0.05$).

CONCLUSION

Combining a hospital–community–family trinity rehabilitation nursing model and motor imagery therapy enhances the motor function and balance ability of patients with cerebral infarction, improving their quality of life.

Key Words: Activities of daily living; Cerebral infarction; Hospital–community–family trinity rehabilitation nursing model; Motor skills; Motor imagery therapy; Postural balance

Core Tip: Various clinical treatments are used for cerebral infarction patients, including motor imagery therapy and rehabilitation nursing. We evaluated a combination of the hospital–community–family trinity rehabilitation nursing model and motor imagery therapy in terms of balance ability, motor ability, and quality of life of cerebral infarction patients. Combined treatment enhanced patients' motor function and balance ability, with concomitant changes in the relevant sensorimotor cortical area brain area. This improved their abilities to conduct activities of daily life as well as in their quality of life, and also resulted in a higher degree of nursing satisfaction.

Citation: Li WW, Li M, Guo XJ, Liu FD. Application of a hospital–community–family trinity rehabilitation nursing model combined with motor imagery therapy in patients with cerebral infarction. *World J Clin Cases* 2023; 11(3): 621-628

URL: https://www.wjgnet.com/2307-8960/full/v11/i3/621.htm

DOI: https://dx.doi.org/10.12998/wjcc.v11.i3.621

INTRODUCTION

Cerebral infarction is a common clinical cerebrovascular disease, accounting for approximately 70% of stroke cases. Cerebral infarction can lead to pyramidal tract damage, causing central paralysis and sensorimotor dysfunction in the human body, which is manifested as decreased muscle strength and motor limitations in a particular limb[1-3].

At present, various clinical treatment methods are used to treat patients with cerebral infarction, including conventional drug therapy, acupuncture, rehabilitation therapy, and motor imagery therapy, and each has therapeutic effects with particular advantages[4-6]. Motor imagery therapy is an intervention administered under the guidance of professionals, in which the patient's own imagination is combined with tactile, auditory, visual, and other associative stimuli to promote motor function improvement in patients with cerebral infarction[7].

In recent years, rehabilitation treatment of patients with cerebral infarction has gradually attracted widespread clinical attention. The importance of rehabilitation nursing has also been reflected. Rehabilitation nursing is considered an indispensable part of cerebral infarction treatment. It is particularly important to select a scientific and reasonable rehabilitation nursing model[8,9]. The hospital-community-family trinity rehabilitation nursing model provides continuous nursing services across hospitals, communities, and families for patients by the cooperation of hospitals and community medical staff, which helps improve the quality of care and promote the rehabilitation of patients[10].

In this study, we explored the application value of a combination of the hospital–community–family trinity rehabilitation nursing model and motor imagery therapy in patients with cerebral infarction, in terms of its effects on balance ability, motor ability, and quality of life of these patients.

MATERIALS AND METHODS

General data

Eighty-eight patients with cerebral infarction who attended our hospital from January 2021 to December 2021 were selected and allocated to a study group and a control group, according to a simple random number table, with 44 cases in each group.

The control group consisted of 21 men and 23 women, aged 39–71 years, with an average age of 55.82 ± 6.15 years. Their body weight ranged from 48 to 79 kg, with an average of 63.79 ± 7.02 kg. In terms of paralysis, 20 cases were affected on the left side and 24 cases on the right side. Ten cases had an education of college degree or above, 23 cases had been educated to junior high school, and 11 cases had an education level of elementary school or below.

The study group consisted of 19 men and 25 women, aged 38–73 years, with an average age of 56.37 ± 5.84. years. Their body weight ranged from 47 to 80 kg, with an average of 64.12 ± 6.80 kg. Twenty-two cases were paralyzed on the left side and 22 cases on the right side. Nine cases had an education of college degree or above, 25 cases had an education up to junior high school, and 10 cases had an education of elementary school or below. Thus, sex, age, site of paralysis, and education level were balanced and comparable between the two groups ($P > 0.05$).

Selection criteria

Patients were included if cerebral infarction was diagnosed by clinical symptoms, brain computed tomography, magnetic resonance imaging, or other imaging examinations; if they had clear consciousness; if they provided informed consent for participation in this study and signed the consent form; and if they had hemiplegic dysfunction. The exclusion criteria were the presence of mental disorders; abnormal coagulation mechanisms; malignant hypertension; malignant tumors; respiratory failure; cognitive dysfunction; severe infection; and limb dysfunction before the occurrence of cerebral infarction.

Treatments

Both groups continued their interventions for 6 mo.

Control group intervention: The control group was given routine nursing and motor imagery therapy. During the treatment, these patients were assisted to perform turning back and patting. They were given cerebral infarction health education, oral care, dietary intervention, daily exercise, and other routine nursing. Combined with the daily exercise content, the patients were verbally guided to imagine a gait using a fixed step, independent step, and lateral step. Dance videos could be played for square dance enthusiasts to guide them in imagining the dance movements and postural changes and feel the comfort of free exercise. Patients were guided to use their imagination through watching videos of walking on the beach, imagining themselves on the beach by touching and listening, walking on the beach, and feeling the comfort of free walking.

Study group intervention: The study group was given hospital–community–family trinity rehabilitation nursing based on the control group. The trinity rehabilitation nursing model included rehabilitation physicians, specialist nurses, community nurses, head nurses, and others. Unified trinity rehabilitation nursing theory training included education on the purpose, significance, and steps of its implementation. We developed a cerebral infarction health education manual, which was composed of the basic knowledge on cerebral infarction, preventive measures, rehabilitation training, home care, basic information on hospital–community–family-related responsible persons (telephone, WeChat), and other contents.

During hospitalization, a self-made cerebral infarction health education manual was distributed to explain the relevant information on cerebral infarction in plain language, emphasize the importance of rehabilitation training, and enhance patients' attention. We conducted one-on-one rehabilitation training, ensuring that rehabilitation training movements were standard and specific. We also played the rehabilitation training-related videos recorded by team members after completion of their training, conducted consolidation exercises, introduced the rehabilitation training effect, and enhance the confidence of patients' rehabilitation exercises. Before discharge, specialist nurses and rehabilitation physicians developed a continuous rehabilitation plan for patients, effectively communicated with the community nurses at discharge, and elaborated the rehabilitation status of patients during hospitalization and the rehabilitation plan after discharge. Community nurses could modify the rehabilitation training plan in real time according to individual circumstances during the rehabilitation training of patients.

Community outpatient sites were constructed. Community nurses were responsible for providing rehabilitation training guidance to patients and, at the same time, visit the patients once a week for follow-up. The follow-up time was controlled at approximately 30 min each time. The psychological status and rehabilitation status of patients were evaluated, and those with negative emotions were guided. Those with non-standard rehabilitation training movements were also corrected, and patients' families were urged to complete the rehabilitation training plan on time. Patients' families were invited to participate in the rehabilitation nursing process. If the implementation of patients' daily rehabilitation exercise plan was recorded, patients were urged to perform rehabilitation exercises actively every day. Rehabilitation exercise videos were distributed. Patients and their families were encouraged to watch these videos repeatedly. Those with non-standard rehabilitation exercise movements were helped to improve performance of their exercises under the guidance of family members and community nurses. Community activities such as patient exchange meetings and expert lectures on cerebral infarction

rehabilitation exercises were conducted once a month, and patients and their families were invited to participate.

Outcome measures

Motor function was evaluated using the Fugl-Meyer Assessment (FMA), while balance ability was assessed using the Berg Balance Scale (BBS). The FMA scale includes 33 upper limb movements and 17 Lower limb movements, with a total score of 0–100 points. Lower scores indicated more severe dyskinesia. The BBS includes 14 items, with a score of 0–4 points for each item and a total score of 0–56 points, where higher scores indicate a stronger balance ability. These scores were compared between the two groups before and after 6 mo of intervention.

Additionally, we compared the activities of daily living using the Barthel Index (BI) as well as the quality of life using the Stroke-Specific Quality of Life scale (SS-QOL) before and after 6 mo of intervention between the two groups. The BI includes 10 items, including dressing, walking on a flat surface, toileting, bathing, and eating. Each item had a score range of 0–10 points and a total score of 0–100 points, with higher scores indicating better ability to conduct activities of daily living. The SS-QOL had a score range of 0–100 points, with higher scores indicating better quality of life.

We compared the activation status of the primary sensorimotor cortical area (SMC) contralateral to the affected side before and after 6 mo of intervention between the two groups. This included assessment of activation frequency and activation volume, in which the activation volume unit is k.

We also compared the satisfaction with nursing between the two groups. The Quality of Service (SERVQUAL) scale was used to assess patients' satisfaction with nursing, including five items: reliability, empathy, responsiveness, assurance, and tangibles. Each item was scored in a range of 1–5 points, with lower scores indicating worse satisfaction with nursing.

Statistical analysis

SPSS v22.0 software (IBM Corp., Armonk, NY, USA) was used to analyze the data. Measurement data were expressed as mean ± SD, t test and enumeration data as n (%). Data were compared using the χ^2 test. $P < 0.05$ indicated statistically significant differences.

RESULTS

Changes in motor function and balance ability

Before intervention, the FMA and BBS scores in the study group were not significantly different from those in the control group (both $P > 0.05$, Table 1). After 6 mo of intervention, the FMA and BBS scores in the study group were higher than those in the control group (both $P < 0.05$), as shown in Table 1.

Changes in activities of daily life and quality of life

The BI and SS-QOL were not significantly different between the study and control groups before intervention (both $P > 0.05$, Table 2). After 6 mo of intervention, the BI and SS-QOL in the study group were higher than those in the control group (both $P < 0.05$, Table 2).

SMC activation state

Prior to the intervention, no significant difference was observed in activation frequency or activation volume between the study and control groups ($P > 0.05$, Table 3). After 6 mo of intervention, the activation frequency and activation volume in the study group were higher than those in the control group ($P < 0.05$, Table 3).

Nursing satisfaction

In the study group, the SERVQUAL scores for the reliability of nursing, empathy, reactivity, assurance, and tangibles were significantly higher than those of the control group (all $P < 0.05$), as shown in Table 4.

DISCUSSION

In this study, we showed that combining a hospital–community–family trinity rehabilitation nursing model and motor imagery therapy enhanced the motor function and balance ability of patients with cerebral infarction, with concomitant changes in the relevant SMC area. This led to improvement in their abilities to conduct activities of daily life as well as in their quality of life and resulted in a higher degree of nursing satisfaction.

Cerebral infarction has a high mortality and disability rate. It can cause neurological deficits after onset, which result in motor, language, and other dysfunctions, to different degrees, which markedly impacts the daily activities and quality of life of patients[11,12]. Promoting the rehabilitation of patients

Table 1 Motor function and balance ability (mean ± SD, points)

Group	FMA		BBS	
	Pre-intervention	After 6 mo of intervention	Pre-intervention	After 6 mo of intervention
Study group (n = 44)	61.58 ± 5.79	78.96 ± 8.44[a]	26.45 ± 4.16	41.89 ± 5.44[a]
Control group (n = 44)	60.87 ± 6.12	70.52 ± 7.68[a]	25.74 ± 5.30	34.62 ± 5.19[a]
t value	0.559	4.906	0.699	6.432
P value	0.578	0.000	0.486	0.000

[a]P < 0.05 *vs* before intervention in the same group. FMA: Fugl–Meyer Assessment, measuring motor function; BBS: Berg Balance Scale, measuring balance ability.

Table 2 Activities of daily living and quality of life (± s, points)

Group	BI		SS-QOL	
	Pre-intervention	After 6 mo of intervention	Pre-intervention	After 6 mo of intervention
Study group (n = 44)	59.86 ± 7.15	78.59 ± 8.33[a]	55.47 ± 6.32	80.17 ± 7.19[a]
Control group (n = 44)	60.82 ± 6.74	70.81 ± 7.52[a]	56.22 ± 5.67	72.18 ± 8.50[a]
t value	0.648	4.599	0.586	4.761
P value	0.519	0.000	0.560	0.000

[a]P < 0.05 *vs* before intervention in the same group. BI: Barthel's index, measuring activities of daily living; SS-QOL: Stroke-Specific Quality of Life, measuring quality of life.

Table 3 Sensorimotor cortical area activation status

Group	Activation frequency, n (%)		Activation Volume (k), (mean ± SD)	
	Pre-intervention	After 6 mo of intervention	Pre-intervention	After 6 mo of intervention
Study group (n = 44)	11 (25.00)	40 (90.91)[a]	105.39 ± 34.51	185.48 ± 44.63[a]
Control group (n = 44)	12 (27.27)	29 (65.91)[a]	108.91 ± 36.44	149.60 ± 42.75[a]
χ^2/t value	0.059	8.122	0.465	3.851
P value	0.808	0.004	0.643	0.000

[a]P < 0.05 *vs* before intervention in the same group.

Table 4 Satisfaction with nursing care

Group	Reliability	Empathy	Reactivity	Assurance	Tangibility
Study group (n = 44)	4.15 ± 0.39	4.26 ± 0.31	4.55 ± 0.20	4.37 ± 0.25	4.18 ± 0.37
Control group (n = 44)	3.80 ± 0.41	3.75 ± 0.43	4.12 ± 0.29	3.81 ± 0.37	3.65 ± 0.49
t value	4.103	6.382	8.097	8.319	5.726
P value	< 0.001	< 0.001	< 0.001	< 0.001	< 0.001

with cerebral infarction has become a crucial topic among clinicians and researchers worldwide. Patients and their families anticipate a scientific and practical rehabilitation nursing model that can reduce the disability rate of stroke and improve the self-care ability of these patients[13-15].

Previous studies have shown that motor imagery therapy can enhance compensatory function at the site of brain injury, activate the central nervous system in specific regions, increase blood flow in functional areas of the brain, promote neurotransmitter release, and reduce limb motor dysfunction[16, 17]. With the development of rehabilitation medicine, rehabilitation nursing has emerged as a discipline

that combines modern rehabilitation concepts with early nursing to promote the maximum functional recovery of patients[18]. The hospital–community–family trinity rehabilitation nursing model provides continuous and comprehensive nursing services for patients, which can significantly eliminate adverse factors of rehabilitation and improve the quality of nursing care[19,20]. In this study, we endeavored to apply the hospital–community–family trinity rehabilitation nursing model in combination with motor imagery therapy in patients with cerebral infarction. After 6 mo of intervention, the FMA and BBS scores in the study group were significantly higher than those in the control group ($P < 0.05$), indicating that the above nursing model could improve the motor function and balance ability of patients with cerebral infarction. This may be because the hospital–community–family trinity rehabilitation nursing model not only imparts cerebral infarction knowledge and functional exercise training to patients during hospitalization but also handles patients *via* community nurses after their discharge from the hospital. Patients' families are invited to participate in the rehabilitation nursing process. Patients receive continuous rehabilitation nursing guidance and supervision, which can improve their motor function and balance ability and promote their rehabilitation.

Moreover, after 6 mo of intervention, the activation frequency and activation volume in the study group were higher than those in the control group ($P < 0.05$), suggesting that the use of a combination of the hospital–community–family trinity rehabilitation nursing model and motor imagery therapy in patients with cerebral infarction enhances the patients' rehabilitation. In this study, repeated drills of motor scenarios in the brain by means of motor imagery therapy could induce the brain to control the trunk muscle groups on the affected side, activate dormant synapses, and enhance compensation for the brain injury site.

Consequently, combined application of hospital–community–family trinity rehabilitation nursing model and motor imagery therapy helped patients obtain continuous and complete professional guidance and care after discharge, correct inaccurate rehabilitation exercise behavior, improve the effect of rehabilitation exercise, and promote the rehabilitation of patients.

After 6 mo of intervention, the BI and SS-QOL scores in the study group were higher than those in the control group ($P < 0.05$), which showed that the application of this combined rehabilitation and therapy in patients with cerebral infarction could significantly improve the ability to conduct activities of daily as well as the quality of life of patients. In addition, we compared the nursing satisfaction of the two groups and found that the reliability, empathy, reactivity, assurance, and tangible scores of the study group were higher than those of the control group ($P < 0.05$). This suggests that the hospital-community-family trinity rehabilitation nursing model combined with motor imagery therapy is suitable for clinical application in patients with cerebral infarction.

The study was limited by the short observation time. Thus, the effect of the above intervention program on the long-term prognosis of patients with cerebral infarction needs to be explored further and confirmed by prolonging the follow-up time.

CONCLUSION

In summary, the application of a combination of the hospital–community–family trinity rehabilitation nursing model with motor imagery therapy in patients with cerebral infarction can improve the motor function and balance ability of patients, cause corresponding changes in the SMC area on the affected side, improving their abilities to conduct the activities of daily life and quality of life of patients, and resulting in a high degree of patient satisfaction with nursing care. In addition, based on the hospital–community–family trinity rehabilitation nursing model, nursing staff are required to ensure close linkage between hospitals, communities, and patients' families and provide continuous and complete professional care to patients.

ARTICLE HIGHLIGHTS

Research background

Cerebral infarction is a common clinical cerebrovascular disease.

Research motivation

Rehabilitation treatment of patients with cerebral infarction has gradually attracted widespread clinical attention.

Research objectives

This study aimed to explored the application value of a combination of the hospital–community–family trinity rehabilitation nursing model and motor imagery therapy in patients with cerebral infarction.

Research methods
Eighty-eight patients with cerebral infarction who attended our hospital.

Research results
After 6 mo' intervention, the activation frequency and volume were higher in the study than in the control group.

Research conclusions
Combining a hospital–community–family trinity rehabilitation nursing model and motor imagery therapy enhances the motor function and balance ability of patients with cerebral infarction, improving their quality of life.

Research perspectives
The effect of the above intervention program on the long-term prognosis of patients with cerebral infarction needs to be explored further and confirmed by prolonging the follow-up time.

FOOTNOTES

Author contributions: Li WW and Liu FD designed the research study; Li WW performed the research; Li M contributed new reagents and analytic tools; Guo XJ analyzed the data and wrote the manuscript; and all authors have read and approve the final manuscript.

Supported by the Key Research and Development Programs of Shaanxi Province, No. 2021SF-059.

Institutional review board statement: The study was reviewed and approved by The First Affiliated Hospital of Xi'an Jiaotong University School of Medicine Institutional Review Board (Approval No. XJTU1AF2021LSK-454).

Informed consent statement: All study participants provided informed written consent prior to study enrollment.

Conflict-of-interest statement: No conflict of interest.

Data sharing statement: No additional data are available.

STROBE statement: The authors have read the STROBE statement checklist of items, and the manuscript was prepared and revised according to the STROBE statement checklist of items.

Country/Territory of origin: China

ORCID number: Wen-Wen Li 0000-0002-1902-1843; Min Li 0000-0003-1142-6739; Xiao-Juan Guo 0000-0002-1398-290X; Fu-De Liu 0000-0001-9803-5225.

S-Editor: Wang JL
L-Editor: A
P-Editor: Wang JL

REFERENCES

1 **Zhen C**, Wang Y, Wang H, Li D, Wang X. Multiple cerebral infarction linked to underlying cancer: a review of Trousseau syndrome-related cerebral infarction. *Br J Hosp Med (Lond)* 2021; **82**: 1-7 [PMID: 34076507 DOI: 10.12968/hmed.2020.0696]
2 **Okuda Y**, Aoike F. Functional recovery of patients with intracerebral haemorrhage and cerebral infarction after rehabilitation. *Int J Rehabil Res* 2021; **44**: 222-225 [PMID: 34034286 DOI: 10.1097/MRR.0000000000000476]
3 **Fu J**, Zeng M, Shen F, Cui Y, Zhu M, Gu X, Sun Y. Effects of action observation therapy on upper extremity function, daily activities and motion evoked potential in cerebral infarction patients. *Medicine (Baltimore)* 2017; **96**: e8080 [PMID: 29049194 DOI: 10.1097/MD.0000000000008080]
4 **Li MH**, Lu H, Du YH, Lu LX, Meng ZH. [Acupotomy combined with Xingnao Kaiqiao acupuncture therapy in treatment of sensory impairment in the recovery stage of cerebral infarction: a randomized controlled trial]. *Zhongguo Zhen Jiu* 2021;

41: 9-12 [PMID: 33559434 DOI: 10.13703/j.0255-2930.20200107-0002]

5 **Chang MC**, Park SW, Lee BJ, Park D. Relationship between recovery of motor function and neuropsychological functioning in cerebral infarction patients: the importance of social functioning in motor recovery. *J Integr Neurosci* 2020; **19**: 405-411 [PMID: 33070518 DOI: 10.31083/j.jin.2020.03.175]

6 **Morishita S**, Hokamura K, Yoshikawa A, Agata N, Tsutsui Y, Umemura K, Kumada T. Different exercises can modulate the differentiation/maturation of neural stem/progenitor cells after photochemically induced focal cerebral infarction. *Brain Behav* 2020; **10**: e01535 [PMID: 31989796 DOI: 10.1002/brb3.1535]

7 **Morioka S**, Osumi M, Nishi Y, Ishigaki T, Ishibashi R, Sakauchi T, Takamura Y, Nobusako S. Motor-imagery ability and function of hemiplegic upper limb in stroke patients. *Ann Clin Transl Neurol* 2019; **6**: 596-604 [PMID: 30911582 DOI: 10.1002/acn3.739]

8 **Chen L**, Han Z, Gu J. Early Path Nursing on Neurological Function Recovery of Cerebral Infarction. *Transl Neurosci* 2019; **10**: 160-163 [PMID: 31637046 DOI: 10.1515/tnsci-2019-0028]

9 **Cao D**, Chu N, Yu H, Sun M. Role of comprehensive nursing care in improving the prognosis and mood of patients with secondary cerebral infarction after craniocerebral injury. *Am J Transl Res* 2021; **13**: 7342-7348 [PMID: 34306503]

10 **Frakking T**, Michaels S, Orbell-Smith J, Le Ray L. Framework for patient, family-centred care within an Australian Community Hospital: development and description. *BMJ Open Qual* 2020; **9** [PMID: 32354755 DOI: 10.1136/bmjoq-2019-000823]

11 **An X**, Zeng L, Shen L, Jiang Y. Influences of a hierarchical nursing model on rescue outcomes and nursing quality of patients with acute cerebral infarction. *Am J Transl Res* 2021; **13**: 6498-6506 [PMID: 34306390]

12 **Liao Y**, Ye T, Liang S, Xu X, Fan Y, Ruan X, Wu M. Clinical nursing pathway improves disease cognition and quality of life of elderly patients with hypertension and cerebral infarction. *Am J Transl Res* 2021; **13**: 10656-10662 [PMID: 34650739]

13 **Jiang X**, Gu Q, Jiang Z, Liao X, Zou Q, Li J, Gan K. Effect of family-centered nursing based on timing it right framework in patients with acute cerebral infarction. *Am J Transl Res* 2021; **13**: 3147-3155 [PMID: 34017483]

14 **Li Z**, Shang N, Fan G, Li M, Zang Z. Effect of nursing based on the hopeless self-esteem theory plus multi-dimensional intensive nursing for elderly patients with acute cerebral infarction complicated with depression. *Am J Transl Res* 2021; **13**: 8450-8457 [PMID: 34377342]

15 **Liu Y**, Qu M, Wang N, Wang L. Effects of an evidence-based nursing intervention on neurological function and serum inflammatory cytokines in patients with acute cerebral infarction: A randomized controlled trial. *Restor Neurol Neurosci* 2021; **39**: 129-137 [PMID: 33935121 DOI: 10.3233/RNN-201080]

16 **Ji EK**, Wang HH, Jung SJ, Lee KB, Kim JS, Jo L, Hong BY, Lim SH. Graded motor imagery training as a home exercise program for upper limb motor function in patients with chronic stroke: A randomized controlled trial. *Medicine (Baltimore)* 2021; **100**: e24351 [PMID: 33546067 DOI: 10.1097/MD.0000000000024351]

17 **Fernandez-Gomez E**, Sanchez-Cabeza A. [Motor imagery: a systematic review of its effectiveness in the rehabilitation of the upper limb following a stroke]. *Rev Neurol* 2018; **66**: 137-146 [PMID: 29480509]

18 **Guerra ZF**, Lucchetti ALG, Lucchetti G. Motor Imagery Training After Stroke: A Systematic Review and Meta-analysis of Randomized Controlled Trials. *J Neurol Phys Ther* 2017; **41**: 205-214 [PMID: 28922311 DOI: 10.1097/NPT.0000000000000200]

19 **Lawler K**, Taylor NF, Shields N. Family-assisted therapy empowered families of older people transitioning from hospital to the community: a qualitative study. *J Physiother* 2019; **65**: 166-171 [PMID: 31204293 DOI: 10.1016/j.jphys.2019.05.009]

20 **Warkentin N**, Wilfling D, Laag S, Goetz K. Experiences of family caregivers regarding a community-based care- and case-management intervention. A qualitative study. *Health Soc Care Community* 2022; **30**: e204-e212 [PMID: 33978280 DOI: 10.1111/hsc.13430]

World Journal of Clinical Cases

Submit a Manuscript: https://www.f6publishing.com

World J Clin Cases 2023 January 26; 11(3): 629-634

DOI: 10.12998/wjcc.v11.i3.629

ISSN 2307-8960 (online)

CASE REPORT

Congenital biliary atresia caused by *GPC1* gene mutation in Chinese siblings: A case report

Yuan-Mei Kong, Ke Yuan, Chun-Lin Wang

Specialty type: Gastroenterology and hepatology

Provenance and peer review: Unsolicited article; Externally peer reviewed.

Peer-review model: Single blind

Peer-review report's scientific quality classification

Grade A (Excellent): 0
Grade B (Very good): 0
Grade C (Good): C
Grade D (Fair): D
Grade E (Poor): 0

P-Reviewer: Gupta MK, Germany; Obando A, Nicaragua

Received: July 18, 2022
Peer-review started: July 18, 2022
First decision: October 17, 2022
Revised: October 21, 2022
Accepted: December 9, 2022
Article in press: December 9, 2022
Published online: January 26, 2023

Yuan-Mei Kong, Ke Yuan, Chun-Lin Wang, Department of Pediatrics, The First Affiliated Hospital of Zhejiang University, Hangzhou 310003, Zhejiang Province, China

Corresponding author: Chun-Lin Wang, PhD, Chief Doctor, Department of Pediatrics, The First Affiliated Hospital of Zhejiang University, No. 79 Qingchun Road, Hangzhou 310003, Zhejiang Province, China. hzwangcl@zju.edu.cn

Abstract

BACKGROUND

Congenital biliary atresia (CBA) is a serious hepatobiliary disease in children with unknown etiology. Its outcome is often liver transplantation or death. Clarifying the etiology of CBA is of great significance for prognosis, treatment, and genetic counseling.

CASE SUMMARY

A male Chinese infant at an age of 6 mo and 24 d was hospitalized because of "yellow skin for more than 6 mo". Soon after birth, the patient developed jaundice, which then progressively intensified. A "laparoscopic exploration" indicated "biliary atresia". After coming to our hospital, genetic testing suggested a *GPC1* mutation [loss 1 (exons 6-7)]. The patient recovered and was discharged after living donor liver transplantation. After discharge, the patient was followed up. The condition was controlled by oral drugs, and the patient's condition was stable.

CONCLUSION

CBA is a complex disease with a complex etiology. Clarifying the etiology is of great clinical importance for treatment and prognosis. This case reports CBA caused by a *GPC1* mutation, which enriches the genetic etiology of biliary atresia. However, its specific mechanism needs to be confirmed by further research.

Key Words: Congenital biliary atresia; Jaundice; Etiology; *GPC1*; Liver transplantation; Case report

Core tip: Congenital biliary atresia (CBA) often results in a poor prognosis. Most patients need liver transplantation as the final treatment. If the opportunity for liver transplantation is missed, death often occurs. However, the etiology of CBA is still unclear. Clarifying the etiology is of great significance for prognosis, treatment, and genetic counseling. Through the report of a patient with a *GPC1* mutation, this paper enriches the genetic etiology of CBA and provides a new basis for clinical and scientific research.

Citation: Kong YM, Yuan K, Wang CL. Congenital biliary atresia caused by *GPC1* gene mutation in Chinese siblings: A case report. *World J Clin Cases* 2023; 11(3): 629-634
URL: https://www.wjgnet.com/2307-8960/full/v11/i3/629.htm
DOI: https://dx.doi.org/10.12998/wjcc.v11.i3.629

INTRODUCTION

Congenital biliary atresia (CBA) is a congenital disease that occurs in infants and young children. Due to the atresia of intrahepatic and extrahepatic bile ducts, the discharge of conjugated bilirubin into the intestine is blocked. This causes inflammation of intrahepatic and extrahepatic bile ducts, resulting in cholestatic cirrhosis. This condition is usually called CBA. The incidence rate of this disease is different in different countries and regions. The incidence rate in Europe is 1/15000-1/19000, and the incidence rate in Japan is 1/9000-1/10000[1]. However, the cause of CBA is not clear. At present, there are many hypotheses, including viral infection (cytomegalovirus, reovirus, rotavirus, human papillomavirus, retrovirus, *etc*.), immune and/or autoimmune injury[2,3], gene-related factors (inversion and *MDR3*[2], *EFEMP1*[4]), abnormal bile duct development, microchimerism, cytokines, miRNA gene expression abnormalities, and biliary malformation[5,6]. In addition, its incidence rate also differs by race, geography, season, and other factors[7]. The main clinical manifestations include the following: (1) Jaundice, which is usually gradually exposed 2-3 wk after birth; and (2) the color of stool becomes lighter, and white pottery-like stool and, is very common in the clinical findings (also it can be just: acholia). The surgical management is the actual approach and it is a by hilar jejunal Roux-Y anastomosis (Kasai operation) within 3 mo after birth. However, the 5-year survival rate of this treatment is low, at approximately 30%-50%[8,9]. Liver transplantation is proposed when the Kassai operation fails to retain the hope of continued survival (as a suggestion you can give the survival rate with transplantation. Clarifying the etiology of CBA have great significance for its treatment and prognosis.

CASE PRESENTATION

Chief complaints

The patient came to our outpatient clinic because of "yellow skin and sclera staining for more than 6 mo".

History of present illness

Soon after birth, there was no obvious incentive for the child to have yellow skin and sclera staining, which gradually intensified. This yellowing was accompanied by a white stool color, but no other discomfort was reported. After many phototherapies at the local hospital, the conditions did not improve, and the yellow skin and sclera staining showed progressive aggravation. Then, the patient went to the local hospital and underwent "laparoscopic exploration suggestive of biliary atresia" (family members complained privately, and no report was found). Later, the family members did not allow further diagnoses and treatments. After discharge, oral symptomatic Chinese patent medicine was administered, but the above symptoms were not relieved. The patient was then admitted to the hospital with "bile duct atresia" for living donor liver transplantation.

History of past illness

Previous "history of laparoscopic surgery".

History of family past illness

The patient's father and mother were in good health. The patient had a sister who had a history of "biliary atresia" and underwent "liver transplantation" at an age of more than 6 mo. This sister died at an age of more than 2 years.

Physical examination

Physical examination results were as follows: T 37°C, P 134 bpm, BP 95/52 mmHg, a clear mind, fair spirit, soft neck, yellow skin and sclera, thick respiratory sounds of both lungs, no dry and wet rales, uniform heart rhythm, no obvious pathological murmur in heart sound, abdominal distention, abdominal circumference of 44 cm, no exposure of abdominal wall vein, touch approximately 7 cm under liver rib, hard texture, blunt edge, 6 cm under spleen rib, negative neurological examination, and limb temperature.

Laboratory examinations

The blood examination on December 18, 2019 results were as follows: Leukocyte count 20.0 × 10^9/L, neutrophils (%) 41.1%, lymphocytes (%) 49.6%, red blood cell 3.08 × 10^{12}/L, hemoglobin 99 g/L, and platelet count 234 × 10^9/L. On December 18, 2019, the plasma D-dimer determination was 4597 μg/L FEU. Examination of coagulation function on December 18, 2019 was as follows: International standardized ratio 2.36, fibrinogen 0.50 g/L, activated partial thromboplastin time 90.5 seconds, thrombin time 26.6 s, and prothrombin time 27.4 s. On December 18, 2019, the liver examination and kidney lipid glucose electrolyte determination were as follows: total protein 78.4 g/L, albumin 59.3 g/L, globulin 19.1 g/L, white globulin ratio 3.1, alanine aminotransferase 16U/L, aspartate aminotransferase 53U/L, total bile acid 522.7 μmol/L, total bilirubin 347.6 μmol/L, direct bilirubin 222.5 μmol/L, indirect bilirubin 125.1 μmol/L, glomerular filtration rate (EPI-cr) 285.95 ml/min, creatinine 14 μmol/L, uric acid 88 μmol/L, total cholesterol 0.93 mmol/L, high-density lipoprotein-c 0.25 mmol/L, low-density lipoprotein-c 0.09 mmol/L, fasting blood glucose 3.54 mmol/L, and potassium 4.86 mmol/L.

Imaging examinations

Full abdominal computed tomography showed that the intrahepatic bile duct and common bile duct were dilated. It also showed signs of exudation around the portal vein and an unclear display of the gallbladder. Thus, effusion of gallbladder fossa and peritoneal effusion were considered. Imaging also showed a patch shadow of the left lower lobe, bilateral pleural effusion, and bilateral hip soft tissue swelling. The biopsy results showed biliary stasis and hepatic cirrhosis (Figure 1).

FINAL DIAGNOSIS

The diagnosis was CBA and cholestatic hepatitis.

TREATMENT

On January 7, 2020, "reduced volume liver transplantation" was performed under general anesthesia. After the operation, meropenem was administered to fight infection, ganciclovir was administered for virus infection prevention, liver protection, and phlegm removal, tacrolimus was administered to fight rejection, and albumin and human immunoglobulin were supplemented. The patient's condition improved. On January 31, 2020, the color Doppler ultrasound of the portal vein system of the transplanted liver (color Doppler ultrasound) revealed that the blood circulation of the transplanted liver was satisfactory, and there was a small amount of effusion near the cutting edge of the liver. On January 31, 2020, the serum drug concentration of FK506 was 8.1 ng/mL. Blood coagulation function was checked, and the international standardized ratio was 2.24. On January 21, 2020, the blood biochemical test results were as follows: Alanine aminotransferase 17 U/L, aspartate aminotransferase 19 U/L, total bilirubin 8.0 μmol/L, and glutamyl transphthalase 77 U/L. The patient recovered, the liver function was stable, and the antirejection drugs and coagulation function reached the standards. On January 10, 2020, whole liver + cholecystectomy specimens were submitted for examination. The liver surface was fine granular, the section was gray-red and gray-yellow, and diffuse fine granular. Microscopically, the structure of normal liver lobules was damaged, hepatocytes and small bile ducts were silted, small bile ducts in the portal area were proliferated, inflammatory cells were infiltrated, pseudolobules of liver tissue were formed, and cholestatic cirrhosis was changed. The first hilar lymph node was reactive hyperplasia. The bile duct indicated chronic cholecystitis. In conclusion, the findings in the total liver and cholecystectomy specimens are consistent with a diagnosis of cholestatic cirrhosis with CBA and chronic cholecystitis.

OUTCOME AND FOLLOW-UP

The patient was discharged after being in a stable condition. Follow-ups occurred regularly in the outpatient department of the liver transplantation department, and the patient took long-term oral

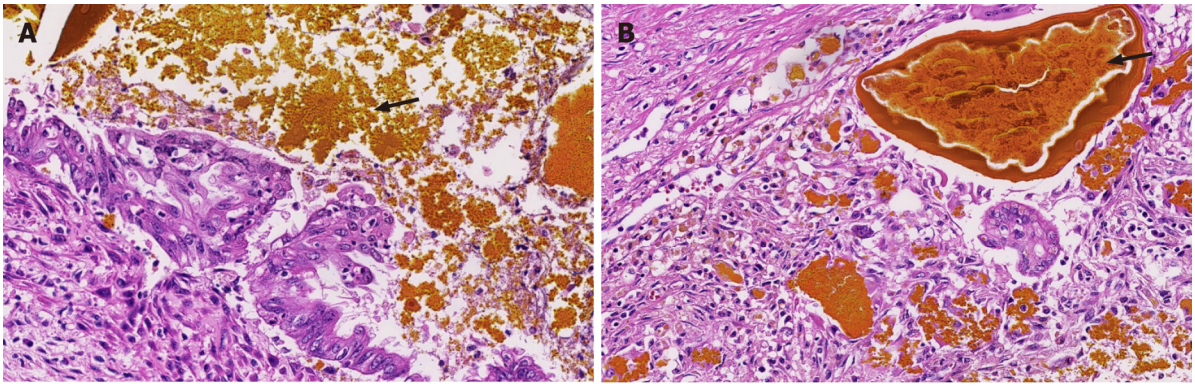

DOI: 10.12998/wjcc.v11.i3.629

Figure 1 The biopsy results showed biliary stasis and hepatic cirrhosis. A: Hematoxylin staining of hepatic tissue; B: Eosin staining of hepatic tissue. Hematoxylin and eosin staining showed biliary stasis and hepatic cirrhosis.

drugs to control the condition after transplantation. At present, there is no obvious yellowing of the skin, the color of stool is normal, the abdominal circumference is significantly reduced, and the functional evaluation of the transplanted liver is basically within the normal range.

DISCUSSION

At present, there is no clear understanding of the etiology of CBA. Clinical scholars have put forward many independent and interrelated hypotheses that mainly focus on the following aspects.

The first aspect is congenital dysplasia. The developmental abnormality hypothesis is mainly aimed at CBA with other organ malformations. It is generally believed that biliary tract lesions begin at 5-6 wk of pregnancy, rather than during the development of the intrahepatic bile duct (7-10 wk of pregnancy). The differentiation and morphogenesis of embryonic cells are key factors of organ development[10]. The most important factor is gene mutations. For example, the inversion mutations in *MDR3*[2], *EFEMP1*[4], and *GPC1* reported in this paper may lead to the production of CBA through corresponding signaling pathways. In addition, in animal experiments of miRNAs, zebrafish lacking miR-30a have abnormal bile duct development. This indicates that genetic factors contribute to the etiology of CBA.

The second aspect is the study of autoimmune-related microchimeras. Kasai hilar jejunostomy after birth in children with CBA can effectively alleviate the development of this disease. However, even if the bile drainage is unobstructed, the process of liver fibrosis does not stop, and histologically, the CBA intrahepatic bile duct is very similar to sclerosing cholangitis, graft-versus-host disease, and other immune diseases. Therefore, some scholars regard CBA as an autoimmune disease. There is also some theoretical and research support for the influence of maternal microchimeras and the second strike theory. In addition, studies have confirmed that there is a large amount of C4d deposition in portal vein blood endothelium[11], indicating that liver fibrosis and portal hypertension in the later stage of CBA are autoimmune reactions that participate in cellular and humoral immunity. Third, the immune imbalance caused by infection may also be an important cause of CBA. Since Benjamin first attributed CBA to viral infection in the liver and biliary system, the mechanism of viral infection immune imbalance has gradually become a hot spot in the etiology of CBA. From the initial discovery of a large amount of monocyte infiltration in the vascular and bile duct endothelium of the hilar region to the establishment of animal models and immune response research, an increasing number of results support this view. The most studied factor is virus infection. At present, research on external infection sources mainly focuses on respiratory enterovirus, cytomegalovirus, and rotavirus[12]. In addition, increasing attention has been given to specific immunity and natural immunity[13]. The presence of bile duct-specific autoantibodies was found in a mouse model infected with rotavirus[14], which also provides a new idea for the exploration of the etiology of CBA.

According to the current paper data, CBA is a serious disease with multiple etiologies and phenotypes, and the etiologies of different types are different. Multiple hypotheses are independent and interdependent and need to be carefully identified in further clinical practice.

CONCLUSION

CBA is a serious childhood disease with a difficult etiology and poor prognosis. *GPC1* mutations are one of the important causes of CBA. Clarifying the etiology of CBA is of great importance for its early

diagnosis and prognosis. It is also of great importance to popularize prenatal gene diagnoses in high-risk groups.

ACKNOWLEDGEMENTS

The authors would like to thank the patient's family for agreeing to participate in this research.

FOOTNOTES

Author contributions: Kong YM and Wang CL conceived and designed the study; Kong YM provided clinical research; Kong YM wrote the paper; Kong YM, and Yuan K reviewed and edited the manuscript; All authors read and approved the manuscript.

Informed consent statement: All study participants, or their legal guardian, provided informed written consent prior to study enrollment.

Conflict-of-interest statement: All the authors declare that they have no competing interests.

CARE Checklist (2016) statement: The authors have read the CARE Checklist (2016), and the manuscript was prepared and revised according to the CARE Checklist (2016).

Country/Territory of origin: China

ORCID number: Yuan-Mei Kong 0000-0002-3250-1892; Ke Yuan 0000-0002-0458-3683; Chun-Lin Wang 0000-0002-4273-1341.

S-Editor: Liu JH
L-Editor: A
P-Editor: Liu JH

REFERENCES

1 **Nakamura K**, Tanoue A. Etiology of biliary atresia as a developmental anomaly: recent advances. *J Hepatobiliary Pancreat Sci* 2013; **20**: 459-464 [PMID: 23567964 DOI: 10.1007/s00534-013-0604-4]
2 **Danial E**, Fleck-Derderian S, Rosenthal P. Has Rotavirus Vaccination Decreased the Prevalence of Biliary Atresia? *J Clin Gastroenterol* 2019; **53**: e348-e351 [PMID: 30222646 DOI: 10.1097/MCG.0000000000001121]
3 **Bednarek J**, Traxinger B, Brigham D, Roach J, Orlicky D, Wang D, Pelanda R, Mack CL. Cytokine-Producing B Cells Promote Immune-Mediated Bile Duct Injury in Murine Biliary Atresia. *Hepatology* 2018; **68**: 1890-1904 [PMID: 29679373 DOI: 10.1002/hep.30051]
4 **Chen Y**, Gilbert MA, Grochowski CM, McEldrew D, Llewellyn J, Waisbourd-Zinman O, Hakonarson H, Bailey-Wilson JE, Russo P, Wells RG, Loomes KM, Spinner NB, Devoto M. A genome-wide association study identifies a susceptibility locus for biliary atresia on 2p16.1 within the gene EFEMP1. *PLoS Genet* 2018; **14**: e1007532 [PMID: 30102696 DOI: 10.1371/journal.pgen.1007532]
5 **Fabris L**, Cadamuro M, Guido M, Spirli C, Fiorotto R, Colledan M, Torre G, Alberti D, Sonzogni A, Okolicsanyi L, Strazzabosco M. Analysis of liver repair mechanisms in Alagille syndrome and biliary atresia reveals a role for notch signaling. *Am J Pathol* 2007; **171**: 641-653 [PMID: 17600123 DOI: 10.2353/ajpath.2007.070073]
6 **Wang JY**, Cheng H, Zhang HY, Ye YQ, Feng Q, Chen ZM, Zheng YL, Wu ZG, Wang B, Yao J. Suppressing microRNA-29c promotes biliary atresia-related fibrosis by targeting DNMT3A and DNMT3B. *Cell Mol Biol Lett* 2019; **24**: 10 [PMID: 30906331 DOI: 10.1186/s11658-018-0134-9]
7 **Muraji T**, Tanaka H, Ieiri S. Ethnic variation in the incidence of biliary atresia correlates with the frequency of the most prevalent haplotype in its population. *Hum Immunol* 2018; **79**: 668-671 [PMID: 30006139 DOI: 10.1016/j.humimm.2018.07.001]
8 **Qisthi SA**, Saragih DSP, Sutowo DW, Sirait DN, Imelda P, Kencana SMS, Makhmudi A, Gunadi. Prognostic Factors for Survival of Patients with Biliary Atresia Following Kasai Surgery. *Kobe J Med Sci* 2020; **66**: E56-E60 [PMID: 33024065]
9 **Shetty NS**, Shah I. Incomplete Kawasaki Disease in an Infant with Cholangitis Post Kasai Surgery for Biliary Atresia. *Ann Hepatol* 2018; **17**: 332-334 [PMID: 29469036 DOI: 10.5604/01.3001.0010.8665]
10 **Keplinger KM**, Bloomston M. Anatomy and embryology of the biliary tract. *Surg Clin North Am* 2014; **94**: 203-217

[PMID: 24679417 DOI: 10.1016/j.suc.2014.01.001]

11 **Muraji T**. Maternal microchimerism in biliary atresia: are maternal cells effector cells, targets, or just bystanders? *Chimerism* 2014; **5**: 1-5 [PMID: 24670921 DOI: 10.4161/chim.28576]

12 **Oetzmann von Sochaczewski C**, Pintelon I, Brouns I, Dreier A, Klemann C, Timmermans JP, Petersen C, Kuebler JF. Rotavirus particles in the extrahepatic bile duct in experimental biliary atresia. *J Pediatr Surg* 2014; **49**: 520-524 [PMID: 24726104 DOI: 10.1016/j.jpedsurg.2013.09.064]

13 **Hadchouel M**, Hugon RN, Odievre M. Immunoglobulin deposits in the biliary remnants of extrahepatic biliary atresia: a study by immunoperoxidase staining in 128 infants. *Histopathology* 1981; **5**: 217-221 [PMID: 7216182 DOI: 10.1111/j.1365-2559.1981.tb01779.x]

14 **Mack CL**, Tucker RM, Lu BR, Sokol RJ, Fontenot AP, Ueno Y, Gill RG. Cellular and humoral autoimmunity directed at bile duct epithelia in murine biliary atresia. *Hepatology* 2006; **44**: 1231-1239 [PMID: 17058262 DOI: 10.1002/hep.21366]

World Journal of Clinical Cases

Submit a Manuscript: https://www.f6publishing.com

World J Clin Cases 2023 January 26; 11(3): 635-644

DOI: 10.12998/wjcc.v11.i3.635

ISSN 2307-8960 (online)

CASE REPORT

Rescuing "hopeless" avulsed teeth using autologous platelet-rich fibrin following delayed reimplantation: Two case reports

Yang Yang, Yan-Li Liu, Lie-Ni Jia, Jun-Jun Wang, Min Zhang

Specialty type: Medicine, research and experimental

Provenance and peer review: Unsolicited article; Externally peer reviewed.

Peer-review model: Single blind

Peer-review report's scientific quality classification

Grade A (Excellent): A
Grade B (Very good): B, B, B
Grade C (Good): C, C
Grade D (Fair): 0
Grade E (Poor): 0

P-Reviewer: Arumugam EAP, India; Capparè P, Italy; Ghaffar KA, Egypt; Heboyan A, Armenia; Sekhar P, India; Simbila AN, Tanzania

Received: August 25, 2022
Peer-review started: August 25, 2022
First decision: November 22, 2022
Revised: December 10, 2022
Accepted: January 9, 2023
Article in press: January 9, 2023
Published online: January 26, 2023

Yang Yang, Yan-Li Liu, Lie-Ni Jia, Jun-Jun Wang, Min Zhang, State Key Laboratory of Military Stomatology & National Clinical Research Center for Oral Diseases & Shaanxi International Joint Research Center for Oral Diseases, Department of General Dentistry and Emergency, School of Stomatology, Fourth Military Medical University, Xi'an 710032, Shaanxi Province, China

Corresponding author: Min Zhang, MD, PhD, Professor, State Key Laboratory of Military Stomatology & National Clinical Research Center for Oral Diseases, Department of General Dentistry and Emergency, School of Stomatology, Fourth Military Medical University, No. 145 Changle West Road, Xincheng District, Xi'an 710032, Shaanxi Province, China.
zhangmin@fmmu.edu.cn

Abstract

BACKGROUND

Tooth avulsion is one of the most severe types of dental trauma. Most avulsed teeth undergo long-term ankylosis and replacement resorption after delayed reimplantation and exhibit a poor prognosis. The aim of this work was to improve the success rate of avulsed teeth after delayed reimplantation using autologous platelet-rich fibrin (PRF).

CASE SUMMARY

Case 1 was a 14-year-old boy who fell and knocked out his left upper central incisor 18 h prior to his arrival at the department. The diagnoses were avulsion of tooth 21, lateral luxation of tooth 11 and alveolar fracture of teeth 11 and 21. In case 2, a 17-year-old boy fell 2 h prior to his presentation to the hospital, and his left upper lateral incisor was completely knocked out of the alveolar socket. The diagnoses included avulsion of tooth 22, complicated crown fracture of tooth 11 and complicated crown-root fracture of tooth 21. The avulsed teeth were reimplanted along with autologous PRF granules and splinted using a semiflexible titanium preshaped labial arch. The root canals of the avulsed teeth were filled with calcium hydroxide paste, and root canal filling was performed 4 wk after reimplantation. The reimplanted teeth showed no symptoms of inflammatory root resorption or ankylosis at the 3-, 6-, and 12-mo follow-up examinations after reimplantation with autologous PRF. In addition to the avulsed teeth, the other injured teeth were treated using corresponding conventional treatment methods.

CONCLUSION

These cases provide examples of the successful use of PRF to reduce pathological

root resorption of the avulsed teeth, and the application of PRF may provide new healing opportunities for traditionally "hopeless" avulsed teeth.

Key Words: Avulsion; Periodontal healing; Platelet-rich fibrin; Ankylosis; Delayed reimplantation; Case report

Core Tip: Tooth avulsion is one of the most severe types of dental trauma. Most avulsed teeth will undergo ankylosis and replacement resorption after delayed reimplantation and generally experience a poor prognosis. We previously demonstrated that autologous platelet-rich fibrin (PRF) could effectively help to control the occurrence and development of initial root resorption. In this report, we presented two clinical cases of avulsed teeth with delayed reimplantation that were treated with autologous PRF. Ideal periodontal healing over 12 mo of follow-up suggested that PRF, as an adjuvant therapy, may provide new insights and perspectives on the management of traditionally hopeless avulsed teeth.

Citation: Yang Y, Liu YL, Jia LN, Wang JJ, Zhang M. Rescuing "hopeless" avulsed teeth using autologous platelet-rich fibrin following delayed reimplantation: Two case reports. *World J Clin Cases* 2023; 11(3): 635-644
URL: https://www.wjgnet.com/2307-8960/full/v11/i3/635.htm
DOI: https://dx.doi.org/10.12998/wjcc.v11.i3.635

INTRODUCTION

Tooth avulsion is defined as a complete displacement of the tooth from its original alveolar socket and is one of the most severe types of dental trauma. Permanent tooth avulsion accounts for 0.5%-3.0% of dental trauma, whereas some studies report an incidence as high as 16.0%[1,2]. A recent study from China showed that 8.0% of all dental injuries were tooth avulsion; these injuries are more likely to occur in individuals 7-20-years-old and generally occur more often in males than females[3]. The prognosis depends on the measures taken at the site of the accident, such as immediate replantation of avulsed teeth, the use of an effective preservation medium for the avulsed tooth, and timely and professional dental treatment performed after avulsion[4]. It was noted that a delay of more than 5 min could be defined as delayed replantation, affecting tooth survival[5]. Unfortunately, in most cases, an avulsed tooth is kept out of the alveolar socket for a significantly long time or is stored under improper conditions, which eventually contribute to periodontal ligament cell necrosis and result in ankylosis and replacement resorption of the tooth root after reimplantation[6]. The commercial enamel matrix protein Emdogain has been used clinically. However, its effectiveness in preventing root resorption has not been demonstrated[7].

Platelet-rich fibrin (PRF) is a second-generation platelet concentrate that is prepared from the patient's own blood without the use of an anticoagulant through a single-step centrifugation process[8,9]. This concentrate is classified as L-PRF or PRF based on its leukocyte content as well as standard PRF or advanced PRF depending on the centrifugation process. In addition, PRF is available in a membrane or injectable form depending on the centrifugation process and consistency of the final product[10]. The main scaffold component of PRF is fibrin, which develops a three-dimensional mesh crossover structure that is visible under a scanning electron microscope with a large interfiber space that contains numerous red blood cells, white blood cells and clusters of platelets[11,12]. The fibrin network of PRF protects platelets from immediate activation but progressively activates them during the process of fibrin degradation, slowly releasing growth factors, eventually prolonging the duration of growth factors in PRF and promoting wound healing effects[13,14]. Thus, PRF has the potential to enhance tissue regeneration, accelerate wound healing and induce stem cell differentiation through the consistent release of multiple growth factors[15,16]. Our previous study demonstrated that autologous PRF could effectively promote the periodontal healing of avulsed teeth after delayed replantation in dogs and thus control the occurrence and development of initial root resorption[15].

In this report, we presented two clinical cases of delayed reimplantation of avulsed teeth using autologous PRF granules with a 12-mo follow-up. In both cases, the avulsed teeth were separated from the alveolar socket for far longer than the optimal reimplantation time of 5 min, and the residual periodontal ligament tissue on the root surface was either damaged or seriously polluted, which would traditionally deem them as "hopeless" teeth. Upon simultaneous reimplantation of avulsed teeth with autologous PRF, the injured teeth showed no symptoms of inflammatory root resorption or ankylosis in both cases, suggesting that the application of PRF may offer new therapeutic opportunities for traditionally "hopeless" avulsed teeth.

CASE PRESENTATION

Chief complaints

Case 1: A 14-year-old boy was referred to the Department of General Dentistry and Emergency of the Fourth Military Medical University with complaints of pain and that his left upper central incisor fell out 18 h prior.

Case 2: A 17-year-old boy visited the Department of General Dentistry and Emergency of the Fourth Military Medical University with complaints that his left upper lateral incisor had completely fallen out 2 h prior.

History of present illness

Case 1: The patient accidentally fell 18 h prior to presentation, and his left upper central incisor was knocked out. The patient was conscious with stable vital signs.

Case 2: The patient suffered avulsion of the left upper lateral incisor from an accidental fall and came to the hospital 2 h later. The patient was conscious with stable vital signs.

History of past illness

The patients did not have a relevant medical history. They did not report any history of drug allergies or systemic diseases and exhibited no apparent dental treatment contraindications.

Personal and family history

There were no specific family health histories.

Physical examination

Case 1: After excluding damage to other important organs, an oral examination was performed. His general medical history did not obviously contribute to the injury, and an examination revealed no evidence of nerve injury. We performed clinical examinations, and the extraoral findings did not reveal serious wounds. Intraoral examination found that tooth 21 was missing, and the alveolar nest was empty. Blood clots had formed in the alveolar socket, and there was no obvious lacerated wound in the gums. The crown of tooth 11 was shifted to the palatal side and exhibited occlusal interference. Tooth H was retained on the lingual side of tooth 13 and was loose (Figure 1A and B). The avulsed tooth was wrapped in dirty dry paper towels (Figure 1C).

Case 2: Intraoral examination found that tooth 22 was missing, and the corresponding alveolar socket was empty with blood clots filling it. The patient had a complicated crown fracture of tooth 11 and a complicated crown-root fracture of tooth 21 with the fracture surfaces being approximately 4 mm below the enamel-dentinal junction (Figure 2A and B). The avulsed tooth was wrapped in dry paper towels, and numerous pollutants were present on the periodontal ligament tissues of the root surface (Figure 2C).

Laboratory examinations

These cases did not undergo any laboratory examinations.

Imaging examinations

Case 1: Digital-X radiograph (FOCUS, Instrumentarium Dental, Finland) revealed that the alveolar socket of tooth 21 was empty, and no high-density foreign body images were noted. The periodontal membrane space was widened in tooth 11 without significant root fracture (Figure 3A). Cone-beam computed tomography (Hires3D, Beijing, China) revealed that the lip side of the alveolar bone wall of tooth 21 was fractured (Figure 3B).

Case 2: Periapical radiography revealed that the alveolar socket of tooth 22 was empty, and no high-density foreign body images were observed (Figure 4A). Cone-beam computed tomography revealed no alveolar fracture around the empty tooth socket (Figure 4B), and the fracture position of tooth 21 was approximately 3 mm above the top of the alveolar crest (Figure 4C).

FINAL DIAGNOSIS

Case 1: Based on the patient's medical history and findings of the imaging examinations, the diagnoses for this patient included lateral luxation of tooth 11, avulsion of tooth 21 and alveolar fracture of teeth 11 and 21.

Case 2: The diagnoses of this patient included avulsion of tooth 22, complicated crown fracture of tooth

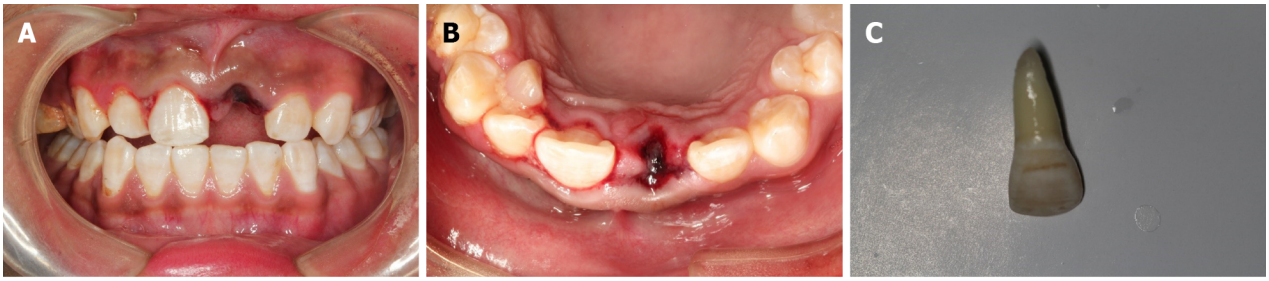

Figure 1 Initial intraoral examination of Case 1. A: Tooth 21 was missing, and the alveolar nest was empty; B: There was no obvious lacerated wound in the gums; C: The root of the avulsed tooth was wiped clean, and no residual periodontal ligament tissue was observed.

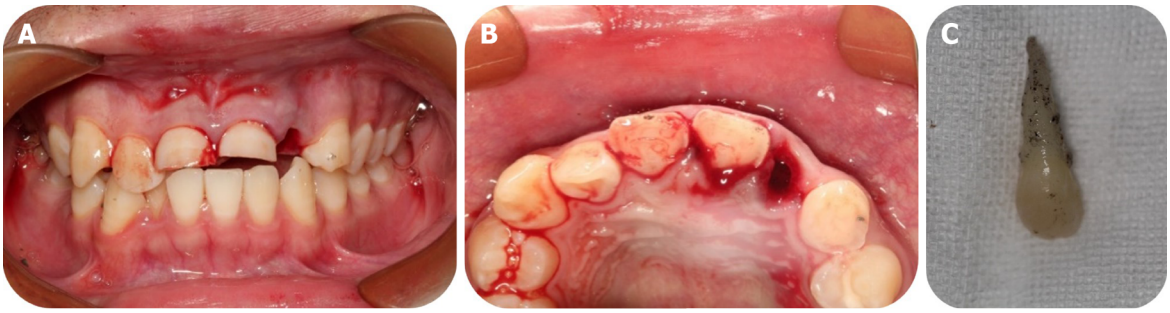

Figure 2 Initial intraoral examination of Case 2. A: Tooth 22 was missing, and the alveolar nest was empty; B: The patient had a complicated crown fracture of tooth 11 and a complicated crown-root fracture of tooth 21; C: The avulsed tooth was wrapped in dry paper towels, and obvious contaminants were present on the root surface.

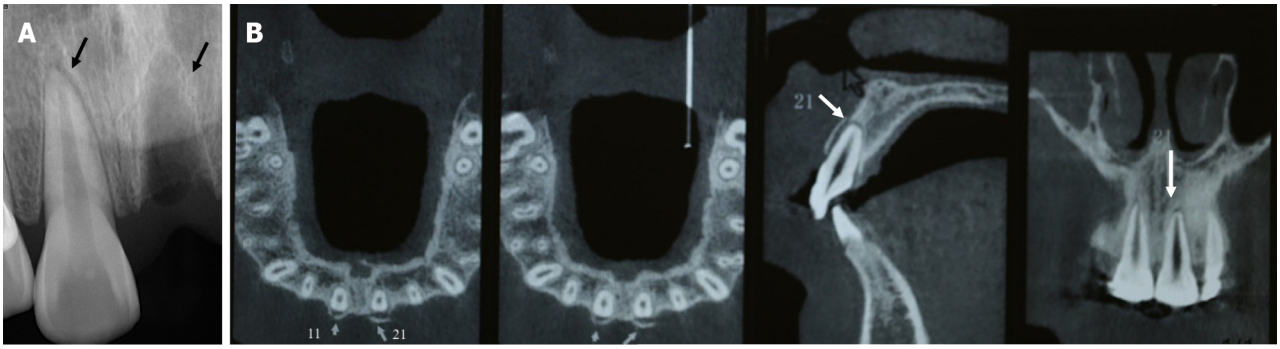

Figure 3 Periapical radiograph and cone beam computed tomography images of Case 1 at the first visit. A: The periodontal membrane space was widened in tooth 11, the alveolar socket of tooth 21 was empty, and no high-density foreign bodies were observed; B: Cone-beam computed tomography images showed that tooth 21 had been completely replanted, and the lip side of the alveolar bone wall of teeth 11 and 21 was fractured.

11, and complicated crown-root fracture of tooth 21.

TREATMENT

Case 1: We obtained a 10-mL blood sample from the median cubital vein and transferred the blood into a 10-mL glass tube without anticoagulation as soon as possible. The tube was immediately centrifuged at 400 × g for 10 min (TD3, CENCE, China) (Figure 5A). The fibrin clot that contains PRF formed in the middle of the tube; thus, the clot was easily separated from the red corpuscles at the bottom (Figure 5B and C). The clot was compressed with sterile dry gauze to remove the fluids trapped in the fibrin matrix. The PRF formed a very resistant autologous fibrin membrane, which was subsequently cut into

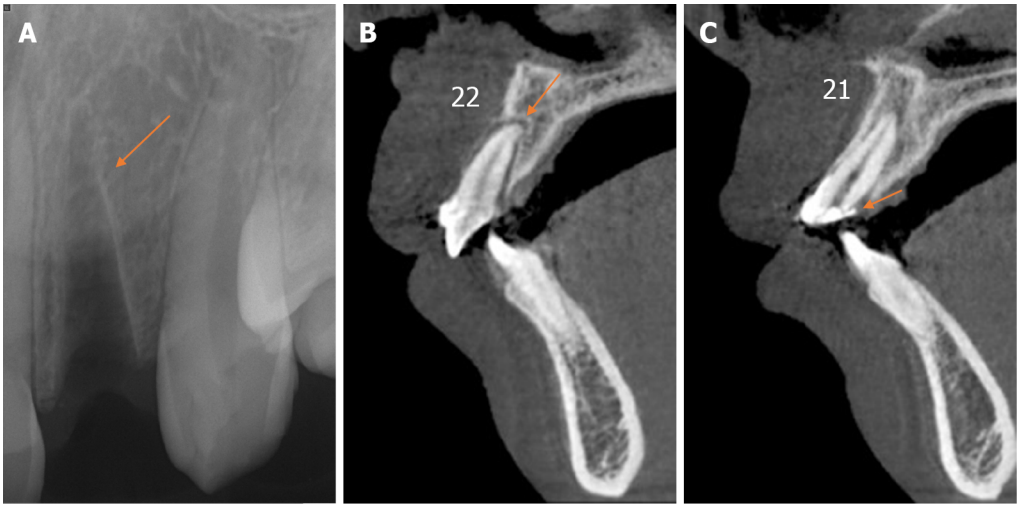

DOI: 10.12998/wjcc.v11.i3.635

Figure 4 Periapical radiograph and cone beam computed tomography images of Case 2 at the first visit. A: The alveolar socket of tooth 22 was empty, and no high-density foreign bodies were present; B: Cone-beam computed tomography image showed that tooth 22 had been replanted completely, and no alveolar fractures were noted around the empty tooth socket; C: Cone-beam computed tomography image showed that the fracture edge of tooth 21 was approximately 3 mm above the top of the alveolar crest.

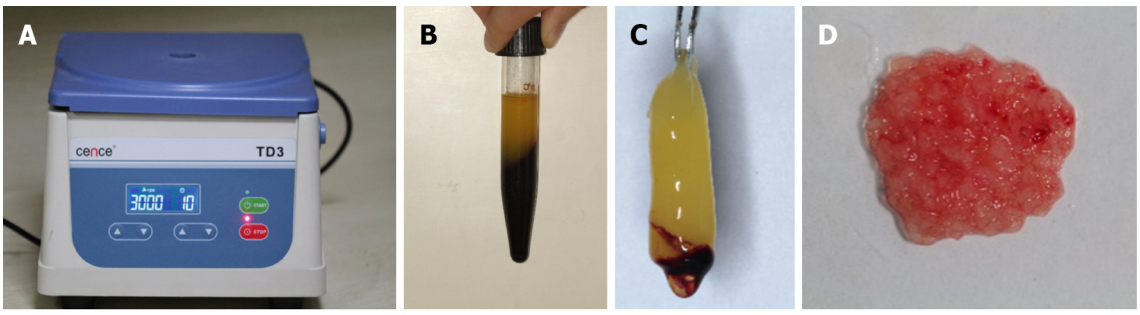

DOI: 10.12998/wjcc.v11.i3.635

Figure 5 Preparation process of the platelet-rich fibrin. A: The tube was immediately centrifuged at 400 × g for 10 min; B: The fibrin clot contained platelet-rich fibrin and was located in the middle of the tube; C: The clot was easily separated from the red corpuscles at the bottom; D: The platelet-rich fibrin membrane was cut into approximately 1 mm^3 granules, and the red and white ends were mixed evenly.

approximately 1 mm^3 granules (Figure 5D). Tooth 21 was reimplanted along with the PRF granules, and tooth 11 received manipulative reduction. Then, the teeth were splinted using a preshaped semiflexible titanium labial arch (Titanium Trauma Splint, Zhongbang Titanium Biological Materials Co., Ltd., Xi'an, China) for 4 wk (Figure 6A). The digital X-ray radiograph obtained immediately after the surgery showed complete reduction of teeth 21 and 11 (Figure 7A). According to the International Association of Dental Traumatology guidelines[17], root canal therapy of avulsed teeth 21 should be started within 7-14 d. For tooth 11, negative dental pulp activity was found. In addition, the tooth was sensitive to percussion, and a small transmission shadow was observed in the apical region at the return visit after 2 wk. Root canal therapy of the laterally dislocated tooth 11 and avulsed tooth 21 was performed 2 wk after the first visit. Calcium hydroxide paste was used as an intracanal medication sealant for 4 wk. Then, a biotype root canal filling sealer and hot-melt gutta-percha (SuperEndo B&L, Korea) were adopted for root canal filling. After root canal treatment, teeth 11 and 21 were restored with nanoment resin (3M Dental Products, MN, United States). The fixtures were removed 4 wk after the first treatment (Figures 6B and 7B).

Case 2: After obtaining informed consent, blood was collected from the patient, and PRF was prepared. Then, tooth 22 was reimplanted with PRF and splinted for 2 wk using a preshaped semiflexible titanium labial arch (Figure 6C). The digital X-ray radiograph obtained immediately after surgery showed complete reduction of tooth 22 (Figure 7C). After pulp vitality assessment, the dental pulp of teeth 11, 21 and 22 was removed after 2 wk, and calcium hydroxide paste was used as an intracanal medication sealant for 4 wk. Then, a biotype root canal filling sealer and hot-melt gutta-percha (SuperEndo B&L, Korea) were adopted for root canal filling. The fixtures were removed after 2 wk, and the root canal was completed after 6 wk (Figure 7D). After root canal treatment, teeth 11 and 21 were filled with fiber piles

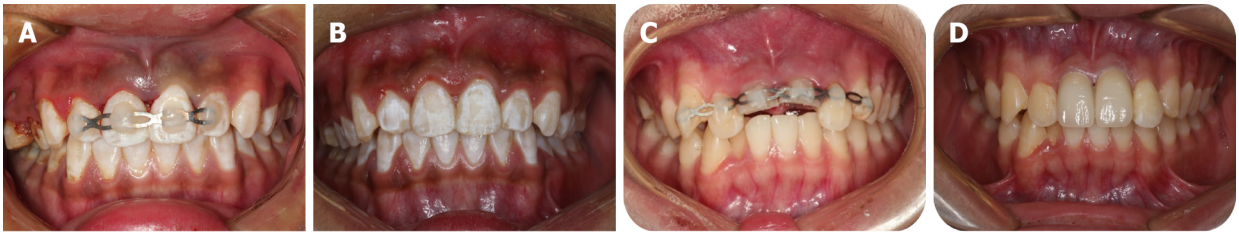

DOI: 10.12998/wjcc.v11.i3.635

Figure 6 Intraoral photographs of replanted tooth fixation. A and C: In Cases 1 and 2, the teeth were splinted using a preshaped semiflexible titanium labial arch; B and D: In Cases 1 and 2, the fixtures were removed.

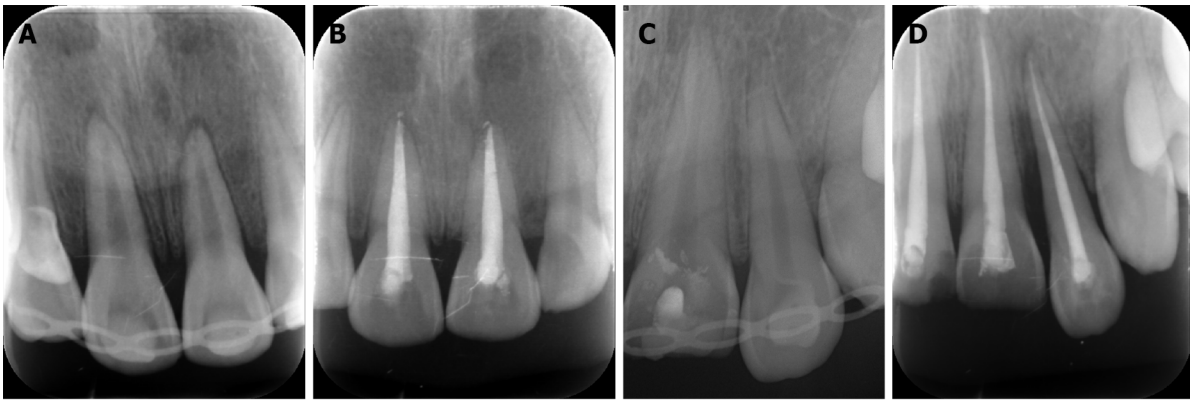

DOI: 10.12998/wjcc.v11.i3.635

Figure 7 Periapical radiograph. A and C: In Case 1 and 2, the teeth were splinted using a preshaped semiflexible titanium labial arch at the first visit; B and D: 6 wk after the initial visit of Case 1 and 2, the fixtures were removed, and the root canal treatment for the injured teeth was accomplished.

(3M Deutschland GmbH, Germany) and resin (3M Dental Products, MN, United States) and finally repaired with full crown restoration. Tooth 22 was restored with nanoment resin (3M Dental Products, MN, United States) (Figure 6D).

OUTCOME AND FOLLOW-UP

Case 1: A follow-up examination was performed 3 mo, 6 mo and 12 mo after the treatment. Clinical examination found no obvious periodontal pockets, tooth discoloration or swelling of the gums around tooth 21 (Figure 8A and B). The radiographic images obtained during the follow-up examination showed that the periodontal membrane space was continuous, and no sign of pathological root absorption was observed (Figure 9A-D).

Case 2: A follow-up examination was performed 3 mo, 6 mo and 12 mo after the treatment. Clinical examination revealed no obvious periodontal pockets, tooth discoloration or swelling of the gums around tooth 22 (Figure 8C and D). Radiographic images obtained during the follow-up examination showed that the periodontal membrane space was continuous, and no sign of pathological absorption was observed (Figure 9E-H).

DISCUSSION

Tooth reimplantation is the most important and fundamental treatment for tooth avulsion. The time interval between avulsion and reimplantation is the most important factor for successful reimplantation and is directly related to the number of live periodontal ligament cells on the root surface of the avulsed teeth[11]. If the tooth is not reimplanted as soon as possible, the residual periodontal ligament tissues on the root surface could be damaged or even exhibit necrosis. These conditions can lead to serious pathologic resorption and loss of the reimplanted tooth. Inflammation and replacement root resorption are the most common causes of reimplantation failure. The development of the lesion greatly depends on pulp vitality. When the root canal becomes infected, microbial toxins can move to the root surface

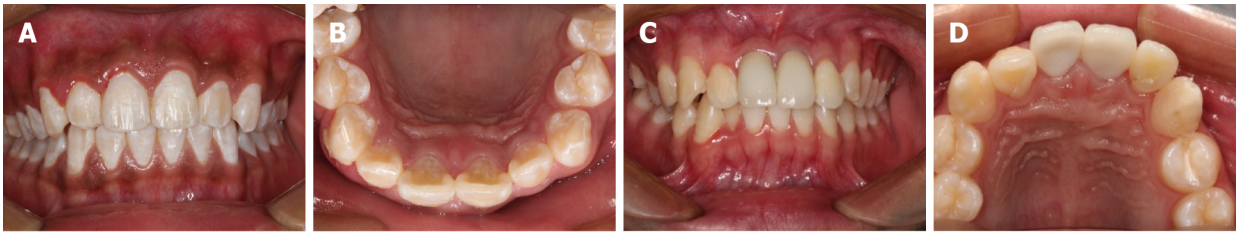

DOI: 10.12998/wjcc.v11.i3.635

Figure 8 Intraoral photographs of the follow-up examination. A and B: There were no obvious periodontal bags, tooth discoloration or swelling of the gums around tooth 21 in Case 1; C and D: There were no obvious periodontal bags, tooth discoloration or swelling of the gums around tooth 22 in Case 2.

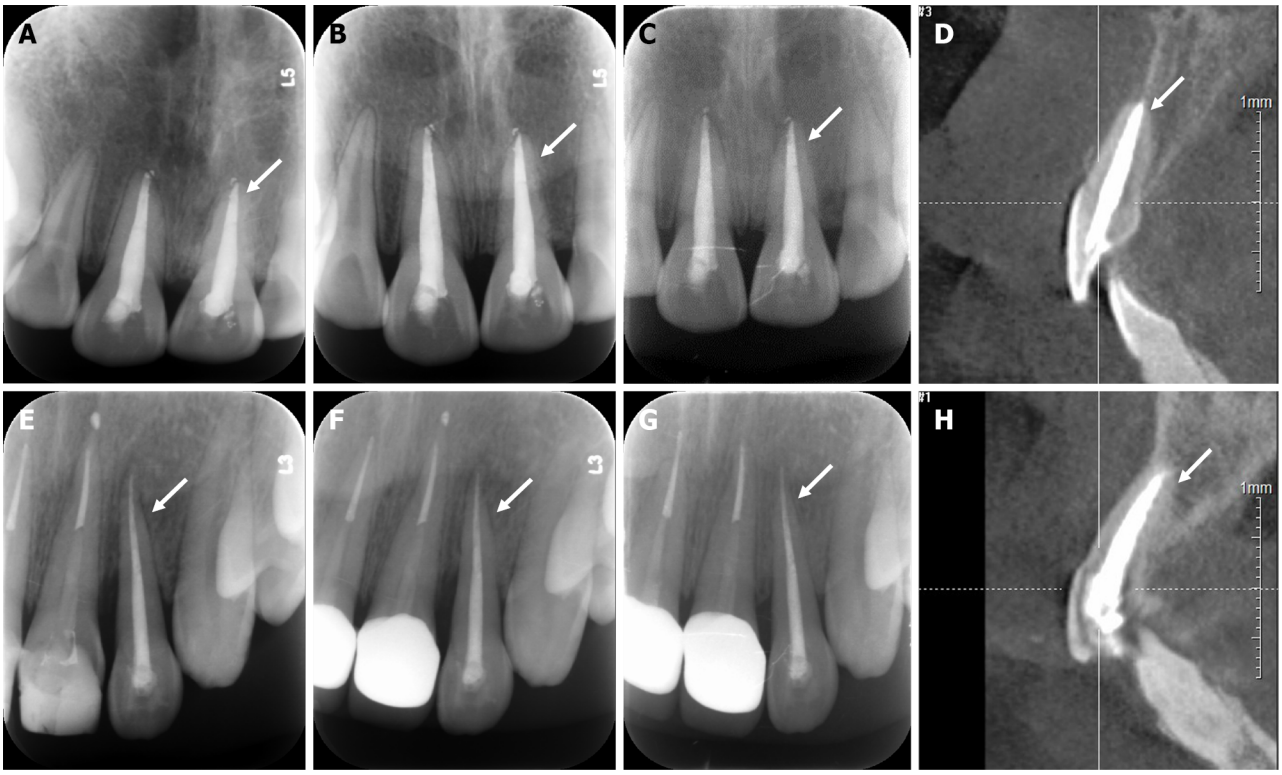

DOI: 10.12998/wjcc.v11.i3.635

Figure 9 Periapical radiograph and cone beam computed tomography images of two cases during follow-up observation. The periodontal membrane space was continuous, and no sign of pathological root absorption was observed in the avulsed teeth. A and E: 3-mo follow-up radiograph images of Cases 1 and 2; B and F: 6-mo follow-up radiograph images of Cases 1 and 2; C and G: 12-mo follow-up radiograph of Cases 1 and 2; D and H: 12-mo follow-up cone-beam computed tomography images of Cases 1 and 2.

through dentinal tubules, leading to the occurrence of root resorption[6,18]. Inflammatory root absorption on the outer surface can be prevented or controlled by the timely removal of the etiological origin, *i.e.* root canal intervention. The most effective method to prevent the replacement absorption of roots is to immediately replant or place the tooth in an appropriate storage medium[19,20].

It has been reported in the literature that ideal periodontal healing can be achieved when the avulsed tooth is reimplanted within 5 min. If reimplantation is delayed for more than 1 h after avulsion, complete necrosis of the injured periodontal ligament tissue is expected[17,21]. The storage of the avulsed tooth is also crucial to the periodontal healing process by affecting the viability of the periodontal ligament cells[22]. Unfortunately, due to the lack of common knowledge of early treatment and preservation of the avulsed teeth, few patients save the avulsed teeth in an ideal media in a timely manner. Studies have shown that 28.6% of patients place dislocated teeth in dry tissues for preservation, and only 11% of dislocated teeth were held in the mouth or placed in milk during transport to the clinic [23]. In the present cases, the patients washed the avulsed tooth with running water, which removed the periodontal tissues from the root surface. The teeth were then wrapped in paper towels, and the patients visited the doctor more than 1 h later (even up to 18 h later). Therefore, periodontal cells, which are essential for periodontal membrane healing, were almost completely destroyed.

In our previous study, we demonstrated that autologous PRF effectively promotes the periodontal healing of avulsed teeth during delayed tooth reimplantation[15]. Similarly, Hiremath *et al*[24] demonstrated that PRF increased the cellular activity of periodontal ligament cells *in vitro*[24,25]. A previous study reported that when a PRF membrane was used to wrap the root surface and condense into the canal, it promoted pulp vitality and periodontal healing of the avulsed teeth, whereas a thick radiolucent area surrounding the root was always obvious even after 24 mo of follow-up[26]. Here, PRF granules instead of PRF membranes were adopted; thus, the problem that the PRF graft might prevent the root from fitting into the alveolar bone was avoided. In case 1, the avulsed tooth was reimplanted after 18 h when its periodontal membrane was necrotic, and the probability of root absorption was greatly increased. Therefore, we used PRF together with tooth replantation to reduce the probability of root resorption. These results were also consistent with our expectations, and no signs of root resorption were noted during the 3-mo, 6-mo and 12-mo postoperative follow-up. To our knowledge, this is the longest successful delayed replantation of an avulsed tooth reported in the literature to date. These results suggest that PRF may provide a new treatment opportunity for traditionally hopeless avulsed teeth.

We assume that PRF promotes the healing of avulsed teeth *via* two mechanisms based on our previous *in vitro* and *in vivo* studies. First, the periodontal ligament tissues remaining within the original alveolar socket contain periodontal ligament cells and stem cells. During the tissue repair process, multiple growth factors are released by PRF. Additionally, cell homing will occur, and host stem cells from the circulation will be recruited to the injury region by factors released by the PRF to promote their proliferation and induce their differentiation toward the periodontal membrane, facilitating the formation of periodontal membrane-like structures[15,27]. Second, we demonstrated that PRF consists of concentrated blood platelets, and the α-granules are activated and degranulated. Thus, many growth factors, such as platelet-derived growth factor, transforming growth factor-β, insulin-like growth factor, epidermal growth factor and vascular endothelial growth factor, can be released for at least a week and up to 4 wk. Thus, PRF supports the regenerative and remodeling environment for a certain period of time[28-31]. These growth factors increase the mitotic activity of periodontal fibroblasts by 20%-37% [19], thereby improving the proliferation and periodontal differentiation of target cells and further promoting periodontal healing of avulsed teeth[15]. We also note that when a variety of growth factors act together, synergistic or even antagonistic effects among them cannot be ruled out. Therefore, the natural proportion of various growth factors is particularly important. This is just one of the important reasons why we chose PRF, which contains numerous active growth factors. The growth factors in PRF are not only rich in content and variety but also maintain natural proportions under normal physiological conditions. Only by their synergistic effects can they jointly maintain the balance of the tissue environment and play an important role in regulating wound healing and tissue regeneration.

Although we did not observe obvious ankylosis in these cases, it is a common finding in patients with avulsed teeth[6,15,32,33]. Previous studies have shown that PRF can inhibit the osteogenic differentiation of periodontal ligament stem cells *in vitro*, which might reduce the possibility of ankylosis based on three reasons. First, PRF promotes cell proliferation to promote the generation of fibroblasts and repair tissue with more seed cells instead of mobilizing bone stromal cells and bone-derived cells. Second, the main component of PRF is collagen fiber, which can act as a physical barrier when placed in the periodontal space. PRF prevents direct contact between the tooth root and the inner wall of the alveolar socket, thus reducing the bone repair between them[15]. Third, PRF inhibits the generation of osteoclasts by promoting osteoprotectin secretion. By inhibiting osteoclast activity, the opportunity for external resorption can be suppressed to some extent[26]. Of course, the present study also has some limitations, such as a short follow-up time and a small sample size. Thus, the long-term effect of PRF in promoting the periodontal healing of avulsed teeth is unclear. Future evaluations including long-term follow-up with a large sample size are planned.

CONCLUSION

Enriched with growth factors and leukocytes, PRF potentially reduces pathological resorption and promotes periodontal wound healing and periodontal ligament regeneration following delayed reimplantation of avulsed teeth. Although the viability of PRF must be demonstrated in more cases, the application of PRF may offer new therapeutic opportunities for traditionally hopeless avulsed teeth.

FOOTNOTES

Author contributions: Yang Y, Jia LN and Wang JJ performed the dental treatment; Yang Y and Liu YL reviewed the literature and contributed to the drafting of the manuscript; Zhang M checked all aspects of this paper, including data collection, data analysis and paper writing; All authors have read and approved the final manuscript.

Supported by Natural Science Foundation of China, No. 31971248; and National Clinical Research Center for Oral

Diseases Project of Military Stomatology, No. LCA202007.

Informed consent statement: Informed written consent was obtained from the patients for publication of this report and any accompanying images.

Conflict-of-interest statement: All authors report having no relevant conflicts of interest for this article.

CARE Checklist (2016) statement: The authors have read CARE Checklist (2016), and the manuscript was prepared and revised according to CARE Checklist (2016).

Country/Territory of origin: China

ORCID number: Yang Yang 0000-0002-3551-6563; Yan-Li Liu 0000-0002-1361-3848; Lie-Ni Jia 0000-0002-4571-5080; Jun-Jun Wang 0000-0002-2788-9685; Min Zhang 0000-0002-7327-3910.

S-Editor: Fan JR
L-Editor: Filipodia
P-Editor: Fan JR

REFERENCES

1 **Andreasen JO**, Andreasen FM. Avulsions. In: Andreasen JO, Andreasen FM, Andersson L. Textbook and Color Atlas of Traumatic Injuries to the Teeth. 4th Edition. Copenhagen: Blackwell Munksgaard, 2007: 444–88
2 **Casaroto AR**, Hidalgo MM, Sell AM, Franco SL, Cuman RK, Moreschi E, Victorino FR, Steffens VA, Bersani-Amado CA. Study of the effectiveness of propolis extract as a storage medium for avulsed teeth. *Dent Traumatol* 2010; **26**: 323-331 [PMID: 20662885 DOI: 10.1111/j.1600-9657.2010.00879.x]
3 **Gong Y**, Xue L, Wang N, Wu C. Emergency dental injuries presented at the Beijing Stomatological Hospital in China. *Dent Traumatol* 2011; **27**: 203-207 [PMID: 21564518 DOI: 10.1111/j.1600-9657.2010.00938.x]
4 **Zhang X**, Gong Y. Characteristics of avulsed permanent teeth treated at Beijing Stomatological Hospital. *Dent Traumatol* 2011; **27**: 379-384 [PMID: 21790974 DOI: 10.1111/j.1600-9657.2011.01024.x]
5 **Petrovic B**, Marković D, Peric T, Blagojevic D. Factors related to treatment and outcomes of avulsed teeth. *Dent Traumatol* 2010; **26**: 52-59 [PMID: 19919541 DOI: 10.1111/j.1600-9657.2009.00836.x]
6 **Heboyan A**, Avetisyan A, Karobari MI, Marya A, Khurshid Z, Rokaya D, Zafar MS, Fernandes GVO. Tooth root resorption: A review. *Sci Prog* 2022; **105**: 368504221109217 [PMID: 35759366 DOI: 10.1177/00368504221109217]
7 **Panzarini SR**, Gulinelli JL, Poi WR, Sonoda CK, Pedrini D, Brandini DA. Treatment of root surface in delayed tooth replantation: a review of literature. *Dent Traumatol* 2008; **24**: 277-282 [PMID: 18410388 DOI: 10.1111/j.1600-9657.2008.00555.x]
8 **Verma UP**, Yadav RK, Dixit M, Gupta A. Platelet-rich Fibrin: A Paradigm in Periodontal Therapy - A Systematic Review. *J Int Soc Prev Community Dent* 2017; **7**: 227-233 [PMID: 29026693 DOI: 10.4103/jispcd.JISPCD_429_16]
9 **Salgado-Peralvo AO**, Mateos-Moreno MV, Uribarri A, Kewalramani N, Peña-Cardelles JF, Velasco-Ortega E. Treatment of oroantral communication with Platelet-Rich Fibrin: A systematic review. *J Stomatol Oral Maxillofac Surg* 2022; **123**: e367-e375 [PMID: 35318134 DOI: 10.1016/j.jormas.2022.03.014]
10 **Castro AB**, Meschi N, Temmerman A, Pinto N, Lambrechts P, Teughels W, Quirynen M. Regenerative potential of leucocyte- and platelet-rich fibrin. Part A: intra-bony defects, furcation defects and periodontal plastic surgery. A systematic review and meta-analysis. *J Clin Periodontol* 2017; **44**: 67-82 [PMID: 27783851 DOI: 10.1111/jcpe.12643]
11 **Miron RJ**, Zucchelli G, Pikos MA, Salama M, Lee S, Guillemette V, Fujioka-Kobayashi M, Bishara M, Zhang Y, Wang HL, Chandad F, Nacopoulos C, Simonpieri A, Aalam AA, Felice P, Sammartino G, Ghanaati S, Hernandez MA, Choukroun J. Use of platelet-rich fibrin in regenerative dentistry: a systematic review. *Clin Oral Investig* 2017; **21**: 1913-1927 [PMID: 28551729 DOI: 10.1007/s00784-017-2133-z]
12 **Mandviwala DK**, Arora AV, Kapoor SV, Shah PB. Internal root resorption: A rare complication of vital pulp therapy using platelet-rich fibrin. *J Oral Maxillofac Pathol* 2022; **26**: 132 [PMID: 35571329 DOI: 10.4103/jomfp.jomfp_389_21]
13 **Wang X**, Yang Y, Zhang Y, Miron RJ. Fluid platelet-rich fibrin stimulates greater dermal skin fibroblast cell migration, proliferation, and collagen synthesis when compared to platelet-rich plasma. *J Cosmet Dermatol* 2019; **18**: 2004-2010 [PMID: 30990574 DOI: 10.1111/jocd.12955]
14 **Chai J**, Jin R, Yuan G, Kanter V, Miron RJ, Zhang Y. Effect of Liquid Platelet-rich Fibrin and Platelet-rich Plasma on the Regenerative Potential of Dental Pulp Cells Cultured under Inflammatory Conditions: A Comparative Analysis. *J Endod* 2019; **45**: 1000-1008 [PMID: 31248700 DOI: 10.1016/j.joen.2019.04.002]
15 **Zhao YH**, Zhang M, Liu NX, Lv X, Zhang J, Chen FM, Chen YJ. The combined use of cell sheet fragments of periodontal ligament stem cells and platelet-rich fibrin granules for avulsed tooth reimplantation. *Biomaterials* 2013; **34**: 5506-5520

[PMID: 23639531 DOI: 10.1016/j.biomaterials.2013.03.079]
16 **Chew JRJ**, Tan BL, Lu JX, Tong HJ, Duggal MS. Cell-Based Therapy for Tooth Replantation Following Avulsion: A Systematic Review. *Tissue Eng Part B Rev* 2022; **28**: 351-363 [PMID: 33593127 DOI: 10.1089/ten.TEB.2021.0016]
17 **Fouad AF**, Abbott PV, Tsilingaridis G, Cohenca N, Lauridsen E, Bourguignon C, O'Connell A, Flores MT, Day PF, Hicks L, Andreasen JO, Cehreli ZC, Harlamb S, Kahler B, Oginni A, Semper M, Levin L. International Association of Dental Traumatology guidelines for the management of traumatic dental injuries: 2. Avulsion of permanent teeth. *Dent Traumatol* 2020; **36**: 331-342 [PMID: 32460393 DOI: 10.1111/edt.12573]
18 **Heboyan A**, Avetisyan AA, Margaryan MM, Azatyan VY. Rare clinical case of tooth root external resorption as a delayed post-traumatic complication. *The New Armenian Med J* 2018; **12**: 93-98
19 **Behnaz M**, Izadi SS, Mashhadi Abbas F, Dianat O, Sadeghabadi S, Akbarzadeh T, Haeri A, Kazem M, Younessian F. The impact of platelet-rich fibrin (PRF) on delayed tooth replantation: A preliminary animal study. *Aust Endod J* 2021; **47**: 457-466 [PMID: 33650725 DOI: 10.1111/aej.12492]
20 **Day PF**, Duggal M, Nazzal H. Interventions for treating traumatised permanent front teeth: avulsed (knocked out) and replanted. *Cochrane Database Syst Rev* 2019; **2**: CD006542 [PMID: 30720860 DOI: 10.1002/14651858.CD006542.pub3]
21 **Wynkoop JR 2nd**, West LA, King JE, Hawley CE. An analysis of dental emergencies during combat and peacetime exercises. *Mil Med* 1986; **151**: 364-367 [PMID: 3092136 DOI: 10.1093/milmed/151.1.364]
22 **Andreasen JO**, Borum MK, Jacobsen HL, Andreasen FM. Replantation of 400 avulsed permanent incisors. 4. Factors related to periodontal ligament healing. *Endod Dent Traumatol* 1995; **11**: 76-89 [PMID: 7641622 DOI: 10.1111/j.1600-9657.1995.tb00464.x]
23 **Hohl TH**, Shapiro PA, Moffett BC, Ross A. Experimentally induced ankylosis and facial asymmetry in the macaque monkey. *J Maxillofac Surg* 1981; **9**: 199-210 [PMID: 6948064 DOI: 10.1016/s0301-0503(81)80045-8]
24 **Hiremath H**, Kulkarni S, Sharma R, Hiremath V, Motiwala T. Use of platelet-rich fibrin as an autologous biologic rejuvenating media for avulsed teeth - an in vitro study. *Dent Traumatol* 2014; **30**: 442-446 [PMID: 24924343 DOI: 10.1111/edt.12119]
25 **Andia I**, Abate M. Platelet-rich plasma: underlying biology and clinical correlates. *Regen Med* 2013; **8**: 645-658 [PMID: 23998756 DOI: 10.2217/rme.13.59]
26 **Johns DA**, Shivashankar VY, Maroli RK, Vidyanath S. Novel management of avulsed tooth by pulpal and periodontal regeneration. *J Endod* 2013; **39**: 1658-1662 [PMID: 24238468 DOI: 10.1016/j.joen.2013.08.012]
27 **Chen FM**, Wu LA, Zhang M, Zhang R, Sun HH. Homing of endogenous stem/progenitor cells for in situ tissue regeneration: Promises, strategies, and translational perspectives. *Biomaterials* 2011; **32**: 3189-3209 [PMID: 21300401 DOI: 10.1016/j.biomaterials.2010.12.032]
28 **Khurshid Z**, Asiri FYI, Najeeb S, Ratnayake J. The Impact of Autologous Platelet Concentrates on the Periapical Tissues and Root Development of Replanted Teeth: A Systematic Review. *Materials (Basel)* 2022; **15** [PMID: 35454469 DOI: 10.3390/ma15082776]
29 **Alves R**, Grimalt R. A Review of Platelet-Rich Plasma: History, Biology, Mechanism of Action, and Classification. *Skin Appendage Disord* 2018; **4**: 18-24 [PMID: 29457008 DOI: 10.1159/000477353]
30 **Suttapreyasri S**, Leepong N. Influence of platelet-rich fibrin on alveolar ridge preservation. *J Craniofac Surg* 2013; **24**: 1088-1094 [PMID: 23851746 DOI: 10.1097/SCS.0b013e31828b6dc3]
31 **Ngah NA**, Dias GJ, Tong DC, Mohd Noor SNF, Ratnayake J, Cooper PR, Hussaini HM. Lyophilised Platelet-Rich Fibrin: Physical and Biological Characterisation. *Molecules* 2021; **26** [PMID: 34885714 DOI: 10.3390/molecules26237131]
32 **Andreasen JO**. Analysis of pathogenesis and topography of replacement root resorption (ankylosis) after replantation of mature permanent incisors in monkeys. *Swed Dent J* 1980; **4**: 231-240 [PMID: 6938062]
33 **Andreasen JO**, Hjorting-Hansen E. Replantation of teeth. II. Histological study of 22 replanted anterior teeth in humans. *Acta Odontol Scand* 1966; **24**: 287-306 [PMID: 5225450 DOI: 10.3109/00016356609028223]

World Journal of Clinical Cases

Submit a Manuscript: https://www.f6publishing.com

World J Clin Cases 2023 January 26; 11(3): 645-654

DOI: 10.12998/wjcc.v11.i3.645

ISSN 2307-8960 (online)

CASE REPORT

Acute diffuse peritonitis secondary to a seminal vesicle abscess: A case report

Kun Li, Nan-Bin Liu, Jiang-Xi Liu, Quan-Ning Chen, Bao-Min Shi

Specialty type: Medicine, research and experimental

Provenance and peer review: Unsolicited article; Externally peer reviewed.

Peer-review model: Single blind

Peer-review report's scientific quality classification

Grade A (Excellent): 0
Grade B (Very good): 0
Grade C (Good): C
Grade D (Fair): D
Grade E (Poor): 0

P-Reviewer: Abd EL hafez A, Egypt; Tomizawa M, Japan

Received: September 26, 2022
Peer-review started: September 26, 2022
First decision: November 11, 2022
Revised: November 18, 2022
Accepted: January 3, 2023
Article in press: January 3, 2023
Published online: January 26, 2023

Kun Li, Nan-Bin Liu, Jiang-Xi Liu, Quan-Ning Chen, Bao-Min Shi, Department of General Surgery, Tongji Hospital of Tongji University, Shanghai 200065, China

Nan-Bin Liu, National and Local Joint Engineering Research Center of Biodiagnosis and Biotherapy, The Second Affiliated Hospital of Xi'an Jiaotong University, Xi'an 710000, Shaanxi Province, China

Corresponding author: Bao-Min Shi, Doctor, MD, PhD, Chief Doctor, Professor, Surgeon, Department of General Surgery, Tongji Hospital of Tongji University, No. 389 Xincun Road, Putuo District, Shanghai 200065, China. tjshibaomin@tongji.edu.cn

Abstract

BACKGROUND

Seminal vesicle abscess (SVA) is the manifestation of a relatively rare urinary system infection. In response to urinary system inflammation, an abscess forms in special locations. However, acute diffuse peritonitis (ADP) induced by SVA is unusual.

CASE SUMMARY

We report a case of a left SVA in a male patient complicated with pelvic abscess, ADP, multiple organ dysfunction syndrome, infectious shock, bacteremia, and acute appendiceal extraserous suppurative inflammation as a result of a long-term indwelling urinary catheter. The patient received a course of morinidazole + cefminol antibiotics but showed no obvious relief, so the perineal SVA underwent puncture drainage and abdominal abscess drainage + appendectomy was performed. The operations were successful. After the operation, anti-infection, anti-shock, and nutritional support treatments were continued and various laboratory indicators were regularly reviewed. The patient was discharged from the hospital after recovery. This disease is a challenge for the clinician because of the unusual spreading path of the abscess. Moreover, appropriate intervention and adequate drainage of abdominal and pelvic lesions are necessary, especially when the primary focus cannot be determined.

CONCLUSION

The etiology of ADP varies, but acute peritonitis secondary to SVA is very rare. In this patient, the left SVA not only affected the adjacent prostate and bladder but also spread retrogradely through the vas deferens, forming a pelvic abscess in the loose tissues of the extraperitoneal fascia layer. Inflammation involving the peritoneal layer led to ascites and pus accumulation in the abdominal cavity, and

appendix involvement led to extraserous suppurative inflammation. In clinical practice, surgeons need to consider the results of various laboratory tests and imaging examinations to make comprehensive judgments involving the diagnosis and treatment plan.

Key Words: Seminal vesicle abscess; Acute diffuse peritonitis; Acute appendicitis; Multiple organ dysfunction syndrome; Case report

Core Tip: Seminal vesicle abscess (SVA) is a relatively rare urinary system infection, and acute diffuse peritonitis (ADP) induced by SVA is unusual. We report a male patient who had a left SVA induced by a long-term indwelling urinary catheter, and this condition was complicated with pelvic abscess, ADP, multiple organ dysfunction syndrome, infectious shock, bacteremia, and acute appendiceal extraserous suppurative inflammation. With no obvious relief by conservative treatment, puncture drainage of the perineal SVA and abdominal abscess drainage + appendectomy was performed. In this case, the left SVA not only affected the adjacent prostate and bladder but also spread retrogradely through the vas deferens, forming a pelvic abscess in the loose tissues of the extraperitoneal fascia layer. Inflammation involving the peritoneal layer led to ascites and pus accumulation in the abdominal cavity, and appendix involvement led to extraserous suppurative inflammation.

Citation: Li K, Liu NB, Liu JX, Chen QN, Shi BM. Acute diffuse peritonitis secondary to a seminal vesicle abscess: A case report. *World J Clin Cases* 2023; 11(3): 645-654
URL: https://www.wjgnet.com/2307-8960/full/v11/i3/645.htm
DOI: https://dx.doi.org/10.12998/wjcc.v11.i3.645

INTRODUCTION

Acute diffuse peritonitis (ADP) is a common acute abdominal complication of general surgery. It has a high risk of mortality due to its rapid onset, rapid progression, and poor prognosis. The causes of ADP vary, but most cases are due to secondary infections. However, emergency surgery is needed regardless of the cause[1]. The main function of the seminal vesicles is to secrete nutrients and dilute the fluid in which the sperm resides. An infection of the seminal vesicle most commonly causes inflammation. Seminal vesicle abscess (SVA) is relatively rare, and diseases that develop from the "SVA–pelvic abscess–ADP" pathogenesis circuit, where the associated bacteria originate from the seminal vesicles and SVA, are even rarer. In 1978, Rajfer *et al*[2] reported the first case of SVA. According to Rajfer *et al*[2], less than 100 cases of SVA have been reported worldwide. Here, we report a male patient who developed a SVA due to a long-term indwelling catheter, analyze the basic condition and outcome, and provide the clinical diagnosis and treatment ideas.

CASE PRESENTATION

Chief complaints

An 86-year-old man was admitted to our hospital for lower abdominal distension and pain that lasted for 5 d. The patient had a sudden high fever of 39 °C.

History of present illness

Five days prior to hospital admission, the patient suffered from intermittent abdominal distension and pain. He did not visit his doctor, the symptoms of lower abdominal pain gradually worsened the night prior, and the symptoms were accompanied by frequent nausea, vomiting, and loose watery stools. After symptomatic treatment in a local hospital, there was no obvious remission, so he came to our hospital for emergency treatment. He had no jaundice or anorexia symptoms.

History of past illness

The patient underwent surgical treatment for benign prostatic hyperplasia 2 years prior and took finasteride + tamsulosin hydrochloride intermittently after the operation. Last year, he had difficulty urinating. Ultrasound examination showed that there was an increase in the residual urine volume and urinary retention. He had an indwelling catheter. The catheter was regularly removed and replaced in

the outpatient clinic, which led to dysuria recurrence. The patient also experienced hypertension for many years, which was partly controlled with medications.

Personal and family history

No relevant family history, travel history, or animal contact was reported.

Physical examination

The patient's initial vital signs at admission were as follows: Blood pressure 146/79 mmHg, pulse 62 bpm, respiratory rate 18 breaths/min, and body temperature 39 °C. He had an altered mental state, slight abdominal distension, slightly weak bowel sounds (3/min), obvious tenderness and rebound pain in the lower abdomen, slightly tense abdominal muscles, and percussive tympany abdominal sounds. He had an indwelling urinary catheter, drainage was unobstructed, urine was dark yellow, and flocculent was visible. Scrotal symmetry, bilateral testis, and epididymis tenderness were observed.

Laboratory examinations

The in-hospital laboratory examination showed the following: White blood cell (WBC) count: 12.61 × 10^9 /L (79.1% neutrophils and 11.7% lymphocytes); C-reactive protein: 82.6 mg/L. The routine urine examination showed red blood cells 85/UL and WBCs 291/UL, indicating hematuria and pyuria. However, the patient's liver and kidney function, electrolytes, myocardial enzymes, and coagulation at the first day of admission were normal.

Imaging examinations

Pelvic magnetic resonance imaging (MRI) was performed 2 d after admission, which showed a lumpy and patchy left lower abdomen, with a high possibility of inflammation, a thickened sigmoid wall, blurred fatty space surrounding the pelvic cavity, and a possible left SVA (Figure 1). Combined pelvic and abdominal computed tomography (CT) showed encapsulated effusion and gas accumulation in the left lower abdomen with peripheral exudative changes, suggesting the possibility of an abscess. The left seminal vesicle was unclear with corresponding cystic foci, suggesting the possibility of an abscess (Figure 2A and B). Chest CT revealed scattered chronic inflammation in both lungs.

FINAL DIAGNOSIS

The discharge diagnoses were: (1) Septic shock; (2) ADP and acute extraserous suppurative appendicitis; (3) Left SVA; (4) Pelvic abscess; and (5) Hypertension grade 3 (high risk).

TREATMENT

After admission, the patient's condition gradually worsened. Morlinidazole + cefminol was administered as anti-infection agents, and fluid resuscitation, abrosia, nutritional support, and other treatments were administered. Four days after admission, puncture drainage of the perineal SVA was performed, and a small amount of purulent fluid (bacterial culture: *Klebsiella pneumoniae*) was drained. Infection with Gram-positive cocci and *Candida parapsilosis* was detected in urine smears. However, multiple cultures were negative, so the possibility of sample contamination was considered. Abdominal pain was not obviously relieved postoperatively, and on the 5th day, blood pressure decreased and septic shock symptoms, such as weak consciousness, liver and kidney insufficiency, and abnormal coagulation function, were observed (Table 1). His vital signs at that time were as follows: Blood pressure 76/40 mmHg, pulse 118 bpm, respiratory rate 22 breaths/min, and body temperature 39 °C. The Acute Physiology and Chronic Health Evaluation II score was 15, and the Sequential Organ Failure Assessment score was 7. Considering that the patient's vital signs were not stable and after communicating with his family, it was decided to perform emergency exploratory laparotomy for active fluid replacement, volume expansion, and vital sign monitoring to identify the focus of infection and to fully drain the abscess.

After preoperative preparation and general anesthesia, the patient underwent surgery in the supine position, and the surgery was performed by the attending physician, who had approximately 25 years of specialized training. During the operation, the intraperitoneal suppurative fluid volume was approximately 100 mL and was mainly found in the intestines and around the appendix. The head and body of the appendix were suppurated, and a large amount of pus was around the surface of the surrounding intestinal canal and sigmoid colon, without obvious intestinal perforation or tumor formation. Thus, abdominal abscess drainage + appendectomy was performed (Figure 3A-C).

After the operation, the patient was transferred to the intensive care unit due to his critical condition. He fasted and underwent electrocardiogram monitoring and continued anti-infection, anti-shock, and nutritional support treatments. The internal environment and water electrolyte balance was maintained.

Table 1 Change trend of the patient's laboratory indexes

Date	Leukocytes (× 10^9/L)	Creatinine (μmol/L)	Albumin (g/L)	Prothrombin time (s)	C-reactive protein (mg/L)
DBO5	13	92	34.3	13.1	151.77
DBO4	11.62	81	31.5	15.7	157.74
DBO2	22.41	157	30.1	17.9	227.71
DBO1	34.67	153	18.2	18.6	239.87
OD	23.85	173	25.0	17.7	177.34
POD1	20.35	158	28.4	16.6	204.14
POD2	14.96	128	34.2	16.0	177.26
POD3	11.29	109	34.4	15.5	141.1
POD4	11.41	104	35.6	14.1	99.55
POD6	16.98	88	35.3	14.2	57.6
POD8	15.39	85	33.5	15.0	37.0
POD10	13.07	91	33.5	14.4	99.3
POD12	7.3	87	30.2	14.3	118.73
POD15	6.78	78	30.6	14.1	66.02

Leukocytes (× 10^9/L); Creatinine (μmol/L); Albumin (g/L); Prothrombin time (s); C-reactive protein (mg/L). DBO: Days before operation, DBO5 refers to the day of admission; OD: Operation day, referring to the date of performing exploratory laparotomy; POD: Postoperative days, POD15 refers to discharge date.

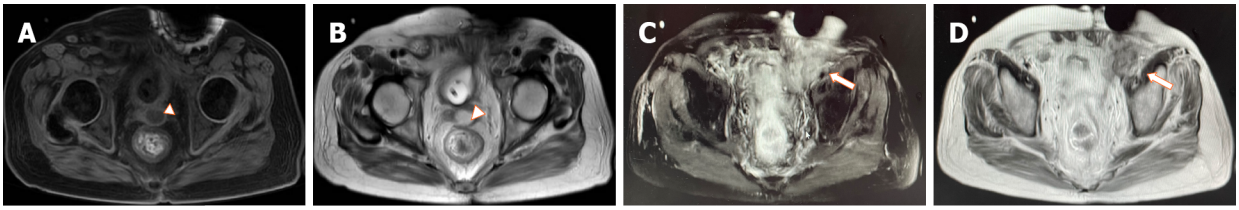

DOI: 10.12998/wjcc.v11.i3.645

Figure 1 Magnetic resonance imaging results of the patient after admission. A and B: Pelvic magnetic resonance imaging (MRI) showed a rounded abnormal signal shadow in the left seminal vesicle, with low signal on T1-weighted imaging (T1WI) and high signal on T2-weighted imaging (T2WI) + lipid inhibition, and a size of approximately 2.3 cm × 1.6 cm; C and D: Pelvic MRI showed a nodular mass in the left inguinal region, with low signal on T1WI and high signal on T2WI + lipid inhibition, and a size of approximately 5.0 cm × 4.0 cm. The white arrowheads show the left seminal vesicle. The white arrows show the pelvic abscess (secondary focus).

The function of various organs was monitored. Plasma was infused to achieve coagulation, and wound dressings were changed regularly. Various laboratory indicators were routinely checked. On the 1st day after the operation, the patient had dyspnea and atrial fibrillation with a fast ventricular rate after taking off the line. He received high flow oxygen inhalation and his heart rate was regulated with amiodarone. Treatment to resolve abdominal distension and promote gastrointestinal motility was performed. The pus culture showed *Klebsiella pneumoniae* infection. A combination of meropenem and linezolid was administered, and the patient's symptoms and signs were gradually resolved. On the 3rd day after the operation, the patient's heart rate returned to normal, oxygen saturation was maintained with low-flow oxygen inhalation, the infection was eradicated, and abdominal distension was relieved. Later, the patient returned to general surgery ward for further treatment. On the 4th day after the operation, a liquid diet was initiated. The amount of intravenous fluid replacement was reduced and he was encouraged to get out of bed to prevent embolization. On the 7th day after the operation, abdominal distension recurred. He continued to fast, and the wound suture was removed. On the 10th day after the operation, the patient complained of hunger but abdominal distension was relieved. Abdominal CT showed less abdominal inflammation than before (Figure 2C and D). Three days later, the patient's diet was changed to a semiliquid diet. Two days later, the patient did not complain of any special discomfort, his body temperature returned to normal, and he was allowed to resume a normal diet. The other catheter was replaced, and the patient was discharged.

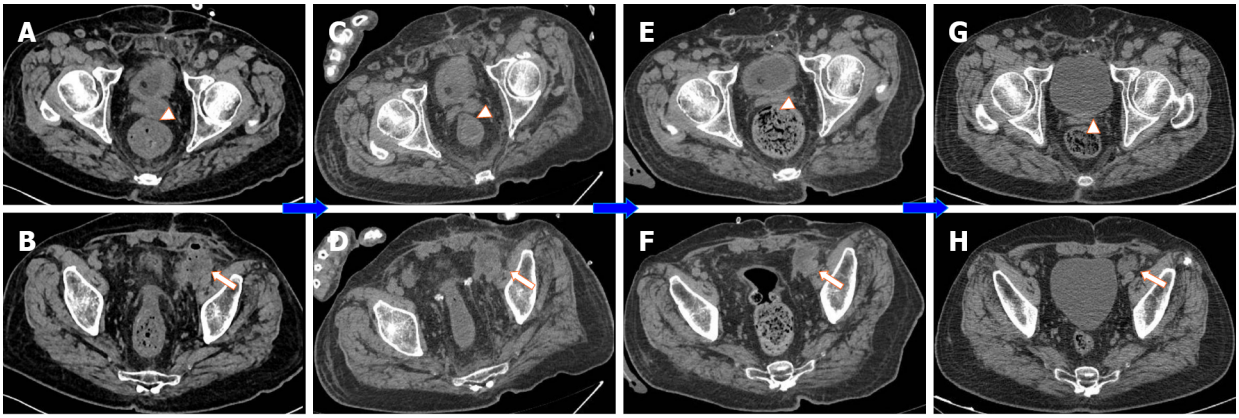

DOI: 10.12998/wjcc.v11.i3.645

Figure 2 Computed tomography results of the patient throughout the diagnosis and treatment processes. A-D: The results of pelvic computed tomography examinations on the 2nd day after admission, on the 10th day after surgery, at 1 mo after discharge, and at 3 mo after discharge; E-H: The primary focus of the left seminal vesicle abscess and the secondary focus of the extraperitoneal fascial abscess were gradually controlled and narrowed after treatment and outpatient and emergency follow-up. The white arrowheads show the left seminal vesicle. The white arrows show the pelvic abscess (secondary focus).

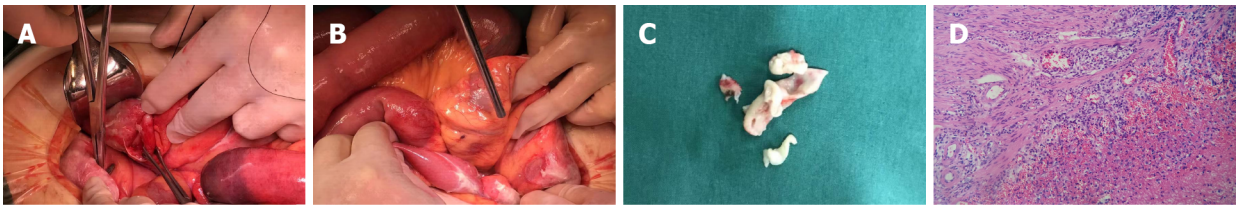

DOI: 10.12998/wjcc.v11.i3.645

Figure 3 The appendix. A and B: During the operation, the appendix was congested and edematous, with accumulation of the surrounding suppurative fluid, and the sigmoid colon was coated with a large amount of pus; C: A section of the appendix with a length of 3.5 cm and a diameter of 0.8-1.2 cm was cut; D: The suppurative inflammation of the appendix was confined outside the serosa (microscopy, × 100).

OUTCOME AND FOLLOW-UP

Postoperative pathology of the appendix showed extraserous suppurative inflammation, AB (+), and PAS (+) (Figure 3D). After discharge, the patient underwent a 1-year follow-up. The two inflammatory foci were managed and their size was gradually reduced after treatment and follow-up (Figure 2E-H).

DISCUSSION

The seminal vesicles are located at the bottom of the bladder and the outer side of the ampulla of the ureter. Together with the ampulla of the vas deferens and the ejaculatory duct, they form the distal structure of the seminal tract[3]. Seminal vesicle secretions account for approximately 60% of the total semen volume and include high concentrations of fructose, prostaglandin, and other substances[4]. SVA is very rare. In 2004, Sağlam *et al*[5] pointed out that a total of 26 related cases were reported in the literature. By searching PubMed, ScienceDirect, and other literature databases, as of August 2022, a total of 51 cases of SVA were idenfied worldwide. Table 2 shows the SVA cases reported since 2004. SVA can occur in all age groups and is more common unilaterally, and *Escherichia coli* is the main pathogenic bacteria. The etiology of SVA is unknown, but long-term indwelling catheters, diabetes, prostate puncture biopsy, and endoscopic operation are factors contributing to the susceptibility to this disease [6,7]. SVAs are mostly secondary to urinary tract infections such as prostatitis. Infections causing a SVA can also involve the blood, lymph, and other pathways[8]. In our case, the patient underwent surgical treatment of benign prostatic hyperplasia. He suffered difficulty urinating and had a long-term indwelling urinary catheter. We speculate that his previous medical history is an important risk factor for SVA.

SVA lacks specific clinical symptoms. Because the vesicles are anatomically adjacent to the bladder and other tissues, dysuria, testicular and groin pain, tenesmus, *etc.* are common clinical manifestations. Pandey *et al*[9] reviewed reports on these clinical manifestations; 74% of patients had fever, 58% had dysuria, and 32% had mild prostatitis[9]. Swollen glands can be found on digital anal examination.

Table 2 Summary of literature on primary seminal vesicle abscess treated by surgery since 2004

Ref.	Year	No.	Age	Complaints	Imaging	Surgery	Pathogens	Location	Underlying causes
Dewani *et al* [15]	2006	1	35	Infertility, hemospermia	CUS, US	Abscess incision, catheterization	Acid-fast bacilli	Unilateral	N/A
Chong *et al* [16]	2014	1	38	Fever, lethargy, rigor, anorexia	N/A	Percutaneous drainage	*Burkholderia pseudomallei*	N/A	Melioidosis, diabetes
Bayne *et al* [11]	2013	1	67	Myalgias, chills	MRI, IVP	Percutaneous drainage	*Escherichia coli*	Left	Transrectal biopsy
Hammad[17]	2006	1	24	Urinary frequency, urgency, urge incontinence	CUS, CT, IVP	Perirectal incision and drainage	N/A	Left	N/A
Fujinaga *et al* [18]	2008	1	2 ms	Fever with leukocyturia	CUS, CT	Percutaneous transrectal aspiration	*Escherichia coli*	Left	Dysplastic left kidney
Wadei *et al* [19]	2008	1	29	Fever, dysuria, right-sided testicular pain	CT, MRI	Transrectal aspiration	*Staphylococcus*, *Proteus mirabilis*, *Clostridium* species	Right	Donor kidney transplant
Talwar *et al* [20]	2021	1	20	Fever, oliguria and uremic symptoms	MRI	Transrectal aspiration	*Escherichia coli*	Left	Zinner syndrome
Monzó *et al* [21]	2005	1	38	Dysuria, frequent urination and fever	US	Transrectal puncture drainage	*Escherichia coli*	Left	Bilateral orchiopexy
Machida *et al* [22]	2008	1	81	Swelling and left inguinal pain	CT	Inguinal canal ligation and percutaneous suprapubic vesical catheterization	*Escherichia coli*	Left	Diabetes
Bradley and Scoular[23]	2021	1	42	Subjective fevers and worsening fatigue	CT	Transurethral resection of the prostate	*Candida parapsilosis*, *Candida glabrata*, *Bacteroides fragilis*	Left	Diabetes
Sağlam *et al* [5]	2004	6	18-47	Rectal discomfort, left inguinal tender-swelling	N/A	Transrectal (2)/Transperineal (4) puncture and aspiration	*Escherichia coli*	Bilateral (4)/Unilateral (2)	2 with rectal cancer
Sihra *et al*[12]	2018	1	29	Right hemiscrotal pain, swelling, and pyrexia	US, CUS	Incision, drainage, transvesical deroofing of abscess	*Staphylococcus aureus*	Right	Elective vasectomy
Saha *et al*[7]	2009	1	49	Gradually enlarging, exquisitely tender groin mass	CT, MRI, CUS, IVP	Laparoscopic drainage of the abscess	*Escherichia coli*	Left	Drainage of perianal abscess
Imperatore *et al*[24]	2017	1	58	Dysuria and fever	CT	Open abdominal pus drainage	N/A	Bilateral	N/A
Zheng *et al* [25]	2015	1	42	Severe dysuria abdominal pain	US, MRI	Percutaneously drainage	*Staphylococcus aureus* and *Candida albicans*	Left	Diabetes
Cui *et al*[26]	2014	3	31-58	N/A	US, CT	F4 single "J" catheterization	N/A	N/A	N/A
Kuribayashi *et al*[27]	2017	1	26	Fever and right seminal vesicle swelling	US, CT	Transperineal needle aspiration	*Staphylococcus aureus*	Right	Zinner syndrome
Somiya *et al* [28]	2018	1	89	Left lower quadrant bulge	CT, CUS	Transperineal needle aspiration	*Streptococcus viridans*	Right	Transurethral prostate resection

US: Ultrasound; CT: Computed tomography; MRI: Magnetic resonance imaging; IVP: Intravenous pyelography; CUS: Cystourethroscopy; N/A: Not applicable.

Ultrasound, CT, and other imaging examinations are the methods used for diagnosing SVA[6]. The typical CT manifestations include unilateral or bilateral seminal vesicle dilation, central irregular low-density areas, and thickening of adjacent organs[5]. On MRI, the abscesses are usually round, with low T1-weighted imaging and high T2-weighted imaging signals[10].

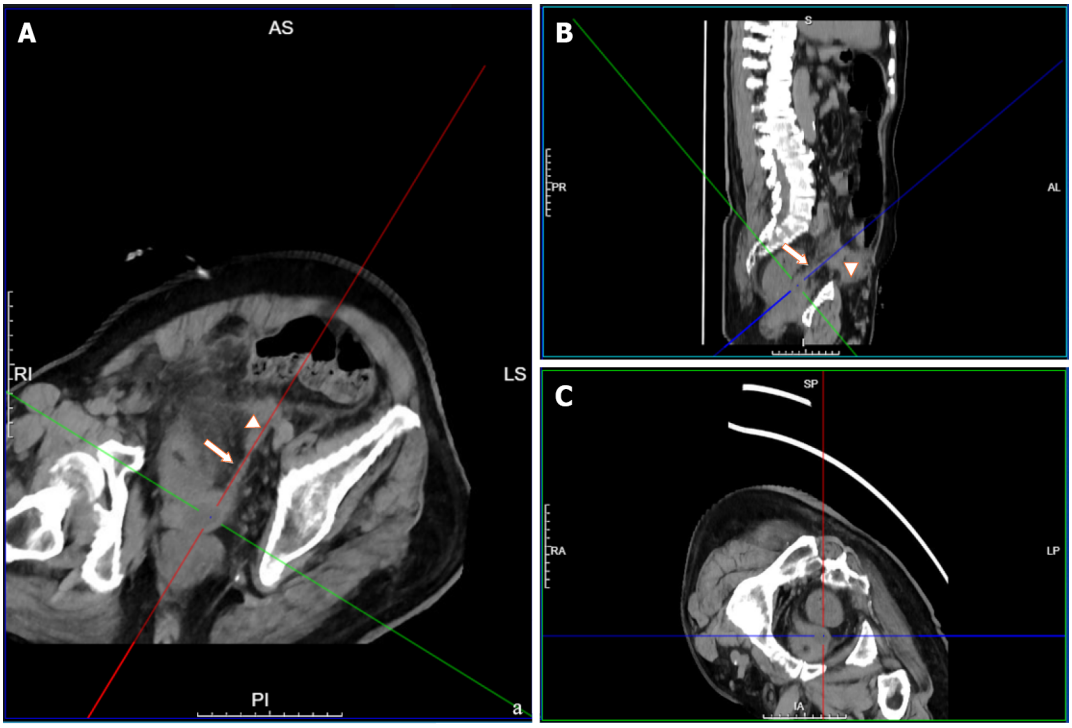

DOI: 10.12998/wjcc.v11.i3.645

Figure 4 Three-dimensional computed tomography reconstruction showing the primary and secondary abscesses. A: Transverse view; B: Sagittal view; C: Coronal view. The primary focus is located at the baseline center, the white arrows indicate the vas deferens, and the arrowheads show the secondary focus.

Infectious diseases can occur in the seminal vesicles, for which antibiotic anti-infective treatment is the first choice. However, once an abscess is formed, conservative treatment is often ineffective[5]. Because of the trauma and long recovery time of open surgery, abscess puncture and drainage is currently the first choice for treatment. The common puncture methods include transurethral/transvesical drainage under cystoscopy and ultrasound-guided transrectal drainage[11,12]. Regarding the diagnosis and treatment of this case, the patient was admitted to the hospital and due to the ineffectiveness of conservative treatment, the left SVA of the perineum was punctured and drained under local anesthesia, and a small amount of purulent fluid was aspirated out. However, the symptoms were not significantly relieved after puncture, and the infection was exacerbated. In addition, abdominal CT showed the possibility of an abdominal abscess, so an exploratory laparotomy was performed.

Abdominal cavity infection is a common and frequently occurring disease in general surgery and is caused by bacteria, chemical stimulation, and other factors. Intraperitoneal organ rupture, perforation, trauma, and other diseases are common causes of peritonitis. The common pathogenic bacteria of peritonitis include hemolytic *Streptococcus*, *Pneumococcus*, and *Escherichia coli*[13,14]. Direct diffusion is one of the main routes by which bacteria enter the abdominal cavity. In this case, neither preoperative imaging examination nor intraoperative exploration revealed perforation or rupture of any abdominal organs that may have led to secondary peritonitis. Culture of the pus showed *Klebsiella pneumoniae*, which is not surprising, considering that this species originates from the urinary system. By repeating the preoperative abdominal imaging examination, we found that the primary foci of the SVA spread through the ejaculatory duct-vas deferens and accumulated in the loose connective tissue of the extraperitoneal fascia to form secondary foci. The transverse abdominis muscle was anterior to the secondary abscess, and the peritoneal reflex was superior, where purulent material contacted the peritoneum, resulting in acute peritonitis and intra-abdominal inflammation (Figures 4 and 5).

CONCLUSION

By reviewing the diagnosis and treatment of this case, we summarize our experience and conclusions as follows: (1) An indwelling urinary catheter increases the risk of urinary tract infection, and the catheter indwelling time should be shortened as much as possible. For patients who must have a long-term indwelling catheter, the catheter should be replaced regularly, and high-quality nursing care should be actively performed. Elderly and frail patients with urinary tract infection should be treated in a timely

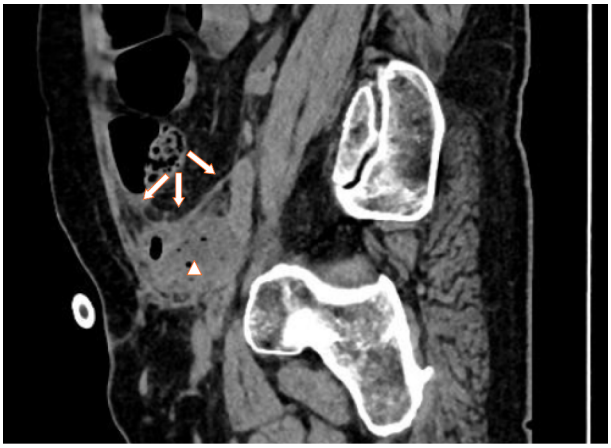

DOI: 10.12998/wjcc.v11.i3.645

Figure 5 Sagittal computed tomography image showing the relationship between the secondary focus and the pelvis and abdominal cavity. The white arrows indicate the peritoneum, and the arrowhead shows the secondary focus.

manner to prevent the occurrence of complications; (2) For bacterial resistance, multiple infections, and other problems, broad-spectrum antibiotics are used for anaerobic bacteria and Gram-negative bacteria; and (3) Early primary disease and complications should be considered at the same time, including the full drainage of SVA in the early stage, as well as active surgical intervention for abdominal infection. Clinicians can use various imaging examinations to fully understand the occurrence, development, and prognosis of the disease. In this case, the general condition of the patient before surgery was poor, and the patient's condition was complicated with sepsis. Early exploratory laparotomy, removal of the abscess, and adequate drainage were the best options.

ACKNOWLEDGEMENTS

We sincerely thank Sheng-Song Huang and Wei Le for their help in the treatment and differential diagnosis of this patient.

FOOTNOTES

Author contributions: Shi BM and Chen QN contributed to the conception and design of the study and performed the operation on the patient; Li K and Liu NB collected the data, performed the data analysis, and wrote the initial draft of the manuscript; Liu JX participated in the clinical management and follow-up of the patient, and analyzed and interpreted the data; all authors contributed to drafting and revising the manuscript and approved the submitted version.

Informed consent statement: Informed written consent was obtained from the patient for publication of this report and any accompanying images.

Conflict-of-interest statement: All the authors report no relevant conflicts of interest for this article.

CARE Checklist (2016) statement: The authors have read the CARE Checklist (2016), and the manuscript was prepared and revised according to the CARE Checklist (2016).

Country/Territory of origin: China

ORCID number: Quan-Ning Chen 0000-0002-3170-9245; Bao-Min Shi 0000-0001-8791-569X.

S-Editor: Fan JR
L-Editor: Wang TQ

P-Editor: Fan JR

REFERENCES

1 **Hoshino N**, Endo H, Hida K, Kumamaru H, Hasegawa H, Ishigame T, Kitagawa Y, Kakeji Y, Miyata H, Sakai Y. Laparoscopic Surgery for Acute Diffuse Peritonitis Due to Gastrointestinal Perforation: A Nationwide Epidemiologic Study Using the National Clinical Database. *Ann Gastroenterol Surg* 2022; **6**: 430-444 [PMID: 35634193 DOI: 10.1002/ags3.12533]

2 **Rajfer J**, Eggleston JC, Sanders RC, Walsh PC. Fever and prostatic mass in a young man. *J Urol* 1978; **119**: 555-558 [PMID: 650769 DOI: 10.1016/s0022-5347(17)57546-1]

3 **Nguyen HT**, Etzell J, Turek PJ. Normal human ejaculatory duct anatomy: a study of cadaveric and surgical specimens. *J Urol* 1996; **155**: 1639-1642 [PMID: 8627842 DOI: 10.1016/s0022-5347(01)66150-0]

4 **Huang YH**, Chen YH, Lin CM, Ciou YY, Kuo SP, Chen CT, Shih CM, Chang EE. Suppression effect of seminal vesicle autoantigen on platelet-activating factor-induced mouse sperm capacitation. *J Cell Biochem* 2007; **100**: 941-951 [PMID: 17131380 DOI: 10.1002/jcb.21050]

5 **Sağlam M**, Uğurel S, Kilciler M, Taşar M, Somuncu I, Uçöz T. Transrectal ultrasound-guided transperineal and transrectal management of seminal vesicle abscesses. *Eur J Radiol* 2004; **52**: 329-334 [PMID: 15643719 DOI: 10.1016/j.ejrad.2003.11.006]

6 **Patel B**, Gujral S, Jefferson K, Evans S, Persad R. Seminal vesicle cysts and associated anomalies. *BJU Int* 2002; **90**: 265-271 [PMID: 12133063 DOI: 10.1046/j.1464-410x.2002.02883.x]

7 **Saha S**, Wright G, Arulampalam T, Corr J. An unusual groin mass. Seminal vesicle abscess: a case report. *Cases J* 2009; **2**: 6531 [PMID: 19829819 DOI: 10.1186/1757-1626-2-6531]

8 **Zhang JQ**, He CC, Yuan B, Liu R, Qi YJ, Wang ZX, He XN, Li YM. Fatal systemic emphysematous infection caused by Klebsiella pneumoniae: A case report. *World J Clin Cases* 2022; **10**: 2610-2615 [PMID: 35434061 DOI: 10.12998/wjcc.v10.i8.2610]

9 **Pandey P**, Peters J, Shingleton WB. Seminal vesicle abscess: a case report and review of literature. *Scand J Urol Nephrol* 1995; **29**: 521-524 [PMID: 8719375 DOI: 10.3109/00365599509180039]

10 **Chen X**, Wang H, Wu RP, Liang H, Mao XP, Mao CQ, Zhu HZ, Qiu SP, Wang DH. The performance of transrectal ultrasound in the diagnosis of seminal vesicle defects: a comparison with magnetic resonance imaging. *Asian J Androl* 2014; **16**: 907-911 [PMID: 25337847 DOI: 10.4103/1008-682X.142768]

11 **Bayne CE**, Davis WA, Rothstein CP, Engel JD. Seminal vesicle abscess following prostate biopsy requiring transgluteal percutaneous drainage. *Can J Urol* 2013; **20**: 6811-6814 [PMID: 23783054]

12 **Sihra N**, Aboelsoud M, Oliyide A, Counsell A, Gall Z. Seminal Vesicle Abscess-An Unusual Complication Following Vasectomy. *Urology* 2018; **116**: 20-22 [PMID: 29305203 DOI: 10.1016/j.urology.2017.12.015]

13 **Labricciosa FM**, Sartelli M, Abbo LM, Barbadoro P, Ansaloni L, Coccolini F, Catena F. Epidemiology and Risk Factors for Isolation of Multi-Drug-Resistant Organisms in Patients with Complicated Intra-Abdominal Infections. *Surg Infect (Larchmt)* 2018; **19**: 264-272 [PMID: 29298133 DOI: 10.1089/sur.2017.217]

14 **Inoue M**, Kako E, Kinugasa R, Sano F, Iguchi H, Sobue K. Necrotizing fasciitis following primary peritonitis caused by Streptococcus pyogenes with covS mutation in a healthy woman: a case report. *JA Clin Rep* 2019; **5**: 29 [PMID: 32025929 DOI: 10.1186/s40981-019-0249-7]

15 **Dewani CP**, Dewani N, Bhatia D. Case report: tubercular cold abscess of seminal vesicle: minimally invasive endoscopic management. *J Endourol* 2006; **20**: 436-442 [PMID: 16808660 DOI: 10.1089/end.2006.20.436]

16 **Chong Vh VH**, Sharif F, Bickle I. Urogenital melioidosis: a review of clinical presentations, characteristic and outcomes. *Med J Malaysia* 2014; **69**: 257-260 [PMID: 25934955]

17 **Hammad FT**. Seminal vesicle cyst forming an abscess and fistula with the rectum review of perianal drainage and treatment. *Scand J Urol Nephrol* 2006; **40**: 426-428 [PMID: 17060091 DOI: 10.1080/00365590600795313]

18 **Fujinaga S**, Hirano D, Hara S, Uchida H, Kitano Y, Kobayashi K, Tada M, Someya T, Ohtomo Y, Shimizu T. Seminal vesicle abscesses associated with ipsilateral multicystic dysplastic kidney in an infant. *Pediatr Nephrol* 2008; **23**: 1551-1554 [PMID: 18458954 DOI: 10.1007/s00467-008-0839-5]

19 **Wadei HM**, Brumble L, Broderick GA, Gonwa TA. Polymicrobial seminal vesical abscess in a kidney transplant recipient. *Urology* 2008; **72**: 296 [PMID: 18468658 DOI: 10.1016/j.urology.2008.03.039]

20 **Talwar HS**, Mittal A, Narain TA, Panwar VK. A wide spectrum of rare clinical variants of Zinner syndrome. *BMJ Case Rep* 2021; **14** [PMID: 33462046 DOI: 10.1136/bcr-2020-239254]

21 **Monzó JI**, Garcia EL, Benavente R, Moralejo Gárate M, Cordero J, Fernández C. Absceso Primario de vesícula seminal: Diagnóstico y tratamiento mediante ecografía transrectal. *ACTAS UROL ESP* 2005; 29 [DOI: 10.4321/S0210-48062005000500015]

22 **Machida H**, Ueno E, Nakazawa H, Fujimura M, Ito F. Spermatic cord abscess with concurrent prostatic abscess involving the seminal vesicle. *Radiat Med* 2008; **26**: 81-83 [PMID: 18301983 DOI: 10.1007/s11604-007-0193-8]

23 **Bradley ME**, Scoular SK. Metastatic Klebsiella pneumoniae Invasive Liver Abscess Syndrome in Denver, Colorado. *J Pharm Pract* 2021; **34**: 332-336 [PMID: 31645222 DOI: 10.1177/0897190019882867]

24 **Imperatore V**, Creta M, Di Meo S, Buonopane R, Spirito L, Mirone V. Seminal vesicle abscess causing unilateral hydroureteronephrosis: A case report. *Arch Ital Urol Androl* 2017; **89**: 321-322 [PMID: 29473388 DOI: 10.4081/aiua.2017.4.321]

25 **Zheng X**, Wang X, Zhou J, Xiang J, Xie L. Diagnosis and treatment of community-associated methicillin-resistant Staphylococcus aureus prostatic abscess involving the seminal vesicle: A case report. *Exp Ther Med* 2015; **9**: 835-838 [PMID: 25667637 DOI: 10.3892/etm.2014.2147]

26 **Cui ZQ**, Wang YC, Du J, Zhou HJ, Yu ZY, Gao EJ, Lu HK. [Transurethral seminal vesiculoscopy combined with finasteride for recurrent hematospermia]. *Zhonghua Nan Ke Xue* 2014; **20**: 536-538 [PMID: 25029861]

27 **Kuribayashi S**, Tanigawa G, Okuda Y, Kawamura M, Kishimoto N, Takezawa K, Tsutahara K, Takao T, Yamaguchi S. [Seminal Vesicle Abscess Associated with Zinner Syndrome]. *Hinyokika Kiyo* 2017; **63**: 439-443 [PMID: 29103260 DOI: 10.14989/ActaUrolJap_63_10_439]

28 **Somiya S**, Tamaki M, Fujikawa S, Yamada Y, Kamiyama Y, Kanaoka T. [A Case of Seminal Vesicle Cyst Incidentally Diagnosed during Rupture of Abdominal Subcutaneous Abscess]. *Hinyokika Kiyo* 2018; **64**: 193-195 [PMID: 29772623 DOI: 10.14989/ActaUrolJap_64_4_193]

World Journal of Clinical Cases

Submit a Manuscript: https://www.f6publishing.com

World J Clin Cases 2023 January 26; 11(3): 655-661

DOI: 10.12998/wjcc.v11.i3.655

ISSN 2307-8960 (online)

CASE REPORT

Young thoracic vertebra diffuse idiopathic skeletal hyperostosis with Scheuermann disease: A case report

Wen-Zheng Liu, Zheng-Qi Chang, Zhe-Ming Bao

Specialty type: Medicine, research and experimental

Provenance and peer review: Unsolicited article; Externally peer reviewed.

Peer-review model: Single blind

Peer-review report's scientific quality classification

Grade A (Excellent): 0
Grade B (Very good): 0
Grade C (Good): C
Grade D (Fair): 0
Grade E (Poor): 0

P-Reviewer: Bains L, India

Received: September 29, 2022
Peer-review started: September 29, 2022
First decision: December 13, 2022
Revised: December 15, 2022
Accepted: January 5, 2023
Article in press: January 5, 2023
Published online: January 26, 2023

Wen-Zheng Liu, The First Clinical Medical College, Shandong University of Traditional Chinese Medicine, Jinan 250000, Shandong Province, China

Wen-Zheng Liu, Zheng-Qi Chang, Zhe-Ming Bao, Department of Orthopedics, 960th Hospital of PLA, Jinan 250031, Shandong Province, China

Corresponding author: Zheng-Qi Chang, MD, Associate Chief Physician, Associate Professor, Department of Orthopedics, 960th Hospital of PLA, No. 25 Shifan Road, Tianqiao District, Jinan 250031, Shandong Province, China. 26766771@qq.com

Abstract

BACKGROUND

Diffuse idiopathic skeletal hyperostosis (DISH) is a disorder characterised by the calcification and ossification of ligaments and entheses. It is a frequent occurrence in elderly males, but rarely encountered in younger individuals.

CASE SUMMARY

A 24-year-old male was admitted to the hospital due to low back pain accompanied with numbness in both lower limbs for 10 d. Upon clinical examination and imaging tests, the patient was diagnosed with DISH with Scheuermann disease and thoracic spinal stenosis. Before the operation and medical treatment, the patient had hypoesthesia of the skin below the xiphoid process. Afterward, a standard laminectomy was conducted using ultrasonic bone curette and internal fixation was applied. Subsequently, the patient was given corticosteroids, neurotrophic drugs, hyperbaric oxygen and electric stimulation. As a result of the treatment, the patient's sensory level decreased to the navel level and there was no major change in the muscle strength of the lower limbs. During follow-up, the patient's skin sensation has returned to normal.

CONCLUSION

This case is a rare instance of DISH co-existing with Scheuermann's disease in a young adult. This provides a valuable reference point for spine surgeons, as DISH is more commonly observed in middle-aged and elder adults.

Key Words: Diffuse idiopathic skeletal hyperostosis; Scheuermann disease; Thoracic spinal stenosis; Case report

Core Tip: This case report presents a rare instance of diffuse idiopathic skeletal hyperostosis in a 24-year-old male patient, which is a condition that is usually seen in elderly males. The patient was also diagnosed with Scheuermann disease. By providing clinical data and treatment experience of this patient, it is hoped that it will help to improve the understanding of related diseases, and reduce the chances of misdiagnosis.

Citation: Liu WZ, Chang ZQ, Bao ZM. Young thoracic vertebra diffuse idiopathic skeletal hyperostosis with Scheuermann disease: A case report. *World J Clin Cases* 2023; 11(3): 655-661
URL: https://www.wjgnet.com/2307-8960/full/v11/i3/655.htm
DOI: https://dx.doi.org/10.12998/wjcc.v11.i3.655

INTRODUCTION

Diffuse idiopathic skeletal hyperostosis (DISH) is an ailment caused by the calcification and ossification of the entheses that primarily affects the spine and other peripheral areas[1]. Primarily, DISH affects the thoracic spine of the axial skeleton; however, other spinal regions are often affected too. Studies demonstrate that DISH is more predominant among middle-aged and elderly individuals and the rate of occurrence increases with age. Moreover, there is a higher rate of male patients than female patients [2]. Scheuermann's disease was initially described by Scheuermann[3], a Danish physician, in 1921. The main symptom of this condition is the formation of three adjacent vertebrae that are angled by at least 5 degrees, resulting in the spine's kyphoscoliosis. Radiographic features of Scheuermann's disease include wedged vertebrae, irregular vertebral endplates, and Schmorl's nodes[4]. In this paper, we present a case of a young patient who was eventually diagnosed with DISH in combination with Scheuermann disease and thoracic spinal stenosis (TSS) in our hospital. While DISH is usually observed in middle-aged and elderly individuals, there is a lack of reports on young DISH patients. Moreover, it is even rarer for young DISH to be associated with Scheuermann disease, thus making this case worth reporting. We have reviewed the characteristics of the case, as well as the diagnosis and treatment process, in order to expand the current knowledge on the diagnosis and treatment of related diseases.

CASE PRESENTATION

Chief complaints

The 24-year-old male patient was hospitalized for 10 d due to lower back pain and numbness in both lower limbs.

History of present illness

The 24-year-old male patient was hospitalized for 10 d due to lower back pain and numbness in both lower limbs. On physical examination, thoracodorsal kyphosis was observed and the skin below xiphoid had hypoesthesia. Furthermore, the muscle strength of the right iliopsoas, quadriceps femoris and biceps femoris was graded as III, while the right tibialis anterior and extensor dorsi were graded as IV. At admission, the patient experienced radiating pain in his waist, which had a VAS score of 8.

History of past illness

The patient reported no other medical history such as hypertension and diabetes.

Personal and family history

The patient denied any personal and family history of illness.

Physical examination

On physical examination, thoracodorsal kyphosis was observed and the skin below xiphoid had hypoesthesia. Furthermore, the muscle strength of the right iliopsoas, quadriceps femoris and biceps femoris was graded as III, while the right tibialis anterior and extensor dorsi were graded as IV. At admission, the patient experienced radiating pain in his waist, which had a VAS score of 8.

Laboratory examinations

To differentiate DISH from ankylosing spondylitis, it is necessary to test for human leukocyte antigen-B27 (HLA-B27). The patient's HLA-B27 index is within the normal range. Additionally, the patient's erythrocyte sedimentation rate, blood routine test and other biochemical indicators are all within the normal range.

Imaging examinations

Anterior-lateral X-ray: Kyphosis of the thoracic spine is present, with calcification of the anterior longitudinal ligament and lamellar ossification/floating bone bridge on the medial-inferior and medial-superior sides of the anterior and lateral edges of vertebral plates. Additionally, there is a local wedge-shaped deformation of the lower thoracic vertebra (Figure 1).

Thoracic computed tomography (CT) scan revealed a kyphosis in the thoracic spine and calcification of the anterior longitudinal ligament of multiple vertebral bodies. The T8-12 vertebral body was wedge-shaped with a narrow front and wide back. The T5/6, T7/8, and T8/9 intervertebral discs were observed to protrude backward, resulting in compression of the corresponding horizontal segment dural sac. Furthermore, the adequate space of the spinal canal was constricted, and the spinal cord was compressed due to hyperplasia and sclerosis of the bilateral facet joints of the T7-9 vertebral body (Figure 2).

Results of a three-dimensional reconstruction revealed calcification of the anterior longitudinal ligament of numerous vertebral bodies, which has formed a bony bridge. The T8-12 vertebral body was found to be wedge-shaped, with a narrow front and wide back, as well as hyperplasia and sclerosis of both facet joints of the T7-9 vertebral body (Figure 3).

Thoracic magnetic resonance imaging showed kyphosis in the local thoracic spine. The T8-12 vertebrae have a wedge-like shape, with a thin anterior side and a wide posterior side. The intervertebral discs between T5/6, T7/8, and T8/9 protrude posteriorly and the adjacent dural sac is compressed. Additionally, no alterations in the spinal cord signal intensity were observed (Figure 4).

FINAL DIAGNOSIS

The patient was diagnosed with DISH with Scheuermann disease and TSS.

TREATMENT

The patient's TSS symptoms were serious, resulting in paraplegia of the lower limbs. To address this, we opted for a laminectomy with an ultrasonic bone curette and internal fixation. After the procedure, we administered corticosteroids, neurotrophic medications, hyperbaric oxygen, and electrical stimulation to the patient for further treatment.

OUTCOME AND FOLLOW-UP

After the surgery and medication, the patient's sensory level decreased to the navel level with no noteworthy alteration in the muscle strength of the lower limbs. The VAS score was also decreased to 2 points. During the follow-up, the lumbar pain was completely gone and the patient's skin sensation was back to normal. The patient was also capable of walking 1.5 kilometers. The postoperative reexamination revealed that the internal fixation position was successful (Figure 5).

DISCUSSION

The diagnosis of DISH is based on radiographic criteria proposed by Resnick and Niwayama[5] in 1976, which include the presence of flowing calcification and ossification along the anterolateral aspects of at least four contiguous vertebral bodies, relative preservation of disc height in the problematic areas, and absence of apophyseal joint bony ankylosis and sacroiliac joint erosion, sclerosis or bony fusion. This patient fulfilled these criteria and was thus diagnosed with DISH. DISH is most commonly found in the thoracic spine, where it presents as wavy ossification in front of the thoracic centrum, forming bone bridges across the intervertebral spaces, and is most commonly located on the right side[6]. It may also occur in the lower cervical spine and the upper lumbar segments[7]. It is important to differentiate DISH from ankylosing spondylitis, which can be done by examining the patient's joint space, inflammatory manifestations of the articular surface, morning stiffness, and limited joint mobility, as well as HLA-B27 values. In this case, the patient did not present with any of these features and had normal HLA-B27 values, thus excluding the possibility of ankylosing spondylitis.

Patients with DISH usually do not present with any noticeable symptoms and rarely require treatment. However, when DISH is accompanied by ossification of the ligamentum flavum and posterior longitudinal ligament, which compresses the spinal cord or nerve, surgery is necessary[8]. This condition is usually discovered incidentally during imaging tests, and the prevalence rate increases with age[6]. Studies have found that the incidence of DISH in males over 50 is more than 25%[2], and is

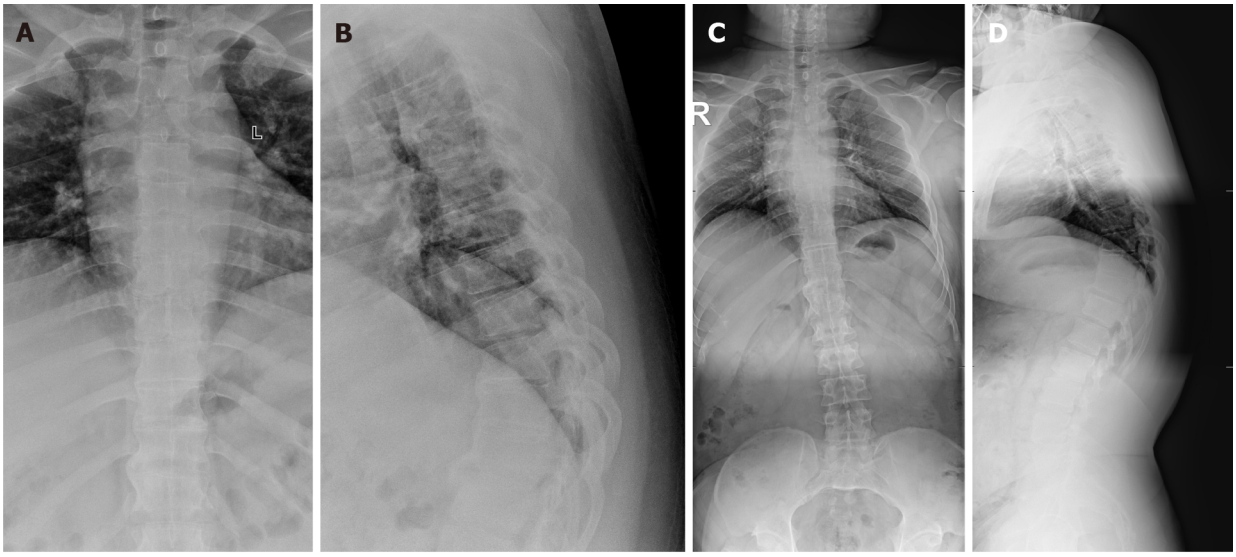

DOI: 10.12998/wjcc.v11.i3.655

Figure 1 X-ray before treatment. A: An anterior X-ray of the thoracic vertebra before operation; B: A lateral X-ray of the thoracic vertebra before operation; C: An anterior X-ray of the full-length of the spine before operation; D: A lateral X-ray of the full-length of the spine before operation.

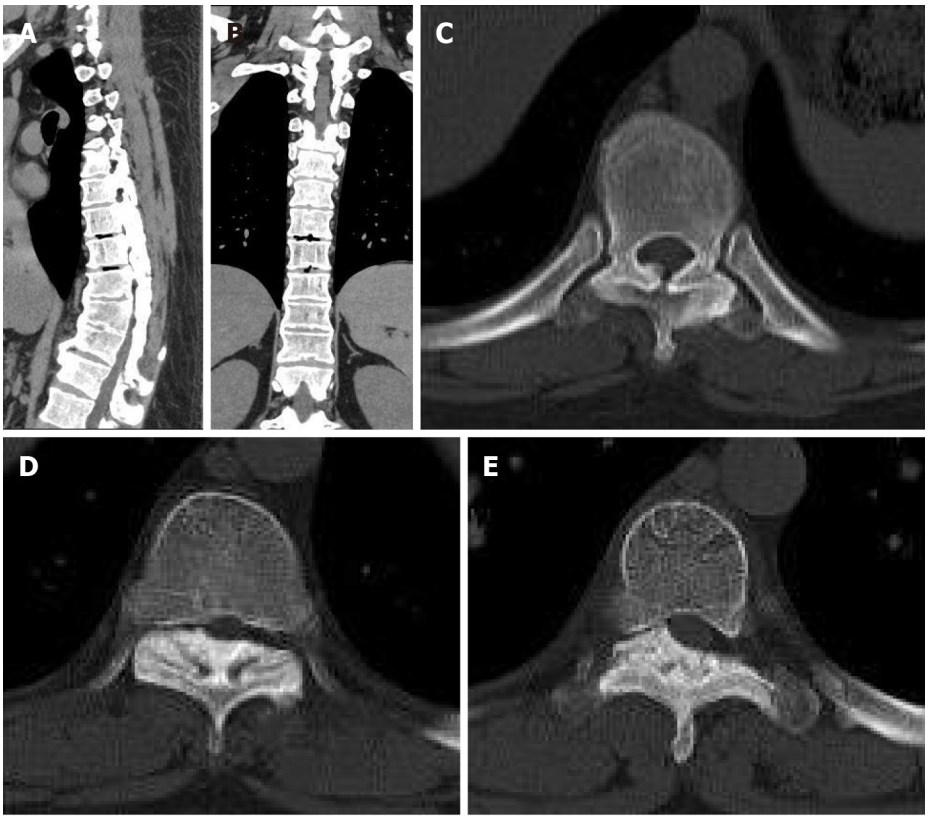

DOI: 10.12998/wjcc.v11.i3.655

Figure 2 Thoracic computed tomography before treatment. A and B: A computed tomography scan of the anterior thorax has revealed calcification of the anterior longitudinal ligament in multiple vertebral bodies; C-E: They were the T5/6, T7/8, and T8/9 intervertebral spaces. The T5/6, T7/8, and T8/9 intervertebral discs protrude backward, and the corresponding horizontal segment of the dural sac is compressed.

associated with age, obesity, and diabetes[9]. In contrast, the incidence of DISH in individuals under 40 is extremely low, with only a few cases reported in the literature[10]. A Japanese study of 345 patients with spinal column diseases revealed that the youngest patient with DISH was 37 years old[11]. Additionally, a study of 1479 patients undergoing chest CT scans showed that the average age of DISH was 54.7 years old, with only one patient under the age of 40[6]. A cross-sectional study of 2000 subjects in China found that the mean age of DISH was 58.7 years old, and there were no cases of DISH in

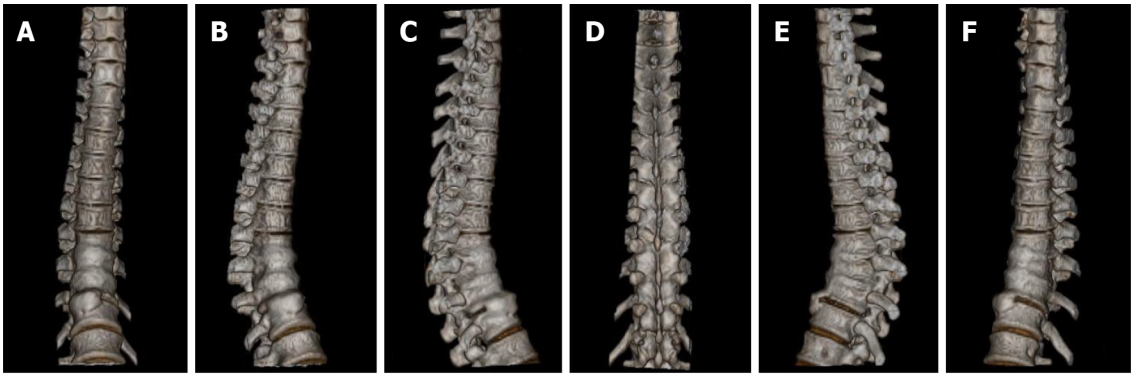

DOI: 10.12998/wjcc.v11.i3.655

Figure 3 Three-dimensional reconstruction before treatment. A-F: Three-dimensional reconstruction.

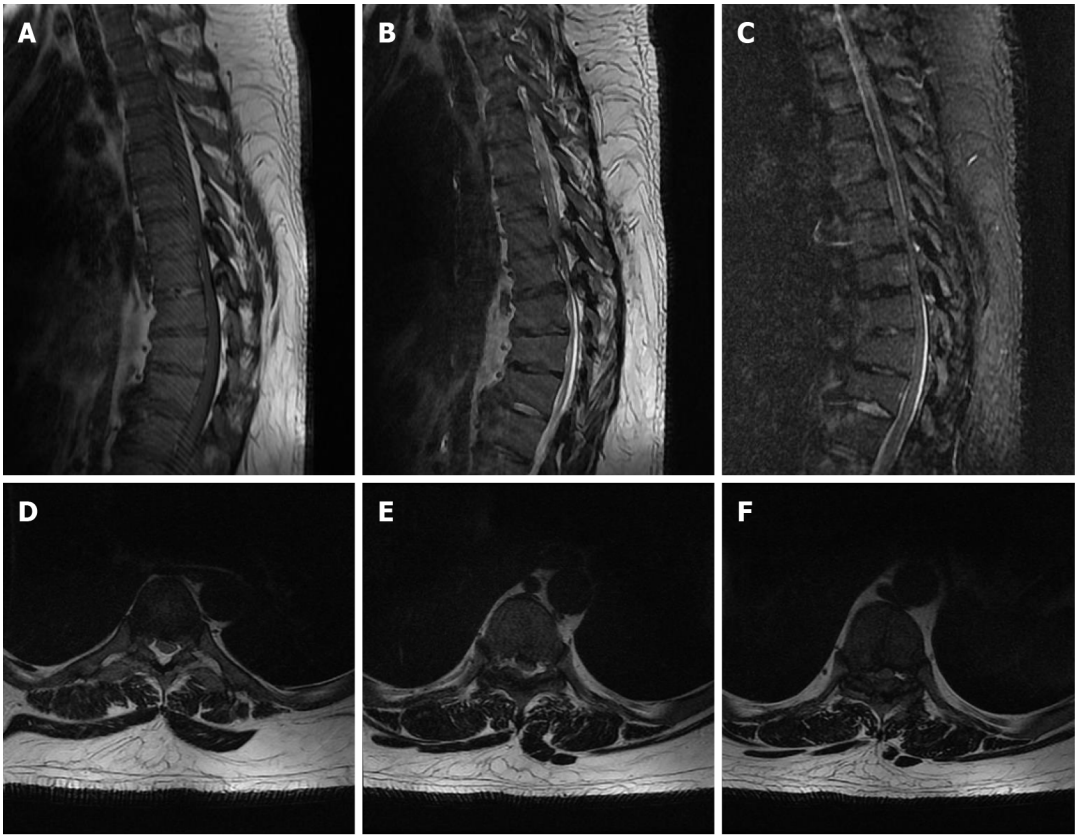

DOI: 10.12998/wjcc.v11.i3.655

Figure 4 Thoracic magnetic resonance imaging before treatment. A-C: An magnetic resonance imaging of the thoracic spine revealed a kyphosis in the local thoracic region. The T8-12 vertebral bodies were observed to have a wedge-like shape, with a narrow front and a wide back; D-F: They were the T5/6, T7/8, and T8/9 intervertebral spaces. The T5/6, T7/8, and T8/9 intervertebral discs protrude backward, and the corresponding horizontal segment of the dural sac is compressed.

subjects under 40[10].

In 1964, Sorensen first proposed X-ray imaging diagnostic criteria for Scheuermann's disease[12], which includes at least three adjacent vertebrae with a minimum of 5° wedging. Subsequent research has expanded the understanding of the condition and refined the diagnostic criteria, which include vertebral body wedging, vertebral endplate irregularity, Schmorl's nodes, and narrowing of intervertebral disk spaces. Common symptoms in the early stages of the disease include chest and back pain. Our patient was a young individual with no prior history of spinal deformity, and they presented with the aforementioned symptoms. Scheuermann's disease is a relatively common condition in adolescents, with an estimated prevalence of 1%-8%[13]. It usually presents as mild kyphosis and does not usually cause functional impairment. However, if the kyphosis worsens and is accompanied by disc herniation or spinal stenosis, prompt surgical intervention may be necessary[12]. Furthermore, a recent study reported a prevalence of syringomyelia of 5.8% in patients with Scheuermann's disease[14], therefore,

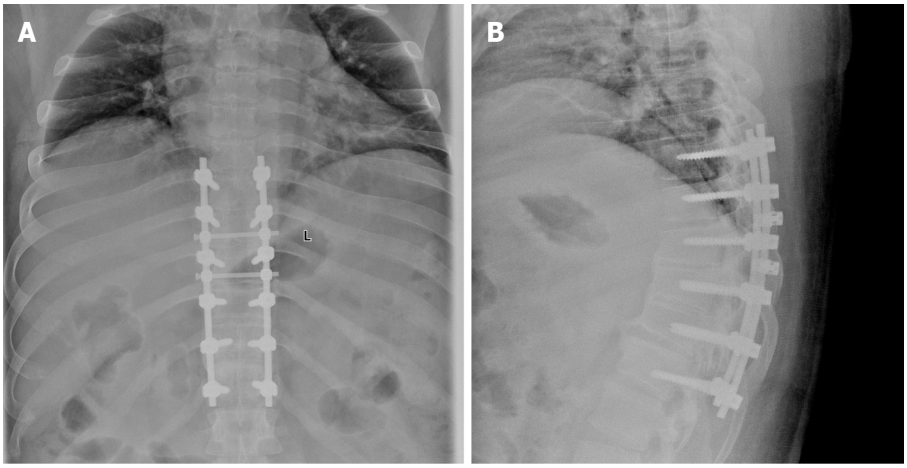

DOI: 10.12998/wjcc.v11.i3.655

Figure 5 X-ray after treatment. A and B: Anterior X-ray of thoracic vertebra before operation. They showed that the internal fixation position was suitable.

any changes in spinal cord signals should be taken seriously and prompt surgical intervention should be considered.

TSS is associated with secondary pathological factors such as ossification of ligamentum flavum and ossification of posterior longitudinal ligament secondary to ankylosing spondylitis and DISH. It is reported that the highest incidence of TSS is seen in individuals aged 50-60 years old[15]. When TSS has resulted in obvious spinal cord compression and deformation (grade IV) and the patient has developed neurologic deficits, decompression surgery should be considered[16]. Depending on the location of the lesion, TSS surgery mainly includes dorsal spinal canal decompression and ventral or annular spinal canal decompression[17]. In the present case, spinal canal decompression and pedicle screw fixation were performed taking into account the patient's medical history and rate of disease progression. Post-operatively, the patient's sensory level decreased without any worsening such as spinal cord ischemia-reperfusion injury. Additionally, the physiological curvature and stability of the spine were restored.

CONCLUSION

The rarity of DISH with Scheuermann disease and TSS in a 24-year-old patient poses a challenge in terms of early detection and diagnosis. Thus, medical practitioners should strive to broaden their knowledge and differential diagnosis skills regarding related diseases in order to improve the accuracy of diagnosis. By studying the clinical data and treatment experience of similar patients, doctors can gain a better understanding of DISH in young patients and reduce the chances of misdiagnosis or delayed diagnosis.

FOOTNOTES

Author contributions: Liu WZ and Chang ZQ conceived the research, performed clinical examinations, and wrote and revised the manuscript; Bao ZM and Chang ZQ evaluated the imaging of the patient; and all authors contributed to the article and approved the final version. Liu WZ and Bao ZM are co-first authors of the article.

Informed consent statement: The patient described in this report provided verbal informed consent.

Conflict-of-interest statement: All the authors report no relevant conflicts of interest for this article.

CARE Checklist (2016) statement: The authors have read the CARE Checklist (2016), and the manuscript was prepared and revised according to the CARE Checklist (2016).

Country/Territory of origin: China

ORCID number: Wen-Zheng Liu 0000-0003-0537-7037; Zheng-Qi Chang 0000-0001-6490-2239; Zhe-Ming Bao 0000-0002-1000-6292.

S-Editor: Wang JJ
L-Editor: A
P-Editor: Wang JJ

REFERENCES

1 **Mader R**, Verlaan JJ, Eshed I, Bruges-Armas J, Puttini PS, Atzeni F, Buskila D, Reinshtein E, Novofastovski I, Fawaz A, Kurt V, Baraliakos X. Diffuse idiopathic skeletal hyperostosis (DISH): where we are now and where to go next. *RMD Open* 2017; **3**: e000472 [PMID: 28955488 DOI: 10.1136/rmdopen-2017-000472]
2 **Holton KF**, Denard PJ, Yoo JU, Kado DM, Barrett-Connor E, Marshall LM; Osteoporotic Fractures in Men (MrOS) Study Group. Diffuse idiopathic skeletal hyperostosis and its relation to back pain among older men: the MrOS Study. *Semin Arthritis Rheum* 2011; **41**: 131-138 [PMID: 21377195 DOI: 10.1016/j.semarthrit.2011.01.001]
3 **Lowe TG**, Line BG. Evidence based medicine: analysis of Scheuermann kyphosis. *Spine (Phila Pa 1976)* 2007; **32**: S115-S119 [PMID: 17728677 DOI: 10.1097/BRS.0b013e3181354501]
4 **Bezalel T**, Carmeli E, Been E, Kalichman L. Scheuermann's disease: current diagnosis and treatment approach. *J Back Musculoskelet Rehabil* 2014; **27**: 383-390 [PMID: 24898440 DOI: 10.3233/BMR-140483]
5 **Resnick D**, Niwayama G. Radiographic and pathologic features of spinal involvement in diffuse idiopathic skeletal hyperostosis (DISH). *Radiology* 1976; **119**: 559-568 [PMID: 935390 DOI: 10.1148/119.3.559]
6 **Hiyama A**, Katoh H, Sakai D, Sato M, Tanaka M, Watanabe M. Prevalence of diffuse idiopathic skeletal hyperostosis (DISH) assessed with whole-spine computed tomography in 1479 subjects. *BMC Musculoskelet Disord* 2018; **19**: 178 [PMID: 29848322 DOI: 10.1186/s12891-018-2108-5]
7 **Mader R**, Baraliakos X, Eshed I, Novofastovski I, Bieber A, Verlaan JJ, Kiefer D, Pappone N, Atzeni F. Imaging of diffuse idiopathic skeletal hyperostosis (DISH). *RMD Open* 2020; **6**: e001151 [PMID: 32111653 DOI: 10.1136/rmdopen-2019-001151]
8 **Le HV**, Wick JB, Van BW, Klineberg EO. Diffuse Idiopathic Skeletal Hyperostosis of the Spine: Pathophysiology, Diagnosis, and Management. *J Am Acad Orthop Surg* 2021; **29**: 1044-1051 [PMID: 34559699 DOI: 10.5435/JAAOS-D-20-01344]
9 **Kuperus JS**, Mohamed Hoesein FAA, de Jong PA, Verlaan JJ. Diffuse idiopathic skeletal hyperostosis: Etiology and clinical relevance. *Best Pract Res Clin Rheumatol* 2020; **34**: 101527 [PMID: 32456997 DOI: 10.1016/j.berh.2020.101527]
10 **Liang H**, Liu G, Lu S, Chen S, Jiang D, Shi H, Fei Q. Epidemiology of ossification of the spinal ligaments and associated factors in the Chinese population: a cross-sectional study of 2000 consecutive individuals. *BMC Musculoskelet Disord* 2019; **20**: 253 [PMID: 31128588 DOI: 10.1186/s12891-019-2569-1]
11 **Toyoda H**, Terai H, Yamada K, Suzuki A, Dohzono S, Matsumoto T, Nakamura H. Prevalence of Diffuse Idiopathic Skeletal Hyperostosis in Patients with Spinal Disorders. *Asian Spine J* 2017; **11**: 63-70 [PMID: 28243371 DOI: 10.4184/asj.2017.11.1.63]
12 **Diaremes P**, Braun S, Meurer A. [Scheuermann's disease]. *Orthopade* 2022; **51**: 339-348 [PMID: 35290495 DOI: 10.1007/s00132-022-04239-4]
13 **Dziewulski M**, Szymanik W. Epidemiology of Scheuermann's disease in children and adolescents. *Ortop Traumatol Rehabil* 2002; **4**: 752-757 [PMID: 18034106]
14 **Demiroz S**, Ketenci IE, Yanik HS, Bayram S, Ur K, Erdem S. Intraspinal Anomalies in Individuals with Scheuermann's Kyphosis: Is the Routine Use of Magnetic Resonance Imaging Necessary for Preoperative Evaluation? *Asian Spine J* 2018; **12**: 697-702 [PMID: 30060379 DOI: 10.31616/asj.2018.12.4.697]
15 **Guo JJ**, Luk KD, Karppinen J, Yang H, Cheung KM. Prevalence, distribution, and morphology of ossification of the ligamentum flavum: a population study of one thousand seven hundred thirty-six magnetic resonance imaging scans. *Spine (Phila Pa 1976)* 2010; **35**: 51-56 [PMID: 20042956 DOI: 10.1097/BRS.0b013e3181b3f779]
16 **Feng FB**, Sun CG, Chen ZQ. Progress on clinical characteristics and identification of location of thoracic ossification of the ligamentum flavum. *Orthop Surg* 2015; **7**: 87-96 [PMID: 26033987 DOI: 10.1111/os.12165]
17 **Dützmann S**, Fernandez R, Rosenthal D. [Thoracic spinal stenosis: Etiology, pathogenesis, and treatment]. *Orthopade* 2019; **48**: 844-848 [PMID: 31041462 DOI: 10.1007/s00132-019-03731-8]

World Journal of Clinical Cases

Submit a Manuscript: https://www.f6publishing.com

World J Clin Cases 2023 January 26; 11(3): 662-668

DOI: 10.12998/wjcc.v11.i3.662

ISSN 2307-8960 (online)

CASE REPORT

Relapsed primary extraskeletal osteosarcoma of liver: A case report and review of literature

Qiu-Yi Di, Xiang-Dang Long, Jing Ning, Zhi-Hong Chen, Zhi-Qun Mao

Specialty type: Medicine, research and experimental

Provenance and peer review: Unsolicited article; Externally peer reviewed.

Peer-review model: Single blind

Peer-review report's scientific quality classification

Grade A (Excellent): 0
Grade B (Very good): 0
Grade C (Good): C, C
Grade D (Fair): D
Grade E (Poor): 0

P-Reviewer: Ariyachet C, Thailand; Dilek ON, Turkey; Garrido I, Portugal

Received: October 31, 2022
Peer-review started: October 31, 2022
First decision: November 14, 2022
Revised: December 1, 2022
Accepted: January 5, 2023
Article in press: January 5, 2023
Published online: January 26, 2023

Qiu-Yi Di, Xiang-Dang Long, Jing Ning, Department of Ultrasound, The First Affiliated Hospital of Hunan Normal University/Hunan Provincial People's Hospital, Changsha 410005, Hunan Province, China

Zhi-Hong Chen, Department of Pathology, The First Affiliated Hospital of Hunan Normal University/Hunan Provincial People's Hospital, Changsha 410005, Hunan Province, China

Zhi-Qun Mao, Department of Radiology, The First Affiliated Hospital of Hunan Normal University/Hunan Provincial People's Hospital, Changsha 410005, Hunan Province, China

Corresponding author: Xiang-Dang Long, PhD, Professor, Department of Ultrasound, The First Affiliated Hospital of Hunan Normal University/Hunan Provincial People's Hospital, No. 61 of Jiefang West Road, Changsha 410005, Hunan Province, China. 376262716@qq.com

Abstract

BACKGROUND

Extraskeletal osteosarcoma (ESOS) is a highly malignant osteosarcoma that occurs in extraskeletal tissues. It often affects the soft tissues of the limbs. ESOS is classified as primary or secondary. Here, we report a case of primary hepatic osteosarcoma in a 76-year-old male patient, which is very rare.

CASE SUMMARY

Here, we report a case of primary hepatic osteosarcoma in a 76-year-old male patient. The patient had a giant cystic-solid mass in the right hepatic lobe that was evident on ultrasound and computed tomography. Postoperative pathology and immunohistochemistry of the mass, which was surgically removed, suggested fibroblastic osteosarcoma. Hepatic osteosarcoma reoccurred 48 d after surgery, resulting in significant compression and narrowing of the hepatic segment of the inferior vena cava. Consequently, the patient underwent stent implantation in the inferior vena cava and transcatheter arterial chemoembolization. Unfortunately, the patient died of multiple organ failure postoperatively.

CONCLUSION

ESOS is a rare mesenchymal tumor with a short course and a high likelihood of metastasis and recurrence. The combination of surgical resection and chemotherapy may be the best treatment.

Key Words: Extraskeletal osteosarcoma; Hepatic; Primary; Relapsed; Case report

Core Tip: Hepatic osteosarcoma is a rare mesenchymal tumor with a short duration and a high likelihood of metastasis and recurrence. Although the imaging examination can help detect lesions, it is difficult to distinguish from other lesions with multiple osteosarcoma-like lesions and make accurate preoperative diagnosis. If hepatic osteosarcoma is suspected, a biopsy and surgery should be performed as soon as possible.

Citation: Di QY, Long XD, Ning J, Chen ZH, Mao ZQ. Relapsed primary extraskeletal osteosarcoma of liver: A case report and review of literature. *World J Clin Cases* 2023; 11(3): 662-668
URL: https://www.wjgnet.com/2307-8960/full/v11/i3/662.htm
DOI: https://dx.doi.org/10.12998/wjcc.v11.i3.662

INTRODUCTION

Extraskeletal osteosarcoma (ESOS) is a highly malignant osteosarcoma that occurs in extraosseous tissues. It is characterized by a low incidence, invasive growth, a high likelihood of metastasis and recurrence, and a poor prognosis[1]. ESOS often involves the soft tissues of the limbs. Few reports of ESOS occurring in organs are available, and relevant publications are mostly case reports[2,3]. The pathogenesis of ESOS is still unclear. The imaging manifestations of hepatic osteosarcoma are not specific, and its diagnosis depends on pathology and immunochemistry. The treatment of ESOS mainly relies on the combination of surgery, radiotherapy, and chemotherapy.

CASE PRESENTATION

Chief complaints

A 76-year-old male was readmitted to the hospital on September 14, 2020, due to abdominal distension and pain.

History of present illness

The patient had a history of resection of malignancy and had undergone surgery for right hemihepatectomy more than a month prior; however, the patient's symptoms improved until significant abdominal distension developed a week ago.

History of past illness

On July 20, 2020, the patient was admitted to the hospital due to aggravation of existing abdominal pain and discomfort. Abdominal color Doppler ultrasound suggested a giant mixed echogenic mass in the right hepatic lobe, and color Doppler flow imaging revealed a small number of blood flow signals in and around the mixed echogenic mass (Figure 1A). Computed tomography (CT) indicated liver enlargement and a giant cystic-solid mass in the right hepatic lobe, and an enhanced scan showed mild to moderate enhancement of the solid component of the mass (Figure 1B). On July 21, 2020, a hospital-wide general consultation was held. After analyzing the patient's imaging data, laboratory findings, and physical signs, doctors concluded that the large intrahepatic mass was malignant and that a mesenchymal origin was probable; furthermore, the patient was in a hypercoagulable state, and blood clots may occur during or after surgery. Ultimately, doctors who participated in the consultation believed that surgical resection and chemotherapy constituted the best treatment for this patient, as did the patient and his family. On July 28, 2020, the patient underwent right hemihepatectomy. During the operation, a cystic-solid mass was observed in the section of the liver next to the liver capsule. The cystic fluid was already lost, and the grayish-red and grayish-yellow solid areas of the tumor were soft with a cut-fish-like surface (Figure 2A). A rapid intraoperative pathology examination suggested mesenchymal sarcoma. Immunohistochemistry yielded the following results: CK (pan) (-), EMA (-), CD34 (-), S-100 (-), SMA (scattered -), STAT6 (-), Ki67 (+, 30%), SATB2 (partially weak +), p16 (-), CD163 (scattered +), CD68 (scattered +), CD56 (-), desmin (-), and H-Cald (-). Postoperative pathology and immunohistochemistry suggested fibroblastic osteosarcoma (Figures 2B and 2C). The patient received capecitabine monotherapy and was discharged on August 30, 2020.

Personal and family history

The patient denied any family history of malignant tumors.

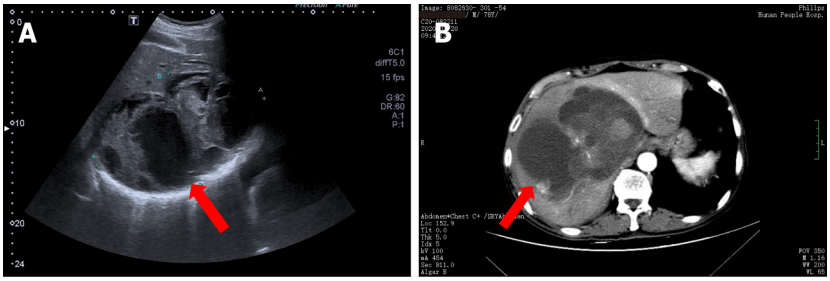

DOI: 10.12998/wjcc.v11.i3.662

Figure 1 Imaging examination. A: Liver ultrasound: A giant mixed echogenic mass (as indicated by the red arrow, approximately 18 cm × 11 cm × 12 cm) was observed in the right lobe of the liver with poorly defined boundary, irregular morphology, and uneven internal echoes. The mass was mainly cystic, with multiple solid parts inside. CDFI: A small number of blood flow signals were visible in and around the mixed echogenic mass, and the intrahepatic and right hepatic veins were compressed and offset; B: Enhanced computed tomography (CT) scans: The liver was enlarged and there was a large cystic-solid mass (as indicated by the red arrow, approximately 17 cm × 13 cm × 12 cm) in the right hepatic lobe with irregular morphology, unclear boundary, uneven attenuation, and CT values ranging from 11 to 62 HU. The solid component of the mass was mildly to moderately enhanced. The arterial branches were observed in the mass. The intrahepatic and right hepatic veins and the right anterior branch of the portal vein were occluded.

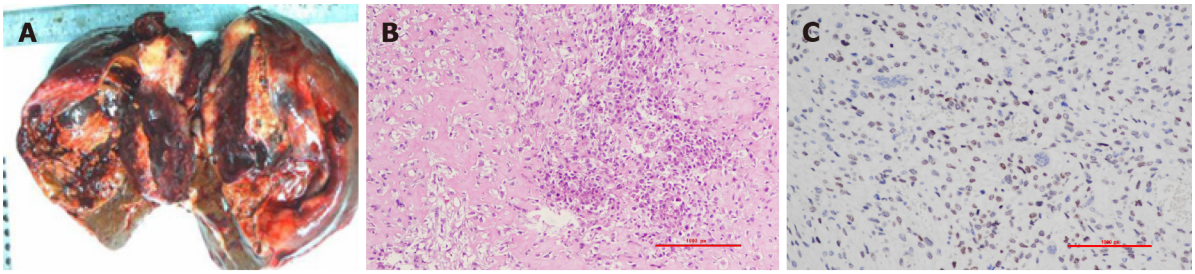

DOI: 10.12998/wjcc.v11.i3.662

Figure 2 Pathology of hepatic osteosarcoma. A: Macroscopic view: A cystic-solid mass was observed in the section of the liver next to the liver capsule. The cystic fluid was already lost, and the grayish-red and grayish-yellow solid area of the tumor was soft with a cut-fish-like surface; B: Pathological microscopy: The short spindle-shaped tumor cells had medium density, an increased nucleus-to-plasma ratio, atypical nuclei, and pathological mitosis. Some tumor cells were converted to osteoblasts. There was osteoid matrix between tumor cells and osteoclast-like giant cells; C: Immunohistochemistry: SATB2 was partially weakly positive.

Physical examination

The abdominal muscles of the upper abdomen were slightly tense, tenderness was noted in the right upper quadrant, and percussion pain was evident in the liver area; the abdominal mass was not touched, and an old scar measuring approximately 14 cm long was visible in the right upper quadrant.

Laboratory examinations

Laboratory tests indicated that inflammatory indicators were elevated, and cancer antigen 125 was slightly increased, suggesting poor liver and coagulation functions. In addition, alpha-fetoprotein was 7.86 ng/mL, a hepatitis B virus (HBV) surface antigen test and hepatitis C antibodies were negative, and HBV-DNA was < 1.00E + 02 IU/mL.

Imaging examinations

Whole-abdomen nonenhanced and contrast-enhanced CT examinations indicated that the residual liver parenchyma had a patchy lesion with mixed attenuation and apparently uneven enhancement near the inferior vena cava and that the hepatic segment of the inferior vena cava was significantly compressed and narrowed (Figure 3), suggesting tumor recurrence.

FINAL DIAGNOSIS

Given the patient's medical history, the final diagnosis was ESOS recurrence.

TREATMENT

Considering that the patient had inferior vena cava compression, stenosis, and a large amount of ascites,

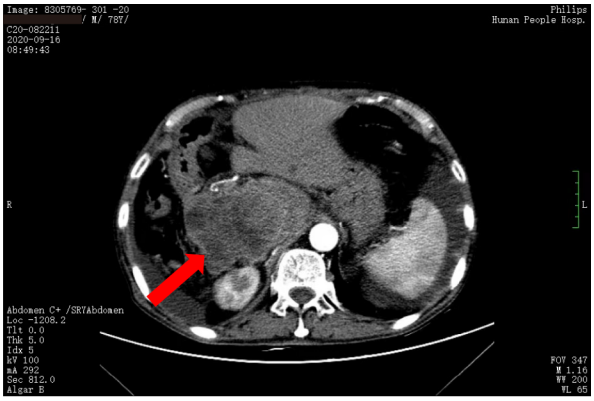

DOI: 10.12998/wjcc.v11.i3.662

Figure 3 Abdominal contrast-enhanced computed tomography. The residual liver parenchyma showed a patchy lesion (as indicated by the red arrow, approximately 11 cm × 8 cm × 10 cm) with mixed attenuation and clear boundary near the inferior vena cava. The lesion grew out of the liver contour and had multiply small, patchy hypoattenuating areas. The lesion showed obviously uneven enhancement, while the hypoattenuating areas of the lesion had no obvious enhancement. The hepatic segment of the inferior vena cava was significantly compressed and narrowed.

inferior vena cava stent implantation and transcatheter arterial chemoembolization were carried out on September 22, 2020.

OUTCOME AND FOLLOW-UP

The patient died on September 29, 2020, due to multiorgan failure after surgery.

DISCUSSION

ESOS is a highly malignant osteosarcoma that occurs in extraosseous tissues. This tumor was first reported in 1941 by Wilson[4]. Its incidence is low, and it occurs primarily in elderly adults. The average age of patients with ESOS is 47.5 to 61 years. ESOS accounts for 1% of all soft tissue sarcomas and 4% of osteogenic osteosarcomas[5]. ESOS is characterized by invasive growth, a high likelihood of metastasis and recurrence, and a poor prognosis[1]. The initial clinical symptom is usually a painless mass[6]. ESOS often involves the soft tissues of the limbs. Few reports of ESOS occurring in organs are available, and most publications are case reports[2,3]. This study reports a primary osteosarcoma occurring on the liver, which is very rare, and only 13 articles were found in the literature search[2,7-18]. Of these patients, ten cases occurred in men, and three occurred in women. Five of the patients had underlying liver cirrhosis. Sumiyoshi and Niho[8] proposed possible tumorigenesis in mesenchymal tissue that proliferates in cirrhosis. However, in our case, the patient had no history of liver cirrhosis or chronic HBV and hepatitis C infection.

The pathogenesis of ESOS is still unclear. Two theories on the pathogenesis of ESOS have been proposed[19]: (1) The tissue residual theory: Residual mesenchymal components from the embryonic development stage form bone and osteosarcomas; and (2) The metaplasia theory: Interstitial fibroblasts in muscle tissues are converted into osteoblasts and chondroblasts in response to internal or external stimuli and then evolve into osteosarcoma. Currently, most scholars support the metaplasia theory. According to their origin, ESOS are classified as primary or secondary ESOS[20]. Primary ESOS occurs in extraskeletal organs and soft tissues and does not attach to the bone or periosteum. No primary ESOS is of bone origin. In contrast, secondary ESOS is mostly metastases from an osteosarcoma of bone origin to the extraskeletal organs and soft tissues or is secondary to certain primary diseases, such as myositis ossificans. In this report, except for the cystic-solid mass in the liver, no evidence of primary tumors or primary bone lesions was found. Therefore, osteosarcomatous foci in other parts of the body were excluded.

Although imaging examinations can help identify lesions, the imaging findings of hepatic osteosarcoma are nonspecific and not different from those of a variety of tumor-like lesions; consequently, hepatic osteosarcoma is difficult to accurately diagnose preoperatively. In this study, the hepatic osteosarcoma manifested as a cystic-solid mass. The histology of hepatic osteosarcoma is similar to that of skeletal osteosarcoma. Although the direct production of osteoid components by osteosarcoma cells has significant diagnostic value, it has no specificity[21]. Pathologists diagnose ESOS based on the appearance of osteoid matrix and osteoblastic-like tumor cells, the differentiation of tumors without fat cells, myogenic or neurogenic properties, and the absence of dedifferentiated or highly differentiated

liposarcoma components at specimen crossover and microscopy[22,23]. In this study, immunohistochemistry suggested SATB2 (partially weak+). Special AT-rich sequence-binding (SATB2) is a nuclear matrix-associated protein. SATB2 expression has tissue and stage specificity, and SATB2 is specifically expressed in glandular cells of the lower digestive tract and osteoblasts of bone tumors, which can be used as a marker for differential diagnosis[18]. This case is morphologically consistent with mesenchymal-derived sarcoma, with tumor cells producing a bone-like stroma, combined with positive immunohistochemical SATB2, which is consistent with the diagnosis of osteosarcoma. Therefore, the diagnosis of hepatic osteosarcoma still relies on pathology and immunochemistry.

At present, the treatment of ESOS mainly relies on the combination of surgery, radiotherapy, and chemotherapy. Radical surgery is considered to reduce local recurrence of ESOS but has no obvious inhibitory effect on the distant metastasis of tumors[24]. As adjuvant therapies for ESOS, radiotherapy and chemotherapy are helpful for improving the tumor resection rate and reducing local recurrence and distant metastasis. Since osteosarcoma is a malignant tumor, ESOS has a short course, rapid progression, a high local recurrence rate, and a high risk of distant metastasis[2]. Lee *et al*[19] reported that the 5-year survival rate of a group of patients diagnosed with ESOS was only 37% and that most of them died within 2 to 3 years after the initial diagnosis. Studies have demonstrated that distant metastasis, large tumors (≥ 10 cm), tumors of the axial skeleton, and advanced age are poor prognostic factors for ESOS, while radiotherapy and chemotherapy have no significant correlation with mortality [25-28]. The patient described in this study was 76 years old. He had a large intrahepatic tumor measuring 17-18 cm. After surgical resection, he underwent chemotherapy. However, local recurrence occurred within a short time after surgery, and the disease progressed rapidly. The patient died within 3 mo after symptom onset. Among the 13 primary hepatic osteosarcoma cases in the literature, most patients died within 2 to 4 mo after initial diagnosis[2,7-15,17,18], but one article reported no tumors within 3 years of surgical resection and adjuvant chemotherapy[16]. At present, the treatment methods for hepatic osteosarcoma are similar to those used for other soft tissue sarcomas. Because this disease is rare, no evidence-based treatment plan has been established to date. Surgical resection combined with adjuvant chemoradiotherapy seems to be the best treatment option[24,25,28-30].

CONCLUSION

Hepatic osteosarcoma is a rare mesenchymal tumor with a short course and a high likelihood of metastasis and recurrence and is difficult to distinguish from other tumors by imaging. Its diagnosis still relies on pathological and immunochemical examinations. Compared with simple surgery or chemotherapy, the combination of surgical resection and chemotherapy may be the best treatment for the disease, which can slow disease progression, reduce the recurrence frequency, and prolong patient survival.

FOOTNOTES

Author contributions: Di QY performed the manuscript writing and the literature collecting; Cheng ZH and Mao ZQ were involved in the operation; Di QY, Ning J and Long XD conceived, designed, and supervised all studies and the drafting and editing of the manuscript; and all the authors have read and approved the final manuscript.

Informed consent statement: Informed written consent was obtained from the patient for publication of this report and any accompanying images.

Conflict-of-interest statement: All the authors report no relevant conflicts of interest for this article.

CARE Checklist (2016) statement: The authors have read the CARE Checklist (2016), and the manuscript was prepared and revised according to the CARE Checklist (2016).

Country/Territory of origin: China

ORCID number: Qiu-Yi Di 0000-0003-3456-2928; Xiang-Dang Long 0000-0001-5251-268X; Zhi-Hong Chen 0000-0002-1030-3289; Zhi-Qun Mao 0000-0003-1218-4479.

S-Editor: Wang JJ
L-Editor: A

P-Editor: Wang JJ

REFERENCES

1 **Usui G**, Hashimoto H, Kusakabe M, Shirota G, Sugiura Y, Fujita Y, Satou S, Harihara Y, Horiuchi H, Morikawa T. Intrahepatic Carcinosarcoma With Cholangiocarcinoma Elements and Prominent Bile Duct Spread. *Int J Surg Pathol* 2019; **27**: 900-906 [PMID: 31203684 DOI: 10.1177/1066896919855766]

2 **Zhang J**, He X, Yu W, Ying F, Cai J, Deng S. Primary Exophytic Extraskeletal Osteosarcoma of the Liver: A Case Report and Literature Review. *Risk Manag Healthc Policy* 2021; **14**: 1009-1014 [PMID: 33737841 DOI: 10.2147/RMHP.S296172]

3 **Bane BL**, Evans HL, Ro JY, Carrasco CH, Grignon DJ, Benjamin RS, Ayala AG. Extraskeletal osteosarcoma. A clinicopathologic review of 26 cases. *Cancer* 1990; **65**: 2762-2770 [PMID: 2160317 DOI: 10.1002/1097-0142(19900615)65:12<2762::aid-cncr2820651226>3.0.co;2-k]

4 **Wilson H**. Extraskeletal ossifying tumors. *Ann Surg* 1941; **113**: 95-112 [PMID: 17857721 DOI: 10.1097/00000658-194101000-00013]

5 **Mc Auley G**, Jagannathan J, O'Regan K, Krajewski KM, Hornick JL, Butrynski J, Ramaiya N. Extraskeletal osteosarcoma: spectrum of imaging findings. *AJR Am J Roentgenol* 2012; **198**: W31-W37 [PMID: 22194512 DOI: 10.2214/AJR.11.6927]

6 **Lee S**, Lee MR, Lee SJ, Ahn HK, Yi J, Yi SY, Seo SW, Sung KS, Park JO, Lee J. Extraosseous osteosarcoma: single institutional experience in Korea. *Asia Pac J Clin Oncol* 2010; **6**: 126-129 [PMID: 20565425 DOI: 10.1111/j.1743-7563.2010.01278.x]

7 **Maynard JH**, Fone DJ. Haemochromatosis with osteogenic sarcoma in the liver. *Med J Aust* 1969; **2**: 1260-1263 [PMID: 5264529 DOI: 10.5694/j.1326-5377.1969.tb103375.x]

8 **Sumiyoshi A**, Niho Y. Primary osteogenic sarcoma of the liver--report of an autopsy case. *Acta Pathol Jpn* 1971; **21**: 305-312 [PMID: 5285824 DOI: 10.1111/j.1440-1827.1971.tb00126.x]

9 **Kitayama Y**, Sugimura H, Arai T, Nagamatsu K, Kino I. Primary osteosarcoma arising from cirrhotic liver. *Pathol Int* 1995; **45**: 320-325 [PMID: 7551004 DOI: 10.1111/j.1440-1827.1995.tb03464.x]

10 **Liony C**, Lemarchand P, Manchon ND, Bécret A, Bercoff E, Pellerin A, Tayot J, Bourreille J. [A case of primary osteosarcoma of the liver]. *Gastroenterol Clin Biol* 1990; **14**: 1003-1006 [PMID: 2289657]

11 **Govender D**, Rughubar KN. Primary hepatic osteosarcoma: case report and literature review. *Pathology* 1998; **30**: 323-325 [PMID: 9770204 DOI: 10.1080/00313029800169556]

12 **von Hochstetter AR**, Hättenschwiler J, Vogt M. Primary osteosarcoma of the liver. *Cancer* 1987; **60**: 2312-2317 [PMID: 3326654 DOI: 10.1002/1097-0142(19871101)60:9<2312::aid-cncr2820600933>3.0.co;2-w]

13 **Craig JR**, Peters RL, Edmondson HA. Atlas of Tumor Pathology: Tumors of the Liver and Intrahepatic Bile Ducts. Second Series, Fascicle 26. Washington: Armed Forces Institute of Pathology, 1989: 223-255

14 **Krishnamurthy VN**, Casillas VJ, Bejarano P, Saurez M, Franceschi D. Primary osteosarcoma of liver. *Europ J Radiol Extra* 2004; **50**: 31-36 [DOI: 10.1016/j.ejrex.2003.12.001]

15 **Park SH**, Choi SB, Kim WB, Song TJ. Huge primary osteosarcoma of the liver presenting an aggressive recurrent pattern following surgical resection. *J Dig Dis* 2009; **10**: 231-235 [PMID: 19659793 DOI: 10.1111/j.1751-2980.2009.00391.x]

16 **Nawabi A**, Rath S, Nissen N, Forscher C, Colquhoun S, Lee J, Geller S, Wong A, Klein AS. Primary hepatic osteosarcoma. *J Gastrointest Surg* 2009; **13**: 1550-1553 [PMID: 19294474 DOI: 10.1007/s11605-009-0852-4]

17 **Tamang TG**, Shuster M, Chandra AB. Primary Hepatic Osteosarcoma: A Rare Cause of Primary Liver Tumor. *Clin Med Insights Case Rep* 2016; **9**: 31-33 [PMID: 27081321 DOI: 10.4137/CCRep.S38384]

18 **Yu L**, Yang SJ. Primary Osteosarcoma of the Liver: Case Report and Literature Review. *Pathol Oncol Res* 2020; **26**: 115-120 [PMID: 30357750 DOI: 10.1007/s12253-018-0483-8]

19 **Lee JS**, Fetsch JF, Wasdhal DA, Lee BP, Pritchard DJ, Nascimento AG. A review of 40 patients with extraskeletal osteosarcoma. *Cancer* 1995; **76**: 2253-2259 [PMID: 8635029 DOI: 10.1002/1097-0142(19951201)76:11<2253::aid-cncr2820761112>3.0.co;2-8]

20 **Murphey MD**, Robbin MR, McRae GA, Flemming DJ, Temple HT, Kransdorf MJ. The many faces of osteosarcoma. *Radiographics* 1997; **17**: 1205-1231 [PMID: 9308111 DOI: 10.1148/radiographics.17.5.9308111]

21 **Hamdan A**, Toman J, Taylor S, Keller A. Nuclear imaging of an extraskeletal retroperitoneal osteosarcoma: respective contribution of 18FDG-PET and (99m)Tc oxidronate (2005:1b). *Eur Radiol* 2005; **15**: 840-844 [PMID: 15858861 DOI: 10.1007/s00330-004-2560-5]

22 **WHO Classification of Tumours Editorial Board**. WHO classification of tumours of soft tissue and bone. 5. Lyon: IARC Press, 2020

23 **Wang H**, Miao R, Jacobson A, Harmon D, Choy E, Hornicek F, Raskin K, Chebib I, DeLaney TF, Chen YE. Extraskeletal osteosarcoma: A large series treated at a single institution. *Rare Tumors* 2018; **10**: 2036361317749651 [PMID: 31508194 DOI: 10.1177/2036361317749651]

24 **Miller BJ**. CORR Insights(®): Should High-grade Extraosseous Osteosarcoma Be Treated With Multimodality Therapy Like Other Soft Tissue Sarcomas? *Clin Orthop Relat Res* 2015; **473**: 3612-3614 [PMID: 26310679 DOI: 10.1007/s11999-015-4519-z]

25 **Fan Z**, Patel S, Lewis VO, Guadagnolo BA, Lin PP. Should High-grade Extraosseous Osteosarcoma Be Treated With Multimodality Therapy Like Other Soft Tissue Sarcomas? *Clin Orthop Relat Res* 2015; **473**: 3604-3611 [PMID: 26197952 DOI: 10.1007/s11999-015-4463-y]

26 **Thampi S**, Matthay KK, Boscardin WJ, Goldsby R, DuBois SG. Clinical Features and Outcomes Differ between Skeletal and Extraskeletal Osteosarcoma. *Sarcoma* 2014; **2014**: 902620 [PMID: 25294959 DOI: 10.1155/2014/902620]

27 **Pisters PW**, Leung DH, Woodruff J, Shi W, Brennan MF. Analysis of prognostic factors in 1,041 patients with localized

soft tissue sarcomas of the extremities. *J Clin Oncol* 1996; **14**: 1679-1689 [PMID: 8622088 DOI: 10.1200/JCO.1996.14.5.1679]

28 **Federman N**, Bernthal N, Eilber FC, Tap WD. The multidisciplinary management of osteosarcoma. *Curr Treat Options Oncol* 2009; **10**: 82-93 [PMID: 19238553 DOI: 10.1007/s11864-009-0087-3]

29 **Berner K**, Bjerkehagen B, Bruland ØS, Berner A. Extraskeletal osteosarcoma in Norway, between 1975 and 2009, and a brief review of the literature. *Anticancer Res* 2015; **35**: 2129-2140 [PMID: 25862869]

30 **Nystrom LM**, Reimer NB, Reith JD, Scarborough MT, Gibbs CP Jr. The Treatment and Outcomes of Extraskeletal Osteosarcoma: Institutional Experience and Review of The Literature. *Iowa Orthop J* 2016; **36**: 98-103 [PMID: 27528844]

World Journal of Clinical Cases

Submit a Manuscript: https://www.f6publishing.com

World J Clin Cases 2023 January 26; 11(3): 669-676

DOI: 10.12998/wjcc.v11.i3.669

ISSN 2307-8960 (online)

CASE REPORT

Heterotopic pregnancy after assisted reproductive techniques with favorable outcome of the intrauterine pregnancy: A case report

Ya-Nan Wang, Lian-Wen Zheng, Lu-Lu Fu, Ying Xu, Xue-Ying Zhang

Specialty type: Reproductive biology

Provenance and peer review: Unsolicited article; Externally peer reviewed.

Peer-review model: Single blind

Peer-review report's scientific quality classification

Grade A (Excellent): 0
Grade B (Very good): 0
Grade C (Good): C, C
Grade D (Fair): 0
Grade E (Poor): 0

P-Reviewer: Ait Addi R, Morocco; Didziokaite G, Lithuania

Received: October 14, 2022
Peer-review started: October 14, 2022
First decision: December 13, 2022
Revised: December 28, 2022
Accepted: January 9, 2023
Article in press: January 9, 2023
Published online: January 26, 2023

Ya-Nan Wang, Lian-Wen Zheng, Lu-Lu Fu, Ying Xu, Xue-Ying Zhang, Department of Obstetrics and Gynecology, Reproductive Medical Center, The Second Hospital of Jilin University, Changchun 130000, Jilin Province, China

Corresponding author: Xue-Ying Zhang, Doctor, Department of Obstetrics and Gynecology, Reproductive Medical Center, The Second Hospital of Jilin University, No. 4026 Yatai Street, Nanguan District, Changchun 130000, Jilin Province, China. zixjocuqo884013@qq.com

Abstract

BACKGROUND

Heterotopic pregnancy (HP) is a rare condition in which both ectopic and intrauterine pregnancies occur. HP is uncommon after natural conception but has recently received more attention due to the widespread use of assisted reproductive techniques (ART) such as ovulation promotion therapy.

CASE SUMMARY

Here, we describe a case of HP that occurred after ART with concurrent tubal and intrauterine singleton pregnancies. This was treated successfully with surgery to preserve the intrauterine pregnancy, resulting in the birth of a low-weight premature infant. This case report aims to increase awareness of the possibility of HP during routine first-trimester ultrasound examinations, especially in pregnancies resulting from ART and even if multiple intrauterine pregnancies are present.

CONCLUSION

This case alerts us to the importance of comprehensive data collection during regular consultations. It is important for us to remind ourselves of the possibility of HP in all patients presenting after ART, especially in women with an established and stable intrauterine pregnancy that complain of constant abdominal discomfort and also in women with an unusually raised human chorionic gonadotropin level compared with simplex intrauterine pregnancy. This will allow symptomatic and timeous treatment of patients with better results.

Key Words: Heterotopic pregnancy; Assisted reproductive techniques; Preterm labor; Premature rupture of membranes; Case report

Core Tip: Extrauterine pregnancies are collectively known as ectopic pregnancies. Heterotopic pregnancy (HP) is a rare type of ectopic pregnancy where both ectopic and intrauterine pregnancies occur. The more frequent use of assisted reproductive technologies (ART) leads to a rise in ectopic pregnancy, consequently leading to an increase in the incidence of HP. We report a case of HP that occurred after ART. Combined with the analysis of the cases indexed in PubMed, we concluded several possible factors related to the correlation. Symptomatic and timeous treatment of patients could lead to improved outcomes.

Citation: Wang YN, Zheng LW, Fu LL, Xu Y, Zhang XY. Heterotopic pregnancy after assisted reproductive techniques with favorable outcome of the intrauterine pregnancy: A case report. *World J Clin Cases* 2023; 11(3): 669-676
URL: https://www.wjgnet.com/2307-8960/full/v11/i3/669.htm
DOI: https://dx.doi.org/10.12998/wjcc.v11.i3.669

INTRODUCTION

Ectopic pregnancies occur in 1%–2% of all pregnancies. Heterotopic pregnancy (HP) is a rare type of ectopic pregnancy that involves the coexistence of both intrauterine and ectopic pregnancies. A recently estimated incidence of HP is about 1/30000[1] in spontaneous pregnancies, increasing to 1/360 to 1/100 [2] in pregnancies resulting from assisted reproductive techniques (ART). ART can result in pelvic inflammatory disease which also contributes to HP. Here, we describe a case of HP after ART in a 26-year-old woman, and through a literature review of previous cases, we summarize the possible causes and related mechanisms accounting for the higher rate of HP after ART.

CASE PRESENTATION

Chief complaints

A 26-year-old Chinese woman presented to the gynecology clinic with a complaint that led to the suspicion of HP.

History of present illness

Suspicion of heterotopic pregnancy after *in vitro* fertilization and embryo transfer cycles (IVF-ET).

History of past illness

Three months before, the patient presented to our reproductive department with a complaint of infertility. After a detailed examination, she was diagnosed with primary infertility, polycystic ovary syndrome, and compound chronic inflammation of the left fallopian tube. Her husband's semen analysis revealed mild asthenospermia. After obtaining their consent, ART was performed.

The patient was pretreated with oral medroxyprogesterone pills (2 mg per pill) given at a dose of 20 mg per day for seven days until the following menses. Controlled ovarian hyperstimulation (COH) was performed on the third day of the period with the use of clomiphene citrate pills (100 mg qd) for five days. After completion of this oral management, the COH was continued with urofollitropin for injection (uFSH) (75 units qd) for four days, with the addition of the same dose of menotrophin for the following four days. Follicle maturation was monitored by ultrasonography. After three days, instead of repeated COH by injection, the patient received further treatment with chorionic gonadotrophin given at a dose of 10000 units and it was suggested that she had sex on that day with the expectation of natural conception.

Two days later, ovulation of the right ovary was detected on the ultrasound scan, and we suggested that the patient take vitamin complex tablets from then onward as well as dydrogesterone starting two days hence to form a habitable place for a fetus and create a suitable internal environment to nurture a growing child.

The urinary pregnancy test was positive 15 days after ovulation and the serum human chorionic gonadotropin (hCG) level was 520 mIU/mL. A transvaginal ultrasound examination showed an intrauterine pregnancy with a 10-mm-thick endometrium at the C stage, with six follicles in the right ovary, four echoless regions in the left ovary, and mild pelvic effusion. Early intrauterine pregnancy with additional ectopic pregnancy in the right tube was strongly suspected due to the enhanced clinical clues. As the patient was strongly in favor of continuing the pregnancy, they decided to anticipate spontaneous abortion of the ectopic pregnancy and treated the intrauterine pregnancy as before.

Six days later, the follow-up serum hCG level was 3754.54 mIU/mL and transvaginal sonography reexamination showed an intrauterine singleton without a clearly visible yolk sac and multiple echoless areas in the bilateral adnexa. Finally, after another six days had passed, the detection of an intrauterine gestational sac (GS) of 14 mm × 6.0 mm, an embryonic bud of 3 mm, an embryonic heartbeat, and a GS of 9 mm × 7 mm with a yolk sac beside the right ovary confirmed the presence of HP. These findings combined with the clinical factors provided the main indications for surgery. (Figure 1) Having taken our advice, the patient (1 gravida, 0 para) presented to the gynecology clinic.

Personal and family history

The patient denied any family history of malignant tumors.

Physical examination

On physical examination, the vital signs were as follows: Body temperature, 36.5°C; blood pressure, 115/85 mmHg; heart rate, 97 beats per min; respiratory rate, 19 breaths per min.

Laboratory examinations

The human chorionic gonadotropin level was 20295.14 mIU/mL.

Imaging examinations

An intrauterine gestational sac appropriate for seven weeks of pregnancy was seen on transvaginal sonography (Figure 2A). Both ovaries were larger than normal, with dimensions of 11 cm × 5 cm for the right and 8 cm × 4 cm for the left. A mass in the right ovary suggested the presence of an ectopic pregnancy (Figure 2B).

FINAL DIAGNOSIS

Combined with the patient's medical history and intraoperative findings, the final diagnosis was HP.

TREATMENT

Laparoscopic surgery was performed. On removal of the blood in the peritoneal cavity (approximately 300 mL), the bilateral ovaries were immediately visible, clearly larger than normal as had been seen on the transvaginal sonography. The right fallopian tube was thickened with a bluish-purple lump of approximately 5.0 cm × 3.0 cm. The left fallopian tube was normal. The uterus was regular in shape and normal in size. After sufficient and short intraoperative communication with her medical authorizer, the surgeon excised the swollen right fallopian tube. During the operation, the estimated blood extravasation was approximately 50 mL. After the operation, the patient was given Ceftizoxime Sodium injection (0.2 g bid) to prevent inflammation which was discontinued after normal WBC counts were obtained on routine blood test reexamination. The patient recovered well during the remaining hospitalization and her reexamination by transvaginal sonography was satisfactory (Figure 3). She was discharged six days after surgery and was monitored for the duration of her pregnancy.

OUTCOME AND FOLLOW-UP

The patient's obstetric follow-ups and fetal assessments were normal showing good fetal growth of her intrauterine singleton. The course of pregnancy was unremarkable until the patient experienced contractions at 30+5 wk of gestation. She was admitted to the hospital and, after confirming premature rupture of membranes, cervical effacement, and complete cervical dilatation, we continued with the delivery process, resulting in a baby boy with a birth weight of 1430 g. He was admitted to the neonatal unit. The postpartum course was uneventful for both the mother and baby.

DISCUSSION

Many recent articles on ART have paid particular attention to the link between ART and an increased incidence of HP, with some reports indicating HP rates as high as 8.6% after ART[3].

HP is diagnosed when ultrasound findings demonstrate an intrauterine pregnancy and a concurrent ectopic pregnancy[4]. As discussed in the Introduction, there is inescapable evidence that the incidence of HP is higher in pregnancies resulting from ART than in spontaneous pregnancies. However, many cases are still clinically misdiagnosed during first-trimester examinations due to poor awareness of this

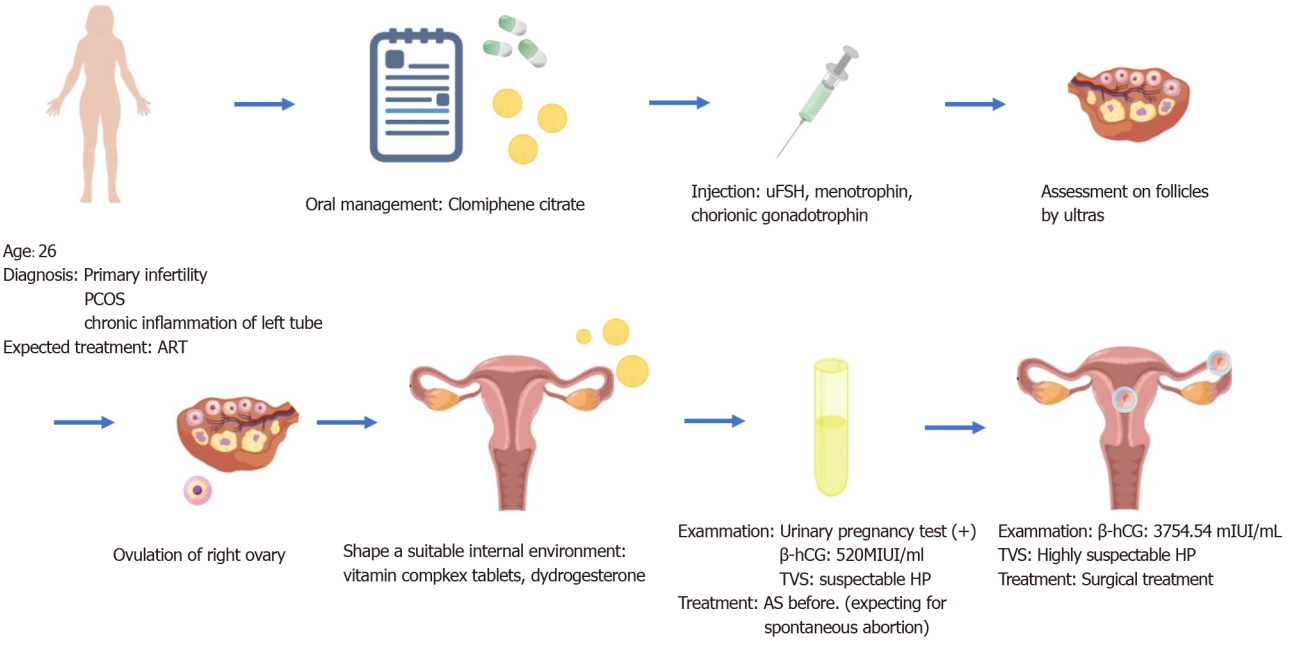

DOI: 10.12998/wjcc.v11.i3.669

Figure 1 The complete process of diagnosis and treatment of the patient. ART: Assisted reproductive techniques; hCG: Human chorionic gonadotropin; HP: Heterotopic pregnancy; PCOS: Polycystic ovary syndrome; TVS: Transvaginal scanning; uFSH: Urofollitropin for injection.

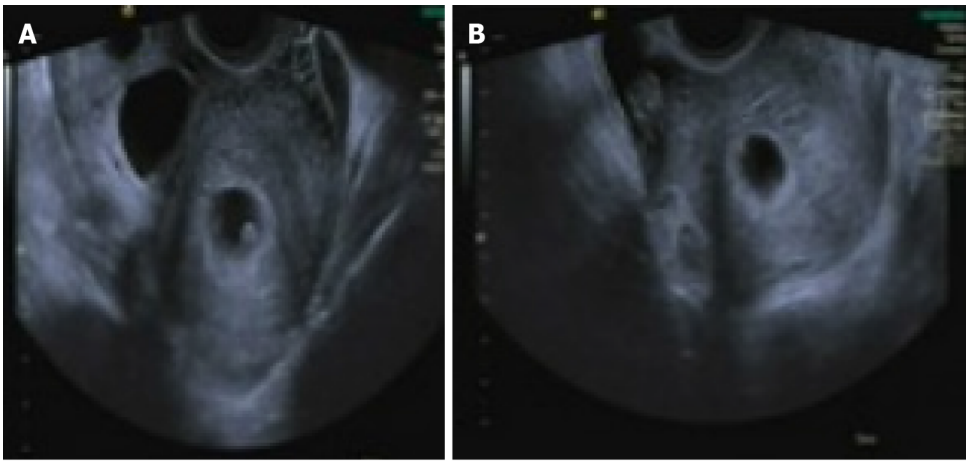

DOI: 10.12998/wjcc.v11.i3.669

Figure 2 Transvaginal sonography. A: The intrauterine gestational sac was about 7 wk of pregnancy; B: The bilateral ovaries were larger than normal. The left ovary measured 8 cm × 4 cm, while the right ovarian mass measured about 11 cm × 5 cm, suggestive of an ectopic pregnancy.

fact[5]. The differences in HP incidence between natural HP and HP after IVF-ET are apparent and present an additional problem, namely, how to explain this phenomenon and how to prevent it.

To answer this question, we first need to understand the ART procedure itself, which includes all clinical fertility treatments. In this respect, after analysis of earlier studies, we focus on the IVF-ET, typically performed by culturing embryos for a few days before transferring them through the cervix to the uterus. IVF-ET consists of four successive steps, commonly stated as stimulation of the growth of multiple ovarian follicles, egg retrieval from the woman's ovaries, fertilization in vitro, and, finally, the transfer of viable embryos into the uterine cavity (Figure 4). However, in many cases, these four steps are not fully performed due to reasons such as allowing the possibility of natural conception, as in the present case[6]. Furthermore, during the steps described above, there are several factors that predispose to higher rates of HP in pregnant women after ART[7].

Firstly, as in the case of the present patient, ovarian induction is widely used for the retrieval of multiple follicles, indicating the presence of often more than one follicle in the body ready to be fertilized after the intervention. Therefore, in the period following attempts at either natural or *in vitro* fertilization, multiple zygotes are often present, implying the availability of more than one embryo ready for implantation, which could occur spontaneously in different places. An experimental study has

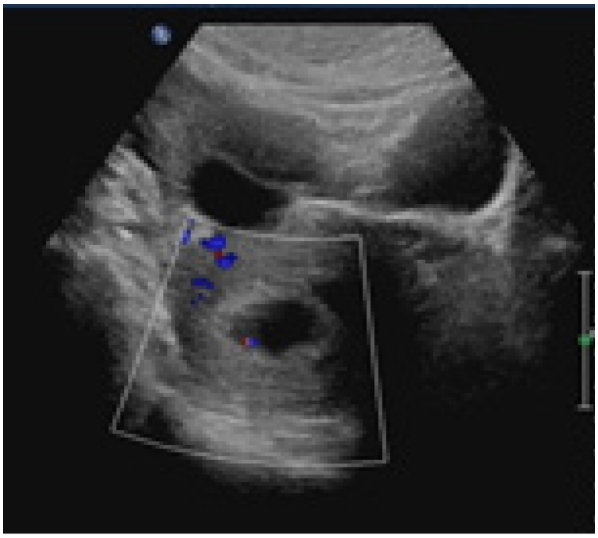

DOI: 10.12998/wjcc.v11.i3.669

Figure 3 Re-examination by transvaginal sonography showing the intact intrauterine gestational sac.

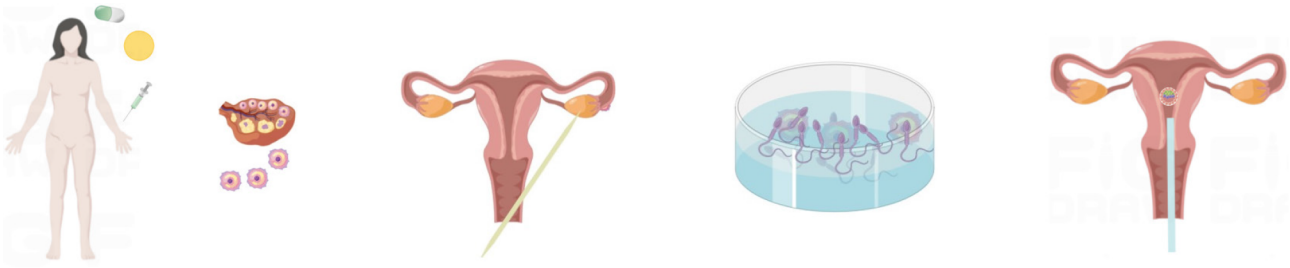

DOI: 10.12998/wjcc.v11.i3.669

Figure 4 Commonly used fertility treatments.

demonstrated that the adhesion of mouse embryos to the human endometrium reduces gradually with increasing concentrations of estradiol (E2)[8]. It has been shown that very high levels of serum E2 influence implantation[9,10]. Recent studies have also shown that normal gene expression in endometrial tissue is disturbed during IVF-ET cycles as a result of high levels of serum E2 or increases in follicular progesterone[11,12].

Secondly, the majority of patients undergoing IVF-ET suffer from one or more types of reproductive dysfunction, with tubal dysfunction accounting for approximately 95% of these[13,14]. Various processes, including ovum and sperm transport, fertilization, and early stages of embryogenesis, occur in the fallopian tubes[15]. Gametes and fertilized embryos are propelled along the tubes by the action of smooth muscles and ciliary beating[5,15], and dysfunction of these systems may affect the correct homing of the oocyte and embryo. A perusal of the recent literature supports the hypothesis that tubal implantation is a result of tubal malfunction, specifically caused by alterations both in tubal transport mechanisms and expression of factors normally responsible for preventing implantation within the fallopian tube[16-19]. Such malfunctions can result from disease, such as chronic salpingitis or the effects of surgery, as well as endocrine disruptions during ovulation induced by hyperstimulation by exogenous gonadotropins or the chronic administration of low-dose progestogen[15]. It is presumed that the amount of administered estrogen is sufficient to prevent increases in progesterone or its tubal effects, delaying the passage of the ovum through the ampulla-isthmus junction for sufficient time to allow hatching of the blastocyst in the ampulla. These mechanisms appear to be associated with an increased risk of HP[14,15].

However, some scientists hold a different perspective, namely, that the increased incidence of embryonic implantation outside the uterus is determined by the embryo itself rather than by tubal factors. E-cadherin is known to be responsible for the anchorage of placental villi and its expression is reduced when differentiation occurs outside of the villi. Previous studies on E-cadherin-knockout mice have shown that the protein is required for normal implantation, as knockout embryos did not form functional trophectoderm and died during implantation[20]. In normal embryos, insulin-like growth

factor 1 receptor (IGF-1R) is present throughout the membrane but on activation, is found exclusively at cell contact sites, colocalizing with E-cadherin. It has been found that abrogation of IGF-1R signaling with specific inhibitors blocks trophectoderm formation and compromises embryo survival during murine blastocyst formation and that E-cadherin is required to maintain the proper activation of IGF-1R. Perturbation of E-cadherin extracellular integrity, independent of its cell-adhesion function, was shown to block IGF-1R signaling, inducing cell death in the trophectoderm, and thus indicating a crucial and non-substitutable role of E-cadherin for these processes[21]. Strong E-cadherin expression is only seen at tubal implantation sites in patients after IVF-ET[13]. E-cadherin staining in the fallopian tubes of IVF-ET patients has been found to be restricted to the trophoblast, supporting the hypothesis of the dominant influence of the embryo in ectopic pregnancy after IVF-ET treatment[13]. Thus, it is possible that ectopic pregnancies in IVF-ET patients with normal fallopian tubes may be associated with reduced abilities of the embryos for implantation.

Furthermore, ARTs, such as ovarian induction and oocyte retrieval, are known to enhance uterine contraction, which could also impede embryonic implantation[22].

The recognized risks of ectopic pregnancy have led clinicians to turn their attention to ways in which these risks can be reduced in clinical practice.

Firstly, to reduce the risk of multiple births, milder and more physiological approaches to ovarian stimulation during IVF-ET are being considered; these have been shown to have several advantages despite the likelihood of producing fewer embryos. The term mild-stimulation IVF (MS-IVF) is defined as the administration of follicle-stimulating hormone or human menopausal gonadotropin at lower doses or shorter durations during a cycle with co-treatment of gonadotropin-releasing hormone antagonists or the administration of oral anti-estrogens or aromatase inhibitors either individually or combined with gonadotropins to collect fewer oocytes[23]. The advantages of MS-IVF, namely, improved safety, tolerance, and affordability, in IVF-ET cycles have been demonstrated, and many studies have shown an association between this gentle stimulation and improved perinatal outcomes [24].

Secondly, to reduce the effects of reproductive disorders such as tubal dysfunction that hinder oocyte and zygote transport within the fallopian tube, it is advisable to instigate treatment to restore the system to its normal state as far as possible before ART[25]. In addition, considering prognosis and perinatal outcomes, salpingectomy is considered a better treatment for women diagnosed with ectopic pregnancy compared with conservative treatment due to the reduced likelihood of future ectopic pregnancies after treatment[26].

Furthermore, it is suggested that the optimum time for embryo transferal is five to six days after oocyte retrieval when the embryo is exactly in the blastocyst stage. This is supported not only by basic experimental studies but also by the consistent results of clinical trials[25-27].

In addition, options for embryo transfer are not only limited to the cleavage or blastocyst phases but also include techniques such as fresh or frozen embryo transfer. It has been found that the transfer of fresh blastocysts does not affect perinatal outcomes in singleton live births compared with the transfer after the cleavage stage[28]. No significant differences were observed in the incidence of ectopic pregnancy between fresh and frozen/thawed cycles in a large patient sample[22]. The risk of recurrent ectopic pregnancy was found to be lower with fresh embryo transfer[26]. However, no definite conclusions on the effects of fresh or frozen embryos on the risk of ectopic pregnancy can be made at this time, and further robust evidence is required.

CONCLUSION

The increased incidence of HP is considered a clinical disadvantage of ART and also alerts us to the importance of collecting comprehensive data during regular consultations. It is important for us to remind ourselves of the possibility of HP in all patients presenting after ART, especially in women with an established and stable intrauterine pregnancy that complain of constant abdominal discomfort and also in women with unusually raised hCG levels compared with simplex intrauterine pregnancy. This will allow symptomatic and timeous treatment of patients leading to improved outcomes.

FOOTNOTES

Author contributions: Zhang XY, Wang YN designed the study and collected data; Xu Y wrote the manuscript; Zheng LW, Xu Y and Fu LL revised the manuscript; All authors read and approved the final manuscript.

Supported by Science and Technology Development Project of Jilin Province, No. YDZJ202201ZYTS060.

Informed consent statement: All study participants, or their legal guardians, provided informed written consent prior to study enrollment.

Conflict-of-interest statement: All the authors declare that they have no conflict of interest to disclose.

CARE Checklist (2016) statement: The authors have read the CARE Checklist (2016), and the manuscript was prepared and revised according to the CARE Checklist (2016).

Country/Territory of origin: China

ORCID number: Ya-Nan Wang 0000-0002-0408-3531; Xue-Ying Zhang 0000-0001-7066-1144.

S-Editor: Liu JH
L-Editor: A
P-Editor: Liu JH

REFERENCES

1 **Dendas W**, Schobbens JC, Mestdagh G, Meylaerts L, Verswijvel G, Van Holsbeke C. Management and outcome of heterotopic interstitial pregnancy: Case report and review of literature. *Ultrasound* 2017; **25**: 134-142 [PMID: 29410688 DOI: 10.1177/1742271X17710965]
2 **Guimarães AC**, Reis LDO, Leite FC, Reis CFDD, Costa AP, Araujo WJB. Spontaneous Heterotopic Triplet Pregnancy with a Two Viable Intrauterine Embryos and an Ectopic One with Right Tubal Rupture. *Rev Bras Ginecol Obstet* 2019; **41**: 268-272 [PMID: 30970384 DOI: 10.1055/s-0039-1683910]
3 **Clayton HB**, Schieve LA, Peterson HB, Jamieson DJ, Reynolds MA, Wright VC. Ectopic pregnancy risk with assisted reproductive technology procedures. *Obstet Gynecol* 2006; **107**: 595-604 [PMID: 16507930 DOI: 10.1097/01.AOG.0000196503.78126.62]
4 **Elson CJ**, Salim R, Potdar N, Chetty M, Ross JA, Kirk EJ. Diagnosis and management of ectopic pregnancy. *BJOG* 2016; **123**: e15-e55 [DOI: 10.1111/1471-0528.14189]
5 **Lin EP**, Bhatt S, Dogra VS. Diagnostic clues to ectopic pregnancy. *Radiographics* 2008; **28**: 1661-1671 [PMID: 18936028 DOI: 10.1148/rg.286085506]
6 **Van Voorhis BJ**. Outcomes from assisted reproductive technology. *Obstet Gynecol* 2006; **107**: 183-200 [PMID: 16394060 DOI: 10.1097/01.AOG.0000194207.06554.5b]
7 **Fauque P**. Ovulation induction and epigenetic anomalies. *Fertil Steril* 2013; **99**: 616-623 [PMID: 23714436 DOI: 10.1016/j.fertnstert.2012.12.047]
8 **Chang KT**, Su YT, Tsai YR, Lan KC, Hsuuw YD, Kang HY, Chan WH, Huang FJ. High levels estradiol affect blastocyst implantation and post-implantation development directly in mice. *Biomed J* 2022; **45**: 179-189 [PMID: 35148258 DOI: 10.1016/j.bj.2021.01.004]
9 **Takeuchi M**, Seki M, Furukawa E, Takahashi A, Saito K, Kobayashi M, Ezoe K, Fukui E, Yoshizawa M, Matsumoto H. Improvement of implantation potential in mouse blastocysts derived from IVF by combined treatment with prolactin, epidermal growth factor and 4-hydroxyestradiol. *Mol Hum Reprod* 2017; **23**: 557-570 [PMID: 28810691 DOI: 10.1093/molehr/gax035]
10 **Fauser BC**, Devroey P. Reproductive biology and IVF: ovarian stimulation and luteal phase consequences. *Trends Endocrinol Metab* 2003; **14**: 236-242 [PMID: 12826330 DOI: 10.1016/s1043-2760(03)00075-4]
11 **Haouzi D**, Assou S, Dechanet C, Anahory T, Dechaud H, De Vos J, Hamamah S. Controlled ovarian hyperstimulation for in vitro fertilization alters endometrial receptivity in humans: protocol effects. *Biol Reprod* 2010; **82**: 679-686 [PMID: 20042535 DOI: 10.1095/biolreprod.109.081299]
12 **Labarta E**, Martínez-Conejero JA, Alamá P, Horcajadas JA, Pellicer A, Simón C, Bosch E. Endometrial receptivity is affected in women with high circulating progesterone levels at the end of the follicular phase: a functional genomics analysis. *Hum Reprod* 2011; **26**: 1813-1825 [PMID: 21540246 DOI: 10.1093/humrep/der126]
13 **Revel A**, Ophir I, Koler M, Achache H, Prus D. Changing etiology of tubal pregnancy following IVF. *Hum Reprod* 2008; **23**: 1372-1376 [PMID: 18385125 DOI: 10.1093/humrep/den018]
14 **Farquhar CM**. Ectopic pregnancy. *Lancet* 2005; **366**: 583-591 [PMID: 16099295 DOI: 10.1016/S0140-6736(05)67103-6]
15 **Jansen RP**. Endocrine response in the fallopian tube. *Endocr Rev* 1984; **5**: 525-551 [PMID: 6094174 DOI: 10.1210/edrv-5-4-525]
16 **Refaat B**, Dalton E, Ledger WL. Ectopic pregnancy secondary to in vitro fertilisation-embryo transfer: pathogenic mechanisms and management strategies. *Reprod Biol Endocrinol* 2015; **13**: 30 [PMID: 25884617 DOI: 10.1186/s12958-015-0025-0]
17 **Shaw JL**, Dey SK, Critchley HO, Horne AW. Current knowledge of the aetiology of human tubal ectopic pregnancy. *Hum Reprod Update* 2010; **16**: 432-444 [PMID: 20071358 DOI: 10.1093/humupd/dmp057]
18 **Refaat B**. Role of activins in embryo implantation and diagnosis of ectopic pregnancy: a review. *Reprod Biol Endocrinol* 2014; **12**: 116 [PMID: 25421645 DOI: 10.1186/1477-7827-12-116]
19 **Refaat B**, Simpson H, Britton E, Biswas J, Wells M, Aplin JD, Ledger W. Why does the fallopian tube fail in ectopic

pregnancy? *Fertil Steril* 2012; **97**: 1115-1123 [PMID: 22425195 DOI: 10.1016/j.fertnstert.2012.02.035]
20 **Larue L**, Ohsugi M, Hirchenhain J, Kemler R. E-cadherin null mutant embryos fail to form a trophectoderm epithelium. *Proc Natl Acad Sci U S A* 1994; **91**: 8263-8267 [PMID: 8058792 DOI: 10.1073/pnas.91.17.8263]
21 **Bedzhov I**, Liszewska E, Kanzler B, Stemmler MP. Igf1r signaling is indispensable for preimplantation development and is activated *via* a novel function of E-cadherin. *PLoS Genet* 2012; **8**: e1002609 [PMID: 22479204 DOI: 10.1371/journal.pgen.1002609]
22 **Decleer W**, Osmanagaoglu K, Meganck G, Devroey P. Slightly lower incidence of ectopic pregnancies in frozen embryo transfer cycles versus fresh in vitro fertilization-embryo transfer cycles: a retrospective cohort study. *Fertil Steril* 2014; **101**: 162-165 [PMID: 24238273 DOI: 10.1016/j.fertnstert.2013.10.002]
23 **Nargund G**, Fauser BC, Macklon NS, Ombelet W, Nygren K, Frydman R; Rotterdam ISMAAR Consensus Group on Terminology for Ovarian Stimulation for IVF. The ISMAAR proposal on terminology for ovarian stimulation for IVF. *Hum Reprod* 2007; **22**: 2801-2804 [PMID: 17855409 DOI: 10.1093/humrep/dem285]
24 **Nargund G**, Datta AK, Fauser BCJM. Mild stimulation for in vitro fertilization. *Fertil Steril* 2017; **108**: 558-567 [PMID: 28965549 DOI: 10.1016/j.fertnstert.2017.08.022]
25 **Santos-Ribeiro S**, Tournaye H, Polyzos NP. Trends in ectopic pregnancy rates following assisted reproductive technologies in the UK: a 12-year nationwide analysis including 160 000 pregnancies. *Hum Reprod* 2016; **31**: 393-402 [PMID: 26724796 DOI: 10.1093/humrep/dev315]
26 **Tan Y**, Bu ZQ, Shi H, Song H, Zhang YL. Risk Factors of Recurrent Ectopic Pregnancy in Patients Treated With in vitro Fertilization Cycles: A Matched Case-Control Study. *Front Endocrinol (Lausanne)* 2020; **11**: 552117 [PMID: 33071969 DOI: 10.3389/fendo.2020.552117]
27 **Pierzynski P**. Oxytocin and vasopressin V(1A) receptors as new therapeutic targets in assisted reproduction. *Reprod Biomed Online* 2011; **22**: 9-16 [PMID: 21130036 DOI: 10.1016/j.rbmo.2010.09.015]
28 **Marconi N**, Raja EA, Bhattacharya S, Maheshwari A. Perinatal outcomes in singleton live births after fresh blastocyst-stage embryo transfer: a retrospective analysis of 67 147 IVF/ICSI cycles. *Hum Reprod* 2019; **34**: 1716-1725 [PMID: 31418775 DOI: 10.1093/humrep/dez133]

World Journal of Clinical Cases

Submit a Manuscript: https://www.f6publishing.com

World J Clin Cases 2023 January 26; 11(3): 677-683

DOI: 10.12998/wjcc.v11.i3.677

ISSN 2307-8960 (online)

CASE REPORT

Periprosthetic knee joint infection caused by *Brucella melitensis* which was first -osteoarticular brucellosis or osteoarthrosis: A case report

Thomas Stumpner, Regina Kuhn, Josef Hochreiter, Reinhold Ortmaier

Specialty type: Medicine, research and experimental

Provenance and peer review: Unsolicited article; Externally peer reviewed.

Peer-review model: Single blind

Peer-review report's scientific quality classification

Grade A (Excellent): 0
Grade B (Very good): 0
Grade C (Good): C, C
Grade D (Fair): 0
Grade E (Poor): 0

P-Reviewer: Li M, China; Ye YP, China

Received: November 24, 2022
Peer-review started: November 24, 2022
First decision: December 13, 2022
Revised: December 26, 2022
Accepted: January 5, 2023
Article in press: January 5, 2023
Published online: January 26, 2023

Thomas Stumpner, Regina Kuhn, Josef Hochreiter, Reinhold Ortmaier, Department of Orthopaedic Surgery, Ordensklinikum Linz Barmherzige Schwestern, Linz 4010, Austria

Corresponding author: Thomas Stumpner, MD, Doctor, Staff Physician, Department of Orthopaedic Surgery, Ordensklinikum Linz Barmherzige Schwestern, Seilerstätte 4, Linz 4010, Austria. thomas.stumpner@ordensklinikum.at

Abstract

BACKGROUND

Brucellosis is the most common zoonosis worldwide and is endemic in the Middle East, Africa, Asia, and Latin America. However, it is uncommon in Central Europe, and periprosthetic infections caused by *Brucella* are therefore rare. Due to the low prevalence and nonspecific clinical presentation of the disease, accurate diagnosis can be challenging; no gold standard currently exists for treating brucellosis.

CASE SUMMARY

Here, we present a 68-year-old Afghan woman living in Austria with a periprosthetic knee infection caused by *Brucella melitensis*. The interval from total knee arthroplasty to septic loosening was five years. A profound medical history and examinations suggested that the patient had been suffering from unrecognized chronic osteoarticular brucellosis prior to total knee arthroplasty. She was successfully treated by two-stage revision surgery and combined antibiotic therapy over three months.

CONCLUSION

Clinicians should consider brucellosis as a possible cause of chronic arthralgia and periprosthetic infection in patients originating from countries with a high brucellosis burden.

Key Words: Brucellosis; Arthroplasty; Infection; Osteoarticular; Knee; Case report

Core Tip: Periprosthetic infections caused by *Brucella* species are rare, difficult to diagnose, and challenging to treat. We present here our experience in treating a 68-year-old Afghan woman with a periprosthetic knee joint infection caused by *Brucella melitensis*. In conclusion we recommend clinicians to consider Brucellosis as a possible cause for chronic arthralgia and periprosthetic infection in patients originating from countries with a high brucellosis burden.

Citation: Stumpner T, Kuhn R, Hochreiter J, Ortmaier R. Periprosthetic knee joint infection caused by *Brucella melitensis* which was first -osteoarticular brucellosis or osteoarthrosis: A case report. *World J Clin Cases* 2023; 11(3): 677-683
URL: https://www.wjgnet.com/2307-8960/full/v11/i3/677.htm
DOI: https://dx.doi.org/10.12998/wjcc.v11.i3.677

INTRODUCTION

Brucellosis is a zoonotic bacterial infection caused by different species of gram-negative coccobacilli *Brucellae*[1]. While it is the most common zoonosis worldwide and endemic in large parts of the Middle East, Mediterranean, Central Asia, Africa, and Latin America, it is rare in Central Europe and Northern America[2].

Transmission usually occurs through the consumption of unpasteurized milk, and less commonly through direct contact with animals or the inhalation of infected particles[3]. Diagnosis is made by serological tests for antibodies against *Brucella* and culture of blood, joint aspirates, or other tissue samples. Cultivation of germs may be hampered by the slow-growing nature of *Brucella* species and therefore culture can require prolonged incubation. Highly sensitive molecular methods (nucleic acid amplification tests) can enable a quick diagnosis; however, they are still under development and no sufficiently validated commercial tests are currently available[4].

The disease itself usually presents with nonspecific symptoms such as fever, fatigue, loss of appetite, and weight loss[3]. Hematogenous spread may affect any organ; however, osteoarticular involvement (arthritis, osteomyelitis) is the most common complication[3,5,6]. Periprosthetic infections due to *Brucella* are extremely rare, and only 30 cases have been reported in the literature to date[6,7].

CASE PRESENTATION

Chief complaints

In December 2020, a 68-year-old female presented with pain, redness, and swelling in her left knee.

History of present illness

At the time of presentation, the complaints had been present for three months, and antibiotic therapy (oral amoxicillin 1 g twice daily) had already been started by her general practitioner.

History of past illness

Total knee arthroplasty (TKA) in the affected joint had been performed five years prior due to osteoarthritis (Figure 1). The initial postoperative course was uneventful. In the following years however the patient repeatedly presented to our outpatient clinic with pain in the operated knee and lumbar spine. Complaints always improved with physiotherapy, oral pain medication, and local cryotherapy to the knee.

Personal and family history

Neither the patient nor her family members had previous episodes of similar symptoms.

Physical examination

There was marked effusion, warming, and swelling in the left knee. The range of motion was quite limited due to pain. The patient was afebrile without any feeling of illness.

Laboratory examinations

The C-reactive protein (CRP) level was 2 mg/dL (norm < 1 mg/dL), and the leukocyte count was within the normal range. No aspirate could be withdrawn by intraarticular puncture.

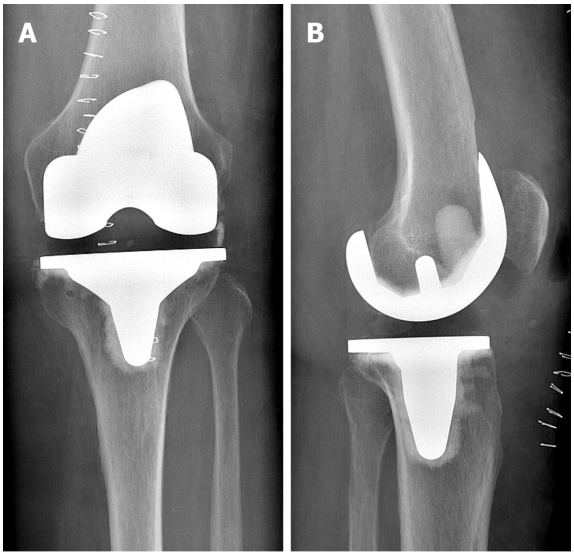

DOI: 10.12998/wjcc.v11.i3.677

Figure 1 Radiograph showing total knee arthroplasty five days after surgery. A: Anterior-posterior view; B: Lateral view.

Imaging examinations

X-ray imaging showed a tilt of the tibial plateau and radiolucent lines around the femoral component (Figure 2).

INITIAL DIAGNOSIS AND TREATMENT

Despite suspicion of septic loosening, an outpatient procedure was initially agreed upon because the patient refused surgical intervention. Therefore, she was fitted with a rigid knee brace and antibiotic therapy with amoxicillin was continued. We scheduled her for a check-up in our orthopedic outpatient clinic.

One week later, the pain and redness were reduced and the CRP level and leukocyte count remained unchanged. However, considerable effusion remained. Ten milliliters of intraarticular serohemorrhagic fluid were aspirated, and qualitative determination of alpha-defensin (Synovasure®, Zimmer Biomet) was positive. The cell count in the aspirate was 9800: 76% of these cells were granulocytes, thus confirming a periprosthetic joint infection. Revision surgery was agreed upon with the patient.

After removal of the prosthesis, a mobile vancomycin- and gentamicin-loaded spacer (VancoGenx™ SPACE Knee,Medix Medical) was implanted (Figure 3). Seven tissue samples were taken intraoperatively for culture and histopathology, and the prosthesis was sent for sonication. The antibiotic regimen was changed to intravenous (*i.v.*) cefuroxime.

Eight days after surgery *Brucella melitensis* was successfully cultivated in synovial fluid. Serological tests were positive for antibodies against *Brucella melitensis* and *Brucella abortus*.

FINAL DIAGNOSIS

The final diagnosis was a periprosthetic knee joint infection caused by *Brucella melitensis.*

TREATMENT

Antibiotic therapy was adapted to oral doxycycline 200 mg daily plus oral rifampicin 450 mg twice daily for 12 wk, and *i.v.* gentamicin was administered for two weeks under the close monitoring of serum levels due to severe renal insufficiency. Six weeks after implant removal a revision TKA was performed. To protect the new prosthesis from superinfection with rifampicin-resistant *staphylococci,* our patient received a single 1.5 g shot of *i.v.* cefuroxime preoperatively and *i.v.* daptomycin 500 mg for 14 d after reimplantation. After a total of 12 wk targeted antibiotic therapy was terminated (Figure 4).

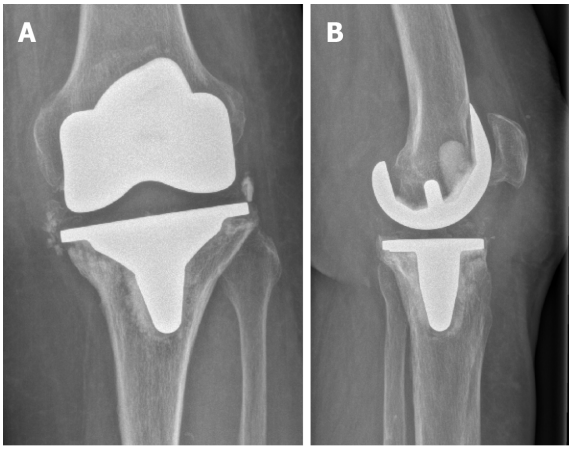

DOI: 10.12998/wjcc.v11.i3.677

Figure 2 Radiograph showing a tilt of the tibial plateau and radiolucent lines around the femoral component. A: Anterior-posterior view; B: Lateral view.

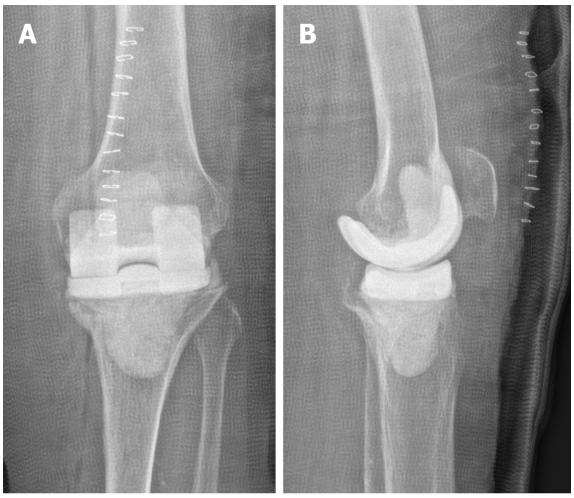

DOI: 10.12998/wjcc.v11.i3.677

Figure 3 Immediate postoperative radiograph showing an antibiotic-loaded spacer. A: Anterior-posterior view; B: Lateral view.

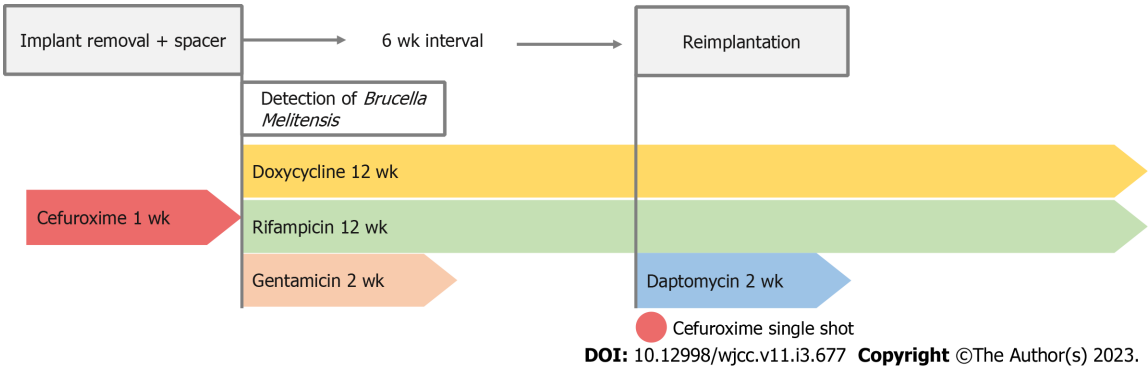

DOI: 10.12998/wjcc.v11.i3.677

Figure 4 Postoperative antibiotic regimen after implant removal.

OUTCOME AND FOLLOW-UP

Nineteen months after reimplantation, the patient was free of pain and walked without crutches. The affected joint showed no swelling, and the active range of motion was 115 degrees without a fixed flexion deformity or extensor lag. Inflammatory markers were within the normal range, and the levels of anti-*Brucella* antibodies had decreased. X-ray imaging showed no signs of loosening (Figure 5).

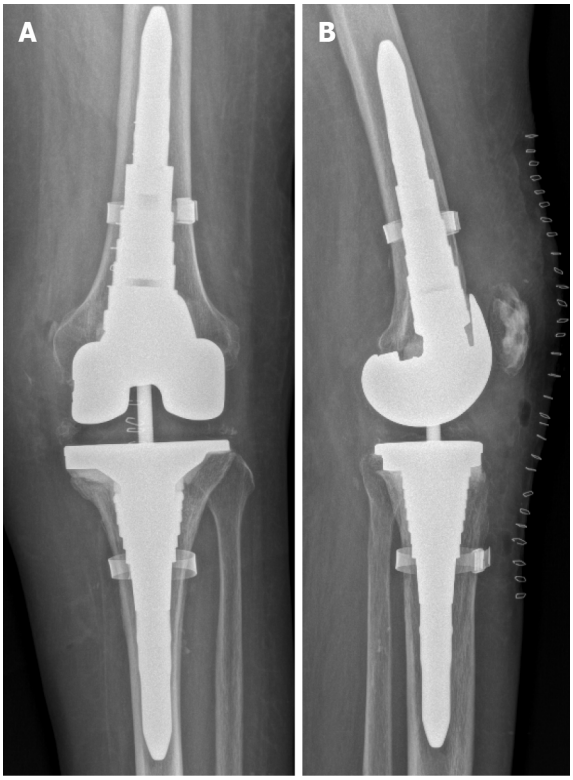

DOI: 10.12998/wjcc.v11.i3.677

Figure 5 Ten-month postoperative radiograph showing a revision knee arthroplasty (Attune® Revision Knee System, J&J Medical Devices). A: Anterior-posterior view; B: Lateral view.

DISCUSSION

Periprosthetic infections with *Brucella* species are rare; therefore, diagnosis can be a challenge especially in nonendemic countries such as Austria. Our patient is originally from Afghanistan and had been living in Austria since 2013. The pain in her left knee started years before she emigrated to Austria, but no cause could be found in Afghanistan. TKA was performed in our department in 2015 after several attempts of conservative treatment for osteoarthritis.

When asked about the possible transmission of *Brucella* species, the patient denied consumption of unpasteurized milk or raw meat, but she reported that she had kept livestock in Afghanistan. The fact that the periprosthetic infection occurred five years after implantation but seven years after the last contact with livestock suggests that the patient had a latent infection with *Brucella melitensis* prior to TKA. Brucellosis has a tendency towards chronicity similar to tuberculosis. By evading the host immune defense, it can persist for long periods in practically any organ system, thus causing chronic granulomatous infections[5,8]. It is debatable whether the real cause of knee pain eventually leading to TKA in 2015 was chronic osteoarticular brucellosis rather than osteoarthrosis. In fact, our patient complained of recurrent load-dependent knee pain after her initial surgery. Minimal effusion was observed in various visits to our department. There was no warming or redness, and the pain always improved with cryotherapy and oral analgesics. Minor radiolucent lines at the anterior and posterior flanges of the femoral component were already evident one year postoperatively (Figure 6). However, such radiological changes are common, and the incidence is reported to be up to 20% for the type of prosthesis used here[9,10]. Therefore, infection was suspected in December 2020 only because the patient had severe pain, and the X-ray showed definite signs of loosening.

After the diagnosis of brucellosis was confirmed we performed magnetic resonance imaging (MRI) of the spine due to the patient's history of chronic lower back pain. The MRI showed depleted intervertebral space in L4/L5 and post-inflammatory alterations indicating a residual state after spondylodiscitis. In conclusion, the history and clinical findings retrospectively and strongly suggest that the patient had suffered from chronic brucellosis with involvement of the knee and lumbar spine for years.

Our case also demonstrates the difficulty in detecting brucellosis especially because the patient was already receiving broad-spectrum penicillin when the diagnostic testing began. Culture was positive in one out of two synovial fluid samples and only one in seven intraoperative tissue samples. It took two weeks of culture until bacterial growth was noted. Sonication was negative. Antibody detection was performed after receiving the microbiological findings and was positive for *Brucella melitensis* and *Brucella abortus*; the latter, however, was considered a serological cross-reaction. Our diagnostic

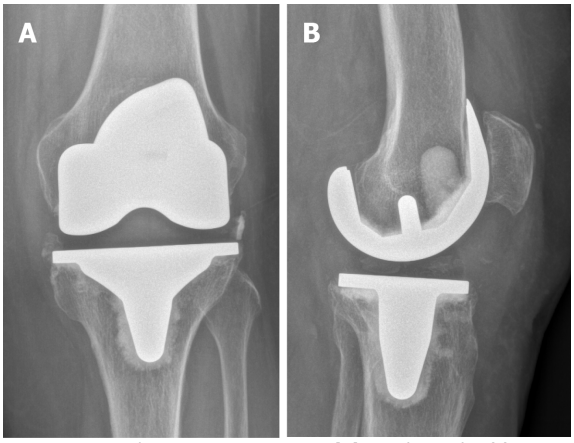

DOI: 10.12998/wjcc.v11.i3.677

Figure 6 Radiograph one year after the initial surgery showing radiolucent lines around the femoral component. A: Anterior-posterior view; B: Lateral view.

experience is consistent with reports in the literature stating that the detection of brucellosis can be challenging and complicated by the long cultivation required due to slow bacterial growth[4,6,7]. We therefore concur with recommendations suggesting screening for anti-*Brucella* antibodies early in patients from endemic countries or in close contact with livestock[6,7]. When serology is positive, invasive procedures such as joint aspiration or surgery should be performed using special protection including an apron, eye protection, and filtering face piece-3 mask to prevent transmission *via* aerosols. Laboratory staff must be informed about special hazards when handling samples[6,7,11].

Treatment of systemic brucellosis requires antibiotic combination therapy for at least six weeks. Monotherapy or a shorter duration of therapy carries a high risk of treatment failure and relapse[3,7,8]. The most common antibiotic combinations are doxycycline plus rifampicin or doxycycline plus streptomycin. Fluoroquinolones, trimethoprim/sulfamethoxazole, or gentamicin are also used. To date, no gold standard in antibiotic combination and duration of therapy has been established[3,7].

Antibiotic therapy for at least 12 wk is recommended in osteoarticular brucellosis[7,12]. Antimicrobial therapy without surgical intervention may be feasible in cases of periprosthetic infection and the absence of radiological loosening[6,13,14]. Thus, successful outcomes have been reported in eight out of nine joints with periprosthetic infections due to *Brucella* and with well-fixed implants when treated solely with antibiotics over six to 52 wk[6]. However, the sample number of patients described is too small to derive firm recommendations. Revision surgery is mandatory in cases of loose implants. Good results have been described for both one-stage and two-stage revision surgery with short or long intervals[6,7]. The prognosis of brucellosis, whether local or systemic, is generally good: Mortality is low but with high morbidity due to the multilocular and often protracted course of disease[3].

We opted for a two-stage revision with a six-week interval given the long history of pain over three months and the profound radiological changes in our case. The antibiotic regimen consisted of doxycycline and rifampicin for 12 wk, gentamicin for two weeks after implant removal, and daptomycin for two weeks after reimplantation. No side effects (changes in blood count or transaminases) were encountered. The treatment of our patient with multiple comorbidities was an interdisciplinary challenge involving orthopedics, internal medicine, and microbiology, and we would like to thank all the disciplines for their contribution to the good outcome.

CONCLUSION

Brucellosis can be easily missed given the low prevalence in nonendemic countries. We recommend that clinicians consider brucellosis as a possible cause for chronic arthralgia, backache, and periprosthetic infection in patients from countries with a high brucellosis burden. If brucellosis is considered, then serological tests should be performed prior to joint aspiration or surgery because those procedures pose a risk of transmission *via* aerosols and therefore require special safety precautions. There is currently no uniform treatment concept in surgical intervention or choice and duration of antibiotic therapy for periprosthetic joint infections caused by *Brucella*; however, our antibiotic regimen was successful and can be used to guide future cases.

FOOTNOTES

Author contributions: Stumpner T performed the follow-up examinations and wrote the manuscript with the support of Kuhn R and Ortmaier R; Kuhn R managed the case and coordinated the involved disciplines; Hochreiter J and Ortmaier R supervised the case; all authors contributed to, read and approved the final manuscript.

Informed consent statement: Informed consent was obtained from the patient for the publication of this case report and any accompanying images.

Conflict-of-interest statement: All authors declare that they have no conflict of interest to disclose.

CARE Checklist (2016) statement: All authors have read the CARE Checklist (2016), and the manuscript was prepared and revised according to the CARE Checklist (2016).

Country/Territory of origin: Austria

ORCID number: Thomas Stumpner 0000-0001-6883-9185; Josef Hochreiter 0000-0002-5378-1811; Reinhold Ortmaier 0000-0002-6684-2513.

S-Editor: Wang LL
L-Editor: A
P-Editor: Wang LL

REFERENCES

1 **González-Espinoza G**, Arce-Gorvel V, Mémet S, Gorvel JP. Brucella: Reservoirs and Niches in Animals and Humans. *Pathogens* 2021; **10** [PMID: 33572264 DOI: 10.3390/pathogens10020186]
2 **Pappas G**, Papadimitriou P, Akritidis N, Christou L, Tsianos EV. The new global map of human brucellosis. *Lancet Infect Dis* 2006; **6**: 91-99 [PMID: 16439329 DOI: 10.1016/S1473-3099(06)70382-6]
3 **Yousefi-Nooraie R**, Mortaz-Hejri S, Mehrani M, Sadeghipour P. Antibiotics for treating human brucellosis. *Cochrane Database Syst Rev* 2012; **10**: CD007179 [PMID: 23076931 DOI: 10.1002/14651858.CD007179.pub2]
4 **Yagupsky P**, Morata P, Colmenero JD. Laboratory Diagnosis of Human Brucellosis. *Clin Microbiol Rev* 2019; **33** [PMID: 31722888 DOI: 10.1128/CMR.00073-19]
5 **Franco MP**, Mulder M, Gilman RH, Smits HL. Human brucellosis. *Lancet Infect Dis* 2007; **7**: 775-786 [PMID: 18045560 DOI: 10.1016/S1473-3099(07)70286-4]
6 **Lewis JM**, Folb J, Kalra S, Squire SB, Taegtmeyer M, Beeching NJ. Brucella melitensis prosthetic joint infection in a traveller returning to the UK from Thailand: Case report and review of the literature. *Travel Med Infect Dis* 2016; **14**: 444-450 [PMID: 27591088 DOI: 10.1016/j.tmaid.2016.08.010]
7 **Flury D**, Behrend H, Sendi P, von Kietzell M, Strahm C. Brucella melitensis prosthetic joint infection. *J Bone Jt Infect* 2017; **2**: 136-142 [PMID: 28540150 DOI: 10.7150/jbji.18408]
8 **Pappas G**, Akritidis N, Bosilkovski M, Tsianos E. Brucellosis. *N Engl J Med* 2005; **352**: 2325-2336 [PMID: 15930423 DOI: 10.1056/NEJMra050570]
9 **Behrend H**, Hochreiter B, Potocnik P, El Baz Y, Zdravkovic V, Tomazi T. No difference in radiolucent lines after TKA: a matched-pair analysis of the classic implant and its evolutional design. *Knee Surg Sports Traumatol Arthrosc* 2020; **28**: 3962-3968 [PMID: 32062683 DOI: 10.1007/s00167-020-05894-w]
10 **Staats K**, Wannmacher T, Weihs V, Koller U, Kubista B, Windhager R. Modern cemented total knee arthroplasty design shows a higher incidence of radiolucent lines compared to its predecessor. *Knee Surg Sports Traumatol Arthrosc* 2019; **27**: 1148-1155 [PMID: 30244340 DOI: 10.1007/s00167-018-5130-0]
11 **Traxler RM**, Lehman MW, Bosserman EA, Guerra MA, Smith TL. A literature review of laboratory-acquired brucellosis. *J Clin Microbiol* 2013; **51**: 3055-3062 [PMID: 23824774 DOI: 10.1128/JCM.00135-13]
12 **Unuvar GK**, Kilic AU, Doganay M. Current therapeutic strategy in osteoarticular brucellosis. *North Clin Istanb* 2019; **6**: 415-420 [PMID: 31909392 DOI: 10.14744/nci.2019.05658]
13 **Kim SJ**, Park HS, Lee DW, Kim JH. Brucella infection following total joint arthroplasty: A systematic review of the literature. *Acta Orthop Traumatol Turc* 2018; **52**: 148-153 [PMID: 29223445 DOI: 10.1016/j.aott.2017.11.003]
14 **Balkhair A**, Al Maskari S, Ibrahim S, Al Busaidi I, Al Amin M, Ba Taher H. Brucella Periprosthetic Joint Infection Involving Bilateral Knees with Negative Synovial Fluid Alpha-Defensin. *Case Rep Infect Dis* 2019; **2019**: 9423946 [PMID: 31396423 DOI: 10.1155/2019/9423946]

World Journal of Clinical Cases

Submit a Manuscript: https://www.f6publishing.com

World J Clin Cases 2023 January 26; 11(3): 684-691

DOI: 10.12998/wjcc.v11.i3.684

ISSN 2307-8960 (online)

CASE REPORT

Recurrent intramuscular lipoma at extensor pollicis brevis: A case report

Je Yeon Byeon, Yong Seon Hwang, Ji Hye Lee, Hwan Jun Choi

Specialty type: Medicine, research and experimental

Provenance and peer review: Unsolicited article; Externally peer reviewed.

Peer-review model: Single blind

Peer-review report's scientific quality classification

Grade A (Excellent): 0
Grade B (Very good): B
Grade C (Good): C
Grade D (Fair): 0
Grade E (Poor): 0

P-Reviewer: Alfaqih MS, Indonesia; Singh M, United States

Received: November 1, 2022
Peer-review started: November 1, 2022
First decision: December 13, 2022
Revised: December 14, 2022
Accepted: January 9, 2023
Article in press: January 9, 2023
Published online: January 26, 2023

Je Yeon Byeon, Yong Seon Hwang, Hwan Jun Choi, Plastic and Reconstructive Surgery, Soonchunhyang University Hospital, Cheonan-si 31151, South Korea

Ji Hye Lee, Department of Pathology, Soonchunhyang University Hospital, Cheonan-si 31151, South Korea

Corresponding author: Hwan Jun Choi, MD, PhD, Professor, Surgeon, Plastic and Reconstructive Surgery, Soonchunhyang University Hospital, No. 31 Sooncheonhyang 6-Gil, Dongnam-gu, Cheonan-si 31151, South Korea. iprskorea@gmail.com

Abstract

BACKGROUND

This report describes and discusses recurrent intramuscular lipoma (IML) of the extensor pollicis brevis (EPB). An IML usually occurs in a large muscle of the limb or torso. Recurrence of IML is rare. Recurrent IMLs, especially those with unclear boundaries, necessitate complete excision. Several cases of IML in the hand have been reported. However, recurrent IML appearing along the muscle and tendon of EPB on wrist and forearm has not been reported yet.

CASE SUMMARY

In this report, the authors describe clinical and histopathological features of recurrent IML at EPB. A 42-year-old Asian woman presented with a slow-growing lump in her right forearm and wrist area six months ago. The patient had a history of surgery for a lipoma of the right forearm one year ago with a scar of 6 cm on the right forearm. magnetic resonance imaging confirmed that the lipomatous mass, which had attenuation similar to subcutaneous fat, had invaded the muscle layer of EPB. Excision and biopsy were performed under general anesthesia. On histological examination, it was identified as an IML showing mature adipocytes and skeletal muscle fibers. Therefore, surgery was terminated without further resection. No recurrence occurred during a follow-up of five years after surgery.

CONCLUSION

Recurrent IML in the wrist must be examined to differentiate it from sarcoma. Damage to surrounding tissues should be minimized during excision.

Key Words: Intramuscular; Lipoma; Recurrence; Wrist; Case report

Core Tip: Lipoma is one of the most common benign tumors. Intramuscular lipoma (IML) is a lipoma that has invaded the muscular layer, sometimes with unclear boundaries. It may recur if complete resection is not performed. IMLs that recur with unclear boundaries might need to be differentiated from soft tissue sarcoma. Therefore, imaging tests such as computed tomography or magnetic resonance imaging should be performed before surgery and a thorough preoperative plan should be established to reduce recurrence and preserve hand function.

Citation: Byeon JY, Hwang YS, Lee JH, Choi HJ. Recurrent intramuscular lipoma at extensor pollicis brevis: A case report. *World J Clin Cases* 2023; 11(3): 684-691
URL: https://www.wjgnet.com/2307-8960/full/v11/i3/684.htm
DOI: https://dx.doi.org/10.12998/wjcc.v11.i3.684

INTRODUCTION

A lipoma is a common benign mesenchymal tumor that can occur anywhere in our body. It is one of the most common soft tissue tumors[1]. Lipomas are usually capsulized and well distinguished from surrounding subcutaneous adipose tissues. However, when they infiltrate structures such as muscles, nerves, or synovium, they are less circumscribed and not-well-distinguished from surrounding tissues than usual lipoma. Among them, cases of invasion of the muscle layer are called intramuscular lipoma (IML) or infiltrating lipoma[2]. As reported in several cases, IML usually occurs in a large muscle of the limb or torso[3-8]. To treat an IML, complete removal including capsules is performed, similar to conventional lipoma treatment methods. However, of all IMLs, 83% are infiltrative and 17% are well-defined. In case of infiltrative IML, it is difficult to distinguish from surrounding tissues[4]. There are also important structures around the periphery of the IML that can make it difficult to achieve complete excision. There is a possibility of recurrence if there is no complete excision[5,8]. Additionally, it might be difficult to differentiate a recurrent IML from well-differentiated liposarcoma, because an IML is clinically or histologically indistinguishable from a well-differentiated liposarcoma[4,9]. Therefore, it is important to perform a preoperative radiology examination. Magnetic resonance imaging (MRI) is a device that can effectively diagnose lipoma. It can also help diagnose IML[10]. In this report, the authors report a recurrent IML in the extensor pollicis brevis (EPB) muscle treated surgically without showing any signs of recurrence after five years of follow-up.

CASE PRESENTATION

Chief complaints

A 42-year-old Asian woman presented with a slow-growing lump in her right forearm and wrist area six months ago.

History of present illness

Symptoms started six months ago with a recurrent lump on the previous operative wounds of wrist and forearm.

History of past illness

The patient had a history of surgery with a lipoma of the right forearm one year ago and had a scar of 6 cm on the right forearm. There was no other medical history or surgical history.

Personal and family history

The patient denied any family history of tumors.

Physical examination

Soft, painless lumps along the EPB of the right thumb were found on physical examination. One had a size of 1 cm × 2 cm in the medial area of the right wrist. One had a size of 2 cm × 5 cm on the medial side of the forearm. Her sensation of fingers and wrists, range of motion, and motor power were all normal (Figure 1).

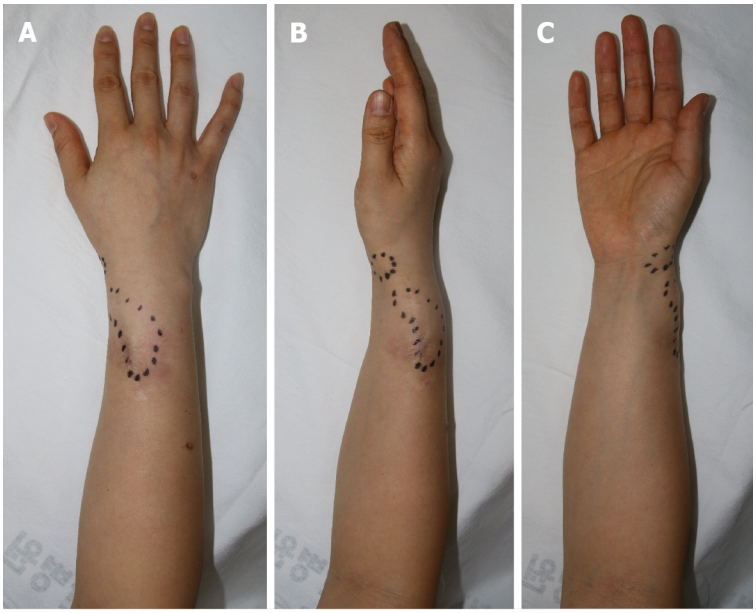

DOI: 10.12998/wjcc.v11.i3.684

Figure 1 Preoperative photographs. A: One 2 cm × 5 cm in size in the medial part of the forearm; B and C: A soft, painless lump was palpated along the extensor pollicis brevis of the right thumb, one 1 cm × 2 cm in size on the medial side of the right wrist. The black dotted line signifies the border of the lump to the touch. The patient's sensation, range of motion of fingers and wrists, and motor power were normal. The previously operated scar is identified about 6 cm on the radial side of the right forearm.

Laboratory examinations

There were no specific findings in laboratory examinations.

Imaging examinations

MRIs showed lumps in muscles and ligaments of EPB that appeared to be due to fat attenuation. Invaded muscles and ligaments showed unclear boundaries (Figure 2).

FINAL DIAGNOSIS

Biopsy results also confirmed the IML of EPB (Figure 3).

TREATMENT

General anesthesia was performed with inhalation anesthesia using sevoflurane after induction using intravascular propofol. After drawing a longitudinal 12 cm incision along the path of the EPB and previous scars, incision was performed with No 15-scalpel blade. Intact presence of the superficial radial nerve and artery running next to the EPB was confirmed. After meticulous dissection of adjacent normal tissues (including muscles, ligaments, nerves, blood vessels, *etc.*), the IML was exposed using sharp mosquito. A lipomatous mass with a lobulated aspect measuring 12 cm × 4 cm × 5 cm was invading muscles and ligaments (Figures 4 and 5). Blunt Metzenbaum scissor and electrocautery were then used to remove the mass. 200cc HemoVAC was inserted after normal saline irrigation. The superficial fascia and subcutaneous layer were sutured layer by layer with 4-0 Maxon and the skin was sutured with 5-0 Nylon.

OUTCOME AND FOLLOW-UP

Immediately after the surgery, her sensory function was intact and circulation was well maintained (Figure 6). Her extension power was slightly weakened by partial excision of the EPB. However, her extension function was preserved. After 5 years of follow-up, there were no recurrences, side effects, or functional limitations.

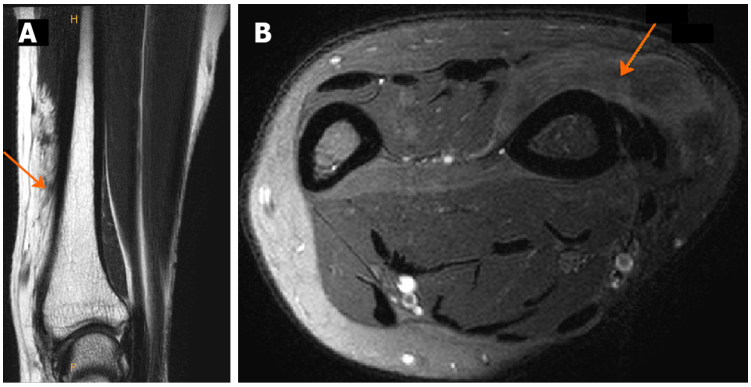

DOI: 10.12998/wjcc.v11.i3.684

Figure 2 Preoperative magnetic resonance imaging showing lipomatous masses with fat-like attenuation in extensor pollicis brevis muscles and ligaments. A: In the coronal view, lipomatous mass infiltrated in the muscle was identified. Boundaries with surrounding muscles and ligaments were unclear; B: In the axial view, lipomatous mass of similar attenuate to fat was identified. An orange arrow indicates a lipomatous mass that infiltrates muscle and ligaments.

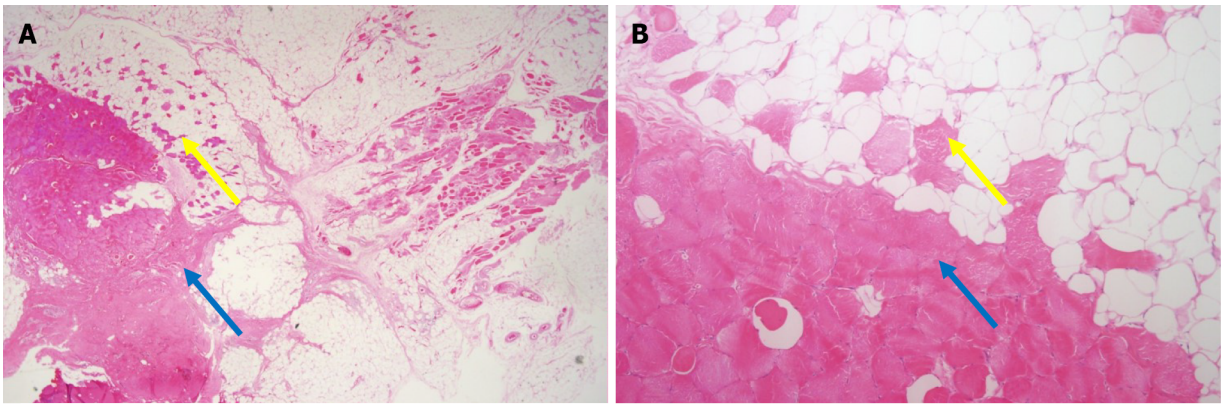

DOI: 10.12998/wjcc.v11.i3.684

Figure 3 Histological findings. A: Microscopic findings of intramuscular lipomas showing mature adipocytes and skeletal muscle fibers (pink color) (× 10.25 magnification, hematoxylin and eosin staining); B: Skeletal muscle fibers (pink color) are observed between mature adipocytes (× 100 magnification, hematoxylin and eosin staining). Yellow arrows indicate muscle components in fat. Blue arrows indicate muscle belly of extensor pollicis brevis.

DISCUSSION

An IML can be distinguished from a conventional lipoma by its rarity and its clinical and pathological characteristics[2]. Histologically, IML can be divided into an infiltrative type, a well-circumscribed type, and a mixed type. Among them, the infiltrative type of IML has distinctive features[11-13]. Clinically, IMLs are characterized by a slow-growing mass that is asymptomatic or accompanied by local edema. Pain is a rare symptom that appears at the end of the course of the disease. It can occur when a deep, huge lipoma causes nerve compression with a mass effect or compresses surrounding soft tissues[12]. In some cases, it has been reported that IML itself is associated with functional limitation of muscles[13, 14]. Paresthesia and nerve distribution caused by nerve impingement are also among symptoms that might appear[15,16]. Trauma, chronic irritation, obesity, developmental disorders, endocrine, dysmetabolic factors, and genetic factors have been suggested to play roles in the pathogenesis of IML [17-19].

Papakostas *et al*[6] have reported cases of IML of the thenar. Lui[7] have reported cases of IML occurring in the abductor digiti minimi. Kim *et al*[1] have presented a lipoma occurring in the flexor tenosynovium. Kostas-Agnantis *et al*[20] have reported a lipoma case in the palmaris longus tendon. Lee *et al*[15] have reported cases of IML occurring in thenar and hypothenar area. However, cases of recurrent IML involving both extensor muscle and tendinous portion at the wrist and forearm level have not been reported yet.

Murphey *et al*[10] have stated that there is no possibility of malignant transformation of lipomas. It was often claimed that the reports were probably sampling errors or misdiagnoses.

Currently, the recurrence rate of IML is believed to be very low[21]. The patient in this case had previously undergone a surgery. However, it was not completely removed during the previous operation, which might have led to the recurrent. Therefore, attention should be paid to complete

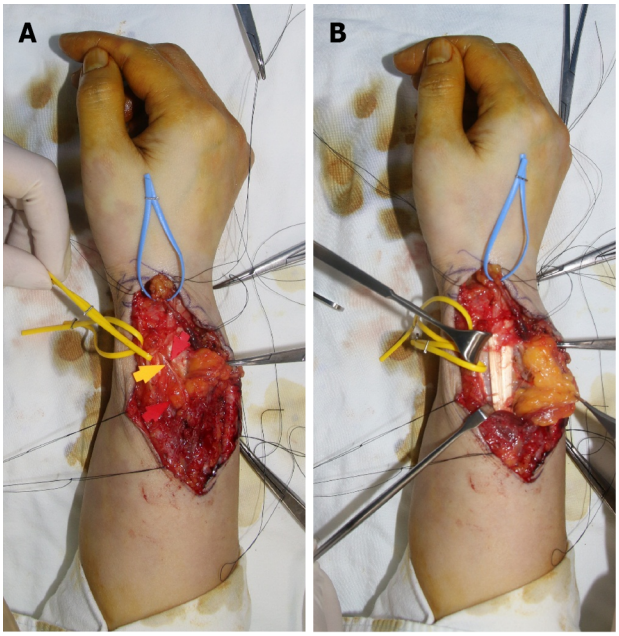

DOI: 10.12998/wjcc.v11.i3.684

Figure 4 Intraoperative photographs. A: The previous surgical scar was used, and an incision was applied along the run of the extensor pollicis brevis (EPB) to expose the lipomatous mass. A radial artery marked with yellow vessel loop and lipoma in the EPB tendon sheath marked with blue vessel loop were identified; B: Lipoma infiltrating into the muscle portion of EPB was removed while preserving the superficial radial nerve marked with yellow and red arrows.

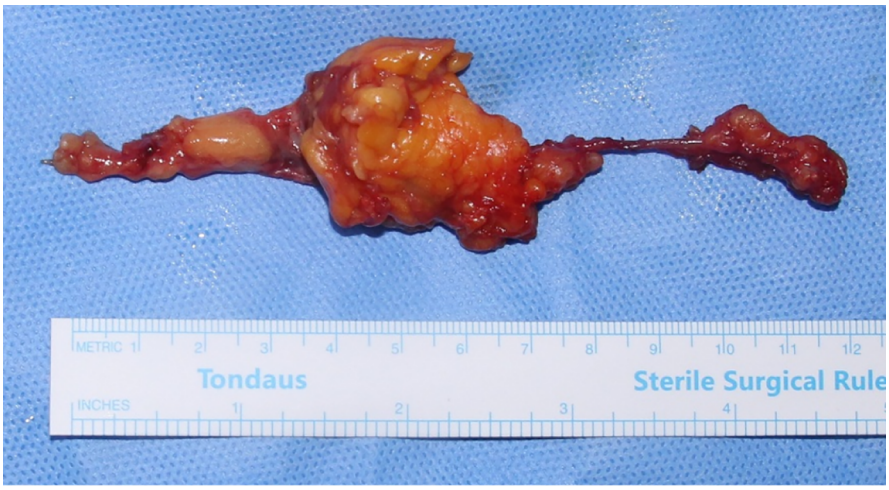

DOI: 10.12998/wjcc.v11.i3.684

Figure 5 Photograph of the specimen. A lipomatous mass of 12 cm × 4 cm × 5 cm was excised. It infiltrated the extensor pollicis brevis (EPB) muscle and tendon sheath. Most of the mass burden was located in the muscle portion of the EPB, presenting as yellow tissue with lobulated aspect and muscular fibers throughout.

excision to reduce the possibility of recurrence and to exclude the possibility of malignancy. By minimizing trauma and meticulous dissection during the surgical procedure, both nerves and blood vessels were preserved with only the area with lipoma invasion removed. The patient has been observed for five years without showing any signs of recurrence.

Computed tomography scan and MRI are both useful for detecting IML and evaluating its invasion in surrounding tissues[10,22]. On computed tomography (CT) scan, IML in the muscle shows a hypodense mass, similar to dense subcutaneous fat[23]. Its morphology can vary widely, ranging from ovoid to fusiform. Its margin might be well-circumscribed or infiltrative[24]. In MRI, IML appears to show a high signal in both T1 and T2, similar to fatty tissue with low signal similar to normal fat in fat-suppressed sequences[10]. MRI can identify IML more specifically than CT. However, results seen on the image might not be exactly the same as actual histological examination results[10].

Histopathologic exam is one of the essential tests for diagnosis. In most cases, there is a uniform appearance of mature uni-vacuolated adipocytes with uniform size and shape. In rare cases, IML can

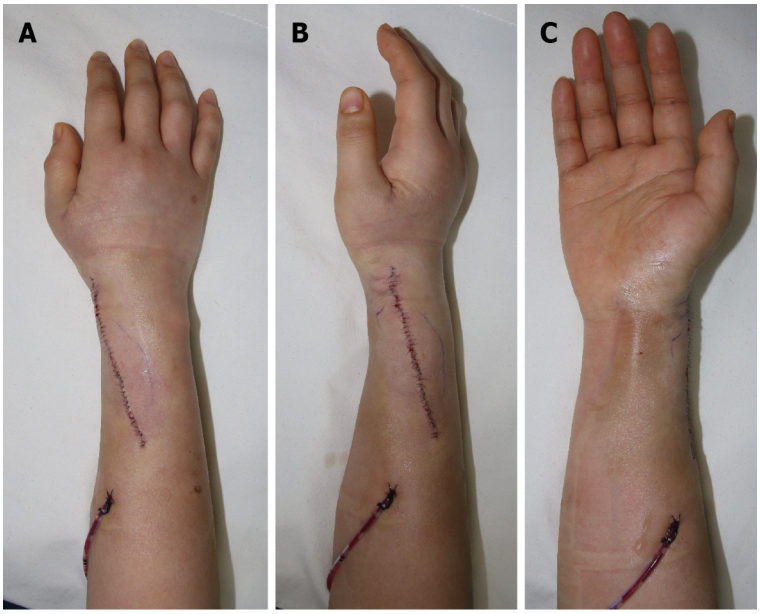

DOI: 10.12998/wjcc.v11.i3.684

Figure 6 Postoperative photographs. A and B: Primary closure was performed after removal of the intramuscular lipoma and 200cc Hemovac was inserted. There was no contour deformity on postoperative physical examination. Sensory function was intact, and circulation was well maintained; C: However, some extensor pollicis brevis motor weakness occurred. Nevertheless, no deformation of the thumb was seen in the neutral state. Other ranges of motion remained intact.

invade muscles, fascia, and tendon[11]. Histological and cytological analyses of IML are extremely important for differentiating it from well-differentiated liposarcoma. Well-differentiated liposarcomas differ from normal IMLs in the presence of atypical cells, vacuolated lipoblasts admixed with fibroblasts-like spindle cells, and several other features[25].

CONCLUSION

In conclusion, considering that IML can occur and recur in hand muscles as observed in this case, careful physical examination and imaging examination should be performed before surgery to diagnose it and completely remove it to reduce the recurrence rate. Additionally, since hands have many important structures, careful attention should be paid to effectively removing the IML s while preserving surrounding nerves, blood vessels, and ligaments.

FOOTNOTES

Author contributions: Byeon JY and Hwang YS contributed to manuscript writing and editing, and data collection; Lee JH contributed to histological examination of specimen; Choi HJ contributed to conceptualization and supervision; all authors have read and approved the final manuscript.

Informed consent statement: Written informed consent was obtained from the patient for publication of this report and any accompanying images.

Conflict-of-interest statement: All the authors report no relevant conflicts of interest for this article.

CARE Checklist (2016) statement: The authors have read the CARE Checklist (2016). The manuscript was prepared and revised according to the CARE Checklist (2016).

Country/Territory of origin: South Korea

ORCID number: Hwan Jun Choi 0000-0002-0752-0389.

S-Editor: Fan JR
L-Editor: A
P-Editor: Fan JR

REFERENCES

1 **Kim HW**, Lee KJ, Choi SK, Jang IT, Lee HJ. A large palmar lipoma arising from flexor tenosynovium of the hand causing digital nerve compression: A case report. *Jt Dis Relat Surg* 2021; **32**: 230-233 [PMID: 33463442 DOI: 10.5606/ehc.2021.75678]
2 **Charifa A**, Azmat CE, Badri T. Lipoma Pathology. 2022 Dec 5. In: StatPearls [Internet]. Treasure Island (FL): StatPearls Publishing; 2022 Jan- [PMID: 29493968]
3 **Wolfe SW**, Bansal M, Healey JH, Ghelman B. Computed tomographic evaluation of fatty neoplasms of the extremities. A clinical, radiographic, and histologic review of cases. *Orthopedics* 1989; **12**: 1351-1358 [PMID: 2798244 DOI: 10.3928/0147-7447-19891001-12]
4 **McTighe S**, Chernev I. Intramuscular lipoma: a review of the literature. *Orthop Rev (Pavia)* 2014; **6**: 5618 [PMID: 25568733 DOI: 10.4081/or.2014.5618]
5 **Khalfe Y**, Orengo I, Buren GV, Rosen T. Intramuscular lipoma of the scapular region. *Dermatol Online J* 2021; **27** [PMID: 34391334 DOI: 10.5070/D327754370]
6 **Papakostas T**, Tsovilis AE, Pakos EE. Intramuscular Lipoma of the Thenar: A Rare Case. *Arch Bone Jt Surg* 2016; **4**: 80-82 [PMID: 26894225]
7 **Lui TH**. Intramuscular lipoma of the abductor digiti minimi mimicking intramuscular haemangioma. *BMJ Case Rep* 2013; **2013** [PMID: 24347498 DOI: 10.1136/bcr-2013-200897]
8 **Su CH**, Hung JK, Chang IL. Surgical treatment of intramuscular, infiltrating lipoma. *Int Surg* 2011; **96**: 56-59 [PMID: 21675621 DOI: 10.9738/1396.1]
9 **Ohguri T**, Aoki T, Hisaoka M, Watanabe H, Nakamura K, Hashimoto H, Nakamura T, Nakata H. Differential diagnosis of benign peripheral lipoma from well-differentiated liposarcoma on MR imaging: is comparison of margins and internal characteristics useful? *AJR Am J Roentgenol* 2003; **180**: 1689-1694 [PMID: 12760945 DOI: 10.2214/ajr.180.6.1801689]
10 **Murphey MD**, Carroll JF, Flemming DJ, Pope TL, Gannon FH, Kransdorf MJ. From the archives of the AFIP: benign musculoskeletal lipomatous lesions. *Radiographics* 2004; **24**: 1433-1466 [PMID: 15371618 DOI: 10.1148/rg.245045120]
11 **Kindblom LG**, Angervall L, Stener B, Wickbom I. Intermuscular and intramuscular lipomas and hibernomas. A clinical, roentgenologic, histologic, and prognostic study of 46 cases. *Cancer* 1974; **33**: 754-762 [PMID: 4815578 DOI: 10.1002/1097-0142(197403)33:3<754::aid-cncr2820330322>3.0.co;2-f]
12 **Patil S**, Goel A, Mandal S. Re: Morsi HA, Mursi K, Abdelaziz AY, Elsheemy MS, Salah M, Eissa MA. Renal pelvis reduction during dismembered pyeloplasty: is it necessary? *J Pediatr Urol* 2013; **9**: 306-307 [PMID: 22749571 DOI: 10.1016/j.jpurol.2012.05.019]
13 **Han HH**, Choi JY, Seo BF, Moon SH, Oh DY, Ahn ST, Rhie JW. Treatment for intramuscular lipoma frequently confused with sarcoma: a 6-year restrospective study and literature review. *Biomed Res Int* 2014; **2014**: 867689 [PMID: 25574469 DOI: 10.1155/2014/867689]
14 **Warner JJ**, Madsen N, Gerber C. Intramuscular lipoma of the deltoid causing shoulder pain. Report of two cases. *Clin Orthop Relat Res* 1990; 110-112 [PMID: 2317963]
15 **Lee YH**, Jung JM, Baek GH, Chung MS. Intramuscular lipoma in thenar or hypothenar muscles. *Hand Surg* 2004; **9**: 49-54 [PMID: 15368626 DOI: 10.1142/s0218810404002005]
16 **Joshua BZ**, Bodner L, Shaco-Levy R. Intramuscular (Infiltrating) Lipoma of the Floor of the Mouth. *Case Rep Med* 2018; **2018**: 3529208 [PMID: 29755529 DOI: 10.1155/2018/3529208]
17 **Awad P**. Rare Intramuscular Lipoma of the Foot: A Case Report. *J Am Podiatr Med Assoc* 2021; **111** [PMID: 34144584 DOI: 10.7547/19-118]
18 **Pichierri A**, Marotta N, Raco A, Delfini R. Intramuscular infiltrating lipoma of the longus colli muscle. a very rare cause of neck structures compression. *Cent Eur Neurosurg* 2010; **71**: 157-159 [PMID: 20358507 DOI: 10.1055/s-0029-1241189]
19 **Copcu E**. Can intramuscular lipoma have a post-traumatic origin? *Br J Dermatol* 2003; **149**: 1084-1085 [PMID: 14632827 DOI: 10.1111/j.1365-2133.2003.05615.x]
20 **Kostas-Agnantis I**, Gkiatas I, Korompilia M, Kosmas D, Motsis E, Pakos E, Korompilias A. Lipoma Arborescens of the Upper Extremity With Anatomic Variation of the Palmaris Longus: A Case Report. *JBJS Case Connect* 2022; **12** [PMID: 36099386 DOI: 10.2106/JBJS.CC.22.00334]
21 **Ramos-Pascua LR**, Guerra-Álvarez OA, Sánchez-Herráez S, Izquierdo-García FM, Maderuelo-Fernández JÁ. [Intramuscular lipomas: Large and deep benign lumps not to underestimated. Review of a series of 51 cases]. *Rev Esp Cir Ortop Traumatol* 2013; **57**: 391-397 [PMID: 24183389 DOI: 10.1016/j.recot.2013.09.010]
22 **Stacy GS**, Bonham J, Chang A, Thomas S. Soft-Tissue Tumors of the Hand-Imaging Features. *Can Assoc Radiol J* 2020; **71**: 161-173 [PMID: 32063006 DOI: 10.1177/0846537119888356]
23 **Pant R**, Poh AC, Hwang SG. An unusual case of an intramuscular lipoma of the pectoralis major muscle simulating a malignant breast mass. *Ann Acad Med Singap* 2005; **34**: 275-276 [PMID: 15902350]
24 **Naruse T**, Yanamoto S, Yamada S, Rokutanda S, Kawakita A, Takahashi H, Matsushita Y, Hayashida S, Imayama N, Morishita K, Yamashita K, Kawasaki G, Umeda M. Lipomas of the oral cavity: clinicopathological and immunohistochemical study of 24 cases and review of the literature. *Indian J Otolaryngol Head Neck Surg* 2015; **67**: 67-73 [PMID: 25621257 DOI: 10.1007/s12070-014-0765-8]
25 **Evans HL**, Soule EH, Winkelmann RK. Atypical lipoma, atypical intramuscular lipoma, and well differentiated

retroperitoneal liposarcoma: a reappraisal of 30 cases formerly classified as well differentiated liposarcoma. *Cancer* 1979; **43**: 574-584 [PMID: 421182 DOI: 10.1002/1097-0142(197902)43:2<574::aid-cncr2820430226>3.0.co;2-7]

World Journal of Clinical Cases

Submit a Manuscript: https://www.f6publishing.com

World J Clin Cases 2023 January 26; 11(3): 692-699

DOI: 10.12998/wjcc.v11.i3.692

ISSN 2307-8960 (online)

CASE REPORT

Imaging features of retinal hemangioblastoma: A case report

Xin Tang, Hai-Ming Ji, Wen-Wen Li, Zhong-Xiang Ding, Sheng-Li Ye

Specialty type: Medicine, research and experimental

Provenance and peer review: Unsolicited article; Externally peer reviewed.

Peer-review model: Single blind

Peer-review report's scientific quality classification

Grade A (Excellent): 0
Grade B (Very good): B, B
Grade C (Good): C
Grade D (Fair): 0
Grade E (Poor): 0

P-Reviewer: Aydin S, Turkey; Urbančič M, Slovenia

Received: November 24, 2022
Peer-review started: November 24, 2022
First decision: December 13, 2022
Revised: December 22, 2022
Accepted: January 5, 2023
Article in press: January 5, 2023
Published online: January 26, 2023

Xin Tang, Department of Radiology, Hangzhou Wuyunshan Hospital, Hangzhou Health Promotion Research Institute, Hangzhou 310008, Zhejiang Province, China

Hai-Ming Ji, Department of Radiology, Liangzhu Hospital, Hangzhou 311112, Zhejiang Province, China

Wen-Wen Li, Department of Radiology, Jingmen No.1 People's Hospital, Jingmen 448000, Hubei Province, China

Zhong-Xiang Ding, Department of Radiology, Key Laboratory of Clinical Cancer Pharmacology and Toxicology Research of Zhejiang Province, Affiliated Hangzhou First People's Hospital, Zhejiang University School of Medicine, Hangzhou 310006, Zhejiang Province, China

Sheng-Li Ye, Department of Radiology, Shulan (Hangzhou) Hospital Affiliated to Zhejiang Shuren University Shulan International Medical College, Hangzhou 310022, Zhejiang Province, China

Corresponding author: Sheng-Li Ye, MD, Professor, Department of Radiology, Shulan (Hangzhou) Hospital Affiliated to Zhejiang Shuren University Shulan International Medical College, No. 848 Dongxin Road, Hangzhou 310022, Zhejiang Province, China.
532382048@qq.com

Abstract

BACKGROUND

Hemangioblastoma typically occurs in the cerebellum, spinal cord, and central nervous system. However, in rare cases, it could occur in the retina or optic nerve. The prevalence of retinal hemangioblastoma is 1 in 73080, and it occurs either alone or as the manifestation of von Hippel Lindau (VHL) disease. Here, we reported a rare case with the imaging features of retinal hemangioblastoma without VHL syndrome, along with the relevant literature review.

CASE SUMMARY

A 53-year-old man had progressive swelling, pain and blurred vision in the left eye without obvious inducement for 15 d. Ultrasonography revealed a possible optic nerve head melanoma. Computed tomography (CT) showed punctate calcification on the posterior wall of the left eye ring and small patchy soft tissue density in the posterior part of the eyeball. Magnetic resonance imaging showed slightly hyperintense signal on T1-weighted images and slightly hypointense-to-isointense signal on T2-weighted images at the medial and posterior edges of the left eyeball, a significant enhancement was observed in the contrast-enhanced scans. Positron emission tomography/CT fusion images showed that the glucose

metabolism of the lesion was normal. Pathology was consistent with hemangioblastoma.

CONCLUSION
Early identification of retinal hemangioblastoma based on imaging features is of great value for its personalized treatment.

Key Words: Ultrasound; Computed tomography; Magnetic resonance imaging; Positron emission tomography; Computed tomography; Case report

Core Tip: We reported a rare case of the imaging features of retinal hemangioblastoma without von Hippel Lindau syndrome, along with the relevant literature review. A 53-year-old man, who had progressive swelling, pain and blurred vision in the left eye without obvious inducement for 15 d. Ultrasonography revealed a possible optic nerve melanoma of the head. Computed tomography (CT) showed punctate calcification on the posterior wall of the left eye ring and small patchy soft tissue density in the posterior part of the eyeball. Magnetic resonance imaging showed slightly hyperintense on T1-weighted images and slightly hypointense-to-isointense on T2-weighted images at the medial and posterior edges of the left eyeball, a significant enhancement was observed after contrast-enhanced scans. positron emission tomography/CT fusion images showed that the glucose metabolism of the lesion was normal. Pathology was consistent with hemangioblastoma. Early identification of retinal hemangioblastoma by imaging features is of great value for its personalized treatment.

Citation: Tang X, Ji HM, Li WW, Ding ZX, Ye SL. Imaging features of retinal hemangioblastoma: A case report. *World J Clin Cases* 2023; 11(3): 692-699
URL: https://www.wjgnet.com/2307-8960/full/v11/i3/692.htm
DOI: https://dx.doi.org/10.12998/wjcc.v11.i3.692

INTRODUCTION

Retinal hemangioblastoma (RCH) is a rare benign tumor that was first reported by Von Hippel, a German ophthalmologist, in 1911. Since then, more than 900 families worldwide have been diagnosed with the disease[1]. RCH has also been shown to be the most common and earliest manifestation in 49%-85% of patients with von Hippel Lindau (VHL) disease, and only a very small number of cases are sporadic. Its diagnosis is mainly based on clinical suspicion and confirmation by molecular testing and imaging techniques[2-4]. Moreover, retinal hemangiomas can be usually observed directly and diagnosed by eye fundus examination, which may be the main reason why radiologists infrequently perform RCH diagnosis. We retrospectively analyzed the relevant literature and found that the imaging features of RCH are rarely reported[1-11]. Herein, we reported the computed tomography (CT), magnetic resonance (MR) imaging, and positron emission tomography (PET)/CT features of a sporadic RCH case.

CASE PRESENTATION

Chief complaints

On February 23, 2022, a 53-year-old male was admitted to our hospital because of 15 d history of progressive swelling, pain and blurred vision in the left eye, in the absence of obvious inducement.

History of present illness

Fifteen days ago, the patient developed swelling, pain and blurred vision in the left eye, and was admitted to the 9th Hospital of Hangzhou. He was diagnosed with "neovascular glaucoma" and was given tobramycin dexamethasone eye drops and pranoprofen eye drops for anti-inflammatory therapy, timolol eye drops and brinzolamide eye drops for ocular hypotensive therapy. However, the disease symptoms did not improve, and he visited the First People's Hospital of Hangzhou on February 23, 2022, for further diagnosis and treatment.

History of past illness

The patient had no past illness.

Personal and family history

The patient had no special personal or family history of illness.

Physical examination

Ophthalmological examination showed that visio oculus dexter was 0.8 and Visus Oculi Sinistri was sensitive to light (mainly contains distorted light that is located above and below the nose). Noncontact tonometer showed that R/L = 16.3/Tn + 3 mmHg. There was no hyperemia of right bulbar conjunctiva. The cornea was clear and the depth of anterior chamber was satisfactory. Pupils were round in shape and reactive to light while light was mixed in the lens of right eye, optic disc boundary was clear and flat, while omentum was located in the fundus, mixed congestion in the conjunctiva of left eye and corneal edema were also noted. There was mild swelling in one-third of the anterior chamber, pupil was round in shape and not reactive to light and it was not extending to posterior chamber of eye, while the other details were unclear.

Laboratory examinations

Relevant antibody tests and other laboratory tests were further performed, and the results were all negative.

Imaging examinations

Ophthalmic ultrasound showed a solid lesion in the left eye, indicating possible optic nerve head melanoma (Figure 1). CT showed patchy slightly hyperdense shadows anterior to the posterior wall of the left eyeball, suggesting a mass (Figure 2A and B). MR imaging showed left eyeball mass with slightly short T1, equal short T2 abnormal signals, about 8 mm × 5 mm in size, which were significantly enhanced after contrast enhancement (Figure 2C-H). PET/CT fusion images showed that the posterior left eyeball was locally thickened. The glucose metabolism of the lesion was normal (Figure 3). No significant abnormality was observed in the pancreas, spinal cord, cerebellum, adrenal gland, or kidney. The patient signed a written informed consent form before the examination. This retrospective study involving human participants was reviewed and approved by the Medical Ethics Committee of Hangzhou First People's Hospital, Zhejiang University School of Medicine (Approval No. 2022-007-01).

FINAL DIAGNOSIS

Postoperative histopathological findings showed that the "left eyeball" lesion was consistent with hemangioblastoma, with a maximum tumor diameter of 0.4 cm and no involvement of the optic nerve resection margin. Immunohistochemical results showed D2-40 focal [+], inhibin focal [+], S-100 few [+], CD34 vessels [+], CD56 [-], NSE [-], CD68 [-], CD163 [-], GFAP [-], CD10 [-], MelanA [-], EMA [-], CK [-], SOX10 [-], and Ki-67 [+] 1%-2% (Figure 4).

TREATMENT

After excluding surgical contraindications, the patient underwent "left eye enucleation" under general anesthesia on March 4, 2022, and received postoperative anti-inflammatory treatment with levofloxacin eye drops and tobramycin dexamethasone eye ointment (TobraDex ointment).

OUTCOME AND FOLLOW-UP

Early identification of retinal hemangioblastoma based on imaging features is of great value for its personalized treatment.

DISCUSSION

The retinal hemangioblastoma in the present case was a solid mass, and ultrasound showed an isoechoic mass. CT showed a mildly hyperdense patchy lesion surrounded by spotty calcifications. MR imaging showed a slightly hyperintense signal on T1-weighted images and slightly hypointense-to-isointense signal on T2-weighted images, and the lesions were significantly enhanced after Gadolinium-

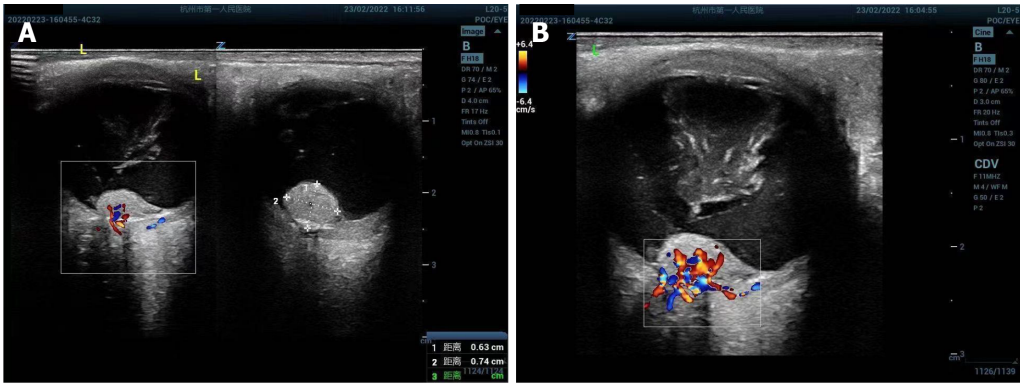

DOI: 10.12998/wjcc.v11.i3.692

Figure 1 Ultrasound images of left retinal hemangioblastoma. A: Ultrasound showed an irregular isoechoic mass of about 6.3 mm × 7.4 mm in front of the left optic nerve head; B: Color doppler flow imaging showed abundant blood flow signals in the lesion.

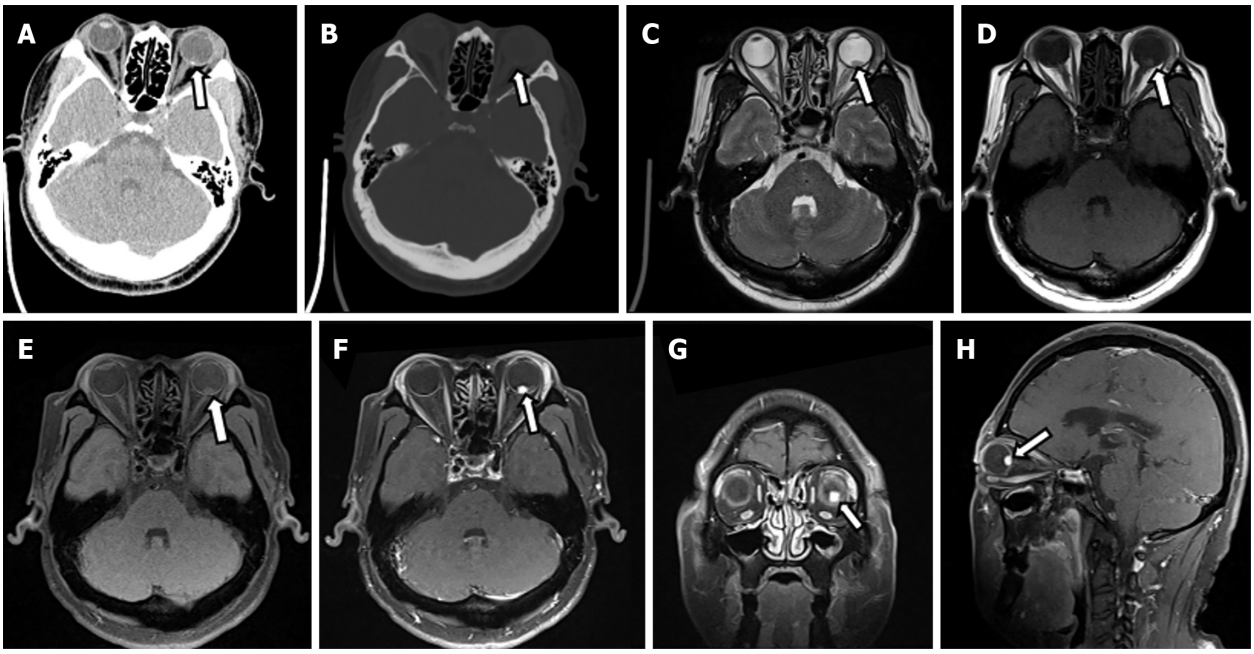

DOI: 10.12998/wjcc.v11.i3.692

Figure 2 Computed tomography and magnetic resonance imaging of left retinal hemangioblastoma. A: Computed tomography (CT) transverse soft tissue window of orbit showed punctate calcification on the posterior wall of the left eye ring and small patchy soft tissue density in the posterior part of the eyeball. The lesion measured about 5 mm × 8 mm, with an ill-defined border; B: CT transverse bone window of orbital showed no obvious abnormal change of orbital bone; C: The lesion was hypointense on transaxial T2-weighted sequence; D and E: The lesion was slightly hyperintense on transaxial T1-weighted images (D) and transaxial T1-weighted + fat-suppression images (E); F-H: Left posterior para-bulbar lesions were significantly enhanced on gadolinium-enhanced T1-weighted + fat-suppression images [mainly included transverse (F), coronal (G), and sagittal sequences (H)] (White arrows represent lesion).

DTPA injection. PET/CT showed no abnormally increased metabolism of the lesion. These imaging features mainly depended on its histological structure. Retinal hemangioblastoma is mainly composed of vacuolar interstitial cells and abundant capillary networks. Interstitial cells are the main component of the tumor, which are rarely associated with necrotic or specific infectious components, while PET metabolism is characterized by minor metabolic changes due to the competition between tumor cells and macrophages[12,13]. Moreover, retinal hemangioblastomas show low levels of 18F-FDG dose that may be associated with over-expression of somatostatin receptors on the surface of tumor cells, and the PET/CT findings are consistent with Papadakis *et al*[9]. Furthermore, retinal hemangioblastoma is essentially a vascular lesion, and these tumors release various angiogenic factors, including vascular endothelial growth factor (VEGR), erythropoietin, and platelet-derived growth factor[14,15]. Vascular endothelial growth factor was significantly increased, which can induce massive capillary proliferation and increase vascular permeability, which leads to significant vascular-like enhancement of the lesion. In addition, hemangioblastoma has different imaging features based on different sites of occurrence. Solid tumors are also the main form of optic nerve hemangioblastoma, but most of the lesions are

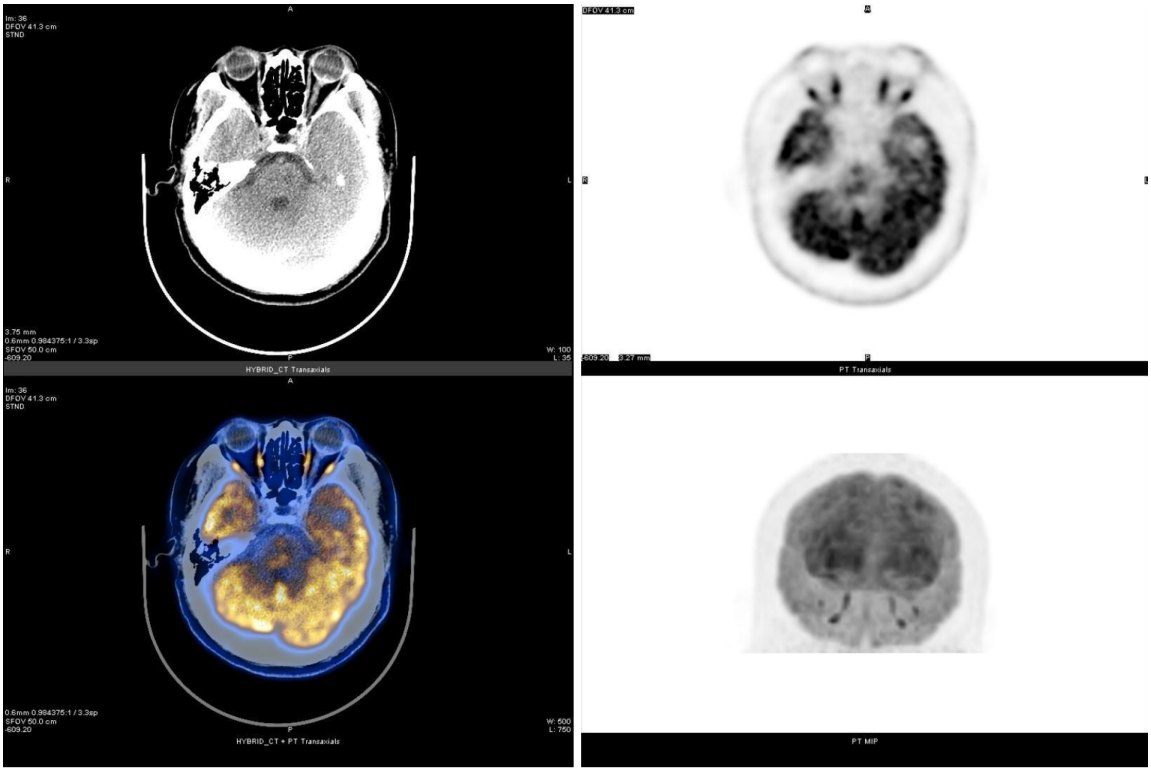

DOI: 10.12998/wjcc.v11.i3.692

Figure 3 Transaxial computed tomography image, transaxial and coronal positron emission tomography metabolograms, color fusion map of positron emission tomography / computed tomography images at the orbital level. The transaxial computed tomography (CT) image at the orbital level showed a patchy slightly hyperdense lesion. The transaxial positron emission tomography (PET) metabologram, coronal PET metabologram and PET/CT color fusion map at the orbital level showed no metabolic changes, and its SUV_{max} was 50.9.

surrounded by edema[16]. Large cysts with small nodules are characteristic of cerebellar and spinal hemangioblastomas, and are mainly associated with intratumoral and peritumoral flow void effects [17]. According to the location and imaging characteristics of the lesion, hemangioblastomas also need to be differentiated from the following diseases. Choroidal melanoma: It is the most common ocular malignancy in adults, wherein CT shows a localized well-defined mass isodense to the extraocular muscles, generally without calcification. MR imaging shows hyperintense signal on T1-weighted images and hypointense signal on T2-weighted images, which is the characteristic feature, because the tumor contains paramagnetic melanin material. It also shows mild to moderate enhancement after contrast enhancement. PET metabolism indicated that glucose uptake was often increased in choroidal melanoma, and its SUVmax was > 10[18,19]. Therefore, it is not difficult to differentiate from this case of retinal hemangioblastoma. Choroidal hemangioma: CT shows local thickening of eyeball wall. It shows progressive significant enhancement after contrast enhancement. MR imaging shows higher signal than vitreous on T1-weighted images and lower than vitreous on T2-weighted images, but isointense signal compared with optic nerve and extraocular muscles on T2-weighted images, 90% of patients have concomitant mild retinal detachment. It shows progressive significant enhancement after contrast enhancement. PET metabolism suggests that choroidal hemangioma usually has no change in glucose uptake[20,21]. Therefore, enhanced dynamic delayed scanning is of great significance in the diagnosis and differentiation of choroidal hemangioma. Retinoblastoma: It occurs in children within 5 years of age and presents with localized thickening or heterogeneous mass shadows of the eye ring on CT, more than 90% of which are mixed with dot-like calcifications. Typical MR imaging features of retinoblastoma include a slightly higher signal on T1-weighted images and low signal on T2-weighted images, with contrast enhancement and diffusion restriction. PET metabolism mostly shows a slight increase in glucose uptake in retinoblastoma[22,23]. Thus, it is not difficult to differentiate from this case. Retinal HB is usually the initial manifestation of VHL. A comprehensive clinical examination of the patient and systematic genetic review of his family revealed that the patient had no other features of VHL syndrome or a family history of genetic diseases. Thus, it was a case of sporadic retinal hemangioblastoma, which may be due to the loss of a tumor suppressor gene similar to retinoblastoma rather than somatic mutations in the *VHL* tumor suppressor gene[24]. Although RHB is inherently benign and slow-growing, it can lead to retinal exudation, detachment, or macular edema resulting in severe visual loss. Advanced cases can present with extensive retinal scarring leading to blind eye pain. Therefore, early detection of retinal hemangioblastoma is important for ocular preservation and long-term visual acuity [25]. Minimally invasive laser photocoagulation is the best early treatment with less side effects, and

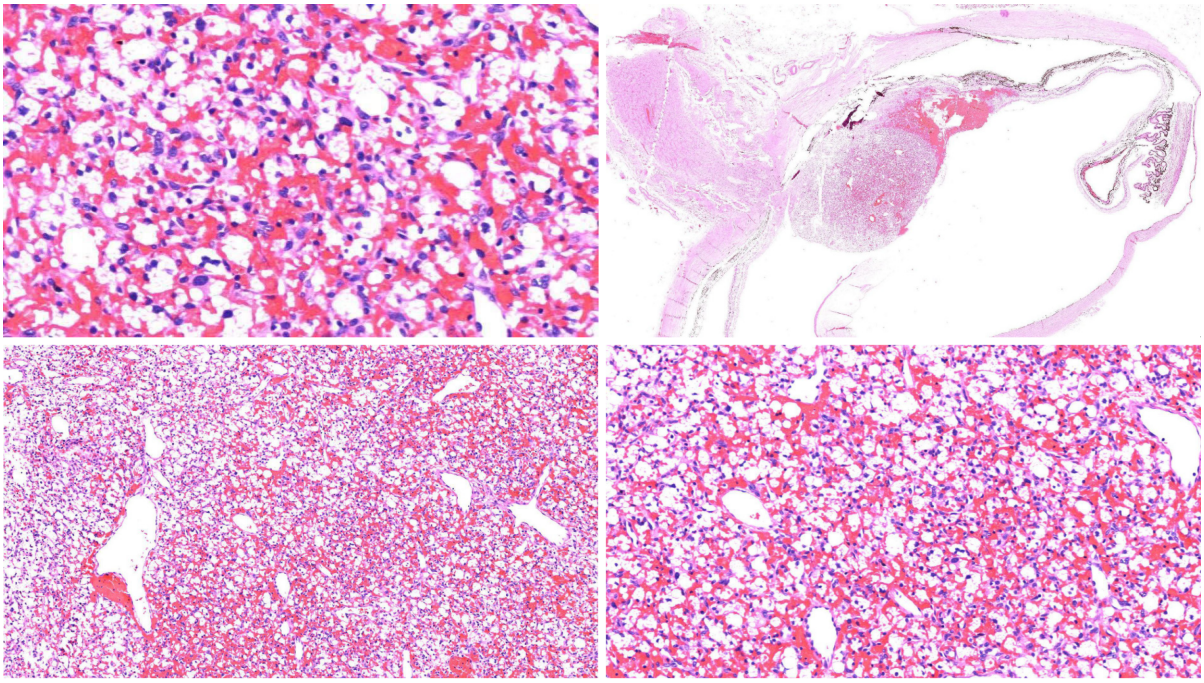

DOI: 10.12998/wjcc.v11.i3.692

Figure 4 Postoperative histopathological and immunohistological images of left retinal hemangioblastoma. The left eyeball lesions were mainly composed of two components, capillaries and interstitial cells surrounded by vacuolated or eosinophilic cytoplasm, which showed epithelioid stromal cells and staghorn dilated thin-walled vessels in capillaries (hematoxylin-eosin staining, magnification × 4).

vitreoretinal surgery is the main treatment in the late stage[1].

CONCLUSION

Retinal hemangioblastoma, as a rare disease type, with or without VHL syndrome, should be used as a routine differential diagnosis when a solid retinal mass is found on ultrasound, CT, or MR imaging in patients with no change in PET/CT metabolic characteristics.

FOOTNOTES

Author contributions: Tang X, Ding ZX and Ye SL designed the research; Tang X, Ji HM and Ding ZX performed the research; Tang X, Ji HM and Li WW contributed new reagents/analytic tools; Tang X, Li WW and Ye SL analyzed the data; Tang X and Ding ZX wrote the paper; all authors contributed to the article and approved the submitted version.

Supported by the National Natural Science Foundation of China, No. 81871337; and the Natural Science Foundation of Zhejiang Province, No. LY16H180007.

Informed consent statement: The study participants, provided informed written consent prior to study enrollment.

Conflict-of-interest statement: All authors declare no conflict of interest, financial or otherwise.

CARE Checklist (2016) statement: The CARE Checklist was done according to the Journal.

Country/Territory of origin: China

ORCID number: Xin Tang 0000-0001-7233-4569; Zhong-Xiang Ding 0000-0001-7691-5571.

S-Editor: Wang LL

L-Editor: A
P-Editor: Wang LL

REFERENCES

1 **Mir Saeid Ghazi AA**, Amouzegar A, Zadeh-Vakili A, Sheikh Rezaei A, Amirbaigloo A, Zarif Yeganeh M, Hashemi H, Azizi F. Clinical and Laboratory Characteristics of a Large Iranian Kindred Afflicted with Von Hippel Lindau Disease. *Int J Endocrinol Metab* 2021; **19**: e105189 [PMID: 34149843 DOI: 10.5812/ijem.105189]
2 **Golas L**, Skondra D, Ittiara S, Bajic N, Jeng-Miller KW, Mukai S, Yonekawa Y, Blair MP. Efficacy of Retinal Lesion Screening in Von Hippel-Lindau Patients With Widefield Color Fundus Imaging Versus Widefield FA. *Ophthalmic Surg Lasers Imaging Retina* 2019; **50**: e260-e265 [PMID: 31755976 DOI: 10.3928/23258160-20191031-12]
3 **Singh B**, Singla M, Singh R, Rathore SS, Gupta A. Von Hippel-Lindau Syndrome: Multi-Organ Involvement Highlighting Its Diverse Clinical Spectrum in Two Adult Cases. *Cureus* 2020; **12**: e9402 [PMID: 32864232 DOI: 10.7759/cureus.9402]
4 **Maher ER**, Yates JR, Harries R, Benjamin C, Harris R, Moore AT, Ferguson-Smith MA. Clinical features and natural history of von Hippel-Lindau disease. *Q J Med* 1990; **77**: 1151-1163 [PMID: 2274658 DOI: 10.1093/qjmed/77.2.1151]
5 **Nabih O**, Hamdani H, El Maaloum L, Allali B, El Kettani A. Retinal angioma of Von hippel-lindau disease: A case report. *Ann Med Surg (Lond)* 2022; **74**: 103292 [PMID: 35145668 DOI: 10.1016/j.amsu.2022.103292]
6 **Russell JF**, Villegas VM, Schwartz SG, Weng CY, Davis JL, Flynn HW Jr, Harbour JW. Multimodal Imaging in the Diagnosis of Exophytic Juxtapapillary Retinal Capillary Hemangioblastoma. *Am J Ophthalmol* 2021; **225**: 128-136 [PMID: 33450232 DOI: 10.1016/j.ajo.2021.01.002]
7 **Nguyen TH**, Pham T, Strickland T, Brewer D, Belirgen M, Al-Rahawan MM. Von Hippel-Lindau with early onset of hemangioblastoma and multiple drop-metastases like spinal lesions: A case report. *Medicine (Baltimore)* 2018; **97**: e12477 [PMID: 30278534 DOI: 10.1097/md.0000000000012477]
8 **Nielsen SM**, Rhodes L, Blanco I, Chung WK, Eng C, Maher ER, Richard S, Giles RH. Von Hippel-Lindau Disease: Genetics and Role of Genetic Counseling in a Multiple Neoplasia Syndrome. *J Clin Oncol* 2016; **34**: 2172-2181 [PMID: 27114602 DOI: 10.1200/jco.2015.65.6140]
9 **Papadakis GZ**, Millo C, Jassel IS, Bagci U, Sadowski SM, Karantanas AH, Patronas NJ. 18F-FDG and 68Ga-DOTATATE PET/CT in von Hippel-Lindau Disease-Associated Retinal Hemangioblastoma. *Clin Nucl Med* 2017; **42**: 189-190 [PMID: 28033220 DOI: 10.1097/rlu.0000000000001511]
10 **Reich M**, Glatz A, Boehringer D, Evers C, Daniel M, Bucher F, Ludwig F, Nuessle S, Lagrèze WA, Maloca PM, Lange C, Reinhard T, Agostini H, Lang SJ. Comparison of Current Optical Coherence Tomography Angiography Methods in Imaging Retinal Hemangioblastomas. *Transl Vis Sci Technol* 2020; **9**: 12 [PMID: 32855859 DOI: 10.1167/tvst.9.8.12]
11 **Ouederni M**, Maamouri R, Sassi H, Nouri S, Cheour M. [Multimodal imaging in the diagnosis of retinal capillary hemangioblastoma]. *J Fr Ophtalmol* 2021; **44**: 912-914 [PMID: 33875238 DOI: 10.1016/j.jfo.2020.10.020]
12 **Hamza HS**, Elhusseiny AM. Submacular sclerosing capillary hemangioblastoma. *Am J Ophthalmol Case Rep* 2018; **11**: 61-63 [PMID: 30003174 DOI: 10.1016/j.ajoc.2018.05.010]
13 **Reinfeld BI**, Madden MZ, Wolf MM, Chytil A, Bader JE, Patterson AR, Sugiura A, Cohen AS, Ali A, Do BT, Muir A, Lewis CA, Hongo RA, Young KL, Brown RE, Todd VM, Huffstater T, Abraham A, O'Neil RT, Wilson MH, Xin F, Tantawy MN, Merryman WD, Johnson RW, Williams CS, Mason EF, Mason FM, Beckermann KE, Vander Heiden MG, Manning HC, Rathmell JC, Rathmell WK. Cell-programmed nutrient partitioning in the tumour microenvironment. *Nature* 2021; **593**: 282-288 [PMID: 33828302 DOI: 10.1038/s41586-021-03442-1]
14 **Custo Greig EP**, Duker JS. Retinal hemangioblastoma vascular detail elucidated on swept source optical coherence tomography angiography. *Am J Ophthalmol Case Rep* 2021; **21**: 101005 [PMID: 33385098 DOI: 10.1016/j.ajoc.2020.101005]
15 **Wiley HE**, Krivosic V, Gaudric A, Gorin MB, Shields C, Shields J, Aronow ME, Chew EY. Management of retinal hemangioblastoma in von hippel-lindau disease. *Retina* 2019; **39**: 2254-2263 [PMID: 31259811 DOI: 10.1097/iae.0000000000002572]
16 **Duan M**, Yang L, Kang J, Wang R, You H, Feng M. Neuroimaging Features of Optic Nerve Hemangioblastoma Identified by Conventional and Advanced Magnetic Resonance Techniques: A Case Report and Literature Review. *Front Oncol* 2021; **11**: 763696 [PMID: 34868983 DOI: 10.3389/fonc.2021.763696]
17 **Huntoon K**, Shepard MJ, Lukas RV, McCutcheon IE, Daniels AB, Asthagiri AR. Hemangioblastoma diagnosis and surveillance in von Hippel-Lindau disease: a consensus statement. *J Neurosurg* 2021; 1-6 [PMID: 34598132 DOI: 10.3171/2021.3.jns204203]
18 **Jiblawi A**, Chanbour H, Tayba A, Khayat H, Jiblawi K. Magnetic Resonance Imaging Diagnosis of Choroidal Melanoma. *Cureus* 2021; **13**: e16628 [PMID: 34458039 DOI: 10.7759/cureus.16628]
19 **Marko M**, Leško P, Jurenová D, Furda R, Greguš M. Importance of PET/CT examination in patients with malignant uveal melanoma. *Cesk Slov Oftalmol* 2020; **76**: 37-44 [PMID: 32917093 DOI: 10.14735/amcsnn2016213]
20 **Sarrafpour S**, Tsui E, Mehta N, Modi YS, Finger PT. Choroidal Hemangioma in a Black Patient With Sturge-Weber Syndrome: Challenges in Diagnosis. *Ophthalmic Surg Lasers Imaging Retina* 2019; **50**: 183-186 [PMID: 30893453 DOI: 10.3928/23258160-20190301-09]
21 **Damento GM**, Koeller KK, Salomão DR, Pulido JS. T2 Fluid-Attenuated Inversion Recovery Imaging of Uveal Melanomas and Other Ocular Pathology. *Ocul Oncol Pathol* 2016; **2**: 251-261 [PMID: 27843906 DOI: 10.1159/000447265]
22 **Abramson DH**, Dunkel IJ, Francis JH. Magnetic Resonance Imaging of Metastatic Retinoblastoma. *J Pediatr Ophthalmol Strabismus* 2022; 1 [PMID: 35938642 DOI: 10.3928/01913913-20220623-02]
23 **Orman G**, Huisman TAGM. A descriptive neuroimaging study of retinoblastoma in children: magnetic resonance imaging

features. *Pol J Radiol* 2022; **87**: e363-e368 [PMID: 35979155 DOI: 10.5114/pjr.2022.118107]

24 **Chang JH**, Spraul CW, Lynn ML, Drack A, Grossniklaus HE. The two-stage mutation model in retinal hemangioblastoma. *Ophthalmic Genet* 1998; **19**: 123-130 [PMID: 9810567 DOI: 10.1076/opge.19.3.123.2185]

25 **Schoen MA**, Shields CL, Say EAT, Douglass AM, Shields JA, Jampol LM. Clinically invisible retinal hemangioblastomas detected by spectral domain optical coherence tomography and fluorescein angiography in twins. *Retin Cases Brief Rep* 2018; **12**: 12-16 [PMID: 27533642 DOI: 10.1097/icb.0000000000000382]

World Journal of Clinical Cases

Submit a Manuscript: https://www.f6publishing.com

World J Clin Cases 2023 January 26; 11(3): 700-708

DOI: 10.12998/wjcc.v11.i3.700

ISSN 2307-8960 (online)

CASE REPORT

Clinical and genetic diagnosis of autosomal dominant osteopetrosis type II in a Chinese family: A case report

Hong-Ping Gong, Yan Ren, Pan-Pan Zha, Wen-Yan Zhang, Jin Zhang, Zhi-Wen Zhang, Chun Wang

Specialty type: Medicine, research and experimental

Provenance and peer review: Unsolicited article; Externally peer reviewed.

Peer-review model: Single blind

Peer-review report's scientific quality classification

Grade A (Excellent): 0
Grade B (Very good): 0
Grade C (Good): C, C
Grade D (Fair): 0
Grade E (Poor): 0

P-Reviewer: Liu X, China; Park J, United States

Received: November 23, 2022
Peer-review started: November 23, 2022
First decision: December 13, 2022
Revised: December 23, 2022
Accepted: January 5, 2023
Article in press: January 5, 2023
Published online: January 26, 2023

Hong-Ping Gong, International Medical Center Ward, General Practice Medical Center, Sichuan University West China Hospital, Chengdu 610041, Sichuan Province, China

Hong-Ping Gong, Yan Ren, Pan-Pan Zha, Chun Wang, Department of Endocrinology and Metabolism, Sichuan University West China Hospital, Chengdu 610041, Sichuan Province, China

Wen-Yan Zhang, Department of Pathology, West China Hospital, Sichuan University, Chengdu 610041, Sichuan Province, China

Jin Zhang, Zhi-Wen Zhang, Department of Endocrinology and Metabolism, The People's Hospital of Leshan, Leshan 614003, Sichuan Province, China

Corresponding author: Chun Wang, Doctor, PhD, Chief Doctor, Department of Endocrinology and Metabolism, Sichuan University West China Hospital, No. 37 Guoxue Lane, Chengdu 610041, Sichuan Province, China. snoopywc@163.com

Abstract

BACKGROUND

Osteopetrosis is a rare genetic disorder characterized by increased bone density due to defective bone resorption of osteoclasts. Approximately, 80% of autosomal dominant osteopetrosis type II (ADO-II) patients were usually affected by heterozygous dominant mutations in the chloride voltage-gated channel 7 (*ClCN7*) gene and present early-onset osteoarthritis or recurrent fractures. In this study, we report a case of persistent joint pain without bone injury or underlying history.

CASE SUMMARY

We report a 53-year-old female with joint pain who was accidentally diagnosed with ADO-II. The clinical diagnosis was based on increased bone density and typical radiographic features. Two heterozygous mutations in the *ClCN7* and T-cell immune regulator 1 (*TCIRG1*) genes by whole exome sequencing were identified in the patient and her daughter. The missense mutation (c.857G>A) occurred in the *CLCN7* gene p. R286Q, which is highly conserved across species. The *TCIRG1* gene point mutation (c.714-20G>A) in intron 7 (near the splicing site of exon 7) had no effect on subsequent transcription.

CONCLUSION

This ADO-II case had a pathogenic *CLCN7* mutation and late onset without the usual clinical symptoms. For the diagnosis and assessment of the prognosis for

osteopetrosis, genetic analysis is advised.

Key Words: Osteopetrosis; Autosomal dominant osteopetrosis type II; Diagnosis; Genetic analysis; Case report

Core Tip: Autosomal dominant osteopetrosis (ADO-II) is an autosomal dominant form of osteopetrosis. In ADO-II patients, the clinical spectrum ranges from nonsymptomatic to recurrent fractures, anemia, and a favorable prognosis. We reported a 53-year-old female patient with persistent joint pain, who was accidentally diagnosed with ADO-II at a later age. Her asymptomatic daughter was also diagnosed with ADO-II, as confirmed by whole exome sequencing.

Citation: Gong HP, Ren Y, Zha PP, Zhang WY, Zhang J, Zhang ZW, Wang C. Clinical and genetic diagnosis of autosomal dominant osteopetrosis type II in a Chinese family: A case report. *World J Clin Cases* 2023; 11(3): 700-708
URL: https://www.wjgnet.com/2307-8960/full/v11/i3/700.htm
DOI: https://dx.doi.org/10.12998/wjcc.v11.i3.700

INTRODUCTION

Osteopetrosis, also known as "marble bone disease," is a rare genetic disease characterized by increased bone mass and density due to bone resorption failure[1]. Dr. Albers-Schonberg, a radiologist in Germany, described it for the first time in 1904[2]. It has a broad clinical spectrum, ranging from asymptomatic to life-threatening bone marrow failure and cranial nerve dysfunction. Based on clinical severity and inheritance patterns, osteopetrosis is classified into three types: a "malignant" autosomal recessive infantile form (ARO), a "benign" autosomal dominant form (ADO type II), and an intermediate recessive form[1,3,4]. To date, mutations in at least ten genes have been identified to cause failure of osteoclast differentiation or function in humans, including the T-cell immune regulator gene (*TCIRG1*), chloride voltage-gated channel 7 (*ClCN7*), tumor necrosis factor (TNF) superfamily member 11, TNF receptor superfamily member 11a, osteopetrosis-associated transmembrane protein, sorting nexin 10 (*SNX10*), pleckstrin homology and RUN domain containing M1, and NF-κB essential modulator genes[3,5].

The most prominent characteristic of ADO-II is its dense yet fragile bones. We present a rare case of limb joint pain that was accidentally diagnosed as ADO-II based on clinical findings and genetic analysis.

CASE PRESENTATION

Chief complaints

A 53-year-old woman was admitted to the hospital with a complaint of limb joint pain for 11 mo.

History of present illness

The patient presented with pain in her shoulder, elbow, wrist, and metacarpophalangeal joints with swelling, tenderness and numbness for 1 mo before pain began in her bilateral knee, ankle, toe and finger joints for approximately 10 mo.

History of past illness

The patient had no history of fractures and bone injury.

Personal and family history

Her parents were not consanguineous. Her father and mother died of bone cancer and esophageal cancer, respectively. She has a daughter, a brother and two sisters who are asymptomatic. The pedigree of her family is shown in Figure 1.

Physical examination

On admission, her blood pressure was 120/70 mmHg, pulse rate 98/min, and respiratory rate 20/min.

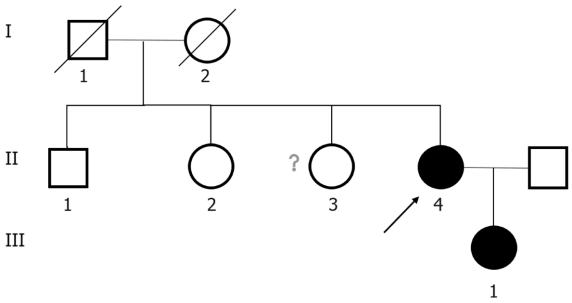

DOI: 10.12998/wjcc.v11.i3.700

Figure 1 Pedigree of a family with osteopetrosis. Circles indicate females, and squares indicate males. The affected individuals are denoted by solid symbols. The arrow indicates the proband (II:4). Diagonal lines represent deceased subjects. The status of II:3 is unknown because this individual did not agree to participate in this study.

Her height and body weight were 155 cm and 63 kg, respectively. Physical examinations showed slight swelling of her wrists, hands, knees and ankles, accompanied by tenderness, limited retral swing of the upper limbs and slightly restricted movement of the lower limbs.

Laboratory examinations

The patient had mild anemia; decreased levels of serum bone alkaline phosphatase (BALP), 25-dihydroxy vitamin D3, urinary calcium and phosphorus; and an elevated level of serum phosphorus. The levels of serum calcium, urinary fluoride, lactate dehydrogenase, creatine kinase, C-telopeptide of type I collagen, N-terminal mid-fragment of osteocalcin, and parathyroid hormone (PTH) were within the normal reference ranges. Her spectrum of antinuclear antibodies, anti-cyclic citrullinated peptide, anti-streptolysin O and rheumatoid factor were negative.

The biochemical measurements of her daughter, brother and sister were normal except that her daughter had mild anemia (partial data not shown). All laboratory findings are summarized in Table 1.

Imaging examinations

The bone mineral density (BMD) was measured by dual-energy X-ray absorptiometry (iDXA, GE Lunar, United States). The results showed that the hips and lumbar spines of the patient and her daughter significantly increased. The T scores of the patient were higher than those of Chinese female youth, and the Z scores of her daughter were also higher than those of the age-matched Chinese women (Table 2). The results of the BMD tests for her brother and sister revealed low bone mass (osteopenia) compared with the Chinese sex-matched adolescents (data not shown).

X-ray images of the limbs, including the wrist and ankle joints of the patient, showed increased bone density in the pelvis, femurs, humerus, knees and shoulder joints; mild degeneration in the hips, knees, ankles, shoulders, elbows and wrist joints; and slight soft tissue swelling around the wrist joints (Figure 2A-C). The chest computerized tomography (CT) scan of the patient showed that bone mineral density increased in the bilateral humeral head, sternum, scapula, ribs and multiple thoracic vertebrae (Figure 2D). Whole-body bone single-photon emission computed tomography of the patient revealed extremely high uptake in the long bone, ribs, and spine with no renal or bladder radioactivity visualization. The features from imaging showed a "bone super scan" (Figure 2E). The results of the ultrasound examination of the patient showed synovitis in both the first metatarsophalangeal joints and the wrist joint, tenosynovitis of the fourth compartment of the left wrist, and joint effusion on the right ankle (data not shown).

X-ray images of the limbs of the patient's daughter showed that the density of the bone tip and flat bone increased, and the marrow cavity became narrow (Figure 2F-H). The CT scan of the lumbar spine of the patient's daughter showed that bone mineral density increased at the upper and lower edges from the twelfth thoracic vertebra to the first sacral vertebra and slightly decreased in their center (Figure 2I).

Pathological study

A bone biopsy of the patient on the right posterior iliac crest showed cortical bone sclerosis, some thickened bone trabeculae, and active proliferation of bone marrow hematopoietic cells (Supplementary Figure 1). Immunohistochemical staining of the bone marrow biopsy showed a few CD20 (+) or CD3 (+) lymphocytes and scattered CD138 (+), IGN (+) or IG λ (+) plasma cells (data not shown).

Genetic analysis

Whole exome sequencing (whole-exome library construction by xGen Exome Research Panel v2.0 (IDT, Iowa, United States), high-throughput sequencing by a DNBSEQ-T7 sequencer (MGI, Beijing, CHN), and not less than 99% of target sequence were sequenced) identified two heterozygous mutations,

Table 1 Laboratory test results for the proband and her daughter

	The proband	The proband's daughter	Reference
Sex	Female	Female	
RBC (10^{12}/L)	3.64	3.55	3.8-5.1
Hb (g/L)	99	105	115-150
PLT (10^{9}/L)	235	110	100-300
ALT (IU/mL)	19	30	< 40
AST (IU/mL)	29	30	< 35
ALP (IU/mL)	89	55	50-135
CK (IU/L)	80	NA	20-140
CK-MB (ng/mL)	0.35	NA	< 2.88
LDH (IU/mL)	232	NA	120-250
Serum uric acid (μmol/L)	313	311	160-380
Cr (μmol/L)	49	58	41-73
eGFR (ml/min/1.73 m^2)	107.16	121	56-122
Ca (mmol/L)	2.22	2.26	2.11-2.52
P (mmol/L)	1.65	1.11	0.85-1.51
25-OH-VD (nmol/L)	34.9	NA	47.7-144
PTH (pmol/L)	2.96	NA	1.6-6.9
B-ALP (μg/L)	10.57	NA	11.4-24.6
CTX (ng/mL)	0.813	NA	0.556-1.008
N-MID OC (ng/mL)	22.7	NA	15-46
Growth hormone (ng/mL)	0.53	NA	0.126-9.88
IGF-1 (ng/mL)	81.78	NA	102-212
ACTH (ng/L)	19.11	NA	5-78
Cortisol (8:00 A.M.) (nmol/L)	260.8	NA	147.3-609.3
Cortisol (12:00 P.M.) (nmol/L)	68.07	NA	/
24 h urinary Ca (mmol/L)	2.45	NA	2.5-7.5
24 h urinary P (mmol/L)	11.84	NA	22-48
24 h urinary Mg (mmol/L)	1.62	NA	3-5

RBC: Red blood cell count; PLT: Blood platelet count; ALT: Alanine transaminase; AST: Aspartate transaminase; ALP: Serum alkaline phosphatase; CK: Creatine kinase; LDH: Lactate dehydrogenase; eGFR: Estimated glomerular filtration rate; 25-OH-VD: 25-hydroxyvitamin D3; PTH: Parathyroid hormone; B-ALP: Bone alkaline phosphatase; CTX: C-terminal telopeptides of type I collagen; N-MID OC: Serum N-terminal mid-fragment of osteocalcin; IGF-1: Insulin-like growth factor-1; ACTH: Adrenocorticotropic hormone; NA: Not available.

including c.857G>A (p. Arg286Gln, rs760956030) in exon 10 of the *CLCN7* gene (NCBI reference sequence: NM_001287) and c.714-20G>A (-, rs200087340) in intron 7 of the *TCIRG1* gene (NCBI reference sequence: NM_006019.4). Her daughter carried the same heterozygous mutation in the *CLCN7* and *TCIRG1* genes by genetic analysis (Figure 3).

Prediction of functional effects of the CLCN7 and TCIRG1 gene mutations

The R286 position was highly conserved among various species in the *CLCN7* gene (Supplementary Figure 2). Moreover, Polymorphism Phenotyping v2 (http://genetics.bwh.harvard.edu/pph) prediction results of p. R286Q in the *CLCN7* gene was probably damaging, with a score of 1.000 (Supplementary Figure 3), and Mutation Taster (https://www.mutationtaster.org/) predicted it to be a disease-causing variant. Mutation Taster predicted c.714-20 (IVS7) G>A in the *TCIRG1* gene as no change in potential splicing sites.

Table 2 Bone mineral density results for the proband and her daughter

	The BMD values of the proband (g/cm²)	T/Z score of the proband	The BMD values of the proband's daughter (g/cm²)	T/Z score of the proband'sdaughter
L1	2.013	8.2/8.8	1.777	5.2/5.4
L2	2.146	8.7/9.4	1.811	5.0/5.1
L3	2.256	9.2/9.9	1.785	4.5/4.7
L4	2.335	9.9/10.4	1.900	5.3/5.5
L1-L4	2.203	9.1/9.7	1.820	5.1/5.2
Femoral neck	1.838	7.6/8.2	1.391	2.5/2.9
Total hip	1.851	6.7/7.2	1.344	2.7/2.9

T scores were calculated by comparison with the age-specific bone mineral density reference value of Chinese adolescents; Z scores were calculated by comparison with age-matched and sex-matched Chinese adults. BMD: Bone mineral density.

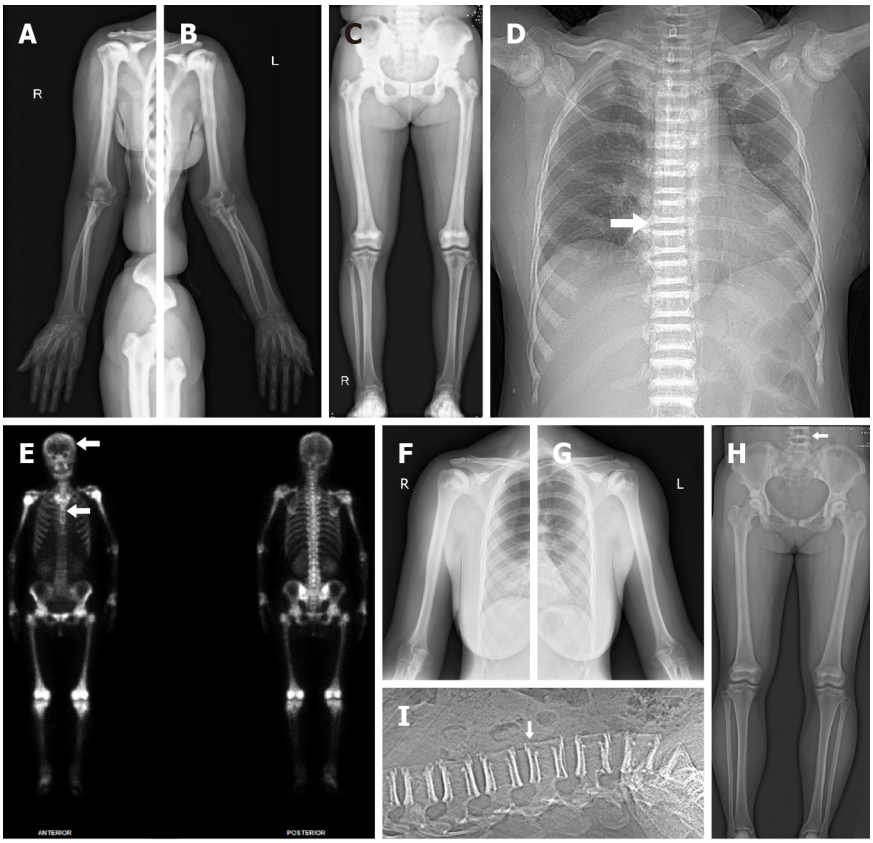

DOI: 10.12998/wjcc.v11.i3.700

Figure 2 The imaging examination of the proband and the proband's daughter. A-C: X-ray image of the proband (II:4) demonstrated increased bone density in the right upper extremity (A), the left upper extremity (B) and the lower extremities (C); D: The chest X-ray of the proband (II:4) showed increased bone density of pelvic, with a "bone-within-bone" appearance in lateral of the spine, indicating classic vertebral endplate thickening (white arrow indicates the "sandwich vertebrae" sign); E: Whole-body bone technetium-99m single-photon emission computed tomography scan revealed extremely high bone uptake of long bone, ribs, and spine with absent renal radioactivity visualization (white arrows indicate "helmet" and "tie" sign); F and G: X-ray image of the proband's daughter (III:1) showed that the bone density of the bone tip, the humerus and the ribs and the medullary cavity became narrow in the right upper extremity (F) and the left upper extremity(G); H and I: X-ray image of the proband's daughter (III:1) in the lower extremities (H) and the lumbar vertebra (I) indicated classic vertebral endplate thickening (white arrow indicates the "sandwich vertebrae" sign).

FINAL DIAGNOSIS

Combined with the patient's medical history and radiological examination results, the final diagnosis was osteopetrosis. In light of genetic typing, the case belonged to ADO II.

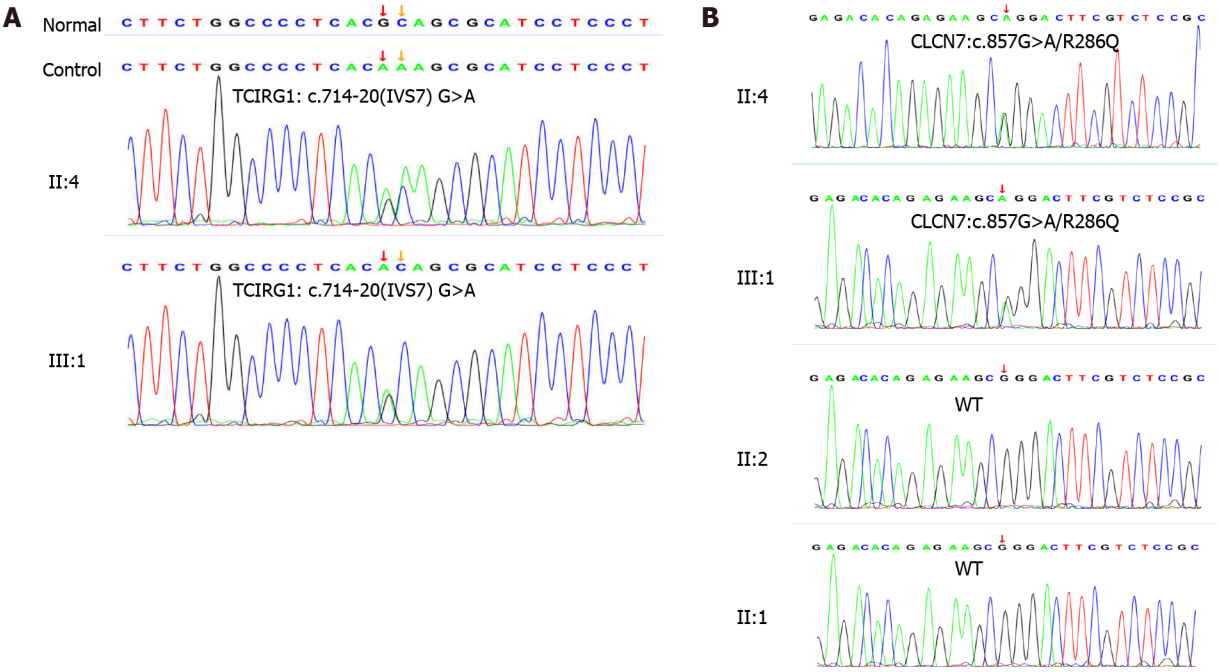

DOI: 10.12998/wjcc.v11.i3.700

Figure 3 Genetic analysis identified mutations in chloride voltage-gated channel 7 and T-cell immune regulator 1 in the osteopetrosis family. A: The proband (II:4) and her daughter (III:1) carried T-cell immune regulator 1-c.714-20 (IVS7) G>A; B: The proband (II:4) and her daughter (III:1) carried *CLCN7*-c.857 (exon10) G>A/R286Q mutations. II:1 and II:2 did not carry any of the two mutations. *CLCN7*: Chloride voltage-gated channel 7; *TCIRG1*: T-cell immune regulator 1; WT: Wild type.

TREATMENT

During hospitalization, celecoxib capsules, wet packing of Liuhedan (a traditional Chinese medicine recipe), ketoprofen gel, and flurbiprofen paste were all given. Her hemoglobin level increased from 99 g/L to 109 g/L with normal serum phosphorus after 16 days of treatment. Her regular activities were unaffected, and the discomfort and swelling in her joints subsided after she was discharged.

OUTCOME AND FOLLOW-UP

After 2 years of follow-up, her joints were no longer painful, and no complications developed. However, her daughter experienced mild lumbar spine discomfort and received analgesic treatment.

DISCUSSION

Osteopetrosis is a rare inherited metabolic bone disorder characterized by a generalized increase in bone density due to osteoclastic insufficiency, impaired bone absorption and poor bone remodeling[4]. Once osteoclasts have defective proton pumps, chloride channels, or carbonic anhydrase II proteins, the mineral matrix is unable to be resorbed effectively[6]. Published studies have shown that most defects in genes result in impaired acidification of bone[7].

With a prevalence of approximately 1:20,000 Live births, ADO is far more common and less severe than ARO[8,9]. The clinical phenotype of osteopetrosis is highly variable, making diagnosis difficult for clinicians. Patients with osteopetrosis may present with no symptoms, fractures following minor trauma, osteomyelitis, early arthritis, anemia, hearing and vision problems due to cranial nerve compression, or all of the above[4]. Some differential diagnoses should be ruled out, such as congenital diseases (*e.g.*, hypoparathyroidism, pseudohypoparathyroidism), chemical poisoning (*e.g.*, with fluoride, lead, or beryllium), and malignancies (leukemias and myeloproliferative diseases). This patient had normal urinary fluoride and PTH serum levels without arthritis, and she was eventually diagnosed with ADO-II. Her daughter was asymptomatic, and ADO-II was confirmed by increased BMD, radiological examination, and the p. R286Q mutation. Their anemia was mild due to relatively sufficient marrow cavity retention for normal hematopoiesis[10]. It is worth noting that, in contrast to ARO, this patient had a mildly decreased BALP concentration. The majority of ADO-II patients have an imbalance in osteoblast serum markers, with low BALP and high osteocalcin levels[11]. As a result, bone

biomarkers may be useful in disease classification.

Increased BMD and radiographic findings are most commonly used to diagnose osteopetrosis. The classic radiographic features of osteopetrosis are the bare minimum for diagnosis[7]. Radiographic features of osteopetrosis include diffuse bone sclerosis with "bone-within-bone" in the pelvis, long bones, phalanges, and vertebrae. A bone marrow biopsy may be required to confirm the diagnosis and differentiate between osteoclast-poor and osteoclast-rich subtypes of osteopetrosis. Bone marrow biopsy can also distinguish hematological disorders such as myelofibrosis, sickle cell disease, leukemia, and osteoblastic bony metastases. It is, however, more invasive to the patient and carries some risks. Whole exome sequencing, on the other hand, is becoming less expensive and faster to obtain a diagnosis and is not invasive. Therefore, therapeutic approaches must be tailored to each patient.

Approximately 80% of ADO-II patients are affected by heterozygous dominant negative mutations of the *CLCN7* gene, while 17% of ARO patients have recessive mutations in the *CLCN7* gene[5,12]. *CLCN7* encodes the chloride channel involved in osteoclast HCl secretion, which is critical in osteoclast dissolution of bone mineral and organic bone matrix[13,14]. A single nucleotide change (c.857G>A, p. R286Q) in exon 10 of *CLCN7* results in a protein with the amino acid glutamine instead of arginine. This variant appears to be located at one of the “hot spots” as the most common *CLCN7* mutations causing ADO and three known disease-related *CLCN7* mutations at the R286 position (p. R286P, p. R286W and p. R286Q) have previously been reported among Caucasians and Asians[15-17]. The mutations (p. R286Q) in the *CLCN7* gene are located in the intramembrane α-helices, creating a positive electrical potential to prevent the fast flux of chloride at the binding site[18]. Approximately 80% of *CLCN7*-dependent ADO-II patients discovered the disease after fractures, implying that osteoblast malfunction likely results in low-quality bone tissue[5,11]. However, no fractures have occurred in this patient thus far. As a result, even if the mutations are identical, the clinical phenotypes may differ.

Osteopetrosis may also be caused by an intronic nucleotide change in the *TCIRG1* gene[19]. *TCIRG1* encodes the a3 subunit of H+ ATPase, and V-ATPase with d2/a3 is a major proton pump of osteoclasts [20]. Mutations in *TCIRG1* account for approximately 50% of ARO cases[5]. The *TCIRG1* variant (c.714-20 G>A) is a point mutation, but there is insufficient evidence to conclude that it is pathogenic. Furthermore, published reports of digenic inheritance suggested that *TCIRG1* and *CLCN7* interact in the two mutations[15,21].

The majority of benign ADO treatments are symptomatic and supportive. Good nutrition is critical for patients with osteopetrosis, especially for those who have hypocalcemia and require calcium and vitamin D supplements[7]. Hematopoietic stem cell transplantation is reserved for osteopetrosis that is malignant[4]. The majority of ADO patients have a better prognosis. Nonetheless, for mild osteopetrosis, it is critical to monitor the disease status and progression by the affected organs.

CONCLUSION

A case of rare ADO-II was accidentally diagnosed in a late-onset patient and her daughter based on increased BMD, classic radiographic features, and a *CLCN7* gene mutation. It was suggested that genetic testing be used to identify precision classifications of osteopetrosis and to provide useful information for therapeutic decisions and prognosis.

ACKNOWLEDGEMENTS

We thank the patient and her relatives for kindly contributing to this study.

FOOTNOTES

Author contributions: Gong HP and Ren Y wrote the manuscript; Gong HP, Ren Y and Wang C revised the manuscript; Gong HP, Ren Y, Zha PP, Zhang J and Zhang ZW contributed to the collection of the clinical data; Zhang WY performed a histopathological review and pathological diagnosis of this case was performed independently; all authors contributed to and approved the final manuscript for publication.

Supported by the Science and Technology Plan Program of Sichuan of China, No. 2018JY0608.

Informed consent statement: Informed written consent was obtained from the patient for publication of this report and any accompanying images.

Conflict-of-interest statement: All authors declare that they have no conflict of interest to disclose.

CARE Checklist (2016) statement: The authors have read the CARE Checklist (2016), and the manuscript was prepared and revised according to the CARE Checklist (2016).

Country/Territory of origin: China

ORCID number: Hong-Ping Gong 0000-0001-5906-2650; Wen-Yan Zhang 0000-0001-6612-6878; Chun Wang 0000-0002-7069-6395.

S-Editor: Wang LL
L-Editor: A
P-Editor: Wang LL

REFERENCES

1 **Stark Z**, Savarirayan R. Osteopetrosis. *Orphanet J Rare Dis* 2009; **4**: 5 [PMID: 19232111 DOI: 10.1186/1750-1172-4-5]
2 **Albers-Schönberg HE**. Röntgenbilder einer seltenen Knockenerkrankung. *Munch. Med. Wochenschr* 1904; **51**: 365-368
3 **Del Fattore A**, Cappariello A, Teti A. Genetics, pathogenesis and complications of osteopetrosis. *Bone* 2008; **42**: 19-29 [PMID: 17936098 DOI: 10.1016/j.bone.2007.08.029]
4 **Bailey JR**, Tapscott DC. Osteopetrosis. In: *StatPearls* [Internet]. Treasure Island (FL): StatPearls Publishing, 2022 [PMID: 32491461]
5 **Palagano E**, Menale C, Sobacchi C, Villa A. Genetics of Osteopetrosis. *Curr Osteoporos Rep* 2018; **16**: 13-25 [PMID: 29335834 DOI: 10.1007/s11914-018-0415-2]
6 **Sobacchi C**, Schulz A, Coxon FP, Villa A, Helfrich MH. Osteopetrosis: genetics, treatment and new insights into osteoclast function. *Nat Rev Endocrinol* 2013; **9**: 522-536 [PMID: 23877423 DOI: 10.1038/nrendo.2013.137]
7 **Wu CC**, Econs MJ, DiMeglio LA, Insogna KL, Levine MA, Orchard PJ, Miller WP, Petryk A, Rush ET, Shoback DM, Ward LM, Polgreen LE. Diagnosis and Management of Osteopetrosis: Consensus Guidelines From the Osteopetrosis Working Group. *J Clin Endocrinol Metab* 2017; **102**: 3111-3123 [PMID: 28655174 DOI: 10.1210/jc.2017-01127]
8 **de Baat P**, Heijboer MP, de Baat C. Osteopetrosis. Classification, etiology, treatment options and implications for oral health. *Ned Tijdschr Tandheelkd* 2005; **112**: 497-503 [PMID: 16385937]
9 **Bollerslev J**, Andersen PE Jr. Radiological, biochemical and hereditary evidence of two types of autosomal dominant osteopetrosis. *Bone* 1988; **9**: 7-13 [PMID: 3377922 DOI: 10.1016/8756-3282(88)90021-x]
10 **Carolino J**, Perez JA, Popa A. Osteopetrosis. *Am Fam Physician* 1998; **57**: 1293-1296 [PMID: 9531912]
11 **Del Fattore A**, Peruzzi B, Rucci N, Recchia I, Cappariello A, Longo M, Fortunati D, Ballanti P, Iacobini M, Luciani M, Devito R, Pinto R, Caniglia M, Lanino E, Messina C, Cesaro S, Letizia C, Bianchini G, Fryssira H, Grabowski P, Shaw N, Bishop N, Hughes D, Kapur RP, Datta HK, Taranta A, Fornari R, Migliaccio S, Teti A. Clinical, genetic, and cellular analysis of 49 osteopetrotic patients: implications for diagnosis and treatment. *J Med Genet* 2006; **43**: 315-325 [PMID: 16118345 DOI: 10.1136/jmg.2005.036673]
12 **Sobacchi C**, Villa A, Schulz A, Kornak U. *CLCN7*-Related Osteopetrosis. In: *GeneReviews®* [Internet]. Seattle (WA): University of Washington, Seattle, 1993 [PMID: 20301306]
13 **Kornak U**, Kasper D, Bösl MR, Kaiser E, Schweizer M, Schulz A, Friedrich W, Delling G, Jentsch TJ. Loss of the ClC-7 chloride channel leads to osteopetrosis in mice and man. *Cell* 2001; **104**: 205-215 [PMID: 11207362 DOI: 10.1016/s0092-8674(01)00206-9]
14 **Kasper D**, Planells-Cases R, Fuhrmann JC, Scheel O, Zeitz O, Ruether K, Schmitt A, Poët M, Steinfeld R, Schweizer M, Kornak U, Jentsch TJ. Loss of the chloride channel ClC-7 leads to lysosomal storage disease and neurodegeneration. *EMBO J* 2005; **24**: 1079-1091 [PMID: 15706348 DOI: 10.1038/sj.emboj.7600576]
15 **Yang Y**, Ye W, Guo J, Zhao L, Tu M, Zheng Y, Li L. CLCN7 and TCIRG1 mutations in a single family: Evidence for digenic inheritance of osteopetrosis. *Mol Med Rep* 2019; **19**: 595-600 [PMID: 30431110 DOI: 10.3892/mmr.2018.9648]
16 **Chu K**, Koller DL, Snyder R, Fishburn T, Lai D, Waguespack SG, Foroud T, Econs MJ. Analysis of variation in expression of autosomal dominant osteopetrosis type 2: searching for modifier genes. *Bone* 2005; **37**: 655-661 [PMID: 16120485 DOI: 10.1016/j.bone.2005.06.003]
17 **Pangrazio A**, Pusch M, Caldana E, Frattini A, Lanino E, Tamhankar PM, Phadke S, Lopez AG, Orchard P, Mihci E, Abinun M, Wright M, Vettenranta K, Bariae I, Melis D, Tezcan I, Baumann C, Locatelli F, Zecca M, Horwitz E, Mansour LS, Van Roij M, Vezzoni P, Villa A, Sobacchi C. Molecular and clinical heterogeneity in CLCN7-dependent osteopetrosis: report of 20 novel mutations. *Hum Mutat* 2010; **31**: E1071-E1080 [PMID: 19953639 DOI: 10.1002/humu.21167]
18 **Pang Q**, Chi Y, Zhao Z, Xing X, Li M, Wang O, Jiang Y, Liao R, Sun Y, Dong J, Xia W. Novel mutations of CLCN7 cause autosomal dominant osteopetrosis type II (ADO-II) and intermediate autosomal recessive osteopetrosis (IARO) in Chinese patients. *Osteoporos Int* 2016; **27**: 1047-1055 [PMID: 26395888 DOI: 10.1007/s00198-015-3320-x]
19 **Pangrazio A**, Caldana ME, Lo Iacono N, Mantero S, Vezzoni P, Villa A, Sobacchi C. Autosomal recessive osteopetrosis: report of 41 novel mutations in the TCIRG1 gene and diagnostic implications. *Osteoporos Int* 2012; **23**: 2713-2718 [PMID: 22231430 DOI: 10.1007/s00198-011-1878-5]
20 **Matsumoto N**, Daido S, Sun-Wada GH, Wada Y, Futai M, Nakanishi-Matsui M. Diversity of proton pumps in osteoclasts: V-ATPase with a3 and d2 isoforms is a major form in osteoclasts. *Biochim Biophys Acta* 2014; **1837**: 744-749 [PMID:

24561225 DOI: 10.1016/j.bbabio.2014.02.011]

21 **Yu T**, Yu Y, Wang J, Yin L, Zhou Y, Ying D, Huang R, Chen H, Wu S, Shen Y, Fu Q, Chen F. Identification of TCIRG1 and CLCN7 gene mutations in a patient with autosomal recessive osteopetrosis. *Mol Med Rep* 2014; **9**: 1191-1196 [PMID: 24535484 DOI: 10.3892/mmr.2014.1955]

World Journal of Clinical Cases

Submit a Manuscript: https://www.f6publishing.com

World J Clin Cases 2023 January 26; 11(3): 709-718

DOI: 10.12998/wjcc.v11.i3.709

ISSN 2307-8960 (online)

CASE REPORT

Soft tissue tuberculosis detected by next-generation sequencing: A case report and review of literature

Yan-Gai He, Ya-Hui Huang, Xiao-Lan Yi, Kao-Liang Qian, Ying Wang, Hui Cheng, Jun Hu, Yuan Liu

Specialty type: Medicine, research and experimental

Provenance and peer review: Unsolicited article; Externally peer reviewed.

Peer-review model: Single blind

Peer-review report's scientific quality classification

Grade A (Excellent): 0
Grade B (Very good): B
Grade C (Good): 0
Grade D (Fair): 0
Grade E (Poor): E

P-Reviewer: Shen TC, Taiwan; Vyshka G, Albania

Received: November 26, 2022
Peer-review started: November 26, 2022
First decision: December 13, 2022
Revised: December 21, 2022
Accepted: January 5, 2023
Article in press: January 5, 2023
Published online: January 26, 2023

Yan-Gai He, Ya-Hui Huang, Xiao-Lan Yi, Ying Wang, Yuan Liu, Department of Infectious Diseases, The First Affiliated Hospital of Nanjing Medical University, Nanjing 210029, Jiangsu Province, China

Kao-Liang Qian, Hui Cheng, Jun Hu, Department of Orthopedics, The First Affiliated Hospital of Nanjing Medical University, Nanjing 210029, Jiangsu Province, China

Corresponding author: Yuan Liu, MD, PhD, Academic Research, Department of Infectious Diseases, The First Affiliated Hospital of Nanjing Medical University, No. 300 Guangzhou Road, Nanjing 210029, Jiangsu Province, China. liuyuan@jsph.org.cn

Abstract

BACKGROUND

Soft tissue tuberculosis is rare and insidious, with most patients presenting with a localized enlarged mass or swelling, which may be factors associated with delayed diagnosis and treatment. In recent years, next-generation sequencing has rapidly evolved and has been successfully applied to numerous areas of basic and clinical research. A literature search revealed that the use of next-generation sequencing in the diagnosis of soft tissue tuberculosis has been rarely reported.

CASE SUMMARY

A 44-year-old man presented with recurrent swelling and ulcers on the left thigh. Magnetic resonance imaging suggested a soft tissue abscess. The lesion was surgically removed and tissue biopsy and culture were performed; however, no organism growth was detected. Finally, Mycobacterium tuberculosis was confirmed as the pathogen responsible for infection through next-generation sequencing analysis of the surgical specimen. The patient received a standardized anti-tuberculosis treatment and showed clinical improvement. We also performed a literature review on soft tissue tuberculosis using studies published in the past 10 years.

CONCLUSION

This case highlights the importance of next-generation sequencing for the early diagnosis of soft tissue tuberculosis, which can provide guidance for clinical treatment and improve prognosis.

Key Words: Mycobacterium tuberculosis; Soft tissue infection; Next-generation sequencing; Extrapulmonary tuberculosis; Diagnosis; Case report

Core Tip: The diagnosis of extrapulmonary tuberculosis can be challenging, especially for tuberculosis in rare sites such as soft tissues. Soft tissue tuberculosis is rare and easily misdiagnosed. A delay in soft tissue tuberculosis diagnosis may worsen the disease, increase tuberculosis transmission, and accelerate the evolution of drug resistance. This case report emphasizes the importance of next-generation sequencing for early diagnosis of soft tissue tuberculosis, which can provide guidance for clinical treatment and improve prognosis.

Citation: He YG, Huang YH, Yi XL, Qian KL, Wang Y, Cheng H, Hu J, Liu Y. Soft tissue tuberculosis detected by next-generation sequencing: A case report and review of literature. *World J Clin Cases* 2023; 11(3): 709-718
URL: https://www.wjgnet.com/2307-8960/full/v11/i3/709.htm
DOI: https://dx.doi.org/10.12998/wjcc.v11.i3.709

INTRODUCTION

Tuberculosis (TB) is a chronic infectious disease caused by mycobacterium TB (MTB). Extrapulmonary TB (EPTB) in China constitutes 15%-20% of all TB cases, it can involve any organ, with the most usual sites of infection being the pleura (49.8%), bronchi (14.8%), lymph nodes (8.56%), meninges (7.6%), thoracic vertebra (2.55%), and skeletal joints (0.56%)[1,2]. Isolated soft tissue TB is rare and accounts for only 1-2% of all pulmonary TB (PTB) and EPTB cases. Current knowledge of soft tissue TB is largely based on the analysis of a single patient and case series[3,4]. Therefore, the low incidence and lack of typical symptoms of soft tissue TB may lead to difficulties and delays in diagnosis.

The traditional gold standard for TB diagnosis is the MTB culture assay, which has a lower positivity rate of 23.03%. In EPTB, the positivity rate is approximately 18.45%[5]. The MTB culture assay demands laboratory biosafety requirements, and rapid diagnosis is challenging. Molecular biology techniques, such as real-time fluorescent polymerase chain reaction (PCR) and cross-primer amplification, have facilitated the rapid diagnosis. However, the diagnostic sensitivity of these methods for EPTB is limited and varies among specimen types[6]. For example, the sensitivity of Xpert MTB/ rifampin (RIF) assay for PTB and EPTB was found to be 95.5% and 76.5%, respectively[7].

Next-generation sequencing (NGS) is an emerging and promising technology that is used for disease diagnosis, drug resistance determination, and epidemiological investigations. It has the potential to significantly reduce response time for the identification of pathogens, such as bacteria, viruses, tuberculosis, fungi, and parasites[8-12]. For TB, next-generation sequencing can be used for early diagnosis, identification of drug resistance gene mutations associated with conventional anti-TB drugs, and detection of mixed infections[13]. However, there are only a few reports on the rapid diagnosis of MTB infection in soft tissue using NGS. In this report, we present a case of soft tissue TB in an immunocompetent patient with no history of TB. We used NGS technology to detect the surgically resected lesion tissue, and the patient was finally diagnosed with soft tissue TB. In addition, we reviewed the main features of soft tissue TB cases reported in the past decade.

CASE PRESENTATION

Chief complaints

A 44-year-old man admitted to Department of Orthopaedics of the First Affiliated Hospital of Nanjing Medical University presented with a history of left thigh ulceration and swelling for 10 d.

History of present illness

The patient showed similar symptoms in 2018, some tests including bacterial and tuberculosis culture, acid-fast staining, and tuberculosis infection T-lymphocyte spot test (T-SPOT). TB tests, were negative at that time. And the patient recovered gradually after debridement. Through careful history investigation, we found that the patient had an open wound on the left thigh caused by trauma 18 years ago, which improved after debridement and suturing.

History of past illness

There is no relevant history of past illness.

Personal and family history

The patient's personal and family histories were unremarkable.

Physical examination

Two old scars were observed on the patient's left thigh, and there was a red and swollen ruptured wound above them. The skin temperature of the limb was normal, and no movement limitation was observed. A physical examination revealed no other positive signs. Breath sounds of both lungs were clear, no obvious dry or wet rales were heard, and there was no pleural friction rub.

Laboratory examinations

On day 2 after admission, laboratory tests, such as routine blood examination, coagulation function tests, erythrocyte sedimentation rate, and serum biochemical indicators, did not show any significant abnormalities.

Imaging examinations

A radiograph of the left femur indicated no bone erosion (Figure 1A). Bone single-photon emission computed tomography did not reveal any abnormalities in bone metabolism (Figure 1B). On day five after admission, magnetic resonance imaging (MRI) of the left hip was performed, which revealed abnormal signals in the soft tissue of the left upper femur and oedema of the subcutaneous soft tissue. In addition, MRI revealed a chronic abscess with sinus tract formation (Figure 1C-E). Computed tomography of the chest showed scattered nodules in both lungs (Figure 1F). But the symptoms of tuberculosis are not obvious.

Further diagnostic work-up

Considering that the abscess was large, we performed abscess resection of the left thigh and vacuum sealing drainage therapy. We observed inflammation and degeneration in subcutaneous tissue and cystic infected tissue wrapped in the deep layer, which had tough capsule walls and a size of approximately 8 cm × 6 cm (Figure 2A and B). After incision of the purulent cyst, gelatinous necrotic tissue which was grey and white, was observed. Furthermore, we performed histological examination, bacterial culture, and NGS testing of the specimen.

Histological examination revealed fibrous connective tissue hyperplasia with necrosis, acute and chronic inflammatory cell infiltration, and focal granulomatous inflammation with multinucleated giant cell formation (Figure 2C). Bacterial culture of the surgically excised specimen was negative on day seven after admission. However, MTB was detected by NGS simultaneously. The distribution of bacteria and fungi identified by NGS revealed that MTB was the main pathogen (Figure 3A), and 24 sequence reads were identified (Figure 3B).

The pathology department was then contacted for an additional acid-fast bacillus staining test of the intraoperative specimen, and scattered suspicious antacid staining positive rods were observed microscopically (Figure 2D). Further, the T-SPOT. TB test results were positive.

FINAL DIAGNOSIS

Combined with the patient's medical history and outcome of NGS, the patient was finally diagnosed with soft tissue tuberculosis.

TREATMENT

We planned a standardized anti-tuberculosis treatment with four drugs, isoniazid, rifampicin, ethambutol, and pyrazinamide, for 2 mo. Further isoniazid and rifampicin were given for four months. But the patient stopped the drug because of gastrointestinal discomfort during the 3rd month of treatment and suspended for 2 wk, then he continued to take the medicine again for 3 mo.

OUTCOME AND FOLLOW-UP

Currently, the wound has healed adequately and the patient is undergoing follow-up. A summary of the timeline is shown in Figure 4.

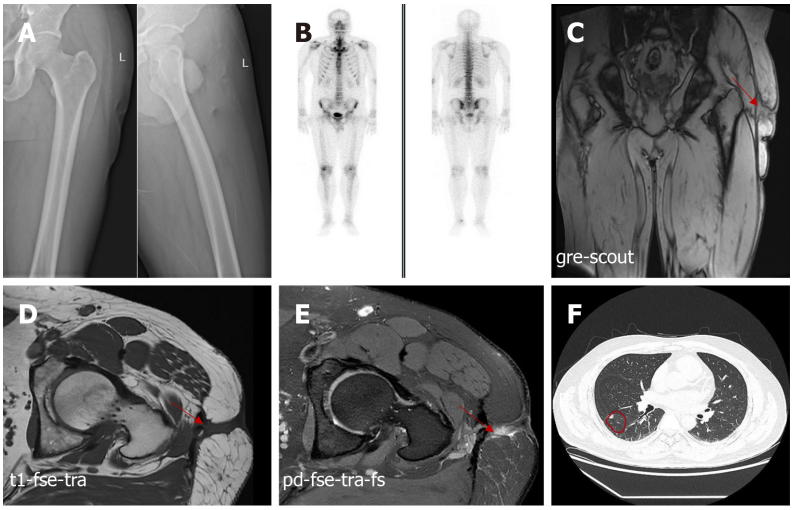

DOI: 10.12998/wjcc.v11.i3.709

Figure 1 Imaging pictures of the patient. A: Anteroposterior and lateral radiographs of the left femur are normal; B: Bone single-photon emission computed tomography did not reveal any abnormalities in bone metabolism; C-E: Magnetic resonance imaging of the left hip showing abnormal signals in the soft tissue of the left upper femur and suggesting a chronic abscess with sinus tract formation; F: Computed tomography of the chest showing scattered nodules in both lungs, the largest nodule in the right lung with a length of 8 mm.

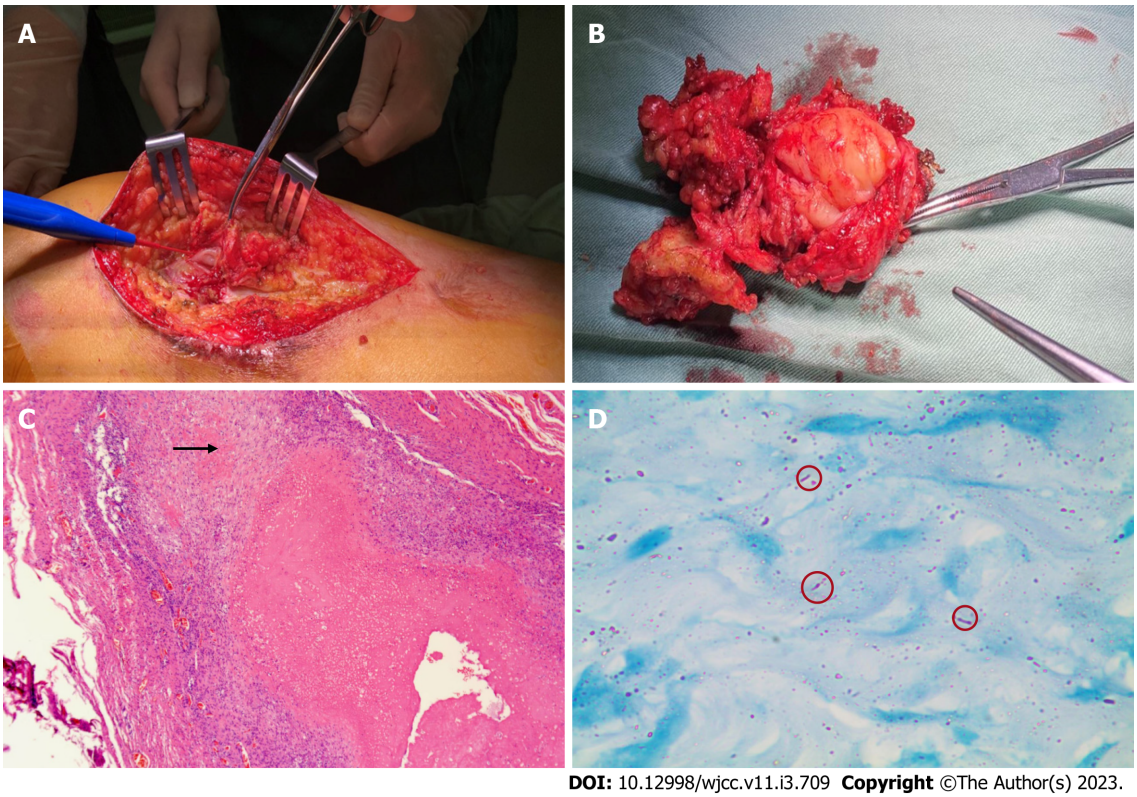

DOI: 10.12998/wjcc.v11.i3.709

Figure 2 Intraoperative photographs of the left thigh and histopathological examination of resected specimens. A: Intraoperative photograph; B: Excised specimen (8 cm × 6 cm); C: Granulomas are embedded among the muscle fibers with lymphocyte infiltration and multinucleated giant cell aggregation (× 40); D: The acid-fast bacilli staining test showed scattered, suspicious antacid staining-positive rods (× 1000).

DISCUSSION

According to a global TB report published by WHO, TB deaths have increased because of reduced access to TB diagnosis and treatment in the face of the COVID-19 pandemic for the first time in over a decade[14]. China has the second-highest number of TB cases worldwide, accounting for approximately 9% of the global TB incidence. One study indicated that the prevalence of smear-positive TB in China decreased from 170/100 000 population in 1990 to 59 /100 000 population in 2010, a reduction of more than 50 percent[15]. Despite past success in controlling TB, the limited epidemiologic information

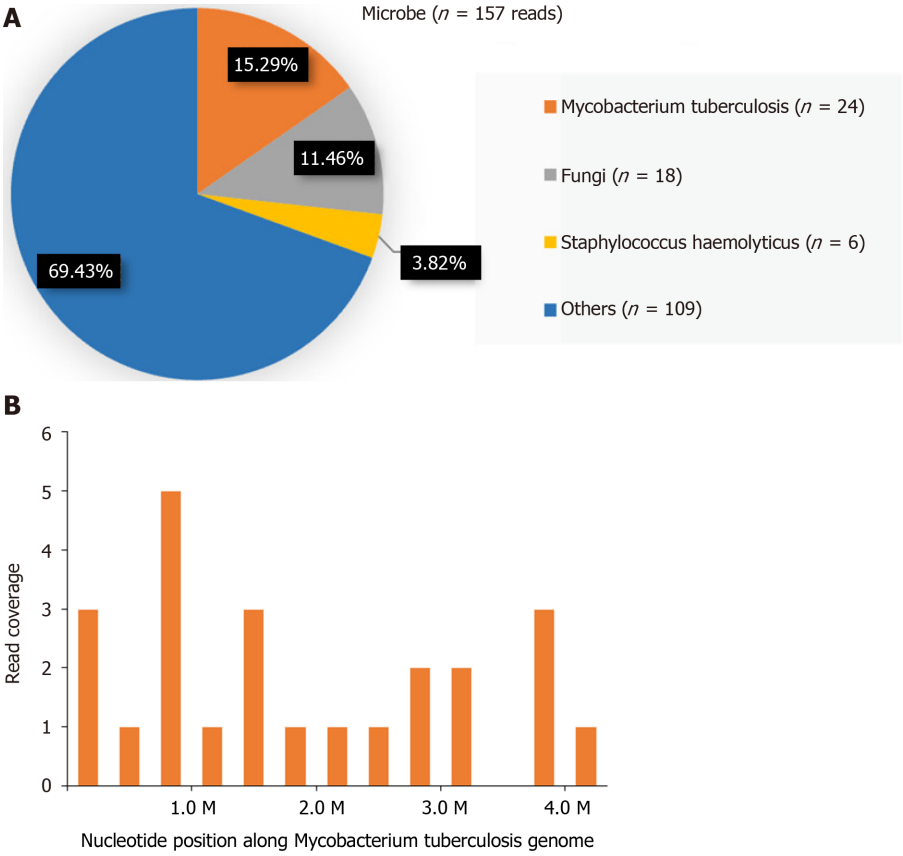

DOI: 10.12998/wjcc.v11.i3.709

Figure 3 Next-generation sequencing results of surgically resected specimen. A: Distribution of the sequences detected by next-generation sequencing of surgically excised specimens; B: Twenty-four sequence reads of mycobacterium tuberculosis are observed, with a coverage rate of 0.005%.

available suggests that the incidence of EPTB may be increasing steadily worldwide, including in China [16,17].

The diagnosis of EPTB can be challenging, especially for TB in rare sites such as soft tissues. A delay in soft tissue TB diagnosis may worsen the disease, increase TB transmission, and accelerate the evolution of drug resistance. The conventional gold standards for TB diagnosis are MTB culture and drug sensitivity tests. However, it is tedious and can take 6-8 wk because of slow growth of MTB[18]. Molecular diagnostic techniques, such as Xpert MTB/RIF, loop-mediated isothermal amplification (LAMP), and line probe assay (LPA), can effectively reduce turnaround time and improve diagnostic performance. However, these techniques have limited diagnostic sensitivity for specimens with low bacterial content, such as EPTB[19,20]. For example, a meta-analysis found that the pooled sensitivity of Xpert MTB/RIF for diagnosing abdominal TB was only 23%[21]. Another meta-analysis reported that the pooled sensitivity of LAMP for detecting EPTB was 77%[22]. Only a few studies have evaluated the role of LPA in EPTB specimens. A study from India reported a sensitivity of 46.1% with a specificity of 91% in EPTB specimens, with liquid culture as the reference standard[23].

Soft tissue TB is rare and easily misdiagnosed. Therefore, rapid, efficient, and accurate diagnosis of soft tissue TB is an urgent clinical problem. NGS is a revolutionary development of first-generation sequencing methods that can sequence millions of DNA fragments simultaneously with high throughput and short detection cycles. A study found that the positivity rate of NGS is approximately 15% higher than that of traditional pathogen culture in a pairwise manner for infectious diseases[24]. Xpert MTB/RIF and NGS tests were performed on various samples of sputum, cerebrospinal fluid, and pus from patients with suspected active TB infection. Compared with Xpert MTB/RIF, NGS showed better sensitivity in all clinical (76.9% *vs* 61.5%), pulmonary (87.5% *vs* 75.0%), and extrapulmonary samples (60.0% *vs* 40.0%)[13]. In this case, NGS rapidly detected the sequence of MTB in the sample, which was important for us to confirm the diagnosis of soft tissue TB early and to treat it with anti-tuberculosis drugs in time. Below, we review the relevant literature on soft tissue TB.

Recent case reports on soft tissue TB published in the past 10 years were identified by searching PubMed (Table 1). We found 17 case reports including 10 males and 7 females. The ages of the patients ranged from 7 to 79 years. There were 12 cases distributed in Asian countries, four cases in African countries and one case in America. No underlying diseases were reported in 10 patients. In 13 patients, the lesions were located on the extremities, including the thigh, calf, forearm, and wrist. The other four patients had lesions in the gluteus, back, thorax, and iliopsoas.

Table 1 Main features of reported cases of soft tissue tuberculosis

Ref.	Gender/age (yr)	Country	Underlying disease	Main clinical manifestations	Involved sites	Diagnostic methods
Arora *et al*[38], 2012	Male/15	India	None	Swelling, anorexia, weight loss	Left thigh	Mycobacterium tuberculosis culture
Lee *et al*[39], 2013	Male/62	Korea	Right total hip arthroplasty	Mass	Right thigh	Histological examination, and culture
Elshafie *et al*[40], 2013	Male/25	Oman	Exposed to suspected tuberculosis, diarrhea	Enlarging swelling	Right gluteus	Histological examination, and culture
Neogi *et al*[41], 2013	Female/11	India	None	Swelling	Right thigh, right calf, and left arm	Histological examination, and culture
Meena *et al*[42], 2015	Male/25	India	None	Swelling, fatigue, weight loss	Right triceps	Mycobacterium tuberculosis PCR
Dhakal *et al*[43], 2015	Female/9	Nepal	None	Swelling	Forearm, right calf	Histological examination
Sbai *et al*[44], 2016	Male/45	Tunisia	None	Pain, swelling	Right wrist	Tissue biopsy and culture
Al-khazraji *et al*[45], 2017	Female/33	America	Lupus nephritis, hormonal therapy	Pain, weakness, swelling, redness	Right calf	Fluid culture
Alaya *et al*[46], 2017	Female/23	Tunisia	None	Swelling, pain	Left thigh	Mycobacterium tuberculosis PCR
Manicketh *et al*[25], 2018	Female/55	India	Pulmonary tuberculosis	Swelling, fever	Left wrist and right calf	A Ziehl-Nielsen stain
Hashimoto *et al*[27], 2018	Male/79	Japan	None	Swelling, erythema	Left wrist	Histological examination
Zeng *et al*[4], 2019	Male/49	China	Pulmonary tuberculosis; steroid treatment	Pain, mass, swelling	Both thighs and calves	Mycobacterium tuberculosis PCR, Tissue biopsy and culture
Zitouna *et al*[47], 2019	Female/42	Tunisia	None	Mass, swelling	Right mid-back	Tissue biopsy and culture
Moyano *et al*[48], 2019	Male/29	Senegal	None	Pain, increase in size of hemithorax	Right hemithorax	Mycobacterium tuberculosis PCR and culture
Fahad *et al*[28], 2020	Female/45	Pakistan	None	Swelling, pain	Right forearm	Histological examination
Murugesh *et al*[49], 2020	Male/31	India	Renal transplant with immuno-suppressants	Fever, pain, swollen erythematous	Right foot and calf	Nucleic acid amplification test
Tone *et al*[26], 2021	Male/29	Japan	Right tuberculous pleurisy	Fever, pain	Right iliopsoas	Mycobacterium tuberculosis PCR

PCR: Polymerase chain reaction.

Soft tissue TB occurs mostly in the extremities, and patients present with local masses, swelling, and weakness. Only a small percentage of patients present with constitutional symptoms such as fever and weight loss[25,26]. Most cases of soft tissue TB reported in the literature were diagnosed by histological examination and MTB culture, whereas some were confirmed by rapid PCR. Although the culture and gene Xpert were negative, two patients recovered after empirical anti-TB therapy[27,28]. Empirical treatment for TB was initiated without a confirmed bacterial diagnosis. Moreover, factors contributing to the probability of a patient developing TB and experiencing adverse outcomes were weighed against the threshold for initiating anti-TB therapy. This threshold is subjective and may vary among the clinicians. Factors considered in empirical anti-TB treatment include the background TB epidemiology in the geographic area, exposure to TB patients, clinical manifestations suggestive of TB disease, comorbidities such as HIV co-infection, and the results of other diagnostic methods such as imaging outcomes if available[29].

There are many traditional tests for TB, including smear, culture, pathological biopsy, imaging, purified protein derivative testing, interferon-gamma release assay, and TB antibody testing[30,31]. Confirmation of TB over the past few decades often requires a combination of these tests. Over the last decade, advances have been made in the field of TB diagnostics in the form of new molecular tests. Often referred to as nucleic acid amplification tests, these assays rely on amplification of a targeted genetic region of the MTB complex, typically by PCR[32]. GeneXpert MTB/RIF is a fully automated

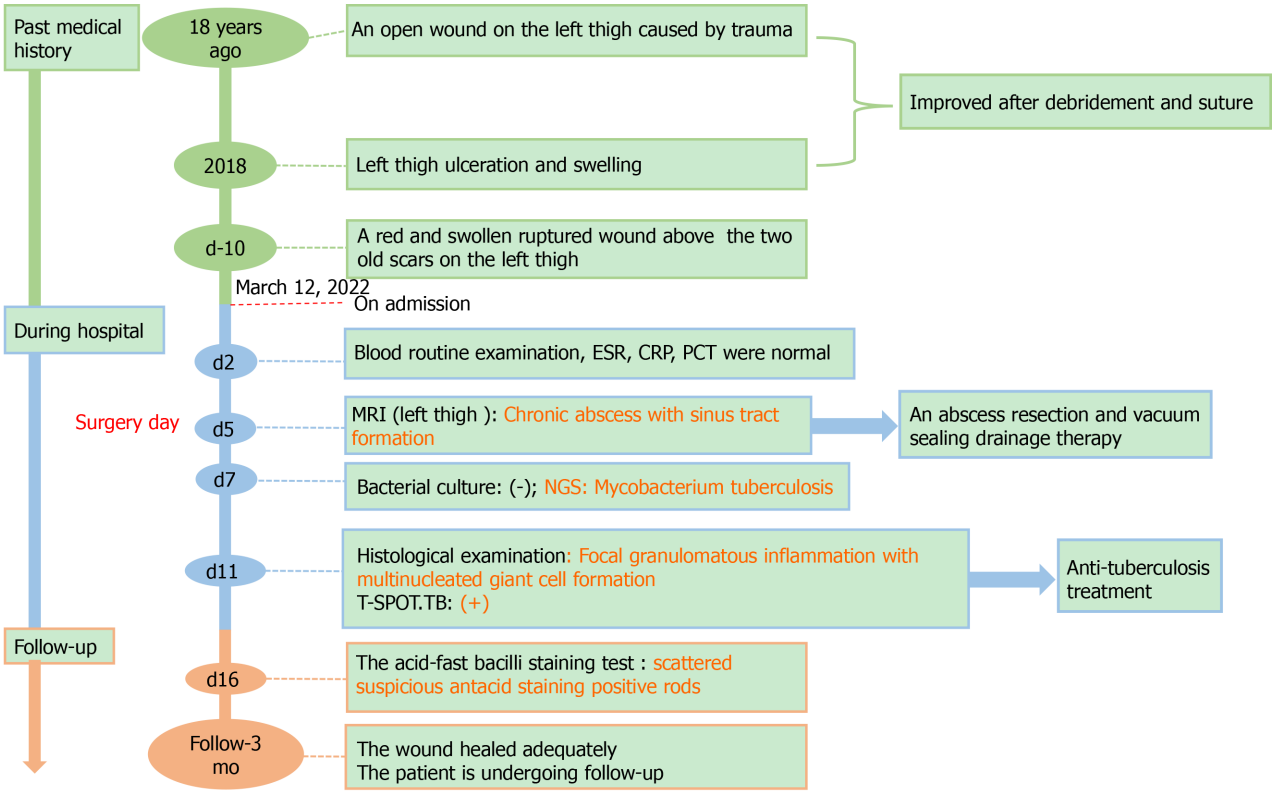

DOI: 10.12998/wjcc.v11.i3.709

Figure 4 A timeline showing the progress of the disease and the patient's treatment and follow-up. ESR: Erythrocyte sedimentation rate; CRP: C-reactive protein; PCT: Procalcitonin; MRI: Magnetic resonance imaging; NGS: Next-generation sequencing.

closed system that performs sample preparation and real-time PCR and produces results within 2 h. This system can detect RIF resistance (targeting the rpoB gene). In 2011, the WHO recommended GeneXpert MTB/RIF for the early diagnosis of drug-resistant TB, which was further expanded in 2013 to replace smear and culture for the rapid diagnosis of EPTB[33]. The new version of Xpert MTB Ultra improved overall sensitivity and was endorsed by the WHO in 2017[34]. In 2017, the UK used NGS for TB diagnosis, drug resistance detection, and MTB typing for the first time[35]. Several studies have shown its advantages in the diagnosis and treatment of EPTB[36,37]. However, the value of NGS in the rapid diagnosis of TB has not been verified in large samples, and there is a lack of unified standards and procedures. Guidelines for the clinical interpretation of NGS reports need to be improved.

CONCLUSION

We reported the case of a patient who was immunocompetent and had no history of TB and was diagnosed with soft tissue TB by NGS. The patient received timely anti-TB treatment, which improved. Clinicians should consider atypical pathogens such as MTB in the diagnosis of patients with local masses or swelling. NGS may be a useful method for identifying the pathogens responsible for soft tissue infections without typical clinical manifestations.

FOOTNOTES

Author contributions: He YG and Huang YH drafted the manuscript, interpreted the patient data. Xi XL, Qian KL, Wang Y, and Cheng H collected information from the patients and searched the related literature. Liu Y and Hu J contributed to supervision and final approval. All authors have read and approved the final manuscript.

Supported by the National Natural Science Foundation of China, No. 82272544.

Informed consent statement: Informed written consent was obtained from the patient and his family for publication of this report and any accompanying images.

Conflict-of-interest statement: All the authors report no relevant conflicts of interest for this article.

CARE Checklist (2016) statement: The authors have read the CARE Checklist (2016), and the manuscript was prepared and revised according to the CARE Checklist (2016).

Country/Territory of origin: China

ORCID number: Yuan Liu 0000-0001-9452-0442.

S-Editor: Wang LL
L-Editor: A
P-Editor: Wang LL

REFERENCES

1 **Baykan AH**, Sayiner HS, Aydin E, Koc M, Inan I, Erturk SM. Extrapulmonary tuberculosıs: an old but resurgent problem. *Insights Imaging* 2022; **13**: 39 [PMID: 35254534 DOI: 10.1186/s13244-022-01172-0]
2 **Kang W**, Liu S, Du J, Tang P, Chen H, Liu J, Ma J, Li M, Qin J, Shu W, Zong P, Zhang Y, Dong Y, Yang Z, Mei Z, Deng Q, Wang P, Han W, Yan X, Chen L, Zhao X, Tan L, Li F, Zheng C, Liu H, Li X, A E, Du Y, Liu F, Cui W, Wang Q, Chen X, Han J, Xie Q, Feng Y, Liu W, Yang S, Zhang J, Zheng J, Chen D, Yao X, Ren T, Li Y, Wu L, Song Q, Shen X, Liu Y, Guo S, Yan K, Yang M, Lei D, Wu M, Li L, Tang S. Epidemiology of concurrent extrapulmonary tuberculosis in inpatients with extrapulmonary tuberculosis lesions in China: a large-scale observational multi-centre investigation. *Int J Infect Dis* 2022; **115**: 79-85 [PMID: 34781005 DOI: 10.1016/j.ijid.2021.11.019]
3 **Franco-Paredes C**, Chastain DB, Allen L, Henao-Martínez AF. Overview of Cutaneous Mycobacterial Infections. *Curr Trop Med Rep* 2018; **5**: 228-232 [PMID: 34164254 DOI: 10.1007/s40475-018-0161-7]
4 **Zeng Y**, Liu Y, Xie Y, Liang J, Kuang J, Lu Z, Zhou Y. Muscular Tuberculosis: A New Case and a Review of the Literature. *Front Neurol* 2019; **10**: 1031 [PMID: 31632334 DOI: 10.3389/fneur.2019.01031]
5 **Sun WW**, Gu J, Fan L. [Application value of metagenomic next-generation sequencing (mNGS) in the diagnosis of different types of tuberculosis]. *Zhonghua Jie He He Hu Xi Za Zhi* 2021; **44**: 96-100 [PMID: 33535323 DOI: 10.3760/cma.j.cn112147-20200316-00343]
6 **Tadesse M**, Abebe G, Bekele A, Bezabih M, Yilma D, Apers L, de Jong BC, Rigouts L. Xpert MTB/RIF assay for the diagnosis of extrapulmonary tuberculosis: a diagnostic evaluation study. *Clin Microbiol Infect* 2019; **25**: 1000-1005 [PMID: 30583052 DOI: 10.1016/j.cmi.2018.12.018]
7 **Allahyartorkaman M**, Mirsaeidi M, Hamzehloo G, Amini S, Zakiloo M, Nasiri MJ. Low diagnostic accuracy of Xpert MTB/RIF assay for extrapulmonary tuberculosis: A multicenter surveillance. *Sci Rep* 2019; **9**: 18515 [PMID: 31811239 DOI: 10.1038/s41598-019-55112-y]
8 **Goelz H**, Wetzel S, Mehrbarzin N, Utzolino S, Häcker G, Badr MT. Next- and Third-Generation Sequencing Outperforms Culture-Based Methods in the Diagnosis of Ascitic Fluid Bacterial Infections of ICU Patients. *Cells* 2021; **10** [PMID: 34831447 DOI: 10.3390/cells10113226]
9 **Sahajpal NS**, Mondal AK, Njau A, Petty Z, Chen J, Ananth S, Ahluwalia P, Williams C, Ross TM, Chaubey A, DeSantis G, Schroth GP, Bahl J, Kolhe R. High-Throughput Next-Generation Sequencing Respiratory Viral Panel: A Diagnostic and Epidemiologic Tool for SARS-CoV-2 and Other Viruses. *Viruses* 2021; **13** [PMID: 34696495 DOI: 10.3390/v13102063]
10 **Oreskovic A**, Waalkes A, Holmes EA, Rosenthal CA, Wilson DPK, Shapiro AE, Drain PK, Lutz BR, Salipante SJ. Characterizing the molecular composition and diagnostic potential of Mycobacterium tuberculosis urinary cell-free DNA using next-generation sequencing. *Int J Infect Dis* 2021; **112**: 330-337 [PMID: 34562627 DOI: 10.1016/j.ijid.2021.09.042]
11 **Tiew PY**, Thng KX, Chotirmall SH. Clinical Aspergillus Signatures in COPD and Bronchiectasis. *J Fungi (Basel)* 2022; **8** [PMID: 35628736 DOI: 10.3390/jof8050480]
12 **Ryan U**, Zahedi A, Feng Y, Xiao L. An Update on Zoonotic Cryptosporidium Species and Genotypes in Humans. *Animals (Basel)* 2021; **11** [PMID: 34828043 DOI: 10.3390/ani11113307]
13 **Zhou X**, Wu H, Ruan Q, Jiang N, Chen X, Shen Y, Zhu YM, Ying Y, Qian YY, Wang X, Ai JW, Zhang WH. Clinical Evaluation of Diagnosis Efficacy of Active Mycobacterium tuberculosis Complex Infection *via* Metagenomic Next-Generation Sequencing of Direct Clinical Samples. *Front Cell Infect Microbiol* 2019; **9**: 351 [PMID: 31681628 DOI: 10.3389/fcimb.2019.00351]
14 **Daley CL**. The Global Fight Against Tuberculosis. *Thorac Surg Clin* 2019; **29**: 19-25 [PMID: 30454918 DOI: 10.1016/j.thorsurg.2018.09.010]
15 **Wang L**, Zhang H, Ruan Y, Chin DP, Xia Y, Cheng S, Chen M, Zhao Y, Jiang S, Du X, He G, Li J, Wang S, Chen W, Xu C, Huang F, Liu X, Wang Y. Tuberculosis prevalence in China, 1990-2010; a longitudinal analysis of national survey data. *Lancet* 2014; **383**: 2057-2064 [PMID: 24650955 DOI: 10.1016/s0140-6736(13)62639-2]
16 **Pang Y**, An J, Shu W, Huo F, Chu N, Gao M, Qin S, Huang H, Chen X, Xu S. Epidemiology of Extrapulmonary Tuberculosis among Inpatients, China, 2008-2017. *Emerg Infect Dis* 2019; **25**: 457-464 [PMID: 30789144 DOI: 10.3201/eid2503.180572]

17 **Chen L**, Fu X, Tian P, Li Q, Lei D, Peng Z, Liu Q, Li N, Zhang J, Xu P, Zhang H. Upward trends in new, rifampicin-resistant and concurrent extrapulmonary tuberculosis cases in northern Guizhou Province of China. *Sci Rep* 2021; **11**: 18023 [PMID: 34504296 DOI: 10.1038/s41598-021-97595-8]

18 **Baker JJ**, Johnson BK, Abramovitch RB. Slow growth of Mycobacterium tuberculosis at acidic pH is regulated by phoPR and host-associated carbon sources. *Mol Microbiol* 2014; **94**: 56-69 [PMID: 24975990 DOI: 10.1111/mmi.12688]

19 **Kohli M**, Schiller I, Dendukuri N, Dheda K, Denkinger CM, Schumacher SG, Steingart KR. Xpert(®) MTB/RIF assay for extrapulmonary tuberculosis and rifampicin resistance. *Cochrane Database Syst Rev* 2018; **8**: CD012768 [PMID: 30148542 DOI: 10.1002/14651858.CD012768.pub2]

20 **Mhimbira FA**, Bholla M, Sasamalo M, Mukurasi W, Hella JJ, Jugheli L, Reither K. Detection of Mycobacterium tuberculosis by EasyNAT diagnostic kit in sputum samples from Tanzania. *J Clin Microbiol* 2015; **53**: 1342-1344 [PMID: 25609720 DOI: 10.1128/jcm.03037-14]

21 **Sharma V**, Soni H, Kumar-M P, Dawra S, Mishra S, Mandavdhare HS, Singh H, Dutta U. Diagnostic accuracy of the Xpert MTB/RIF assay for abdominal tuberculosis: a systematic review and meta-analysis. *Expert Rev Anti Infect Ther* 2021; **19**: 253-265 [PMID: 32845790 DOI: 10.1080/14787210.2020.1816169]

22 **Yu G**, Shen Y, Zhong F, Ye B, Yang J, Chen G. Diagnostic accuracy of the loop-mediated isothermal amplification assay for extrapulmonary tuberculosis: A meta-analysis. *PLoS One* 2018; **13**: e0199290 [PMID: 29944682 DOI: 10.1371/journal.pone.0199290]

23 **Sharma SK**, Kohli M, Chaubey J, Yadav RN, Sharma R, Singh BK, Sreenivas V, Sharma A, Bhatia R, Jain D, Seenu V, Dhar A, Soneja M. Evaluation of Xpert MTB/RIF assay performance in diagnosing extrapulmonary tuberculosis among adults in a tertiary care centre in India. *Eur Respir J* 2014; **44**: 1090-1093 [PMID: 25063241 DOI: 10.1183/09031936.00059014]

24 **Miao Q**, Ma Y, Wang Q, Pan J, Zhang Y, Jin W, Yao Y, Su Y, Huang Y, Wang M, Li B, Li H, Zhou C, Li C, Ye M, Xu X, Li Y, Hu B. Microbiological Diagnostic Performance of Metagenomic Next-generation Sequencing When Applied to Clinical Practice. *Clin Infect Dis* 2018; **67**: S231-S240 [PMID: 30423048 DOI: 10.1093/cid/ciy693]

25 **Manicketh I**, Panjwani P, Ravikumar G, Prince Mathan L. Soft tissue tuberculosis - An unusual presentation of a common disease. *Indian J Tuberc* 2018; **65**: 96-97 [PMID: 29332661 DOI: 10.1016/j.ijtb.2017.04.002]

26 **Tone K**, Hirano Y, Kuwano K. Iliopsoas gravity abscess secondary to a tuberculous empyema. *Int J Mycobacteriol* 2021; **10**: 335-337 [PMID: 34494577 DOI: 10.4103/ijmy.ijmy_129_21]

27 **Hashimoto K**, Nishimura S, Oka N, Kakinoki R, Akagi M. Tuberculoma with phlegmon-like symptoms mimicking soft tissue sarcoma in the wrist: A case report. *Mol Clin Oncol* 2018; **9**: 207-210 [PMID: 30101023 DOI: 10.3892/mco.2018.1652]

28 **Fahad S**, Baloch N, Din NU. Tuberculosis of the flexor carpi radialis muscle - a case report. *J Pak Med Assoc* 2020; **70**: 1645-1647 [PMID: 33040129 DOI: 10.5455/jpma.40799]

29 **Dartois VA**, Rubin EJ. Anti-tuberculosis treatment strategies and drug development: challenges and priorities. *Nat Rev Microbiol* 2022; **20**: 685-701 [PMID: 35478222 DOI: 10.1038/s41579-022-00731-y]

30 **Nishimura T**, Hasegawa N, Mori M, Takebayashi T, Harada N, Higuchi K, Tasaka S, Ishizaka A. Accuracy of an interferon-gamma release assay to detect active pulmonary and extra-pulmonary tuberculosis. *Int J Tuberc Lung Dis* 2008; **12**: 269-274 [PMID: 18284831]

31 **Procop GW**. Laboratory Diagnosis and Susceptibility Testing for Mycobacterium tuberculosis. *Microbiol Spectr* 2016; **4** [PMID: 28087944 DOI: 10.1128/microbiolspec.TNMI7-0022-2016]

32 **Acharya B**, Acharya A, Gautam S, Ghimire SP, Mishra G, Parajuli N, Sapkota B. Advances in diagnosis of Tuberculosis: an update into molecular diagnosis of Mycobacterium tuberculosis. *Mol Biol Rep* 2020; **47**: 4065-4075 [PMID: 32248381 DOI: 10.1007/s11033-020-05413-7]

33 **WHO Guidelines Approved by the Guidelines Review Committee**. Xpert MTB/RIF Implementation Manual: Technical and Operational 'How-To'; Practical Considerations. Geneva: World Health Organization, 2014

34 **Chakravorty S**, Simmons AM, Rowneki M, Parmar H, Cao Y, Ryan J, Banada PP, Deshpande S, Shenai S, Gall A, Glass J, Krieswirth B, Schumacher SG, Nabeta P, Tukvadze N, Rodrigues C, Skrahina A, Tagliani E, Cirillo DM, Davidow A, Denkinger CM, Persing D, Kwiatkowski R, Jones M, Alland D. The New Xpert MTB/RIF Ultra: Improving Detection of Mycobacterium tuberculosis and Resistance to Rifampin in an Assay Suitable for Point-of-Care Testing. *mBio* 2017; **8** [PMID: 28851844 DOI: 10.1128/mBio.00812-17]

35 **Satta G**, Lipman M, Smith GP, Arnold C, Kon OM, McHugh TD. Mycobacterium tuberculosis and whole-genome sequencing: how close are we to unleashing its full potential? *Clin Microbiol Infect* 2018; **24**: 604-609 [PMID: 29108952 DOI: 10.1016/j.cmi.2017.10.030]

36 **Sun W**, Lu Z, Yan L. Clinical efficacy of metagenomic next-generation sequencing for rapid detection of Mycobacterium tuberculosis in smear-negative extrapulmonary specimens in a high tuberculosis burden area. *Int J Infect Dis* 2021; **103**: 91-96 [PMID: 33227518 DOI: 10.1016/j.ijid.2020.11.165]

37 **Yu G**, Wang X, Zhu P, Shen Y, Zhao W, Zhou L. Comparison of the efficacy of metagenomic next-generation sequencing and Xpert MTB/RIF in the diagnosis of tuberculous meningitis. *J Microbiol Methods* 2021; **180**: 106124 [PMID: 33321144 DOI: 10.1016/j.mimet.2020.106124]

38 **Arora S**, Sabat D, Sural S, Dhal A. Isolated tuberculous pyomyositis of semimembranosus and adductor magnus: a case report. *Orthop Surg* 2012; **4**: 266-268 [PMID: 23109314 DOI: 10.1111/os.12011]

39 **Lee HJ**, Kim KW, Kim KS, Ryu SH, Ha YC. Primary musculoskeletal mycobacterium infection with large cystic masses after total hip arthroplasty. *J Arthroplasty* 2013; **28**: 374.e1-374.e3 [PMID: 22749661 DOI: 10.1016/j.arth.2012.05.009]

40 **Elshafie KT**, Al-Hinai MM, Al-Habsi HA, Al-Hattali MS, Hassan O, Al-Sukaiti R. A massive tuberculosis abscess at the erector spinae muscles and subcutaneous tissues in a young man. *Sultan Qaboos Univ Med J* 2013; **13**: 601-605 [PMID: 24273676 DOI: 10.12816/0003325]

41 **Neogi DS**, Bandekar SM, Chawla L. Skeletal muscle tuberculosis simultaneously involving multiple sites. *J Pediatr Orthop B* 2013; **22**: 167-169 [PMID: 22561909 DOI: 10.1097/BPB.0b013e328354b04d]

42 **Meena M**, Dixit R, Samaria JK, Vijayakandeepan Kumaresan SH. Tuberculosis of the triceps muscle. *BMJ Case Rep* 2015; **2015** [PMID: 25564636 DOI: 10.1136/bcr-2014-207032]

43 **Dhakal AK**, Shah SC, Shrestha D, Banepali N, Geetika KC. Tuberculosis presenting as multiple intramuscular nodules in a child: a case report. *J Med Case Rep* 2015; **9**: 72 [PMID: 25885776 DOI: 10.1186/s13256-015-0543-6]

44 **Sbai MA**, Benzarti S, Msek H, Boussen M, Khorbi A. Pseudotumoral form of soft-tissue tuberculosis of the wrist. *Int J Mycobacteriol* 2016; **5**: 99-101 [PMID: 26927998 DOI: 10.1016/j.ijmyco.2015.08.001]

45 **Al-Khazraji A**, Takher J, Alkhawam H, Fabbri M. Primary Tuberculous Pyomyositis of the Calf Muscles. *Am J Med Sci* 2017; **353**: 187-188 [PMID: 28183421 DOI: 10.1016/j.amjms.2016.05.010]

46 **Alaya Z**, Osman W. Isolated muscular tuberculosis: unusual location of the Koch bacillus. *Pan Afr Med J* 2017; **26**: 158 [PMID: 28533881 DOI: 10.11604/pamj.2017.26.158.11795]

47 **Zitouna K**, Riahi H, Goubantini A, Barsaoui M. Isolated tuberculous abscess in longissimus muscle. *Int J Mycobacteriol* 2019; **8**: 403-405 [PMID: 31793514 DOI: 10.4103/ijmy.ijmy_139_19]

48 **Moyano-Bueno D**, Blanco JF, López-Bernus A, Gutiérrez-Zubiaurre N, Gomez Ruiz V, Velasco-Tirado V, Belhassen-García M. Cold abscess of the chest wall: A diagnostic challenge. *Int J Infect Dis* 2019; **85**: 108-110 [PMID: 31163270 DOI: 10.1016/j.ijid.2019.05.031]

49 **Murugesh Anand S**, Edwin Fernando M, Srinivasaprasad ND, Sujit S, Thirumalvalavan K. Tuberculous myositis and cellulitis in a renal transplant recipient. *Indian J Tuberc* 2020; **67**: 353-356 [PMID: 32825866 DOI: 10.1016/j.ijtb.2019.04.010]

Published by **Baishideng Publishing Group Inc**
7041 Koll Center Parkway, Suite 160, Pleasanton, CA 94566, USA
Telephone: +1-925-3991568
E-mail: bpgoffice@wjgnet.com
Help Desk: https://www.f6publishing.com/helpdesk
https://www.wjgnet.com